The role of tissue-resident memory T cells in immunity to *Bordetella pertussis*

Trinity College Dublin
Coláiste na Tríonóide, Baile Átha Cliath
The University of Dublin

Lucy Curham

B.Sc. Human Health and Disease

A thesis submitted to

Trinity College Dublin

As completion of the degree of Doctor of Philosophy

2022

Supervisor: Professor Kingston Mills

Immune Regulation Research Group

School of Biochemistry and Immunology

Trinity College Dublin

Declaration of Authorship

I declare that this thesis has not been submitted as an exercise for a degree at this or any other university and it is entirely my own work, except where otherwise stated.

I agree to deposit this thesis in the University's open access institutional repository or allow the library to do so on my behalf, subject to Irish Copyright Legislation and Trinity College Library conditions of use and acknowledgement.

_____

Lucy Curham

School of Biochemistry and Immunology

Trinity College Dublin

Abstract

Whooping cough (pertussis) is a severe respiratory disease cause by the Gram-negative bacterium *Bordetella pertussis*. Despite high vaccine coverage, a resurgence of pertussis has been observed over recent years. Although current acellular pertussis vaccines protect against severe disease, they do not induce sterilising immunity in the nasal cavity and this may contribute to asymptotic transmission of *B. pertussis*. Therefore, a better understanding of the mechanisms of protective immunity against *B. pertussis* in the nasal cavity is required to help inform the design of next generation pertussis vaccines.

The results of this study found that CD4 tissue-resident memory T (T_{RM}) cells, a population of memory T cells that express CD69 with or without CD103, accumulate and persist in the nasal mucosa of mice following *B. pertussis* infection. CD4 T_{RM} cells were a major source of IL-17A in the nasal cavity. Furthermore, CD4 T_{RM} cells expanded locally during re-challenge and this was associated with rapid clearance of the secondary infection with *B. pertussis* from the nasal cavity. Protection against primary and secondary infection of the nasal cavity with *B. pertussis* was lost in IL-$17^{-/-}$ mice and in mice depleted of CD4 T cells. Expansion of IL-17A-producing CD4 T_{RM} cells was accompanied by the infiltration of a novel neutrophil population expressing Siglec-F, which exhibited high NETosis capacity. Accumulation of Siglec-F^{+} neutrophils was reduced in IL-$17^{-/-}$ mice and mice depleted of CD4 T cells. CXCL1, a chemokine required for neutrophil recruitment, was decreased in the nasal cavity of IL-$17^{-/-}$ mice, whereas intranasal IL-17A administration induced CXCL1 production in the nasal cavity. Furthermore, depletion of neutrophils significantly curtailed bacterial clearance from the nasal cavity during infection with *B. pertussis*.

This study also revealed that respiratory CD4 T_{RM} cells induced by natural infection or immunisation with a whole cell pertussis (wP) vaccine can produce IL-17A in the absence of TCR activation. CD4 T_{RM} cells could be activated directly by the cytokines IL-23 with IL-1β or IL-18 or when cultured with innate immune cells stimulated with PAMPs or the unrelated pathogen *Klebsiella pneumoniae*. Furthermore, immunisation of mice with a wP vaccine conferred non-specific protection against *K. pneumoniae* infection of the nasal cavity. These findings demonstrated that CD4 T_{RM} cells are a major source of protective IL-17A in the nasal cavity and can be maintained by non-specific activation, probably by unrelated pathogens, and should be considered when informing future immunisation strategies to control the transmission of *B. pertussis* in humans.

Acknowledgements

First and foremost, I would like to thank my supervisor Prof. Kingston Mills for his guidance and support throughout my PhD. You have been an incredible supervisor throughout my time in the lab. I am so thankful for all of your encouragement and motivation, especially when experiments didn't go to plan. These last few years were difficult for everyone, but you always remained optimistic. Your door was always open and I appreciate all of the advice you have given me. I have thoroughly enjoyed my time and am grateful to you for giving me the opportunity to pursue a PhD in your lab.

I would also like to give a huge thank you to Mieszko and Lisa for all of their help and support over the years. Mieszko, you were a great mentor when I started in the lab and taught me so much. I wouldn't be the scientist I am today without your expertise and advise. Lisa, I couldn't have asked for a better person to work with on the IL-17 project. I am so appreciative of all of your help and advice, and have learned so much from working with you (specifically, how to be more organised with experiments!).

I feel so lucky to not only work with great scientists, but also with such incredible people. Charlotte, I am so fortunate to have you as a friend and don't know how I would have got through the PhD without you! You have always been the voice of reason whenever I was being completely irrational and I'm so grateful for your support over these last few months. Kyle, you made me feel so welcome when I joined the lab and have been an amazing friend ever since. I miss sharing a lab bench and having the chats with you, but I'm sure I'll meet you for a pint soon! Caitlín, you have brought such a lovely and positive energy to the lab, and I'm so grateful for your help with experiments and more importantly for your friendship.

To the current members of the Mills' lab, you have been so helpful to me during my PhD. To Pauline and Béré, you have both been such a great addition to the lab and always so helpful with experiments. To Caroline, Karen, and Davoud, thank you for all of the support and advice. I would also like to give a huge thanks to Paula and Catherine, who do so much work to keep the lab up and running. Also a big thank you goes to Barry, I don't know what TBSI would do without you! Thank you for all your help and patience with flow cytometry, it has been invaluable throughout my project. I would also like to thank former members of the Mills' lab - Alicja, Joey, Mark, Bill, Mathilde, and Sarah - who made it such a welcoming environment when I started. To Aoife, Rob, and Shauna, I have such great memories from when you were all in the lab, Friday night pints aren't the same without you! Also to current and past members of the Loane lab: David, Janeen,

Isabella, Nico, and Marie – you have all been so great to work with. I also owe a huge thanks to Jenny for all of your help with the *Klebsiella* project.

To my PhD pals, Hannah and Jamie, we've finally made it! Hannah, thank you so much for being such an amazing friend – I couldn't think of a better person to go through the PhD process with. You have always been there for me and I have so many great memories from the last nine (!) years of our friendship. To Jamie, you are always a welcome distraction to work and are always able to put a smile on my face. I really value your friendship, especially over the last few years. To Luke and Stephen, thank you for being amazing friends, I have such great memories from Madrid and can't wait for Barcelona! I would also like to acknowledge all of the friends I've made in the Biochemistry and Immunology Department – I couldn't have asked for a nicer department to work in and have met so many great people. I would also like to thank my friends from home, especially Sarah, who was always around for a coffee and a chat when needed.

And finally, the biggest thank you to my family. Ellen and Hannah, thank you for always being so supportive (even if you didn't really know what I was doing for the last four years!). To Grace, your strength and resilience over this last year has made doing a PhD look easy in comparison. I'm so lucky to have you all as sisters. Mum and dad, words can't describe how grateful I am for your support and encouragement throughout my life. I wouldn't be the person I am today without you both. Thank you for everything you have done for me.

Publications

Borkner L, **Curham LM**, Wilk MM, Moran B, Mills KHG. IL-17 mediates protective immunity against nasal infection with *Bordetella pertussis* by mobilizing neutrophils, especially Siglec-F^+ neutrophils. Mucosal Immunol. 2021 Sep;14(5):1183-1202. doi: 10.1038/s41385-021-00407-5. Epub 2021 May 11.

Quinn SM, Cunningham K, Raverdeau M, Walsh RJ, **Curham L**, Malara A, Mills KHG. Anti-inflammatory Trained Immunity Mediated by Helminth Products Attenuates the Induction of T Cell-Mediated Autoimmune Disease. Front Immunol. 2019 May 21;10:1109. doi: 10.3389/fimmu.2019.01109.

Wilk MM, Borkner L, Misiak A, **Curham L**, Allen AC, Mills KHG. Immunization with whole cell but not acellular pertussis vaccines primes CD4 T_{RM} cells that sustain protective immunity against nasal colonization with *Bordetella pertussis*. Emerg Microbes Infect. 2019;8(1):169-185. doi: 10.1080/22221751.2018.1564630.

Fitzpatrick JM, Minogue E, **Curham L**, Tyrrell H, Gavigan P, Hind W, Downer EJ. MyD88-dependent and -independent signalling via TLR3 and TLR4 are differentially modulated by Δ^9-tetrahydrocannabinol and cannabidiol in human macrophages. J Neuroimmunol. 2020 Jun 15;343:577217. doi: 10.1016/j.jneuroim.2020.577217. Epub 2020 Mar 20.

Abbreviations

AMP	Antimicrobial peptide
ANOVA	Analysis of variance
aP	Acellular pertussis
APC	Antigen presenting cell
ATP	Adenosine 5'-triphosphate
BAL	Aronchoalveolar lavage
BCG	Bacillus Calmette-Guerin
BCL6	B cell lymphoma 6
BCR	B cell receptor
BMDC	Bone marrow-derived dendritic cell
BSA	Bovine serum albumin
cAMP	Cyclic adenosine monophosphate
cDC	Conventional DC
CFU	Colony forming unit
cLN	Cervical lymph node
cMoP	Common monocyte precursor
CNS	Central nervous sytem
CTL	Cytotoxic T lymphocyte
CXCL	C-X-C Motif Chemokine Ligand
CyaA	Adenylate cyclase
DAMP	Damage-associated molecular pattern
DAPI	4',6- diamidino-2-phenylindole
DC	Dendritic cell
DN	Double negative
DNAse I	Deoxyribonuclease I
EAE	Experimental autoimmune encephalomyelitis
EAU	Experimental autoimmune uveitis
ECP	Eosinophil cationic protein
EDTA	Ethylenediaminetetraacetic acid
ELISA	Enzyme Linked Immunosorbent Assay
ETT	Eosinophil extracellular trap
FACS	Fluorescence-activated cell sorting
FCS	Foetal calf serum
FHA	Filamentous hemagglutinin

FIM	Fimbriae
Foxp3	Forkhead box P3
G-CSF	Granulocyte colony-stimulating factor
GM-CSF	Granulocyte macrophage colony-stimulating factor
GPCR	G-protein coupled receptor
HLA	Human leukocyte antigen
HRP	Horseradish peroxidase
HSC	Hematopoietic stem cell
HSD	Honestly significant difference
HSV	Herpes simplex virus
i.m.	Intramuscular
i.n.	Intranasal
i.p.	Intraperitoneal
i.v.	Intravenous
ICAM-1	Intercellular adhesion molecule 1
ICOS	Inducible T cell co-stimulator
IFN	Interferon
Ig	Immunoglobulin
IL	Interleukin
IL-17R	IL-17 receptor
ILC	Innate-like lymphocyte
ITAM	Immunoreceptor tyrosine-based activation motif
iTreg	Inducible Treg
LCMV	Lymphocytic choriomeningitis virus
LCN2	Lipocalin-2
LIAV	Live attenuated influenza vaccine
LPS	Lipopolysaccharide
MAC-1	Macrophage receptor-1
MAIT	Mucosal-associated invariant T
MBP	Major basic protein
MCP-1	Monocyte chemoattractant protein-1
M-CSF	Macrophage colony-stimulating factor
MDDC	Monocyte-derived DC
MHC	Major histocompatibility complex
MIP-2	Macrophage inflammatory protein-2
Mtb	*Mycobacterium tuberculosis*

NALT	Nasal-associated lymphoid tissue
NET	Neutrophil extracellular trap
NF-κB	Nuclear factor kappa-light-chain-enhancer of activated B cells
NK cell	Natural killer cell
NO	Nitric oxide
nTreg	Natural Treg
OD	Optical density
OMV	Outer membrane vesicle
OVA	Ovalbumin
PAMP	Pathogen associated mollecular pattern
PBMC	Peripheral blood mononuclear cells
PBS	Phosphate buffered saline
PD1	Programmed cell death-1
pDC	Plasmacytoid DC
PFA	Paraformaldehyde
P.i.	Post infection
PMA	Phorbol 12-myristate 13-acetate
PMN	Polymorphonuclear
Poly I:C	Polyinosinic-polycytidylic acid
PRN	Pertactin
PRR	Pattern recognition recepto
PT	Pertussis toxin
RORγT	Retinoic acid-related orphan receptor gamma-T
ROS	Reactive oxgen species
RPMI	Roswell Park Memorial Institute
RSV	Respiratory syncytial virus
RT-qPCR	Real-Time Quantitative Polymerase Chain Reaction
RTX	Repeat in toxin
S1P	Sphingosine 1 phosphate
sBP	Sonicated *B. pertussis*
SD	Standard deviation
SEM	Standard error of the mean
STAT	Signal transducer and activator of transcription
STING	Stimulator of interferon genes
T-bet	T-box transcription factor
T_{CM}	T central memory

TCR	T cell receptor
TCT	Tracheal cytotoxin
T_{EM}	T effector memory
Tfh	Follicular helper T
Th	T helper
TLR	Toll-like receptor
TNF	Tumour necrosis factor
Treg	Regulatory T cell
T_{RM}	Tissue-resident memory T cell
TSA	Tryptic Soy Agar
WHO	World Health Organisation
wP	Whole cell pertussis
WT	Wild type

Table of Contents

List of Figures

Chapter 1: General Introduction

Chapter 2: Materials and Methods

Chapter 3: IL-17-producing CD4 T_{RM} cells mediate protective immunity against *B. pertussis* in the nasal cavity by mobilising Siglec-F^{+} neutrophils

Chapter 4: CD4 T_{RM} cells mediate adaptive immunity against re-infection with *B. pertussis* in the nasal cavity

Chapter 5: Bystander activation of CD4 T_{RM} cells induced by previous infection with *B. pertussis*

Chapter 6: Bystander activation of CD4 T_{RM} cells induced by intranasal immunisation with a wP vaccine

Chapter 7: General Discussion

Chapter 1: General Introduction

1.1 Background and disease course of pertussis

Whooping cough (pertussis) is a highly communicable, acute respiratory infection caused by the Gram-negative coccobacillus *Bordetella pertussis* [1]. *B. pertussis* is a strictly human pathogen and unlike other contagious infectious diseases, such as smallpox, measles, and polio, pertussis has no ancient history [2]. Transmission of disease is believed to occur through aerosols droplets [3]. Once in the respiratory tract, *B. pertussis* attaches to ciliated epithelial cells and releases toxins that contribute to disease pathogenesis [4]. Classical pertussis illness typically occurs following infection of unimmunised children and has three distinct stages, lasting for a period of 6 to 12 weeks [3]. The initial stage, known as the catarrhal stage, exhibits symptoms similar to that of a common cold, including rhinorrhoea and a mild cough. However, over a period of 7 to 14 days, the cough worsens in both frequency and intensity, and the disease enters the second stage, known as the paroxysmal stage. The paroxysmal stage is characterised by repeated coughing fits with 5 to 10 or more forceful coughs during a single expiration (paroxysm), often followed by a characteristic high-pitched 'whoop' that occurs as air re-enters the lungs when patients gasp to breath. The paroxysmal stage generally lasts for 2 to 8 weeks. The final, or convalescent, stage is accompanied by a decrease in the frequency and severity of the paroxysms and generally lasts for 1 to 2 weeks [3, 4]. Pertussis is commonly treated with antibiotics such as azithromycin, clarithromycin, and erythromycin [5]. Despite the availability of a vaccine since the 1940s, whooping cough is still a major public health concern, with the World Health Organisation (WHO) reporting over 150,000 pertussis cases globally in 2018, and estimating 89,000 deaths based on 2008 data [6]. In Ireland, there were 165 reported cases of pertussis in 2019 [7].

1.2 Vaccines against *B. pertussis*

Following the isolation of *B. pertussis* by Bordet and Gengou in 1906, efforts were made to generate an effective pertussis vaccine [2]. Prior to mass vaccination, significant morbidity and mortality was associated with pertussis, with around 1.7 million reported cases and 73,000 deaths due to pertussis in the United States (US) between 1922 and 1931 [8]. Candidate whole-cell (wP) pertussis vaccines, prepared from killed whole cell *B. pertussis* organisms, were first developed in the 1930s. Universal use of wP vaccines commenced in the 1940s. Initial vaccines were mono-component, but have been combined with diphtheria and tetanus toxoids since 1947 [3, 9]. Mass vaccination was incredibly effective at reducing pertussis incidence, reducing the average rate of reported

pertussis cases from 157 in 100 000 in the pre-vaccine era to < 1 in 100 000 in the 1970s in the US alone [9]. However, use of the wP vaccine was associated with side effects ranging from mild injection site reactions to more severe systemic effects including whole-limb swelling, febrile seizures and persistent crying [10]. The reactogenicity of the wP vaccine was attributed to its endotoxin/lipopolysaccharide (LPS) content, which is highly inflammatory [1]. More ominous reports began to emerge, with a publication from 1974 describing an association between wP vaccination and severe neurological complications [11]. However, later studies did not find a strong causal relationship between wP immunisation with infantile spasms [12], encephalopathy [13], or acute neurological illness [14]. Nonetheless, these early studies, alongside exaggerated media reports, resulted in markedly reduced wP vaccine uptake in several countries, such as the United Kingdom (UK) and Japan, and discontinuation of use in countries such as Sweden [9]. This led to the development of a subunit-based acellular pertussis (aP) vaccine, which contains purified, inactivated components of *B. pertussis* cells [10]. In contrast to the wP vaccine, which contains more than 3000 antigens, the aP vaccine contains up to 5 purified *B. pertussis* antigens [9]. The first aP vaccine was developed in Japan by Sato and colleagues [15]. The aP vaccines were found to be less reactogenic because they contain virtually no LPS and subsequently replaced the wP vaccine in most industrialised countries by the mid-late 1990s [9]. All aP vaccines approved for use today contain inactivated pertussis toxin (PT) with combinations of filamentous hemagglutinin (FHA), pertactin (PRN), and some also include fimbriae (FIM) types 2 and 3 [4]. However, despite an estimated 86% worldwide coverage of pertussis vaccines, the WHO reported almost 151,000 cases globally in 2018. Furthermore, global vaccine coverage for pertussis fell from 86% in 2019 to 83% in 2020, most likely due to the COVID-19 pandemic and associated disruptions to health systems [16].

1.3 Resurgence in pertussis

The incidence of pertussis has been on the rise in recent years, coinciding with the introduction of the aP vaccine. Recent outbreaks have been reported in multiple industrialised countries, including Australia and the US [17]. Ireland reported a large increases in pertussis cases in 2012, with 458 cases recorded that year, up from 229 cases reported in 2011 and 114 cases reported in 2010 [18]. Although pertussis typically only causes mild or asymptomatic disease in older children and adults, circulating *B. pertussis* poses most risk to infants who have either not commenced or completed their vaccination schedule, where disease can become serious and potentially fatal [19]. In

the 2012 outbreak in Ireland, 45% of cases were less than six months of age therefore not eligible for three doses of pertussis vaccine in the Irish schedule. However, 24% of cases were completely vaccinated for their age [18]. There are multiple factors contributing to the recent resurgence in pertussis. Increased pertussis incidence could be an artefact of improved diagnostic techniques. Although highly selective, the use of culture methods display low sensitivity compared with molecular techniques, such as real-time polymerase chain reaction (RT-PCR), which are now routinely used in clinical settings [17]. However, as the increase in the incidence of pertussis is found mainly in age groups in which immunity has waned, such as older children and adolescents, the failure of currently used aP vaccines to induce long-lasting immunity is thought to be a major contributing factor to the resurgence of pertussis [19]. Protective immunity induced following natural infection with *B. pertussis* is estimated to persist for between 4 – 20 years, whereas immunity acquired after vaccination with a wP vaccine is estimated to wane after 4 – 12 years [20]. However, there is evidence to suggest that the duration of immunity after immunisation with aP vaccines is even shorter. A US study demonstrated that protection following 5 doses of a 3-component aP vaccine was estimated to wane 27% per year on average, with cases of pertussis amongst vaccinated children increasing in those furthest away from their last booster dose [21, 22].

Another possible contributing factor to recent outbreaks are genetic modifications of circulating *B. pertussis* strains, which may facilitate the organism to evade vaccine-induced immunity or become more virulent [23]. Although it cannot be ruled out that this is simply part of the natural evolutionary course of *B. pertussis*, it has been proposed that it might be a consequence of *B. pertussis* adaption to widespread use of the aP vaccine, resulting in vaccine-induced selective pressure. Genes encoding the limited number of antigens included in the aP vaccine have been found to evolve at higher rates then those not included in the vaccine [17]. The most striking example of this is the emergence of PRN-deficient strains in countries where PRN is one of the key antigens used in aP vaccines. Prior to widespread use of the aP vaccine, PRN-deficient isolates were rarely found [24]. However, PRN-deficient strains have recently been detected in multiple European countries including Norway [24] and France [25], in addition to the US [23], Australia [26], and Japan [27]. In contrast, PRN-deficient strains have not been identified in Denmark, where PRN is not one of the antigens included in the aP vaccine [24].

An emerging hypothesis for the resurgence of whooping cough is that the currently used aP vaccines fail to prevent asymptomatic transmission. Recent studies from a baboon model have revealed that although aP vaccines are effective at preventing pertussis

disease, these vaccines fail to protect against *B. pertussis* colonisation of the upper respiratory tract, and that animals immunised with an aP vaccine are still capable of transmitting disease [28]. The mechanisms and implications of aP vaccine-mediated asymptomatic transmission will be discussed later in this chapter. However, current aP vaccine schedules are insufficient at curtailing pertussis outbreaks and highlights the need for the development of third generation pertussis vaccines.

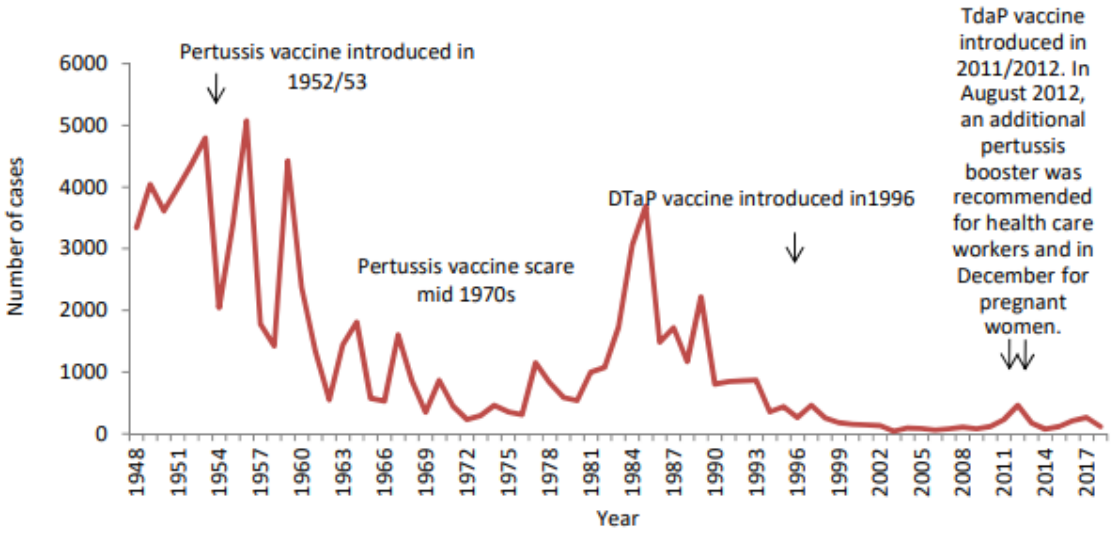

Figure 1.1 Number of notified pertussis cases in Ireland by year, 1948-2018

The reported number of cases of notified pertussis in Ireland, from 1948-2018. The single arrow indicates the year the wP or aP vaccine programme was introduced into Ireland. The double arrow indicates the year a booster aP was introduced and recommended for health care workers and pregnant women. Data from 1948-2000 collected by Department of Health, Ireland. Data from 2000-2018 collected by Health Protection Surveillance Centre, Ireland. (Figure taken from [29])

1.4 The innate immune response to *B. pertussis*

1.4.1 Overview of the innate immune system

The innate immune system is the first line of defence against infection. It consists of a wide range of protective mechanisms, such as physical barriers, soluble proteins, and cellular components, which aim to restrict and eliminate an invading organism, and subsequently activate an adaptive immune response [30, 31]. The innate immune response is non-specific, and can recognise a range of conserved microbial components which are commonly expressed on invading organisms but not by the host, termed

pathogen associated molecular patterns (PAMPs), by non-clonal, germline-encoded receptors, termed pattern recognition receptors (PRRs) [31, 32]. PRRs can be found on the cellular or endosomal membrane, or in the cytosol. Additionally, they can be found extracellularly in secreted forms. There are four major sub-families of PRRs—the Toll-like receptors (TLRs), the nucleotide-binding oligomerization domain (NOD)- Leucin Rich Repeats (LRR)-containing receptors (NLRs), the retinoic acid-inducible gene 1 (RIG-1) -like receptors, and the C-type lectin receptors (CLRs) [33]. Recognition of pathogens by PRRs results marks the initiation of an innate immune response [32, 34].

1.4.2 Barrier immunity in the respiratory tract

B. pertussis is considered mainly to be an upper respiratory tract pathogen, with infection initiated by the attachment of *B. pertussis* organisms to the cilia of epithelial cells of the upper respiratory tract. However, lower respiratory tract infections can occur [3]. As the respiratory tract is constantly exposed to a range of inhaled pathogens, irritants, pollutants and toxic particles, it has developed a range of innate immune mechanisms to promptly remove invading organisms [35]. Conversely, *B. pertussis* is a strongly host-adapted pathogen, and has evolved to produce a number of virulence factors to counter most host immune responses in the respiratory tract [36].

The respiratory tract can be divided into two distinct anatomical sites: the upper respiratory tract, which comprises of the nares, pharynx, and larynx, and the lower respiratory tract, which consists of the trachea, bronchi, and lungs [37]. The upper respiratory tract is the first site encountered by many pathogens and is lined by ciliated pseudostratified columnar epithelium composed of ciliated, goblet, club, and basal cells [38]. The epithelial layer functions primarily as a physical barrier between the lumen and vasculature through the formation of tight junctions involving claudins, occludins and adherens, such as E-cadherin and β-catenin [35]. Furthermore, a secreted mucous layer which entraps inhaled pathogens and particles overlays the ciliated epithelial cells, which beat in metachronal waves to propel the entrapped pathogens out of the airways in a process known as mucociliary clearance [39, 40]. Additionally, epithelial cells express multiple types of PRRs [41]. *B. pertussis* produces a number of virulence factors which enable adherence to the respiratory tract and disruption host clearance mechanisms. FHA, which is a 220 kDa surface-associated protein, functions predominantly as an adhesion molecule to ciliated epithelial cells [42]. Furthermore, tracheal cytotoxin (TCT), a muramyl tetrapeptide bacterial cell wall fragment, has been shown to paralyse respiratory epithelial cilia when combined with LPS [43]. Additionally, adenylate cyclase (CyaA) toxin has been shown to upregulate mucin production in *B. pertussis*-infected

airway epithelia, altering its viscosity and elasticity and thereby compromising the capacity of the mucociliary escalator to eliminate entrapped *B. pertussis* [44]. CyaA can also disrupt epithelium tight junction functional integrity [45]. *B. pertussis* has been shown to induce cytokine and chemokine production, such as interleukin-6 (IL-6), IL-8, and monocyte chemoattractant protein-1 (MCP-1), from airway epithelial cells [43]. Although *B. pertussis* is generally considered an extracellular pathogen, intracellular survival of *B. pertussis* has been reported in human epithelial cells [46].

Respiratory tract epithelial cells are also a major source of antimicrobial peptides (AMPs). AMPs are a class of small peptides which exhibit a wide range of inhibitory effects against bacteria, fungi, parasites and viruses [47]. However, *B. pertussis* has evolved to avoid the antimicrobial activity of cationic AMPs (CAMPs). LPS is a major component of the outer membrane of Gram-negative bacteria and enables susceptibility to CAMPs, however modification of the Lipid A region of LPS as seen in *B. pertussis* increases resistance to numerous CAMPs, including LL-37 [48].

The complement system is another soluble mediator of the innate immune response and consists of a cascade of enzymatic reactions which activate proteins present in serum, as well as on mucosal surfaces including the respiratory tract [49, 50]. Activation of the complement cascade results in opsonisation and lysis of invading pathogens, in addition to promoting pro-inflammatory responses. Complement can be activated through three pathways: the classical, lectin, or alternative pathway, however, they all converge in the formation of the convertases which cleave and subsequently activate the major effectors of the complement system: anaphylatoxins (C4a/C3a/C5a) [51]. As a consequence of co-evolution with its host, *B. pertussis* has developed various methods to avoid killing by complement such as producing complement evasion proteins including BrkA (*Bordetella* resistance to killing) protein [36]. Furthermore, *B. pertussis* has been shown to recruit C1 esterase inhibitor (C1inh), a major regulator of complement, from human serum in order to avoid complement-mediated killing [52].

1.4.3 Cellular components of the innate immune response to B. pertussis infection

Phagocytes are the major cellular arm of the innate immune system and are highly conserved throughout evolution. Phagocytes are specialised cells that engulf and kill invading pathogens to protect the host against microorganisms [53]. Phagocytes include granulocytes such as neutrophils and eosinophils, and mononuclear leukocytes such as monocytes, macrophages and dendritic cells (DCs).

1.4.4 Neutrophils

Neutrophils are the most abundant cell type in circulation and are one of the first cells to arrive at the site of infection [54, 55]. Neutrophils are also known as polymorphonuclear (PMN) leukocytes due to their multi-lobulated nucleus [56]. They are also characterised by the abundance of granules in their cytoplasm, and belong to the granulocyte lineage of circulating immune cells [57]. Neutrophils are generated in the bone marrow at a rate of 10^{11} per day, however this can increase to 10^{12} per day during a bacterial infection [53]. Neutrophils and other granulocytes such as basophils and eosinophils are generated from hematopoietic stem cells (HSCs) in a process called granulopoiesis [57, 58]. Granulopoiesis can be divided into two stages. The first stage involves the conversion of HSCs into a granulocyte precursor cell, the myeloblast. The second stage involves the irreversible conversion of the myeloblast into a committed PMN leukocyte. This process is controlled by a range of external stimuli such as growth factors and cytokines, principally granulocyte colony-stimulating factor (G-CSF). Granulopoieses is also controlled by a range of internal factors, such as activation of different transcription factors, including Runx1, C/EBP-α, and C/EBP-ε, and microRNAs [58, 59]. Once mature, neutrophils can leave the bone marrow into circulation, however this process is tightly controlled under normal homeostatic conditions, where only 1 - 2% of all neutrophils in the body are found in the blood at any one time [54].

In healthy individuals, circulating neutrophils are found in a ‘dormant state’ and their activation is a defining step in the inflammatory response [53, 60]. During an infection, mature neutrophils reach sites of tissue inflammation in response to chemokines such as C-X-C Motif Chemokine Ligand 1 (CXCL1) via the vasculature [61]. Recruitment of neutrophils from the circulation into inflamed tissue involves a cascade mediated by the sequential interactions between receptors expressed on neutrophils and ligands expressed on the surface of activated endothelium [53]. The classical multistep adhesion cascade involves the initial attachment and subsequent rolling of the neutrophils along the endothelium. Rolling is mediated by selectins, such as L-, P-, and E-selectin, which are expressed on inflamed endothelium cells, interreacting with ligands such as P-selectin glycoprotein ligand 1 (PSGL1) and CD44 expressed on neutrophils [62]. This is followed by neutrophil arrest with accompanying cell spreading [63]. The final stages of the neutrophil recruitment cascade involves paracellular crawling of the neutrophil along the endothelium in a macrophage receptor 1 (MAC-1) and intercellular adhesion molecule 1 (ICAM1)-dependent manner, and finally the transmigration of the neutrophil through venular walls into the tissue [64].

Once neutrophils enter the inflamed tissue, they are able to recognise and phagocytose invading microorganisms and subsequently execute antimicrobial functions through a combination reactive oxygen species (ROS) generation, release of AMPs, and release of nuclear material to form neutrophil extracellular traps (NETs) [53, 54]. Neutrophils also contribute to the regulation of an inflammatory response through the production of pro-inflammatory cytokines, such as IL-1β, IL-18, and IL-6, and chemokines, including CXCL1, CXCL2, and macrophage inflammatory protein-2 (MIP-2) [65].

Neutrophils express a wide range of PRRs, ligation of which results in the activation of neutrophil killing mechanisms. Neutrophils are professional phagocytes and can rapidly internalise pathogens coated or opsonised with serum antibodies in an Fcγ Receptor-mediated manner. The nascent phagosome containing the internalised pathogen rapidly fuses with preformed granules found in the cytosol of neutrophils which contain a range of antimicrobial mediators including hydrolytic enzymes, proteinases, AMPs, and NADPH oxidase subunits that initiate killing mechanisms [53, 66]). Assembly and activation of the NADPH complex results in the generation superoxide anion (O_2^-), which subsequently leads to the generation of ROS, such as hydrogen peroxide (H_2O_2), hydroxyl radical ($OH^\bullet$) and hypochlorous acid (HOCl), which all contributing microbial destruction within the phagosome, in a process termed ‘oxidative burst’ [60].

Zychlinsky and colleagues described another method of neutrophil-mediated cell killing, by which neutrophils release modified chromatin structures decorated with histones, in addition to granule-derived AMPs and enzymes, called NETs [57, 67]. NETs are released upon neutrophil cell death in a process known as ‘NETosis’. During NETosis, the nucleus delobulates and cytosolic granules disappear. This is followed by chromatin decondensation, histone modification and destruction of the nuclear envelope. The chromatin is subsequently released into the cytosol where it binds to granular proteins. Finally, the cytoplasmic membrane ruptures and the NET is released into the extracellular space [57, 68]. NETs subsequently capture the invading organism with a sticky meshwork of chromatin and subsequently kills them by exposure to highly concentrated AMPs and enzymes [69]. Neutrophils are generally considered short-lived cells, with a lifespan of < 1 day and an estimated circulating half-life of approximately 8 hours in humans [70]. However there are reports using *in vivo* labelling with ^2H_2O that human neutrophils can last up to five days [71]. Nonetheless, removal of neutrophils from tissue once infection has subsided is essential in preventing excessive tissue damage [72]. Recruited neutrophils are primarily removed by macrophages, however DCs have also been implicated [73].

Murine models of *B. pertussis* infection have revealed that neutrophil influx to the lungs peaks at day 7 post infection, which is relatively delayed compared to that observed during infection with other Gram-negative respiratory pathogens [74]. This suggests a defective neutrophil response during the acute stages of a *B. pertussis* infection. Furthermore, the exact role of neutrophils during the early stages of *B. pertussis* infection remains unclear, with studies suggesting that they may play a greater role in the later stages of infection or during re-exposure to the bacterium. A study by Kirimanjeswara and colleagues suggested that opsonisation of *B. pertussis* by antibodies is required for the protective effects of neutrophils during *B. pertussis* infection. Adoptive transfer of convalescent phase serum from mice previously infected with *B. pertussis* enhanced bacterial clearance from the lungs, and this protection was lost following depletion of neutrophils [75]. Furthermore, a study by Andreasen et al. demonstrated that depletion of neutrophils did not affect bacterial clearance from the lungs of mice during a primary infection with *B. pertussis*. However, depletion of neutrophils in convalescent mice during a secondary challenge did impair clearance of *B. pertussis* from the lungs, as did depletion of neutrophils from mice receiving convalescent phase serum and subsequently infected [76]. These studied suggest that neutrophils exert their protective effects through FcγR-mediated phagocytosis, and require the presence of circulating antibodies to execute their protective effects. As circulating antibodies are only generated towards the later stages of an infection, this may explain why neutrophils appear redundant in the acute stages.

Furthermore, the neutrophil response to *B. pertussis* infection is highly influenced by the virulence factors such as CyaA and PT expressed by the bacterium, which may contribute to the delayed response observed in animal models. CyaA is a 1706 residue long bi-functional leukotoxin released over the course of *B. pertussis* infection that impairs a variety of neutrophil functions [77]. The N-terminal domain contains adenylate cyclase activity, whereas the C-terminus possesses pore-forming RTX (repeat in toxin) motifs that disturbs ion homeostasis by disrupting the permeability barrier of the plasma membrane [77, 78]. CyaA uses the integrin CD11b/CD18 (CR3), which is highly expressed on neutrophils, as a toxin receptor to translocate its adenylate cyclase catalytic domain across the plasma membrane where it converts ATP to excessive levels of cyclic adenosine monophosphate (cAMP) [74, 79]. The CyaA-mediated increase in intracellular cAMP levels has been shown to disrupt a number of neutrophil functions, such as phagocytosis [80], ROS generation [81], and NETosis [82].

PT is an AB-toxin composed of five subunits and is a member of the ADP-ribosylating toxin family. Through the B-oligomer, PT binds to any sialic acid-containing glycoprotein

at the cellular surface. Following internalisation, the A-promoter, which contains the enzymatically active S1 subunit, is separated and translocate to the cytosol where ADP-ribosylation of the α-subunit of G_i proteins impairs their interaction with their cognate G-protein coupled receptors (GPCRs), consequently disrupting downstream signalling transduction. Furthermore, $G_{i\alpha}$ ADP-ribosylation by PT inhibits regulation of adenylate cyclase activity, thus increasing intracellular cAMP levels [78, 83]. Chemokine receptors belong to the GPCR superfamily and PT has been demonstrated to inhibit neutrophil chemotaxis to the lungs, with infection of mice with a PT-deficient mutant strain of *B. pertussis* exhibiting enhanced neutrophil recruitment to the lungs [75, 84]. Furthermore, PT has also be shown to inhibit early transcription of chemokines involved in neutrophil recruitment by alveolar macrophages and other cells present in the lungs, including CXCL1 and CXCL2 (MIP-2) [84].

1.4.5 Eosinophils

Eosinophils are another member of the granulocyte family that develop in the bone marrow. Eosinophils can be distinguish from neutrophils by virtue of their bilobed nucleus and large specific granules containing cationic proteins, including the major basic protein (MBP), eosinophil peroxidase (EPX), and eosinophil cationic protein (ECP). Unlike neutrophils, relatively few eosinophils are found in the peripheral blood of healthy humans, with eosinophils mainly residing within tissues [85, 86]. During granulopoiesis, pluripotent progenitor cells commit to the myeloid lineage though expression of GAT-1, PU.1, and c/EBP transcription factors and develop into mature eosinophils when stimulated with IL-13, GM-CSF, and IL-5 [87]. Eosinophils are classically associated with Th2 responses to parasites or immune hyper-reactive states, such as asthma or allergies [86]. However, there is emerging evidence that eosinophils are capable of recognising, ingesting, and killing bacteria such as *Escherichia coli* and *Staphylococcus aureus*, however intracellular killing by eosinophils is reported to be lower than that observed by neutrophils [87, 88]. Furthermore, eosinophils are also capable of releasing their genetic material bound with granule proteins into the extracellular space to trap and subsequently kill invading pathogens in a similar manner to NETs released by neutrophils. Eosinophils can release their nuclear contents using one of two mechanisms. They can release either mitochondrial DNA in a ROS-dependent manner which is not accompanied by cell death [89]. Alternately, eosinophils can release nuclear DNA, which is accompanied by cell death in a process referred to as ‘eosinophil extracellular trap cell death’ (EETosis) [90]. The role of eosinophils during *B. pertussis*

infection is not well defined. There is peer reviewed evidence suggesting a history of whooping cough increases risk of asthma and allergic sensitisation disease, suggesting that *B. pertussis* triggers a hyper-reactive eosinophilic state [91]. In contrast, eosinophils have been reported to be protective during an infection with *Bordetella bronchiseptica*, a closely related species for which rodents are a natural host. Eosinophil-deficient mice failed to clear *B. bronchiseptica* from the nasal cavity and trachea, and had significantly delayed clearance from the lungs. This was associated with defective recruitment of T and B cells, in addition to reduced production of IL-17, IL-6, and IL-1β, which are implicated in protective immunity against *Bordetella* species [92].

1.4.6 Monocytes

Monocytes are innate immune cells of the myeloid lineage that are produced throughout life and play a key role in immunity and homeostasis. Monocytes are present in all vertebrates and comprise 4% and 10% of nucleated cells in the blood of mice and humans, respectively [93, 94]. There are two main types of monocytes found in the circulation. The first subtype consists of classical monocytes, which are originally derived from a common monocyte precursor (cMoP) cell in the bone marrow, and are identified as Ly6C^{hi} in mice, and CD14^{+} in humans. Ly6C^{hi} classical monocytes are relatively short lived, with a half-life of 20 hours. Classical Ly6C^{hi} monocytes function as a precursor for a heterogenous population of mononuclear phagocytes such as monocyte-derived macrophages and monocyte-derived DCs. During steady state, there is a continuous influx of monocytes into tissues, however this is substantially increased during inflammation [94-96]. The second subtype are non-classical monocytes, which are classified as Ly6C^{low} in mice, or CD14^{low} in humans. Ly6C^{low} monocytes are derived from classical Ly6C^{hi} monocytes in peripheral blood. In contrast to classical monocytes, non-classical monocytes have a relatively long half-life of 5 days, and remain in blood vessels where they patrol the vascular wall [94-96]. Monocytes are among the first cells recruited to the lungs in response to *B. pertussis* infection [97]. However, *B. pertussis* virulence factors are known to modulate monocyte function. CyaA has been demonstrated to block macrophage colony-stimulating factor (M-CSF)-mediated differentiation of monocytes to macrophages, which CyaA exposure preventing M-CSF-induced upregulation of macrophage maturation markers such as CD11b, CD36, CD206, and CD204 [98]. PT has also been shown to decrease the ability of monocytes to phagocytose *B. pertussis* [97].

1.4.7 Macrophages

Macrophages are a population of highly heterogeneous phagocytic cells which are strategically located with tissues throughout the body [99]. Macrophages play an important role in tissue homeostasis, surveillance, and resolution of inflammation [94]. It was originally hypothesised that the maintenance of tissue-resident macrophages relies on constant influx of blood-derived monocytes. This model, termed the monocyte phagocyte system (MPS), was first proposed by van Furth and Cohn in 1968 [100]. However, advancements in fate-mapping technologies have demonstrated that circulating monocytes minimally contribute to most tissue macrophage populations [101]. It is now understood that the majority of tissue macrophages are maintained predominantly through self-renewal and are derived from embryonic progenitors such as yolk sac-derived macrophages and foetal monocytes which migrate to peripheral tissue once circulation is established, with maintenance dependent on M-CSF and IL-34 [96].

Alveolar macrophages are the dominant immune cell in the lungs in the steady state and are located in close contact with the type I and II epithelial cells of alveoli [102]. Alveolar macrophages are predominantly derived from primitive yolk sac-derived macrophages which are seeded in the lung during the first week after birth in mice. They exhibit a typical phenotype that is highly auto-fluorescent, expressing low levels of CD11b, and high levels of the integrin CD11c and the lectin Siglec-F [103]. Alveolar macrophages exhibit a wide range of functions including the phagocytosis of apoptotic cells and antibody-opsonised bacteria. Furthermore, alveolar macrophages express a range of PRRs to detect PAMPS, in addition to damage-associated molecular patterns (DAMPS), and can coordinate an immune response to invading pathogens and tissue damage [102]. Interstitial macrophages constitute a second macrophage population in the lungs and reside in the parenchyma between the microvascular endothelium and alveolar epithelium [104]. Interstitial macrophages exhibit a phenotype distinct from alveolar macrophages and are described as non-auto-fluorescent Siglec-F^{-}CD11c$^{+/-}$CD11b^{+} and are implicated in the maintenance of lung homeostasis [105].

Alveolar macrophages have been demonstrated to play a protective role in immunity against *B. pertussis* infection. Challenge of mice deficient in the TLR adaptor protein MyD88 adaptor-like protein (Mal) with *B. pertussis* resulted in the depletion of alveolar macrophages, but not other innate immune cells such as neutrophils, inflammatory monocytes, or infiltrating macrophages. The reduced alveolar macrophage numbers observed in the MAL$^{-/-}$ mice was accompanied by increased bacterial load in the lungs, bacterial dissemination to the liver, and increased mortality. Furthermore, MAL$^{-/-}$ mice

were defective in an early burst of proinflammatory cytokine production which included IL-1β, tumour necrosis factor (TNF), and MIP-2α, and also had reduced ability to constrain intracellular growth of *B. pertussis*, demonstrating that alveolar macrophages play a protective role against *B. pertussis* infection [106]. Furthermore, depletion of alveolar macrophages by intranasal (i.n.) administration of clodronate liposomes prior to *B. pertussis* infection was found to enhance bacterial burden in the respiratory tract of mice [107]. Alveolar macrophages can also influence the subsequent adaptive immune response to *B. pertussis* and can contribute to respiratory tolerance. Conditioned medium from both human and murine alveolar macrophages was shown to induce Foxp3 expression in naïve CD4 T cells [108]. Foxp3 is the master transcription factor for regulatory T (Treg) cells which play a key role in modulating immune responses during infection [109]. However, the ability of alveolar macrophages to influence adaptive immune responses can be inhibited by virulence factors released by *B. pertussis*. A T helper (Th) 1 response is essential for protective immunity against *B. pertussis* and IL-12 is a key cytokine required for the generation of a Th1 response [110]. However, FHA reduces *B. pertussis*-derived LPS induced IL-12 production from alveolar macrophages in an IL-10-depedent manner [111]. Furthermore, survival of *B. pertussis* has been reported in both human and murine alveolar macrophages, with virulence factors such as CyaA, FHA, and PT implicated in promoting their intracellular survival [112, 113].

1.4.8 Dendritic cells

DCs are sentential leukocytes that play a key role in the initiation and regulation of adaptive immune responses [114]. DCs are professional antigen presenting cells (APCs) that function to translate innate information into adaptive immunity by inducing the clonal expansion of antigen-specific naïve T cells and promoting their differentiation into effector T cells [115-117]. DCs were first described by Steinman and Cohn in 1973 who termed them ‘dendritic cells’ due to their ability to ‘assume a variety of branching forms’ [118]. There are two main types of DCs - plasmacytoid DCs (pDCs) and ‘classical’ or ‘conventional’ DCs (cDCs), and can be distinguished based on morphology and function [115, 119]. As the name suggests, the morphology of pDCs resembles that of a plasma cells, however they acquire dendrites after activation [117]. pDCs promote antiviral immune responses and can produce large amounts of type I and type III interferons (IFNs) following recognition of viruses or self-nucleic acids through the intracellular PRRs TLR7 and TLR9 [115, 120].

cDCs resemble the cells originally described by Steinman and Cohn and are characterised by a stellate morphology and the capacity to uptake antigens and migrate to draining lymph nodes to prime naïve T cells following activation [114, 119]. cDCs can be further subdivided into either cDC1s or cDC2s. cDC1s are identified as $CD8\alpha^+CD103^+$ and are capable of cross-presenting antigens to CD8 T cells. Furthermore, cDC1s produce high levels of IL-12, which promotes cytotoxic T cell and Th1 cell responses. cDC2s are identified as $CD11b^+CD172a^+$ and are superior at presenting antigens on MHC class II and inducing Th1, Th2, and Th17 differentiation [96, 115]. cDCs originally develop in the bone marrow from a common DC precursor which gives rise to an intermediate cell known as a pre-cDC. After leaving the bone marrow, pre-cDCs travel through the blood to colonise either lymphoid tissue, including the spleen and lymph nodes, or non-lymphoid tissues, such as the skin, intestine and lungs, where they differentiate into resting cDCs. cDCs have a relatively short half-life of 3-5 days in lymphoid tissue, with this being slightly longer in non-lymphoid tissue, and are continuously replenished from bone marrow hematopoietic progenitor cells in a manner that depends on the cytokine Flt3 ligand [114, 115, 117].

In a steady-state, cDCs are described as resting or immature and exhibit characteristic dynamic stellate-like extensions that allow cell to exhibit sweeping movement to sample the local environment for foreign- and self-antigens. Immature cDCs are further characterised by low surface expression of both major histocompatibility complex (MHC) class II molecules and co-stimulatory molecules, such CD80, CD86, and CD40 [117, 119]. cDCs express a large repertoire of PRRs, ligation of which during an insult induces profound functional and phenotypic changes in DCs, termed ‘DC activation/maturation’ [116]. DC maturation is accompanied by the upregulation of surface markers such as MHC class II and co-stimulatory molecules such as CD80 and CD86, in addition to the CC-chemokine receptor 7 [119]. cDCs then carry ingested antigens and pathogens from the site of infection to T cell rich zones in lymphoid organs in a CCR-7-dependent manner [121]. DCs have been demonstrated to play a protective role in mediating immunity against *B. pertussis* infection in the lungs. $CD11c^+CD8\alpha^+CD103^+$ cells were found to peak in the lungs on day 6 post *B. pertussis* infection. Antibody-mediated depletion of either $CD8\alpha^+$ or $CD103^+$ DCs in the early stages of infection was found to significantly delay clearance of *B. pertussis* from the lungs, indicating that $CD11c^+CD8\alpha^+CD103^+$ cells directly contribute to protective immunity against *B. pertussis* [122].

1.5 The adaptive immune response to *B. pertussis* infection

In contrast to the innate immune system, which is non-specific and relatively short-lived, the adaptive immune response demonstrates a high degree of specificity and exhibits long-lived memory. The adaptive immune system consists of a cellular arm mediated by T cells and a humoral arm mediated by B cells. Both B and T cells arise in the bone marrow, and while B cells remain in the bone marrow to mature, T cells migrate to the thymus for further maturation. T cells are defined by their expression of a unique heterodimeric antigen-binding molecule known as the T cell receptor (TCR). In the thymus, the TCR chains undergo somatic recombination, resulting in a unique amino acid sequence in the antigen-binding region capable of recognising antigens from nearly all pathogens. When they leave the thymus, mature T cells are still considered naïve until they are exposured to their cognate antigen [123]. Mature T cells can be further subdivided into either helper T (Th) cells based on the expression of the CD4 co-receptor, or cytotoxic T lymphocytes (CTLs) based on expression of the CD8 co-receptor [124]. T cells are key mediators of protective immunity against *B. pertussis*, with nude mice, which are deficient in T cells, unable to clear *B. pertussis* after challenge [125].

1.5.1 T cell activation by DCs

An adaptive immune response is initiated following the interaction between DCs and T cells, leading to the activation and clonal expansion of naïve T cells [126]. It was first proposed by Lafferty and colleagues in 1980 that two signals are required for effective activation of naïve T cells. Signal-1 is provided by the interaction of an antigenic peptide-loaded MHC presented by an APC with the TCR expressed on the corresponding cognate T cell. CD4 T cells recognise antigens presented by an MHC class II molecule. Following phagocytosis of the invading pathogen by APCs, internalised antigens are degraded in endo/lysosomal compartments by proteases, such as cathepsins, to achieve a specific length of approximately 12 amino acids prior to loading onto MHC class II molecules. The peptide-MHC II complexes are then transported to the cell surface of professional APCs, such as DCs, where they can be recognised by antigen-specific CD4 T helper cells [126, 127]. In contrast, CD8 T cells recognise antigens cross-presented by MHC class I molecules [127]. Unlike MHC class II molecules, which are expressed exclusively by APCs, MHC class I molecules are expressed on all nucleated cells [124]. The TCR is a heterodimer consisting of an α and β chain. Each chain contain an immunoglobulin (Ig)-like extracellular variable (V) and constant (C) domain, a

membrane-proximal connecting peptide (CP), a single transmembrane (TM) region, and a short cytoplasmic tail [128]. The TCR itself does not contain signalling domains, but rather is non-covalently coupled to a multi-subunit signalling apparatus, termed the CD3 complex, that comprises the CD3εγ, CD3εδ, and CD3ζζ dimers [129]. The specificity of the TCR for antigen is located in the V domain of the two TCR polypeptides. Ligation of the TCR with the peptide-MHC complex induces the phosphorylation of the immunoreceptor tyrosine-based activation motif (ITAM) on CD3 by the Src kinase Lck, initiating a downstream signalling cascade that results in the activation of transcription factors required for T cell activation [126, 128]. Signal-2, termed 'co-stimulation' involves the interactions between co-stimulatory receptors expressed on T cells and corresponding ligands expressed APCs [130, 131]. Activation of the TCR in the absence of co-stimulation results in the T cell becoming non-responsive to subsequent stimulation, a phenomenon termed T cell anergy [131, 132]. Co-stimulatory receptor-ligand pairs such as CD28 expressed on T cells interacting with either CD80 or CD86 on DCs can induce positive signals, promoting T cell activation. However, interaction of the CTLA-4 co-receptor on T cells with either of these ligands can induce inhibitory signals, thus negatively regulating T cell activation [126]. In addition to signal-1 and signal-2, a third signal in the form of cytokines secreted by mature DCs and other innate immune cells promote naïve CD4 T cells to further differentiate into Th1, Th2, Th17, or Treg cells subsets [126].

1.5.2 Cytotoxic T lymphocytes

Upon activation, resting naïve CD8 T cells undergo massive expansion to generate a large pool of CTLs, which play an important role anti-viral and anti-tumour immunity [133]. In addition to TCR activation and co-stimulation, pro-inflammatory cytokines such as type I IFNs and IL-12 play a key role in the terminal differentiation of CD8 effector T cells [134]. Once activated, CTLs contribute to the elimination of infected or malignant cells using a range of contact-dependent and independent mechanisms, including secretion of cytotoxic effector molecules such as perforin and granzymes, or engagement of the Fas receptor expressed on infected cells, ligation of which induces apoptosis in target cells. Furthermore, CTLs produce chemokines and effector cytokines including IFNγ and TNF [124, 133].

The role of CD8 T cells in mediating immunity against *B. pertussis* is not well-defined. FHA-specific IFNγ-production has been detected from CD8 T cells isolated from the

peripheral blood of *B. pertussis*-infected individuals and from vaccinated children. This study found that FHA-specific IFNγ production by CD8 T cells was mediated in part by CD4 T cells. Conversely, IFNγ production by CD4 T cells was somewhat inhibited by the presence of CD8 T cells, suggesting that CD8 T cells may play a potential regulatory role in immunity against *B. pertussis* [135]. The potential negative role of CD8 T cells during *B. pertussis* infection has been demonstrated in murine models, with adoptive transfer of immune CD8 T cells resulting in higher bacterial load in the lungs of recipient mice following *B. pertussis* challenge compared with control mice that received non-immune T cells [110]. Treatment of mice with a depleting anti-CD8α antibody during the initial stages of a *B. pertussis* infection or throughout the course of infection was found to significantly enhance the bacterial load in the lungs, however, this was attributed to the depletion of $CD8\alpha^{+}CD11c^{+}$ DCs. To assess the potential contribution of CD8 T cells to this observation, this study commenced treatment with a depleting anti-CD8α antibody from day 6 during an active infection, which preceded the infiltration of CD8 T cells into the lungs. Interesting, treatment with a depleting anti-CD8α antibody during the later stages of *B. pertussis* challenge resulted in a lower bacterial load in the lung, suggesting once again a possible negative role for CD8 T cells in immunity to *B. pertussis* [122].

1.5.3 Role of CD4 T cells

CD4 T helper cells are a heterogeneous population which play a central role in mediating both innate and adaptive immune responses. CD4 T cells are termed 'helper T cells' due to their ability to help or facilitate the activation of other cells, including those of the innate immune system, CTLs, B cells, and non-immune cells, in addition to regulating an immune response, thereby protecting against immunopathology [136]. Murine models have demonstrated that CD4 T cells are key mediators of protective immunity against *B. pertussis*, with adoptive transfer of purified CD4 T cells from immune mice to sub-lethally irradiated recipient mice conferring protection following infection with *B. pertussis* [110]. Following activation, naïve CD4 T cells differentiate into specific subtypes which are characterised by the cytokines they produce and/or the expression of characteristic lineage-defining transcription factors [137]. These subsets include Th1, Th2, and Th17 cells in addition to regulatory T (Treg) cells and follicular helper T (Tfh) cells. The differentiation of CD4 T cells into different effector lineages depends primarily on the cytokine-milieu generated by APCs at the time of activation [136]. Naïve CD4 T cells demonstrate incredible plasticity, exhibiting almost stem cell-like properties, and have

the potential to differentiate into virtually all types of effector subtypes, depending on the combination of cytokines present during their activation stage [138].

1.5.4 Th1 cell differentiation and function during B. pertussis infection

Th1 cells play a key role in mediating protective immunity against intracellular pathogens [138]. T-box transcription factor (T-bet) is the master transcription factor regulating Th1 differentiation, activation of which results in a significant enhancement of IFNγ production by Th1 cells. Other transcription factors that regulate Th1 differentiation include signal transducer and activator of transcription 4 (STAT4) and STAT1 [136]. The main cytokines involved in Th1 differentiation are IL-12p70 and IFNγ [139, 140]. In both humans and mice, IL-12p70 is composed of a p40 subunit linked to a p35 subunit, and the heterodimer signals through the IL-12p70 receptor [141]. IL-12p70 is secreted in large amounts by APCs and induces IFNγ production from CD4 T cells through STAT4 activation [140]. Secreted IFNγ can subsequently act in a positive feedback loop to activate STAT1 in CD4 T cells, which in turn promotes T-bet expression and enhancing Th1 differentiation [136]. It has been shown that *B. pertussis* fails to induce IL-12p70 production from human monocyte-derived DCs (MDDCs). However, *B. pertussis*-treated MDDCs were still able to drive Th1 polarisation, suggesting that *B. pertussis* induces Th1 differentiation in an IL-12-independendent manner [142]. Conversely, *B. pertussis* was able to induce IL-23 production from MDDCs, a cytokine classically associated with Th17 differentiation which shares a common p40 subunit with IL-12. Although *B. pertussis* was found to induce p40 expression, the *B. pertussis* virulence factor CyaA inhibited p35 expression in MDDCs, and consequently inhibited functional IL-12p70 production, thus representing a potential mechanism of bacterial escape [143].

Th1 cells mediate the majority of their protective effects through secretion of IFNγ. There are a number of studies which have detected *B. pertussis* antigen-specific IFNγ production from total peripheral blood mononuclear cells (PBMCs) and peripheral blood CD4 T cells isolated from infants and children acutely infected with *B. pertussis*, as well as convalescent individuals [135, 144, 145]. As recovery from whooping cough is associated with a high level of immunity against subsequent infection, these studies suggest a role for Th1 cells in natural immunity to *B. pertussis* in humans. Murine models have also demonstrated a protective role of Th1 cells and IFNγ in protective immunity against *B. pertussis*. CD4 T cells from infected or convalescent mice were found to secrete *B. pertussis*-specific IFNγ [110]. Furthermore, adoptive transfer of polarised *B.*

pertussis-specific Th1 cells enhanced clearance of *B. pertussis* from the lungs of the recipient mice [146]. Challenge of IFNγ$^{-/-}$ mice with *B. pertussis* resulted in significantly higher bacterial load in the lungs compared with wild type (WT) mice. Furthermore, *in vivo* neutralisation of IFNγ during *B. pertussis* infection was also found to significantly delay bacterial clearance from the lungs [147]. Infection of mice with targeted disruption of the genes for the IFN-γ receptor did not significantly impair clearance of *B. pertussis* from the lungs. However, IFNγ receptor-deficient mice did exhibit atypical disease, which bacterial dissemination to the liver and reduced survival, suggesting that IFNγ is important for maintaining *B. pertussis* to the respiratory tract [148]. IFNγ is capable of orchestrating numerous protective functions, such as enhancing antigen presentation, and boosting anti-microbial functions, such as promoting the rapid acidification of phagolysosomes within infected macrophages and enhancing ROS production [149]. IFNγ has been demonstrated to reduce intracellular survival of *B. pertussis* within macrophage by inducing nitric oxide (NO) production [150]. Furthermore, IFNγ was also shown to enhance neutrophil-mediated killing of *B. pertussis* [146]. Combined, these results demonstrate that Th1 cells are a key mediator of protective immunity against *B. pertussis* through the production of IFNγ.

1.5.5 Th17 cell differentiation

Th17 cells play a key role in protective immunity against fungi and extracellular pathogens, in addition to contributing to the pathogenesis of autoimmunity. Th17 cells are characterised by their ability to produce IL-17A, in addition to other cytokines such as IL-17F and IL-22, which can promote an inflammatory response to infection, including chemokine production, neutrophil recruitment, and AMP production [151]. The major cytokines involved in Th17 differentiation include IL-6, transforming growth factor β (TGF-β), IL-21, IL-1β and IL-23, which initiate an intricate network of signalling pathways resulting in the activation of transcription factors which regulate Th17 differentiation [136, 151]. The retinoic acid-related orphan receptor gamma-T (RORγT) was discovered by Littman and colleagues to be the master transcription factor orchestrating Th17 differentiation [152]. The closely related transcription factor RORα was subsequently identified as an important transcription factor, synergising with RORγT to enhance Th17 differentiation [153]. Induction of RORγT is dependent upon STAT3, which is activated in response to Th17 polarising cytokines such as IL-6 and IL-23 [151]. Th17 differentiation involves multiple steps. The initial differentiation stage is promoted by

TGF-β and IL-6 [136]. Alone, TGF-β promotes naïve CD4 T cells to express Foxp3 and differentiate into inducible Treg cells. However, the presence of IL-6 in the inflammatory milieu inhibits TGF-β-induced Foxp3 expression and promotes Th17 differentiation, a process which is amplified by the presence of IL-1β and TNF [154, 155]. IL-6 induces the production of IL-21 by CD4 T cells, which can act in an autocrine manner to promote a self-amplification stage [156, 157]. Activation of Th17 cells is accompanied by the upregulation of the IL-23 receptor (IL-23R) [136]. IL-23 contributes to the maintenance of the Th17 phenotype and the ability of differentiated Th17 cells to produce IL-17A [157, 158].

1.5.6 Th17 cells and IL-17 family

IL-17A is the signature cytokine of Th17 cells and plays a key role in host defence against pathogens at mucosal sites. IL-17A is part of the larger IL-17 cytokine family, a group of cytokines that share a highly conserved C-terminus containing a cysteine-knot fold structure [159]. The IL-17 family currently consists of 6 members (IL-17 A-F), which signal via their corresponding receptors to activate downstream pathways to induce the expression of inflammatory mediators. IL-17F is also produced by Th17 cells and shares the greatest sequence homology (56%) with IL-17A [160]. Both IL-17A and IL-17F exist as homodimers, however an IL-17A/F heterodimer which is capable of regulating inflammatory responses has also been reported [161, 162]. IL-17 cytokines signal via the IL-17 receptor family which currently consists of 5 members (IL-17RA, RB, RC, RD, and RE), all of which share sequence homology to the earliest identified member, IL-17RA [160]. Both IL-17A and IL-17F signal through a heterodimeric receptor complex, the IL-17R, composed of IL-17RA and IL-17RC, both of which belong to the SEFIF protein family and contain a conserved cytoplasmic SEFIR domain. The proximal adaptor protein Act1 is a key mediator of IL-17R signalling, and is recruited to the IL-17R through SEFIR-dependent interactions after IL-17 stimulation. Act1 subsequently engages with TNF receptor–associated factor (TRAF) family members, activating the NF-κB, C/EBP, and MAPK signalling pathways to induce pro-inflammatory gene expression in target cells [159, 163]. IL-17RA is constitutively expressed on a wide variety of cell types and tissue, whereas IL-17RC expression is limited mainly to non-hematopoietic cells, including stromal cells and epithelial cells [164]. Both IL-17A and IL-17F bind to IL-17RC with comparable affinities, however the affinity by with IL-17F binds to IL-17RA is ~100 – 1000 times lower than that of IL-17A [160].

IL-17A and IL-17R signalling contribute to host defence against a variety of bacterial and fungal pathogens at barrier sites including *Klebsiella pneumoniae* infection in the lung, cutaneous *S. aureus* infection, and *Candida albicans* infection in the oral mucosa [165-167]. IL-17A mediates its protective effects through the induction of immune mediators including cytokines, chemokines, acute phase proteins, mucins, and matrix metalloproteinases, which result in neutrophil infiltration, inflammation, and microbial killing [160]. IL-17A is a potent activator of neutrophils, inducing both neutrophil proliferation and recruitment of neutrophils to the site of infection via chemokines [161]. Ectopic expression of IL-17 was found to stimulate granulopoiesis in mice, resulting in a 10-fold increase in the numbers of circulating neutrophils [168]. Additionally, mice deficient in IL-17RA are highly susceptible to extracellular bacteria and fungi infections, including *Porphyromonas gingivalis* and *C. albicans*, and this was associated with decreased expression of neutrophil-attracting CXC chemokines and reduced neutrophil recruitment [167, 169]. Furthermore, direct stimulation of human airway epithelial cells with IL-17 promoted the upregulation of CXCL8, CXCL1, and G-CSF [170]. IL-17A also promotes the expression of various antimicrobial genes [161]. IL-17A can directly induce expression of Lipocalin-2 (LCN2) in a variety of non-immune cells, and this is synergistically enhanced in the presence of TNF [171]. LCN2 is an acute phase protein which contributes to host defences by inhibiting catecholate-type siderophores which are used by bacteria such as *E. coli* and *K. pneumoniae* to sequester iron required for bacterial survival [172]. Furthermore, IL-17 has also been shown to induce the production of β-defensins in primary human airway epithelial cells [173].

1.5.7 IL-17 in immunity to B. pertussis

There are numerous studies suggesting that Th17 cells are key mediators of protective immunity against *B. pertussis*. Murine models have revealed that IL-17A^{+} CD4 T cells peak in the lungs 2 weeks after *B. pertussis* infection [146]. IL-17A$^{-/-}$ mice were found to exhibit impaired clearance of *B. pertussis* from the lungs, and this was accompanied by reduced concentrations of the neutrophil-chemoattractant CXCL1, as well as decreased neutrophil infiltration to the lungs [146, 174]. Furthermore, adoptive transfer of polarised *B. pertussis*-specific Th17 cells conferred protection against *B. pertussis* in the lungs of the recipient mice [146]. IL-1 receptor signalling contributes to Th17 differentiation. Infection of IL-1R type I-deficient (IL-1R$^{-/-}$) mice with *B. pertussis* resulted in an impaired pathogen-specific IL-17A response accompanied by significantly exacerbated bacterial burden in the lungs throughout the entire course of the infection [174]. Although i.n.

administration of a neutralising anti-IL-17 antibody only moderately impaired bacterial clearance in the lungs, it did significantly reduce CXCL1 expression in the lungs and the number of neutrophils recovered from the bronchoalveolar lavage (BAL) fluid post *B. pertussis* challenge [175]. Furthermore, treatment with IL-17A, but not IL-17F, was found to significantly enhance neutrophil-mediated killing of *B. pertussis in vitro* [146]. A non-human primate model of *B. pertussis* infection exhibited a strikingly similar phenotype to that seen in the murine model. Measurement of cytokines in the nasaopharyngeal mucosa of baboons over the course of *B. pertussis* infection revealed a significant increase in IL-17A expression, which was preceded by an increase in the Th17-polarising cytokines IL-6 and IL-23. Additionally, expression of IL-17A-inducible targets, such as G-CSF, CXCL8, MCP-1, and MIP-1α, were also promoted during the course of infection. Furthermore, *B. pertussis*-specific IL-17A and IFNγ responses were detected from PBMCs up to two years post initial infection [176]. *B. pertussis* infection results in near sterilising immunity in the nasal cavity of baboons against a secondary *B. pertussis* challenge, suggesting that Th17 responses are essential in protective immunity against *B. pertussis*. However, aside from the non-human primate model, the aforementioned murine studies only examined the role of IL-17A in the lungs of mice, and did not address the role of IL-17A in the upper respiratory tract. Furthermore, there is limited data examining Th17 responses in humans following natural infection with *B. pertussis*.

1.5.8 Th2 cell differentiation and function during B. pertussis infection

Th2 cells orchestrate a protective type 2 immune response against extracellular parasites such as helminths and contribute to tissue repair. However, immune responses elicited by Th2 cells can also be pathogenic in nature, and contribute to chronic inflammatory diseases such as allergy and allergic asthma [177]. The signature cytokines produced by Th2 cells include IL-4, IL-5, and IL-13, all of which contribute towards mediating a type 2 immune response through promoting B cell proliferation and Ig class-switching to IgE, recruitment of eosinophils, macrophage polarisation to an M2 phenotype and smooth muscle contraction [138]. IL-4 and IL-2 are critical cytokines for Th2 differentiation. IL-4 induces STAT6 activation, which in turn upregulates the master transcription factor for Th2 differentiation, GATA3. IL-2 and subsequent activation of STAT5 is also required for Th2 polarisation [136, 178]. Together, STAT5 and GATA3 promotes further IL-4 expression, which can act in an autocrine manner to amplify Th2 differentiation [177].

Little or no Th2 cells are induced following infection of mice with *B. pertussis*, nor does infection of IL-4$^{-/-}$ mice impair the clearance of *B. pertussis* from the lungs, suggesting that Th2 cells do not contribute to protective natural immunity [179]. It is classically thought that the immune system of infants is initially skewed towards Th2 immunity [180]. However, no antigen-specific IL-13 was detected from PBMCs isolated from infants acutely infected with *B. pertussis,* further suggesting that Th2 cells are not involved in a natural immune response to *B. pertussis* infection [145]. Cross-regulation exists between Th1 and Th2 cells, where the cytokines secreted by each respective T cell subtype can reciprocally inhibit the proliferation of the other subtype, and this can greatly impact the outcome of an infection dependent of a protective Th1 response [181]. In agreement with this, co-infection with *B. pertussis* and *Fasciola hepatica,* a helminth parasite which induces a Th2 response, was found to significantly delay clearance of *B. pertussis* from the lungs of mice and supress *B. pertussis*-specific Th1 responses. Furthermore, the immunomodulatory effect of *F. hepatica* on Th1 responses was partially reversed in IL-4$^{-/-}$ mice [182]. Combined, these studies demonstrated that a Th2 response is not promoted during natural infection with *B. pertussis*, and induction of Th2 immunity can negatively impact a protective Th1 immune response.

1.5.9 Treg cell differentiation and function during B. pertussis infection

Another key feature of the adaptive immune system is the ability to tightly regulate an immune response in order to prevent excessive inflammation and maintaining peripheral tolerance towards self-antigens. Treg cells are key mediators of this response [181]. There are two major subsets of Treg cells – 'natural' Treg (nTreg) cells and 'inducible' Treg (iTreg) cells [183]. nTreg cells develop in the thymus and exhibit a diverse TCR repertoire that is specific for self-antigens. In contrast, iTreg cells arise in the periphery and can be 'induced' from effector T cells during inflammatory processes [184]. Murine Treg cells are identified by their expression of CD25, the alpha chain for the IL-2 receptor, and expression of the forkhead/winged helix transcription factor Foxp3 [183]. Both IL-2 and TGF-β are required to generate iTreg cells [185]. TGF-β promotes the expression of Foxp3 from peripheral naïve CD4^{+}CD25^{-} T cells and promotes a suppressor phenotype [186]. IL-2 promotes the activation of the Foxp3 locus through STAT5 and constrains the differentiation of activated CD4+ T cells into Th17 cells, in addition to contributing to Treg cell survival, proliferation, and stability [183, 185]. In addition to cytokines, other factors contribute to Treg cell induction, including TCR stimulation with either low dose or high affinity ligands, suboptimal co-stimulation, and metabolites such as all-trans retinoic acid

[183]. The main effector cytokines of Treg cells include IL-10, TGF-β, and IL-35 [136]. In addition to secreting immunosuppressive cytokines, Treg-mediated suppressive activity can be achieved through direct cell-cell contact mechanisms. Treg cells constitutively express CTLA4, which is an inhibitory relative of the costimulatory molecule CD28. CTLA4 and CD28 interact with the same shared ligands, CD80 and CD86, which are expressed on APCs. CTLA4 exhibits superior affinity to CD80 and CD86, thus can inhibit T cell responses by out-competing CD28 for shared ligands [187]. Furthermore, Treg cells can also supress immune responses through outcompeting for growth factors. Treg cells constitutively express CD25, whereas naïve T cells only express CD25 after TCR stimulation, thus giving Treg cells an initial competitive advantage for the consumption of IL-2, consequently depriving naïve T cells of this essential T cell growth factor [181].

The induction of a Treg cell response and subsequent IL-10 production may play a regulatory role during *B. pertussis* infection. On one hand, manipulation of the host's immune response by *B. pertussis* virulence factors to produce the anti-inflammatory cytokine IL-10 may permit the bacteria to avoid immune detection and elimination. However, a lack of a Treg cell response may also result in uncontrolled inflammation and tissue pathology. The *B. pertussis* virulent factor FHA induces IL-10 from murine DCs, which in turn promoted Treg cell differentiation from naïve T cells. Furthermore, IL-10-producing Treg clones specific for FHA were generated from the lungs of mice acutely infected with *B. pertussis*, and these were found to suppress Th1 responses against *B. pertussis* both *in vitro* and *in vivo* [188]. CD25 is one of the main identifying markers for Treg cells, however a $CD4^+Foxp3^+CD25^-$ population was found to be the dominant population of Treg cells in the lungs of naïve mice. Over the course of *B. pertussis* infection, $CD4^+Foxp3^+$ cells acquired CD25 expression in the lung. Both $CD25^+$ and $CD25^-$ Treg populations produced IL-10 in the lungs during *B. pertussis* infection, with prolonged IL-10 production detected in the $CD25^-$ Treg cell population. Clearance of *B. pertussis* from the lungs was not affected by antibody-mediated depletion of $CD25^+$ cells prior to infection or in $IL\text{-}10^{-/-}$ mice. However, bacterial clearance was significantly enhanced in $IL\text{-}10^{-/-}$ mice treated with a depleting anti-CD25 antibody, and this was accompanied by increased IFNγ production in the lungs, suggesting that the induction of Treg cells permits prolonged *B. pertussis* infection by supressing Th1 responses [189]. Furthermore, infection of TLR4-deficient C3H/HeLJ mice with *B. pertussis* had delayed bacterial clearance from the lungs despite enhanced antigen-specific IFNγ responses [190]. This was attributed to significantly reduced innate IL-10 production by DCs and subsequently reduced antigen-specific Treg responses, which resulted in increased proinflammatory cytokine production and enhanced inflammatory pathology in the lungs

of the TLR4-deficient mice. These studies demonstrate that Treg cell responses must be carefully balanced during *B. pertussis* infection in order to achieve bacterial clearance but avoid tissue damage.

1.5.10 T follicular helper cells

T follicular helper (Tfh) cells play a significant role in promoting and regulating humoral immunity through their interaction with B cells [136]. Tfh are maintained in secondary lymphoid organs where they play an essential role in germinal centre formation, in addition to promoting survival, affinity maturation and class switch recombination of B cells [191, 192]. Tfh cells express high levels of programmed cell death-1 (PD-1), inducible T cell co-stimulator (ICOS), and the chemokine receptor CXCR5, which facilitates the localisation of Tfh cells to B cell-rich areas in secondary lymphoid organs. B cell lymphoma 6 (Bcl6) is the master transcription factor regulating Tfh cell differentiation [192]. Tfh differentiation is a multi-step, multi-signal process which requires interactions with both DCs and B cells. Tfh differentiation is initiated by DC priming of a naïve CD4 T cell and is regulated by IL-6, ICOS, IL-27, type I IFN, and TCR signal strength in murine models. IL-6 signals via STAT3 to transiently induce Bcl6 expression by newly activated CD4 T cells, which in turn promotes early CXCR5 expression on differentiating cells [191]. In the absence of further interactions with an activated B cell, these nascent Tfh cells dissipate. However, interaction with an antigen-specific B cell induces a ‘committed’ Tfh cell that has the ability to enter the germinal centre and modulate humoral responses [192]. However, the contribution of Tfh cells to protective immunity against *B. pertussis* has not been extensively investigated.

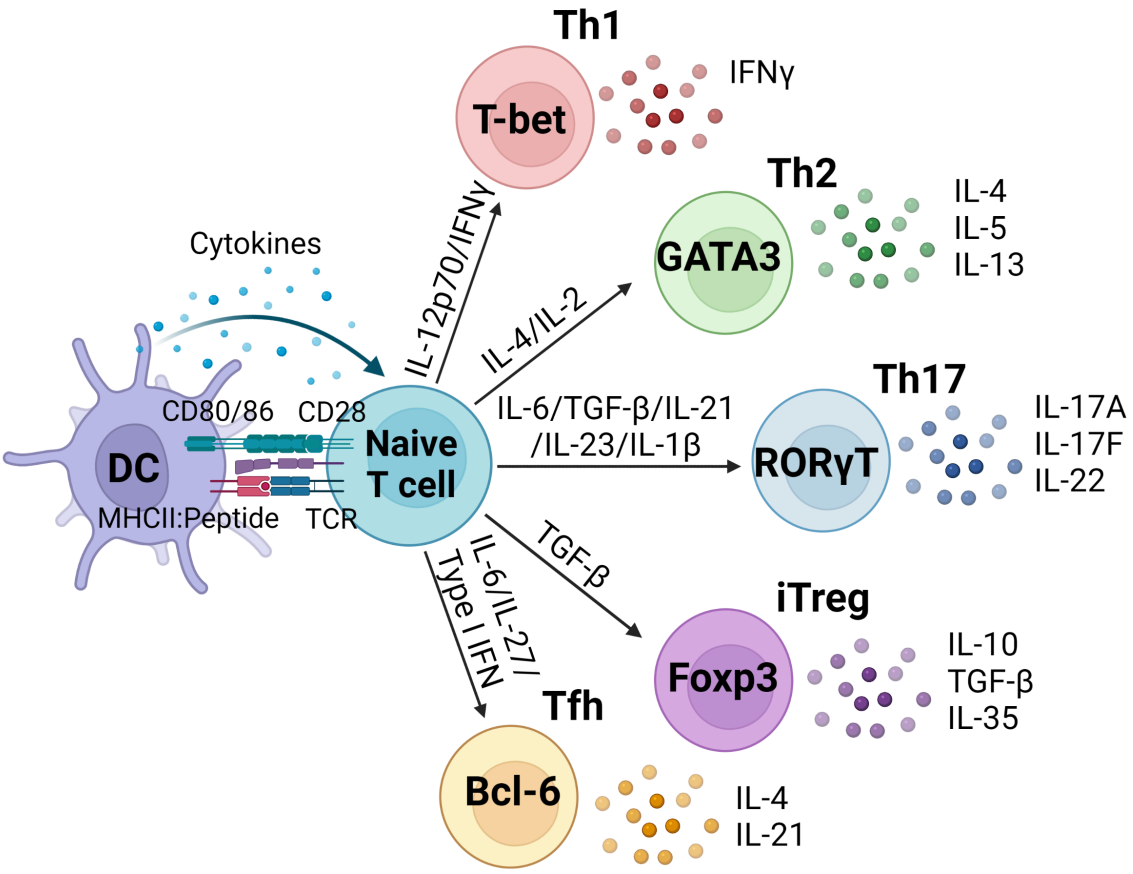

Figure 1.2 Activation and differentiation of CD4 T cells by DCs.

The TCR expressed on the surface of CD4 T cells recognises antigens presented by an MHC class II molecule expressed on activated DCs. The co-stimulatory receptor CD28 expressed on T cells interacts with co-stimulatory ligands, CD80 or CD86, expressed on DCs, which initiates T cell proliferation. Naïve T cells differentiate into Th subsets in response to cytokines produced by DCs and other immune cells. T-bet-expressing Th1 cells develop in response to IL-12p70 and IFNγ. IL-2 and IL-4 are involved in the differentiation of GATA3-expressing Th2 cells. IL-6, TGF-β, IL-21, IL-23, and IL-1β promotes the development of RORγT-expressing Th17 cells. TGF-β promotes the development of Foxp3-expressing iTregs. IL-4 and IL-21 are involed in the differentiation of Bcl-6 expressing Tfh cells.

1.5.11 Immune memory

One of the cardinal features of the adaptive immune system is its propensity to form immunological memory after an initial encounter with a pathogen. Immunological memory can be defined as the capacity of the adaptive immune system to generate a more rapid and functionally enhanced response towards a previously encountered pathogen. Adaptive immune memory is considered long-lived, and can be maintained independent of antigen stimulation [193]. Studies in mouse and baboon models have demonstrated that natural infection with *B. pertussis* induces a strong Th1 and Th17 immune response that prevents re-infection with *B. pertussis*, resulting in sterilising immunity in both the lung and nasal cavity [176, 194]. As immunological memory provides the basis for successful vaccines, understanding the mechanisms that underlie a protective immune response that prevents re-infection with *B. pertussis* is key to informing next-generation pertussis vaccine design.

During a primary infection, antigen-specific CD4 T cells differentiate and proliferate into polarised effector T cells which eliminate the invading pathogen. Once the infection has cleared, the majority of effector T cells (up to 90%) die, however a small residual pool remain as long-term memory CD4 T cells. Upon reencounter with the same pathogen, memory CD4 T cells exhibit a rapid qualitatively different and quantitatively enhanced response to prevent re-infection [195, 196]. Sallusto and colleagues identified two types of memory T cells in humans based on their expression of the chemokine receptor CCR7 and the cell-adhesion molecule CD62L (L-selectin), both of which are involved in migration through lymph nodes. $CCR7^{+}CD62L^{+}$ cells were identified as central memory T (T_{CM}) cells and $CCR7^{-}CD62L^{-}$ cells were defined as effector memory T (T_{EM}) cells [197]. In addition to surface marker expression, memory subtypes can also be distinguished from each other based on homing capacities and effector function. T_{EM} circulate between blood and secondary lymphoid organs, and express homing receptors that facilitate migration to nonlymphoid sites of inflammation, where they rapidly produce cytokines within several hours of TCR stimulation [196]. In contrast, T_{CM} cells are restricted to secondary lymphoid tissues and blood, have little or no effector function immediately after TCR stimulation, however readily produce IL-2 and later differentiate to effector cells after activation [196, 198].

1.5.12 Tissue resident memory T cells

Around the time that the T_{CM}/T_{EM} paradigm was being established, there were emerging studies describing the preferential localisation of memory T cells to non-lymphoid tissues. As T_{EM} cells were known to recirculate between tissue and blood, these cells were originally identified as such [199]. After clearance of both viral and bacterial infections, antigen-specific CD8 T cells were found to persist in peripheral tissue, including the lungs, liver and small intestines, of mice at a higher percentage than that observed in secondary lymphoid organs, with antigen-specific CD8 T cells in the spleen, lymph nodes, and blood declining rapidly. Furthermore, CD8 memory T cells isolated from non-lymphoid tissues exhibited enhanced effector functions compared with their splenic counterparts [200]. Parabiosis experiments, which involve the surgical union of two mice resulting in a shared circulatory system, revealed that although certain organs, such as the liver, permitted memory T cell recirculation through peripheral tissue, memory T cells founds in other tissues, such as the brain and intestinal lamina propria, did not readily equilibrate with those found in the blood, suggesting that memory T cells are restricted within tissues to form a long-surviving resident population [201]. This led to the identification of a third type of memory T cell, termed tissue-resident memory T (T_{RM}) cells, which reside in tissues without recirculation.

T_{RM} cells were found to be enriched at barrier sites such as the skin, lungs, and intestinal mucosa, where they act as a 'first line' of defence and can rapidly respond and orchestrate a protective localised immune response following re-encounter with a pathogen [202]. Both CD8 and CD4 T_{RM} cells have been identified in multiple tissues using various techniques such as the aforementioned parabiosis model in addition to intravital staining methods. Intravital staining involves the use of fluorescent antibody labelling *in vivo* to discriminate between blood-borne cells, which become labelled, and tissue-localised cells which are protected from labelling [203]. Both CD4 and CD8 T_{RM} cells can be further identified by high expression of the surface marker CD69, a membrane-bound type II C-lectin receptor which directly contributes to T_{RM} cell retention in peripheral tissues [202]. It was shown that CD69 surface expression by skin-infiltrating CD8 T cells was accompanied by the transcriptional downregulation of the sphingosine-1-phosphate receptor $S1P_1$. $S1P_1$-dependent chemotaxis is essential for both T cell and B cell egression from peripheral lymphoid organs. However, expression of CD69 was found to physically interact with $S1P_1$, resulting in inhibition of $S1P_1$ surface expression, therefore facilitating the prolonged retention T cells in peripheral tissue and the formation of a local memory pool [204, 205]. CD8 T_{RM} cells can also be identified by surface

expression of CD103, the α-chain of the integrin $\alpha E\beta 7$ which binds E-cadherin expressed on epithelial cells. However, CD103 is not consistently expressed on CD4 T_{RM} cells [199].

The majority of the early research investing T_{RM} cells focused predominantly on CD8 T_{RM} cells, however there is emerging evidence using murine models that their CD4 counterparts play an important role in mediating protective immunity at barrier sites [202]. Lung CD4 T_{RM} cells were found to mediate localised protective immunity against influenza infection. Teijaro and colleagues demonstrated that adoptive-transfer of antigen-specific lung CD4 T cells home to the lungs of recipient mice, and this was accompanied by enhance survival and viral clearance following influenza challenge compared with mice who received antigen-specific memory CD4 T cells isolated from the spleen [206]. CD4 T_{RM} cells also mediate protective immune responses against a variety of other pathogens including *Leishmania major*, *Listeria monocytogenes*, and herpes simplex virus (HSV) 2 in a range of tissues, including the skin, intestinal tissue, and reproductive tract [207-209]. The functional diversity and heterogenous nature of CD4 helper T cells has made it difficult to identify a distinct CD4 T_{RM} precursor and it remains unknown if all CD4 Th effector cells possess the same potential to differentiate into long-lived memory cells [202]. A study using IL-17A tracking-fate mouse models revealed a significant fraction of lung CD4 T_{RM} cells induced following immunisation with a *K. pneumoniae* vaccine were derived from effector Th17 cells, and that ex Th17 T_{RM} cells contributed to protective immunity following infection with *K. pneumoniae* [210].

CD4 and CD8 T_{RM} cells expressing CD69 and/or CD103 have also been identified in a range of human tissues, including lungs, intestines, salivary glands, and tonsils, obtained from deceased organ donors. $CD69^+$ tissue-resident T cells were shown to be transcriptionally, phenotypically and functionally distinct from $CD69^-$ memory T cells in tissues and blood, with enhanced expression of genes involved in adhesion, migration, and immune regulation in $CD69^+$ tissue-resident T cells. Functionally, both $CD4^+$ and $CD8^+$ $CD69^+$ memory T cells in the lung and spleen produced a higher proportion of IL-2 and IL-10 compared with their $CD69^-$ counterparts. Interestingly, lung $CD69^+$ memory $CD4^+$ T cells produced significantly more IL-17 compared with lung $CD69^-$ memory $CD4^+$ T cells, with spleen memory T cells failing to produce significant levels, highlighting the importance of IL-17 in mucosal immunity. Furthermore, the core transcriptional profile of human $CD69^+$ tissue-resident memory T cells exhibited key homologies with murine T_{RM} cells [211]. The localisation of T_{RM} cells within tissues has rendered them difficult to study in humans. However, a study by Snyder and colleague assessing BAL samples collected longitudinally from human leukocyte antigen (HLA)-disparate lung transplant recipients revealed that T cells persist specifically in the lung and do not recirculate in the blood of

the recipients for up to 1 year post transplantation and expressed high levels of the T_{RM} signature markers CD69 and CD103. Furthermore, lung-infiltrating host T cells were found to gradually acquire a T_{RM} phenotype over months *in vivo*. Functional studies revealed that donor CD4 T cells produced a higher frequency of IL-17 and IFNγ compared with recipient T cells [212]. The retention of CD4 T_{RM} cells in human tissues has been further demonstrated following treatment of cutaneous T cell lymphoma (CTLCL) patients with alemtuzumab. Alemtuzumab, a humanised anti-CD52 antibody, was found to deplete circulating T cells, however a population of non-recirculating CD4 T cells persisted in the skin of patients. These cells displayed a classical CD4 T_{RM} phenotype, expressing CD69 and lacking CD103, and also exhibited enhanced effector function. Alemtuzumab requires the presence of neutrophils and/or natural killer (NK) cells in order to deplete T cells using antibody-dependent cellular cytotoxicity mechanisms. As neutrophils are rare in human skin but numerous in blood, this study speculated that circulating T cells are more susceptible to alemtuzumab-mediated depletion, whereas skin T_{RM} cells are resistant [213]. Furthermore, there was a marked lack of infections in the alemtuzumab-treated CTCL patients despite the complete absence of T cells in the blood, suggesting the skin-resident T cells protected the skin from pathogens even in absence of T cell recruitment from circulation [214].

1.5.13 Role of CD4 T_{RM} cells in immunity to B. pertussis infection

Natural immunity to *B. pertussis* is considered long-lasting and effective at preventing reinfection. Wilk et al. identified that CD4 T_{RM} cells are key mediators of protective acquired immunity against *B. pertussis* in a murine model. It was demonstrated that CD4 T cells accumulated in the lungs over the course of *B. pertussis* infection and acquired a T_{RM} phenotype. CD4 T_{RM} cells produced IL-17A and IFNγ and expanded rapidly during re-infection, which was accompanied by enhanced bacterial clearance from the lung. Treatment of mice previously infected with *B. pertussis* with FTY720, an immunomodulatory drug which modulates the S1P receptor and inhibits lymphocyte egression from lymph nodes [215], did not affect the expansion of CD4 T_{RM} cells in the lungs following a secondary challenge with *B. pertussis* nor did it compromise bacterial clearance, demonstrating that the resident CD4 T_{RM} cell population expanded locally and mediated a protective immune response without the contribution of circulating T cells. [216]. IL-17A-producing CD4 T_{RM} cells are also induced in the nasal tissue following infection with *B. pertussis*, expansion of which was strongly correlated with rapid clearance of *B. pertussis* from the nasal cavity following re-infection [194]. The

importance of IL-17A-producing CD4 T_{RM} cells in mediating protective immunity in the nasal cavity was further demonstrated in a study by Dubois et al. which showed that infection of IL-17A$^{-/-}$ mice, but not IFN$\gamma^{-/-}$ mice, was accompanied by significantly delayed clearance of *B. pertussis* from the nasal cavity. However, transfer of CD4 T_{RM} cells isolated from the nasal tissue of immune mice restored protection against *B. pertussis* in the nasal cavity of IL-17A$^{-/-}$ recipients, and this was associated with enhanced neutrophil recruitment [217]. It has recently been reported that virulence factors secreted by *B. pertussis,* such as PT, can influence the development of T_{RM} cells in the respiratory tract of mice. Mice infected with a *B. pertussis* mutant strain deficient in PT were found to have significantly less CD4 T_{RM} cells in the lungs compared with mice infected with a WT strain. However co-administration of PT with a PT-deficient *B. pertussis* strain was sufficient to generate lung T_{RM} cells [218]. Combined, these studies highlight the important role of CD4 T_{RM} cells, in particular IL-17A-producing CD4 T_{RM} cells in mediating naturally acquired immunity against *B. pertussis*.

1.6 Non-conventional lymphocytes

The dichotomy between the innate and adaptive immune system has been revised since the discovery of lymphocytes that exhibit both innate-like and adaptive-like properties, for example the ability to produce Th-like cytokines in a non-MHC-restricted manner. Cells that exhibit these properties include $\gamma\delta$ T cells, NK cells, NK T cells, mucosa-associated invariant T (MAIT) cells, and innate-like lymphocytes (ILCs). These cells are strategically positioned in barrier tissues where they provide a first line of defence against invading pathogens. In addition to their privileged anatomical location, non-conventional lymphocytes respond faster to insults compared with their conventional $\alpha\beta$ T cell counterparts, with the capacity to produce cytokines within hours of activation in contrast to the days required for naïve $\alpha\beta$ T cells to differentiate into effector Th cells [219].

1.6.1 $\gamma\delta$ T cells and B. pertussis infection

T cells which express the $\gamma\delta$ T cell receptor represent a relatively small population of T cells in blood and secondary lymphoid organs, but are enriched at mucosal sites, accounting for ~10-20% of total T cells in the reproductive tract and ~50-70% of skin dermal T cells [220]. Distinct subsets of $\gamma\delta$ T cells are characterised by expression of specific Vγ TCR chains, however the antigen specificity of $\gamma\delta$ T cells remains largely

unknown and rarely involves antigen presentation via classical MHC molecules [221]. Unlike classical αβ T cells, which are dependent on cognate antigens for their activation, γδ T cells are readily activated in a TCR-independent manner by proinflammatory cytokines especially IL-1β, IL-18, and IL-23, and can promptly produce Th effector cytokines including IL-17A and IFNγ [222-224]. By rapidly producing large amounts of cytokines, γδ T cells make key contributions to immune responses at mucosal barrier sites, and mediate direct cell killing, activation of phagocytes, and neutrophil recruitment [225].

γδ T cells are involved in the immune response to *B. pertussis* infection in both humans and mice. Analysis of peripheral blood obtained from children infected with *B. pertussis* revealed that although the number of total $CD4^+$ and $CD8^+$ T cells were enhanced, the number of circulating γδ T cells was significantly reduced compared with healthy age-matched controls [226]. The authors of this study speculated that the reduced proportion of γδ T cells might be due to increased influx of γδ T cells to sites of inflammation. Furthermore, murine models have revealed that lung γδ T cells provide an early source of IL-17A during *B. pertussis* infection, with depletion of this early IL-17A associated with enhanced bacterial load and reduced AMP production in the lung [227]. Although γδ T cells are classically considered innate-like cells, lung γδ T cells induced during *B. pertussis* infection were found to acquire a T_{RM} phenotype ($CD69^+CD103^+$), with the Vγ4 subset also capable of producing *B. pertussis*-specific IL-17A. Furthermore, γδ T cells from mice previously infected with *B. pertussis* exhibited significantly enhanced IL-17A production during a secondary challenge compared with γδ T cells from infected un-primed mice [227]. These results suggest that in addition to providing an early source of IL-17A, γδ T cells also contribute to the adaptive immune response to *B. pertussis*.

1.6.2 Natural killer cells and B. pertussis infection

NK cells are innate lymphocytes with cytolytic activity that mediate both anti-viral and anti-tumour responses. NK cells do not express polymorphic clonotypic receptors but rather express a sophisticated repertoire of activating and inhibitory receptors that regulate NK cell activity, enabling them to recognise 'self' from 'non-self' [228]. NK cells can be described as the 'innate-like' equivalent of CD8 T cells, with the ability to produce IFNγ and TNF, in addition to exhibiting cytolytic functions. However, in contrast to CD8 T cells, NK cells do not require prior antigen exposure for activation, and can be activated

directly in response to cytokines such as IL-12, IL-15, and IL-18 [221]. Although classically associated with viral infections, NK cells have been shown to infiltrate the lungs of mice during *B. pertussis* infection and are a major cellular source of IFNγ during the acute stage of the infection [229]. Infection of IFNγ receptor-deficient mice with *B. pertussis* resulted in bacterial dissemination to the liver and reduced survival [148]. A similar phenotype was observed following antibody-mediated depletion of NK cells during *B. pertussis* infection, with bacterial dissemination to the liver, reduced survival, and a significantly higher bacterial load in the lungs of the NK-depleted mice [229]. NK cells are the largest cellular source of *B. pertussis*-induced IFNγ in the peripheral blood of healthy subjects, however IFNγ production by NK cells in response to *B. pertussis* requires the presence of either IL-15 or IL-18 [230, 231]. Furthermore, NK-derived IFNγ was found to induce expression of CXCL9 and CXCL10 by human respiratory epithelial cells, with these cytokine involved in the CXCR3-dependent recruitment of NK and T cells [230].

1.7 Bystander activation of T cells

Just as non-conventional lymphocytes exhibit adaptive-like qualities, conventional T cells also demonstrate innate-like functions. It is classically thought that T cell activation is strictly dependent on the TCR engaging with peptide-MHC complexes, in addition to co-stimulation. However, there is emerging evidence that T cells can be activated in a TCR-independent manner, in what is referred to as ‘bystander activation’. During bystander activation, T cells can rapidly proliferate and secrete effector cytokines in response to a cytokine milieu generated during infection with an unrelated pathogen, independent of direct MHC-TCR interaction. Non-specific activation of T cells may confer protection against an unrelated pathogen, in what is referred to as ‘heterologous immunity’ by amplifying host immune responses and contributing to pathogen clearance. Furthermore, bystander activation of T cells may contribute to the long-term homeostatic maintenance of memory T cells in the absence of cognate antigen. However, uncontrolled activation of T cells can also be pathogenic, and may contribute to the development of auto-inflammatory and autoimmune disease. While bystander activation has been well-characterised in CD8 T cells, evidence surrounding this phenomenon in CD4 T cells is limited [232, 233].

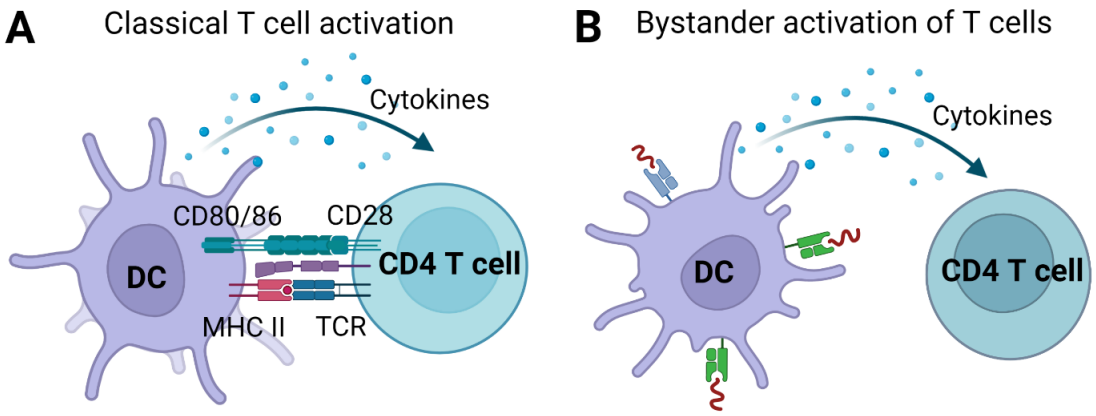

Figure 1.3 Classical and bystander activation of CD4 T cells.

Classical activation of CD4 T cells requires 3 signals. Signal-1 involves the interaction of the TCR expressed on T cells with the peptide-MHC II complex expressed on activated DCs or others APCs. Signal-2 involves the binding of co-stimulatory receptors, such as CD28, expressed on T cells with corresponding ligands, such as CD80 and CD86, expressed on activated DCs, which initates T cell proliferation. Signal-3 comprises of cytokines produced by DCs and other immune cells, which promote the differentiation of naïve T cells into one of several Th subsets (A). During bystander activation, cytokines produced by activated innate immune cells such as DCs can activate CD4 T cells directly in the absence of TCR engagement (B).

1.7.1 Bystander activation of CD8 T cells

Early *in vivo* studies investigating bystander activation demonstrated that injection of mice with LPS or the synthetic analogue of double-stranded RNA, polyinosinic-polycytidylic acid (Poly I:C), induced proliferation of memory ($CD44^{hi}$) CD8 T cells. It was speculated that this was mediated indirectly by LPS or Poly I:C-induced type I IFN production by APCs. Evidence in support of this hypothesis was provided by the demonstration of enhanced proliferation of memory CD8 T cells in response to injection of mice with purified Type I IFN [234, 235]. Combinations of IL-12 and IL-18 have been shown to induce IFNγ production from both human and murine CD8 T cells *in vitro*, with IFNγ production further enhanced by the addition of IL-15 [236, 237].

Multiple murine models have demonstrated that non-cognate antigens can induce IFNγ production from memory CD8 T cells in a bystander manner *in vivo* and that this can

substantially influence subsequent immune responses. Infection with the intracellular bacterium *L. monocytogens* was shown to promote rapid IFNγ production from memory CD8 T cells specific for ovalbumin protein (OVA). Furthermore, adoptive transfer of OVA-specific CD8 T cells conferred protection against *L. monocytogens* infection in IFNγ-deficient mice which would otherwise succumb to *L. monocytogens* infection [238]. Conversely, *L. monocytogens*-specific memory CD8 T cells in the lung produced IFNγ in response to the unrelated pathogen *Streptococcus pneumonia in vivo*, and this was shown to be mediated indirectly by IL-18 and IL-15 produced by inflammatory monocytes in response to *S. pneumonia* [239]. Lung-residing memory CD8 T cells induced following lymphocytic choriomeningitis virus (LCMV) infection produce IFNγ in response to acute infection with vaccinia virus. Non-cognate activation of LCMV-specific memory CD8 T cells preferentially occurred in non-lymphoid tissue such as the lungs. Furthermore, TCR-independent activation of LCMV-specific memory CD8 T cells was associated with enhanced survival and reduced mortality following vaccinia virus infection [240]. In addition to promoting a pro-inflammatory response to a non-cognate pathogen, bystander activation of CD8 T cells can also play a regulatory role. Memory CD8 T cells retained in the lung following infection with influenza virus were shown to supress allergic airway inflammation induced by *Nippostrongylus brasiliensis*-derived allergen (NES) in a IFNγ-dependent manner. NES promoted non-specific IFNγ production by airway-resident CD8 T cells, which subsequently reduced the infiltration of eosinophils and IL-4 producing Th2 cells to the lungs. The suppressive effects of previous influenza infection on allergic airway inflammation was reversed following antibody-mediated neutralisation of IFNγ [241].

1.7.2 Bystander activation of CD4 T cells

Bystander activation of CD4 T cells has also been reported, however the mechanisms surrounding these events are less well understood. Early studies on human PBMCs demonstrated that supernatants from LPS-stimulated macrophages in combination with recombinant IL-2 induced proliferation of both naïve ($CD45RA^+$) and memory ($CD45RO^+$) CD4 T cells. Furthermore, stimulation with TNF and IL-6 in combination with IL-2 induced proliferation and IFNγ and IL-4 production from memory, but not naïve, human CD4 T cells [242].

Bystander activation has been demonstrated in multiple Th subsets, including Th1, Th2, and Th17 cells, resulting in both immuno-protective and immuno-pathogenic outcomes.

Similar to CD8 T cells, IL-12 and IL-18 induces non-specific IFNγ production from murine Th1 cells *in vitro* [243]. TCR-independent IFNγ production has also been demonstrated in human Th1 Cells. Stimulation of whole blood samples obtained from Thai school children with dengue virus antigens induced IFNγ production from CD4 T cells. Although treatment with cylosporin A (CsA), which inhibits TCR-dependent activation of T cells, reduced total IFNγ production, a residual population of CsA-resistant IFNγ-producing CD4 T cells remained. Conversely, direct stimulation with IL-12 and IL-15 promoted IFNγ production from CD4 T cells [244]. Non-cognate activation of Th1 cells has also been demonstrated in multiple studies *in vivo*. Injection of LPS was found to induce rapid IFNγ production from CD4 T cells of mice previously infected with *Salmonella* in an MHC II-independent but IL-18-dependent manner [245]. Rapid IFNγ production following LPS injection has also been reported in CD4 T cells from mice previously infected with *Chlamydia muridarum* [246]. However, non-specific activation of Th1 cells may also have a detrimental impact on the host. Antigen-independent activation of CD4 T cells was found to contribute to the development of Lyme arthritis which develops following *Borrelia burgdorferi* infection. SMARTA mice, which have CD4 T cells with monoclonal specificity for the MHC class II-restricted epitope of LCMV gp_{61-80} , infected with *B. burgdorferi* still developed severe arthritis and pathological lesions, and this was accompanied by the expansion of IFNγ-producing CD4 T cells [232]. Furthermore, injection of LPS was found to exacerbate relapses of experimental autoimmune encephalomyelitis (EAE), a murine model of multiple sclerosis, and this was mediated by IFNγ produced by autoreactive CD4 T cells in a TCR-independent manner [247].

Th2 cells are also susceptible to bystander activation by cytokines. Guo and colleagues demonstrated that the combination of IL-33 with either of the STAT5 activators IL-2, IL-7, or thymic stromal lymphopoietin (TSLP), induced innate IL-13 and IL-5, but not IL-4, production from CD4 T cells primed under Th2 differentiation conditions [243]. Innate activation of Th2 cells has been implicated in the development of allergic airway inflammation *in vivo*. Th2 cells were found to produce IL-13 in response to either papain or house dust mite extract (HDM) and promoted eosinophilic inflammation in a TCR-independent but IL-33-dependent manner [248].

Combinations of the Th17-polarising cytokines IL-1β, IL-18,IL-23, IL-21, and IL-6, have been shown to induce IL-17A, IL-17F, and IL-22 production from primed Th17 cells in a TCR-independent manner *in vitro* [243]. However, the evidence surrounding bystander activation of Th17 cells *in vivo* is limited. Mice immunised with the autoantigen interphotoreceptor retinoid-binding peptide ($IRBP_{1-20}$) in complete Freund's adjuvant

were found to exhibit two distinct Th17 populations – one specific for the immunising autoantigen ($IRBP_{1-20}$) and another 'bystander-Th17' population that was not reactive with antigen, but rather produced IL-17, IL-22, and IFNγ in Th17-polarising conditions. Furthermore, only bystander Th17 cells were capable of producing IL-10. Bystander Th17 cells were found to confer protective effects, with adoptive transfer of bystander Th17 cells into syngeneic naïve mice attenuating the pathogenic uveitogenic activity of IRBP-specific Th17 cells, significantly delaying the symptom onset of experimental autoimmune uveitis (EAU) [249]. Although this study suggests that bystander Th17 cells can be protective in EAU, bystander activation of Th17 cells has also been shown to be pathogenic in other autoimmune models such as EAE. A study by Lee and colleagues demonstrated that OVA-specific memory-like Th17 cells were found to infiltrate the spinal cord following the induction of EAE, produce IL-17A, IFNγ, and GM-CSF, and contribute to significantly enhanced EAE pathogenicity in an IL-1R1-dependent manner [250].

Bystander activation of memory CD4 T cells induced during natural infection with *B. pertussis* has not been extensively examined. *B. pertussis* has been shown to exert immunomodulatory effects on the development of EAE, with acute infection attenuating EAE disease severity in an IL-10 dependent manner. Although infection with *B. pertussis* significantly reduced the infiltration of IL-17A and IFNγ-producing CD4 T cells into the CNS of mice with EAE, infection with *B. pertussis* enhanced MOG-specific IL-17A production from spleen and lymph node cells. This suggests that infection with a non-cognate respiratory tract pathogen enhances peripheral autoantigen-specific T cell responses, and this could be mediated through bystander mechanisms [251]. Due to the anatomical localisation of CD4 T_{RM} cells, one could speculate that they may be susceptible to bystander activation due to their constant exposure to inhaled pathogens and may act as a bridge between innate and adaptive responses at mucosal surfaces. However, this has yet to be confirmed.

1.8 Humoral immune response to *B. pertussis* infection

The humoral immune response makes up the second branch of the adaptive immune system and is characterised by the production of antibodies by B cells. B cells are derived from pluripotent hematopoietic stem cells in a series of distinct steps in the bone marrow [252]. During B cell development, gene recombination in the immunoglobulin locus occurs, which results in the surface expression of a unique B cell receptor (BCR) [253]. These gene rearrangements continue throughout life, generating a vast B cell repertoire capable of recognising a wide range of self and foreign antigens [252]. After development

in the bone marrow, naïve B cells migrate to the blood and peripheral lymphoid organs [253]. Naïve mature B cells first encounter antigens in the B cell follicles of secondary lymphoid organs. Antigen binding to the BCR results in the internalisation, processing, and presentation of BCR-bound antigen on MHC class II molecules. B cells subsequently migrate to the boarder of the T cell zone and interact with T_{FH} cells. Activation of naïve B cells results in one of three fates. B cells can differentiate into either short lived-plasma cells which produce antibodies of relatively low affinity, or into long-lived plasma cells. Plasma cells are terminally differentiated B cells whose main function is to produce and secrete antibodies, with each plasma cell producing antibodies of one specificity. Alternatively, activated B cells can differentiate into long-lived memory B cells [253, 254].

Antibodies are heterodimeric proteins that consist of two heavy chains and two light chains linked to each other by disulphide bonds. They can be separated functionally into variable (V) domains that binds antigen and constant (C) domains that specify effector functions [255]. Antibodies contribute to pathogen clearance by various mechanisms, such as direct neutralisation, activation of the complement cascade, or by interacting with other immune cells in an Fc receptor-mediated fashion [253]. There are five main classes, or isotypes, of antibodies - IgM, IgD, IgG, IgA, and IgE - which are identified by their C-terminus, also known as the Fc region [255]. IgM is the first immunoglobulin expressed during B cell development and expressed as a monomeric form on the surface of naïve B cells. Following antigenic stimulation, IgM is secreted mainly in a pentameric form, with individual monomers linked together by disulphide bonds. IgM is the first antibody to appear in response to initial antigen exposure. Circulating IgD is found at very low levels and the function of circulating IgD remains elusive. IgG is the predominant isotype found in the body and has the longest serum half-life of all immunoglobulin isotypes. IgG can be further divided into four subclasses – IgG1, IgG2, IgG3, and IgG4. Whilst circulating levels of IgA are lower than IgG, IgA is enriched at mucosal surfaces and in secretions. In the serum IgA exists as a monomer, however IgA at the mucosa, termed secretory IgA (sIgA), exists predominantly as a dimer, where it plays a critical role in direct neutralisation of invading pathogens and in the prevention of pathogen-binding to mucosal surfaces. IgE is present at lowest serum concentration with the shortest half-life of all the immunoglobulins. Nonetheless, IgE is a very potent immunoglobulin, binding with extremely high affinity to the FcεRI which is expressed on mast cells, basophils, and eosinophils, and is involved in hypersensitivity and allergic reactions [256].

Natural infection with *B. pertussis* in humans is accompanied by the production of *B. pertussis*-specific IgA and IgG, suggesting that antibody production may be important in

the control of *B. pertussis* infection [257]. A controlled human infection study in which healthy subjects were inoculated intranasally with non-attenuated *B. pertussis* found a significant rise in serum IgG concentrations again PT, PRN, and FHA at the highest inoculum dose [258]. The presence of serum antibodies against the *B. pertussis* antigens PRN, FIM 2/3, and PTx, but not FHA, has been correlated with clinical protection in children following exposure to *B. pertussis* [259]. Antibodies against PRN has also been associated with prevention of illness after household exposure to *B. pertussis* [260]. IgA is the predominant antibody isotype at mucosal surfaces, with *B. pertussis*-specific IgA detectable in nasopharyngeal secretions during the second or third weeks of illness and persist for at least 3 months [261]. Anti-adherence activity was detected in the serum of individuals previously infected with *B. pertussis*, with both IgA and IgG antibody classes inhibiting the adherence of *B. pertussis* to human respiratory epithelial cells [262]. Furthermore, IgA purified from immune sera of individuals previously infected with *B. pertussis* was found to enhance phagocytosis and killing of *B. pertussis* by human polymorphonuclear leukocytes in an FcαRI-mediated manner [263].

Immunoglobulin treatment for pertussis predates the antibiotic era, beginning with the observation that convalescent serum administered during the incubation period attenuated the subsequent disease [264]. A study by Lucchesi et al. in 1949 found that patients treated during the first week of disease with serum from healthy adults previously infected with *B. pertussis* in childhood and boosted with a phase I pertussis vaccine demonstrated a more regular decline in the rate of paroxysms than did the patients in the control group. However, these differences were not significant if the treatment was started at a later stage in the disease [265]. Modern clinical trials with pertussis immunoglobulin have yielded inconsistent results. A study by Granstrom and colleagues demonstrated that treatment of patients with immunoglobulin raised by immunisation of donors with a mono-component or a two-component aP vaccine significantly reduced the duration of whoops post treatment compared with the patients treated with a placebo control [266]. However, a multicentre, randomised, placebo-controlled clinical trial by Halperin and colleagues found no benefit of intravenous (i.v.) immunoglobulin treatment on disease progression compared with the placebo control [264].

Animal models have also yielded conflicting evidence on the role of antibodies and B cells in protective immunity against *B. pertussis*. A baboon model has demonstrated that a primary infection with *B. pertussis* induces serum IgG against PT, FHA, PRN, and FIM 2/3, with a moderate increase in IgG antibodies against *B. pertussis* antibodies following re-infection [28]. Challenge of mice lacking B cells with *B. pertussis* resulted in a chronic

lung infection, demonstrating the requirement of B cells to effectively clear *B. pertussis* from the respiratory tract [148]. Conversely, passive transfer of immune serum from convalescent mice only marginally reduced bacterial load in the lungs of recipient mice in the early stages of *B. pertussis* challenge [110]. Furthermore, infection of $IgA^{-/-}$ mice with *B. pertussis* did not impair bacterial clearance in either the upper or lower respiratory tract compared with WT control mice. However, clearance from the upper respiratory tract was impaired in $IgA^{-/-}$ mice following infection with the closely related species *Bordetella bronchioseptica* [267].

1.9 Immune response induced by wP and aP vaccination

Murine models have highlighted clear differences in the immune response elicited following immunisation with either a wP or an aP vaccine, with initial studies demonstrating that immunisation with a wP vaccine inducing a predominantly Th1 response whereas immunisation with an aP vaccine promotes a predominantly Th2 response. This was accompanied by the finding that mice immunised with an aP vaccine exhibit moderately delayed clearance of *B. pertussis* from the lungs compared with mice immunised with a wP vaccine or mice previously exposed to a natural infection with *B. pertussis* [268]. The immune response induced following immunisation with a wP vaccine is similar to that induced following natural infection and is dependent on cell-mediated immunity [125]. Immunisation with a wP vaccine results in the generation of peripheral *B. pertussis*-specific IFNγ-producing CD4 T cells [268]. Protective immunity afforded by the wP vaccine is mediated in part by Th1 responses, as demonstrated by impaired clearance of *B. pertussis* from the lungs of $IFN\gamma^{-/-}$ mice following immunisation with a wP vaccine [146, 269]. In addition to a Th1 response, wP priming also induces a robust *B. pertussis*-specific Th17 immune response [270]. Antibody-mediated neutralisation of IL-17A significantly impaired clearance of *B. pertussis* from the lungs of mice immunised with a wP vaccine [271]. Furthermore, immunisation of $IL\text{-}17A^{-/-}$ with a wP vaccine displayed moderately impaired clearance of *B. pertussis* from the lungs [146], demonstrating that both Th1 and Th17 cells mediate protective immunity induced by wP vaccination. In contrast, immunisation with an aP vaccine induces a predominantly Th2 response in mice, with *B. pertussis*-specific T cells primarily producing the Th2-related cytokines IL-4 and IL-5 [268]. Evidence from murine models also suggest that humoral responses make a greater contribution to protective immunity generated by an aP vaccine then that generated following wP vaccination. Although passive transfer of immune serum from convalescent mice only moderately enhanced clearance of *B.*

pertussis from the lungs, passive transfer of serum from mice immunised with either a wP or an aP vaccine conferred significant protection in the lungs of recipient mice, with the results most striking for the mice receiving serum raised against an aP vaccine [269]. However, limited Th2 responses are induced following natural infection of mice with *B. pertussis* suggesting that they may not be of benefit to the host [179]. In contrast, Th17 responses have also been reported in mouse models following immunisation with an aP vaccine. Whilst immunisation of IL-4$^{-/-}$ mice with an aP vaccine did not impair clearance of *B. pertussis* from the lungs, immunisation of IL-17A$^{-/-}$ mice with an aP vaccine did exhibit delayed bacterial clearance [146]. There is evidence to suggest that Th2 and Th17 inflammatory pathways are reciprocally regulated in the lung [272]. One could speculate that the lack of regulation by IL-4 enables the protective effects of IL-17A to persist in the lungs of IL-4$^{-/-}$ mice following aP priming, whereas the lack of regulation of IL-4 enables a potentially pathogenic response seen in the lungs of the IL-17A$^{-/-}$ mice.

1.10 Evidence for waning immunity after aP vaccination

The Th1/Th2 dichotomy of the wP and aP vaccine has also been well documented in humans. Numerous studies have demonstrated how immunisation with a wP vaccine induces *B. pertussis*-specific Th1 responses from human PBMCs, whereas immunisation with an aP vaccine induces *B. pertussis*-specific Th2 responses [273-275]. Despite high vaccine coverage globally, the switch from the wP to the aP vaccine has been associated with a rise in pertussis incidence in several industrialised countries and this has been attributed in part to more rapid waning immunity after immunisation with aP vaccines [17]. The APERT study highlighted how antibody responses decline rapidly in adolescents and adults following a booster with an aP vaccine, with the initial increase of IgG and IgA antibodies to PT, FHA, and PRN reducing substantially by 18 months post booster [276]. The limited durability of immunity induced following immunisation with aP vaccines has been demonstrated following outbreaks of pertussis, particularly amongst preadolescents who would have received an aP vaccine during early childhood. Observations by Witt and colleagues reported that the highest incidence of disease during a pertussis outbreak in the US was among previously vaccinated children aged 8–12 years. The vaccination rate among PCR-positive preadolescents was found to be equal to that of unvaccinated controls, suggesting that the current aP vaccine schedule is insufficient to prevent outbreaks of pertussis [277].

1.11 Evidence for asymptomatic transmission after aP vaccination

In addition to waning immunity, there is emerging evidence that recent outbreaks of pertussis may be due to the failure of currently used aP vaccines to prevent asymptomatic transmission. Asymptomatic carriers are individuals who are infected with a pathogen but do not show classical symptoms of infection, such as rhinorrhoea or a paroxysmal cough in the case of *B. pertussis* infection. Asymptomatic carriers can subsequently transmit the disease to uninfected individuals in a process termed 'asymptomatic transmission'. As asymptomatic carriers remain largely undetected in a population, the exact contribution of asymptomatic transmission in disease outbreaks is difficult to assess, with incidence data often only reflecting symptomatic cases of infecteion [278]. The link between asymptomatic transmission and resurgence of pertussis has been demonstrated using mathematical modelling based on data obtained from the US and UK [279]. Furthermore, a systematic review published by Craig et al. revealed a high prevalence of subclinical infection in household contacts of pertussis cases, and that mild and asymptomatic infection may contribute to the ongoing transmission of disease [280]. Additionally, a controlled human infection model demonstrated that nasopharyngeal carriage of *B. pertussis* was inducible in humans without causing pertussis symptoms, providing further evidence that *B. pertussis* can exist in a human carrier state in the upper respiratory tract. However, this study commenced antibiotic treatment in subjects on day 14 post-inoculation. Therefore, the duration of which *B. pertussis* can asympotomatically colonise the nasaopharyngeal cavity in humans remains unknown at present [258]. The link between immunisation with an aP vaccine and the asymptomatic transmission of *B. pertussis* has been demonstrated in a baboon model in a landmark study by Warfel and colleagues. Previous infection with *B. pertussis* induced sterilising immunity of the nasal cavity of baboons following a secondary *B. pertussis* challenge. Furthermore, baboons immunised with a wP vaccine exhibited enhanced clearance of *B. pertussis* from the nasal cavity compaired with unimmunised baboons. This was accompanied by *B. pertussis*-specific IL-17A production from PBMCs isolated from convalescent or wP-primed primates. In contrast, baboons immunised with an aP vaccine exhibited significantly delayed clearance of *B. pertussis* from the nasal cavity, despite the absence of clinical symptoms of disease. Furthermore, infected aP-vaccinated animals were able to transmit *B. pertussis* to unvaccinated cage-mates, providing empirical evidence for asymptomatic transmission of *B. pertussis* in aP vaccinated populations. PBMCs from aP-primed baboons produced *B. pertussis*-specific IL-5, but failed to produce *B. pertussis*-specific

IL17A, highlighting an important link between immune protection in the nasal cavity and the induction of a Th17 response [28].

A study by Wilk et al. showed that while previous infection of mice with *B. pertussis* or immunisation with a wP vaccine promoted rapid clearance of *B. pertussis* from the nasal cavity of mice, immunisation with an aP vaccine failed to prevent *B. pertussis* colonisation in the nasal cavity. The inability of the aP vaccine to induce sterilising mucosal immunity in the upper respiratory tract was attributed to the failure of the aP vaccine to induce IL-17A-producing CD4 T_{RM} cells in the nasal mucosa [194] Furthermore, a study by Dubois and colleagues demonstrated that priming with an aP vaccine suppresses the development of nasal CD4 T_{RM} following infection with *B. pertussis*, with un-primed mice accumulating significantly more CD4 T_{RM} cells in the nasal mucosa post *B. pertussis* challenge compared with mice previously immunised with an aP vaccine [217].

1.12 Strategies to improve current pertussis vaccines

The association of asymptomatic nasopharyngeal carriage and subsequent transmission has highlighted the need to better understand the mechanisms underlying protective immunity in the upper respiratory tract. Although *B. pertussis* is a strictly mucosal pathogen, the protective role of mucosal immunity and the role of IL-17A in the nasal cavity has often been overlooked in previous vaccine studies. A study by Antunes et al. demonstrated that the Th17/Th1 response induced following immunisation with wP vaccines persists in humans up to fifteen years after original wP priming despite repeated boosters with an aP vaccine [281]. However, as with most human studies, only peripheral T cell responses were assessed due to the difficulty in accessing mucosal samples. This highlights the need to better understand the mechanisms of protective immunity in the nasal cavity in preclinical animal models to inform the design of improved pertussis vaccines.

The ability of vaccines to generate protective T_{RM} cells at mucosal barriers has been demonstrated in numerous other models with vaccines targeted against influenza virus, *S. aureus*, and *Helicobacter pylori* [282-284]. Experimental pertussis vaccines currently in development are employing multiple strategies with the aim of inducing mucosal CD4 T_{RM} cells. Locht and colleagues developed a live attenuated *B. pertussis* vaccine from the Tohama-1 strain, termed BPZE1, in which three major toxins, PT, dermonecrotic toxin (DNT) and TCT are genetically removed or modified. BPZE1 is designed for i.n.

administration in order to induce long-lasting and protective mucosal immunity [285]. Murine models demonstrated that immunisation with BPZE1 confers protection in the nasal cavity against *B. pertussis*, and this is associated with the induction of nasal IL-17A-producing CD4 T_{RM} and subsequent sIgA production [286]. A phase 1b clinical trial demonstrated that BPZE1 induces a safe and immunogenic response in healthy participants [287]. Other potential vaccine candidates include those containing outer membrane vesicles (OMV) derived from *B. pertussis*. OMVs are vesicles between 20 and 300 nm in diameter consisting of a single lipid bilayer derived from the outer membrane of Gram-negative bacteria. OMVs are promising structures for vaccine development since these vesicles contain many surface antigens present in the bacterial strain from which they were derived [288]. OMV-based vaccines have been shown to confer protection in the lungs of mice against multiple *B. pertussis* strains, including a PRN-deficient strain, in addition to inducing a sizable CD4 T_{RM} cell population similar to that seen following immunisation with a wP vaccine [289]. An alternative approach involves formulating currently used aP vaccine with new adjuvants which promote the development of T_{RM} cells. Adjuvants function by activating innate immune cells, which in turn promotes and instructs the adaptive immune response [290]. Addition of a novel adjuvant combination comprising of the intracellular stimulator of interferon genes (STING) agonist c-di-GMP, and the TLR2 agonist LP1569, which is derived from *B. pertussis*, was found to induce IL-17A-producing CD4 T_{RM} cells in the nasal cavity and conferred a high level of protection against nasal colonisation [291].

1.13 Aims of the project

Currently licenced aP vaccines fail to prevent nasal colonisation with *B. pertussis*, with evidence suggesting that this may contribute to asymptomatic transmission and the increased incidence of pertussis observed in recent years. It is clear that next generation pertussis vaccines should promote sterilising immunity in the nasal cavity. However, the upper respiratory tract has oftentimes been overlooked, and the mechanisms involved in protective immunity in the nasal cavity have not been fully elucidated. The goal of this study was to understand the mechanisms of protective immunity against *B. pertussis* in the upper respiratory tract which in turn could help inform the design of improved pertussis vaccines. In detail, the specific aims of this project were:

- To investigate the innate immune response in the nasal cavity to *B. pertussis* infection, with a particular focus on the role of neutrophils
- To examine the accumulation and persistence of *B. pertussis*-specific CD4 T_{RM} cells in the nasal cavity
- To determine if CD4 T cells contribute to protective immunity in the nasal cavity
- To investigate if IL-17A contributes to protective immunity in the upper respiratory tract and the mechanisms by with this protection is mediated
- To examine if CD4 T_{RM} cells induced following natural infection with *B. pertussis* are susceptible to bystander activation both *in vitro* and *in vivo*
- To investigate if CD4 T_{RM} cells induced following immunisation with a pertussis vaccine can be activated in a bystander manner

Chapter 2: Materials and Methods

2.1 Materials

2.1.1 Buffers, media, and solutions

Complete Roswell Park Memorial Institute (cRPMI) medium

RPMI-1640 medium (RPMI; Sigma-Aldrich)

10% heat inactivated foetal calf serum, filter-sterilised (FCS; Sigma-Aldrich)

100 mM L-glutamine (Sigma-Aldrich)

100 U/ml penicillin / 100 µg/ml streptomycin (Sigma-Aldrich)

50 µM β-mercaptoethanol (Sigma-Aldrich)

Complete Ham's F-12 Nutrient Mixture medium

Ham's F-12 Nutrient Mixture medium (with L-glutamine) (Sigma-Aldrich)

10% heat inactivated foetal calf serum, filter-sterilised (FCS; Sigma-Aldrich)

100 U/ml penicillin / 100 µg/ml streptomycin (Sigma-Aldrich)

Red blood cell lysis buffer

0.87% Ammonium chloride (NH_4Cl; Sigma-Aldrich)

Dissolved in dd$H_2$0 (pH 7.3-7.4) and filter sterilised.

Stainer-Scholte liquid medium

Reagent	**g/L**	**Supplier**
L-glutamic acid (monosodium salt) ($C_5H_8NNaO_4.xH_2O$)	10.72	Sigma-Aldrich
L-proline ($C_5H_9NO_2$)	0.24	Sigma-Aldrich
Sodium chloride (NaCl)	2.5	Sigma-Aldrich
Potassium phosphate monobasic (KH_2PO_4)	0.5	Sigma-Aldrich
Potassium chloride (KCl)	0.2	Sigma-Aldrich
Magnesium chloride hexahydrate ($MgCl_2.6H_2O$)	0.1	Sigma-Aldrich
Calcium chloride dehydrate ($CaCl_2.2H_2O$)	0.02	Sigma-Aldrich
Tris (Trizma base; $C_{14}H_{11}NO_3$)	1.525	Sigma-Aldrich

Made up to 1 litre with ddH_2O (pH 7.3-7.4) and sterilised by autoclaving.

Supplement (200X)

0.4 g L-cystine ($C_6H_{12}N_2O_4S_2$) – Dissolved in 1 mL 37% Hydrogen chloride (HCl; Sigma-Alrich)

0.1 g Ferrous sulfate heptahydrate ($FeSO_4.7H_2O$; Sigma-Aldrich)

0.2 g L-ascorbic acid ($C_6H_8O_6$; Sigma-Aldrich)

0.04 g Nicotinic acid ($C_6H_5NO_2$; Sigma-Aldrich)

1.0 g L-glutathione (reduced) ($C_{10}H_{17}N_3O_6S$; Sigma-Aldrich)

Make up to 50 ml with ddH_2O and filter sterilised.

1% Casein salt solution

6.0 g NaCl

10.0 g BactoCasamino acids (Becton Dickinson)

Made up to 1 L with ddH_2O (pH 7.0-7.2) and autoclaved at 115°C for 20 minutes.

Phosphate buffered saline (PBS) 20X

320 g NaCl (1.4 M)

46 g Sodium hydrogen phosphate (Na_2HPO_4; 0.08 M)

8 g KH_2PO_4 (0.01 M)

Made up to 2 L with dH_2O (pH 7.0)

Fluorescence-activated cell sorting (FACS) FACS Buffer

2% FCS

1 M HEPES (Thermo-Fischer)

0.1 M Ethylenediaminetetraacetic acid (EDTA; Sigma)
Prepared in 1X PBS, stored at 4°C

Stock isotonic Percoll

Percoll (GE Healthcare) was made isotonic by diluting 9:1 with 10X PBS (Sigma). Stock isotonic Percoll was then diluted to 30% with PBS.

2% Paraformaldehyde (PFA)

1 ml PFA (Thermo-Fischer) diluted in 7 ml 1X PBS

Fixation/Permeabilization Buffer

1 part Fixation/Permeabilization Concentrate (Invitrogen) diluted with 3 parts Fixation/Permeabilization Diluent (Invitrogen)

Permeabilization Buffer

Permeabilization Buffer 10X (Invitrogen) dilute 1:10 in dH_2O

ELISA Wash Buffer

0.5% Tween-20 (Sigma-Aldrich)

Prepared in 1X PBS

ELISA blocking solutions

BD kits: 10% (w/v) milk (Marvel)

R&D kits: 1% (w/v) Bovine serum albumin (BSA; Sigma-Aldrich)

ELISA stop solution

26.74 mL 18M Sulfuric acid (H_2SO_4; Sigma Aldrich)

473.26 L dH_2O

Protease Inhibitor

1 cOmplete, Mini, EDTA-free tablet (Roche) was dissolved in 7 mL 1X PBS

2.1.2 Agar

Bordet-Gengou blood agar plates

5 mL Glycerol ($C_3H_8O_3$; Fisher Chemical)

15 g Bordet-Gengou agar (Becton Dickenson)

Made up to 500 mL with ddH_2O and autoclaved at 121°C for 20 minutes.

2 ml Cephalexin (10 mg/ml; Sigma-Aldrich)

100 mL horse blood (pre-warmed to 37°C; Cruinn)

Tryptic Soy Agar (TSA) plates (in house)

2.1.3 Mouse Cytokine ELISA kits

Cytokine	Supplier
IL-1β	R&D
IL-12p70	R&D
IL-17A	R&D
IL-23	R&D
CXCL1	R&D
MIP2	R&D
LCN2	R&D
IL-6	BD Biosciences
IFNγ	BD Biosciences

2.1.4 Mouse Antibody ELISA kits

Antibody	Supplier
IgA (HRP-conjugated)	Southern Biotech
IgG2c (HRP-conjugated)	Bio-Rad Laboratories

2.1.5 Other ELISA reagents

Reagent	Supplier
Streptavidin-HRP	BD Pharmingen
1X TMB Substrate Solutions	Life Technologies

2.1.6 Fluorochrome-conjugated antibodies for flow cytometry

Antibody	Clone	Source	RRID
Alexa Fluor 700-CD45.1	A20	BioLegend	AB_493733
Alexa Fluor 700-CD45R/B220	RA3-6B2	eBioscience	AB_469907
Alexa Fluor 700-CD8a	53-6.7	eBioscience	AB_494005
APC-CD121a (IL-1 R, Type I/p80)	JAMA-147	BioLegend	AB_2264757
APC-CD69	H1.2F3	BioLegend	AB_492843
APC-eFluor 780-CD3e	145-2C11	eBioscience	AB_11149861
APC-eFluor780-CD11b	M1/70	eBioscience	AB_1603193
APC-eFluor780-CD4	RM4-5	eBioscience	AB_1272183
APC-eFluor780-CD62L (L-Selectin)	MEL-14	eBioscience	AB_1603256
APC-Foxp3	FJK-16s	eBioscience	AB_469457
APC-MHCII (I-A/I-E)	M5/114.15.2	eBioscience	AB_469455
BB515-IL-23R	O78-1208	BD Biosciences	AB_2739602
BV421-CD11c	HL3	BioLegend	AB_11219593
BV421-CD182 (CXCR2)	V48-2310	BD Biosciences	AB_2864336
BV421-CD4	GK1.4	BioLegend	AB_10900241
BV421-Ly6G	1A8	BioLegend	AB_10897944
BV605-CD11c	N418	BioLegend	AB_11204262
BV605-CD11c	N418	BioLegend	AB_11204262
BV605-CD44	IM7	BioLegend	AB_2562451
BV650-CD3	17A2	BioLegend	AB_11204249
BV650-IL-17A	TC11-18H10.1	BioLegend	AB_11126980
BV650-Ly6G	1A8	BioLegend	AB_2565881
BV650-RORgt	Q31-378	BD Biosciences	AB_2738915
BV711-CD45.2	104	BioLegend	AB_2616859
BV711-CD45R/B220	RA3-6B2	BioLegend	AB_2563491
BV711-CD49d	9C10 (MFR4.B)	BD Biosciences	AB_2740360
BV711-IFNg	XMG1.2	BioLegend	AB_11219588
BV711-MHCII (I-A/I-E)	M5/114.15.2	BD Biosciences	AB_2738191
BV711-NK-1.1	PK136	BioLegend	AB_2563286
BV785-CD11c	N418	BioLegend	AB_2565268
BV785-CD4	RM4-5	BioLegend	AB_2563053

BV786-CD103	M290	BD Biosciences	AB_2738744
eFluor450-CD218a (IL-18Ra)	P3TUNYA	Thermo Fisher Scientific	AB_2574069
eFluor 450-CD11c	N418	eBioscience	AB_1548654
eFluor 450-CD3e	145-2C11	eBioscience	AB_10735092
eFluor 660-CD170 (Siglec F)	1RNM44N	eBioscience	AB_2574187
FITC-CD69	H1.2F3	BioLegend	AB_313109
FITC-Ly6C	AL-21	BD Biosciences	AB_394628
FITC-TNF	MP6-XT22	BD Biosciences	AB_395379
FITC-γδ T-Cell Receptor	GL3	BD Biosciences	AB_394688
Pacific Blue-Ly-6G	1A8	BioLegend	AB_2251161
Pe/Cy7-CD192 (CCR2)	SA203G11	BioLegend	AB_2616983
Pe/Cy7-CD25	PC61.5	eBioscience	AB_469608
Pe/Cy7-CD27	LG.7F9	eBioscience	AB_1724035
Pe/Cy7-CD3e	145-2C11	BioLegend	AB_312685
PE/Cy7-F4/80	BM8	eBioscience	AB_469653
Pe/Cy7-IL-2	JES6-5H4	BioLegend	AB_2561750
PE/Cyanine5-CD11c	N418	BioLegend	AB_493566
PE/Cyanine5-CD45R (B220)	RA3-6B2	BioLegend	AB_312995
PE/Cyanine5-CD62L	MEL-14	BioLegend	AB_313097
PE/Cyanine5-F4/80	BM8	eBioscience	AB_468798
PE/Dazzle594-CD80	16-10A1	BioLegend	AB_2564175
PE-CD45	30-F11	eBioscience	AB_465669
PE-CF594-CD103	M290	BD Biosciences	AB_2739377
PE-CF594-CD62L	MEL-14	BD Biosciences	AB_11154046
PE-CF594-IFNg	XMG1.2	BD Biosciences	AB_11153140
PE-CF594-Siglec-F	E50-2440	BD Biosciences	AB_2687994
PerCP-Cy5.5-Ly-6C	HK1.4	eBioscience	AB_2723343
PerCPCyanine5.5-CD62L (L-Selectin)	MEL-14	eBioscience	AB_996667
PerCPCyanine5.5-F4/80	BM8	BioLegend	AB_893484
PerCPCyanine5.5-GM-CSF	MP1-22E9	BioLegend	AB_2562376
PerCPCyanine5.5-NK1.1	PK136	eBioscience	AB_914361
PerCP-eFluor710-TCR gamma/delta	eBioGL3 (GL-3,GL3)	eBioscience	AB_2016707

Purified Rat Anti-Mouse CD16/CD32 (Mouse BD Fc Block)	2.4G2	BD Biosciences	AB_394657
V450-IL17A	TC11-18H10	BD Biosciences	AB_1727540

2.1.7 Other FACS reagents

Reagent	**Concentration**	**Supplier**
Collagenase-D	1 mg/ml	Sigma-Aldrich
Deoxyribonuclease I (DNAse I)	20 U/ml	Sigma-Aldrich
LIVE/DEAD Fixable Aqua dead cell stain kit	1:600 (PBS)	Thermo Fischer Scientific
Propidium Iodide Ready Flow Reagent		Thermo Fischer Scientific
OneCompeBeads		Invitrogen
Phorbol 12-myristate 13-acetate (PMA)	50 ng/ml	Sigma-Aldrich
Ionomycin	500 ng/ml	Sigma-Aldrich
Brefeldin A	5 µg/ml	Sigma-Alrdich
CountBright™ Absolute Counting Beads		Invitrogen
ArC™ Amine Reactive Compensation Bead Kit		Invitrogen
SYTOX Green	0.3 µM	Thermo Fisher Scientific
4’,6-diamidino-2-phenylindole (DAPI)	0.1 µM	Sigma-Aldrich

2.1.8 Recombinant Cytokines

Cytokine	**Concentration *in vitro***	**Concentration *in vivo***	**Supplier**
Recombinant mouse IL-1β	10 ng/ml		ImmunoTools
Recombinant mouse IL-23	10 ng/ml		Miltenyl Biotec
Recombinant mouse IL-12	10 ng/ml		R&D Systems
Recombinant mouse IL-18	10 ng/ml		Biolegend
Recombinant mouse IL-7	10 ng/ml		Immunotools
Recombinant mouse GM-CSF	10 – 20 ng/ml		Immunotools
Recombinant mouse IL-17A	10 ng/ml	500 ng/mouse	Immunotools
Recombinant mouse TNF	10 ng/ml		Immunotools
Recombinant mouse IFNγ	10 ng/ml		Immunotools

2.1.9 Ligands and antigens

Reagent	**Concentration *in vitro***	**Concentration *in vivo***	**Supplier**
Sonicated *B. pertussis* Strain BP338	5 µg/ml	-	In house
Heat-killed *Staphylococcus aureus* Strain PS80	1 - 10 µg/ml	-	Kindly supplied by Tracey Claxton, TCD
Heat-killed *Mycobacterium Tuberculosis*	10 µg/ml	-	Invivogen
Ultrapure Lipopolysaccharide – derived from *Escherichia coli*	100 ng/ml	1 - 5 µg/mouse	Invivogen
Heat-killed *Klebsiella pneumoniae* Strain ATCC 43816	1 - 5 µg/ml	10 µg/mouse	Kindly supplied by Jenny Mannion, TCD
Poly I:C	50 µg/ml	-	Sigma-Aldrich

2.1.10 In vivo antibodies and reagents

Reagent	Clone	Concentration *in vivo*	Supplier
Anti-Mouse IL-17A	17F3	50 µg/mouse (i.n.) – 200 µg/mouse (i.p.)	BioXCell
Anti-Mouse Ly6G	1A8	100 µg/mouse	BioXCell
Rat IgG2a isotype control, anti-trinitrophenol	2A3	100 µg/mouse	BioXCell
Anti-Ly6G			
Anti-rat Kappa Immunoglobulin Light Chain	MAR 18.5	100 µ/mouse	BioXCell
Mouse IgG1 isotype control, unknown specificity	MOPC-21	50 µg/mouse (i.n.) – 200 µg/mouse (i.p.)	BioXCell
Anti-Mouse CD4	GK1.5	50 µg/mouse (i.n.) – 200 µg/mouse (i.p.)	BioXCell
Rat IgG2b isotype control, anti-keyhole limpet hemocyanin	LTF-2	50 µg/mouse (i.n.) – 200 µg/mouse (i.p.)	BioXCell
Anti-Mouse IL-12 p40	C17.8	50 µg/mouse (i.n.) – 200 µg/mouse (i.p.)	BioXCell
FTY720	-	0.3 mg/kg/day	Santa Cruz Biotechnology
Pertussis Vaccine (Whole Cell) WHO International Standard 94/532	-	1/20th human dose/mouse	National Institute for Biological Standards and Control (NIBSC)

2.1.11 In vitro antibodies

Reagent	Clone	Concentration *in vitro*	Application	Supplier
Anti-Mouse CD3ε	145-2C11	1 µg/ml	Plate bound	BD Biosciences
Anti- Mouse CD28	37.51	1 µg/ml	Soluble	BD Biosciences
Anti-Mouse CD49d	R1-2	1 µg/ml	Soluble	BD Biosciences
Anti-Mouse MHC Class II (I-A/I-E)	M5/114.15.2	2 µg/ml	Soluble	Invitrogen
Anti-Mouse IL-23 p19	N71-1183	10 µg/ml	Soluble	BD Biosciences
Anti-Mouse IL-1β	B122	10 µg/ml	Soluble	BD Biosciences
Anti-Mouse IL-12 p40	C17.8	10 µg/ml	Soluble	BioXCell
Anti-Rat IgG2a Isotype Control	2A3	10 µg/ml	Soluble	BioXCell
Anti-RatIgG1, κ Isotype Control	R3-34	10 µg/ml	Soluble	BD Biosciences

2.1.12 Mouse RT-PCR Primers

Oligonucleaotide	Product code	Supplier
Euk 18S r RNA	4319413E	Applied Biosystems
Il1β	Mm00434228_m1	Applied Biosystems
Csf3	Mm00438334_m1	Applied Biosystems
Cxcl1	Mm04207460_m1	Applied Biosystems
Lcn2	Mm01324470_m1	Applied Biosystems
Nos2	Mm00440502_m1	Applied Biosystems
Pigr	Mm00465049_m1	Applied Biosystems
Il17a	Mm00439618_m1	Applied Biosystems

2.1.13 Other RT-PCR reagents

Reagent	Supplier
Trizol	Life Technologies
High Capacity cDNA Reverse Transcription Kit	Applied Biosystems
Isopropanol	Sigma-Aldrich
Chloroform	Honeywell
Ethanol	Sigma-Aldrich
RNAse Free H_2O	Invitrogen
RNALater Solution	Sigma-Aldrich

2.2 Methods

2.2.1 Mice

Specific pathogen-free C57BL/6 mice were bred in-house in the Comparative Medicine Unit in Trinity College Dublin. IL-17A$^{-/-}$ mice were bred in-house. Female mice were used in experiments and were 6 – 12 weeks old at initiation of experiment. Mice were euthanised by asphyxiation with CO_2. All animal experiments were conducted in accordance to European Union regulations and under licence (AE19136/P042) from the Irish Health Products Regulatory Authority with approval from the Trinity College Dublin Bioresources Ethics Committee.

2.2.2 B. pertussis respiratory challenge

The common laboratory *B. pertussis* strain BP338 was used throughout this study. BP338 is a derivative of the Tohama I strain, which was originally isolated from a case of whooping cough in Japan in the 1950s and was used to formulate the wP vaccine used for mass vaccination in Japan until 1975 [292, 293]. BP338 has been used in multiple *in vitro* and *in vivo* models to study the immune response to *B. pertussis*, and has been demonstrated to be virulent in a murine model of *B. pertussis* [194, 227]. Stock *B. pertussis* (BP338 strain; stored at -80°C) was spread on warm Bordet-Genou Agar plates (100 µl/plate) and cultured for 3 days at 37°C. Using an inoculation loop, bacteria from each plate was transferred to 100 ml of supplemented Stainer and Scholte liquid medium and incubated overnight at 37°C in an Innova 4330 Incubator Shaker set at 190 rpm. Liquid culture was then centrifuged at 3500 RPM for 30 minutes at room temperature. Bacterial pellets were re-suspended in 1% casein salts solution and pooled. To calculate the concentration of bacteria in the liquid culture, aliquots of cultured bacteria were diluted in 1% casein salt solution (1:20 and 1:50 dilutions) and the optical density of the diluted bacteria was read at 600 nm using an Eppendorf BioPhotometer, with 1% casein salt solution used to obtain a blank reading. The average colony forming units (CFUs) of the liquid culture was obtained by applying the obtained absorbance values to an established standard curve. The liquid culture was diluted with 1% casein salt solution to 1 x 10^9 CFU/ml. Respiratory challenge was performed by exposing mice to *B. pertussis* aerosol for 10 minutes in a Perspex chamber followed by a 10 minutes rest in the chamber using a PARI TurboBOY SX nebulizer.

2.2.3 B. pertussis CFU counts of lungs, nasal wash, and nasal tissue

The left and post-caval lung lobes were aseptically removed and homogenised in 500 µl of 1% casein solution and serially diluted in 1% casein solution. To harvest nasal wash, the head was cut from body of the mouse, followed by the aseptic removal of the mandible (lower jaw) to expose the trachea. A 23 G needle was placed in the trachea and 700 µl of sterile PBS was slowly flushed through the nasal cavity and collected in an Eppendorf tube placed beneath the tip of the nose. Nasal wash was serially diluted in 1% casein solution. Nasal tissue, including the nasal cavity and nasal turbinates, was collected in 500 µl of sterile PBS. Collagenase-D and DNase I in PBS was added to the nasal tissue, bringing the volume up to 1 ml, and samples were incubated for 1 h at 37 °C with agitation. After incubation, the digested nasal tissue was flushed through 70 µM cell strainers using 4 ml of PBS. An aliquot of the sample was serially diluted in 1% casein solution, with the remaining cells processed further for flow cytometry analysis. Undiluted and serially diluted lung, nasal wash, and nasal tissue samples (100 µl) were lawned onto Bordet-Gengou agar plates and the number of CFU was calculated after 5-6 days incubation at 37°C. The counts were converted into Log_{10}CFU for graphical representation of bacterial load. The remaining lung homogenate was centrifuged at 14,500 rpm for 10 minutes. Supernatants were collected and 10 µl protease inhibitor was added to each lung sample as well as remaining nasal wash before storing at -80°C for ELISA analysis.

2.2.4 Intranasal Klebsiella pneumoniae challenge

Stock *K. pneumoniae* (ATCC 43816 strain) was spread on warm trypic soy agar (TSA) plates and grown over-night at 37°C. Using an inoculation loop, bacteria was collected from the plate and suspended in 1 ml of sterile PBS. The OD 600 of the suspension was adjusted 1.0 (containing 1 X 10^9 CFU/ml). For i.n. administration, a 1:20 dilution in PBS was performed such that 20 µl contained 1 X 10^6 CFU. Mice were infected by placing 10 µl of *K. pneumoniae* onto each nares or the mouse, so that each mouse received a total volume of 20 µl, and waiting for the mouse to inhale the bacteria.

2.2.5 K. pneumoniae CFU counts of lungs, nasal wash, and nasal tissue

The left and medial lobe of the mouse lung, nasal wash, and nasal tissue was collected in PBS as previously described. Samples were serially diluted in sterile PBS and 20 µl of neat and diluted samples were dotted in triplicate onto TSA plates. The number of CFU was calculated after overnight incubation at 37°C. The counts were converted into Log_{10}CFU for graphical representation of bacterial load.

2.2.6 Preparation of sonicated B. pertussis

Stock *B. pertussis* (BP338 strain; stored at -80°C) was spread on warm Bordet-Genou Agar plates (100 µl/plate) and cultured for 3 days at 37°C. Using an inoculation loop, bacteria from each plate was transferred to 100 ml of supplemented Stainer and Scholte liquid medium and incubated overnight at 37°C in an Innova 4330 Incubator Shaker set at 190 rpm. The *B. pertussis* liquid culture was centrifuged at 4,000 rpm for 30 minutes. Pelleted bacteria was washed with sterile PBS and centrifuged again at 4,000 rpm for 30 minutes. Bacteria pellet was resuspended in sterile PBS and diluted to 1 x 10^{10} CFU/ml in sterile PBS. Diluted bacteria was aliquoted into 15 ml falcons (3 ml of bacterial suspension/falcon) and sonicated on ice using 10 x 15 second pulses using a Branson Sonifier 250. The sonicated *B. pertussis* suspension (sBP) was centrifuged at 10,000 rpm for 15 minutes and the supernatants were collected. The Pierce Bicinchoic BCA assay (Pierce Thermo Scientific) was used to measure protein concentration and sBp was stored at -80°C.

2.2.7 Intranasal administration of PAMPs, killed pathogens, and cytokines

Mice were first anesthetised by sub-cutaneous injection of a mixture of Anaestamine (ketamine; 90 – 100 mg/kg) and Sedaxylan (xylazine; 7.5 – 16 mg/kg) prepared to a volume of 150 µl in PBS according to weight of mouse. Mice received either ultrapure LPS derived from *Escherichia coli* (1 – 5 µg/mouse), heat-killed *K. pneumoniae* (10 µg/mouse), or recombinant murine IL-17A (500 ng/mouse) in a volume of 40 µl PBS (20 µl per nares) by the i.n. route. Control mice received 40 µl of PBS by the i.n. route.

2.2.8 Immunisation with a whole cell pertussis vaccine

For i.n. immunisations, mice were anesthetised by sub-cutaneous injection of ketamine/xylazine as previously described. The wP vaccine (Pertussis Vaccine Whole Cell WHO International Standard 94/532) was prepared in 20 µl PBS to give 1/20th of one human dose per mouse, and 10 µl was administered to each nares. For intraperitoneal (i.p.) immunisations, 1/20th of one human dose was prepared in 200 µl PBS per mouse and injected via the i.p. route.

2.2.9 In vivo treatment with antibodies

For IL-17A neutralisation during *B. pertussis* challenge, mice were injected i.p. with anti-IL-17A antibody at either 100 µg/mouse or 200 µg/mouse (stated in figure legends) in 200 µl PBS 1 day prior to infection and every 3 days during challenge. Control mice were injected with the appropriate isotype control (mouse IgG1 isotype control, unknown specificity).

For depletion of neutrophils, a double antibody-based depletion strategy adapted from Boivin et al. was employed [294]. Mice were injected i.p. every day with an anti-Ly6G antibody (100 µg/mouse), commencing treatment 1 day prior to or on day 7 post *B. pertussis* challenge. Control mice were treated every day with the corresponding isotype control (Rat IgG2a isotype control, anti-trinitrophenol). A secondary antibody, anti-rat Kappa immunoglobulin light chain (100 µg/mouse) was injected i.p into mice every second day after anti-Ly6G or isotype control treatment.

For depletion of CD4 T cells during a primary *B. pertussis* challenge, mice were treated with anti-CD4 antibody, 200 µg/mouse i.p. and 50 µg/mouse i.n. administered simultaneously, every 4 days, starting the depletion on day 7 post *B. pertussis* challenge. For depletion of CD4 T cells during the re-challenge of convalescent mice, convalescent mice were treated with anti-CD4, 200 µg/mouse i.p. and 50 µg/ mouse i.n. administered simultaneously, 5 and 1 day before and every 4 days after secondary *B. pertussis* challenge. A corresponding isotype antibody (Rat IgG2b, κ isotype control, anti-keyhole limpet hemocyanin) was used as a control.

For neutralisation of IL-12/IL-23p40 during i.n. administration of LPS, mice were injected i.p. with an anti-IL-12p40 antibody (200 µg/mouse) 1 day prior to LPS administration. Mice were treated i.n. with an additional dose of anti-IL-12p40 (50 µg/mouse) during LPS challenge. A corresponding isotype antibody (Rat IgG2a isotype control, anti-trinitrophenol) was used as a control.

For neutralisation of IL-17A during i.n. administration of heat-killed *K. pneumoniae*, mice were injected i.p. with an anti-IL-17A antibody (200 µg/mouse) 1 day prior to heat-killed *K. pneumoniae* administration. Mice were treated i.n. with an additional dose of anti-IL-17A (50 µg/mouse) during heat-killed *K. pneumoniae* challenge. A corresponding isotype antibody (mouse IgG1 isotype control, unknown specificity) was used as a control.

2.2.10 FTY720 treatment

Drinking water consumption by mice was monitored for one week and the average volume of water consumed per mice per day was calculated and weights of individual mice was measured. FTY720 was administered to mice orally in the drinking water at a concentration of 0.3 mg/kg/day for a period of 10 days before infection and until the cessation of the experiment.

2.2.11 In vivo Intravascular Staining

To discriminate circulating from tissue-resident lymphocytes by flow cytometry, mice were injected i.v. with 200µl of a fluorochrome-conjugated antibody against CD45 (7.5 µg/ml in PBS) into the tail veins 10 minutes prior to euthanasia. Circulating lymphocytes are exposed to the antibody and labelled CD45 i.v.$^{+}$, while tissue-resident lymphocytes within the tissue are protected from i.v. labelling, therefore are identified as CD45 i.v.$^{-}$ (Figure 2.1).

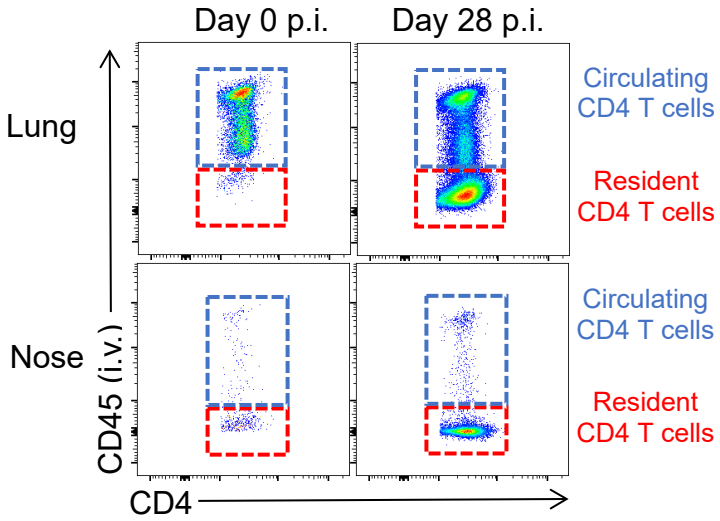

Figure 2.1 *In vivo* intravascular staining of lung and nasal CD4 T cells on the day of and 28 days post *B. pertussis* challenge.

2.2.12 Isolation of lungs, nasal tissue, and lymph nodes for staining for flow cytometry

The nasal tissue was obtained by first separating the head from the body of the mouse. The lower jaw, tongue, and connective tissue was removed to expose the upper pallet which contains the nasal associated lymphoid tissue (NALT) (Figure 2.2). The front incisors were cut away and the upper pallet was carefully peeled from the upper jaw using forceps and discarded (Figure 2.2). The nasal tissue, including the nasal cavity and turbinates, was harvested by cutting down the vertical plane of the skull using a scalpel and scraping out the tissues and small bones from both sides of the nasal passage using forceps [295]. The superior, middle and inferior lobes of the lungs were harvested from mice and chopped using a scalpel to facilitate enzymatic digestion of the lung tissue. The nasal tissue and lungs were digested with collagenase-D and DNAse I for 1 h at 37 °C, continuously rotating to facilitate tissue break down and release of cells. Digested nasal tissue and lungs were passed through a 70- µm cell strainer to obtain a single-cell suspension. Cervical lymph nodes (cLNs) were passed through a 40- µm cell strainer to obtain a single cell suspension. Cells were centrifuged at 1350 rpm for 5 minutes and pellet was re-suspended in 1 m of 0.87 % ammonium chloride to lyse red blood cells. After 2 minutes, 10 ml of cRPMI was added to neutralise the reaction. Cells were centrifuged and re-suspended in cRPMI.

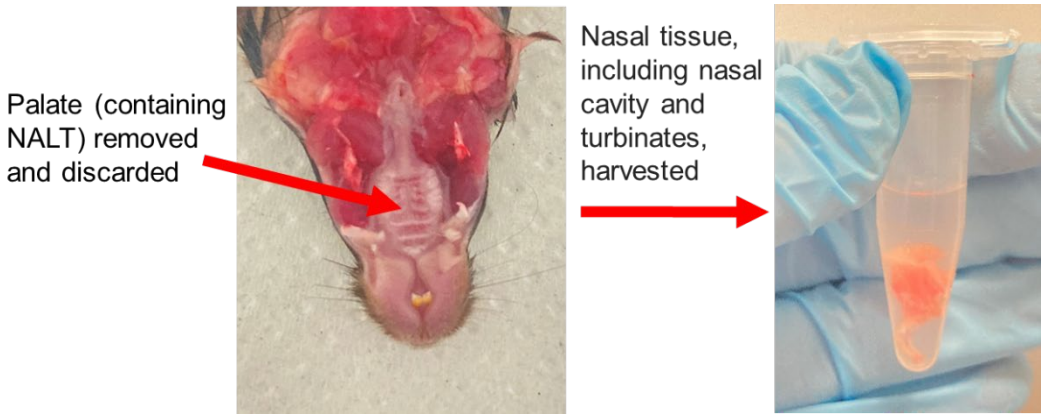

Figure 2.2 Dissection of murine nasal tissue.

To detect intracellular cytokine production directly *ex vivo* without any additional stimulation, cells were incubated with brefeldin A (5 µg/ml) at 37°C in 5% CO_2 during the digestion stage, followed by an addition 1 hour incubation of the isolated mononuclear cells with brefeldin A (5 µg/ml). To detect *B. pertussis*-specific intracellular cytokine

production, isolated mononuclear cells were stimulated for 18–20 hours at 37°C in 5% CO_2 with sonicated *B. pertussis* (sBP; 5 µg/mL), anti-CD28 and anti-CD49d (1 µg/mL each), with brefeldin A (5 µg/mL) added for the final 4 hours of culture. Alternatively, intracellular cytokine production was also detected following stimulation of cells with PMA (50 ng/ml) and ionomycin (500 ng/ml) in the presence of brefeldin A (5 µg/ml) for 4 hours at 37°C. To detect TCR-independent cytokine production by CD4 T cells, isolated mononuclear cells were first rested for 2 hours at 37°C in 5% CO_2 and cells in suspension were subsequently harvested and stimulated with combinations of recombinant murine IL-1β, IL-23, IL-18, and IL-12 (all at 10 ng/ml) for 20 hours at 37°C in 5% CO_2, with brefeldin A (5 µg/mL) added for the final 4 hours of culture.

Cells for staining were washed with PBS and incubated in 50 µl of PBS with LIVE/DEAD Aqua (1:600 dilution) for 25 minutes in the dark at 4°C. Cells were then washed with PBS and pelleted by centrifugation. The supernatant was discarded and cells were incubated in the presence of Fc block (αCD16/CD32 FcγRIII) (1:200 in FACS buffer) for 15 minutes in the dark at 4°C. Cells were then washed with FACS buffer and stained for surface markers with fluorochrome-conjugated anti-mouse antibodies at appropriate dilutions in FACS buffer, and incubated for 25 minutes in the dark at 4°C. After staining for surface markers, cells were washed twice with FACS buffer prior to fixation. For samples subjected to surface staining only, cells were fixed in 50 µl PBS with 2% PFA in the dark at 4°C for 10 minutes. Cells were then washed twice with FACS buffer and re-suspended in 200 µl FACS buffer and kept at 4°C until analysed.

For detection of intracellular cytokines and transcription factors, cells were fixed, permeabilised and stained using eBioscience™ Foxp3/Transcription Factor Staining Buffer Set according to the manufacturer's instructions. Following extracellular staining, samples were incubated with Foxp3 Fixation/Permeabilization working solution at 4°C for 45 minutes or overnight (up to 18 hours). Cells were then washed twice with 1X Permeabilization Buffer. Cells were then stained with fluorochrome-conjugated antibodies specific for intracellular and intra-nuclear proteins made in 1X Permeabilization Buffer. Cells were stained in the dark at 4°C for 1 hour. Cells were then washed twice with 1X Permeabilization Buffer, followed by one wash with FACS buffer. Cells were then re-supended with 200ul FACS buffer and kept at 4°C until Analysis. Flow cytometric analysis was performed on an LSRFortessa or a Cytek Aurora, and data was acquired using Diva software (BD Biosciences) or SpectroFlo® software (Cytek Biosciences), respectively. Data was analysed using FlowJo software (Tree Star). ImageStream analysis was acquired on an Amnis® ImageStream®^{X} MK II Imaging Flow Cytometer (Luminex). Doublet cells and dead cells were excluded by their pulse width

profile and LIVE/DEAD Aqua staining, respectively. Percentages and absolute number of cells were calculated on the basis of live single cells. Fluorescence-minus-one (FMO) controls were used as a guide for gating strategies.

2.2.13 Detection of NET activity by flow cytometry

A technique adapted by Zharkova et al. using a combination of the cell-impermeable nucleic acid dye, SYTOX Green, and 4',6- diamidino-2-phenylindole (DAPI), which is membrane-semipermeable, was employed for two-colour visualization of NETs on flow cytometry [296]. Single cell suspensions were obtained from nasal tissue and added to U-bottom 96-well polypropylene plates. Cells were incubated for 30 min at 37 °C in 5% CO_2 prior to stimulating with heat-killed *B. pertussis* (1×10^7 CFU/mL), PMA (50 ng/mL), or medium for 4 hours. Cells were fixed by adding PFA at a final concertation of 1.3% and incubated for 15 min at RT. PFA concentrations below 4% are thought to fix, but not permeate the plasma membrane, thus reducing artificial "NET formation". Samples were then centrifuged at 100 × g for 10 min at RT and supernatants were carefully aspirated [297]. Samples were stained with the following: DAPI (0.1 µg/mL), SYTOX Green (0.3 µM), CD11b-APCeFluor780, Ly6G-BV650, and Siglec-FPECF594. Flow cytometric analysis was performed on a Cytek Aurora, and data were acquired using SpectroFlo® software (Cytek Biosciences). Data were analysed using FlowJo software (Tree Star).

2.2.14 Fluorescence-activated cell sorting of tissue-resident $CD4^+$ T cells

Mice were injected i.v. with 200 ul of a PE-conjugated antibody against CD45 (7.5 µg/ml in PBS) to discriminate circulating from resident cell populations. Lungs and nasal tissue were harvested. Mononuclear cells were isolated and pooled from lungs or nasal tissue as described above. After red blood cell lysis, cells were re-suspended 30% Percoll in PBS (GE Healthcare) and centrifuged at 1500 RPM at room temperature for 20 minutes. The interface was carefully removed and cells were washed once with cRPMI and centrifuged at 1350 rpm for 5 minutes. The cell pellet was washed with sterile FACS buffer and cells were stained with fluorochrome-conjugated antibodies specific for the surface markers CD3 and CD4, in addition to CD8, B220, and γδ TCR which served as a dump gate, in 200 ul of FACs buffer in the presence of Fc Block to prevent non-specific binding. Cells were stained in the dark at 4°C for 25 minutes. Cells were then washed twice prior to isolation of target population using the BD FACSAria Fusion High Performance Cell Sorter. Propidium Iodide Ready Flow reagent was added prior to cell

sort to discriminate live from dead cells. From the lungs, both circulating (CD45 i.v.$^+$) and tissue-resident (CD45 i.v.$^-$) CD4$^+$CD3$^+$ T cells (CD8$^-$B220$^-$γδTCR$^-$) were isolated. Due to the low number of circulating CD4 T cells in the nasal tissue, only tissue-resident (CD45 i.v.$^-$) CD4$^+$CD3$^+$ T cells (CD8$^-$B220$^-$γδTCR$^-$) were isolated from the nose (Figure 2.3).

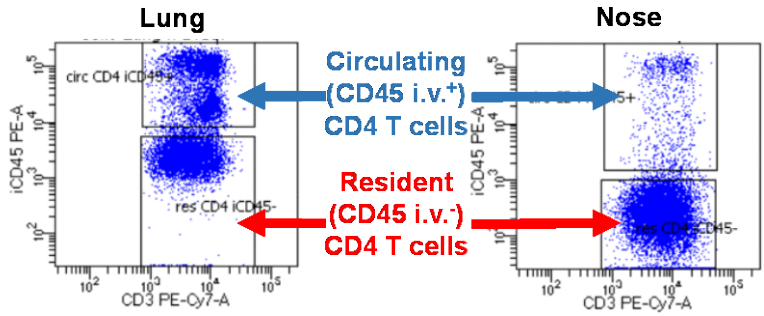

Figure 2.3 Resident (CD45 i.v.$^-$) and circulating (CD45 i.v.$^+$) CD4 T cell populations isolated from mouse lung and nasal tissue.

2.2.15 Cytokine stimulation of purified CD4$^+$ T cells

Isolated tissue-resident CD4$^+$ T cells were plated in round-bottomed 96-well plate (200 µl/well; refer to figure legend for seeding densities). Cells were stimulated with 50 µl of combinations of IL-1β, IL-23, IL-18, IL-12, and IL-7 (all at 10 ng/ml). Plate-bound anti-CD3ε (1 µg/ml) and soluble anti-CD28 (1 µg/ml) were added to selected wells as a positive control. Cells were cultured for 72 hours at 37°C in 5% CO_2 and supernatants were removed for quantification of cytokine concentrations by ELISA.

2.2.16 Generation of bone marrow-derived dendritic cells (BMDCs)

The femurs and tibiae were aseptically removed from mice and separated from the surrounding muscle and tissue. The tips of the epiphysis were removed to expose the bone marrow. The bone marrow was flushed using a 27G needle attached to a 20 ml syringe containing cRMPI. Any cell aggregates were broken down by syringing the cells up and down using a 19 G needle. Cells were pelleted by centrifugation (1350 rpm for 5 minutes) and re-suspended in 1ml of 0.87% ammonium chloride for 2 minutes to lyse red blood cells, followed by neutralization with 10 mL of RPMI. Cells were pelleted by centrifugation (1350 rpm, 5 min) and were re-suspended in an appropriate volume of media for counting. The cells were seeded at a concentration of 1 x 10^6 cells/ml in T175 flasks (15 ml/flask) in cRPMI supplemented with 20 ng/ml of GM-CSF. An additional 20 ml of GM-CSF-supplemented (20 ng/ml) media was added to flasks after 3 days of

culture. On day 6 of culture the supernatants were gently removed and discarded from flasks and replaced with 20 ml of sterile PBS warmed to 37°C. Flasks were agitated to remove loosely adherent cells. The PBS containing the loosely adherent cells was removed from the flask and added to 10 ml of RPMI in 50 ml tubes and pelleted by centrifugation. The remaining adherent cells were incubated for a further 10 minutes (37°C, 5% CO_2) in 15 mls of EDTA. After incubation, the EDTA was pipetted up and down the base of the flasks, then collected and transferred to a 50 ml falcon containing 10 ml of cRPMI, followed by centrifugation (1350 rpm, 5 min). Pellets were then pooled, re-suspended in an appropriate volume of cRPMI, and the cells were counted. The cells were seeded at a concentration of 1 x 10^6 cells/ml in T175 flasks (15 ml/flask) in GM-CSF-supplemented (20 ng/ml) cRPMI. Two days later, 20 ml of GM-CSF (20 ng/ml) - supplemented cRPMI was added to flasks. On day 10 loosely adherent cells were harvested, counted, and plated in GM-CSF (10 ng/ml)-supplemented cRPMI in 96-well plates and rested overnight at 37°C in 5% CO_2 before use.

2.2.17 Stimulation of BMDCs with PAMPs and pathogens

BMDCs were seeded at 0.2 x 10^6 cells/well in flat-bottom 96-well plates and stimulated with LPS (100 ng/ml), sBp (5 µg/ml), heat-killed *S. aureus* (1 - 10 µg/ml), heat-killed *M. tuberculosis* (10 µg/ml), poly I:C (50 µg/ml), heat-killed *K. pneumoniae* (1 – 5 µg/ml) or medium alone for 24 hours at 37°C in 5% CO_2. Supernatants were harvested for quantification of cytokine concentrations by ELISA.

2.2.18 Co-culture of isolated $CD4^+$ T cells with BMDCs

BMDCs were seeded at 0.2 x 10^6 cells/well in round-bottom 96-well plates in a volume of 150 µl to permit space for addition of CD4 T cells. When blocking antibodies were used, BMDCs were pre-incubated with either anti-IL-12 p40 (10 µg/ml), anti-IL-1β (10 µg/ml), anti-IL-23 p19 (10 µg/ml), anti-MHC class II (2 µg/ml) or appropriate isotype control for 1 hour prior to the addition of T cells. Purified CD4+ T cells were added to each well (refer to figure legend for seeding densities) and stimulated with LPS (100 ng/ml), sBp (5 µg/ml), heat-killed *S. aureus* (10 µg/ml), heat-killed *M. tuberculosis* (10 µg/ml), poly I:C (50 µg/ml), heat-killed *K. pneumoniae* (1 – 5 µg/ml), or medium alone. Cells were cultured for 48 hours at 37°C in 5% CO_2 and supernatants were removed for quantification of cytokine concentrations by ELISA.

2.2.19 Adoptive transfer of nose- and lung-resident CD4 T cells

CD45.2 mice on a C57BL/6 background were infected with *B. pertussis* (1 x 10^9 CFU/ml) and left to clear the infection from the respiratory tract. On day 60 post infection (p.i.) mice were injected i.v. with a fluorochrome-conjugated anti-CD45 antibody and euthanised 10 min later. Tissue-resident (CD45 i.v.$^-$) $CD4^+CD3^+$ T cells were FACS purified from pooled nasal tissue and lungs (n=15 mice), as described previously. Isolated cells were washed x2 in sterile PBS, counted, and prepared at a ratio of 1:4 nose:lung CD4 T cells in sterile PBS. Naïve recipient CD45.1 mice on a C57BL/6 background were irradiated (4.5 Gy) 1 day before cell transfer using a Nordian Gammacell 3000 Elan irradiator. A total of 1 × 10^5 CD4 cells were transferred i.p. 1 day before infection with *B. pertussis* (1 x 10^8 CFU/ml).

2.2.20 LA4 cell culture

The LA4 cell line, derived from a murine lung adenoma, shows characteristics of type II pneumocytes and was obtained from the European Collection of Authenticated Cell Cultures (ECACC). LA4 cells were cultured in complete Ham's F-12 Nutrient Mix medium in T75 flasks at 37 °C in an atmosphere maintained at 95 % humidity and 5 % CO_2. Every fourth day, supernatants were gently removed and discarded from flasks and cells were washed twice with sterile PBS warmed to 37°C. Cells were then trypsinized by adding 10 ml of Trysin-EDTA Solution (Sigma) to adherent cells and incubating for 10 minutes at 37°C, 5 % CO_2. The reaction was stopped by adding an excess of culture medium and pipetted up and down the base of the flasks. Supernatants were collected and transferred into falcon tubes. Cells were pelleted by centrifugation (1350 rpm, 5 min). Cell pellets were combined and re-suspended in complete Ham's F-12 Nutrient Mix medium for counting. Cells were split 1:2 to 1:3, depending on confluency. For experiments, LA4 cells were plated at 0.25 x 10^6 cells/ml in 96 well flat-bottom tissue culture plates. Cells were left to adhere overnight prior to stimulation.

2.2.21 Cytokine Enzyme Linked Immunosorbent Assay (ELISA)

ELISA kits (R&D and BD Biosciences) were used for the quantitative analysis of various cytokines in cell culture supernatants, nasal washes, and lung homogenates. High-

binding certified 96-well micro-titre plates (Grenier Bio-one) were coated overnight at 4°C with 50 µl/well of capture antibody in PBS. Capture antibody was then removed and plates were washed three times in ELISA wash buffer. Non-specific binding was prevented by incubating plates with 150 µl/well of blocking buffer (1% BSA for R&D ELISA kits; 10% milk for BD Biosciences ELISA kits) for 2 hours at room temperature. Plates were then washed three times, followed by adding 50 µl/well of samples, either neat or diluted in 1% BSA, in in triplicate onto plates. Standards were prepared by serially diluting a specific top working standard in 1% BSA and added to the plate in triplicate. Each plate also contained three blank wells containing 1% BSA only. Plates were incubated overnight at 4°C. Samples were removed by washing plates three times with ELISA wash buffer, followed by adding 50 µl/well of biotinylated anti-mouse detection antibody diluted in 1% BSA and incubating for 1 hour (BD Biosciences ELISA kits) or 2 hours (R&D ELISA kits), both at room temperature. Plates were washed three times, and 50 µl/well of horseradish peroxidase (HPR)-conjugated streptavidin diluted in 1% BSA (1:1000) was added and plates were incubated for 20 minutes at room temperature in the dark. Plates were then washed five times and 50 µl/well of substrate solution (TMB) was added. When the standard curve had developed sufficiently the enzyme reaction was stopped by adding 25 µl/well of stop solution (1 M H_2SO_4). The absorbance was read at 450 nm on a Versamax Tunable Microplate Reader using SoftMax Pro software. Cytokine concentration in each unknown sample was determined by reference to the standard curve prepared using recombinant cytokine of a known concentration and following subtraction of the blank absorbance reading from each sample on the plate.

2.2.22 Antibody ELISA

Medium binding certified 96-well plates were coated 50 µl/well of sBP (1 µg/ml) and incubated overnight at 4°C. Plates were washed in wash buffer three times and non-specific binding was prevented by incubating plates with 150 µl/well of blocking buffer (1% BSA in PBS) for 2 hours at room temperature. Plates were washed in wash buffer three times and 50 µl of serum (diluted 1:50 for IgG2c or 1:20 for IgA), lung homogenates (diluted 1:20), or nasal wash (dilute 1:2) was added to the first column of wells on the 96 well plate. Samples were serially diluted 1:2 in 1% BSA across the plate to generate an 11-point titration curve and plates were incubated overnight at 4°C. Plates were washed four times in wash buffer, followed by addition of 50 µl/well of HRP-conjugated IgG2c or IgA diluted in 1% BSA and incubated for 2 hours at room temperature. Plates were then washed four times in wash buffer and developed by adding 50 µl/well of substrate

solution (TMB). When plates had developed sufficiently the reaction was stopped by adding 25 µl/well of stop solution (1 M H_2SO_4). The absorbance was read at 450 nm on a Versamax Tunable Microplate Reader using SoftMax Pro software.

2.2.23 Real-Time Quantitative Polymerase Chain Reaction (RT-qPCR)

Nasal tissue was excised and stored in RNAlater solution at -80°C until RNA extraction. Tissue was thawed and transferred to RNAse-free tubes containing 1 ml of Trizol and homogenising beads previously decontaminated in DEPC water. Tissue was lysed using a TissueLyserII (Qiagen). Once tissue was homogenised in Trizol, 200 µl of chloroform was added to each tube and shaken vigorously for 30 seconds. Tubes were rested at room temperature for 5 minutes, then centrifuged at 13,000 rpm for 15 min at 4°C. The top aqueous layer containing the RNA was carefully removed and transferred to a fresh RNAse-free tube and 500 µl of isopropanol was added to each sample. Samples were then mixed by inversion for 30 seconds and allowed to rest at room temperature for 10 minutes. Samples were then centrifuged at 13,000 rpm for 10 minutes at 4°C. The supernatants were carefully removed and 1 ml of 75% ethanol was added to each tube and vortexed. Samples were centrifuged at 8,000 rpm for 10 minutes at 4°C. Supernatants were entirely removed and pellet was left to dry for 15 minutes. Once all ethanol was evaporated, the RNA pellet was re-suspended in 30 µl of RNAse-free water. The RNA concentration in each sample was determined using a Nanodrop spectrophotometer (Applied Biosystems) and concentration was equalized across samples. The purified RNA was stored at -80°C until conversion to complementary DNA (cDNA).

RNA samples were reverse transcribed into cDNA using the Applied Bioscience High Capacity cDNA Reverse Transcription Kit according to manufacturer's instructions. The cDNA was then synthesized using a DNA Engine Dyad Cycler under the conditions indicated in Table 2.1. The cDNA reverse transcription product was then diluted 1:5 with RNAse-free water and stored at -80°C before further analysis.

Table 2.1 cDNA Reverse Transcription Cycle

	Temperature (°C)	Time (min)
Step 1	25	10
Step 2	37	120
Step 3	85	5
Step 4	4	∞

Real-time PCR for the detection of mRNA was performed using TaqMan Fast Universal Master Mix (Applied BioSystems) according to the manufacturer's instructions. Briefly, 4.5 µl of cDNA was mixed with 5.5 µl of master mix consisting of 4.5 µl master mix reagent, 0.5 µl reaction primers, and 0.5 µl endogenous primers. The RT-qPCR reaction was carried out on Applied Biosystem 7500 fast Real-Time PCR machine. The ΔΔCt method was used to calculate relative changes in gene expression which were normalised to 18S rRNA expression.

2.2.24 Statistical analysis

Statistical analysis was carried out using Graphpad Prism 9 software. Unpaired two-tailed Student's t-test was used to compare the statistical difference between the mean values of two groups. One-way or two-way analysis of variance (ANOVA) test followed by Dunnett's (to compare every mean to a control mean), Sidak's (to compare selected pairs of means), or Tukey's (to compare every mean to every other mean) honestly significant difference (HSD) post-hoc test was used to determine the statistical difference between more than two groups. Error bars indicate the mean ± standard error of the mean (SEM) or standard deviation (SD) as indicated in individual figure legends. *P* values equal to or less than 0.05 were considered statistically significant.

2.3 Flow cytometry gating strategies

2.3.1 IL-17A$^+$ and IFNγ$^+$ CD4 T_{RM} cells

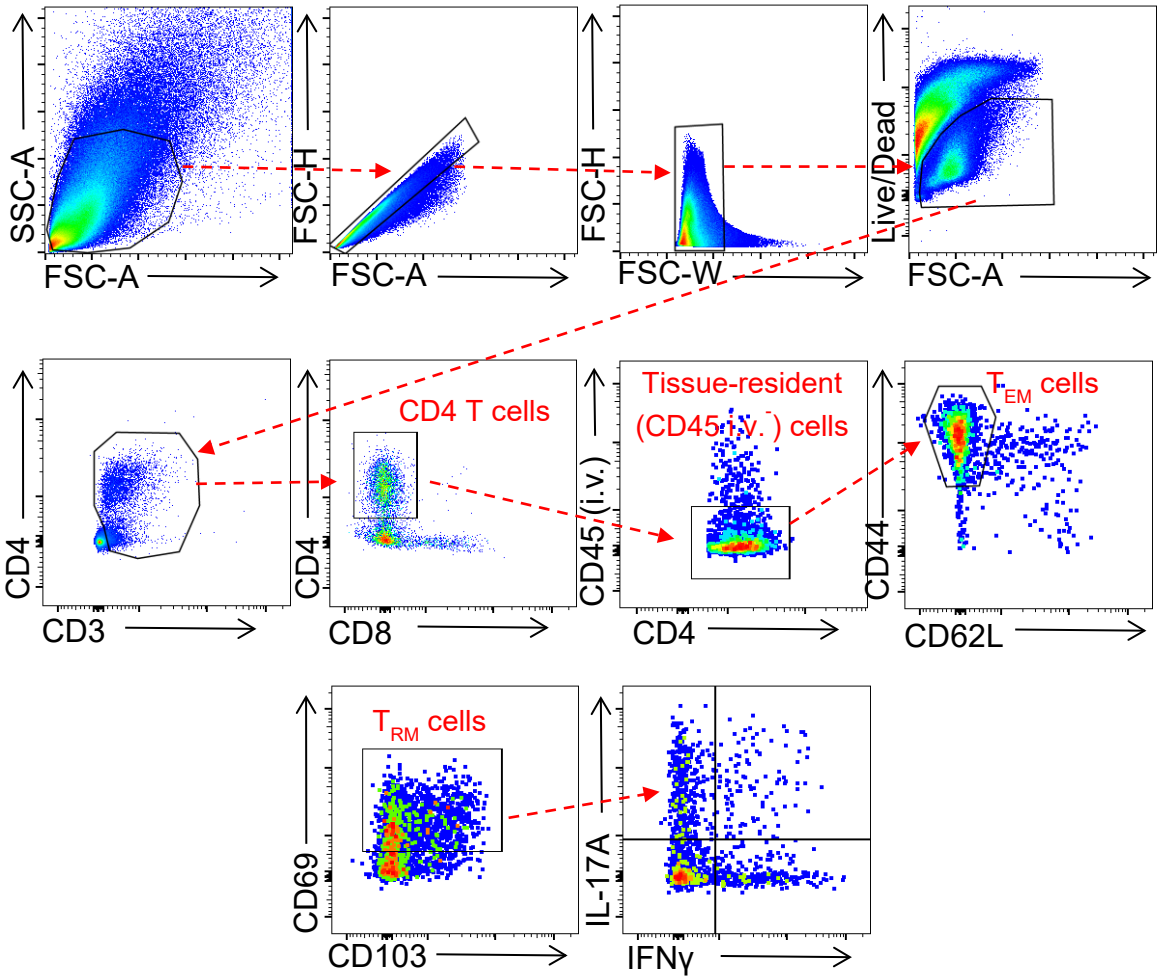

2.3.2 Total neutrophils, infiltrated (CD45 i.v.$^-$) Siglec-F$^+$ and Siglec-F$^-$ neutrophils, and infiltrated MHCII$^+$Ly6C$^+$CD11b$^+$ monocytes in the nasal tissue

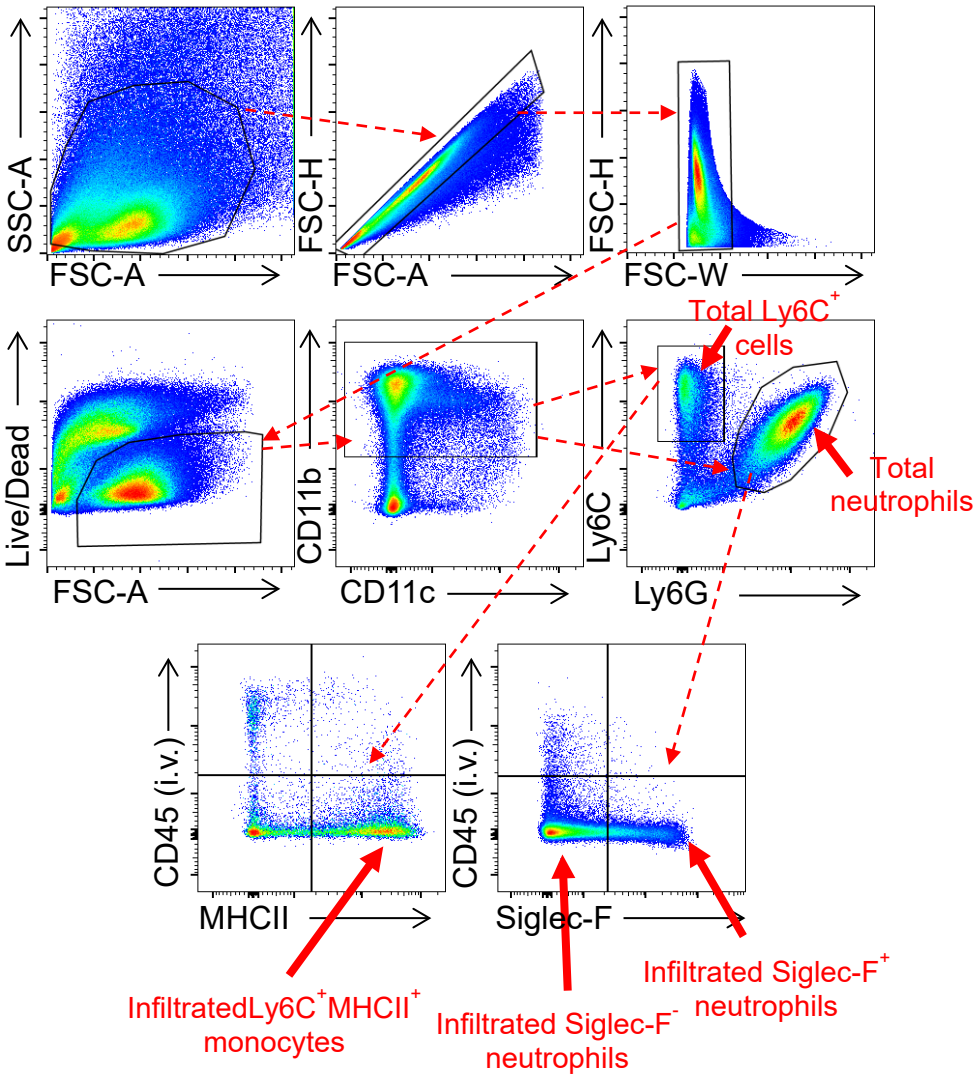

2.3.4 Alveolar macrophages, Ly6C$^+$CD11b$^+$ monocytes, and total and tissue-infiltrated (CD45 i.v.$^-$) neutrophils in the lungs

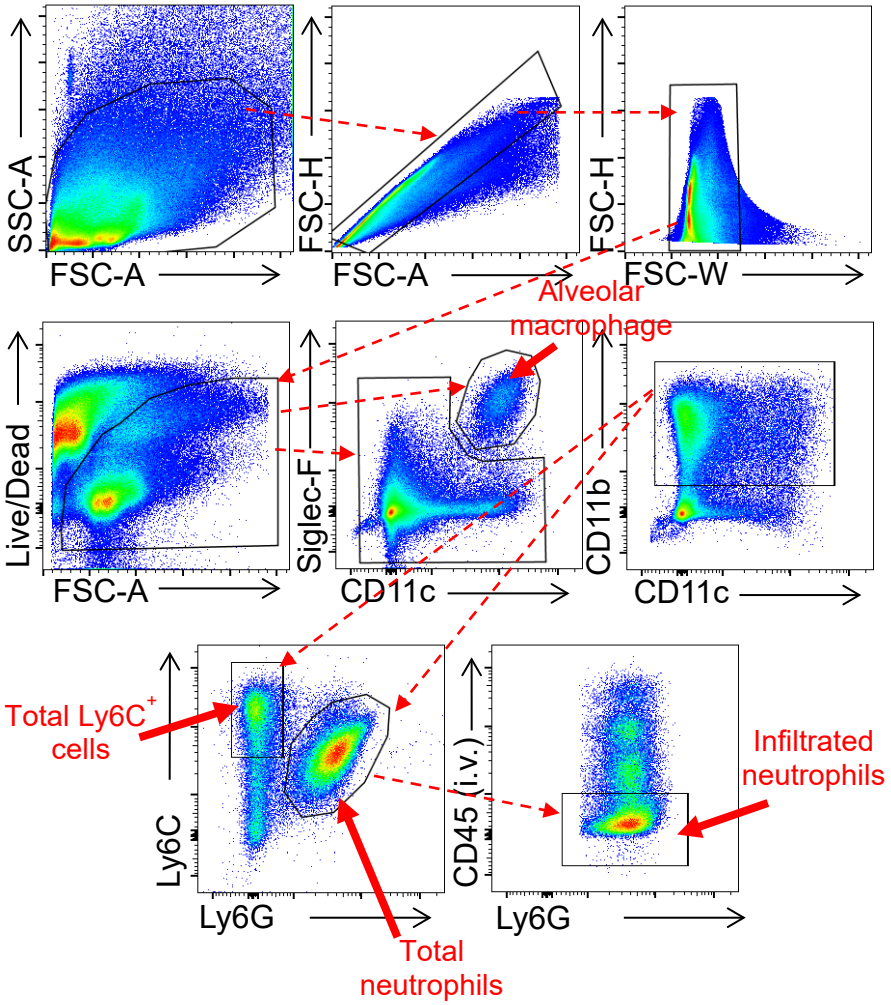

Chapter 3: IL-17-producing CD4 T_{RM} cells mediate protective immunity against *B. pertussis* in the nasal cavity by mobilising Siglec-F^+ neutrophils

3.1 Introduction

Whooping cough, also known as pertussis, is a highly contagious acute respiratory disease caused by the Gram-negative bacterium *B. pertussis* [3]. Despite the routine use of vaccines, incidence of whooping cough has been rising slowly since the 1970s, and accelerating sharply since the introduction of aP vaccines in the 1990s [298]. The potential cause for this increase is multifactorial, including improved detection methodology and the evolution of circulating *B. pertussis* strains to evade vaccine-induced immunity. However, there is emerging evidence that a major contributing factor to increased pertussis incidence is the failure of current aP vaccines to induce sterilising mucosal immunity in the nasal cavity [4]. In order for next generation pertussis vaccines to be effective, they must generate sterilising immunity in the nasal cavity. This highlights the need to better understand the mechanisms of protective mucosal immunity in the upper respiratory tract.

Mucosal immunity can be defined as any process that leads to a protective immune response on a mucosal surface, even if the origin of that response may not reside locally within the mucosa itself [298]. *B. pertussis* is mainly an upper respiratory tract pathogen, with dissemination outside of the respiratory tract almost unheard of in humans [299]. The immune response to *B. pertussis* in the lungs has been well characterised using murine models. During infection with *B. pertussis* innate immune cells, such as neutrophils, monocytes, and $CD11c^{+}CD8\alpha^{+}$ DCs, infiltrate the lungs [122, 146]. Innate-like lymphoid cells, such as γδ T cells and NK cells, also expand in the lungs [227, 229]. The adaptive immune response to *B. pertussis* is predominantly mediated by CD4 helper T cells [110], with Th1- and Th17-associated cytokines, especially IFNγ and IL-17A, shown to play a critical role in the induction of a protective immune response in the lower respiratory tract [146, 148].

It has been shown that a type of memory CD4 T cell, termed T_{RM} cells, remain for extended periods within the lungs once *B. pertussis* infection has cleared [216]. Unlike T_{CM} and T_{EM} cells, which recirculate through lymphoid tissue or non-lymphoid tissue, respectively [300], T_{RM} cells persist in peripheral tissues and do not re-enter the circulation. T_{RM} cells are abundant in many non-lymphoid tissues such as the lung and skin, where they can survey the local environment and rapidly respond upon re-exposure to a pathogen and mediate a protective and localised immune response [301]. CD4 T_{RM} cells can be identified by surface expression of CD69 and CD44, which is also a defining marker for T_{EM} cells [206, 300]. CD103 is a relatively robust marker for identification of CD8 T_{RM} cells, but it is less uniformly expressed on CD4 T_{RM} cells [302]. The Mills' lab

have demonstrated that CD4 T_{RM} cells accumulate in the lungs following infection with *B. pertussis*. IL-17A-producing CD4 T_{RM} cells were shown to expand rapidly following re-infection with *B. pertussis*, and this was associated with rapid clearance of bacteria from the lungs [216].

IL-17A is the signature cytokine of Th17 cells, a subset of CD4 helper T cells which are characterised by expression of the master transcription factor RORγT [303]. IL-17A has been shown to mediate protective immunity in the nasal cavity against *S. aureus* and *Streptococcus pneumoniae* by enhancing neutrophil recruitment to the nasal mucosa and promoting AMP production within the nasal tissue [304, 305]. Furthermore, IL-17A has been shown to play a role in protection against *B. pertussis* in the lungs [146], however its role in protective immunity against *B. pertussis* in the nasal cavity has not been fully characterised.

Given the emerging evidence that the resurgence in pertussis may be due to the inability of current aP vaccines to induce sterilising mucosal immunity in the nasal cavity, there is increased interest in uncovering the mechanism of protective immunity in the upper respiratory tract. The upper respiratory tract has often been overlooked, thus the immune response to *B. pertussis* in the nasal cavity is not fully understood. Wilk et al. demonstrated that immunisation with a wP vaccine or previous infection with *B. pertussis* induced long-lived IL-17A-producing CD4 T_{RM} cells in the nasal tissue of mice, and this correlated with enhanced protection against *B. pertussis* in the nasal cavity. Conversely, the aP vaccine failed to protect against nasal colonisation with *B. pertussis* and this was associated with the failure to induce CD4 T_{RM} cells in the nasal mucosa [194]. Studies in non-human primate models mirrored these findings, and demonstrated that aP-immunised baboons had significantly delayed bacterial clearance in the nasal cavity following *B. pertussis* challenge. In contrast, previous infection with *B. pertussis* or immunisation with a wP vaccine conferred significant protection against *B. pertussis* infection in the nasal cavity, and protection was associated with mucosal and systemic IL-17A responses [28, 176, 306]. Together, these results highlight a role of CD4 T_{RM} cells and IL-17A in protective immunity against *B. pertussis* in the nasal cavity. However, the mechanisms by which CD4 T cells and IL-17A mediate these protective effects in the nasal tissue have yet to be fully elucidated.

The objective of this chapter was to characterise the immune response in the nasal cavity during a primary infection with *B. pertussis*, and compare it to what is already known about the protective immune response in the lungs. Using a murine aerosol challenge model of live *B. pertussis*, both the innate and adaptive immune response were

examined in the nose. As previous studies have demonstrated that CD4 T_{RM} cells and IL-17A are associated with enhanced clearance of *B. pertussis* from the upper respiratory tract, the goal of this study was to uncover the mechanism by which this is achieved. Uncovering the mechanisms of protective immunity in the upper respiratory tract could contribute in the development of next-generation pertussis vaccines that can elicit sterilising immunity in the nasal cavity.

3.2 Results

3.2.1 The innate immune response to B. pertussis differs between the lungs and nasal cavity.

In order to examine the innate immune response to *B. pertussis* in the upper and lower respiratory tract, C57BL/6 mice were aerosol challenged with *B. pertussis* and multi-colour flow cytometry was used to identify innate immune cell populations in both the nasal tissue and lungs at various time points post infection. In order to quantify tissue-resident cells using flow cytometry, a validated i.v. labelling approach was used [203], where mice are injected i.v. with fluorochrome-conjugated anti-CD45 antibody 10 min before euthanasia. Circulating cells become labelled with the antibody (CD45 i.v.$^{+}$), whereas the antibody cannot penetrate the tissue, therefore immune cells within the tissue remain unstained (CD45i.v.$^{-}$). In the lungs, the absolute number of alveolar macrophages (Siglec-F^{+}CD11c^{+}) decreased until day 7 post challenge, and expanded from day 14 onwards (Figure 3.1 *A, B*). Furthermore, the absolute number of alveolar macrophages expressing MHC II significantly increased on day 14 and day 21 post challenge (Figure 3.1 *C*). This was accompanied by an early burst in IL-1β production in the lung homogenates 2 hours post *B. pertussis* infection, with a secondary increase from day 7 post challenge, and peaking on day 14 (Figure 3.1 *D*). There was a similar significant increase in IL-17A production in the lung homogenates on day 7 and day 14 post challenge (Figure 3.1 *E*).

Conventional neutrophils, defined by Ly6G and CD11b expression, infiltrated (CD45 i.v.$^{-}$) the lungs and nose from day 7 post *B. pertussis* challenge (Figure 3.2 *A, B*). Interestingly, recruitment of a novel neutrophil population, defined by surface expression of Sialic acid-binding, Ig-like lectin (Siglec-F), was observed in the nasal cavity on day 14 and 21 post infection, with only minor numbers of these cells detected in the lungs (Figure 3.2 *C*). A population of MHCII^{+}Ly6C^{+}CD11b^{+} monocytes infiltrated (CD45 i.v.$^{-}$) both the lungs and nasal cavity during *B. pertussis* infection, peaking in the lungs on day 7 and in the nasal cavity on day 14 post challenge (Figure 3.2 *D, E*). These data demonstrate that the innate immune response to *B. pertussis* infection differs between the upper and lower respiratory tract, with distinct cell populations and kinetics observed in the nasal cavity and lungs.

3.2.2 Siglec-F$^+$ neutrophils expand in the nasal tissue during B. pertussis infection, and exhibit an activated phenotype and high NET activity.

Assessment of the NALT, spleen, bone marrow, lungs and nasal tissue of mice revealed that the frequency of Siglec-F$^+$ neutrophils was significantly higher in the nasal tissue compared with the other tissues examined on day 20 days post *B. pertussis* challenge. A minor population of Siglec-F$^+$ neutrophils was detected in the lungs, whereas no Siglec-F$^+$ neutrophils were detected in the NALT, spleen, or bone marrow. In contrast, conventional Siglec-F$^-$ neutrophils were found in the bone marrow, lungs, spleen, and nasal tissue of naïve mice and mice infected with *B. pertussis* (Figure 3.3 *A*-*C*). ImageStream analysis of nasal mononuclear cells harvested from mice on day 13 post *B. pertussis* challenge confirmed co-expression of the surface markers Siglec-F and Ly6G on a population of CD11b$^+$ cells (Figure 3.3 *D*).

Analysis of neutrophil activation markers revealed that surface expression of the chemokine receptor CXCR2, as well as surface markers CD11c and CD49d, was enhanced on Siglec-F$^+$ compared with Siglec-F$^-$ neutrophils in the nasal tissue of naïve mice and mice 20 days post *B. pertussis* challenge. In contrast, expression of CD44 and CD62L was lower on Siglec-F$^+$ neutrophils in the nasal tissue of naïve mice, with no significant difference in surface expression of CD44 or CD62L detected 20 days post challenge (Figure 3.4 *A, B*).

NETosis is a major mechanism by which neutrophils entrap extracellular bacteria. To compare NET activity in Siglec-F$^+$ and Siglec-F$^-$ neutrophils, isolated mononuclear cells from the nasal tissue of mice up to one month post *B. pertussis* challenge were stimulated with heat-killed *B. pertussis*, PMA, or medium only for 4 hours. Cells were then stained with the intracellular DNA dye, DAPI, and the cell-impermeable DNA dye, SYTOXgreen. Cells undergoing NETosis were identified as being double positive for DAPI and SYTOXgreen. Siglec-F$^+$ neutrophils had a higher frequency of NETosis$^+$ cells compared with conventional Siglec-F$^-$ neutrophils following stimulation with heat-killed *B. pertussis* or PMA (Figure 3.5 *A, B*).

Gene expression for *Il1*β was significantly higher in Siglec-F$^+$ compared with Siglec-F$^-$ neutrophils isolated from the nasal tissue of naïve mice, however no significant difference was seen post *B. pertussis* challenge. Furthermore, Siglec-F$^+$ neutrophils isolated from the nasal tissue of naïve mice or mice infected with *B. pertussis* had significantly less mRNA expression of *Lcn2* and *S100a8* compared with Siglec-F$^-$ neutrophils (Figure 3.5 *C*).

3.2.3 IL-17A-producing CD4 T_{RM} cells accumulate in the nasal cavity and lungs during B. pertussis infection.

As neutrophil recruitment is enhanced by T cell-derived cytokines, such as IL-17A [307], the accumulation of T cells in the nasal cavity and lungs, and their pathogen-specific cytokine production, was assessed over the course of *B. pertussis* infection. Infection of mice with *B. pertussis* was accompanied by the infiltration of a population of CD4 T cells into the nasal tissue (Figure 3.6 *A, B*) and lungs (Figure 3.7 *A, B*) which exhibit a T_{RM} phenotype ($CD4^+CD3^+CD45$ i.v.$^-CD44^+CD62L^-CD69^+CD103^{\pm}$), and produced IL-17A, IFNγ, and TNF in response to *ex vivo* stimulation with sonicated *B. pertussis* (sBP) and anti-CD28 and anti-CD49d, indicating that these T_{RM} cells are pathogen-specific. In the nasal cavity, there was a significant increase in absolute number of IL-$17A^+$ CD4 T_{RM} cells on day 28 post challenge, with IL-17A-producing CD4 T_{RM} cells detected in the nasal cavity up to 100 days post challenge. In contrast, only a small population of pathogen-specific IFNγ-producing CD4 T_{RM} cells were detected in the nasal cavity throughout the course of infection (Figure 3.6 *A, B*). SPICE analysis confirmed that IL-17A is the predominant cytokine produced by CD4 T_{RM} cells in the nasal cavity during *B. pertussis* infection, with minor populations producing IFNγ and TNF or combinations of these cytokines in response to stimulation with sBP (Figure 3.6 *C*).

IL-$17A^+$ CD4 T_{RM} cells also accumulated in the lungs over the course of *B. pertussis* infection, with significant increases seen on day 14 and day 28 post challenge, and a moderate population of IL-$17A^+$ CD4 T_{RM} cells detected in the lungs up to 100 days post challenge. In contrast, no significant increase in $IFN\gamma^+$ CD4 T_{RM} cells is seen in the lungs (Figure 3.7 *A, B*). SPICE analysis of lung CD4 T_{RM} cells revealed a comparable phenotype to CD4 T_{RM} cells seen in the nasal cavity, with IL-17A being the predominant cytokine produced by lung CD4 T_{RM} cells, with minor populations producing IFNγ or TNF, or combinations of two or three of the aforementioned cytokines (Figure 3.7 *C*). These results demonstrate that *B. pertussis*-specific CD4 T cells with a T_{RM} phenotype accumulate and persist in both the nasal cavity and lung during *B. pertussis* infection, and display a predominantly Th17 phenotype.

3.2.4 IL-17A$^{-/-}$ mice have significantly delayed clearance of B. pertussis from the nasal cavity and this is accompanied by reduced infiltration of Siglec-F^{+} neutrophils into the nasal tissue.

Having shown that IL-17A was the predominant cytokine produced by *B. pertussis*-specific nose and lung CD4 T_{RM} cells, the role of IL-17A in protective immunity against *B. pertussis* in the nasal cavity and lungs was examined by infecting IL-17A$^{-/-}$ and WT mice with *B. pertussis* and monitoring the course of infection. Significantly higher CFU counts were detected in the nasal washes of IL-17A$^{-/-}$ compared with WT mice up to day 35 post challenge, with IL-17A$^{-/-}$ mice failing to clear *B. pertussis* completely from the nasal cavity by day 60 post challenge (Figure 3.8 *A*). In contrast, only moderately higher CFU counts were detected in the lungs of IL-17A$^{-/-}$ compared with WT mice over the course of infection (Figure 3.8 *B).* These results were confirmed in co-housed WT and IL-17A$^{-/-}$ mice, with significantly higher CFU counts detected in the nasal washes and lungs of IL-17A$^{-/-}$ mice on day 28 post *B. pertussis* infection, with this delay most dramatic in the nasal mucosa (Figure 3.9 *A, B*). These results demonstrate that IL-17A plays an essential role in protective immunity against *B. pertussis* infection in the nasal cavity.

Analysis of the CD4 T cell response revealed that IL-17A$^{-/-}$ mice had enhanced numbers of CD4 T_{RM} cells in the nasal cavity and lungs compared with WT mice over the course of infection (Figure 3.10 *A*-*D*). In the absence of IL-17A, increased numbers of *B. pertussis*-specific IFNγ^{+} CD4 T_{RM} cells were observed in the nasal tissue and lungs of IL-17A$^{-/-}$ mice, with a significant increase seen on day 28 post challenge in both tissues (Figure 3.11 *A*-*C*). These results demonstrate that in the absence of IL-17A, nasal and lung CD4 T_{RM} cells induced during *B. pertussis* infection exhibit a predominant Th1 phenotype.

As IL-17A is involved in antibody class switching and secretion at mucosal surfaces [286, 308], *B. pertussis*-specific IgA and IgG2c was quantified in the nasal washes, lung homogenates, and blood sera of WT and IL-17A$^{-/-}$ mice on the day of and 35 days post *B. pertussis* challenge. The results showed that IL-17A$^{-/-}$ mice had significantly higher *B. pertussis*-specific IgA (Figure 3.12 *A*) and IgG2c (Figure 3.12 *B*) in the nasal washes, lung homogenates, and sera, suggesting that IL-17A does not confer its protective effects against *B. pertussis* infection by promoting antibody production.

To investigate if IL-17A confers its protective effects by promoting AMP, cytokine, or chemokine production, nasal tissue was harvested from WT and IL-17A$^{-/-}$ mice over the course of *B. pertussis* infection and RNA was extracted for analysis by RT-qPCR. IL-17A$^{-/-}$ mice exhibited reduced mRNA expression of *Cxcl1* and *Il1β* 2 hours post *B.*

pertussis challenge. No significant difference in mRNA expression of *Csf3*, *Lcn2*, or *Pigr* was observed between WT and IL-17A$^{-/-}$ mice post *B. pertussis* challenge. In contrast, *Nos2* mRNA expression was significantly enhanced in IL-17A$^{-/-}$ compared with WT mice on day 17 post challenge (Figure 3.13).

An examination of innate cell recruitment in the absence of IL-17A revealed no significant difference between WT and IL-17A$^{-/-}$ mice in the infiltration (CD45 i.v.$^{-}$) of conventional Siglec-F^{-} neutrophils into the nasal tissue post *B. pertussis* challenge (Figure 3.14 *A*, *C*). In contrast, there was a significant reduction in the infiltration (CD45 i.v.$^{+}$) of Siglec-F^{+} neutrophils into the nasal cavity of IL-17A$^{-/-}$ mice on days 7, 21, 28 and 60 post challenge (Figure 3.14 *B*). Furthermore, there was a significant enhancement in the infiltration of inflammatory MHCII^{+}Ly6C^{+}CD11b^{+} monocytes into the nasal cavity IL-17A$^{-/-}$ mice on days 21, 28, and 35 post challenge (Figure 3.14 *D, E*). An examination of the lungs revealed that IL-17A$^{-/-}$ mice had enhanced numbers of total neutrophils on day 28 post challenge and increased lung-infiltrated (CD45 i.v.$^{-}$) neutrophils on days 21 and 28 post challenge (Figure 3.15 *A*-*C*). In contrast, there were reduced numbers of alveolar macrophages in the lungs of IL-17A$^{-/-}$ compared with WT mice, with a significant reduction seen on day 28 post challenge (Figure 3.15 *D, E*). The results suggest that IL-17A exerts its protective effects in the nasal cavity by promoting chemokine production and subsequent recruitment of Siglec-F^{+} neutrophils to the nasal mucosa.

3.2.5 IL-17A directly induces chemokine production in vitro and in vivo.

As impaired CXCL1 expression was observed in IL-17A$^{-/-}$ mice during *B. pertussis* infection, it was next investigated if IL-17A can directly induce chemokine production both *in vitro* and *in vivo*. IL-17A, and to a lesser extent IL-17F, synergised with TNF to induce CXCL1, MIP2, and LCN2 production from LA4 cells, a murine lung epithelial cell line, in the presence and absence of sBP (Figure 3.16). Furthermore, i.n. administration of recombinant murine IL-17A to mice induced a significant upregulation of *Cxcl1* mRNA expression in the nasal tissue, and significantly increased CXCL1 protein levels the nasal wash and lung homogenates within 2 hours (Figure 3.17 *A*-*C*). These results demonstrate that IL-17A induces CXCL1 production *in vitro* and *in vivo.*

3.2.6 Continuous FTY720 treatment during a primary B. pertussis infection significantly delays bacterial clearance in the lungs, but only moderately delays clearance in the nasal cavity.

In order to assess the relative contribution of circulating versus tissue-resident CD4 T cells in protective immunity against *B. pertussis* infection in the nasal cavity, mice were treated with FTY720, which inhibits lymphocyte egression from secondary lymphoid organs [309], 10 days prior to and throughout the course of *B. pertussis* infection. Control mice received normal drinking water. Congruent with previously published data [216], continuous administration of FTY720 over the course of infection with *B. pertussis* significantly impaired bacterial clearance from the lungs. In contrast, only moderately higher CFU counts were observed in the nasal washes of mice treated with FTY720 compared with untreated control mice (Figure 3.18 *A, B*).

The efficacy of FTY720 treatment was investigated by assessing lymphocyte egression from cLNs. Continuous treatment of mice with FYT720 significantly reduced the absolute number of circulating (CD45 i.v.$^+$) and resident (CD45 i.v.$^-$) CD4 T cells in the cLNs throughout the course of *B. pertussis* infection (Figure 3.19 *A*). Furthermore, treatment of mice with FTY720 significantly reduced the absolute number of circulating and resident CD8 T cells, and circulating B220$^+$ cells in the cLNs post *B. pertussis* challenge (Figure 3.19 *B, C*).

FTY720 treatment had a moderate effect on reducing the number of circulating CD4 T cells in the nasal cavity (Figure 3.20 *A*). However, there was no significant difference in the number of nose-resident CD4 T cells in mice treated with FTY720 compared with untreated control mice (Figure 3.20 *B, C*). Furthermore, nose-resident CD4 T cells acquired a T_{RM} phenotype (CD4$^+$CD3$^+$CD45i.v.$^-$CD44$^+$CD62L$^-$CD69$^+$CD103$^{+/-}$) and expanded following *B. pertussis* challenge despite continuous FTY720 treatment (Figure 3.20 *D, E*). Treatment of mice with FTY720 resulted in a moderate reduction in the number of *B. pertussis*-specific IL-17A$^+$ CD4 T_{RM} cells in the nasal cavity, with a significant reduction compared with the untreated control mice observed on day 28 post challenge (Figure 3.21 *A, C*).

FTY720 treatment had a more striking effect in the lungs of mice, significantly reducing the number of circulating CD4 T cells in the lungs up to day 56 post *B. pertussis* challenge (Figure 3.22 *A*). Furthermore, FTY720 treatment significantly reduced the number of circulating CD8 T cells and B220$^+$ cells in the lungs (Figure 3.22 *B, C*). Despite continuous FTY720 treatment, the persisting CD4 T cells in the lungs acquired a T_{RM} phenotype and expanded at a similar rate to those in the untreated control mice (Figure

3.23 *A, B*). However, there was a significant reduction in the absolute number of *B. pertussis*-specific IL-17A$^+$ CD4 T_{RM} cells in the lungs of mice treated with FTY720 on days 21 and 28 post *B. pertussis* challenge (Figure 3.23 *C-E*). Taken together, these results suggest that nasal CD4 T_{RM} cells arise locally within the nasal cavity during *B. pertussis* infection with minimal contribution from circulating CD4 T cells.

3.2.7 CD4 T cells mediate protective immunity in the nasal cavity and lungs during B. pertussis infection.

The results so far have demonstrated that circulating CD4 T cells minimally contribute to protective immunity against *B. pertussis* in the nasal cavity. In order to investigate the relative contribution of resident CD4 T cells in protective immunity against *B. pertussis* in the upper and lower respiratory tract, an antibody-based strategy was used to deplete CD4 T cells from day 7 post *B. pertussis* challenge. Mice treated with a depleting anti-CD4 antibody had significantly higher CFU counts in both the nasal cavity and lungs compared with mice treated with the isotype control antibody on days 14 and 21 post *B. pertussis* challenge, indicating that resident CD4 T cells play an important role in protective immunity against *B. pertussis* in both tissues (Figure 3.24 *A, B*). Treatment of mice with an anti-CD4 antibody effectively depleted total CD4 T cells in the nasal cavity (Figure 3.25 *A, D*), lungs (Figure 3.26 *A, D*), and cLNs (Figure 3.27 *A, D*). Furthermore, antibody-mediated depletion of CD4 T cells was accompanied by increased CD8 T cells in the nasal cavity (Figure 3.25 *B*), lungs (Figure 3.26 *B*), and cLNs (Figure 3.27 *B*). Depletion of CD4 T cells had no effect on the number of B220$^+$ cells, which is a marker for mature B cells, in the nasal cavity (Figure 3.25 *C*) or cLNs (Figure 3.27 *C*). In contrast, there was significant reduction in the number of B220$^+$ cells in the lungs of mice treated with a depleting anti-CD4 antibody compared with mice treated with the isotype control antibody (Figure 3.26 *C*).

Expansion of total CD4 T_{RM} cells, and RORγT$^+$ and Foxp3$^+$ CD4 T_{RM} cells, in the nasal cavity of mice treated with the isotype control antibody following *B. pertussis* challenge was significantly reduced in mice treated with a depleting anti-CD4 antibody (Figure 3.28 *A-E*). Furthermore, IL-17A-producing CD4 T_{RM} cells were reduced to background in the nasal tissue of anti-CD4 treated mice on days 14 and 21 post challenge (Figure 3.29 *A, B*). The expansion of total CD4 T_{RM} cells and IL-17A$^+$ CD4 T_{RM} cells observed in the lungs of mice treated with the isotype control antibody following *B. pertussis* challenge

was also significantly reduced in mice treated with an anti-CD4 antibody (Figure 3.30 *A-D*).

Given that IL-17A production is not exclusive to CD4 T cells, the number of total live IL-17A-producing cells and the cellular composition of this population was investigated following antibody-mediated depletion of CD4 T cells during *B. pertussis* infection. Treatment of mice with a depleting anti-CD4 antibody significantly reduced the number of total live IL-17A-producing cells in the nasal cavity and lungs, but not in the cLNs, post *B. pertussis* challenge. CD4 T cells were the dominant source of IL-17A from day 14 post challenge in the nasal tissue, lungs, and cLNs of mice treated with the isotype control antibody. Following treatment of mice with a depleting anti-CD4 antibody, CD8 T cells and other un-identified $CD4^{-}CD8^{-}\gamma\delta^{-}$ cells were major sources of IL-17A in the nasal tissue, lungs, and cLNs (Figure 3.31 *A-C*).

In order to examine if CD4 T cells contribute to humoral responses in the respiratory tract, *B. pertussis*-specific IgA and IgG2c was quantified in in the nasal washes and lung homogenates of naïve mice and mice infected with *B. pertussis* (21 days p.i.) treated with an anti-CD4 antibody or an isotype control antibody. No significant difference in *B. pertussis*-specific IgA or IgG2c was detected in the nasal washes between mice treated with a depleting anti-CD4 antibody and those treated with the isotype control antibody (Figure 3.32 *A*). However, there was a significant reduction in *B. pertussis*-specific IgA and IgG2c in the lung homogenates of anti-CD4 treated mice treated on day 21 post challenge (Figure 3.32 *B*). These results suggest that CD4 T cells are involved in generating effective antibody responses in the lung during a primary infection with *B. pertussis*.

The effect of anti-CD4 treatment on the recruitment of innate immune cells to the respiratory tract during *B. pertussis* challenge was next investigated. Mice treated with a depleting anti-CD4 antibody had significantly reduced numbers of tissue-infiltrated (CD45 i.v.$^{-}$) Siglec-F^{+} neutrophils, conventional Siglec-F^{-} neutrophils, and $MHCII^{+}Ly6C^{+}$ monocytes in the nasal tissue compared with mice treated with the isotype control antibody on day 14 post challenge (Figure 3.33 *A-E*). In the lungs, anti-CD4 treated mice exhibited a significant increase in the number of total neutrophils and lung-infiltrated (CD45 i.v.$^{-}$) neutrophils on day 21 post challenge (Figure 3.34 *A-C*). In contrast, treatment of mice with a depleting anti-CD4 antibody significantly reduced the infiltration of $MHCII^{+}Ly6C^{+}$ monocytes into the lungs on day 14 post challenge and reduced the number of alveolar macrophages on day 14 and 21 post *B. pertussis* challenge (Figure 3.35 *A-D*). Combined, these results demonstrate that resident CD4 T cells contribute to

protective immunity against *B. pertussis* by promoting Siglec-F$^+$ neutrophil recruitment to the nasal cavity and alveolar macrophage expansion and antibody production in the lungs.

3.2.8 Treatment with a depleting anti-Ly6G antibody from the onset of B. pertussis infection significantly delays clearance of bacteria from the nasal cavity.

The results so far suggest that resident CD4 T cells mediate protective immunity in the nasal cavity by producing IL-17A which promotes the recruitment of Siglec-F$^+$ neutrophils to the nasal mucosa. To clarify the role of neutrophils in protective immunity against *B. pertussis* in the nasal cavity, a double antibody-based depletion strategy developed by Boivin and colleagues [294] was employed. Mice were injected with a depleting anti-Ly6G antibody or a corresponding isotype control antibody one day before *B. pertussis* infection, and every day post challenge. Every alternative day, mice were injected with a secondary antibody specific for the rat kappa immunoglobulin. The administration of a secondary antibody results in an isotype switch, changing the anti-Ly6G antibody from a rat IgG2a isotype, which mediates neutrophil depletion through Fc-dependent macrophage opsonisation, to an IgG2b isotype, which mediates neutrophil depletion through the more effective complement pathway. Significantly higher CFU counts were detected in the nasal wash of the mice treated with an anti-Ly6G antibody compared with mice treated with the isotype control antibody on day 14 post challenge (Figure 3.36 *A*). In contrast, anti-Ly6G treatment had no significant effect on clearance of *B. pertussis* from the lungs (Figure 3.36 *B*).

As antigen masking can be an issue in assessing the efficacy of antibody-mediated cell depletion strategies, where the antibody used *in vivo* will prevent the binding of a fluorochrome-labelled antibody used to identify the cell by targeting the same epitope *ex vivo*, a double-staining technique for Ly6G was employed. As Ly6G can be expressed on the cell surface and intracellularly, surface and intracellular Ly6G were sequentially stained using differently labelled fluorochrome-conjugated antibodies [294]. Neutrophils were identified based on intracellular expression of Ly6G. Administration of a depleting anti-Ly6G antibody significantly reduced the absolute number of total neutrophils, as well as Siglec-F$^+$ neutrophils, in the nasal cavity on day 14 post *B. pertussis* challenge, with Siglec-F$^+$ neutrophils appearing to be more susceptible to this depletion strategy (Figure 3.37 *A*-*D*). A similar trend was also seen in the lungs, with absolute number of total neutrophils and Siglec-F$^+$ neutrophils significantly reduced in the mice treated with an anti-Ly6G antibody compared with mice treated with the isotype control antibody on day 14 post challenge (Figure 3.38 *A*-*C*). Interestingly, the numbers of alveolar macrophages

were also reduced in the lungs of mice treated with an anti-Ly6G antibody on day 14 post challenge (Figure 3.38 *D*).

Neutrophils are a source of source of Th17-polarising cytokines such as IL-1β and IL-23 [65], however, treatment of mice with a depleting anti-Ly6G antibody had no effect on the expansion of IL-17A-producing CD4 T_{RM} cells in the nasal tissue or in the lungs post *B. pertussis* challenge. In contrast, there was a significant increase in the number of IFNγ$^+$ CD4 T_{RM} cells in the nasal tissue and lungs of mice treated with anti-Ly6G antibody on day 14 post challenge (Figure 3.39 *A*-*C*).

3.2.9 Administration of an anti-Ly6G antibody from day 7 of B. pertussis infection significantly delays clearance of B. pertussis from both the nasal cavity and lungs.

The effect of depleting neutrophils in the later stages of *B. pertussis* challenge was next investigated by commencing antibody-mediated neutrophil depletion on day 7 post *B. pertussis* challenge. There was a significant increase in CFU counts in the nasal wash and lungs in mice treated with an anti-Ly6G antibody compared with the mice treated with the isotype control antibody on day 21 post challenge (Figure 3.40 *A, B*). Commencement of the anti-Ly6G depletion treatment on day 7 post challenge was sufficient to reduce the absolute number of total neutrophils and Siglec-F$^+$ neutrophils in the nasal cavity, with a more sustained depletion observed for Siglec-F$^+$ neutrophils (Figure 3.41 *A*-*D*). A significant reduction in total neutrophils and Siglec-F$^+$ neutrophils was also seen in the lungs of mice treated with an anti-Ly6G antibody (Figure 3.42 *A*-*C*). A moderate reduction in alveolar macrophages was also observed in the lungs of mice treated with a depleting anti-Ly6G antibody on day 21 post challenge (Figure 3.42 *D*). Administration of a depleting anti-Ly6G antibody from day 7 of *B. pertussis* infection had no significant effect on the absolute number of IL-17A$^+$ or IFNγ$^+$ CD4 T_{RM} cells in either the nasal cavity or the lungs (Figure 3.43 *A*-*D*). These results demonstrate that neutrophils, in particular Siglec-F$^+$ neutrophils, contribute to protective immunity in the nasal cavity and lungs during the later stages of *B. pertussis* infection.

3.3 Discussion

The key finding of the present study is that CD4 T cells accumulate in the nasal cavity during *B. pertussis* infection, acquire a T_{RM} phenotype, and produce IL-17A in response to antigen stimulation with *B. pertussis*. IL-17A was found to mediate protective immunity against *B. pertussis* in the nasal cavity by promoting chemokine production and the subsequent recruitment of a novel neutrophil population expressing Siglec-F, which directly contributed to bacterial clearance. These finding uncover a key mechanism of protective immunity to *B. pertussis* in the upper respiratory tract.

The results highlighted key differences in the innate immune response to *B. pertussis* between the upper and lower respiratory tract. In accordance with previously published studies, *B. pertussis* infection is accompanied by an expansion of alveolar macrophages and infiltration of neutrophils into the lungs [106, 146]. This study also demonstrated that $Ly6C^{+}CD11b^{+}$ inflammatory monocytes expressing MHC II infiltrate the lungs during *B. pertussis* infection. $Ly6C^{hi}$ monocytes have been implicated in protective immunity against other pulmonary pathogens, such as *K. pneumoniae,* where they provided a source of TNF to amplify a protective IL-17-mediated response [310]. Neutrophils and $Ly6C^{+}CD11b^{+}MHCII^{+}$ inflammatory monocytes were also found to infiltrate the nasal tissue during *B. pertussis* infection. However, a novel neutrophil population expressing Siglec-F was found to significantly expand in the nasal cavity during *B. pertussis* infection. These cells were primarily located in the tissue, as evident by intravascular staining. Only a minor population of $Siglec\text{-}F^{+}$ neutrophils were detected in the lungs, suggesting that recruitment of these cells is a unique feature of the nasal mucosa during *B. pertussis* infection.

Siglec-F is a member of the sialic-acid-binding immunoglobulin-like lectins family, which mediates both cell-cell interactions and signalling functions [311]. Siglec-F was first described as an eosinophil marker and is thought to function as an inhibitory receptor on these cells [312]. However, Siglec-F is now known to be expressed on many other cell types such as alveolar macrophages [313], intestinal microfold (M) cells [314], and subsets of myeloid progenitor cells [315]. A subset of neutrophils expressing Siglec-F have been described in multiple other models, including a murine allergic rhinitis model [316], a diesel exhaust particulates exposure model [317], and in a murine lung cancer model [318]. The results presented in this study are the first to describe the expansion and potential role of $Siglec\text{-}F^{+}$ neutrophils in the nasal cavity in response to a bacterial infection. $Siglec\text{-}F^{+}$ neutrophils induced in the nose during *B. pertussis* infection were found to exhibit an activated phenotype, with significantly higher surface expression of

CXCR2, CD11c, and CD49d compared with conventional Siglec-F$^-$ neutrophils. CXCR2 is a prominent chemokine receptor on neutrophils [319], and is a marker of mature neutrophils [318]. Enhanced CXCR2 expression, in addition to increased CD11c and CD49d expression, was also observed on Siglec-F$^+$ neutrophils expanded during an allergic rhinitis model [316], lung tumour-infiltrating Siglec-F$^+$ neutrophils [318], and on Siglec-F$^+$ neutrophils found in olfactory neuroepithelium [320]. In addition to phenotypic differences, this study also demonstrated functional differences between Siglec-F$^+$ and Siglec-F$^-$ neutrophils, with Siglec-F$^+$ neutrophils exhibiting a greater capacity for NET formation. This finding is in agreement with a study by Shin and colleagues, who found that lung Siglec-F$^+$ neutrophils had increased expression of genes related to NET formation such as *Atk, Mtor, Map3k,* and *Ctsa* [317].

Neutrophils have been demonstrated to play a protective role in immunity to infection with several different respiratory pathogens, including *Pseudomonas aeruginosa* [321], *Legionella pneumophila* [322], and *K. pneumoniae* [323]. However, the role of neutrophils in protective immunity against *B. pertussis* is unclear. A study by Andreasen and colleagues found that depletion of neutrophils had no effect on clearance of *B. pertussis* from the lungs of naïve mice [76]. However, this study used an anti-GR-1 antibody, which recognises Ly6G and Ly6C, the latter of which is also expressed on monocytes, macrophages, T cells and eosinophils. The study presented in this chapter utilised a novel neutrophil depletion method developed by Boivin et al. which used an antibody specific for Ly6G, which is expressed exclusively on neutrophils, in addition to a secondary antibody that results in more effective neutrophil depletion by complement-mediated mechanisms [294]. This method resulted in a significant, however not complete, reduction in total neutrophils in the respiratory tract. Interestingly, Siglec-F$^+$ neutrophils were more susceptible to this depletion strategy, especially in the nasal cavity. The results presented in this chapter demonstrated that depleting neutrophils at the start of *B. pertussis* infection significantly impaired bacterial clearance in the nasal cavity, but not the lungs. However, commencing the neutrophil depletion on day 7 post *B. pertussis* challenge significantly impaired bacterial clearance in both the nasal cavity and lungs. These results complement those by Andreasen and colleagues who only found an impairment in bacterial clearance from the lungs following depletion of neutrophils during the re-infection of immune mice or in naïve mice treated with immune serum, suggesting that the presence of opsonising antibodies in immune mice are important for the ability of neutrophils to control *B. pertussis* infection in the lower respiratory tract [76]. The results presented in this study are the first to demonstrate that neutrophils, particularly Siglec-F$^+$, directly contribute to clearance of *B. pertussis* from

the nasal cavity. Furthermore, Siglec-F$^+$ neutrophils were found to be selectively reduced in the nasal cavity in the absence of IL-17A or CD4 T cells, suggesting that IL-17A and CD4 T cells mediate the recruitment of Siglec-F$^+$ neutrophils to the nasal mucosa.

This study revealed that nasal CD4 T_{RM} cells which accumulate in the nose during *B. pertussis* infection exhibit a strong Th17 phenotype and are the predominant source of IL-17A in the nasal cavity. Infection of mice lacking CD4 T cells or IL-17A with *B. pertussis* resulted in significantly impaired bacterial clearance from the nasal cavity. In contrast, infection of IL-17A$^{-/-}$ mice with *B. pertussis* resulted in a moderate delay in bacterial clearance from the lungs. Similar findings were reported by Dubois and colleagues, who described significantly impaired clearance of *B. pertussis* from the nasal cavity of IL-17A$^{-/-}$ mice but minimal impairment in the lungs of IL-17A$^{-/-}$ mice [217]. Despite impaired bacterial clearance from the nasal cavity, IL-17A$^{-/-}$ mice exhibited significantly higher numbers of IFNγ-producing CD4 T_{RM} cells in both the nasal cavity and lungs. IL-17A has been shown to attenuate IFNγ expression, with enhanced IFNγ protein production from lung lymphocyte populations also observed in IL-17A$^{-/-}$ mice in other infection models, such as nematode infection [324]. IFNγ is essential for constraining *B. pertussis* to the respiratory tract, with infection of IFNγ receptor-deficient mice resulting in atypical disease dissemination in the blood and liver, and reduced survival compared with WT mice [148]. However, infection of IFNγ$^{-/-}$ mice with *B. pertussis* resulted in only a mild delay in bacterial clearance in the nasal cavity [217]. Thus, it could be speculated that the enhanced IFNγ production observed in the respiratory tract of IL-17A$^{-/-}$ mice is sufficient to protect against severe disease in lungs, however, is redundant in protection against *B. pertussis* in the nasal cavity.

IL-17A is known to target a range of cells including epithelial cells, keratinocytes, and synoviocytes, in addition to immune cells, such as neutrophils, macrophages, dendritic cells, and T cells, to induce a myriad of inflammatory mediators, ranging from cytokines, such as IL-1β and IL-6, and chemokines, including CXCL1 and CXCL2, to inflammatory effectors such as acute-phase proteins, complement, and AMPs [325]. The results presented in this study demonstrated that IL-17A$^{-/-}$ mice have reduced *Cxcl1* mRNA expression in the nasal tissue post *B. pertussis* challenge and this was accompanied by reduced infiltration of Siglec-F$^+$ neutrophils to the nasal mucosa. Furthermore, intranasal administration of IL-17A induced rapid CXCL1 protein and mRNA expression in the nasal tissue. These findings are in agreement with a study by Ross et al. who found decreased CXCL1 in the lungs of IL-17A$^{-/-}$ mice during *B. pertussis* challenge, which was accompanied by reduced neutrophil influx [146]. The role of IL-17A in promoting chemokine production and subsequent neutrophil recruitment has been described in

other respiratory tract infections. Studies have shown that mice deficient in the IL-17 receptor have impaired clearance of *K. pneumoniae* from the lung and this was attributed to reduced expression of chemokines such as CXCL5 and MIP2, and consequently reduced neutrophil recruitment [326].

IgA is the most abundant antibody isotype in the mucosal immune system [327] and there is evidence that IL-17A contributes to secretion of IgA at mucosal surfaces. Intranasal administration of IL-17A was found to directly induce expression of the polymeric immunoglobulin receptor (pIgR) by the epithelium, which mediates the delivery of IgA to the apical surface of epithelial cells via transcytosis [328]. Furthermore, it was found that a Group A streptococcal C5a peptidase vaccine with the Th1/Th17-inducing adjuvant CAF01 induced tissue-resident Th17 cells and a strong local IgA response in the lungs, with IgA significantly reduced following neutralisation of IL-17A [329]. BPZE1, a live attenuated vaccine for i.n. administration, confers protection in the nasal cavity against *B. pertussis* and this protection was lost in IgA-deficient and IL-17A$^{-/-}$ mice [286]. Surprisingly, results presented in this chapter demonstrated that IL-17A$^{-/-}$ mice had significantly higher *B. pertussis*-specific IgA and IgG2c in the nasal wash, lung homogenate, and blood serum compared with WT mice, indicating that IL-17A is not essential for antibody production during *B. pertussis* infection. This enhanced antibody response may reflect the higher bacterial load detected in the IL-17A$^{-/-}$ mice. Antibody production has been shown to be required for clearance of *B. pertussis* from the lung during natural infection, with immunoglobulin μ-chain (Ig$^{-/-}$) mice failing to clear *B. pertussis* from the lungs [148]. Therefore, this enhanced antibody response observed in the IL-17A$^{-/-}$ may be sufficient to confer protection in the lungs in the absence of IL-17A. In contrast, as seen with IFNγ, this enhanced antibody response in IL-17A$^{-/-}$ mice appears to be redundant in protection against *B. pertussis* in the nasal cavity.

IL-17A is produced by a variety of immune cells including γδ T cells, ILCs, CD8 T cells, macrophages, and NK cells [325], however CD4 T cells were found to be the dominant source of IL-17A in the nasal tissue and lungs post *B. pertussis* infection. Interestingly, in the absence of CD4 T cells, CD8 T cells acquired the ability to produce IL-17A. IL-17-producing CD8 T cells, also called Tc17 cells, have been implicated in a range of conditions, such as autoimmunity and cancer [330].

The results presented in this chapter demonstrated that CD4 T cells expand in the nasal cavity and lungs during *B. pertussis* infection and acquire a T_{RM} phenotype. CD4 T_{RM} cells generated during *B. pertussis* infection were found to produce pathogen-specific IL-17A, which mediated protective immunity against *B. pertussis* by enhancing chemokine

production and promoting the recruitment of a novel neutrophil population expressing Siglec-F to the nasal cavity. Siglec-F$^+$ neutrophils were found to exhibit an activated phenotype and have a high capacity for NET formation. Utilising a neutrophil depletion method to which Siglec-F$^+$ neutrophils were more susceptible to, this study demonstrated that Siglec-F$^+$ neutrophils directly contributed to bacterial clearance in the nasal cavity. Understanding the mechanisms of protective immunity against *B. pertussis* in the upper respiratory tract may inform the design of next generation pertussis vaccines capable of inducing sterilising immunity in the nasal cavity.

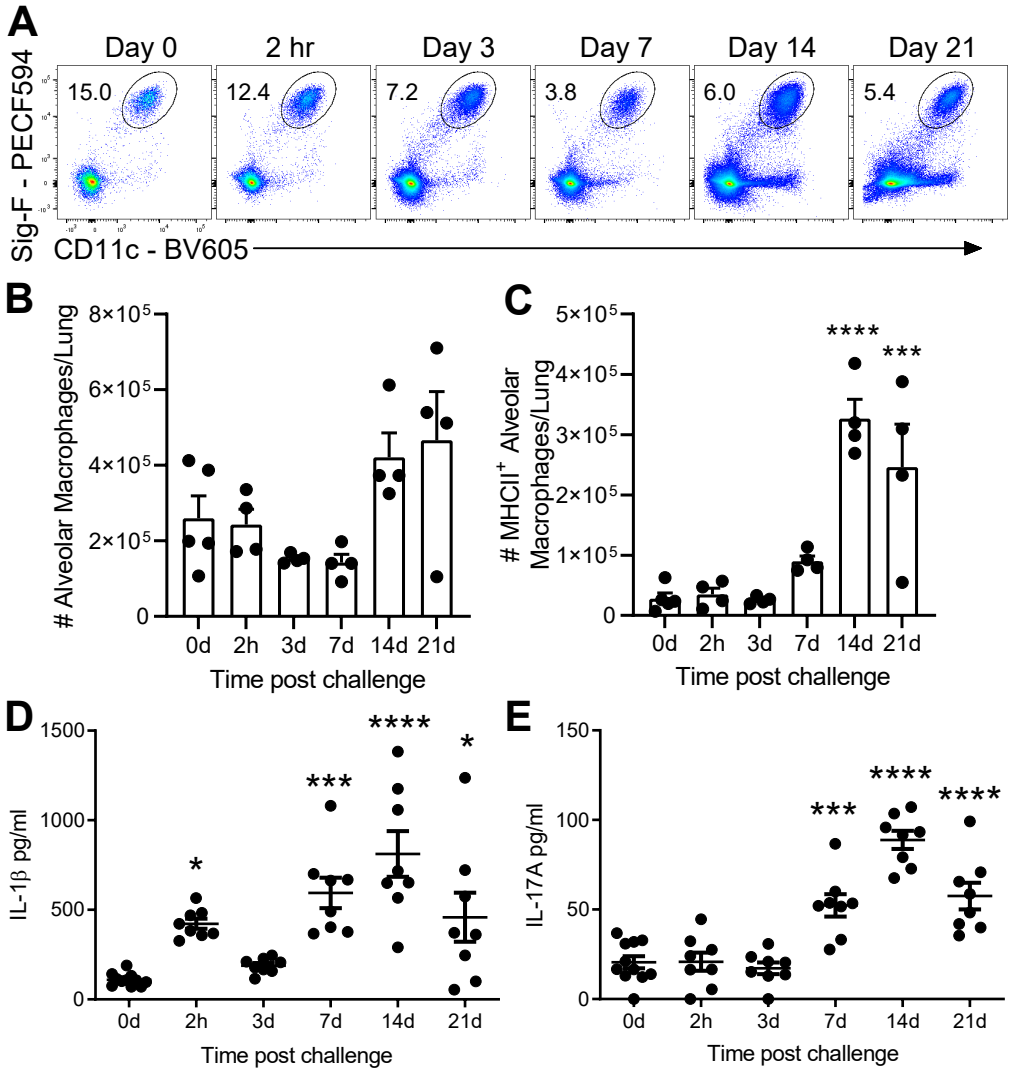

Figure 3.1 Kinetics of alveolar macrophage expansion and cytokine production in the lungs during *B. pertussis* infection.

C57BL/6 mice were infected with live *B. pertussis* and lungs were harvested at indicated time points. Mononuclear cells were isolated and stained for CD11b, CD11c, Siglec-F, and MHC II, and analysed by flow cytometry. Representative flow cytometry plots (A) and absolute number (B) of alveolar macrophages (Siglec-F$^+$CD11c$^+$) over the course of infection. Absolute number (C) of MHC II$^+$ alveolar macrophages at indicated time points. Data are mean ± SEM (n=4-5 mice per time point). ***p < 0.001, ****p < 0.0001 naïve versus infected mice by one-way ANOVA followed by Dunnett's post hoc analysis. The concentration of IL-1β (D) and IL-17A (E) in lung homogenates over the course of *B. pertussis* infection were quantified by ELISA. Results are combined from two independent experiments. Data are mean ± SEM (n=8-11 mice per time point). *p < 0.05, ***p < 0.001, ****p < 0.0001 naïve versus infected mice by one-way ANOVA followed by Dunnett's post-hoc analysis.

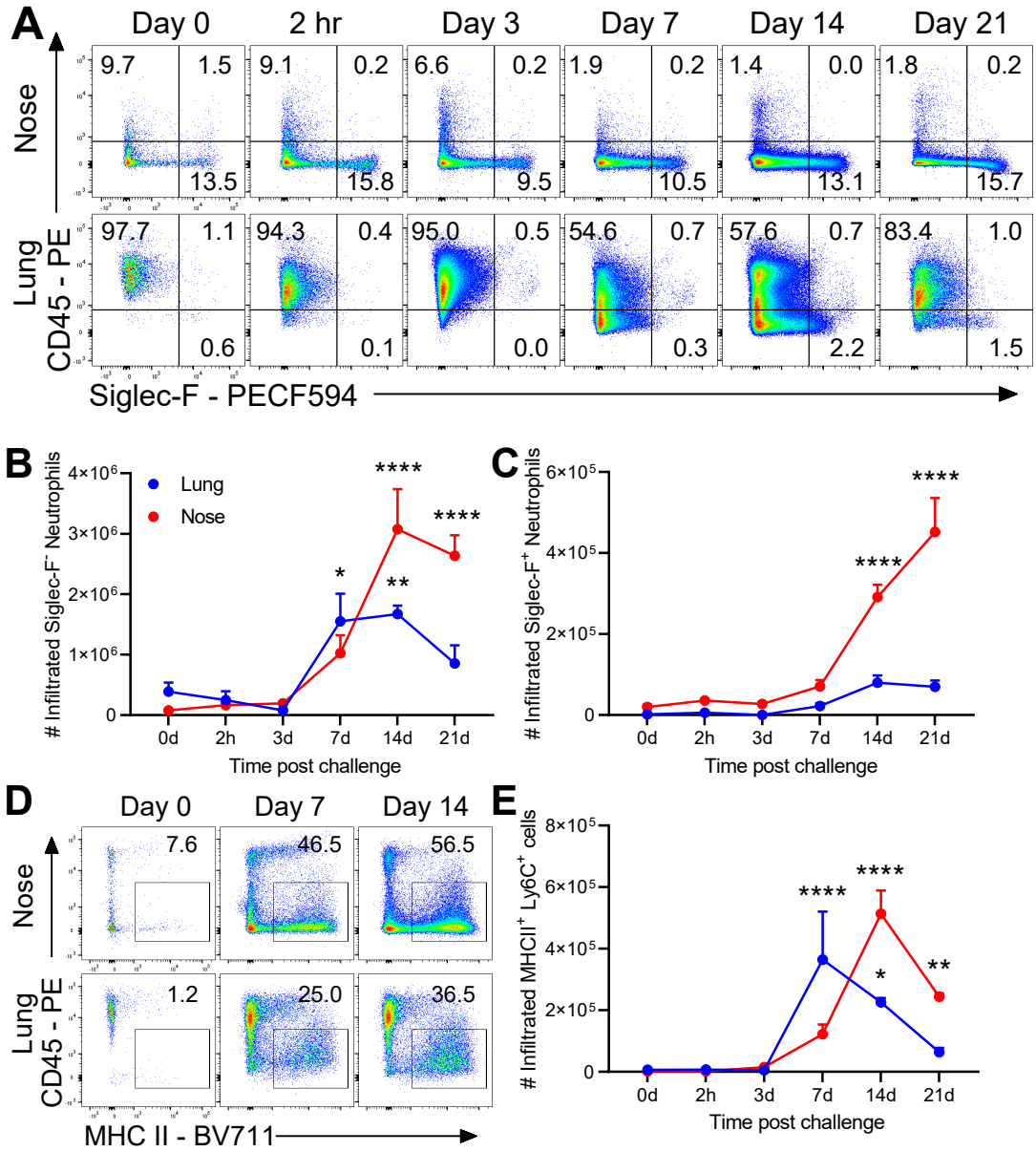

Figure 3.2 Siglec-F⁺ neutrophils and MHCII⁺Ly6C⁺ monocytes infiltrate the nasal cavity during *B. pertussis* infection.

C57BL/6 mice were aerosol infected with live *B. pertussis*. At indicated time points mice were injected i.v. with a fluorochrome-conjugated anti-CD45 antibody and euthanised 10 min later. Cell suspensions were prepared from nasal tissue and lungs and stained for CD11b, Ly6G, Ly6C, Siglec-F, and MHC II, and analysed by flow cytometry. Representative flow cytometry plots (A) and absolute number of tissue-infiltrated (CD45 i.v.⁻) Siglec-F⁻ (B) and Siglec-F⁺ (C) neutrophils (Ly6G⁺CD11b⁺) in the nasal tissue and lungs over the course of *B. pertussis* infection. Representative flow cytometry plots (D) and absolute number (E) of tissue-infiltrated MHCII⁺Ly6C⁺CD11b⁺ monocytes in the nasal cavity and lungs. Data are mean ± SEM (n=4-5 mice per time point). *$p < 0.05$, **$p < 0.01$, ****$p < 0.0001$ naïve versus infected mice by two-way ANOVA followed by Dunnett's post-test.

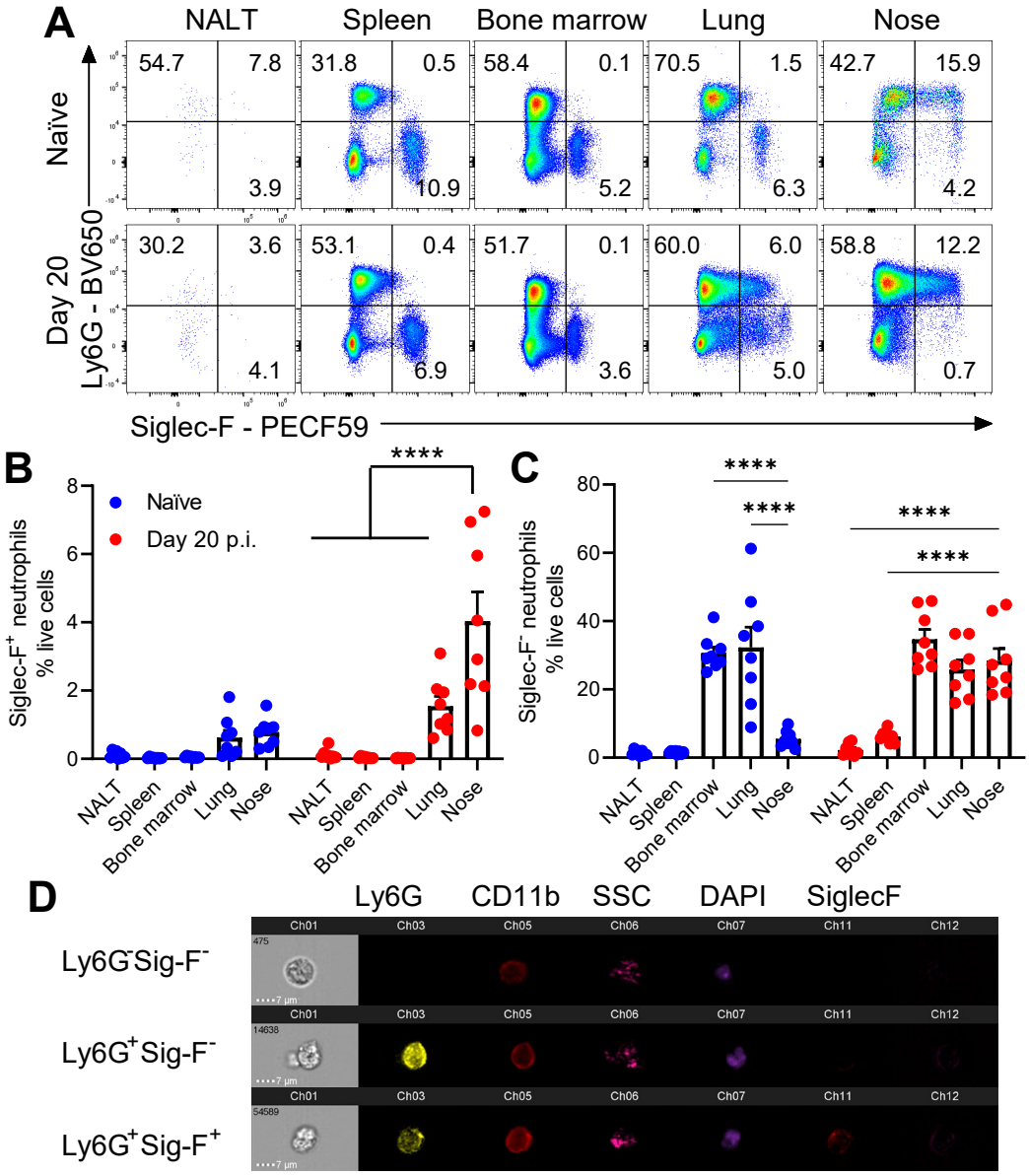

Figure 3.3 Siglec-F$^+$ neutrophils preferentially expand in the nasal cavity during *B. pertussis* infection.

C57BL/6 mice were aerosol infected with live *B. pertussis*. On day 20 post challenge, NALT, spleen, bone marrow, lungs and nasal tissue were harvested from infected mice and naïve control mice. Cell suspensions were prepared and stained for CD11b, Ly6G, and Siglec-F, and analysed by flow cytometry. Representative flow cytometry plots (A) and relative frequencies of Siglec-F$^+$ (B) and Siglec-F$^-$ (C) Ly6G$^+$ neutrophils (pre-gated on CD11b$^+$ cells) in the NALT, spleen, bone marrow, lungs, and nasal tissue of naïve and infected mice. Results are combined of two independent experiments. Data shown are mean ± SEM (n=8 mice per group). ****$p < 0.0001$ nose versus other tissues by two-way ANOVA followed by Dunnett's post-test. ImageStream analysis of nasal mononuclear cells (n=1) on day 13 p.i., pre-gated on total CD11b$^+$ cells (D).

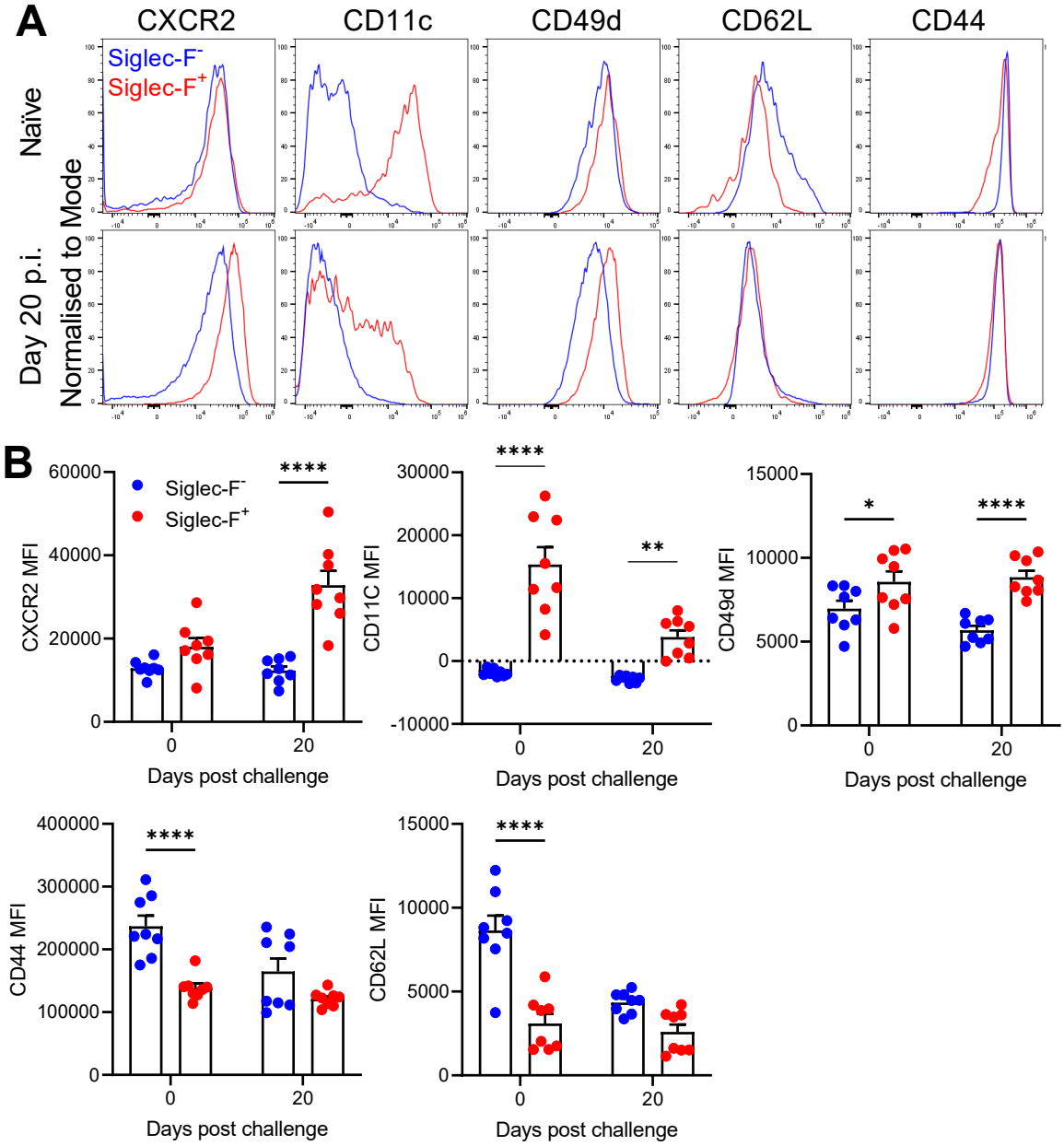

Figure 3.4 Siglec-F$^+$ neutrophils in the nasal tissue have an activated phenotype.

C57BL/6 mice were aerosol infected with live *B. pertussis*. On day 20 post challenge nasal tissue was harvested from infected mice and naïve control mice. Nasal mononuclear cells were isolated and stained for surface CD11b, Ly6G, Siglec-F, CXCR2, CD11c, CD49d, CD44, and CD62L, and analysed by flow cytometry. Representative histograms (A) and mean fluorescent intensity (MFI) (calculated using geometric mean) (B) of CXCR2, CD11c, CD49d, CD62L, and CD44 expression on Siglec-F$^+$ and Siglec-F$^-$ neutrophils (Ly6G$^+$CD11b$^+$) in the nasal cavity of naïve and *B. pertussis*-infected mice. Results are combined from two independent experiments. Results shown are mean ± SEM (n=8 mice per group). *p < 0.05, **p < 0.01, ****p < 0.0001 Siglec-F$^+$ versus Siglec-F$^-$ neutrophils by two-way ANOVA followed by Sidak's post-test.

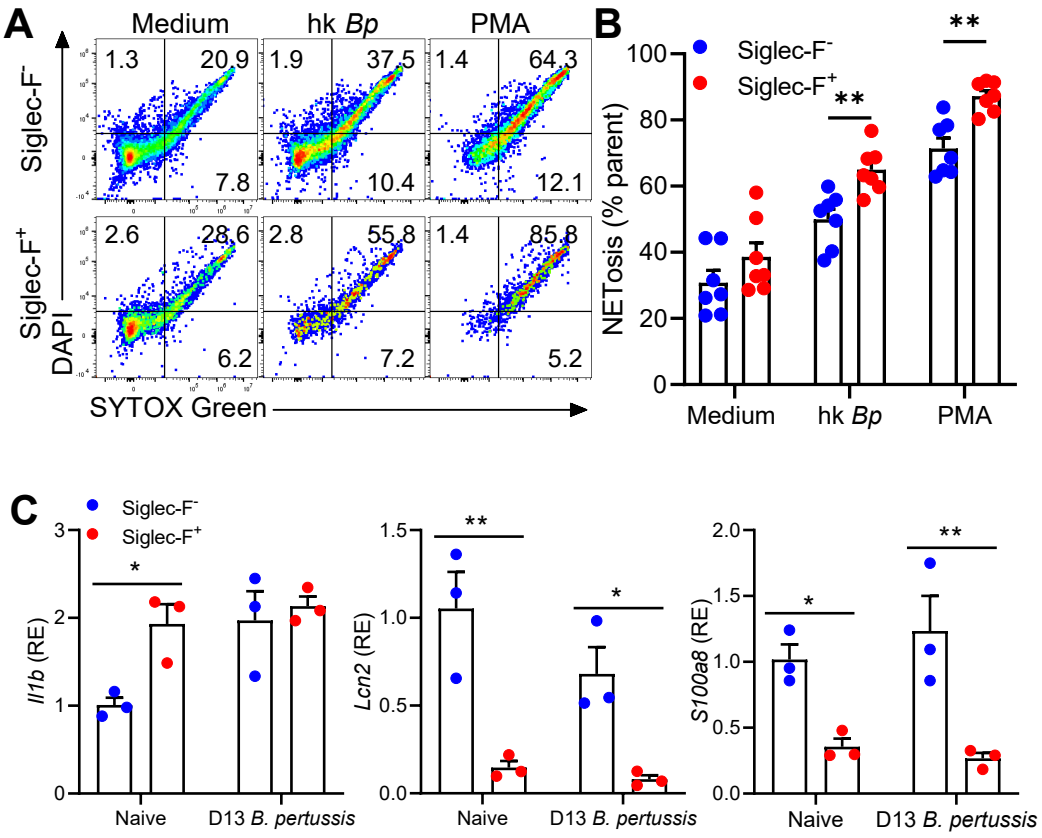

Figure 3.5 Siglec-F$^+$ neutrophils exhibit significantly higher NET activity compared with conventional Siglec-F$^-$ neutrophils.

Nasal mononuclear cells isolated from mice infected with *B. pertussis* were stimulated with heat-killed *B. pertussis* (hk *Bp*; 1x10^7 CFU/ml), PMA (50 ng/ml), or media alone for 4 hours and then stained with an intracellular DNA dye (DAPI) and a cell-impermeant DNA dye (SYTOXgreen), in addition to staining for surface Ly6G and CD11b, and analysed by flow cytometry. Representative flow cytometry plots (A) and percentage (B) of Siglec-F$^+$ and Siglec-F$^-$ neutrophils in the nasal tissue undergoing NETosis (double positive for DAPI and SYTOXgreen). Results are combined from 2 independent experiments. Data are mean ± SEM (n=7 mice per group). $^{**}p < 0.01$ Siglec-F$^+$ versus Siglec-F$^-$ neutrophils by two-way ANOVA followed by Sidak's post-test. Nasal tissue was harvested from naïve and infected mice (13 days p.i.). Nasal mononuclear cells were pooled from 2 mice per group and Siglec-F$^+$ and Siglec-F$^-$ neutrophils (Ly6G$^+$CD11b$^+$) were FACS purified and *Il1b, S100a8,* and *Lcn2* mRNA expression was evaluated by RT-qPCR, normalised to 18S rRNA and relative to Siglec-F$^-$ neutrophils day 0 (C). Data are mean ± SEM (n=2 mice per data point, with 3 data points per group). $^{*}p < 0.05$, $^{**}p < 0.01$ Siglec-F$^+$ versus Siglec-F$^-$ neutrophils by two-way ANOVA followed by Sidak's post-test.

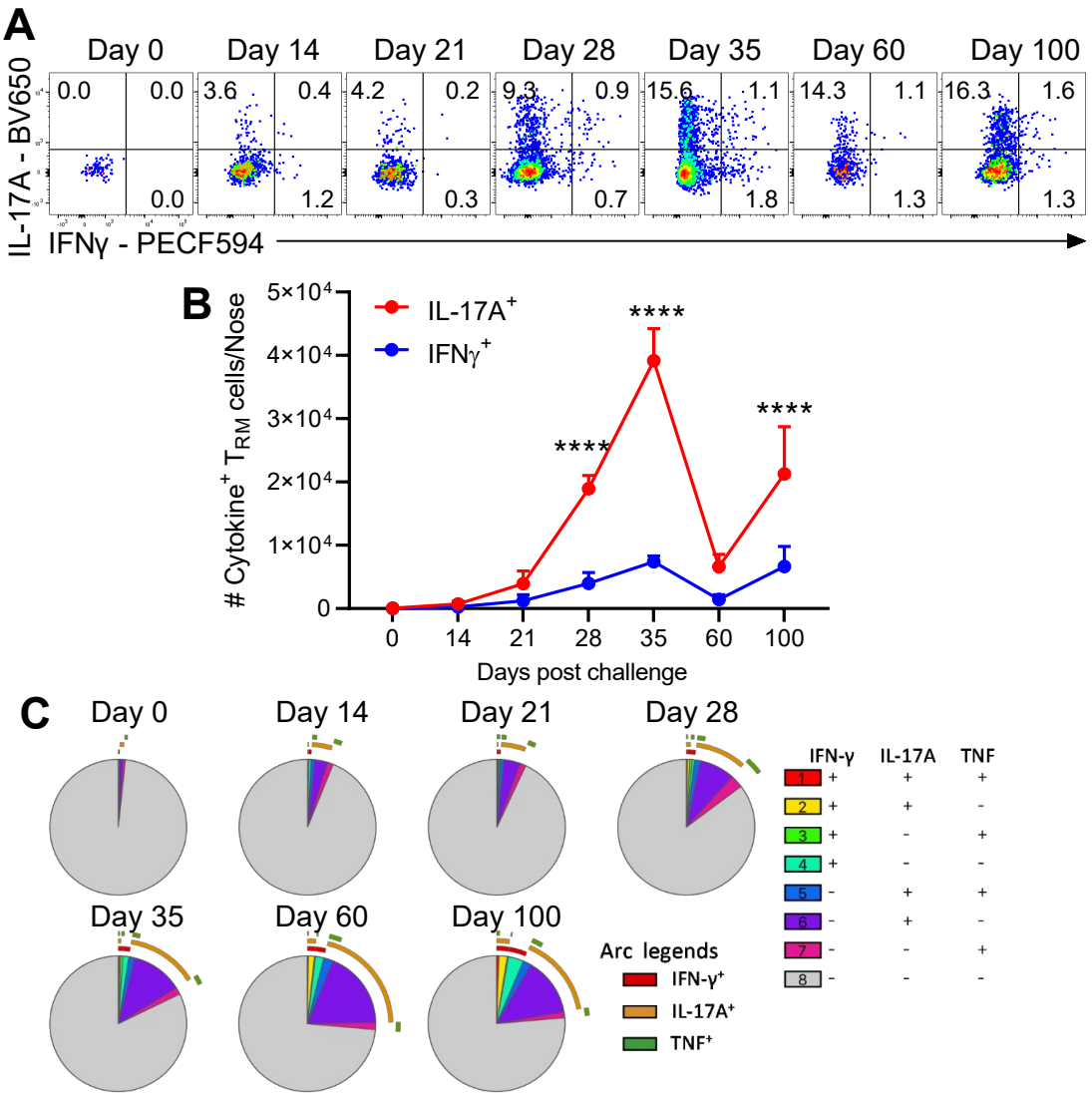

Figure 3.6 Pathogen-specific CD4 T_{RM} cells accumulate in the nasal cavity during *B. pertussis* infection and exhibit a predominantly Th17 phenotype.

C57BL/6 mice were aerosol challenged with live *B. pertussis*. At the indicated time points, mice were injected i.v. with a fluorochrome-conjugated anti-CD45 antibody and euthanised 10 min later. Cell suspensions were prepared from nasal tissue and cells were stimulated with sBP (5 µg/ml) and anti-CD28 and CD49d (both at 1 µg/ml) for 20 hours. Brefeldin A (5 µg/ml) was added for the final 4 hours of culture. Cells were stained for surface CD4, CD3, CD44, CD62L, CD69, CD103, and intracellular IL-17A and IFNγ, and analysed by flow cytometry. Representative flow cytometry plots (A) and absolute number (B) of IL-17A$^+$ and IFNγ$^+$ CD4 T_{RM} cells (CD4$^+$CD3$^+$CD45i.v.$^-$ CD44$^+$CD69$^+$CD103$^\pm$) in the nasal cavity of mice at the prior to and post *B. pertussis* challenge. SPICE analysis of cytokine producing nasal CD4 T_{RM} cells over the course of infection (C). Data are mean ± SEM (n=4 mice per time point). ****p < 0.0001 naïve versus infected mice by two-way ANOVA followed by Dunnett's post-test.

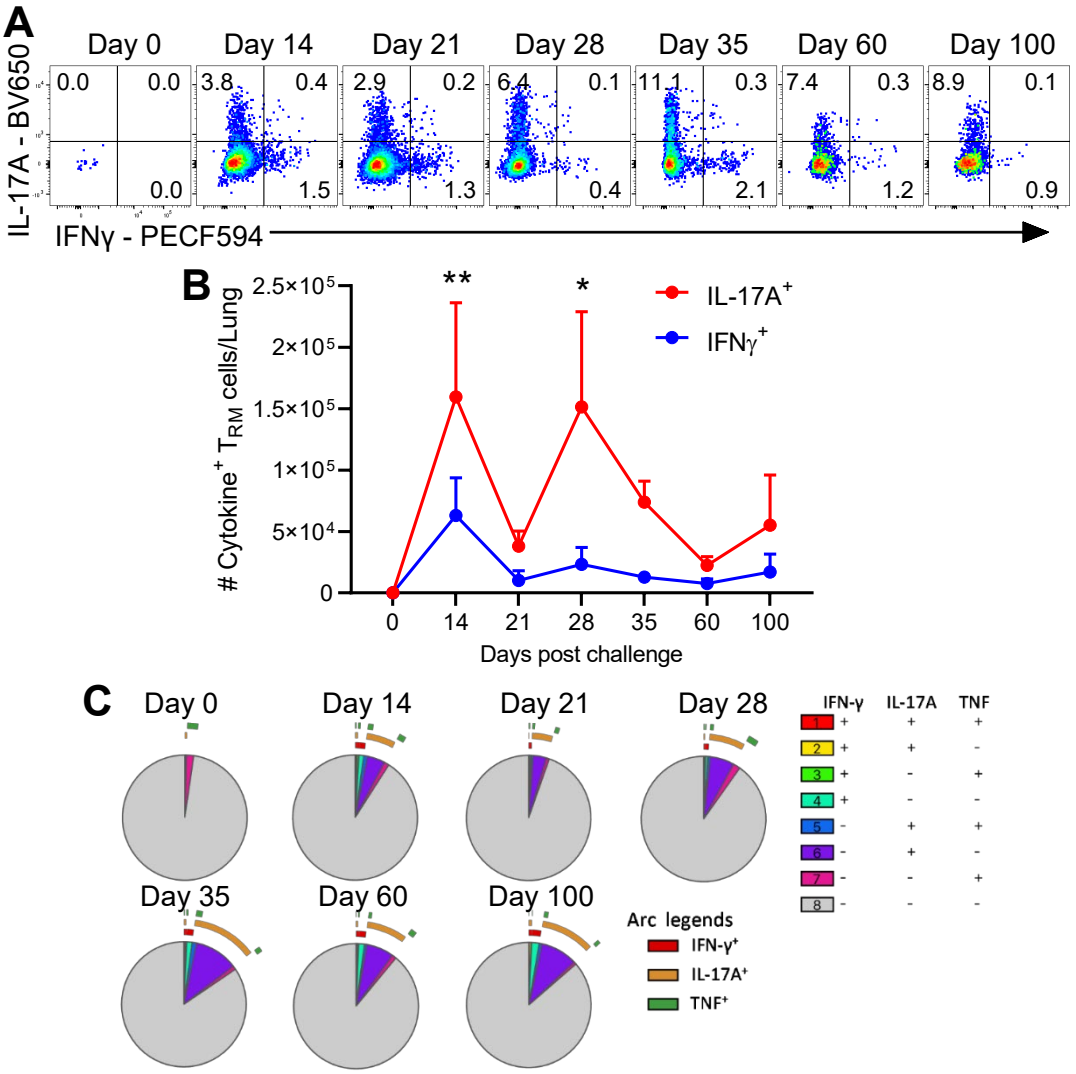

Figure 3.7 Pathogen-specific CD4 T_{RM} cells accumulate in the lungs during *B. pertussis* infection and exhibit a predominantly Th17 phenotype.

C57BL/6 mice were infected with live *B. pertussis.* At the indicated time points, a fluorochrome-labelled anti-CD45 antibody was administered i.v. to mice 10 min prior to euthanasia. Cell suspensions were prepared from lungs and cells were stimulated with sBP (5 µg/ml) and anti-CD28 and anti-CD49d (both at 1 µg/ml) for 20 hours. Brefeldin A (5 µg/ml) was added for the final 4 hours of culture. Cells were stained for surface CD4, CD3, CD44, CD62L, CD69, and CD103, and intracellular IL-17A and IFNγ, and analysed by flow cytometry. Representative flow cytometry plots (A) and absolute number (B) of IL-17A$^+$ and IFNγ$^+$ CD4 T_{RM} cells (CD4$^+$CD3$^+$CD45i.v.$^-$CD44$^+$CD62L$^-$CD69$^+$CD103$^\pm$) in the lungs of mice prior to and post *B. pertussis* challenge. SPICE analysis of cytokine producing lung CD4 T_{RM} cells over the course of infection (C). Data are mean ± SEM (n=4 mice per time point). *$p < 0.05$, **$p < 0.01$, naïve versus infected mice by two-way ANOVA followed by Dunnett's post-test.

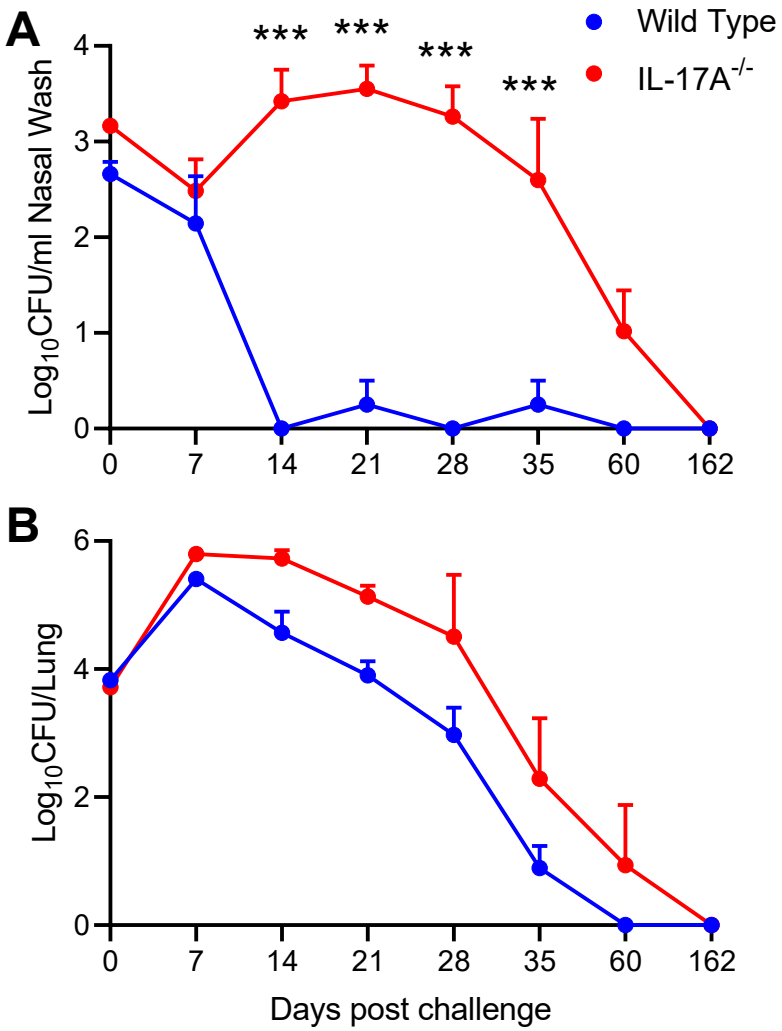

Figure 3.8 IL-17A$^{-/-}$ mice have significantly delayed bacterial clearance from the nasal cavity, and moderately delayed clearance from the lungs, following *B. pertussis* infection.

C57BL/6 WT and IL-17A$^{-/-}$ mice were aerosol infected with live *B. pertussis* and nasal washes and lungs were harvested at indicated time points. The number of viable bacteria was estimated by performing CFU counts on serially diluted nasal washes (A) and lung homogenates (B) from individual mice. Results shown are mean ± SEM CFU counts (n=4 mice per group). ***$p < 0.001$ WT versus IL-17A$^{-/-}$ by two-way ANOVA followed by Sidak's post-test. Experiment conducted in collaboration with Dr. Lisa Borkner at Trinity Biomedical Sciences Institute, Trinity College Dublin.

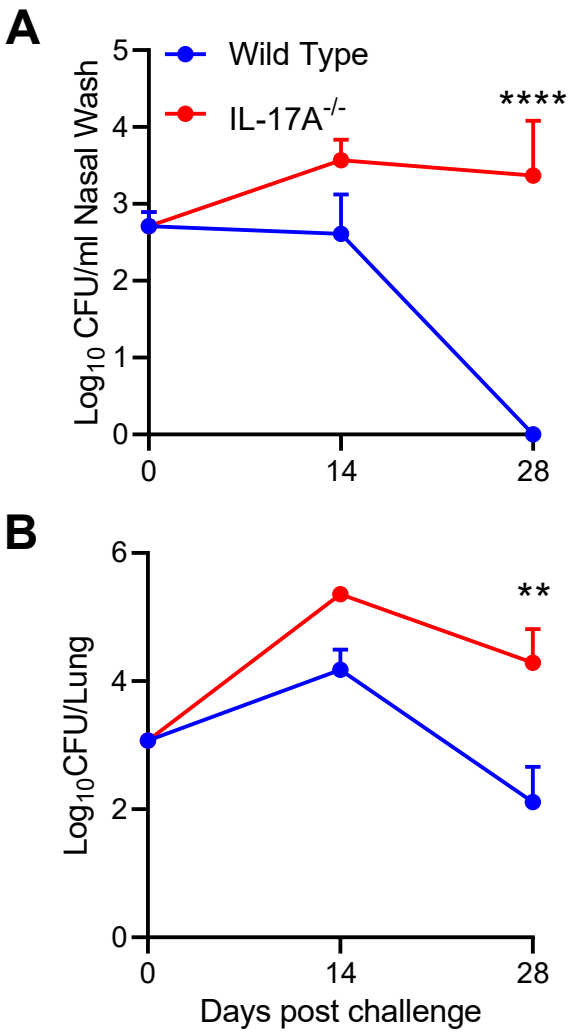

Figure 3.9 IL-17A$^{-/-}$ mice co-housed with corresponding WT control mice have significantly delayed clearance of *B. pertussis* from the nasal cavity and lungs.

C57BL/6 WT and IL-17A$^{-/-}$ mice were co-housed prior to and during the course of infection with live *B. pertussis.* The number of viable bacteria in the nasal wash (A) and lung homogenates (B) was estimated by performing CFU counts on serially diluted nasal washes and lung homogenates from individual mice on days 14 and 28 post challenge. Results shown are mean ± SEM CFU counts (n=4-5 mice per group). $^{**}p < 0.01$, $^{****}p < 0.0001$ WT versus IL-17A$^{-/-}$ mice by two-way ANOVA followed by Sidak's post-test.

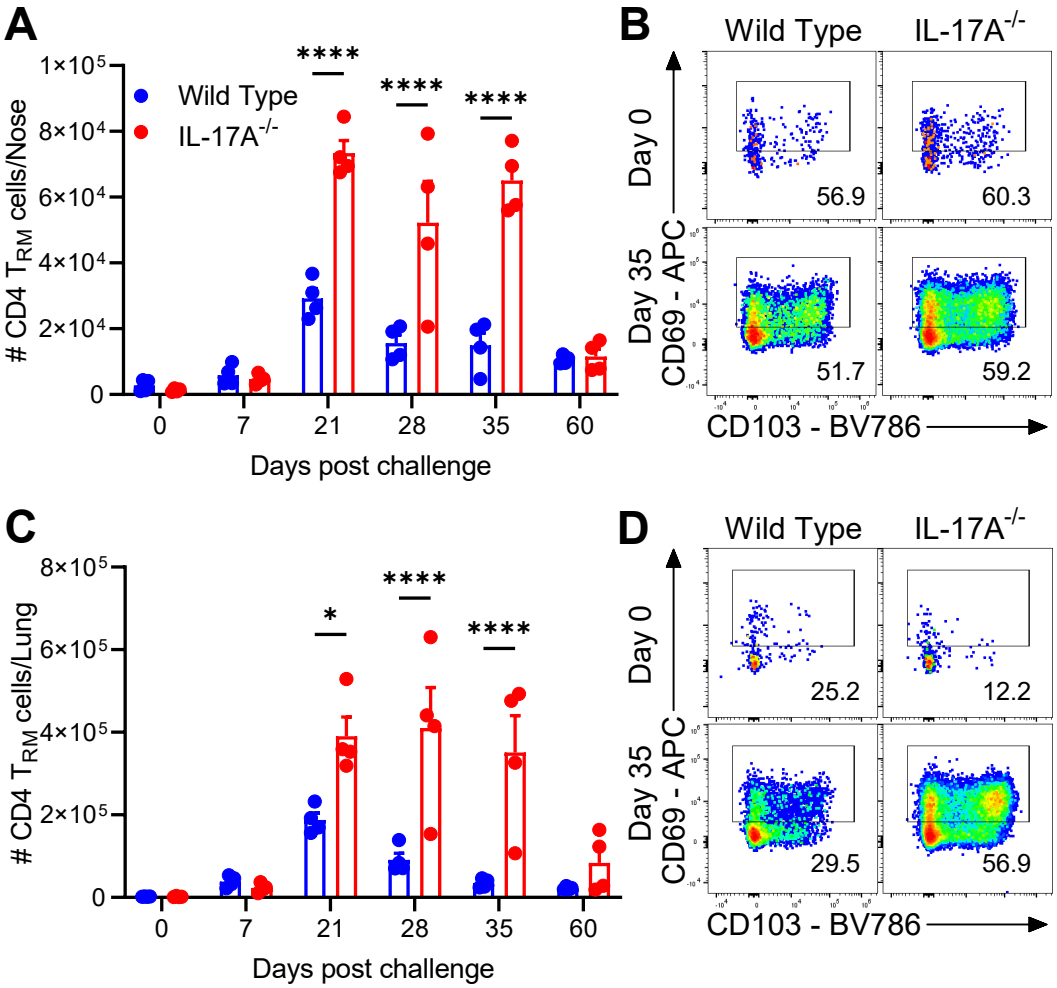

Figure 3.10 IL-17A$^{-/-}$ mice have significantly increased number of CD4 T_{RM} cells in the nasal cavity and lungs during *B. pertussis* infection.

C57BL/6 WT and IL-17A$^{-/-}$ mice were aerosol challenged with live *B. pertussis*. Mice were injected with a fluorochrome-labelled anti-CD45 antibody at indicated time points and euthanised 10 min later. Nasal tissue and lungs were harvested and mononuclear cells were isolated and stained for CD4, CD3, CD44, CD62L, CD69, and CD103, and analysed by flow cytometry. Absolute number (A) with representative flow cytometry plots (B) of nasal CD4 T_{RM} cells ($CD4^+CD3^+CD45$ i.v.$^-CD44^+CD62L^-CD69^+CD103^\pm$), and absolute number (C) and representative flow cytometry plots (D) of lung CD4 T_{RM} cells in WT and IL-17A$^{-/-}$ mice. Results shown are mean ± SEM (n=4 mice per group). *p < 0.05, ****p < 0.0001, WT versus IL-17A$^{-/-}$ by two-way ANOVA followed by Sidak's post-test.

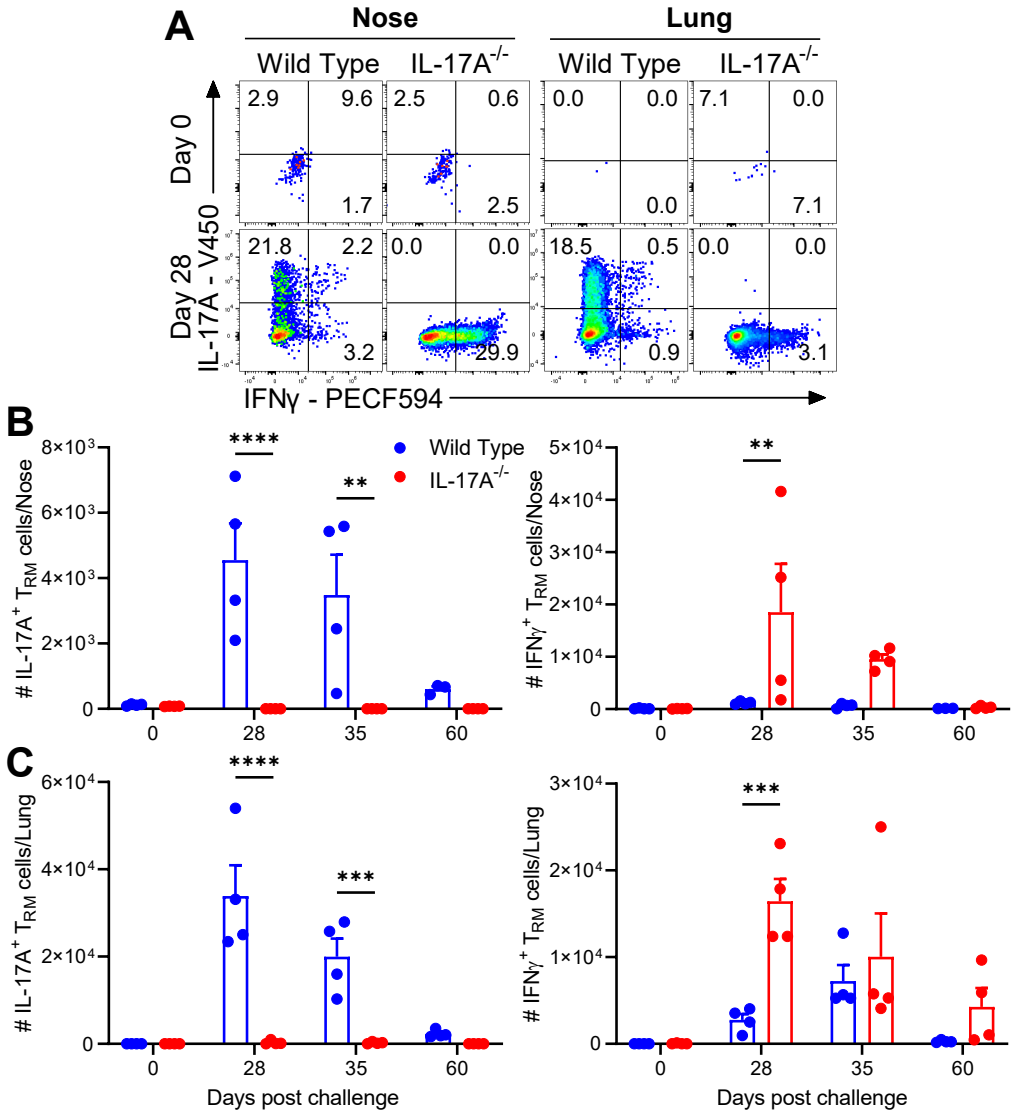

Figure 3.11 Enhanced pathogen-specific IFNγ⁺ CD4 T_{RM} cells in the nasal cavity and lungs of IL-17A$^{-/-}$ mice during *B. pertussis* infection.

C57BL/6 WT and IL-17A$^{-/-}$ mice were aerosol challenged with live *B. pertussis*. At the indicated time points, a fluorochrome-conjugated anti-CD45 antibody was administered i.v. to mice 10 min before euthanasia. Cell suspensions were prepared from nasal tissue and lungs and cells were stimulated with sBP (5 µg/ml) and anti-CD28 and anti-CD49d (both at 1 µg/ml) for 20 hours. Brefeldin A (5 µg/ml) was added for the final 4 hours of culture. Cells were stained for surface CD4, CD3, CD44, CD69, and CD103, and intracellular IL-17A and IFNγ, and analysed by flow cytometry. Representative flow cytometry plots (A) and absolute number of nasal (B) and lung (C) IL-17A⁺ and IFNγ⁺ CD4 T_{RM} cells ($CD4^+CD3^+CD45i.v.^-CD44^+CD62L^-CD69^+CD103^±$) in WT and IL-17A$^{-/-}$ mice. Data are mean ± SEM (n=4 mice per group). $^{**}p < 0.01$, $^{***}p < 0.001$, $^{****}p < 0.0001$ WT versus IL-17A$^{-/-}$ by two-way ANOVA followed by Sidak's post-test.

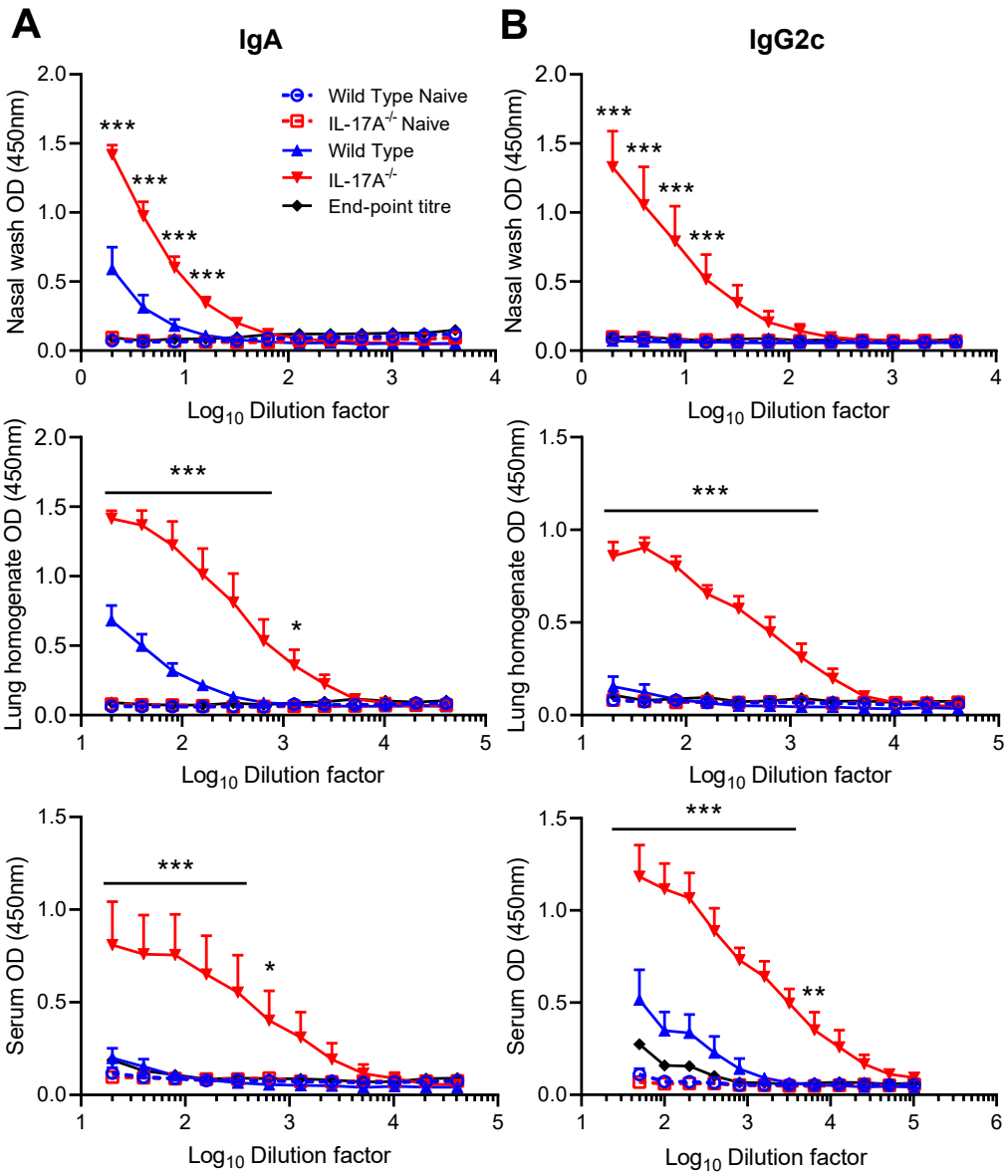

Figure 3.12 IL-17A$^{-/-}$ mice have significantly enhanced *B. pertussis*-specific antibody responses.

C57BL/6 WT and IL-17A$^{-/-}$ mice were infected with live *B. pertussis*. *B. pertussis*-specific IgA (A) and IgG2c (B) in the nasal washes, lung homogenates, and serum of WT and IL-17A$^{-/-}$ mice on day 35 post infection was quantified by ELISA. Data are mean ± SEM (n=4 mice per group). *$p < 0.05$, **$p < 0.01$, ***$p < 0.001$ WT versus IL-17A$^{-/-}$ by two-way ANOVA followed by Sidak's post-test.

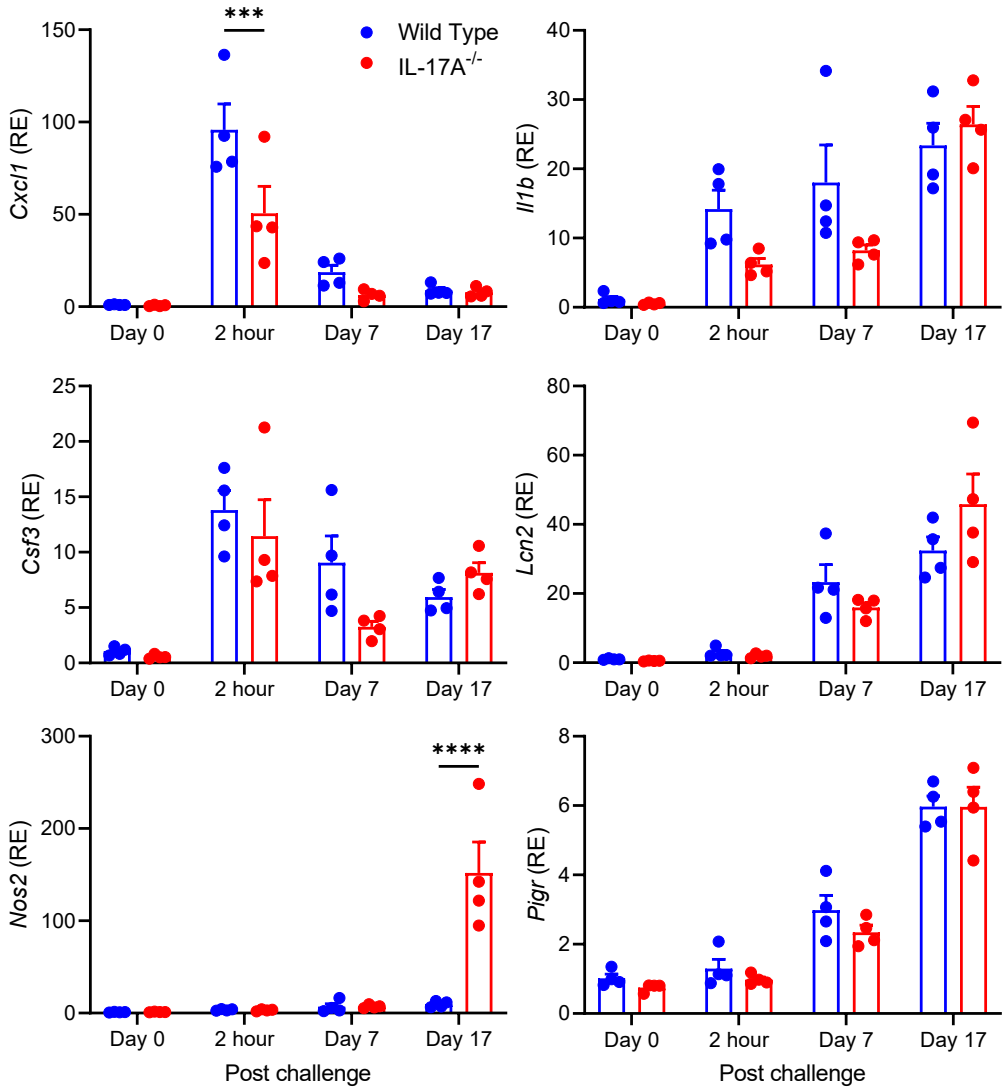

Figure 3.13 Reduced early CXCL1 expression and enhanced late NOS2 expression in the nasal tissue of IL-17A$^{-/-}$ mice during *B. pertussis* infection.

C57BL/6 WT and IL-17A$^{-/-}$ mice were aerosol infected with live *B. pertussis*. Nasal tissue was collected over the course of infection and *Cxcl1, Il1b, Csf3, Lcn2, Nos2,* and *Pigr* mRNA expression was evaluated by RT-qPCR, normalised to 18S rRNA and relative to WT mice day 0. Data are mean ± SEM (n=4 mice per group). ***$p < 0.001$, ****$p < 0.0001$ WT versus IL-17A$^{-/-}$ by two-way ANOVA followed by Sidak's post-test.

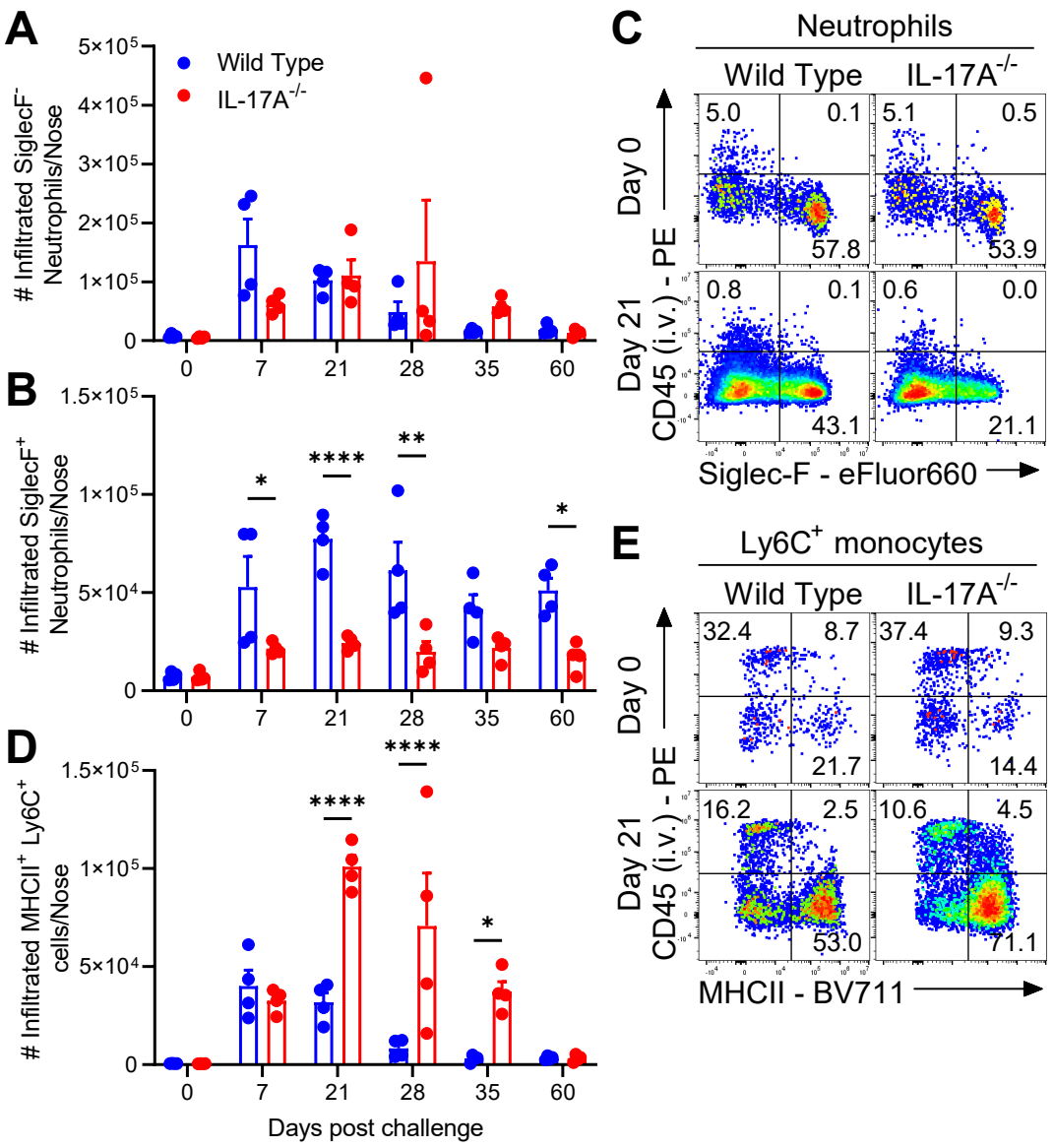

Figure 3.14 Reduced infiltration of Siglec-F$^+$ neutrophils and enhanced infiltration of MHCII$^+$Ly6C$^+$ monocytes into the nasal cavity of IL-17A$^{-/-}$ mice during *B. pertussis* infection.

C57BL/6 WT and IL-17A$^{-/-}$ mice were aerosol challenged with live *B. pertussis*. At the indicated time points, mice were injected i.v. with a fluorochrome-labelled anti-CD45 antibody 10 min prior to euthanasia. Nasal tissue was harvested and mononuclear cells were isolated and stained for CD11b, Ly6C, Ly6G, Siglec-F, and MHCII, and analysed by flow cytometry. Absolute number of tissue-infiltrated (CD45 i.v.$^-$) conventional Siglec-F$^-$ (A) and Siglec-F$^+$ (B) neutrophils in the nasal cavity with representative flow cytometry plots (C). Absolute number (D) of tissue-infiltrated MHCII$^+$Ly6C$^+$CD11b$^+$ monocytes in the nasal tissue of WT and IL-17A$^{-/-}$ mice with representative flow cytometry plots (E). Results shown are mean ± SEM (n=4 mice per group). *p < 0.05, **p < 0.01, ****p < 0.0001 WT versus IL-17A$^{-/-}$ by two-way ANOVA followed by Sidak's post-test.

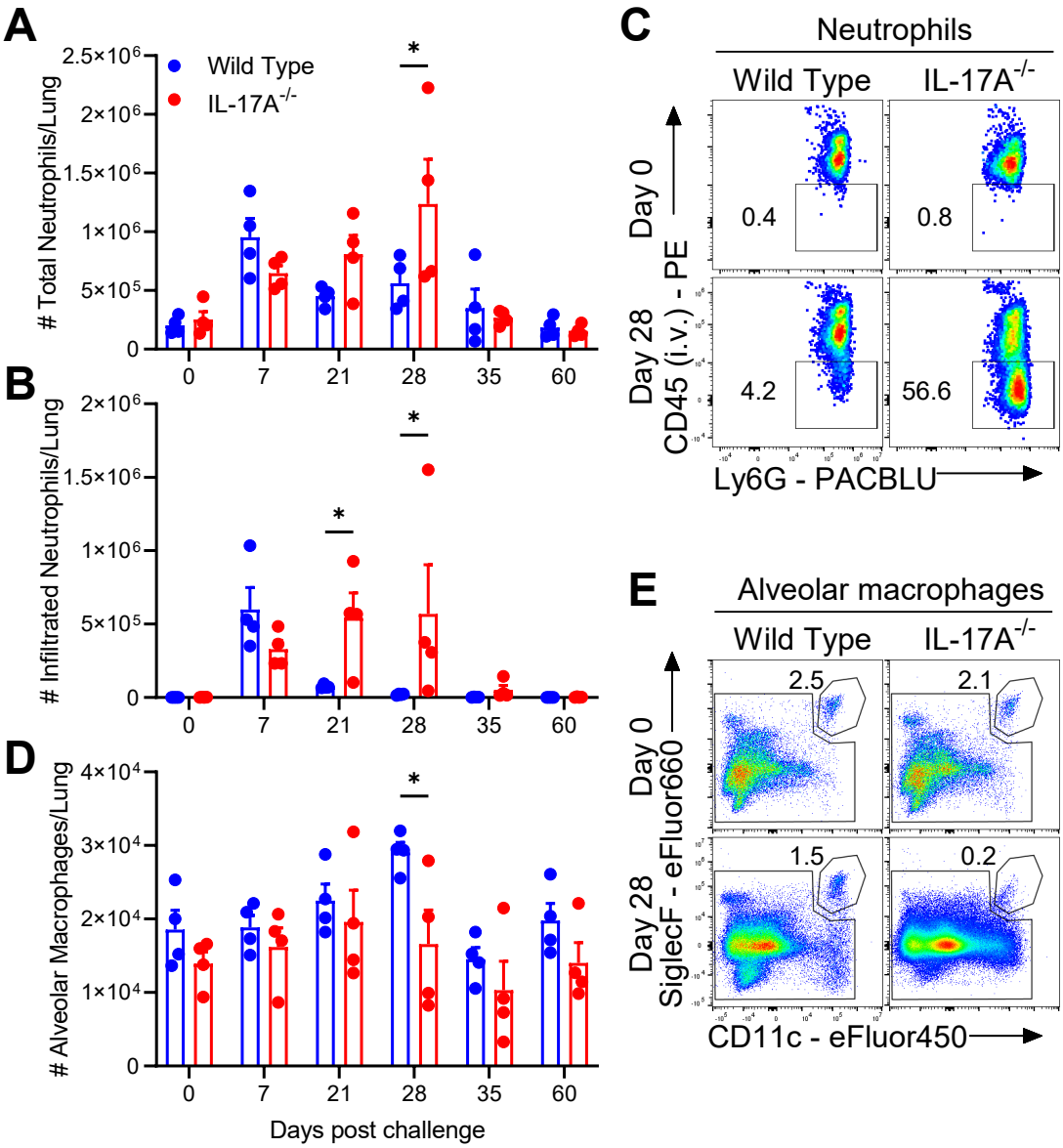

Figure 3.15 Enhanced number of total and tissue-infiltrated neutrophils, and reduced number of alveolar macrophages, in the lungs of IL-17A$^{-/-}$ mice during *B. pertussis* infection.

C57BL/6 WT and IL-17A$^{-/-}$ mice were aerosol challenged with live *B. pertussis*. At the indicated time points, mice were injected i.v. with a fluorochrome-conjugated anti-CD45 antibody and euthanised 10 min later. Lungs were harvested and mononuclear cells were isolated and stained for CD11c, CD11b, Siglec-F, and Ly6G, and analysed by flow cytometry. Absolute number of total neutrophils (CD11b^{+}Ly6G^{+}) (A), and tissue-infiltrated (CD45 i.v.$^{-}$) neutrophils (B) in the lungs, with representative flow cytometry plots (C). Absolute number (D) and representative flow cytometry plots (E) of alveolar macrophages (Siglec-F^{+}CD11c^{+}) in the lungs of WT and IL-17A$^{-/-}$ mice. Data are mean ± SEM (n=4 mice per group). *$p < 0.05$ WT versus IL-17A$^{-/-}$ by two-way ANOVA followed by Sidak's post-test.

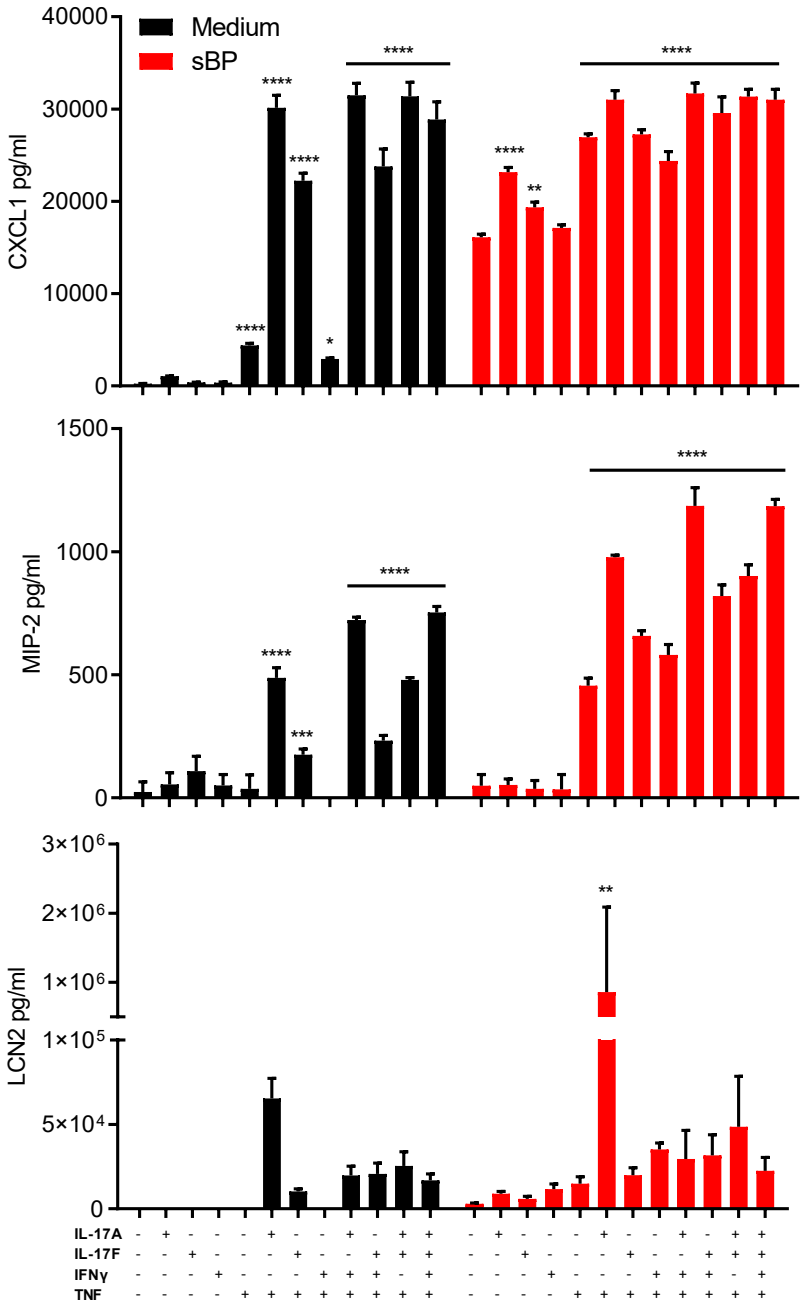

Figure 3.16 IL-17A, and to a lesser extent IL-17F, synergises with TNF to induce CXCL1, MIP-2, and LCN2 production from LA4 cells in the presence and absence of sBP.

LA4 cells were stimulated with combinations of IL-17A, IL-17F, IFNγ, or TNF (all at 10 ng/ml) in the presence or absence of sBP (5 µg/ml) for 24 hours. The concentration of CXCL1, MIP-2, and LCN2 in the supernatants was quantified by ELISA. Data presented are means ± SD of triplicate culture and are representative of one independent experiment. Statistical assessment was performed by two-way ANOVA with Dunnett's post hoc test. *$p < 0.05$, **$p < 0.01$, ***$p < 0.001$, ****$p < 0.0001$ vs medium control.

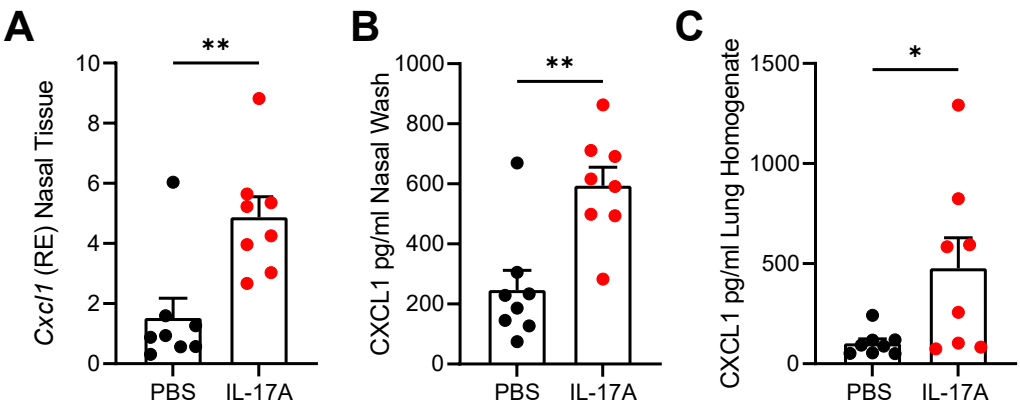

Figure 3.17 Intranasal IL-17A induces CXCL1 production in the nasal cavity and lungs.

Recombinant IL-17A (500 ng/mouse) or PBS was administered i.n. into C57BL/6 mice and nasal washes, nasal tissue, and lungs were harvested 2 hours later. *Cxcl1* mRNA expression in the nasal tissue of PBS or IL-17A treated mice was analysed by RT-PCR and normalised to 18S RNA (A). CXCL1 concentration in nasal washes (B) and lung homogenates (C) was determined by ELISA. Results shown are mean ± SEM, combined from two independent experiments (n=8 mice per group). *$p < 0.05$, **$p < 0.01$ PBS versus IL-17A by Student's t-test.

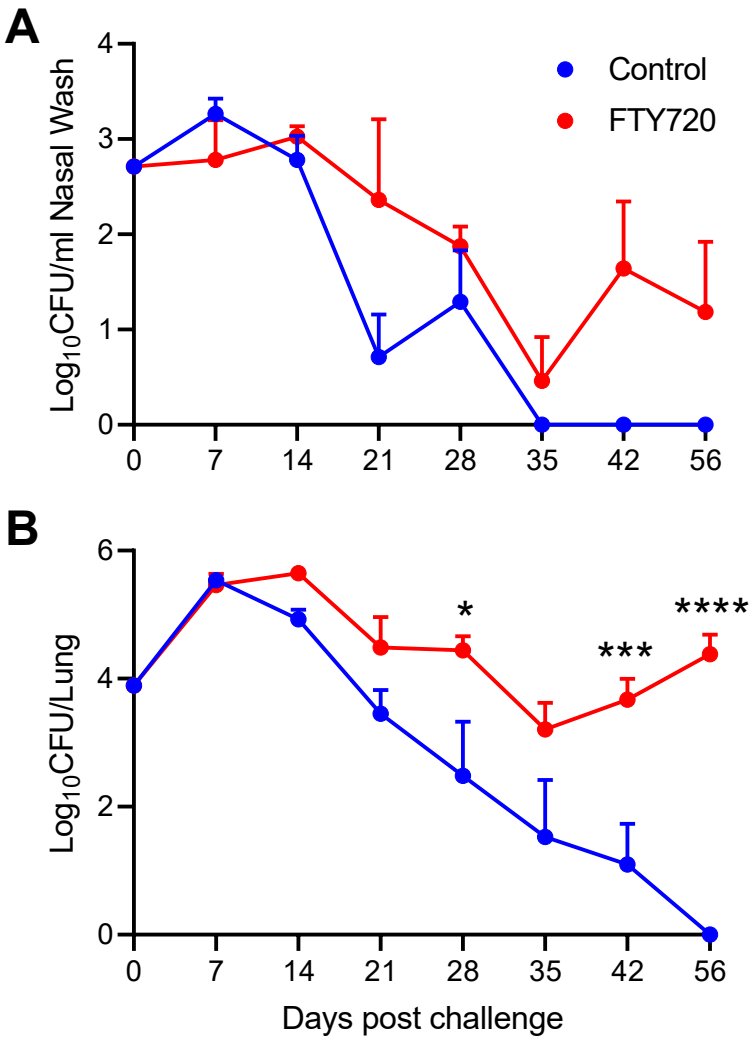

Figure 3.18 Treatment of mice with FTY720 during *B. pertussis* infection significantly delays bacterial clearance from the lungs but only moderately impairs bacterial clearance from the nasal cavity.

C57BL/6 mice were given FTY720 in drinking water for 10 days prior to and during *B. pertussis* infection. Nasal washes and lungs were harvested at selected time points and the number of viable bacteria in the nasal cavity (A) and lungs (B) was estimated by performing CFU counts on serially diluted nasal washes and lung homogenates from individual mice. Results shown are mean ± SEM CFU counts (n=4 mice per group). *$p < 0.05$, ***$p < 0.001$, ****$p < 0.0001$ control versus FTY720 treatment by two-way ANOVA followed by Sidak's post-test.

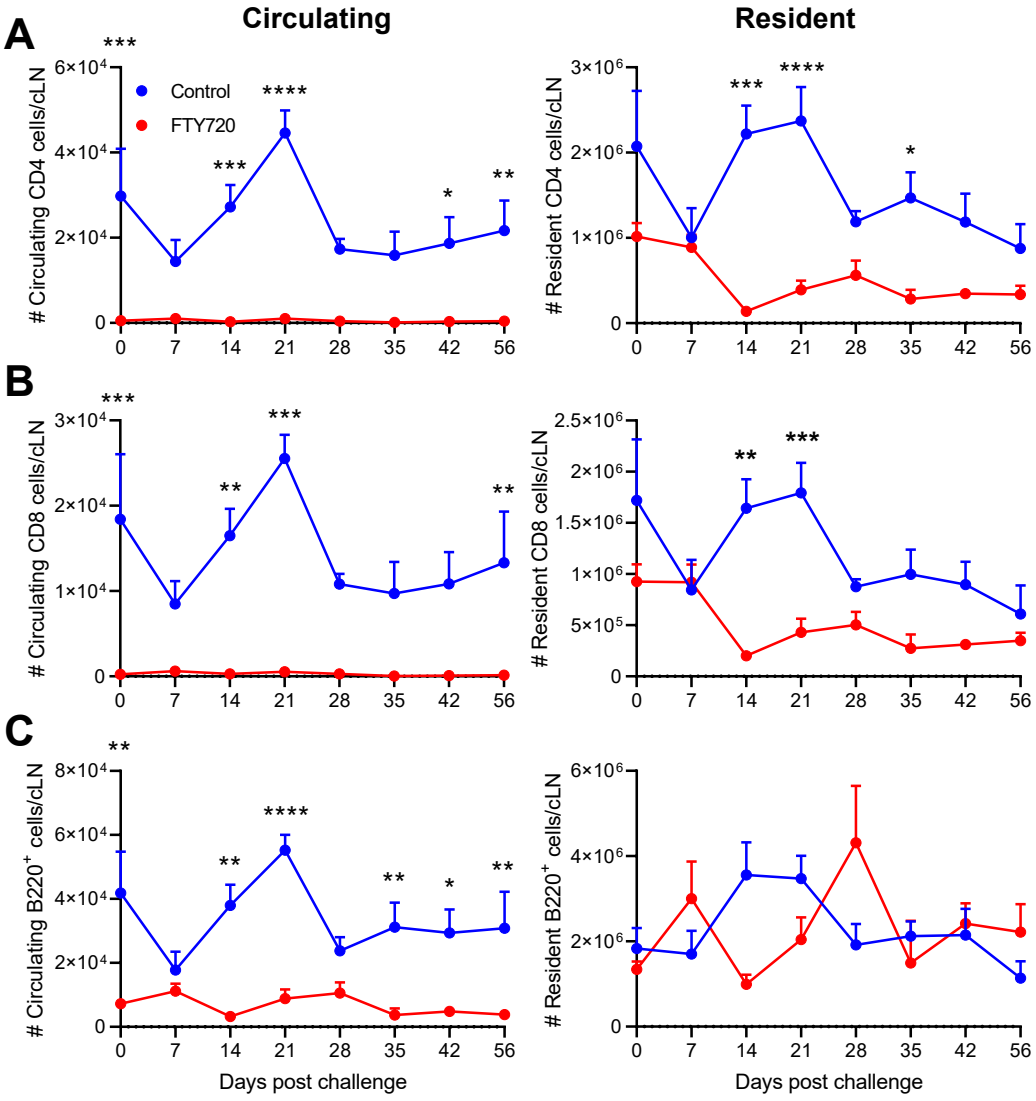

Figure 3.19 Treatment of mice with FTY720 during *B. pertussis* challenge significantly reduces the number of circulating CD4 T cells, CD8 T cells, and B220⁺ cells in the cLNs.

C57BL/6 mice were given FTY720 in drinking water for 10 days prior to and during infection with *B. pertussis*. At the indicated time points, mice were injected i.v. with a fluorochrome-labelled anti-CD45 antibody 10 min prior to euthanasia. Cell suspensions were prepared from cLNs and cells were stained for CD3, CD4, CD8, and B220 and analysed by flow cytometry. Absolute numbers of circulating (CD45 i.v.⁺) and resident (CD45 i.v.⁻) CD4 T cells (A), CD8 T cells (B), and B220⁺ cells (C) in the cLNs of untreated control and FTY720-treated mice. Data are mean ± SEM (n=4 mice per group). *$p < 0.05$, **$p < 0.01$, ***$p < 0.001$, ****$p < 0.0001$ control versus FTY720 treatment by two-way ANOVA followed by Sidak's post-test.

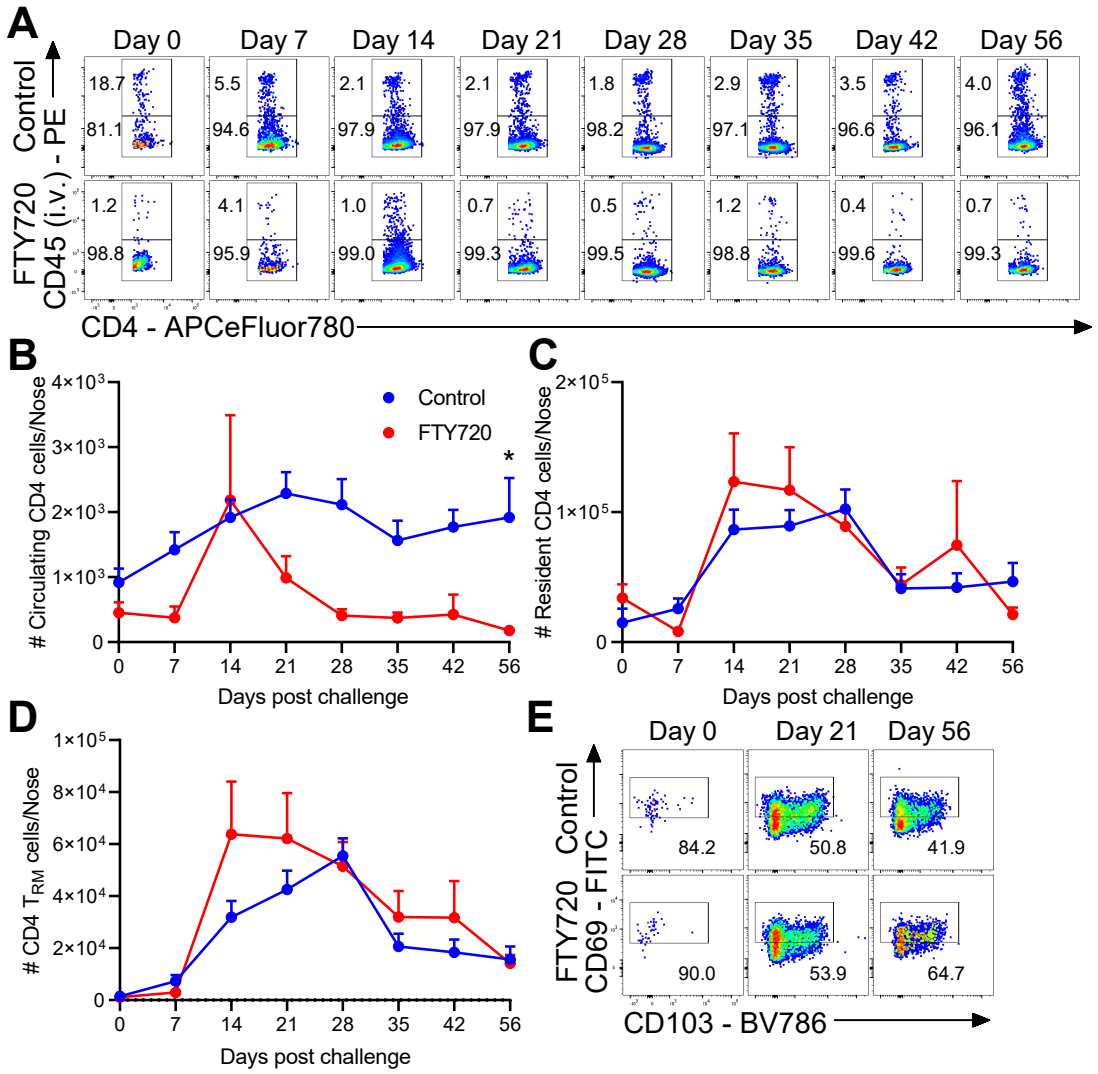

Figure 3.20 FTY720 treatment during *B. pertussis* challenge reduces circulating, but not resident, CD4 T cells in the nasal cavity and does not affect expansion of nasal CD4 T_{RM} cells in mice.

C57BL/6 mice were given FTY720 in drinking water for 10 days prior to and during infection with *B. pertussis*. At the indicated time points, mice were injected i.v. with a fluorochrome-labelled anti-CD45 antibody 10 min prior to euthanasia. Cell suspensions were prepared from nasal tissue and cells were stained for CD4, CD3, CD44, CD62L, CD69, and CD103, and analysed by flow cytometry. Representative flow cytometry plots (A) and absolute number of circulating ($CD45\ i.v.^+$) (B) and resident ($CD45\ i.v.^-$) (C) $CD4^+CD3^+$ T cells in the nasal cavity of control and FTY720-treated mice. Absolute number (D) and representative flow cytometry plots (E) of nasal CD4 T_{RM} cells ($CD4^+CD3^+CD45i.v.^-CD44^+CD62L^-CD69^+CD103^\pm$). Results shown are mean ± SEM (n=4 mice per group). *$p < 0.05$ control versus FTY720 treatment by two-way ANOVA followed by Sidak's post-test.

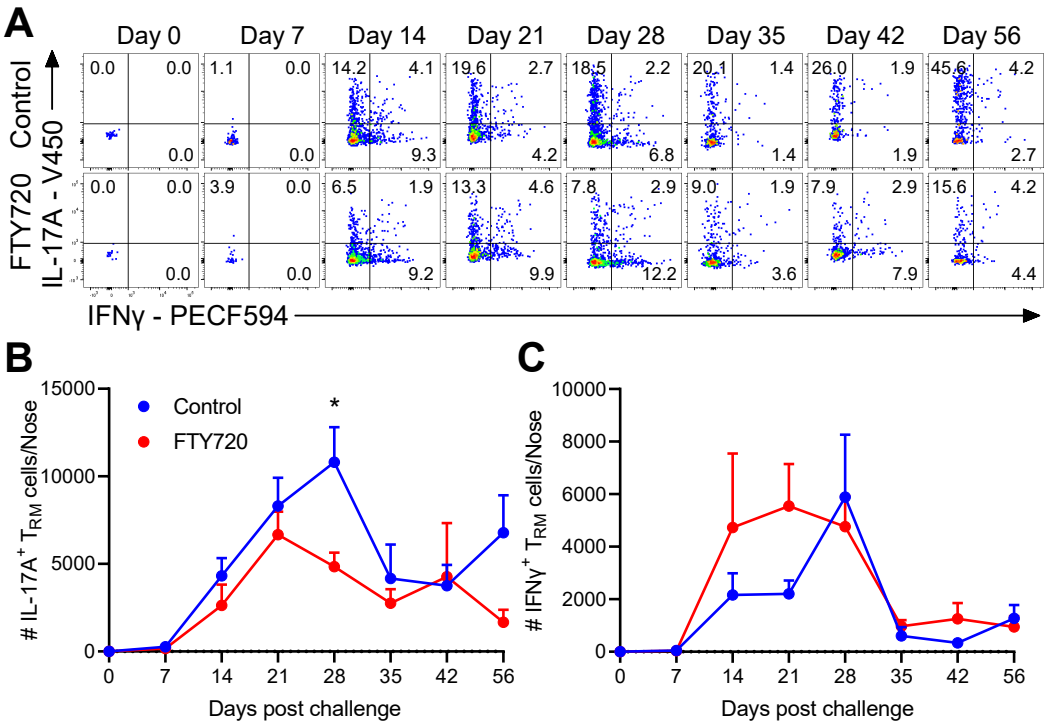

Figure 3.21 Continuous FTY720 treatment during *B. pertussis* challenge reduces the number of *B. pertussis*-specific IL-17A$^+$ CD4 T_{RM} cells in the nasal cavity.

C57BL/6 mice were given FTY720 in drinking water for 10 days prior to and during infection with *B. pertussis*. At the indicated time points, mice were injected i.v. with a fluorochrome-labelled anti-CD45 antibody 10 min prior to euthanasia. Cell suspensions were prepared from nasal tissue and cells were stimulated with sBP (5 µg/ml) and anti-CD28 and anti-CD49d for 20 hours. Brefeldin A (5 µg/ml) was added for the final 4 hours of culture. Cells were stained for surface CD4, CD3, CD44, CD62L, CD69, CD103, and intracellular IL-17 and IFNγ, and analysed by flow cytometry. Representative flow cytometry plots (A) and absolute number of IL-17A$^+$ (B) and IFNγ$^+$ (C) CD4 T_{RM} cells (CD4$^+$CD3$^+$CD45i.v.$^-$CD44$^+$CD62L$^-$CD69$^+$CD103$^\pm$) in the nasal cavity of control and FTY720-treated mice. Results shown are mean ± SEM (n=4 mice per group). *$p < 0.05$ control versus FTY720 treatment by two-way ANOVA followed by Sidak's post-test.

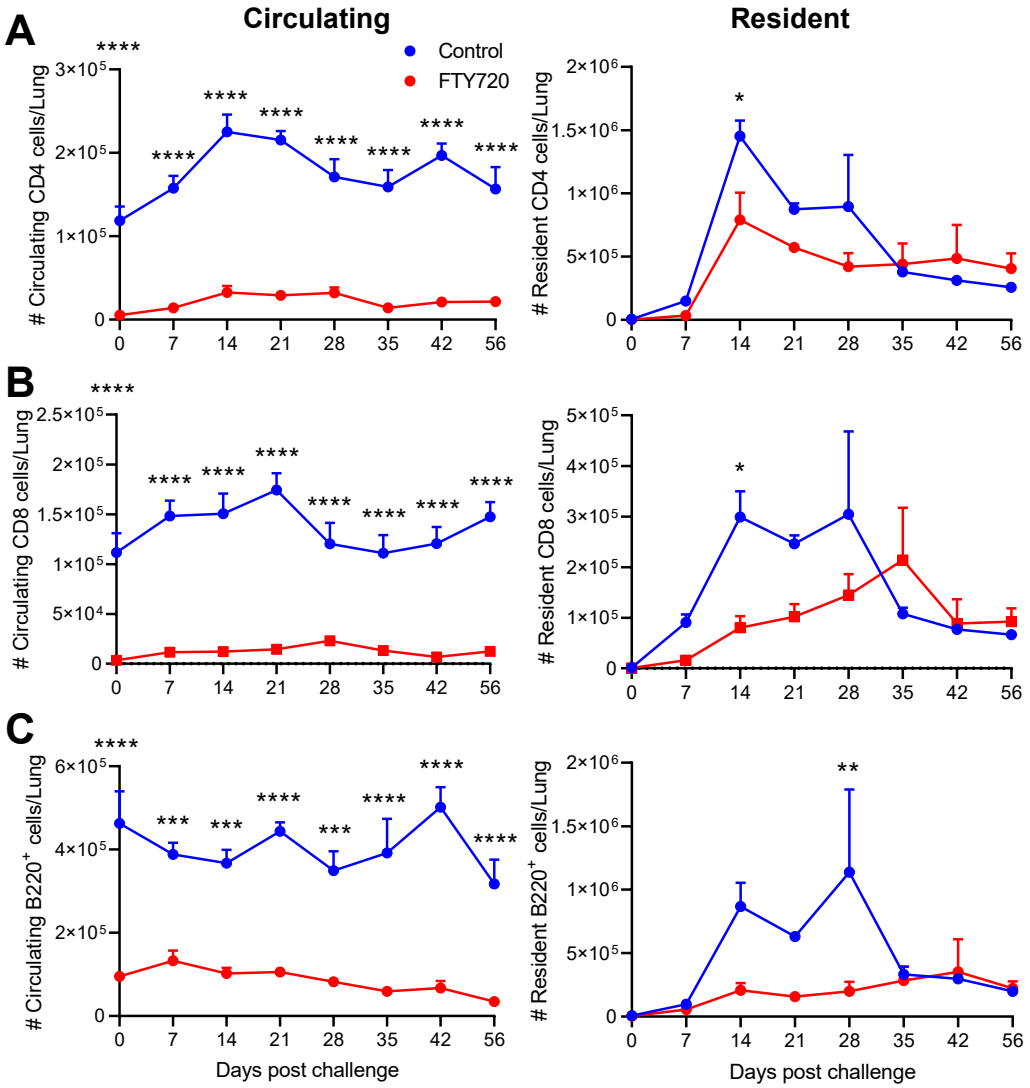

Figure 3.22 FTY720 treatment during *B. pertussis* challenge reduces circulating and tissue-resident CD4 T cells, CD8 T cells, and B220⁺ cells in the lungs of mice.

C57BL/6 mice were treated orally with FTY720 for 10 days prior to and during infection with *B. pertussis*. At the indicated time points, mice received an i.v. injection of fluorochrome-conjugated anti-CD45 antibody 10 min prior to euthanasia. Lungs were harvested and mononuclear cells were isolated and stained for CD3, CD4, CD8, and B220, and analysed by flow cytometry. Absolute numbers of circulating (CD45 i.v.⁺) and resident (CD45 i.v.⁻) CD4 T cells (A), CD8 T cells (B), and B220⁺ (C) cells in the lungs of control and FTY720-treated mice. Data are mean ± SEM (n=4 mice per group). **p* < 0.05, ***p* < 0.01, ****p* < 0.001, *****p* < 0.0001 control versus FTY720 treatment by two-way ANOVA followed by Sidak's post-test.

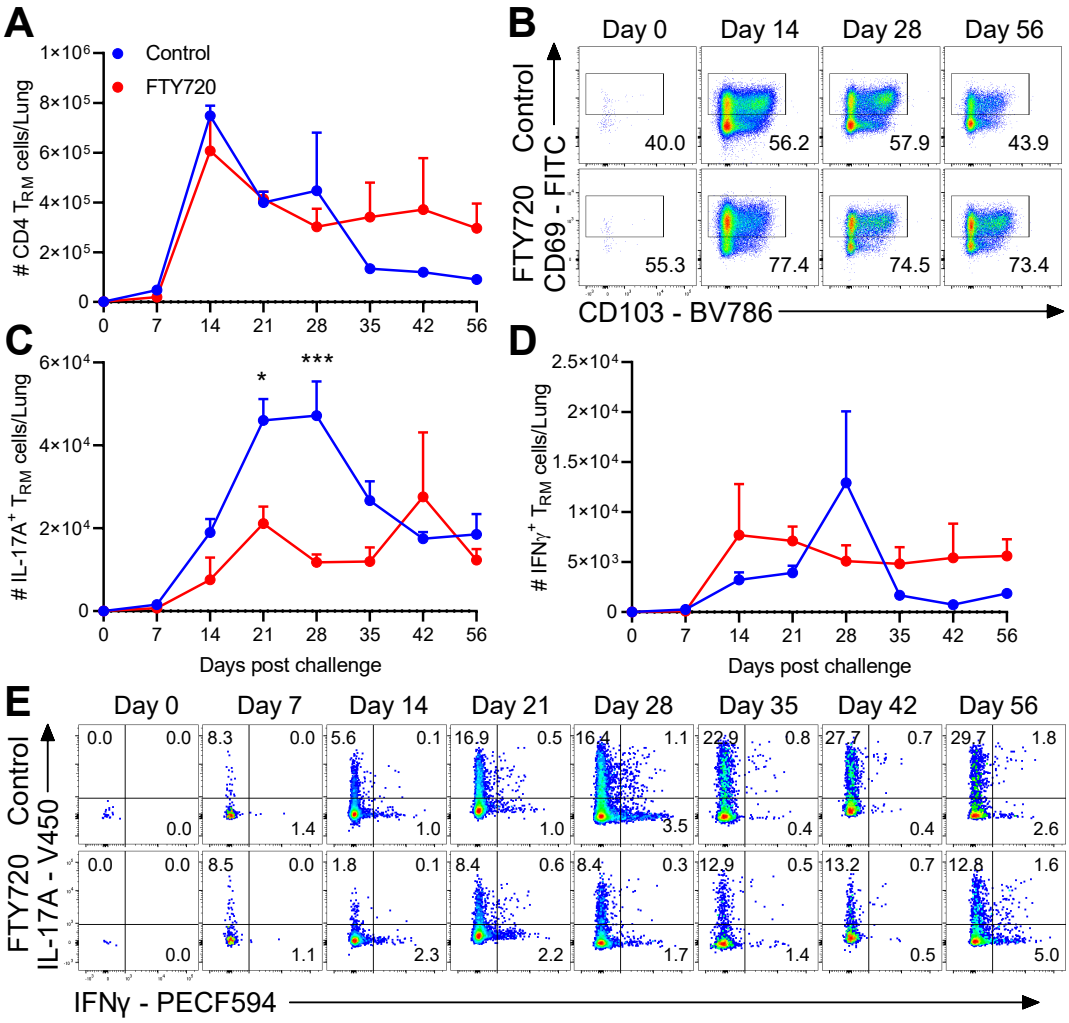

Figure 3.23 FTY720 treatment during *B. pertussis* challenge does not affect the expansion of total CD4 T_{RM} cells but significantly reduces the number of pathogen-specific IL-17A$^+$ CD4 T_{RM} cells in the lungs.

C57BL/6 mice were treated orally with FTY720 for 10 days prior to and during infection with *B. pertussis*. At the indicated time points, mice were injected i.v. with a fluorochrome-conjugated anti-CD45 antibody and euthanised 10 min later. Cell suspensions were prepared from lungs and cells were stained for CD4, CD3, CD44, CD62L, CD69, and CD103, and analysed by flow cytometry. Absolute number (A) and representative flow cytometry plots (B) of unstimulated lung CD4 T_{RM} cells (CD4$^+$CD3$^+$CD45i.v.$^-$CD44$^+$CD62L$^-$CD69$^+$CD103$^\pm$). Mononuclear cells isolated from lungs were stimulated with sBP (5 µg/ml) and anti-CD28 and anti-CD49d for 20 hours, with brefeldin A (5 µg/ml) added for the final 4 hours of culture. Cells were stained for surface CD4, CD3, CD44, CD62L, CD69, CD103, and intracellular IL-17A and IFNγ, and analysed by flow cytometry. Absolute number of IL-17A$^+$ (C) and IFNγ$^+$ (D) CD4 T_{RM} cells in the lungs of control and FTY720-treated mice with representative flow cytometry plots (E). Results shown are mean ± SEM (n=4 mice per group). *p < 0.05, ***p < 0.001 control versus FTY720 treatment by two-way ANOVA followed by Sidak's post-test.

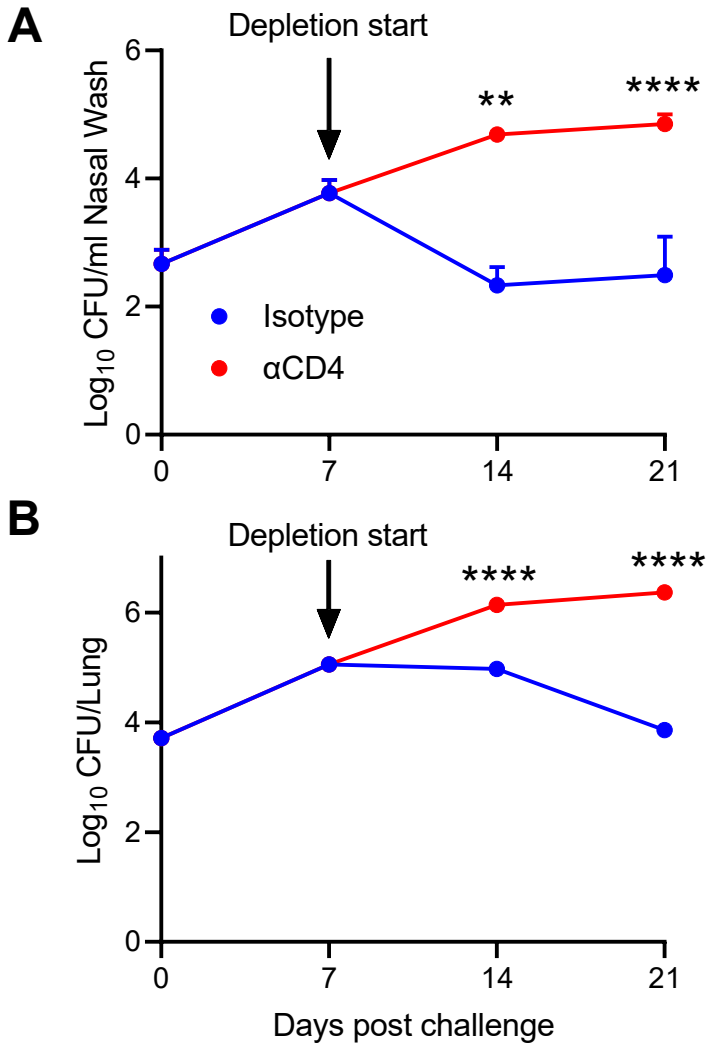

Figure 3.24 Depleting CD4 T cells during an active *B. pertussis* infection significantly delays clearance of *B. pertussis* from the nasal cavity and lungs.

C57BL/6 mice were aerosol challenged with live *B. pertussis*. Mice were treated with a depleting anti-CD4 antibody or isotype control administered both i.p. (200 µg/mouse) and i.n. (50 µg/mouse) on days 7, 11, 15 and 19 post challenge. The number of viable bacteria in the nasal cavity (A) and lungs (B) was estimated by performing CFU counts on serially diluted nasal washes and lung homogenates from individual mice on days 7, 14, and 21 post challenge. Results shown are mean ± SEM CFU counts (n=6 per group). $^{**}p < 0.01$, $^{****}p < 0.0001$ isotype control versus anti-CD4 treatment by two-way ANOVA followed by Sidak's post-test.

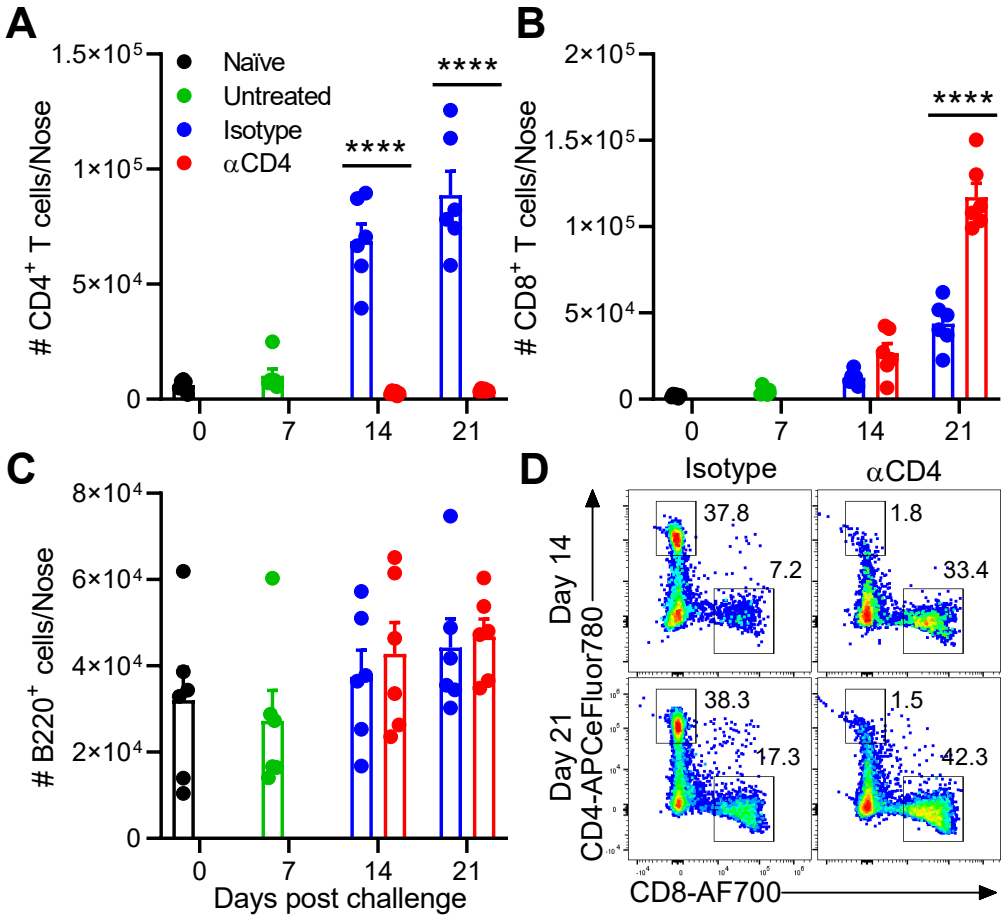

Figure 3.25 Depletion of CD4 T cells is accompanied by increased CD8 T cells, but not B220⁺ cells, in the nasal cavity during *B. pertussis* infection.

C57BL/6 mice were aerosol challenged with live *B. pertussis* and treated with a depleting anti-CD4 antibody or isotype control administered both i.p. (200 µg/mouse) and i.n. (50 µg/mouse) on days 7, 11, 15 and 19 post challenge. Untreated mice which did not receive an anti-CD4 antibody or isotype control were also infected with *B. pertussis*. Nasal tissue was harvested at indicated time points and mononuclear cells were isolated and stained for surface CD3, CD4, CD8, and B220, and analysed by flow cytometry. Absolute number of CD4⁺ (A), CD8⁺ (B), and B220⁺ (C) cells in the nasal tissue with representative flow cytometry plots of CD4 and CD8 populations (gated on CD3⁺ cells) (D). Data are mean ± SEM (n=4-6/group). ****$p < 0.0001$ isotype control versus anti-CD4 treatment by two-way ANOVA followed by Sidak's post-test.

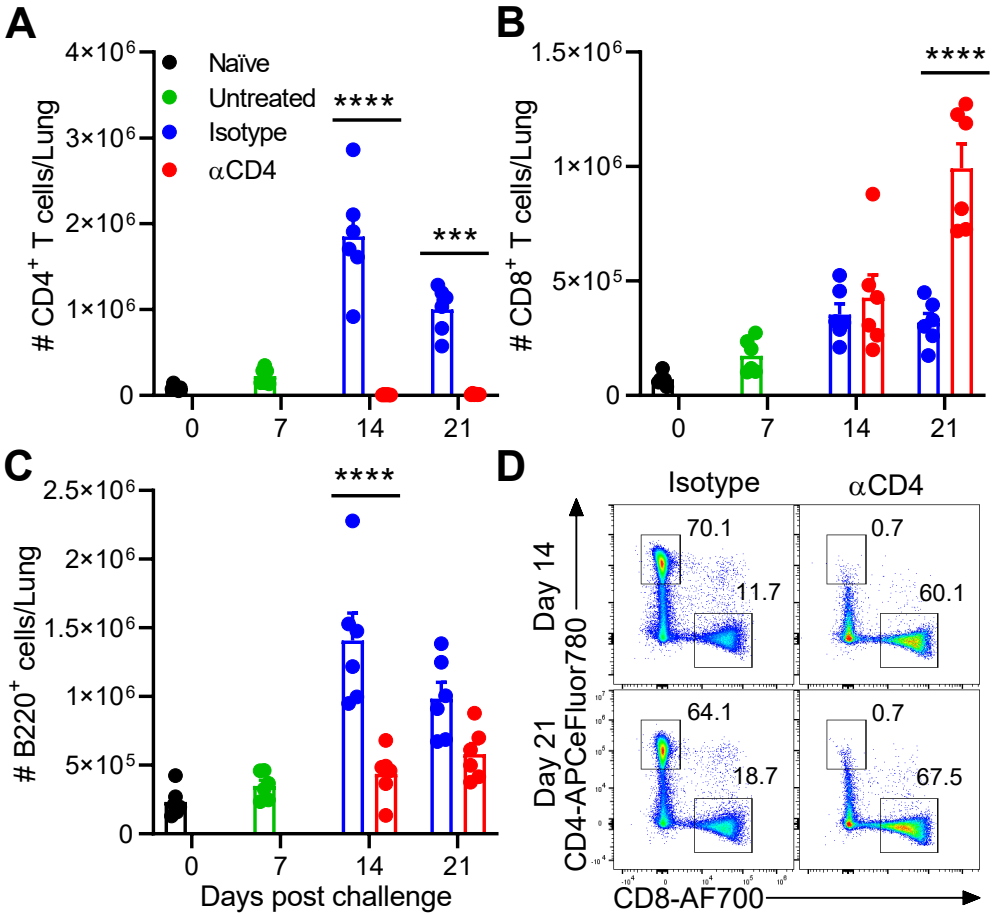

Figure 3.26 Depletion of CD4 T cells is accompanied by increased CD8 T cells and reduced B220⁺ cells in the lungs during *B. pertussis* infection.

C57BL/6 mice were aerosol challenged with live *B. pertussis* and treated with a depleting anti-CD4 antibody or isotype control administered both i.p. (200 µg/mouse) and i.n. (50 µg/mouse) on days 7, 11, 15, and 19 post challenge. Untreated mice which did not receive an anti-CD4 antibody or isotype control were also infected with *B. pertussis*. Lungs were harvested at indicated time points and mononuclear cells were isolated and stained for surface CD3, CD4, CD8, and B220, and analysed by flow cytometry. Absolute numbers of CD4⁺ (A), CD8⁺ (B), and B220⁺ (C) cells in the lungs with representative flow cytometry plots of CD4 and CD8 populations (gated on CD3⁺ cells) (D). Data are mean ± SEM (n=4-6/group). ***$p < 0.001$, ****$p < 0.0001$ isotype control versus anti-CD4 treatment by two-way ANOVA followed by Sidak's post-test.

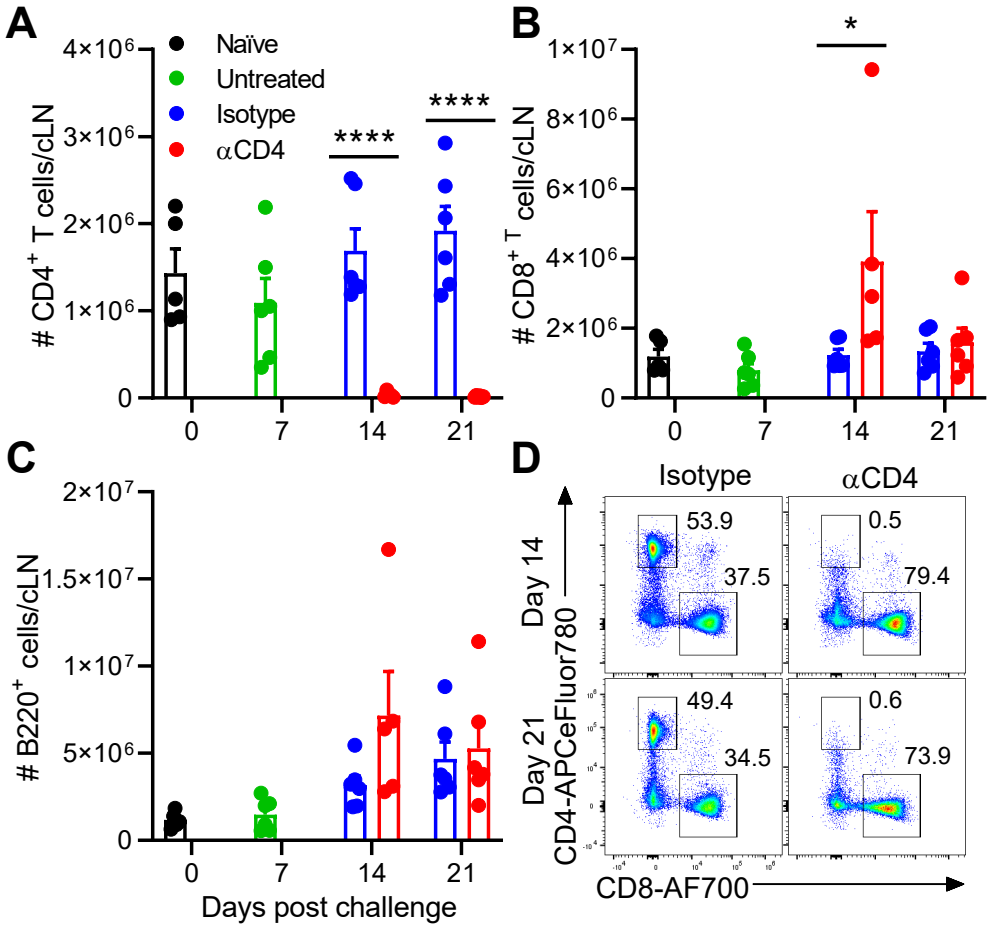

Figure 3.27 Depletion of CD4 T cells is accompanied by increased CD8 T cells in the cLNs nodes during *B. pertussis* infection.

C57BL/6 mice were aerosol challenged with live *B. pertussis* and treated with a depleting anti-CD4 antibody or isotype control administered both i.p. (200 µg/mouse) and i.n. (50 µg/mouse) on days 7, 11, 15, and 19 post challenge. Untreated mice which did not receive an anti-CD4 antibody or isotype control were also infected with *B. pertussis*. cLNs were harvested at indicated time points and mononuclear cells were isolated and stained for surface CD3, CD4, CD8, and B220, and analysed by flow cytometry. Absolute number of total CD4⁺ (A), CD8⁺ (B), and B220⁺ (C) cells in the cLNs over the course of infection. Representative flow cytometry plots of CD4⁺ and CD8⁺ cells, pre-gated on total CD3⁺ cells (D). Results shown are mean ± SEM (n=4-6/group). *$p < 0.05$, ****$p < 0.0001$ isotype control versus anti-CD4 treatment by two-way ANOVA followed by Sidak's post-test.

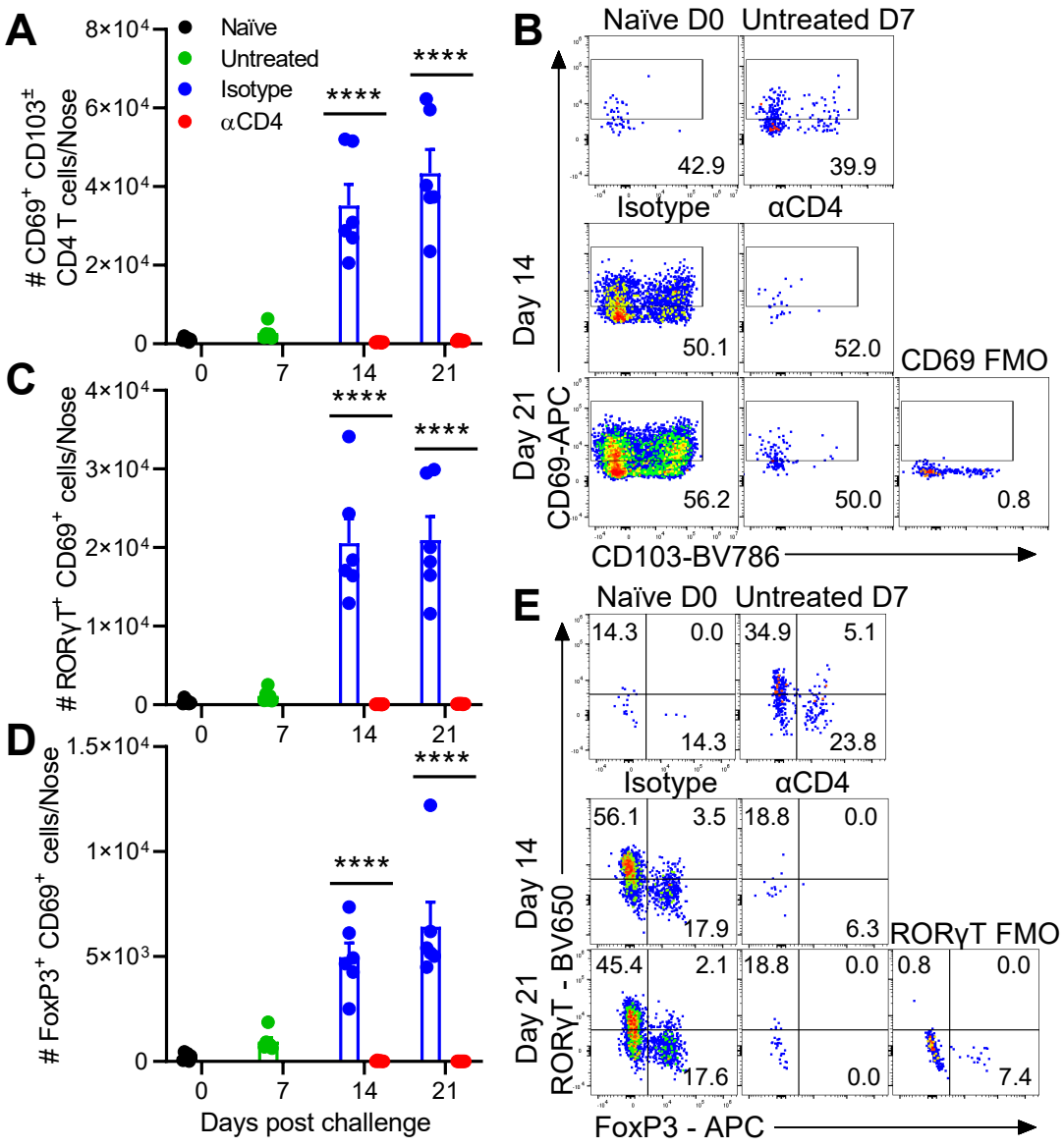

Figure 3.28 Reduced number of total CD4 T_{RM} cells and RORγT$^+$ and Foxp3$^+$ T_{RM} cells in the nasal cavity of mice treated with depleting anti-CD4 antibody during *B. pertussis* infection.

C57BL/6 mice were aerosol challenged with live *B. pertussis* and treated with a depleting anti-CD4 antibody or isotype control administered both i.p. (200 µg/mouse) and i.n. (50 µg/mouse) on days 7, 11, 15, and 19 post challenge. Untreated mice which did not receive an anti-CD4 antibody or isotype control were also infected with *B. pertussis*. At selected time points, mice were injected i.v. with fluorochrome-labelled anti-CD45 antibody and euthanised 10 min later. Cell suspensions were prepared from nasal tissue and cells were stained for surface CD3, CD4, CD44, CD62L, CD69, and CD103, and intracellular RORγT and Foxp3, and analysed by flow cytometry. Absolute number (A) and representative flow cytometry plots (B) of nasal CD4 T_{RM} cells (CD4$^+$CD8$^-$ CD3$^+$CD45i.v.$^-$CD44$^+$CD62L$^-$CD69$^+$CD103$^±$). Absolute numbers of nasal RORγT$^+$ (C) and Foxp3$^+$ (D) CD4 T_{RM} cells with representative flow cytometry plots (E). Results shown are mean ± SEM (n=4-6/group). ****$p < 0.0001$ isotype control versus anti-CD4 treatment by two-way ANOVA followed by Sidak's post-test.

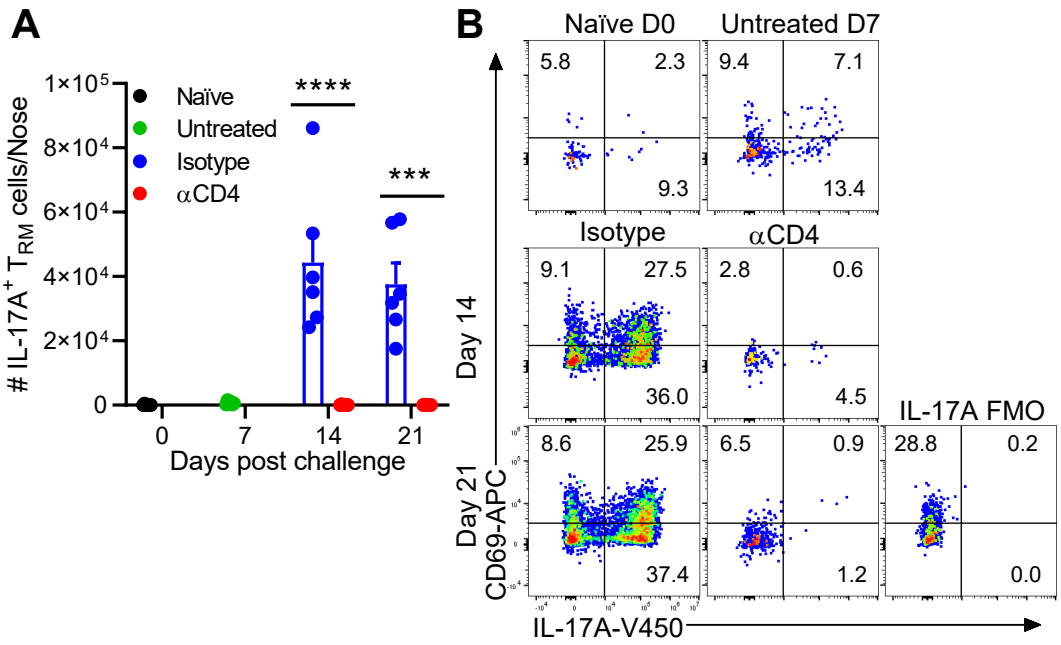

Figure 3.29 Reduced number of IL-17A-producing CD4 T_{RM} cells in the nasal cavity of mice treated with a depleting anti-CD4 antibody during *B. pertussis* infection.

C57BL/6 mice were aerosol challenged with live *B. pertussis* and treated with a depleting anti-CD4 antibody or isotype control administered both i.p. (200 µg/mouse) and i.n. (50 µg/mouse) on days 7, 11, 15, and 19 post challenge. Untreated mice which did not receive an anti-CD4 antibody or isotype control were also infected with *B. pertussis*. At selected time points, mice were injected i.v. with fluorochrome-labelled anti-CD45 antibody and euthanised 10 min later. Mononuclear cells were isolated from nasal tissue and stimulated with PMA (50 ng/ml), ionomycin (500 ng/ml), and brefeldin A (5 µg/ml) for 4 hours. Cells were stained for surface CD4, CD3, CD44, CD69, and intracellular IL-17A, and analysed by flow cytometry. Absolute number (A) and representative flow cytometry plots (B) of nasal IL-17A$^+$CD69$^+$ CD4 T_{RM} cells (pre-gated on CD4$^+$CD3$^+$CD45i.v.$^-$CD44$^+$ cells). Data are mean ± SEM (n=4-6/group). ***p < 0.001, ****p < 0.0001 isotype control versus anti-CD4 treatment by two-way ANOVA followed by Sidak's post-test.

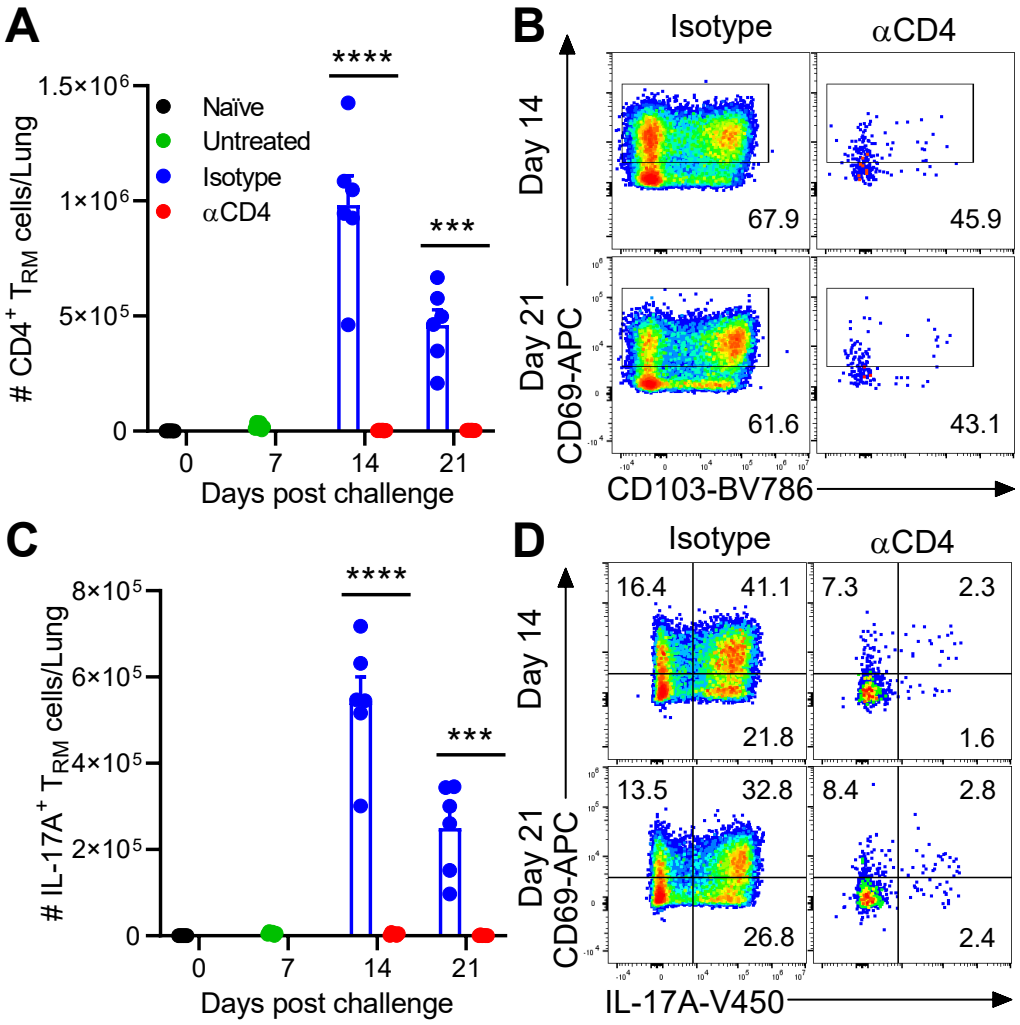

Figure 3.30 Reduced number of CD4 T_{RM} cells and IL-17A-producing CD4 T_{RM} cells in the lungs of mice treated with a depleting anti-CD4 antibody during *B. pertussis* infection.

C57BL/6 mice were aerosol challenged with live *B. pertussis* and treated with a depleting anti-CD4 antibody or isotype control administered both i.p. (200 µg/mouse) and i.n. (50 µg/mouse) on days 7, 11, 15, and 19 post challenge. Untreated mice which did not receive an anti-CD4 antibody or isotype control were also infected with *B. pertussis*. At selected time points, mice were injected i.v. with fluorochrome-labelled anti-CD45 antibody and euthanised 10 min later. Mononuclear cells were isolated from lungs and cells were stimulated with PMA (50 ng/ml), ionomycin (500 ng/ml), and brefeldin A (5 µg/ml) for 4 hours. Cells were stained for surface CD4, CD3, CD44. CD69, and intracellular IL-17A, and analysed by flow cytometry. Absolute number (A) and representative flow cytometry plots (B) of unstimulated lung CD4 T_{RM} cells ($CD4^+CD3^+CD45i.v.^-CD44^+CD62L^-CD69^+CD103^±$). Absolute number (C) and representative flow cytometry plots (C) of lung IL-17A$^+$CD69$^+$ CD4 T_{RM} cells (gated on $CD4^+CD3^+CD45i.v.^-CD44^+$ cells). Results shown are mean ± SEM (n=4-6/group). ****p < 0.0001 isotype control versus anti-CD4 treatment by two-way ANOVA followed by Sidak's post-test.

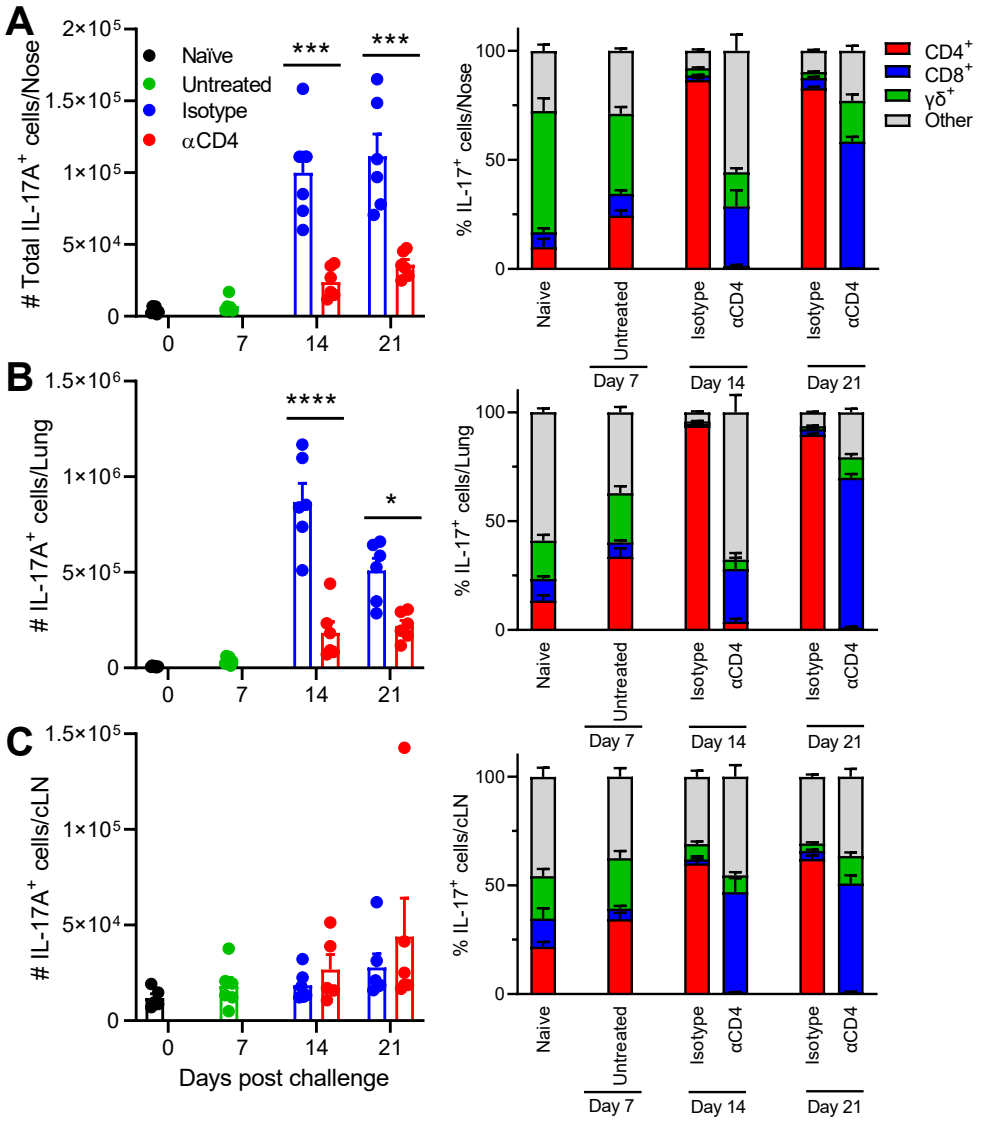

Figure 3.31 CD4 T cells are the dominant source of IL-17A in the nasal cavity, lungs, and cLNs during primary *B. pertussis* infection, however CD8 T cells are the dominant source in the absence of CD4 T cells.

C57BL/6 mice were aerosol challenged with live *B. pertussis* and treated with a depleting anti-CD4 antibody or isotype control administered both i.p. (200 µg/mouse) and i.n. (50 µg/mouse) on days 7, 11, 15, and 19 post challenge. Untreated mice which did not receive an anti-CD4 antibody or isotype control were also infected with *B. pertussis*. Cell suspensions were prepared from nasal tissue, lungs, and cLNs, at indicated time points and cells were stimulated with PMA (50 ng/ml), ionomycin (500 ng/ml), and Brefeldin A (5 µg/ml) for 4 hours. Cells were stained for surface CD3, CD4, CD8, γδ, and intracellular IL-17A, and analysed by flow cytometry. Absolute number of IL-17A$^+$ cells, gated on total live cells, with frequencies of CD4$^+$, CD8$^+$, and γδ$^+$ cells, gated on the total IL-17A$^+$ cells, in the nose (A), lungs (B), and cLNs (C). Data are mean ± SEM (n=4-6/group). *$p < 0.05$, ***$p < 0.001$. ***$p < 0.0001$ isotype control versus anti-CD4 treatment by two-way ANOVA followed by Sidak's post-test.

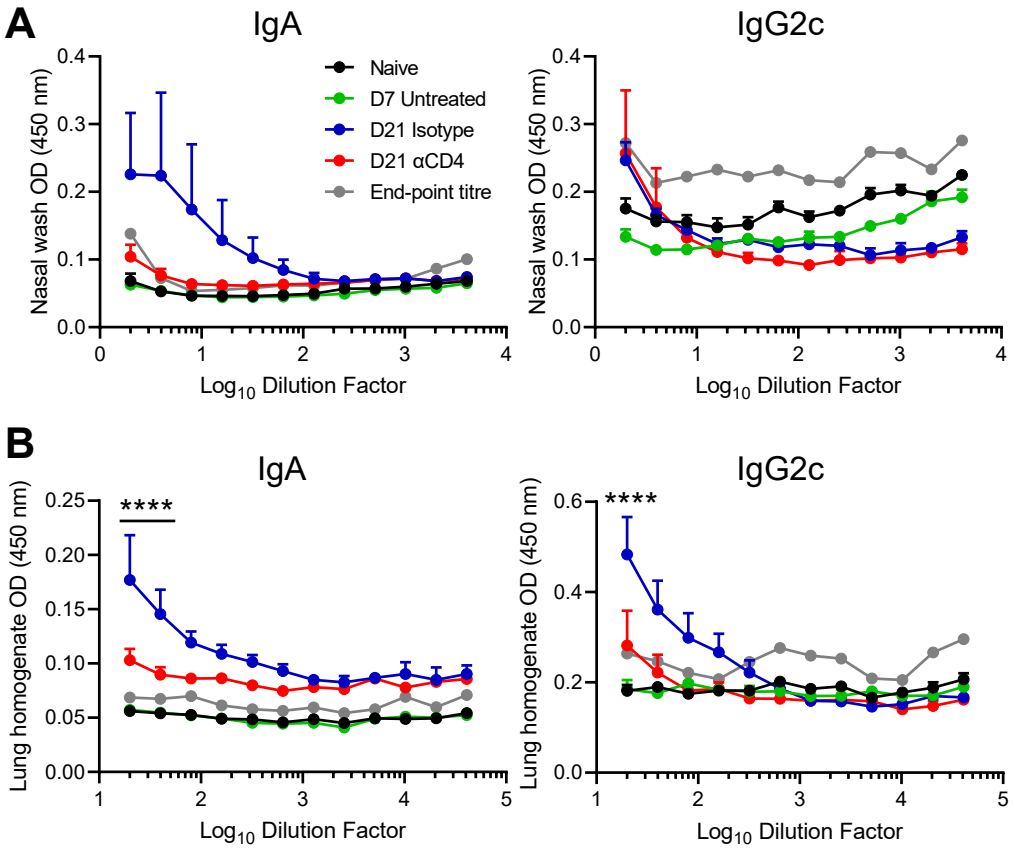

Figure 3.32 *B. pertussis*-specific antibody responses are significantly reduced in the lungs following treatment with a depleting anti-CD4 antibody.

C57BL/6 mice were aerosol challenged with live *B. pertussis* and treated with a depleting anti-CD4 antibody or isotype control administered both i.p. (200 µg/mouse) and i.n. (50 µg/mouse) on days 7, 11, 15, and 19 post challenge. Untreated mice which did not receive an anti-CD4 antibody or isotype control were also infected with *B. pertussis*. *B. pertussis*-specific IgA and IgG2c antibody titres were quantified in nasal washes (A) and lung homogenates (B) from individual mice by ELISA. Results shown are mean ± SEM (n=4-6/group). ****$p < 0.0001$ isotype control versus anti-CD4 treatment by two-way ANOVA followed by Sidak's post-test.

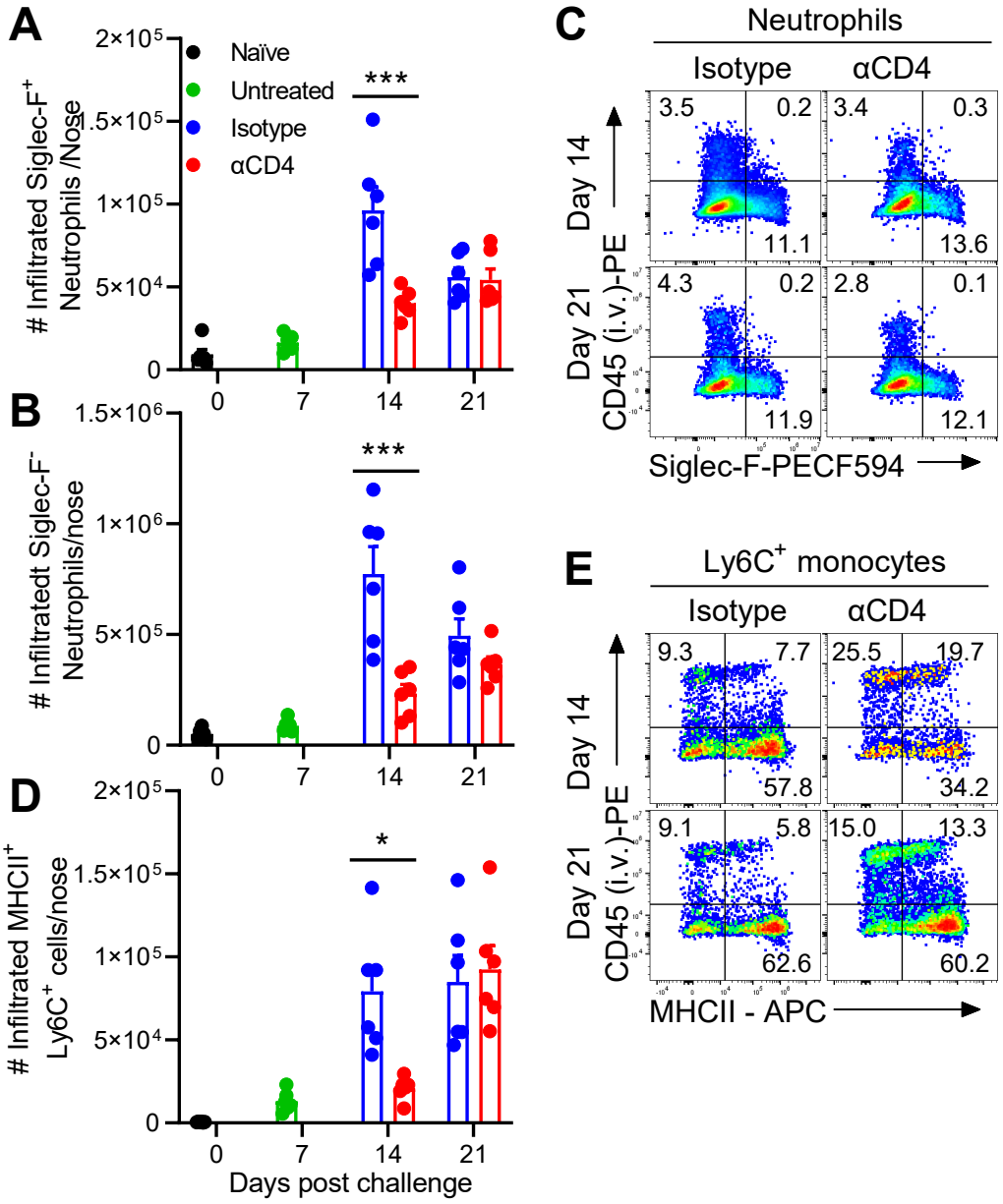

Figure 3.33 Anti-CD4 treatment reduces the infiltration of Siglec-F⁺ neutrophils, conventional neutrophils, and MHCII⁺Ly6C⁺ monocytes into the nasal cavity during *B. pertussis* infection.

C57BL/6 mice were infected with live *B. pertussis* and treated with a depleting anti-CD4 antibody or isotype control administered both i.p. (200 µg/mouse) and i.n. (50 µg/mouse) on days 7, 11, 15, and 19 post challenge. Untreated mice which did not receive an anti-CD4 antibody or isotype control were also infected with *B. pertussis*. At the indicated time points, mice were injected i.v. with fluorochrome-labelled anti-CD45 antibody and euthanised 10 min later. Nasal tissue was harvested and mononuclear cells were isolated and stained for CD11b, Ly6G, Ly6C, Siglec-F, and MHCII and analysed by flow cytometry. Absolute number of infiltrated (CD45 i.v.⁻) Siglec-F⁺ (A) and Siglec-F⁻ (B) neutrophils (Ly6G⁺CD11b⁺) with representative flow cytometry plots (C). Absolute numbers (D) and representative flow cytometry plots (E) of tissue-infiltrated MHCII⁺Ly6C⁺CD11b⁺ monocytes in the nasal cavity. Data are mean ± SEM (n=4-6/group). *$p < 0.05$, ***$p < 0.001$ isotype control versus anti-CD4 treatment by two-way ANOVA followed by Sidak's post-test.

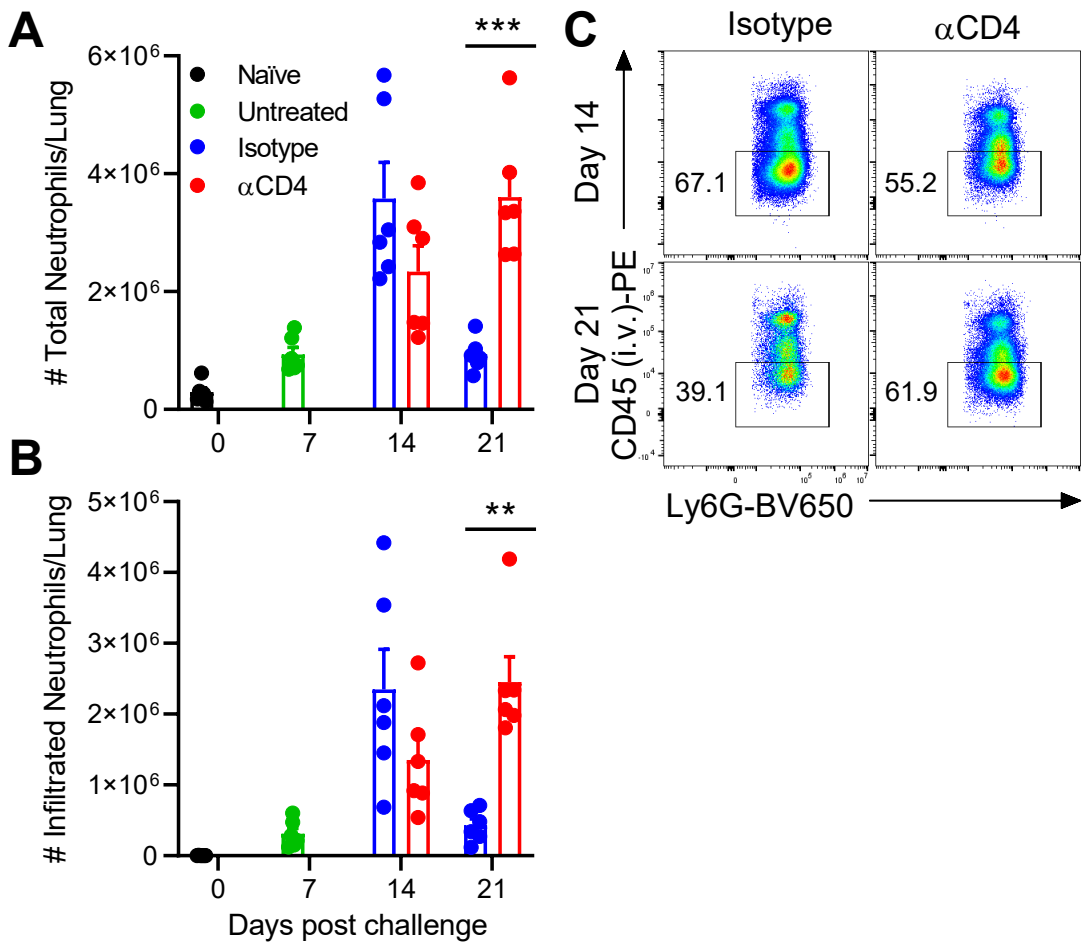

Figure 3.34 Depletion of CD4 T cells initially delays, then significantly enhances, neutrophil recruitment to the lungs during *B. pertussis* infection.

C57BL/6 mice were aerosol challenged with live *B. pertussis* and treated with a depleting anti-CD4 antibody or isotype control administered both i.p. (200 µg/mouse) and i.n. (50 µg/mouse) on days 7, 11, 15, and 19 post challenge. Untreated mice which did not receive an anti-CD4 antibody or isotype control were also infected with *B. pertussis*. At the indicated time points, mice were injected with fluorochrome-labelled anti-CD45 i.v. and euthanised 10 min later. Lungs were harvested and monocuclear cells were isolated and stained for surface CD11b and Ly6G, and analysed by flow cytometry. Absolute number of total (A) and lung-infiltrated (CD45 i.v.$^-$) (B) neutrophils with corresponding representative flow cytometry plots (C). Data are mean ± SEM (n=4-6/group). $^{**}p < 0.01$, $^{***}p < 0.001$ isotype control versus anti-CD4 treatment by two-way ANOVA followed by Sidak's post-test.

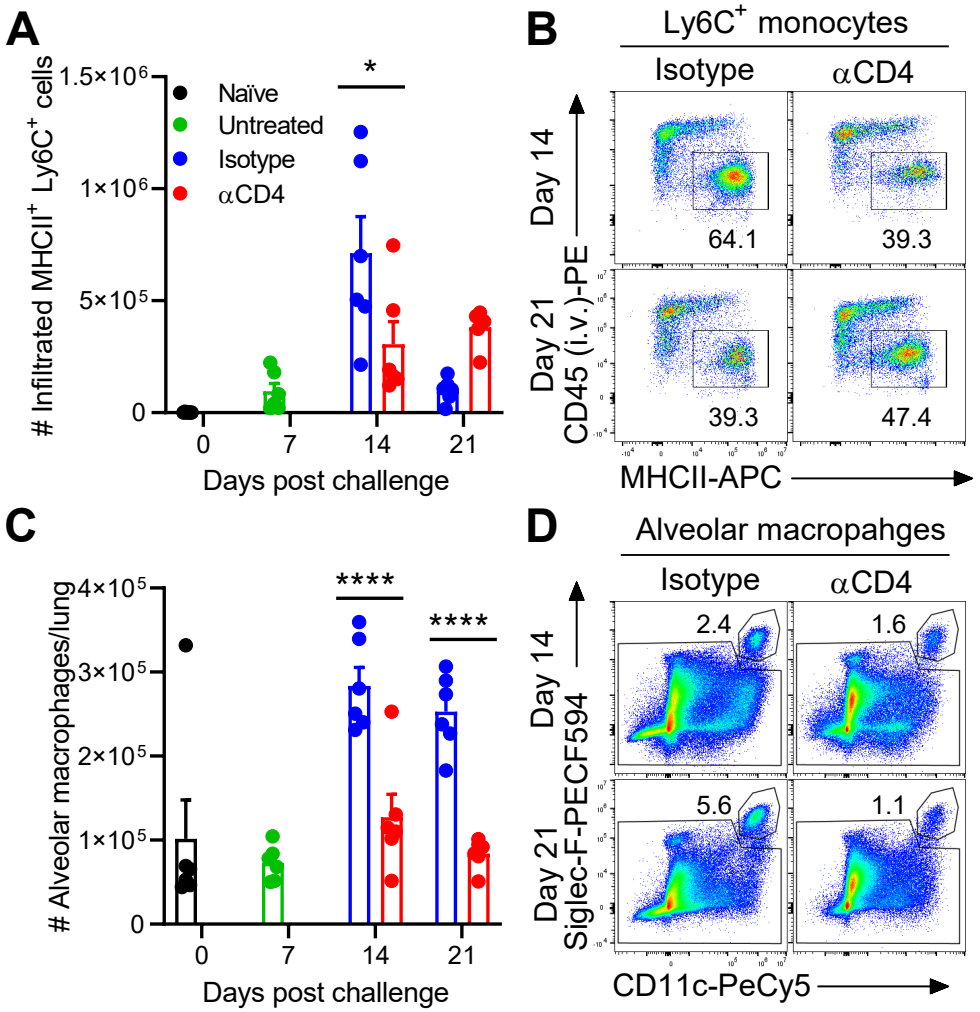

Figure 3.35 Depletion of CD4 T cells reduces the number of infiltrated MHCII$^+$Ly6C$^+$ monocytes and alveolar macrophages in the lungs during *B. pertussis* infection.

C57BL/6 mice were aerosol challenged with live *B. pertussis* and treated with a depleting anti-CD4 antibody or isotype control administered both i.p. (200 µg/mouse) and i.n. (50 µg/mouse) on days 7, 11, 15, and 19 post challenge. Untreated mice which did not receive an anti-CD4 antibody or isotype control were also infected with *B. pertussis*. At selected time points, mice were injected with fluorochrome-labelled anti-CD45 antibody i.v. 10 min prior to euthanasia. Lungs were harvested and mononuclear cells were isolated and stained for CD11b, Ly6C, MHCII, CD11c, and Siglec-F, and analysed by flow cytometry. Absolute number (A) and representative flow cytometry plots (B) of lung-infiltrated (CD45 i.v.$^-$) MHCII$^+$Ly6C$^+$CD11b$^+$ cells. Absolute number (C) and representative flow cytometry plots (D) of alveolar macrophages (Siglec-F$^+$ CD11c$^+$). Results shown are mean ± SEM (n=4-6/group). *$p < 0.05$, ****$p < 0.0001$ isotype control versus anti-CD4 treatment by two-way ANOVA followed by Sidak's post-test.

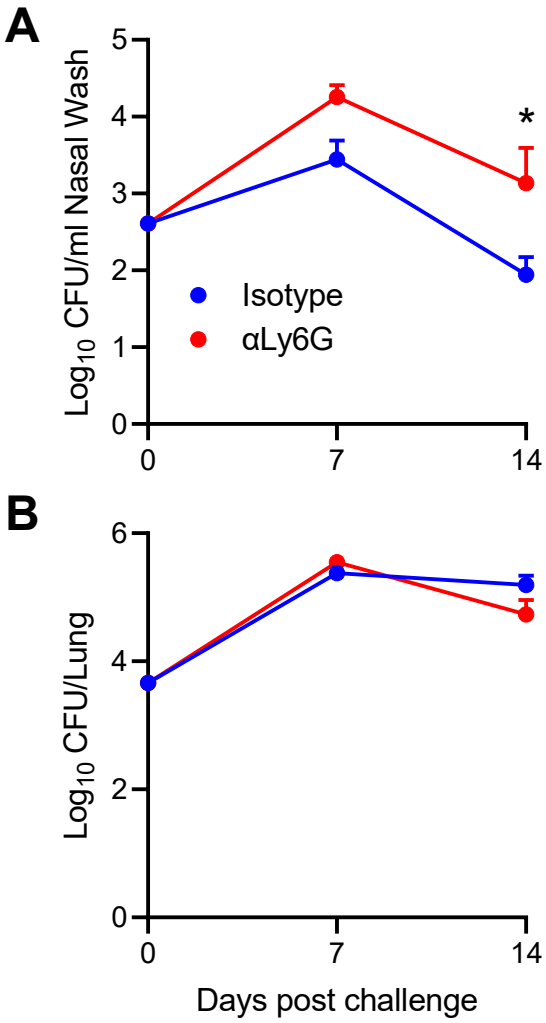

Figure 3.36 Mice treated with a depleting anti-Ly6G antibody at the onset of *B. pertussis* infection have significantly delayed bacterial cleared from the nasal cavity but not from the lungs.

C57BL/6 mice were injected i.p. with a depleting anti-Ly6G antibody (100 µg/mouse) or corresponding isotype control 1 day prior to and every day after *B. pertussis* challenge. Every second day, anti-Ly6G- or isotype control-treated mice received an i.p. injection of a secondary antibody specific for the rat kappa immunoglobulin (100 µg/mouse). The number of viable bacteria in the nasal cavity (A) and lungs (B) was estimated by performing CFU counts on serially diluted nasal washes and lung homogenates from individual mice on days 7 and 14 post challenge. Results shown are mean ± SEM CFU counts (n=4 mice per group). *$p < 0.05$ isotype control versus anti-Ly6G treatment by two-way ANOVA followed by Sidak's post-test.

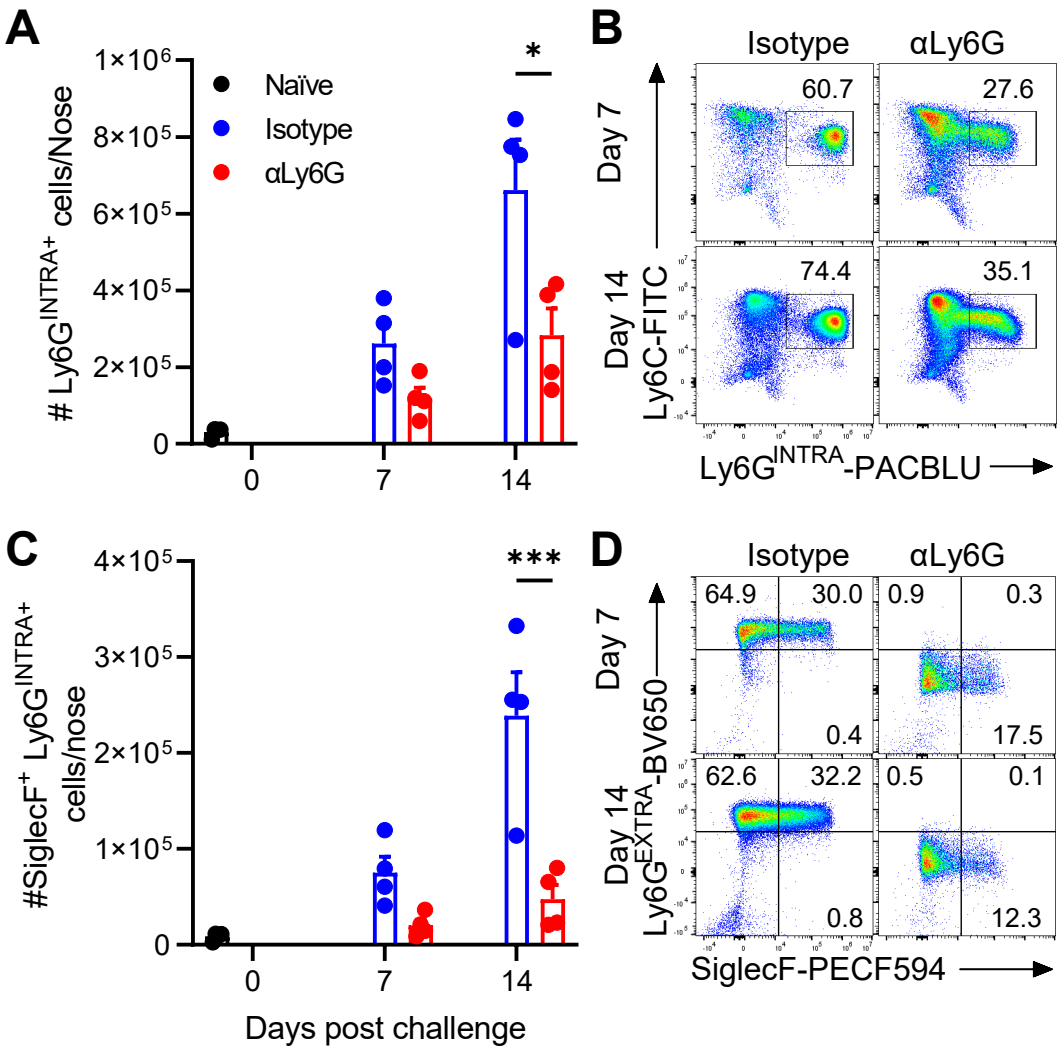

Figure 3.37 Reduced number of total neutrophils and Siglec-F$^+$ neutrophils in the nasal cavity of mice treated with a depleting anti-Ly6G antibody during *B. pertussis* infection.

C57BL/6 mice were injected i.p. with a depleting anti-Ly6G antibody or isotype control (100 µg/mouse) one day prior to and every day after *B. pertussis* challenge. Mice were injected i.p. with a secondary antibody specific for the rat kappa immunoglobulin (100 µg/mouse) every second day. Nasal tissue was harvested at the indicated time points. Cell suspensions were prepared and cells were stained for surface expression of CD11b, Ly6C, Siglec-F, and Ly6G, and intracellular Ly6G expression using a different fluorochrome-conjugated antibody, and analysed by flow cytometry. Absolute number (A) and representative flow cytometry plots (B) of total neutrophils, based on intracellular Ly6G expression (pre-gated on CD11b$^+$ cells), in the nasal cavity of isotype and anti-Ly6G treated mice during *B. pertussis* challenge. Absolute number (C) and representative flow cytometry plots (D) of Siglec-F$^+$ neutrophils, pre-gated on total Ly6G^{INTRA+}CD11b$^+$ cells. Results shown are mean ± SEM (n=4 mice per group). *p < 0.05, ***p < 0.001 isotype control versus αLy6G treatment by two-way ANOVA followed by Sidak's post-test.

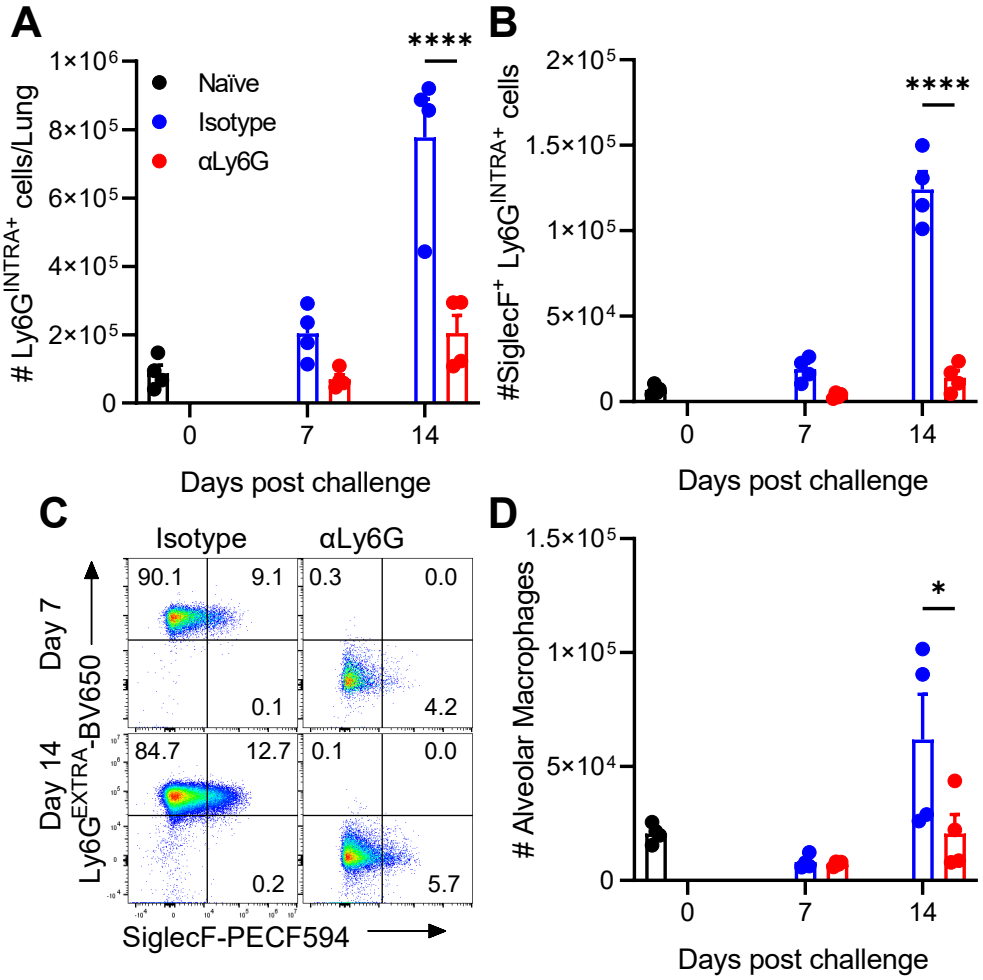

Figure 3.38 Reduced number of total neutrophils, Siglec-F⁺ neutrophils, and alveolar macrophages in the lungs of mice treated with a depleting anti-Ly6G antibody during *B. pertussis* infection.

C57BL/6 mice were injected i.p. with a depleting anti-Ly6G antibody or isotype control (100 µg/mouse) one day prior to and every day after *B. pertussis* challenge. Mice were injected i.p. with a secondary antibody specific for the rat kappa immunoglobulin (100 µg/mouse) every second day. Lungs were harvested at indicated time points. Cell suspensions were prepared from lungs and cells were stained for surface expression of CD11b, CD11c, Ly6C, Siglec-F, and Ly6G, and intracellular expression of Ly6G on a different fluorochrome-conjugated antibody, and analysed by flow cytometry. Absolute number of total neutrophils identified by intracellular expression of Ly6G (pre-gated on CD11b⁺ cells) (A). Absolute number (B) and representative flow cytometry plots (C) of Siglec-F⁺ neutrophils, pre-gated on Ly6G^{INTRA+}CD11b⁺ cells. Absolute number of alveolar macrophages (Siglec-F⁺CD11b⁺) in the lungs of isotype control and anti-Ly6G treated mice (D). Results shown are mean ± SEM (n=4 mice per group). *$p < 0.05$, ****$p < 0.0001$ isotype control versus anti-Ly6G treatment by two-way ANOVA followed by Sidak's post-test.

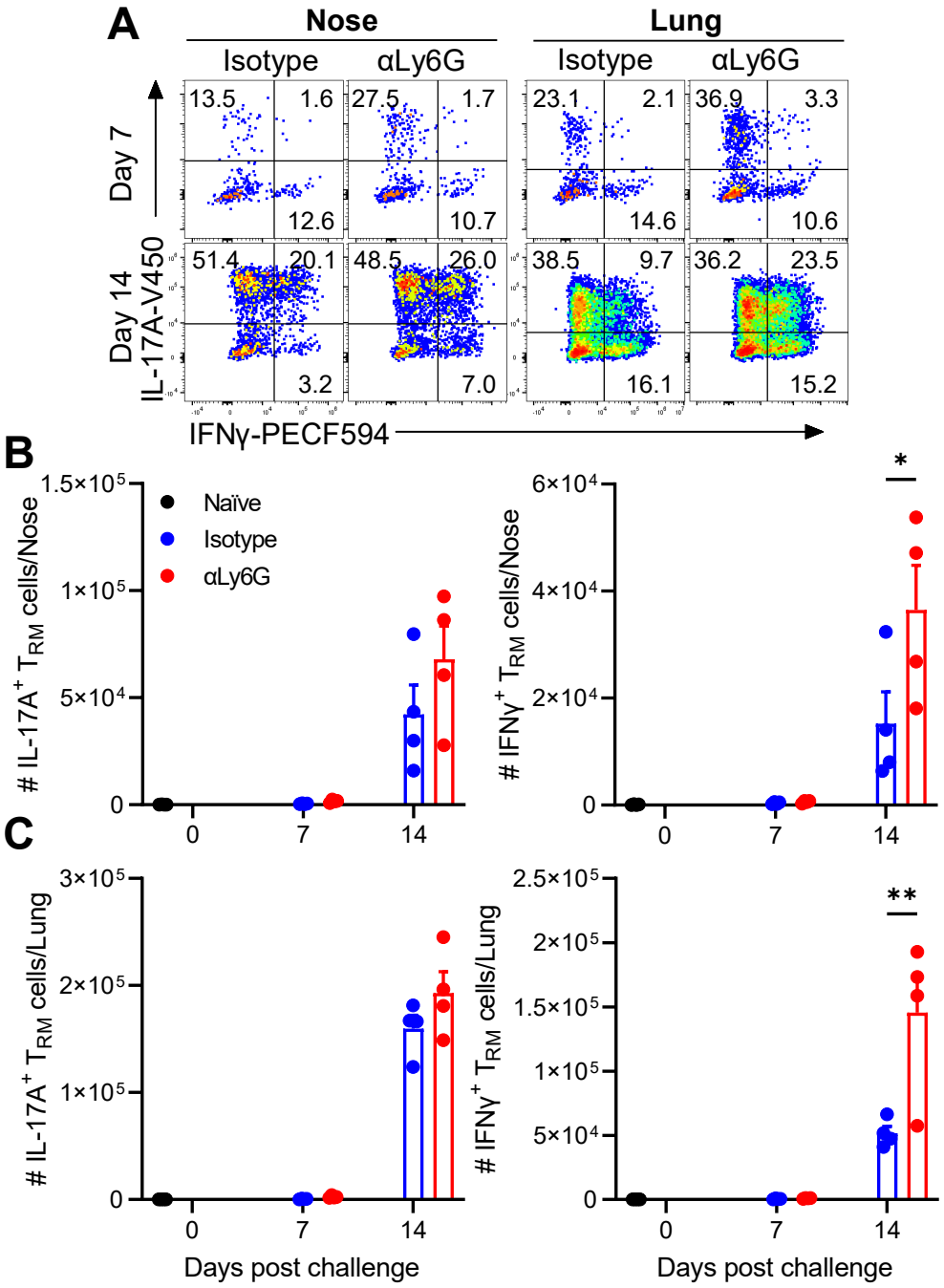
A
Nose
Lung
Isotype
αLy6G
Isotype
αLy6G
Day 7
Day 14
IL-17A-V450
IFNγ-PECF594
13.5
1.6
12.6
27.5
1.7
10.7
23.1
2.1
14.6
36.9
3.3
10.6
51.4
20.1
3.2
48.5
26.0
7.0
38.5
9.7
16.1
36.2
23.5
15.2
B
Naïve
Isotype
αLy6G
IL-17A+ TRM cells/Nose
IFNγ+ TRM cells/Nose
1.5×10^5
1×10^5
5×10^4
0
6×10^4
4×10^4
2×10^4
*
0
7
14
C
IL-17A+ TRM cells/Lung
IFNγ+ TRM cells/Lung
3×10^5
2×10^5
1×10^5
2.5×10^5
1.5×10^5
5×10^4
**
Days post challenge
Days post challenge

Figure 3.39 Increased number of IFNγ$^+$ CD4 T_{RM} cells in the nasal cavity and lungs of mice treated with an anti-Ly6G antibody during *B. pertussis* infection.

C57BL/6 mice were injected i.p. with a depleting anti-Ly6G antibody or isotype control (100 µg/mouse) one day prior to and every day after *B. pertussis* challenge. Mice were injected i.p. with a secondary antibody specific for the rat kappa immunoglobulin (100 µg/mouse) every second day. On the day of and 7 and 14 days post challenge, mice were injected i.v. with a fluorochrome-conjugated anti-CD45 antibody 10 min before euthanasia. Cell suspensions were prepared from nasal tissue and lungs and cells were stimulated with PMA (50 ng/ml), ionomycin (500 ng/ml), and brefeldin A (5 µg/ml) for 4 hours. Cells were stained for surface CD4, CD3, CD44, CD69, CD103, and intracellular IL-17A and IFNγ, and analysed by flow cytometry. Representative flow cytometry plots (A) and absolute number of nasal (B) and lung (C) IL-17A$^+$ and IFNγ$^+$ CD4 T_{RM} cells ($CD4^+CD3^+CD45i.v.^-CD44^+CD69^+CD103^±$). Data are mean ± SEM (n=4 mice per group). **p* < 0.05, ***p* < 0.01, isotype control versus αLy6G treatment by two-way ANOVA followed by Sidak's post-test.

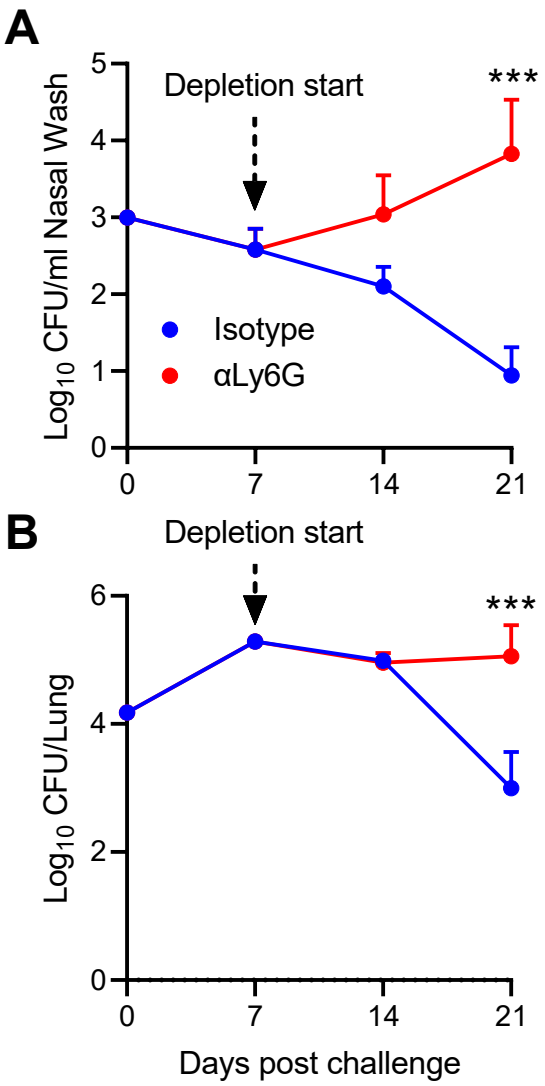

Figure 3.40 Administration of an anti-Ly6G antibody from day 7 of *B. pertussis* infection significantly impairs bacteria clearance from the nasal cavity and lungs.

C57BL/6 mice were aerosol challenged with live *B. pertussis*. Beginning day 7 post infection, mice were injected i.p. everyday with a depleting anti-Ly6G antibody (100 µg/mouse) or isotype control. Mice were injected i.p. with a secondary antibody specific for the rat kappa immunoglobulin (100 ug/mouse) every second day. The number of viable bacteria in the nasal cavity (A) and lungs (B) was estimated by performing CFU counts on serially diluted nasal washes and lung homogenates from individual mice on days 7, 14 and 21 post challenge. Results shown are mean ± SEM (n=4 mice per group). ***$p < 0.001$ isotype control versus anti-Ly6G treatment by two-way ANOVA followed by Sidak's post-test.

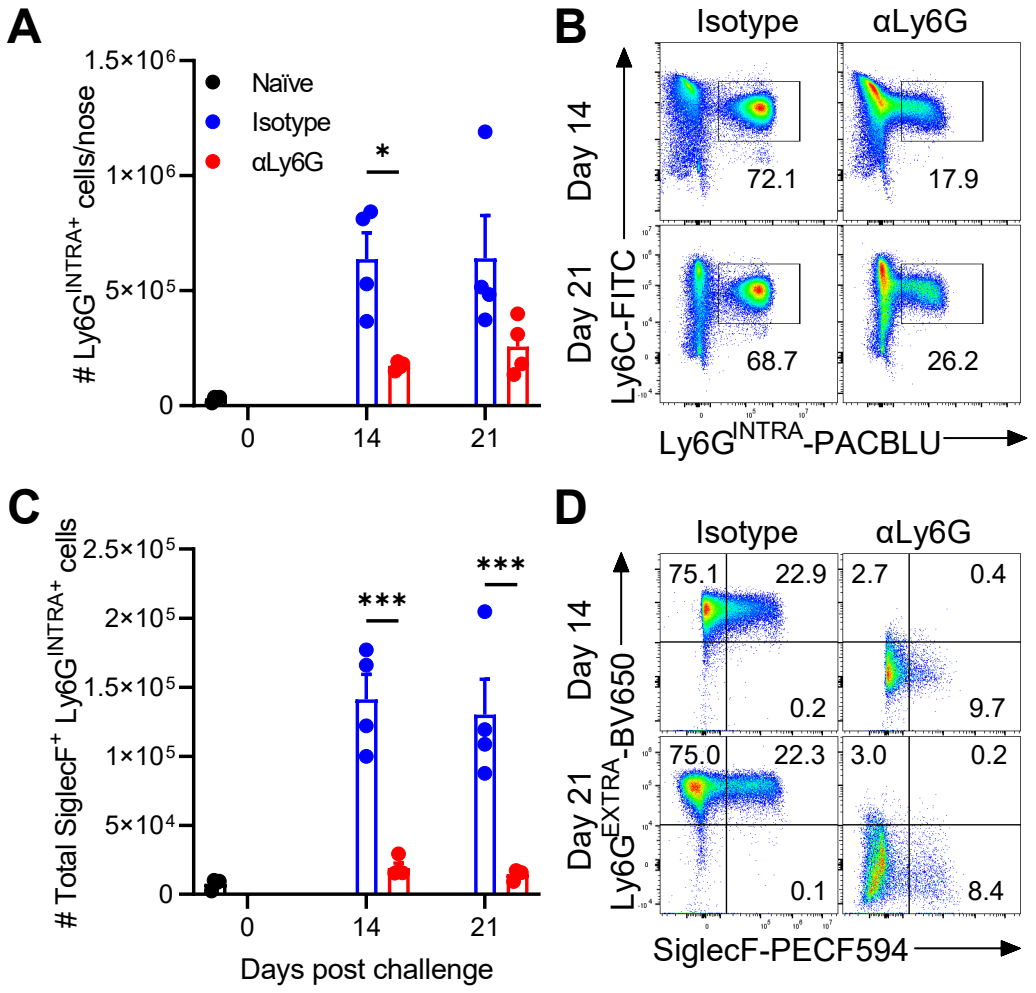

Figure 3.41 Administration of an anti-Ly6G antibody from day 7 of *B. pertussis* infection significantly reduces the number of total neutrophils and Siglec-F$^+$ neutrophils in the nasal cavity of mice.

C57BL/6 mice were aerosol challenged with live *B. pertussis*. Beginning day 7 post infection, mice were injected i.p. everyday with a depleting anti-Ly6G antibody (100 µg/mouse) or isotype control. Mice were injected i.p. with a secondary antibody specific for the rat kappa immunoglobulin (100 ug/mouse) every second day. At selected time points nasal tissue was harvested. Mononuclear cells were isolated and stained for surface expressions of CD11b, Ly6C, Siglec-F, Ly6G, and intracellular Ly6G expression using a different fluorochrome-conjugated antibody, and analysed by flow cytometry. Absolute number (A) and representative flow cytometry plots (B) of total neutrophils, based on intracellular Ly6G expression (pre-gated on CD11b$^+$ cells), in the nasal cavity of isotype and anti-Ly6G treated mice during *B. pertussis* challenge. Absolute number (C) and representative flow cytometry plots (D) of Siglec-F$^+$ neutrophils, pre-gated on total Ly6G^{INTRA+}CD11b$^+$ cells. Results shown are mean ± SEM (n=4 mice per group). *p < 0.05, ***p < 0.001 isotype control versus anti-Ly6G treatment by two-way ANOVA followed by Sidak's post-test.

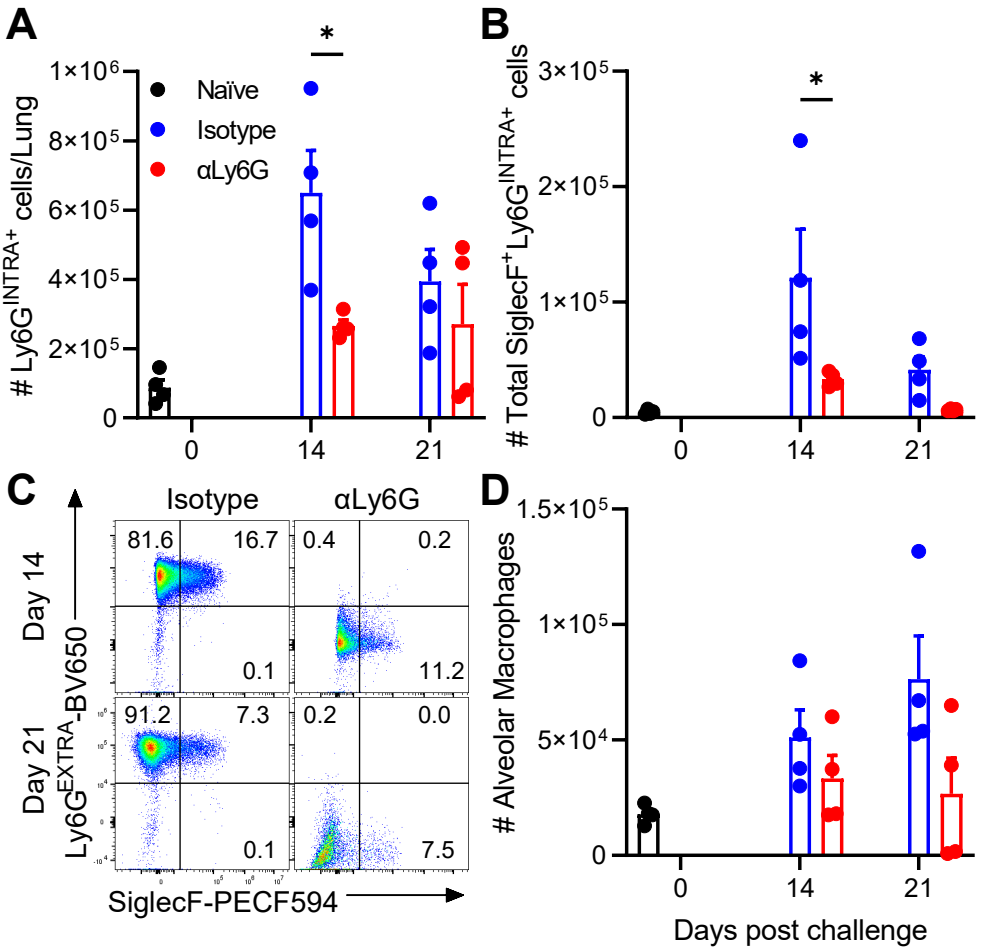

Figure 3.42 Administration of an anti-Ly6G antibody from day 7 of *B. pertussis* infection significantly reduces total neutrophils and Siglec-F$^+$ neutrophils in the lungs of mice.

C57BL/6 mice were aerosol challenged with live *B. pertussis*. Beginning day 7 post infection, mice were injected i.p. everyday with a depleting anti-Ly6G antibody (100 µg/mouse) or isotype control. Mice were injected i.p. with a secondary antibody specific for the rat kappa immunoglobulin (100 ug/mouse) every second day. At indicated time points lungs were harvested. Mononuclear cells were isolated from the lungs and stained for surface expressions of CD11b, CD11c, Ly6C, Siglec-F, and Ly6G, and intracellular expression of Ly6G on a different fluorochrome-conjugated antibody, and analysed by flow cytometry. Absolute number of total Ly6G^{INTRA+} neutrophils in the lungs (pre-gated on CD11b$^+$ cells) (A). Absolute numbers of Siglec-F$^+$ neutrophils (B), pre-gated on Ly6G^{INTRA+}CD11b$^+$ neutrophils, with representative flow cytometry plots (C). Absolute number of alveolar macrophages (Siglec-F$^+$CD11b$^+$) in isotype control and anti-Ly6G treated mice (D). Results shown are mean ± SEM (n=4 mice per group). *$p < 0.05$ isotype control versus anti-Ly6G treatment by two-way ANOVA followed by Sidak's post-test.

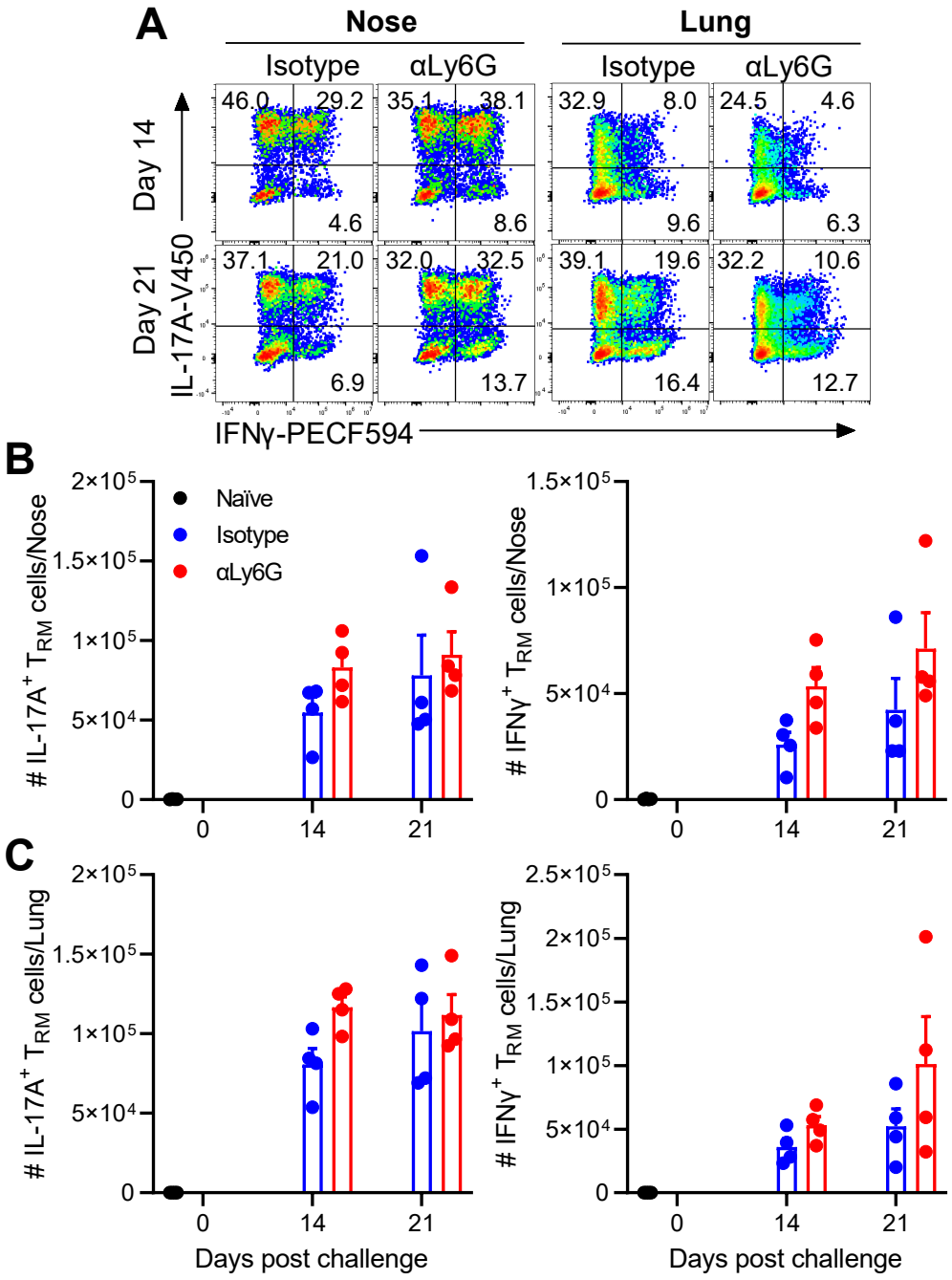
A
Nose
Lung
Isotype
αLy6G
Isotype
αLy6G
Day 14
Day 21
IL-17A-V450
IFNγ-PECF594
46.0
29.2
4.6
35.1
38.1
8.6
32.9
8.0
9.6
24.5
4.6
6.3
37.1
21.0
6.9
32.0
32.5
13.7
39.1
19.6
16.4
32.2
10.6
12.7
B
Naïve
Isotype
αLy6G
IL-17A+ TRM cells/Nose
IFNγ+ TRM cells/Nose
C
IL-17A+ TRM cells/Lung
IFNγ+ TRM cells/Lung
Days post challenge
Days post challenge

Figure 3.43 Administration of an anti-Ly6G antibody from day 7 of *B. pertussis* infection has no significant effect on IL-17A- or IFNγ-producing CD4 T_{RM} cells in the nasal cavity.

C57BL/6 mice were aerosol challenged with live *B. pertussis*. Beginning day 7 post infection, mice were injected i.p. everyday with a depleting anti-Ly6G antibody (100 µg/mouse) or isotype control. Mice were injected i.p. with a secondary antibody specific for the rat kappa immunoglobulin (100 ug/mouse) every second day. At the indicated time points, mice were injected i.v. with a fluorochrome-labelled anti-CD45 antibody 10 min before euthanasia. Cell suspensions were prepared from nasal tissue and lungs and cells were stimulated with PMA (50 ng/ml), ionomycin (500 ng/ml), and brefeldin A (5 µg/ml) for 4 hours. Cells were stained for surface CD4, CD3, CD44, CD69, CD103, and intracellular IL-17A and IFNγ, and analysed by flow cytometry. Representative flow cytometry plots (A) and absolute number of nasal (B) and lung (C) IL-17A$^+$ and IFNγ$^+$ CD4 T_{RM} cells (CD4$^+$CD3$^+$CD45i.v.$^-$CD44$^+$CD69$^+$CD103$^\pm$). Data are mean ± SEM (n=4 mice per group). No significant difference between isotype or anti-Ly6G treatment PBS by two-way ANOVA followed by Sidak's post-test.

Chapter 4: CD4 T_{RM} cells mediate adaptive immunity against re-infection with *B. pertussis* in the nasal cavity

4.1 Introduction

A key feature of the adaptive immune system is the capacity for memory, which results in a more rapid and efficient immune response upon recognition of a cognate antigen. Adaptive immunity provides life-long protection from infection by establishing a long-lived reservoir of memory cells, consisting of antigen-specific T cells, which are activated and proliferate in response to cognate antigen presentation by APCs, and B cells, which mediate a humoral immune response [210, 331]. Memory T cells were originally classified as either T_{CM} cells, which circulate between secondary lymphoid tissue, or as T_{EM} cells, which circulate between non-lymphoid tissue [196]. However, following the observation that a population of T_{EM} cells preferentially localised to non-lymphoid tissue following infection [200], a third class of memory T cells was identified, termed T_{RM} cells. T_{RM} cells do not re-enter circulation, but rather persist at barrier sites and expand locally in response to pathogen re-exposure [332].

The results presented in chapter 3 demonstrated that CD4 T cells accumulated in the upper and lower respiratory tract of mice during *B. pertussis* infection and were a major source of IL-17A in the nasal cavity. IL-17A was shown to mediate protective immunity in the nasal cavity by promoting chemokine production and the recruitment of a novel neutrophil population expressing Siglec-F to the nasal mucosa. Over the course of infection, infiltrated CD4 T cells acquired a T_{RM} phenotype characterised by the expression of the markers CD69, CD103, and CD44, and were found to persist in the nasal cavity once the infection had cleared. T_{RM} cells expand rapidly upon re-encounter with cognate antigen to mediate a protective and localised immune response, and are now considered key players in adaptive immunity at mucosal surfaces [333]. However, the relative contribution of nasal CD4 T_{RM} cells to acquired immunity against *B. pertussis* and the mechanisms by which this is achieved are not fully elucidated.

Although studies on nasal CD4 T_{RM} cells are limited, there have been multiple studies on the role of lung-resident CD4 T_{RM} cells in the adaptive immune response to infection. Using different models, it has been demonstrated that CD4 T_{RM} cells are retained in the lungs and expand locally within the tissue to confer protective immunity. Parabiosis models, which involve the surgical union of the circulatory system of an immune mouse containing a CD4 T_{RM} population with a naïve mouse lacking CD4 T_{RM} cells, have revealed that CD4 T_{RM} cells are irreversibly retained in the lungs of immune mice, and not found in the lungs of the naïve partner [206, 334]. Furthermore, challenge of parabiotic pairs with *K. pneumoniae* demonstrated that mice previously immunised with killed *K. pneumoniae* had reduced bacterial burden in the lungs compared with their

naïve parabiotic partner, despite sharing circulating *K. pneumoniae*-specific antibodies and circulating memory T cells [210].

FTY720, an agonist of the sphingosine 1-phosphate receptor which prevents lymphocyte egression from lymphoid tissue to peripheral tissue [335], has also been used in multiple models to demonstrate that CD4 T_{RM} cells expand locally within the lungs to mediate protective immune responses without the contribution of circulating lymphocytes. Intranasal administration of a live-attenuated influenza virus vaccine was found to induce lung CD4 T_{RM} and virus-specific CD8 T_{RM} cells and this was accompanied by protection in the lungs against a subsequent influenza challenge. This protection persisted despite FTY720 treatment during the influenza challenge, demonstrating that T_{RM}-mediated protection is independent of circulating memory T cells [282]. Similar results were reported with lung CD4 T_{RM} cells induced following immunisation of mice with recombinant influenza A viruses vaccine expressing *M. tuberculosis* peptides; immunised mice were protected against *M. tuberculosis* infection despite a reduction in circulating T cells by FTY720 treatment [336].

Studies from the Mills' lab have used FTY720 to highlight the role of lung CD4 T_{RM} cells induced following natural infection in protective immunity against re-infection with *B. pertussis*. Treatment of convalescent mice, who had cleared *B. pertussis* infection from the respiratory tract, with FTY720 prior to and during re-infection with *B. pertussis* did not impair bacterial clearance from the lungs [216]. Furthermore, mice immunised with a wP vaccine effectively cleared *B. pertussis* from the lungs despite continuous treatment with FTY720 during challenge [194]. This protection was associated with the local expansion of IL-17A-producing CD4 T_{RM} cells in the lungs. Wilk et al. also demonstrated that adoptive transfer of CD4 T cells isolated from the lungs of either convalescent mice or mice previously immunised with a wP vaccine conferred protection against *B. pertussis* in the lungs of the naïve recipients, with transferred cells seeding in the lungs, adopting a T_{RM} phenotype and producing IL-17A in recipient mice [194, 216]. Despite demonstrating a strong correlation between nasal IL-17A-producing CD4 T_{RM} cells and protective immunity in the upper respiratory tract, these studies did not examine the effect of FTY720 treatment or adoptive transfer of tissue-resident CD4 T cells on acquired immunity against *B. pertussis* in the nasal cavity [194]. Nor did these studies fully elucidate the mechanisms by which CD4 T_{RM} cells orchestrate acquired immunity against *B. pertussis* in the nasal cavity. Studies examining the lungs revealed that antibody-mediated neutralisation of IL-17A significantly impaired clearance of *B. pertussis* from the lungs of mice previously immunised with a wP vaccine [271].

Furthermore, IL-17A$^{-/-}$ mice immunised with a wP vaccine had delayed clearance of *B. pertussis* from the lungs compared to wP-immunised WT control mice [146].

Together, these studies provide strong evidence supporting the hypothesis that adaptive immunity elicited by CD4 T_{RM} cells is mediated by IL-17A. The aim of this chapter was to assess the role of nasal CD4 T_{RM} cells in protective acquired immunity against *B. pertussis* re-infection. The persistence and expansion of *B. pertussis*-specific CD4 T_{RM} cells in the upper and lower respiratory tract was examined. The results in chapter 3 revealed that CD4 T_{RM} cells exhibited a predominantly Th17 phenotype, and that IL-17A was required for clearance of *B. pertussis* from the nasal cavity during a primary infection. This study examined the role of IL-17A in acquired immunity against a secondary infection with *B. pertussis*. Furthermore, this study examined if protective immunity in the nasal cavity conferred by wP vaccination is mediated by IL-17A. As asymptomatic transmission has been linked to increased incidence of pertussis [279], understanding the mechanisms of persistent and durable immunological memory in the nasal cavity is beneficial in informing the design of next generation pertussis vaccines.

4.2 Results

4.2.1 Acquired protective immunity in the nose and lungs persists up to one year post B. pertussis infection, and is associated with the expansion of IL-17A$^+$ CD4 T_{RM} cells and recruitment of Siglec-F$^+$ neutrophils to the nasal cavity.

The results from chapter 3 demonstrated that CD4 T cells with a T_{RM} phenotype accumulated and persisted in the nasal cavity and lungs following *B. pertussis* infection. In order to assess the persistence of *B. pertussis*-specific CD4 T_{RM} cells in the respiratory tract and their role in protective acquired immunity, C57BL/6 mice were infected with *B. pertussis*, left to clear the infection from the respiratory tract, and re-infected with *B. pertussis* 12 months after the primary infection. Once mice have cleared *B. pertussis* from the respiratory tract, which takes up to 60 days, they are considered convalescent. Convalescent mice had significantly reduced CFU counts in the nasal wash and lungs compared with age-matched un-primed naïve control mice on day 7 post challenge, demonstrating that protective immunity persists for up to one year after initial exposure to *B. pertussis* (Figure 4.1 *A, B*). *B. pertussis*-specific IL-17A$^+$ CD4 T_{RM} cells were detected in both the nasal cavity (Figure 4.2 *A, B*) and lungs (Figure 4.2 *C*) up to one year post primary infection with *B. pertussis*. The number of *B. pertussis*-specific IL-17A$^+$ and IFNγ$^+$ CD4 T_{RM} cells expanded in the nose and lungs of convalescent mice by day 7 post challenge. This was accompanied by significantly enhanced number of conventional neutrophils (Siglec-F$^-$Ly6G$^+$CD11b$^+$) and Siglec-F$^+$ neutrophils (Siglec-F$^+$Ly6G$^+$CD11b$^+$) in the nasal mucosa of convalescent mice on day 7 post re-challenge (Figure 4.3 *A*-*C*). There were significantly more alveolar macrophages in the lungs of convalescent mice compared with naïve mice on day 7 post *B. pertussis* challenge (Figure 4.4 *A, B*). In contrast, there was a significant increase of Ly6C$^+$CD11b$^+$ monocytes and neutrophils in the lungs of naïve mice on day 7 post challenge (Figure 4.4 *C*-*E*). These results demonstrate that acquired protective immunity against *B. pertussis* persists in the nasal cavity and lungs for up to one year post primary infection and that *B. pertussis*-specific IL-17A+ T_{RM} cells are long-lived and expand after re-exposure to *B. pertussis*.

4.2.2 CD4 T_{RM} cells expand in the nasal cavity and lung during re-infection with B. pertussis despite continuous FTY720 treatment.

To examine if the increase of *B. pertussis*-specific IL-17A$^+$ CD4 T_{RM} cells is due to local expansion of tissue-resident CD4 T cells or due to the infiltration of effector memory T cells, convalescent C57BL/6 mice (>60 days post primary infection) were treated with FTY720 orally in their drinking water 10 days prior to and during the course of *B. pertussis* re-infection. Control convalescent mice received untreated drinking water. Un-primed naïve mice were included as an additional control. Although there were significantly higher CFU counts in the nasal washes and lungs of the un-primed naïve mice, there was no significant difference in CFU counts between FTY720-treated convalescent mice and untreated convalescent mice, with both groups of mice clearing *B. pertussis* from the lungs and nasal cavity at similar rates (Figure 4.5 *A, B*).

FTY720 treatment in convalescent mice significantly reduced the number of circulating (CD45 i.v.$^+$) CD44$^-$ and CD44$^+$ CD4 T cells in the nasal tissue (Figure 4.6 *A*-*C*) and lungs (Figure 4.7 *A*-*C*) prior to and post *B. pertussis* challenge. However, nose- (Figure 4.6 *E*) and lung-resident (Figure 4.7 *E*) CD44$^+$ CD4 T cells (CD45 i.v.-) remained unaffected by FTY720 treatment and expanded following re-infection with *B. pertussis*.

The expansion of total CD4 T_{RM} cells, and RORγ$^+$ and Foxp3$^+$ CD4 T_{RM} cells in the nasal cavity (Figure 4.8 *A*-*E*) and lungs (Figure 4.9 *A*-*E*) of convalescent mice on day 7 post *B. pertussis* re-infection was not affected by FTY720 treatment, demonstrating that these cells expand locally without the contribution of circulating CD4 T cells. Furthermore, the persistence and subsequent expansion of *B. pertussis*-specific IL-17A$^+$ and IFNγ$^+$ CD4 T_{RM} cells in the nasal cavity (Figure 4.10 *A*-*C*) or lungs (Figure 4.11 *A*-*C*) of convalescent mice was not affected by FTY720 treatment. SPICE analysis of cytokine production by CD4 T_{RM} cells in the nasal tissue (Figure 4.10 *D*) and lungs (Figure 4.11 *D*) revealed that IL-17A was the dominant cytokine produced by CD4 T_{RM} cells both prior to and 7 days after *B. pertussis* re-challenge, with minor populations producing IFNγ, TNF, or multiple cytokines at once, and this was not altered by FTY720 treatment.

It was next investigated if FTY720 treatment impaired innate cell recruitment to the respiratory tract during re-infection with *B. pertussis*. Untreated convalescent mice had a significantly higher number of infiltrated (CD45 i.v.$^-$) Siglec-F$^+$ neutrophils in the nasal cavity compared with un-primed naïve control mice on day 7 post challenge, and this was not affected by FTY720 treatment (Figure 4.12 *A*-*C*). Furthermore, FTY720 treatment did not inhibit the expansion of alveolar macrophages or impair the infiltration of neutrophils into the lungs of convalescent mice during *B. pertussis* re-infection (Figure

4.13 *A-E*). Together, these results demonstrate that *B. pertussis*-specific CD4 T_{RM} cells expand locally in the nasal cavity and lungs without the contribution of circulating lymphocytes to mediate a localised and protective immune response against re-infection with *B. pertussis*.

4.2.3 Treatment of convalescent mice with a depleting anti-CD4 antibody significantly delays clearance of B. pertussis from the nasal cavity.

As FTY720 also inhibits migration of other lymphocyte populations, including CD8 T cells and $B220^{+}$ cells, the specific role of CD4 T cells in acquired protective immunity to *B. pertussis* in the respiratory tract was examined by depleting CD4 T cells. Convalescent mice (70 days p.i.) were treated with a depleting anti-CD4 antibody or an isotype control antibody prior to and during re-infection of mice with *B. pertussis*. PBS-treated naïve mice were included as an additional control. There were significantly higher CFU counts in the nasal washes of the convalescent mice treated with a depleting anti-CD4 antibody compared with convalescent mice treated with the isotype control antibody on day 10 post re-challenge (Figure 4.14 *A*). In contrast, depleting CD4 T cells had no significant effect on clearance of *B. pertussis* from the lungs during a secondary challenge (Figure 4.14 *B*).

Treatment of convalescent mice with a depleting anti-CD4 antibody but not with an isotype control antibody effectively depleted CD4 T cells in the nasal cavity (Figure 4.15 *A, D*), lungs (Figure 4.16 *A, D*), and cLNs (Figure 4.17 *A, D*) over the course of the re-infection. A significant increase in the number of CD8 T cells was observed in the nasal cavity of the anti-CD4-treated convalescent mice on day 10 post re-challenge (Figure 4.15 *B*). In the lungs, anti-CD4 treatment significantly reduced the number of CD8 T cells and B220+ cells (Figure 4.16 *A-D*). Re-infection with *B. pertussis* resulted in an expansion of total CD4 T_{RM} cells and IL-17A-producing CD4 T_{RM} cells in the nasal cavity (Figure 4.18 *A-C*) and lungs (Figure 4.19 *A-C*) of convalescent mice treated with an isotype control, and these cell populations were reduced to background following treatment with a depleting anti-CD4 antibody.

CD4 T cells were found to be the predominant source of IL-17A in the nasal tissue, lungs, and cLNs, prior to and post *B. pertussis* re-challenge. However, depletion of CD4 T cells did not reduce the number of total live IL-17A-producing cells in the nose or cLNs during *B. pertussis* re-infection (Figure 4.20 *A-C*). Analysis of the IL-17A-producing population revealed that in the absence of CD4 T cells, an unidentified $CD4^{-}CD8^{-}\gamma\delta^{-}$ cell population

was the main producer of IL-17A in the nasal tissue, lungs, and cLNs, of convalescent mice during re-infection with *B. pertussis*. CD8 T cells also contributed to IL-17A production in the nasal tissue and cLNs in the absence of CD4 T cells (Figure 4.20 *A-C*).

It was next investigated if depletion of CD4 T cells impaired antibody production in convalescent mice. Anti-CD4 treatment significantly reduced *B. pertussis*-specific IgA and IgG2c in the nasal washes and IgG2c in the lung homogenates of convalescent mice on day 4 post challenge. However, *B. pertussis*-specific IgG2c increased in the nasal mucosa and lungs of the anti-CD4 treated convalescent mice on day 10 post challenge (Figure 4.21 *A, B*).

Analysis of the innate immune response on day 4 post re-infection revealed a significant reduction in the infiltration (CD45 i.v.$^-$) of Siglec-F$^+$ neutrophils, but not conventional Siglec-F$^-$ neutrophils, into the nasal cavity of convalescent mice treated with a depleting anti-CD4 antibody compared with convalescent mice treated with the isotype control antibody (Figure 4.22 *A-C*). Furthermore, anti-CD4 treatment in convalescent mice significantly reduced the concentration of LCN2 in the nasal washes on day 4 post re-infection (Figure 4.22 *D*). Analysis of the lungs revealed that anti-CD4 treatment in convalescent mice significantly reduced the infiltration (CD45 i.v.$^-$) of neutrophils into the lungs compared with convalescent mice treated with an isotype control on day 4 post *B. pertussis* re-challenge (Figure 4.23 *A-C*). Anti-CD4 treatment did not affect the number of alveolar macrophages in the lungs of convalescent mice but did significantly reduce the number of infiltrated MHCII$^+$Ly6C$^+$CD11b$^+$ monocytes in the lung (Figure 4.23 *D, E*). The concentration of LCN2 and IL-1β in the lung homogenates was significantly reduced in convalescent mice treated with an anti-CD4 antibody on day 4 post re-challenge (Figure 4.23 *F, G*). Together, these results demonstrate that CD4 T cells play a role in acquired immunity in the nasal cavity against re-infection with *B. pertussis* by enhancing the recruitment of Siglec-F$^+$ neutrophils to the nasal cavity and promoting AMP production. In the lungs, compensatory mechanisms may be sufficient to mediate protective immunity in the absence of CD4 T cells.

4.2.4 Transfer of lung- and nose-resident CD4 T cells from convalescent mice confers protective immunity in the respiratory tract of recipient hosts.

Since depletion of CD4 T cells in convalescent mice impaired clearance of *B. pertussis* from the nasal cavity during re-infection, it was next investigated if protective immunity against *B. pertussis* could be conferred in the respiratory tract by transfer of tissue-

resident CD4 T cells from donor convalescent mice to naïve recipient mice. A 1:4 mixture of lung:nose-resident (CD45 i.v.$^-$) CD4 T cells from convalescent (60 days post *B. pertussis* challenge) CD45.2 mice were injected i.p. to sublethally irradiated naïve CD45.1 recipient mice. Control mice received an i.p. injection of PBS. Recipient mice were challenged with a low dose of *B. pertussis* ($1x10^8$ CFU/ml) 1 day later. A lower dose was used to allow examination of later time points in sub-lethally irradiated mice where the disease is more severe. Adoptive transfer of lung/nose-resident CD4 T cells resulted in enhanced bacterial clearance in the nasal cavity on day 21 and in the lungs on days 13 and 21 post *B. pertussis* challenge compared with mice that received PBS only (Figure 4.24 *A, B*). Donor CD4 T cells, identified by surface expression of CD45.2, homed to nasal cavity and lungs of recipient mice and produced pathogen-specific IL-17A (Figure 4.25 *A-D*).

4.2.5 Protective acquired immunity against B. pertussis in the nasal cavity is mediated through IL-17A.

Using both antibody depletion methods and cell transfer approaches, the results so far have suggested that protective acquired immunity in the nasal cavity is mediated by CD4 T_{RM} cells. The results have also shown that CD4 T_{RM} cells are a major source of IL-17A, and that *B. pertussis*-specific IL-17A$^+$ CD4 T_{RM} cells expand locally in the nasal tissue during *B. pertussis* re-infection. In Chapter 3 it was demonstrated that IL-17A$^{-/-}$ mice have significantly impaired bacterial clearance from the nasal cavity following a primary infection with *B. pertussis*. In order to examine the role of IL-17A in protective immunity against re-infection with *B. pertussis*, IL-17A$^{-/-}$ and WT control mice were infected with *B. pertussis* and left for 6 months to clear the infection completely from the respiratory tract. Convalescent IL-17A$^{-/-}$ and WT control mice were re-infected with *B. pertussis* and bacterial clearance in the nasal cavity and lungs was assessed over the course of the re-infection. There were significantly higher CFU counts in the nasal wash of IL-17A$^{-/-}$ compared with WT mice on day 14 post re-challenge (Figure 4.26 *A*). Furthermore, there was a significant delay in clearance of *B. pertussis* from the lungs of IL-17A$^{-/-}$ compared with WT mice on day 7 post re-challenge (Figure 4.26 *B*).

It was next investigated if a lack of IL-17A affected the maintenance and expansion of CD4 T_{RM} cells during *B. pertussis* re-infection. The lack of IL-17A in the IL-17A$^{-/-}$ mice had no significant effect on the maintenance of CD4 T_{RM} cells in the nasal cavity or lungs compared with convalescent WT mice prior to *B. pertussis* re-challenge. However, IL-

17A$^{-/-}$ mice had significantly more CD4 T_{RM} cells in both the nasal tissue and lungs following *B. pertussis* re-infection (Figure 4.27 *A-D*). As expected, nasal or lung CD4 T_{RM} cells from convalescent IL-17A$^{-/-}$ mice did not produce IL-17A following stimulation with sBP. However, there was a significant increase in the number of *B. pertussis*-specific IFNγ^{+} CD4 T_{RM} cells in the nose (Figure 4.28 *A, B*) and lungs (Figure 4.28 *C*) of IL-17A$^{-/-}$ compared with WT mice after *B. pertussis* re-infection.

Analysis of *B. pertussis*-specific IgA and IgG2c production revealed significantly enhanced *B. pertussis*-specific IgA (Figure 4.29 *A-C*) and IgG2c (Figure 4.30 *A-C*) in the nasal washes, lung homogenates, and sera of convalescent IL-17A$^{-/-}$ compared with WT mice prior to and 7 days after *B. pertussis* re-infection.

An examination of chemokine and cytokine production found a significant reduction in the concentration of CXCL1 in the nasal wash and lung homogenates of IL-17A$^{-/-}$ compared with WT mice post *B. pertussis* re-challenge (Figure 4.31 *A*). A significant reduction in the concentration of IL-1β was also observed in the nasal wash of convalescent IL-17A$^{-/-}$ mice on day 7 post re-challenge. In contrast, there was a marked increase in the concentration of IL-1β in the lung homogenates of IL-17A$^{-/-}$ mice 7 days after re-infection with *B. pertussis* (Figure 4.31 *B*).

Analysis of innate cell recruitment to the respiratory tract revealed a significant reduction in the infiltration (CD45 i.v.$^{-}$) of Siglec-F^{+} neutrophils to the nasal cavity of convalescent IL-17A$^{-/-}$ compared with WT mice on day 14 post re-challenge (Figure 4.32 *A, D*). In contrast, there was a moderate increase in the infiltration of conventional Siglec-F^{-} neutrophils and a significant increase in the infiltration of MHCII^{+}Ly6C^{+}CD11b^{+} monocytes to the nasal cavity of IL-17A$^{-/-}$ mice after re-infection with *B. pertussis* (Figure 4.32 *B, C*). In the lungs, there was a significant reduction in the number of total neutrophils, lung-infiltrated (CD45 i.v.$^{-}$) neutrophils, and alveolar macrophages in convalescent IL-17A$^{-/-}$ mice post re-challenge (Figure 4.33 *A-E*). Together, these results suggest that IL-17A contributes to protective immunity against re-infection with *B. pertussis* in both the nasal cavity and lungs by impairing Siglec-F^{+} neutrophil recruitment to the nose and alveolar macrophage expansion in the lungs.

4.2.6 Neutralisation of IL-17A during a secondary infection with B. pertussis impairs bacterial clearance from the nasal cavity.

A limitation of using cytokine-deficient mice to assess the role of IL-17A in protective immunity against a re-infection with *B. pertussis* is that the primary infection was also significantly affected by the absence of IL-17A, thus may complicate interpreting the role

of IL-17A in protection against a secondary infection. In order to examine the role of IL-17A in acquired protective immunity during a secondary infection where the primary challenge remained unaffected by cytokine deficiency, a neutralising anti-IL-17A antibody or a corresponding isotype control antibody was administered to convalescent C57BL/6 mice (6 months post primary infection) one day before *B. pertussis* re-infection and every 3 days after challenge. PBS-treated naïve mice were used as an additional control and bacterial clearance in the nasal cavity and lungs was assessed over the course of the re-infection. Clearance *of B. pertussis* was significantly delayed in the nasal cavity of the convalescent mice treated with the anti-IL-17A antibody compared with convalescent mice treated with the isotype control antibody, with significantly higher CFU counts in the nasal wash of the anti-IL-17A treated mice on day 7 post re-challenge (Figure 4.34 *A*). However, treatment of convalescent mice with an anti-IL-17A antibody had no significant effect on bacterial clearance in the lungs (Figure 4.34 *B*). Administration of an anti-IL-17A antibody to convalescent mice had no significant effect on the expansion of *B. pertussis*-specific IL-17A$^+$ CD4 T_{RM} cells in the nasal cavity (Figure 4.35 *A, B*) or lungs (Figure 4.35 *C*) following re-challenge with *B. pertussis*. However, treatment of convalescent mice with an anti-IL-17A antibody resulted in a significant increase in *B. pertussis*-specific IFNγ$^+$ CD4 T_{RM} cells in the nasal cavity on day 14 post re-challenge (Figure 4.35 *A*), with a moderate increase also seen in the lungs on day 7 post re-infection (Figure 4.35 *B*).

An examination of the innate immune response revealed a significant reduction in the infiltration of Siglec-F$^+$ neutrophils, as well as conventional Siglec-F$^-$ neutrophils, into the nasal cavity of convalescent mice treated with an anti-IL-17A antibody during *B. pertussis* re-infection (Figure 4.36 *A-C*). In the lungs, anti-IL-17A treatment reduced the number of tissue-infiltrated (CD45 i.v.$^-$) neutrophils on day 7 post challenge (Figure 4.37 *A, B, D*). Furthermore, blocking IL-17A in convalescent mice resulted in a significant reduction in the absolute number of alveolar macrophages on day 7 post challenge (Figure 4.37 *C, E*). Together these results demonstrate that protective adaptive immunity against re-infection with *B. pertussis* in the nasal cavity is mediated by IL-17A.

4.2.7 Protective immunity in the nasal cavity conferred by immunisation with a wP vaccine is mediated by IL-17A.

To further elucidate the role of IL-17A in protective acquired immunity against *B. pertussis*, wP-immunised C57BL/6 mice were treated with an anti-IL-17A antibody or an isotype control antibody one day prior to and every 3 days after *B. pertussis* challenge. PBS-immunised naïve mice were used as an additional control. Neutralisation of IL-17A

in mice primed with a wP vaccine resulted in significantly impaired clearance of *B. pertussis* from the nasal cavity, but not the lungs, compared with wP-immunised mice treated with the isotype control antibody (Figure 4.38 *A, B*). Anti-IL-17A treatment of mice immunised with a wP vaccine had no significant effect on the expansion of IL-17A$^+$ or IFNγ$^+$ CD4 T_{RM} cells in the nasal cavity (Figure 4.39 *A*-*C*). However, neutralising IL-17A in wP-immunised mice significantly reduced the infiltration of Siglec-F$^+$ neutrophils and the concentration of LCN2 in the nasal cavity on day 7 post challenge (Figure 4.40 *A*-*D*). Together, these results demonstrate that protective immunity in the nasal cavity against *B. pertussis* conferred by a wP vaccine is mediated by IL-17A.

4.3 Discussion

The key finding of the present study is that IL-17A-producing CD4 T_{RM} cells play a critical role in rapid resolution of a secondary infection with *B. pertussis* in the nasal cavity. Pathogen-specific IL-17A$^+$ CD4 T_{RM} cells were found to expand locally in the nasal mucosa following re-infection with *B. pertussis* and this was accompanied by enhanced bacterial clearance in the nose, in addition to accelerated recruitment of Siglec-F$^+$ neutrophils to the nasal cavity. Protection in the nasal cavity was lost following the antibody-mediated depletion of CD4 T cells or neutralisation of IL-17A. Furthermore, re-infection of convalescent IL-17A$^{-/-}$ mice who had previously cleared *B. pertussis* from the respiratory tract exhibited delayed bacterial clearance from the nasal cavity following re-infection with *B. pertussis*.

The generation of T_{RM} cells has been shown to be an essential aspect of protective immunity at mucosal surfaces. Research from the Mills' lab has demonstrated that CD4 T_{RM} cells accumulate in the lungs following infection with *B. pertussis* and expand locally within the tissue to mediate protective adaptive immunity. Local expansion of lung CD4 T_{RM} cells was confirmed by treating mice with FTY720, which prevents lymphocyte egression from secondary lymphoid organs, prior to and during the re-infection of convalescent mice with *B. pertussis* [216]. The results presented in this chapter utilising FTY720 during a secondary *B. pertussis* challenge demonstrated that IL-17A-producing CD4 T_{RM} cells specific for *B. pertussis* expanded locally in the nasal tissue during re-infection and this was associated with rapid bacterial clearance from the nasal cavity. IL-17A-producing CD4 T_{RM} cells have been implicated in protective immunity against other bacterial pathogens in the nose. Infection of mice with *S. pneumoniae* was found to promote the accumulation of antigen-specific IL-17A$^+$ CD4 T_{RM} cells in the nasal mucosa which expanded following re-exposure to *S. pneumonia*, and this was accompanied by accelerated bacterial clearance from the upper respiratory tract [337].

However, FTY720 does not specifically inhibit the migration of CD4 T cells from secondary lymphoid tissue, but also prevents the migration of CD8 T cells and B cells [309]. Therefore the potential contribution of tissue-resident CD8 T cells and B cells in protective immunity against *B. pertussis* cannot be ruled out when using FTY720. In order to overcome the non-specific effects of FTY720, the current study employed alternative approaches, including adoptive transfer of purified CD4 T cells and antibody-mediated depletion of CD4 T cells, to examine the specific role of CD4 T_{RM} cells in acquired immunity to *B. pertussis* in the nasal cavity. Wilk et al. demonstrated that adoptive transfer of lung CD4 T cells isolated from convalescent mice adopted a T_{RM}

phenotype and conferred protection against *B. pertussis* in the lungs of naïve recipient hosts [216]. However, the aforementioned study did not examine infection of the nasal cavity. Data from the present study revealed that lung- and nose-resident CD4 T cells purified from convalescent mice re-populated the nasal cavity and lungs of naive recipient mice, produced pathogen-specific IL-17A, and conferred protection against *B. pertussis* infection in the nasal cavity and lungs of recipient mice. These results are in agreement with a study by Dubois et al. which demonstrated that adoptive transfer of *B. pertussis*-specific nasal CD4 T_{RM} cells restored protective immunity against *B. pertussis* in the nasal cavity of IL-17 knock-out mice, and this was accompanied by enhanced neutrophil recruitment to the nasal mucosa [217].

The results presented in this study demonstrated that antibody-mediated depletion of CD4 T cells or neutralisation of IL-17A resulted in impaired bacterial clearance from the nasal cavity following challenge of convalescent mice with *B. pertussis*. Delayed bacterial clearance was also observed in the nasal cavity of convalescent IL-17A$^{-/-}$ mice following re-infection with *B. pertussis*. In these studies, impaired bacterial clearance was associated with reduced CXCL1 production and delayed Siglec-F^{+} neutrophil recruitment to the nasal cavity. In contrast, depletion of CD4 T cells or neutralisation of IL-17A did not impair bacterial clearance in the lungs of convalescent mice following re-infection with *B. pertussis*, suggesting that alternative immune mechanisms, such as humoral responses, may also contribute to protective acquired immunity in the lower respiratory tract.

The results from the present study suggest that the recruitment of Siglec-F^{+} neutrophils to the nasal mucosa during the re-infection of mice with *B. pertussis* is selectively modulated by IL-17A. IL-17A has been shown to promote neutrophil recruitment to the nasal cavity in other infection and inflammatory murine models. Infection of mice with *S. aureus* was associated with an upregulation of CXCL1 and IL-17A in the nasal cavity. Mice lacking T cells or IL-17A$^{-/-}$ mice failed to effectively eliminate *S. aureus* from the upper respiratory tract and this was accompanied by reduced neutrophil influx. Furthermore, antibody-mediated depletion of neutrophils resulted in reduced clearance of *S. aureus* from the nasal cavity [305]. Additionally, i.n. treatment of mice with a neutralising anti-IL-17A antibody was found to reduce neutrophil recruitment to the nasal mucosa and improve symptoms in a murine allergic rhinitis model [338].

Depletion of CD4 T cells in convalescent mice was accompanied by reduced LCN2 concentrations in the nasal wash following re-infection with *B. pertussis*. LCN2 is an AMP that plays a key role in preventing iron acquisition by bacteria that use catecholate-type

siderophores, such as *E. coli* and *K. pneumoniae*, and is a known downstream target of IL-17A [172, 339]. However, the role of LCN2 in protective immunity against *B. pertussis* has not been fully elucidated. The relationship between IL-17A and AMP production in protective immunity in the nasal cavity has been observed in other infection models. Infection of IL-17A$^{-/-}$ mice with *S. aureus* exhibited impaired bacterial clearance from the nasal cavity and this was accompanied by reduced expression of the AMPs CRAMP, mBD-3, and mBD-14 [340].

Interestingly, depletion of CD4 T cells did not reduce the total number of IL-17A-producing cells in the nasal cavity of convalescent mice following re-exposure to *B. pertussis*, suggesting that CD4 T_{RM} cells may also contribute to protective immunity to *B. pertussis* through mechanisms other than IL-17A production. CD4 T cells were the dominant source of IL-17A in the nasal cavity and lungs of convalescent mice prior to and post re-infection with *B. pertussis*. However, in the absence of CD4 T cells, an unidentified CD4^{-}CD8^{-}γδ^{-} cell population was the main source of IL-17A in the nasal cavity and lungs. Although not further characterised in this study, this population could consist of ILC3s, MAIT cells, or a recently described lymphocyte population expressing CD3 but lacking CD4 or CD8 co-receptors termed double-negative (DN) T cells. These unconventional lymphocyte populations have been shown to produce IL-17A at mucosal surfaces [341-343]. MAIT cells are a population of unconventional lymphocytes that recognise riboflavin-derivative antigens presented by the MHC class I-like protein MR1, with Il-17A-producing MAIT cells expressing tissue-resident markers such as CD69 and CD103 identified in sinonasal tissue obtained from patients with chronic rhinosinusitis [344, 345]. ILC3 cells are a subset of innate lymphoid cells which lack an antigen receptor but produce IL-17 and IL-22 in response to Th17 polarising cytokines [346]. ILC3s in the lung have been implicated in the host response to bacterial pathogens including *K. pneumoniae* and *P. aeruginosa* through IL-17-dependent mechanisms [310, 347]. However, the role of these cells in protective immunity to *B. pertussis* in the nasal cavity remains to be elucidated.

Studies have demonstrated that immunisation with a wP vaccine conferred protection in nasal cavity and this was associated with the induction and expansion of IL-17A-producing CD4 T_{RM} cells in the nasal cavity, however the mechanisms by which IL-17A mediates protective immunity was not elucidated [194, 306]. The results presented in this study confirmed that protection against *B. pertussis* in the nasal cavity generated following priming with a wP vaccine is mediated by IL-17A. Impaired bacterial clearance was observed in the nasal cavity, but not the lungs, following neutralisation of IL-17A during infection with *B. pertussis*, and this was accompanied by reduced LCN2 and

decreased infiltration of Siglec-F^{+} neutrophils into the nasal cavity. The findings presented in this study complement those by Dubois et al. which showed that immunisation with a wP vaccine failed to confer protection in the nasal cavity of the IL-17A$^{-/-}$ mice [217]. Furthermore, BPZE1, a live attenuated *B. pertussis* vaccine designed for i.n. administration, failed to protect IL-17A$^{-/-}$ mice against nasal colonisation by *B. pertussis*. However this study attributed the impaired bacterial clearance to reduced secretory IgA production in the nasal cavity in the absence of IL-17A [286]. Nonetheless, these studies highlight the need for next generation pertussis vaccines to induce IL-17A responses in the nasal cavity.

Taken together, the present study demonstrates that infection with *B. pertussis* generates long-lasting CD4 T_{RM} cells in the nasal mucosa which expand locally following re-infection to orchestrate a rapid and localised protective immune response. CD4 T_{RM} cells induced following natural infection or immunisation with a wP vaccine mediate their protective effects in the nasal cavity by producing IL-17A, which subsequently promotes CXCL1 and LCN2 production and accelerates Siglec-F^{+} neutrophil influx into the nasal mucosa. This study suggests that strategies to develop more effective pertussis vaccines should consider the induction IL-17-producing T_{RM} cells that recruit Siglec-F+ neutrophils to control infection of the nasal mucosa. Together, these results highlight a role of CD4 T_{RM} cells and IL-17 in protective immunity against *B. pertussis* in the nasal cavity.

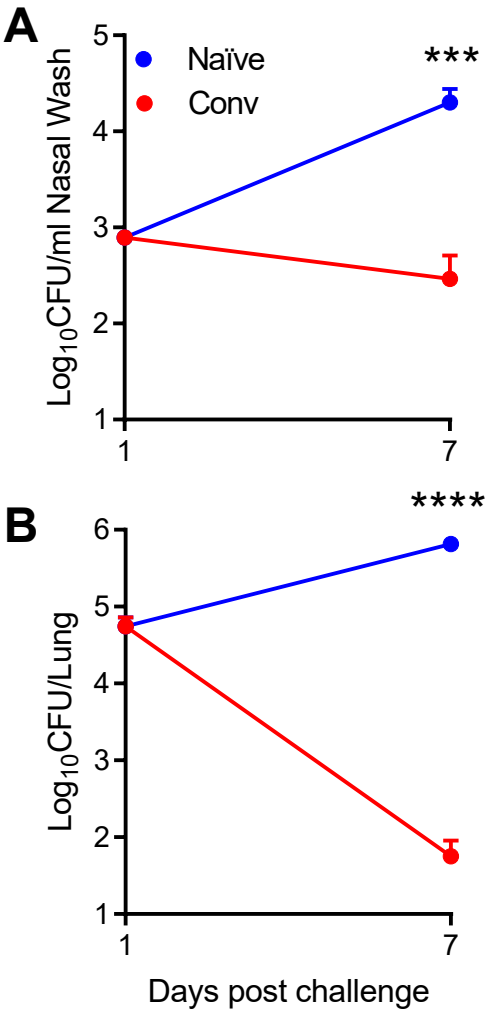

Figure 4.1 Acquired protective immunity persists the nasal cavity and lungs up to one year post primary *B. pertussis* challenge.

C57BL/6 mice were aerosol challenged with live *B. pertussis* and allowed to clear the infection. Convalescent (conv) and naïve control mice were re-challenged with *B. pertussis* 12 months later. The number of viable bacteria on day 7 post challenge was estimated by performing CFU counts on serially diluted nasal washes (A) and lung homogenates (B) from individual mice. Results shown are mean ± SEM CFU counts (n=3 mice per group). ***$p < 0.001$, ****$p < 0.0001$ Naïve versus convalescent mice by two-way ANOVA followed by Sidak's post-test.

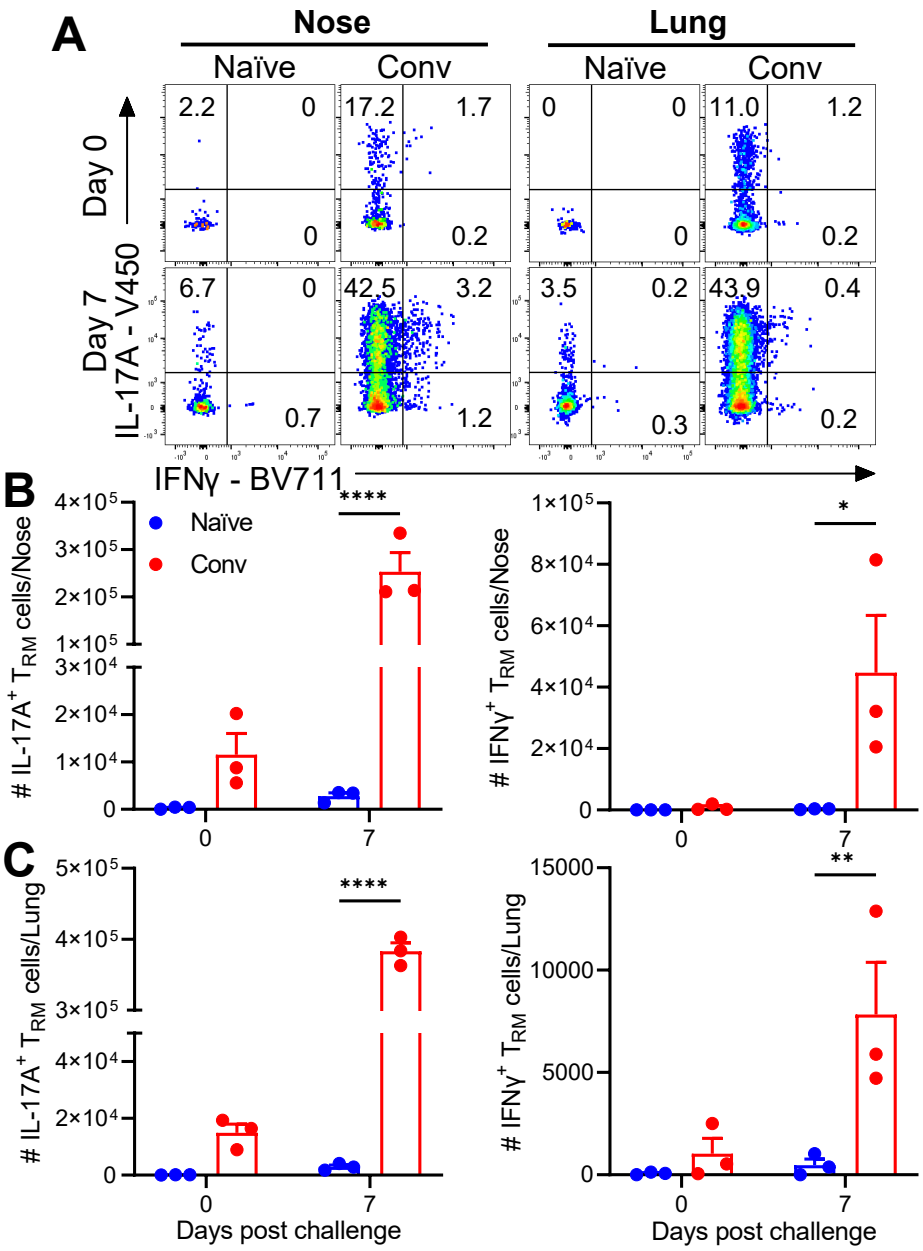
A
Nose
Lung
Naïve
Conv
Naïve
Conv
Day 0
Day 7
IL-17A - V450
IFNγ - BV711
2.2
0
0
17.2
1.7
0.2
0
0
0
11.0
1.2
0.2
6.7
0
0.7
42.5
3.2
1.2
3.5
0.2
0.3
43.9
0.4
0.2
B
IL-17A+ TRM cells/Nose
Naïve
Conv
****
IFNγ+ TRM cells/Nose
*
C
IL-17A+ TRM cells/Lung
****
IFNγ+ TRM cells/Lung
**
Days post challenge
Days post challenge

Figure 4.2 *B. pertussis*-specific CD4 T_{RM} cells persist in the nasal cavity and lungs up to one year post challenge and expand following re-infection with *B. pertussis*.

C57BL/6 mice were aerosol challenged with live *B. pertussis* and allowed to clear the infection. Convalescent (conv) and naïve control mice were re-challenged with *B. pertussis* 12 months later. Nasal tissue and lungs were harvested on the day of and 7 days post challenge. Cell suspensions were prepared and cells were stimulated with sBP (5 µg/ml) and anti-CD28 and anti-CD49d (both at 1 µg/ml) for 20 hours, with brefeldin A (5 µg/ml) added for the final 4 hours of culture. Cells were stained for surface CD4, CD3, CD44, CD62L, CD69, CD103, intracellular IL-17A and IFNγ, and analysed by flow cytometry. Representative flow cytometry plots (A) and absolute number of nasal (B) and lung (C) IL-17A$^+$ and IFNγ$^+$ CD4 T_{RM} cells (CD4$^+$CD3$^+$CD44$^+$CD62L$^-$CD69$^+$CD103$^\pm$) on the day of and 7 days post challenge. Results shown are mean ± SEM (n=3 mice per group). *$p < 0.05$, **$p < 0.01$, ****$p < 0.0001$ Naïve versus convalescent mice by two-way ANOVA followed by Sidak's post-test.

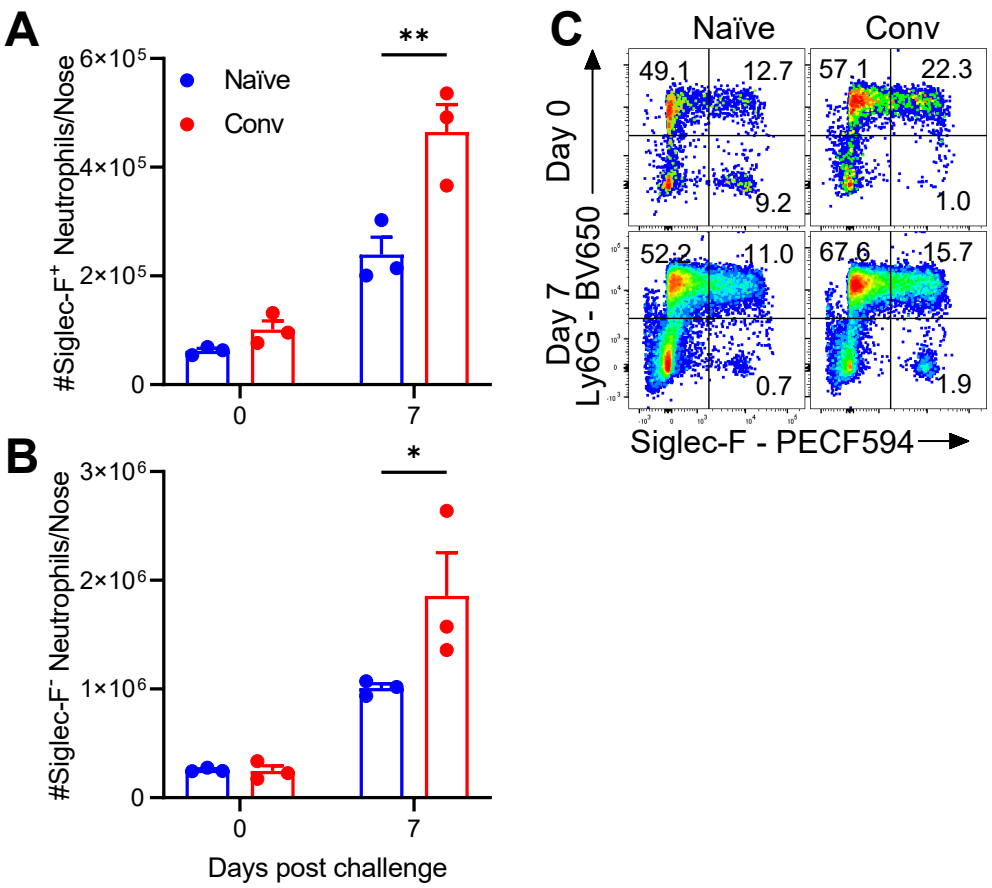

Figure 4.3 Enhanced recruitment of conventional and Siglec-F$^+$ neutrophils to the nasal cavity of convalescent mice following re-infection with *B. pertussis*.

C57BL/6 mice were aerosol challenged with live *B. pertussis* and allowed to clear the infection. Convalescent (conv) and naïve control mice were re-challenged with *B. pertussis* 12 months later. Nasal tissue was harvested on the day of and 7 days post challenge. A single cell suspension was prepared from nasal tissue and cells were stained for CD11b, Ly6G, and Siglec-F, and analysed by flow cytometry. Absolute number of Siglec-F$^+$ neutrophils (Ly6G$^+$CD11b$^+$) (A) and conventional (Siglec-F$^-$) neutrophils (B) in the nasal cavity of naïve and convalescent mice on the day of and 7 days post challenge, with representative flow cytometry plots (C). Data are mean ± SEM (n=3 mice per group). *$p < 0.05$, **$p < 0.01$ Naïve versus convalescent mice by two-way ANOVA followed by Sidak's post-test.

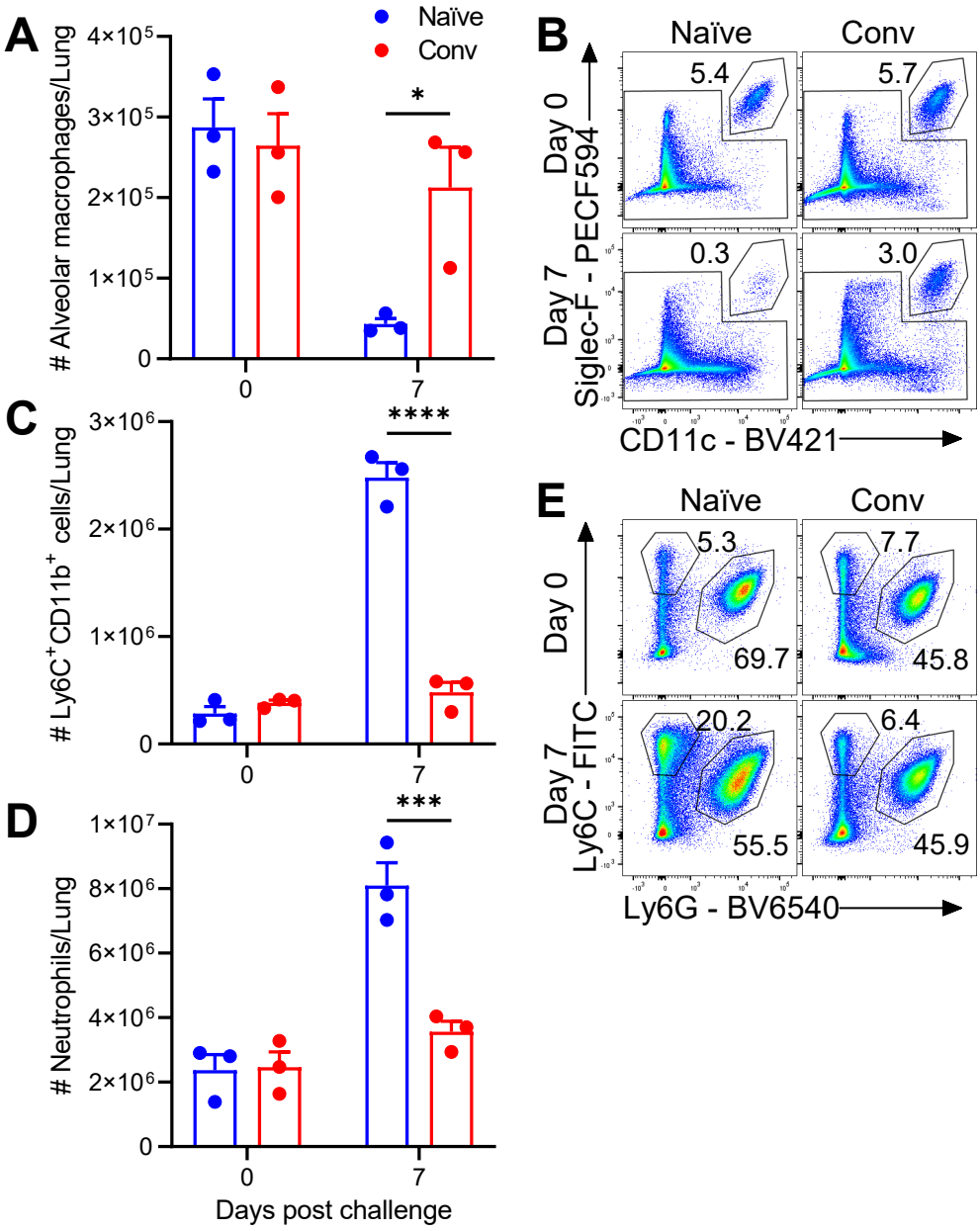

Figure 4.4 Enhanced number of alveolar macrophages but reduced number of Ly6C$^+$CD11b$^+$ monocytes and neutrophils in the lungs of convalescent mice following re-infection with *B. pertussis*.

C57BL/6 mice were aerosol challenged with live *B. pertussis* and allowed to clear the infection. Convalescent (conv) and naïve control mice were re-challenged with *B. pertussis* 12 months later. Lungs were harvested on the day of and 7 days post challenge. Cell suspensions were prepared from the lungs and cells were stained for CD11b, CD11c, Siglec-F, Ly6C, and Ly6G, and analysed by flow cytometry. Absolute number (A) with representative flow cytometry plots (B) of alveolar macrophages (Siglec-F$^+$CD11c$^+$) in the lungs of naïve and convalescent mice on the day of and 7 days post re-challenge. Absolute number of Ly6C$^+$CD11b$^+$ monocytes (C) and neutrophils (Ly6G$^+$CD11b$^+$) (D) in the lungs with representative flow cytometry plots (E). Data are mean ± SEM (n=3 mice per group). *$p < 0.05$, ***$p < 0.001$, ****$p < 0.0001$ Naïve versus convalescent mice by two-way ANOVA followed by Sidak's post-test.

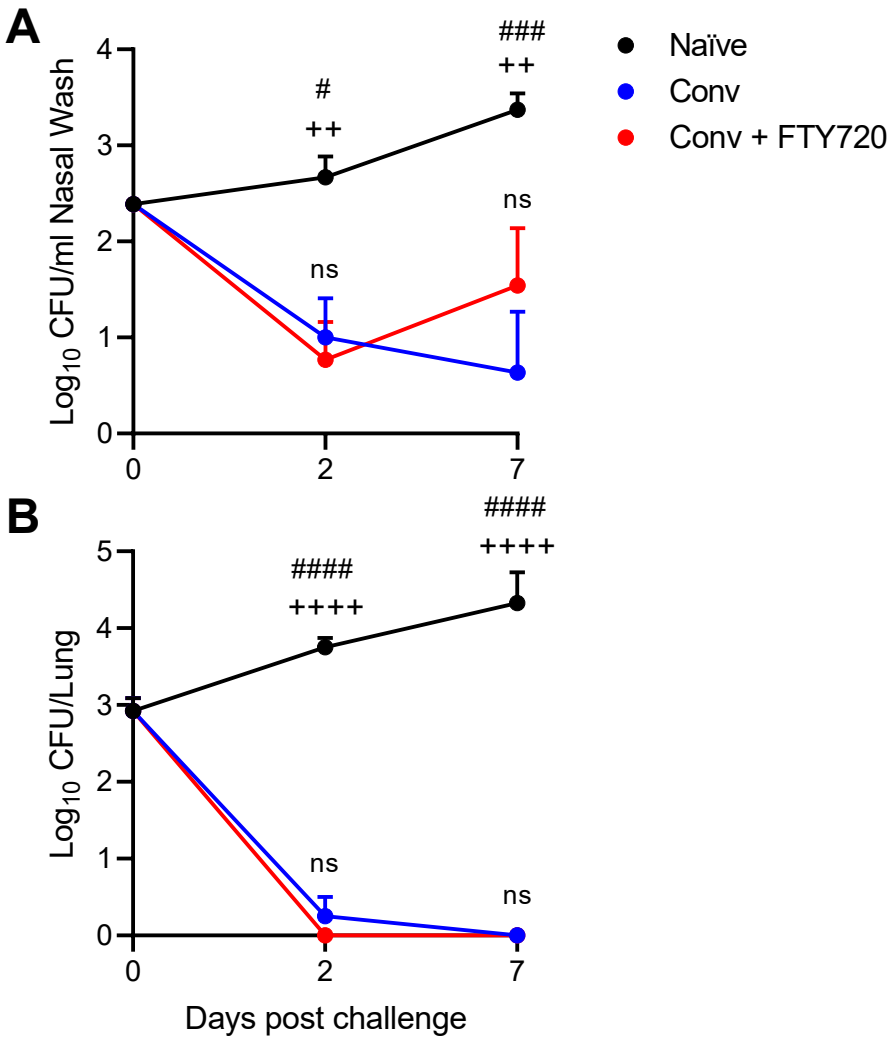

Figure 4.5 FTY720 treatment during a secondary *B. pertussis* infection has no significant effect on bacterial clearance from the nasal cavity or lungs of convalescent mice.

C57BL/6 mice were aerosol challenged with *B. pertussis* and allowed to clear the infection. Convalescent (conv) mice (day 60 p.i.) were given FTY720 in drinking water for 10 days prior to and during re-challenge with *B. pertussis*. Nasal washes and lungs were harvested on day 2 and 7 after re-challenge from convalescent mice or from naïve control mice given a primary challenge on the same day. The number of viable bacteria in the nasal cavity (A) and lungs (B) was estimated by performing CFU counts on serially diluted nasal washes and lung homogenates from individual mice. Results shown are mean ± SEM CFU counts (n=4 mice per group). #$p < 0.05$, ###$p < 0.001$, #### $p < 0.0001$ Naïve versus convalescent mice; ++ $p < 0.01$, ++++ $p < 0.0001$ Naïve versus Convalescent + FTY720 mice by two-way ANOVA with Tukey post-test. No significant difference between convalescent versus convalescent + FTY720 mice by two-way ANOVA followed by Tukey's post-test.

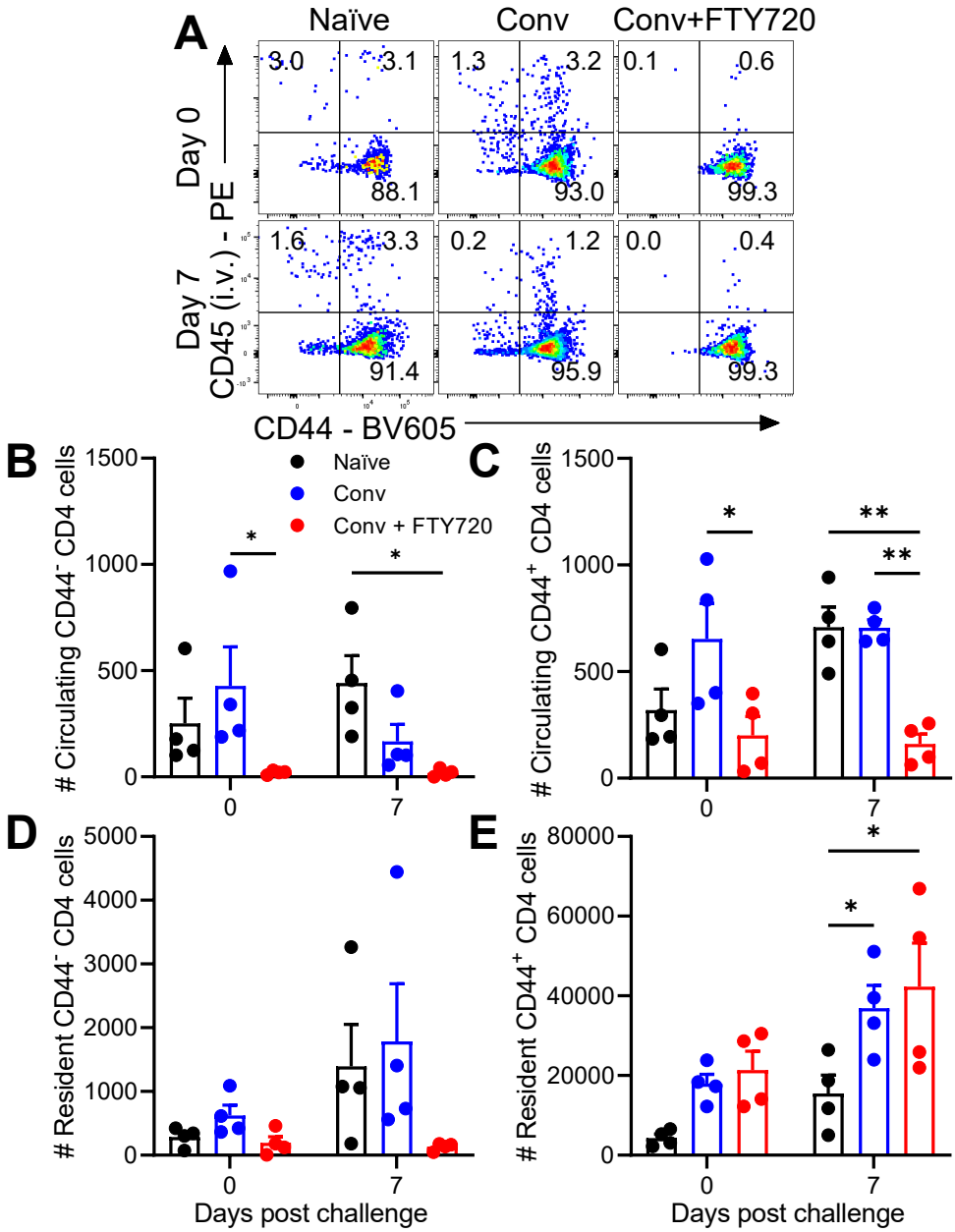

Figure 4.6 Treatment of convalescent mice with FTY720 during *B. pertussis* re-infection significantly reduces the number of circulating CD44$^-$ and CD44$^+$ CD4 T cells in the nasal cavity.

C57BL/6 mice were aerosol challenged with *B. pertussis* and allowed to clear the infection. Convalescent (conv) mice (day 60 p.i.) were given FTY720 in drinking water for 10 days prior to and during re-challenge with *B. pertussis*. On the day of and 7 days after re-challenge, convalescent mice or naïve control mice given a primary challenge on the same day were injected i.v. with a fluorochrome-conjugated anti-CD45 antibody and euthanised 10 min later. Nasal tissue was harvested and mononuclear cells were isolated and stained for CD4, CD3, and CD44, and analysed by flow cytometry. Representative flow cytometry plots (A) and absolute number of circulating (CD45 i.v.$^+$) CD44$^-$ (B) and CD44$^+$ (C) CD4 T cells, and tissue-resdient (CD45 i.v.$^-$) CD44$^-$ (D) and CD44$^+$ (E) CD4 T cells in the nasal cavity. Results shown are mean ± SEM (n=4 mice per group). *p < 0.05, **p < 0.01 by two-way ANOVA followed by Tukey's post-test.

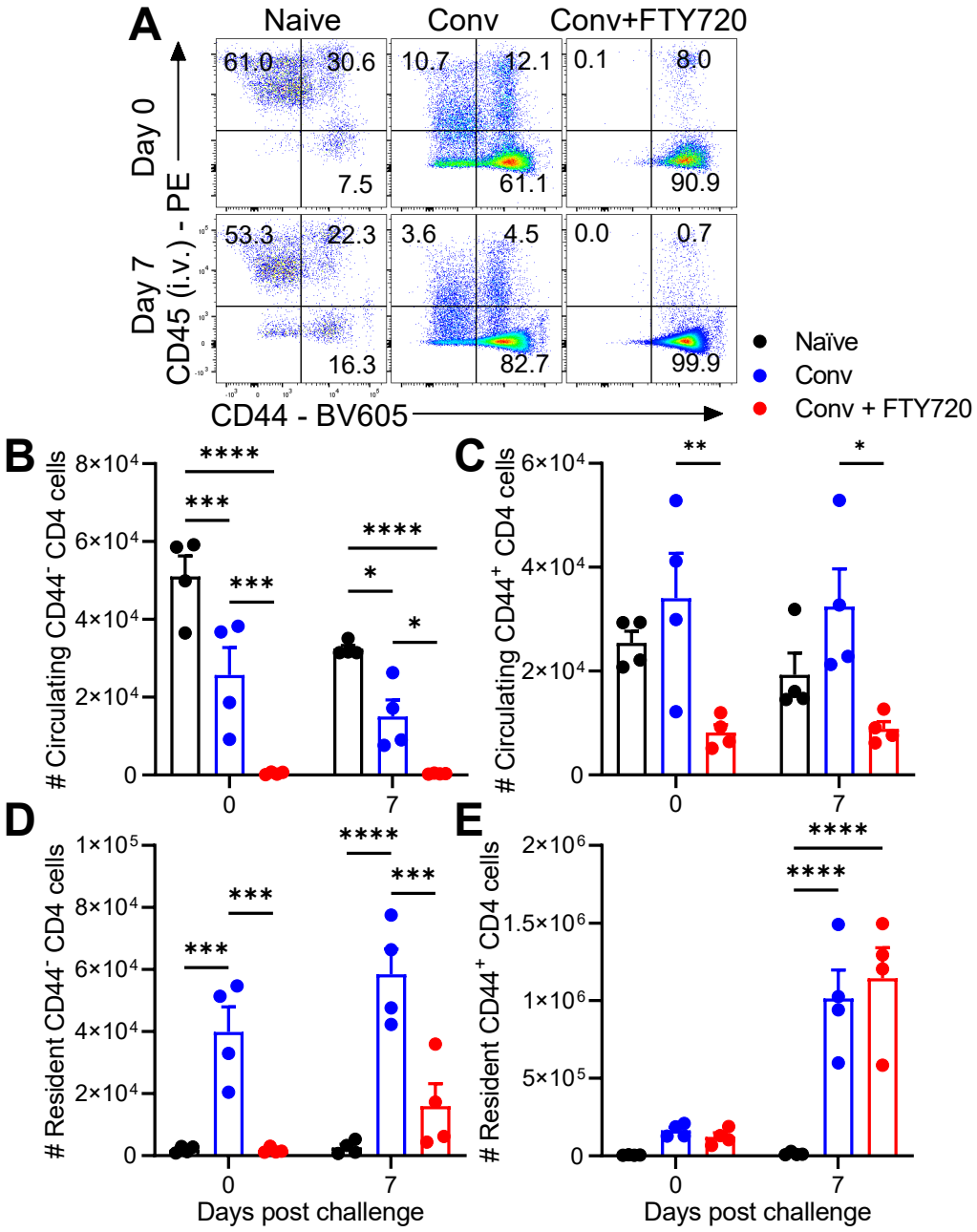

Figure 4.7 Treatment of convalescent mice with FTY720 during *B. pertussis* re-infection does not impair the expansion of lung-resident CD44⁺ CD4 T cells.

C57BL/6 mice were aerosol challenged with *B. pertussis* and allowed to clear the infection. Convalescent (conv) mice (day 60 p.i.) were given FTY720 in drinking water for 10 days prior to and during re-challenge with *B. pertussis*. On the day of and 7 days after re-challenge, convalescent mice or naïve control mice given a primary challenge on the same day were treated with a fluorochrome-conjugated anti-CD45 antibody i.v. and euthanised 10 min later. Lungs were harvested and mononuclear cells were isolated and stained for CD4, CD3, and CD44, and analysed by flow cytometry. Representative flow cytometry plots (A) and absolute number of circulating (CD45 i.v.⁺) CD44⁻ (B) and CD44⁺ (C) CD4 T cells, and tissue-resident (CD45 i.v.⁻) CD44⁻ (D) and CD44⁺ (E) CD4 T cells in the lungs. Results shown are mean ± SEM (n=4 mice per group). *$p < 0.05$, **$p < 0.01$, ***$p < 0.001$, ****$p < 0.0001$ by two-way ANOVA followed by Tukey's post-test.

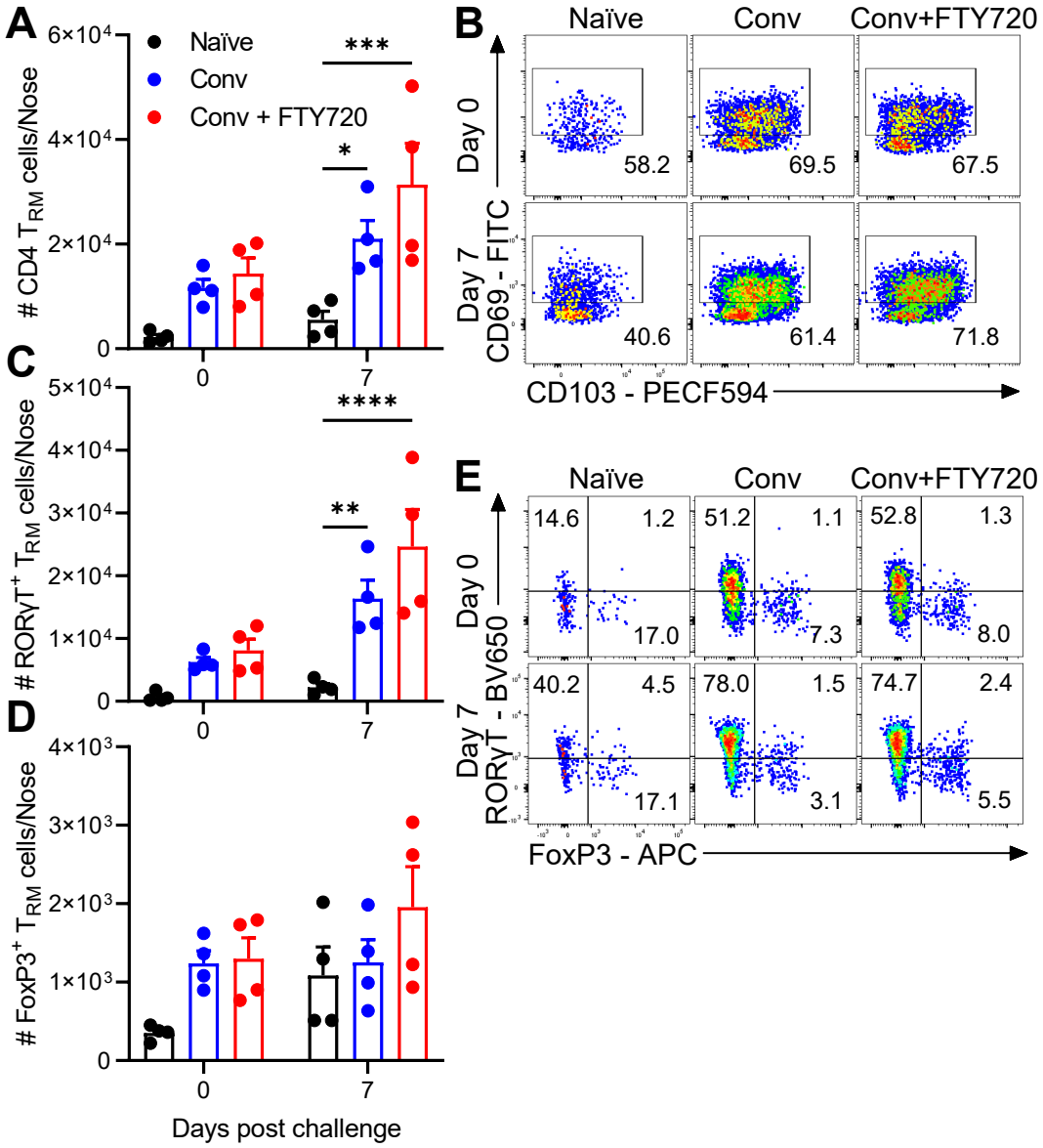

Figure 4.8 Treatment of convalescent mice with FTY720 during *B. pertussis* re-infection does not impair the expansion CD4 T_{RM} cells, or RORγT⁺ or Foxp3⁺ T_{RM} cells in the nasal cavity.

C57BL/6 mice were aerosol challenged with *B. pertussis* and allowed to clear the infection. Convalescent (conv) mice (day 60 p.i.) were given FTY720 in drinking water for 10 days prior to and during re-challenge with *B. pertussis*. On the day of and 7 days after re-challenge, convalescent mice or naïve control mice given a primary challenge on the same day were injected i.v. with a fluorochrome-conjugated anti-CD45 antibody and euthanised 10 min later. Nasal tissue was harvested and mononuclear cells were isolated and stained for surface CD4, CD3, CD44, CD62L, CD69, CD103, and intracellular RORγT and Foxp3, and analysed by flow cytometry. Absolute number of nasal T_{RM} cells ($CD4^+CD3^+CD45i.v.^-CD44^+CD62L^-CD69^+CD103^±$) (A) and representative flow cytometry plots (B). Absolute number of RORγT⁺ (C) and Foxp3⁺ (D) CD4 T_{RM} cells in the nasal cavity, with representative flow cytometry plots (E). Data are mean ± SEM (n=4 mice per group). *$p < 0.05$, **$p < 0.01$, ***$p < 0.001$, ****$p < 0.0001$ by two-way ANOVA followed by Tukey's multiple-comparison test.

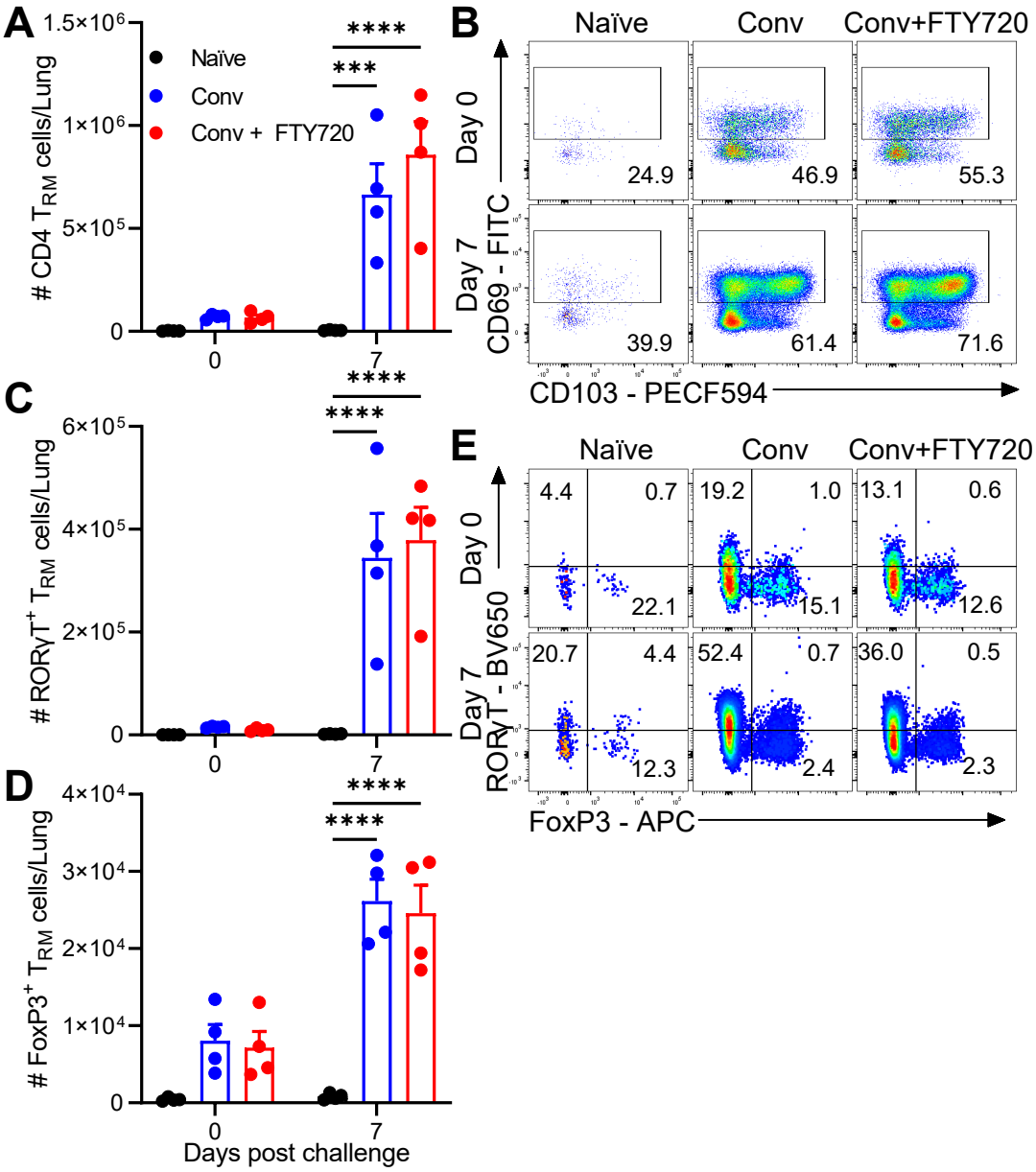

Figure 4.9 Treatment of convalescent mice with FTY720 during *B. pertussis* re-infection does not inhibit the expansion of CD4 T_{RM} cells in the lungs.

C57BL/6 mice were aerosol challenged with *B. pertussis* and allowed to clear the infection. Convalescent (conv) mice (day 60 p.i.) were given FTY720 in drinking water for 10 days prior to and during re-challenge with *B. pertussis*. On the day of and 7 days after re-challenge, convalescent mice or naïve control mice given a primary challenge on the same day were treated with a fluorochrome-conjugated anti-CD45 antibody i.v. and euthanised 10 min later. Lungs were harvested and mononuclear cells were isolated and stained for surface CD4, CD3, CD44, CD62L, CD69, CD103, and intracellular RORγT and Foxp3, and analysed by flow cytometry. Absolute number of lung CD4 T_{RM} cells ($CD4^+CD3^+CD45i.v.^-CD44^+CD62L^-CD69^+CD103^±$) (A) with representative flow cytometry plots (B). Absolute number of $RORγT^+$ (C) and $Foxp3^+$ (D) T_{RM} cells with representative flow cytometry plots (E). Data are mean ± SEM (n=4 mice per group). ***p < 0.001, ****p < 0.0001 by two-way ANOVA followed by Tukey's post hoc test.

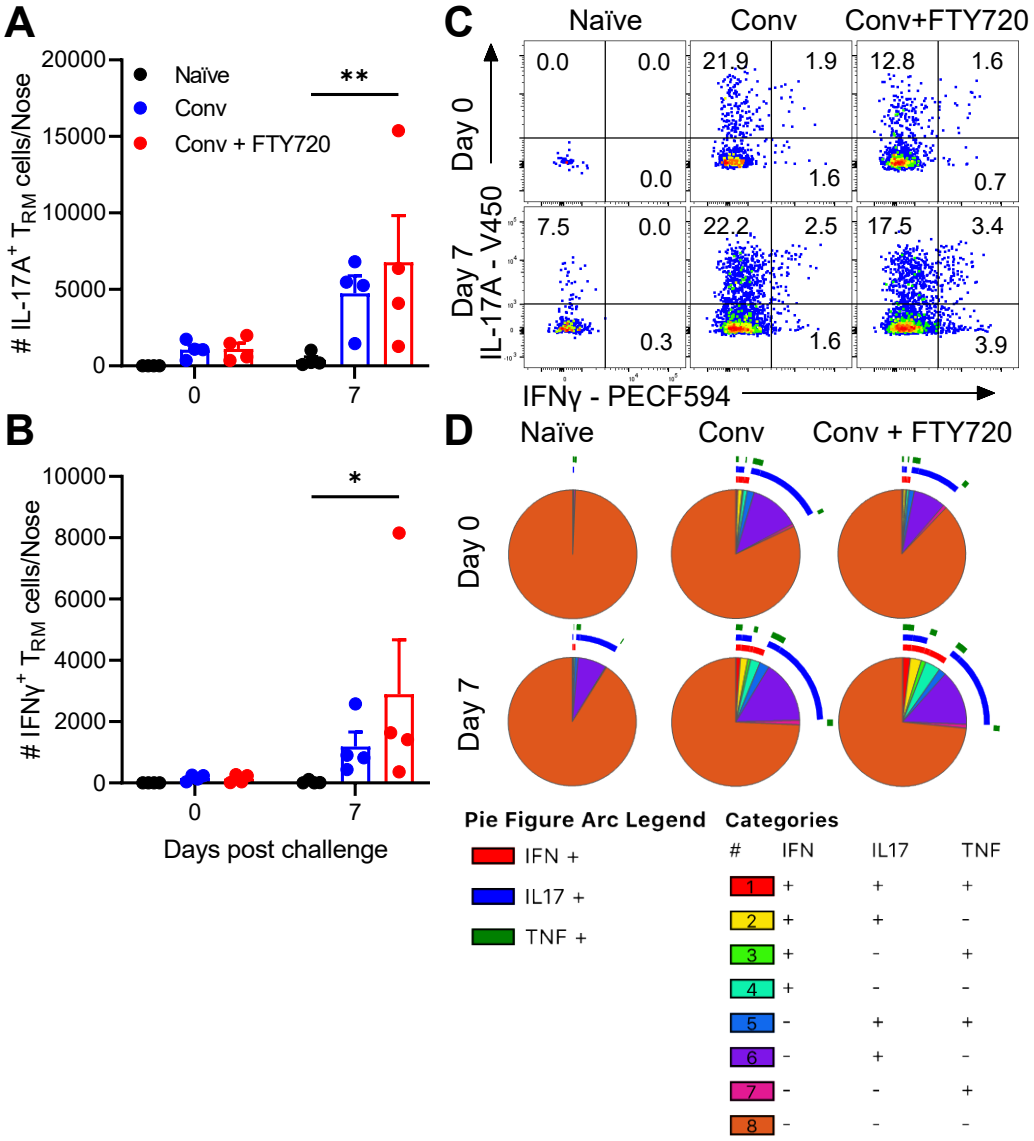

Figure 4.10 FTY720 treatment does not impair the expansion of pathogen-specific IL-17A⁺ or IFNγ⁺ CD4 T_{RM} cells in the nasal cavity of convalescent mice.

C57BL/6 mice were aerosol challenged with *B. pertussis* and allowed to clear the infection. Convalescent (conv) mice (day 60 p.i.) were given FTY720 in drinking water for 10 days prior to and during re-challenge with *B. pertussis*. On the day of and 7 days after re-challenge, convalescent mice or naïve control mice given a primary challenge on the same day were treated with a fluorochrome-conjugated anti-CD45 antibody i.v. and euthanised 10 min later. Nasal tissue was harvested and mononuclear cells were isolated and stimulated with sBP (5 µg/ml) and anti-CD28 and anti-CD49d (both at 1 µg/ml) for 20 hours, with brefeldin A (5 µg/ml) added for the final 4 hours of culture. Cells were stained for surface CD4, CD3, CD44, CD62L, CD69, CD103, and intracellular IL-17A and IFNγ, and analysed by flow cytometry. Absolute numbers of IL-17A⁺ (A) and IFNγ⁺ (B) T_{RM} cells ($CD4^+CD3^+CD45i.v.^-CD44^+CD62L^-CD69^+CD103^\pm$) in the nasal cavity, with representative flow cytometry plots (C). SPICE analysis of cytokine producing nasal CD4 T_{RM} cells (D). Data are mean ± SEM (n=4 mice per group). *$p < 0.05$, **$p < 0.01$ by two-way ANOVA followed by Tukey's post hoc test.

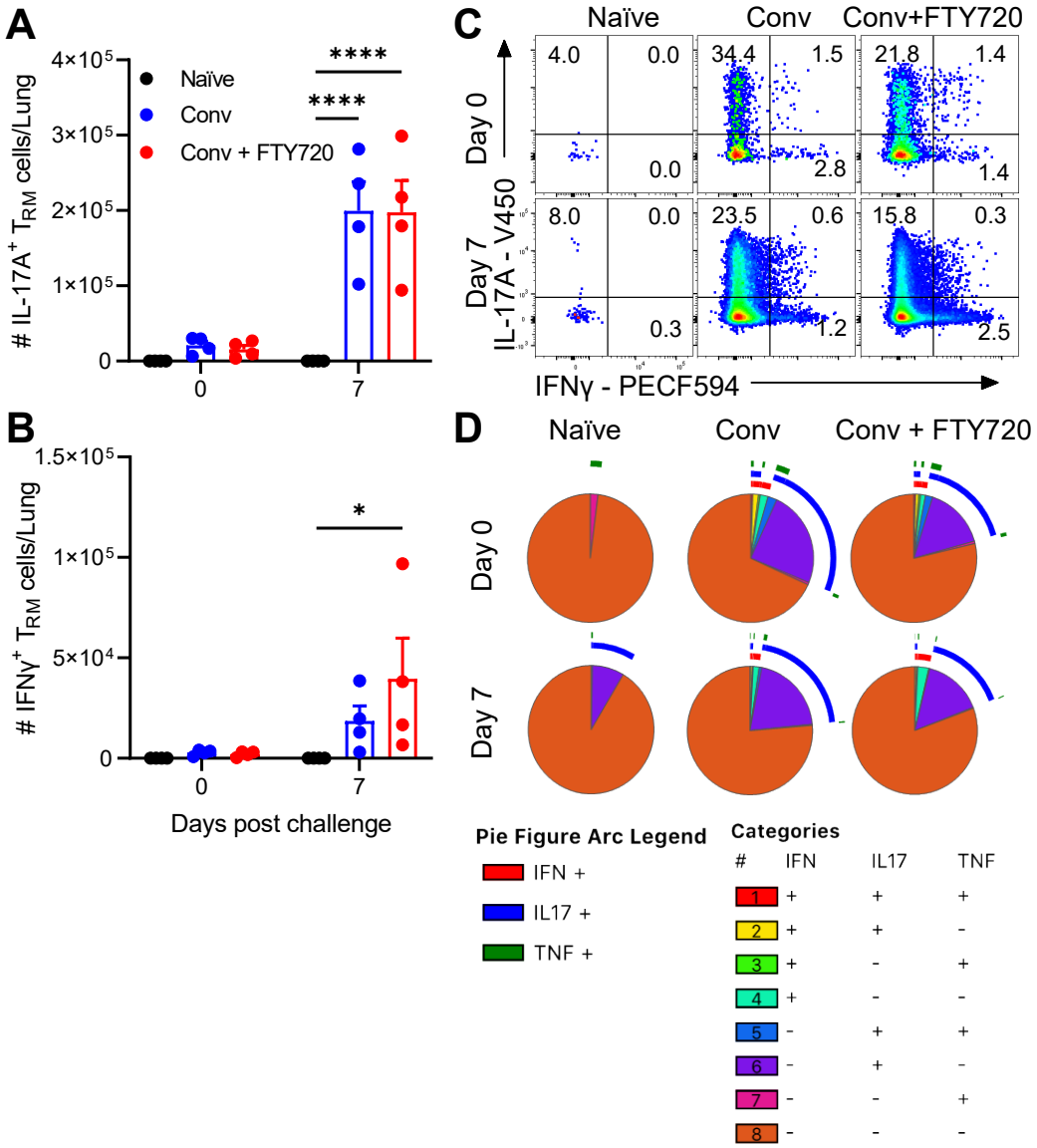

Figure 4.11 FTY720 treatment does not inhibit the expansion of *B. pertussis*-specific IL-17A$^+$ or IFNγ$^+$ CD4 T_{RM} cells in the lungs of convalescent mice.

C57BL/6 mice were aerosol challenged with *B. pertussis* and allowed to clear the infection. Convalescent (conv) mice (day 60 p.i.) were given FTY720 in drinking water for 10 days prior to and during re-challenge with *B. pertussis*. On the day of and 7 days after re-challenge, convalescent mice or naïve control mice given a primary challenge on the same day were treated with a fluorochrome-conjugated anti-CD45 antibody i.v. and euthanised 10 min later. Cell suspensions were prepared from the lungs and cells were stimulate with sBP (5 µg/ml) and anti-CD28 and anti-CD49d (both at 1 µg/ml) for 20 hours, with brefeldin A (5 µg/ml) added for the final 4 hours of culture. Cells were stained for surface CD4, CD3, CD44, CD62L, CD69, CD103, and intracellular IL-17A and IFNγ, and analysed by flow cytometry. Absolute number of IL-17A$^+$ (A) and IFNγ$^+$ (B) T_{RM} cells (CD4$^+$CD3$^+$CD45i.v.$^-$CD44$^+$CD62L$^-$CD69$^+$CD103$^\pm$) in the lungs, with representative flow cytometry plots (C). SPICE analysis of cytokine producing lung CD4 T_{RM} cells (D). Data are mean ± SEM (n=4 mice per group). *$p < 0.05$, ****$p < 0.0001$ by two-way ANOVA followed by Tukey's post hoc test.

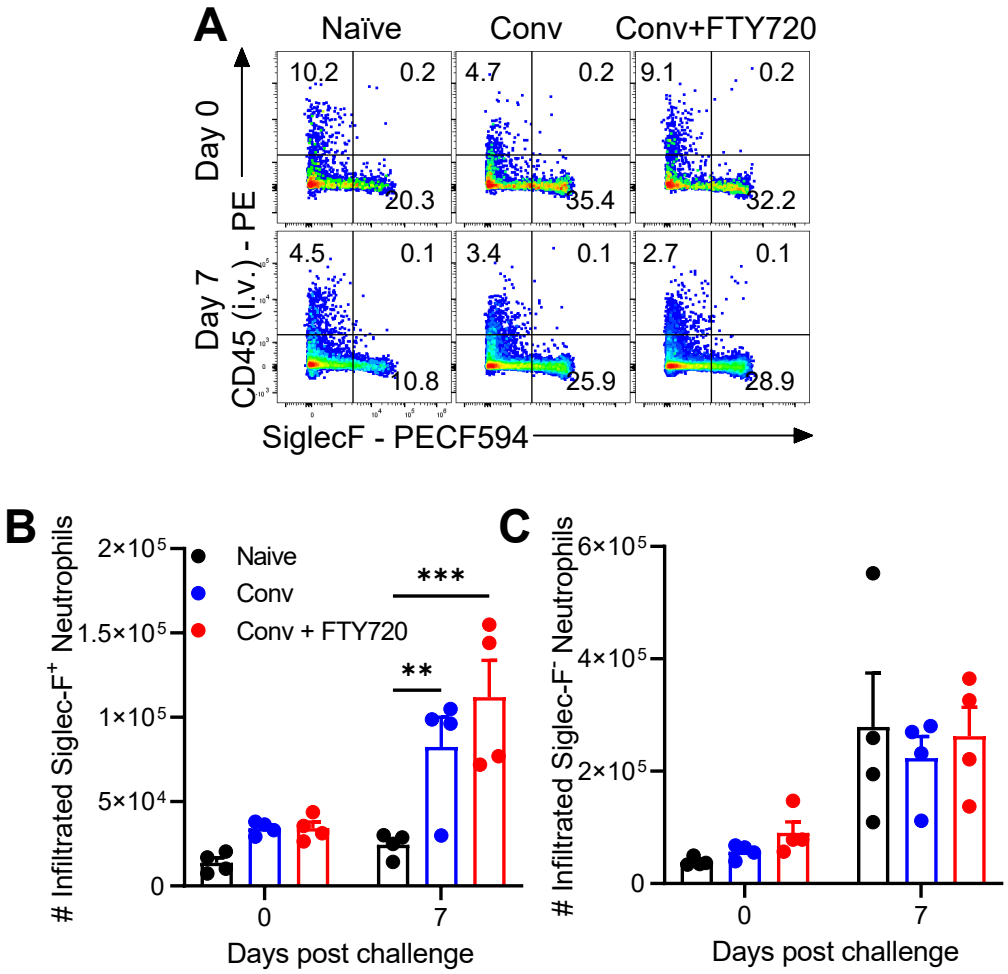

Figure 4.12 Treatment of convalescent mice with FTY720 during *B. pertussis* re-infection does not impair the recruitment of Siglec-F$^+$ neutrophils or conventional neutrophils to the nasal cavity.

C57BL/6 mice were aerosol challenged with *B. pertussis* and allowed to clear the infection. Convalescent (conv) mice (day 60 p.i.) were given FTY720 in drinking water for 10 days prior to and during re-challenge with *B. pertussis*. On the day of and 7 days after re-challenge, convalescent mice or naïve control mice given a primary challenge on the same day were injected i.v. with a fluorochrome-conjugated anti-CD45 antibody and euthanised 10 min later. Nasal tissue was harvested and mononuclear cells were isolated and stained for CD11b, Ly6G, Ly6C, MHCII, and Siglec-F, and analysed by flow cytometry. Representative flow cytometry plots of Siglec-F expression of nose-infiltrating (CD45 i.v.$^-$) neutrophils (Ly6G$^+$CD11b$^+$) (A). Absolute number of tissue-infiltrated (CD45 i.v.$^-$) Siglec-F$^+$ (B) and Siglec-F$^-$ (C) neutrophils (Ly6G$^+$CD11b$^+$) in the nasal cavity. Data are mean ± SEM (n=3-4 mice per group). $^{**}p < 0.01$, $^{***}p < 0.001$ by two-way ANOVA followed by Tukey's post hoc test.

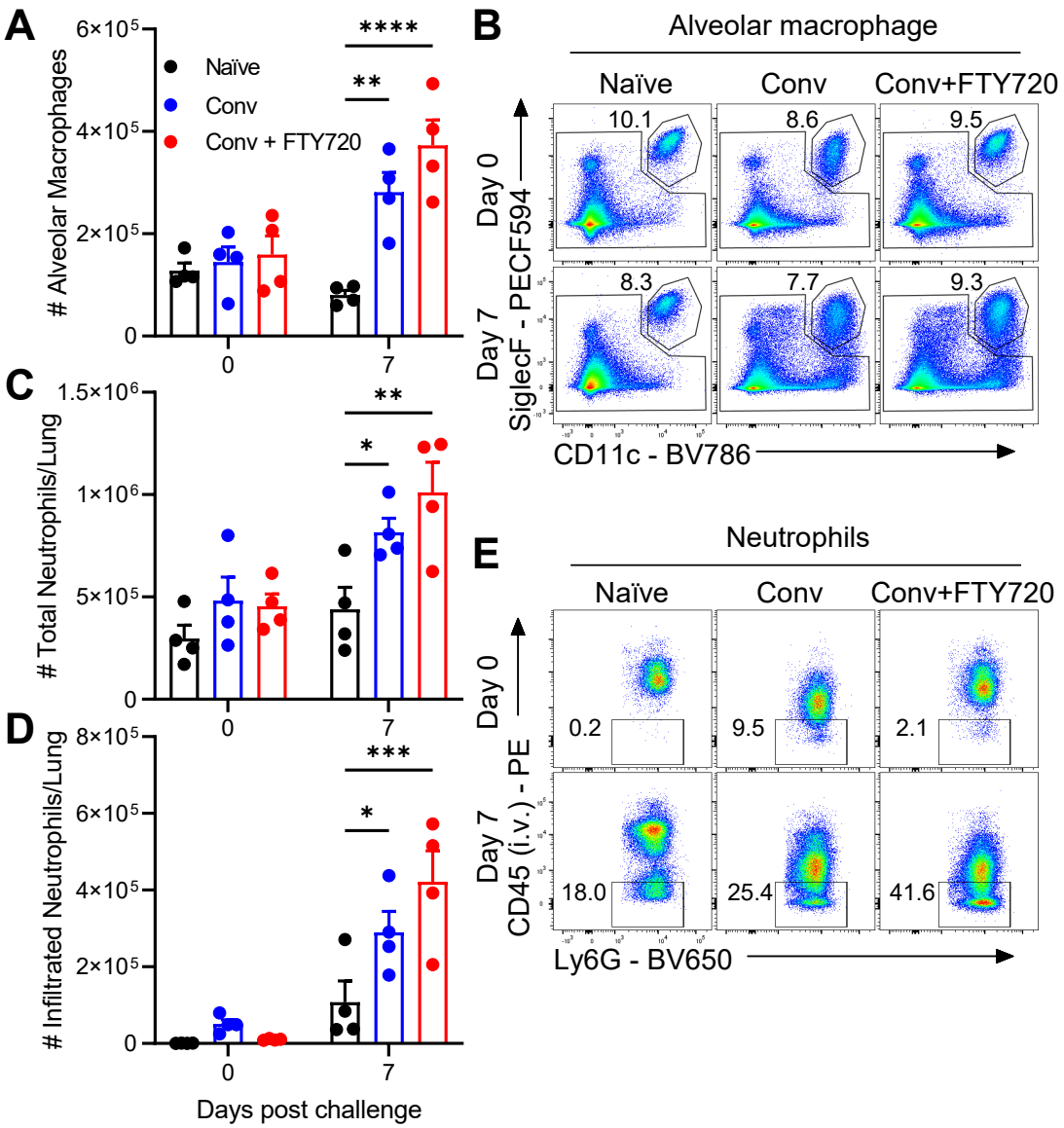

Figure 4.13 Treatment of convalescent mice with FTY720 during *B. pertussis* re-infection has no significant effect on the expansion alveolar macrophages or the infiltration of neutrophils into the lungs.

C57BL/6 mice were aerosol challenged with *B. pertussis* and allowed to clear the infection. Convalescent mice (day 60 p.i.) were given FTY720 in drinking water for 10 days prior to and during re-challenge with *B. pertussis*. On the day of and 7 days after re-challenge, convalescent mice or naïve control mice given a primary challenge on the same day were treated with a fluorochrome-conjugated anti-CD45 antibody i.v. and euthanised 10 min later. Lungs were harvested and mononuclear cells were isolated and stained for CD11b, CD11c, Siglec-F, and Ly6G, and analysed by flow cytometry. Absolute number (A) and representative flow cytometry plots (B) of alveolar macrophages (Siglec-F$^+$CD11c+) in the lungs. Absolute number of total neutrophils (Ly6G$^+$CD11b$^+$) (C) and lung-infiltrated (CD45 i.v.$^-$) neutrophils (D) with representative flow cytometry plots (E). Data are mean ± SEM (n=4 mice per group). *p < 0.05, **p < 0.01, ***p < 0.001, ****p < 0.0001 by two-way ANOVA followed by Tukey's post-test.

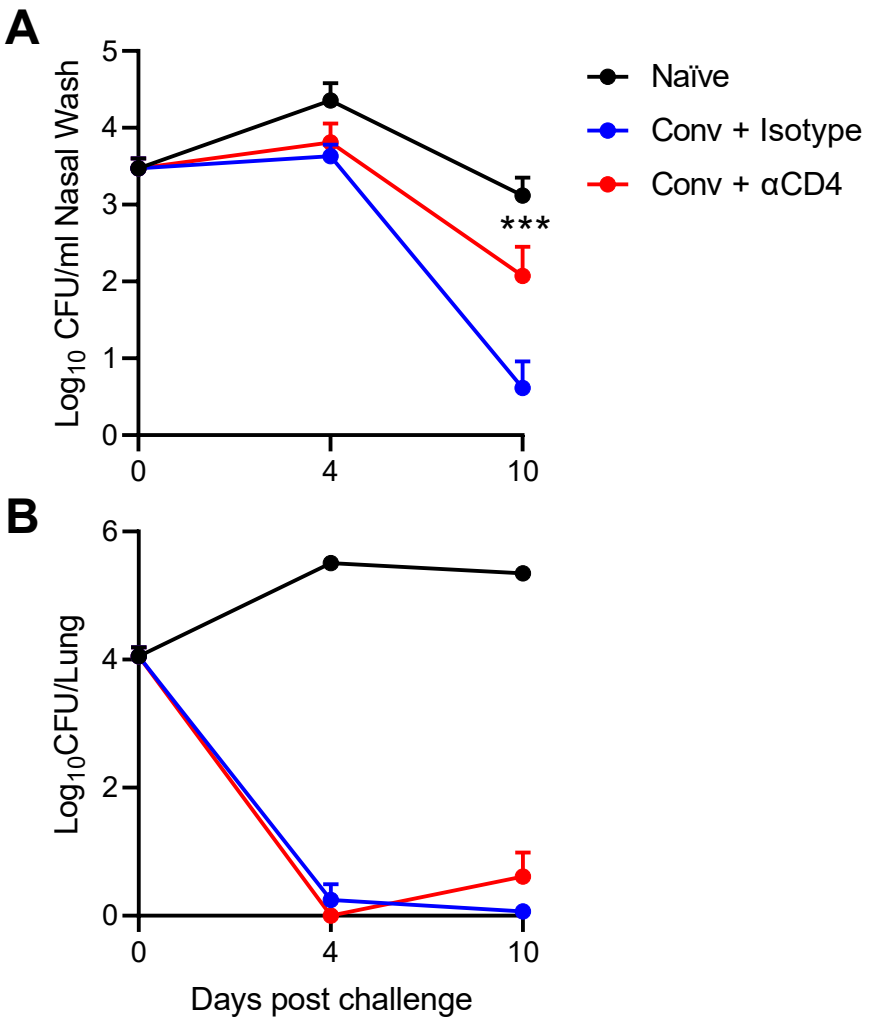

Figure 4.14 Treatment of convalescent mice with a depleting anti-CD4 antibody during a secondary *B. pertussis* infection delays bacterial clearance from the nasal cavity.

C57BL/6 mice were aerosol challenged with *B. pertussis* and allowed to clear the infection. Convalescent (conv) mice (day 70 p.i.) were treated with an anti-CD4 antibody or isotype control administered i.p. (200 µg/mouse) and i.n. (50 µg/mouse) 5 and 1 day before and every 4 days after a secondary *B. pertussis* challenge. The number of viable bacteria in the nasal cavity (A) and lungs (B) was estimated by performing CFU counts on serially diluted nasal washes and lung homogenates harvested on days 4 and 10 post challenge. Results combined from 2 independent experiments. Data are mean ± SEM CFU counts (n=6-10 mice per group). ***$p < 0.001$ isotype control versus anti-CD4 treatment by two-way ANOVA followed by Sidak's post-test.

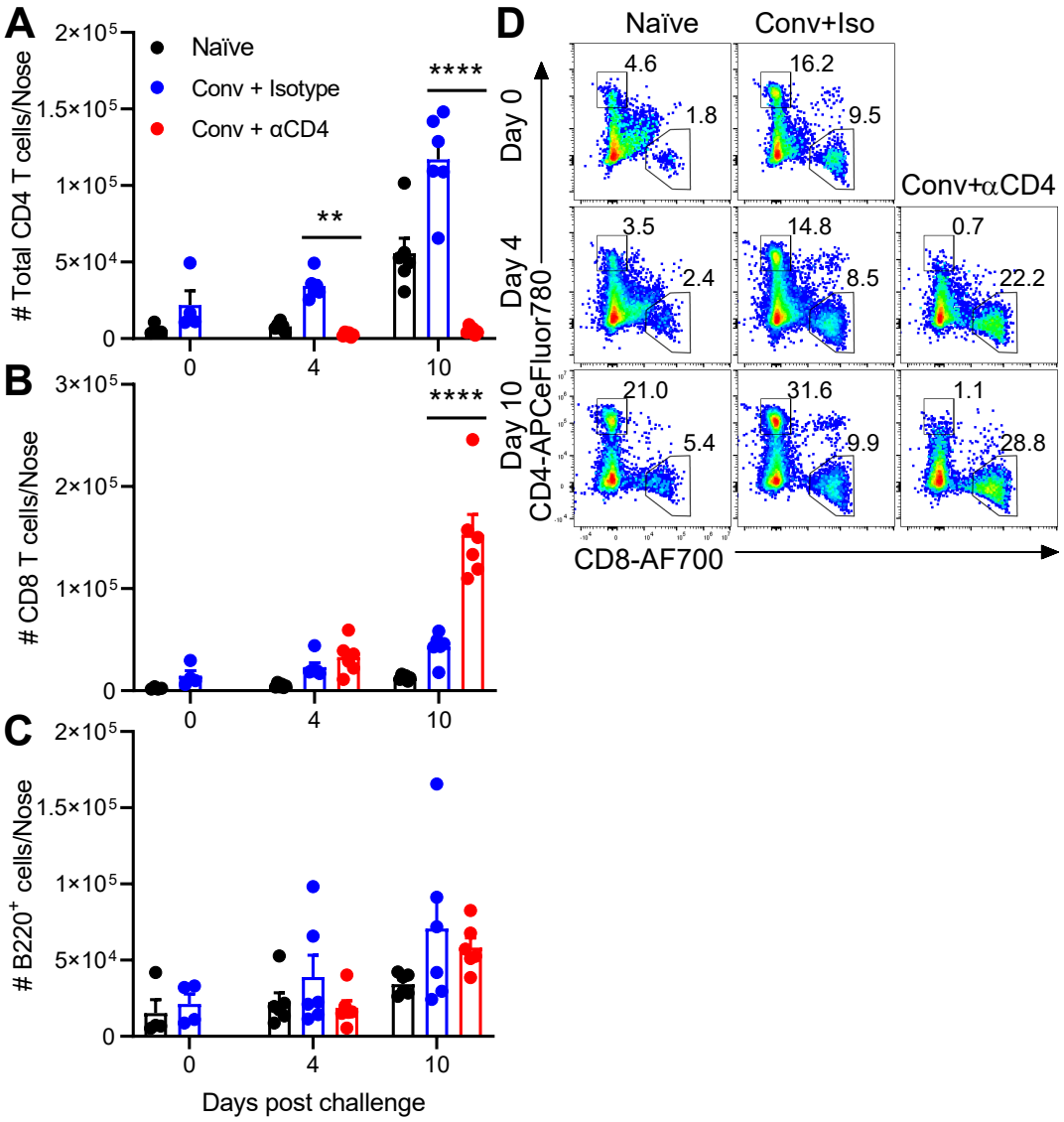

Figure 4.15 Anti-CD4 treatment significantly reduces CD4 T cells and enhances CD8 T cells, but has no effect on B220⁺ cells, in the nasal cavity of convalescent mice during *B. pertussis* re-infection.

Convalescent (conv) mice (70 days p.i.) were treated with an anti-CD4 antibody or isotype control administered i.p. (200 µg/mouse) and i.n. (50 µg/mouse) 5 and 1 day before and every 4 days after a secondary *B. pertussis* challenge. Nasal tissue was harvested on the day of and 4 and 10 days after re-challenge from convalescent mice or from naïve control mice given a primary challenge on the same day. Cell suspensions were prepared from nasal tissue and cells were stained for CD3, CD4, CD8 and B220, and analysed by flow cytometry. Absolute number of CD4⁺ T cells (A), CD8⁺ T cells (B), and B220⁺ cells (C) in the nasal tissue with representative flow cytometry plots of CD4 and CD8 populations, pre-gated on CD3⁺ cells (D). Data are mean ± SEM (n=4-6/group). $^{**}p < 0.01$, $^{****}p < 0.0001$ isotype control versus anti-CD4 treatment by two-way ANOVA followed by Sidak's post-test.

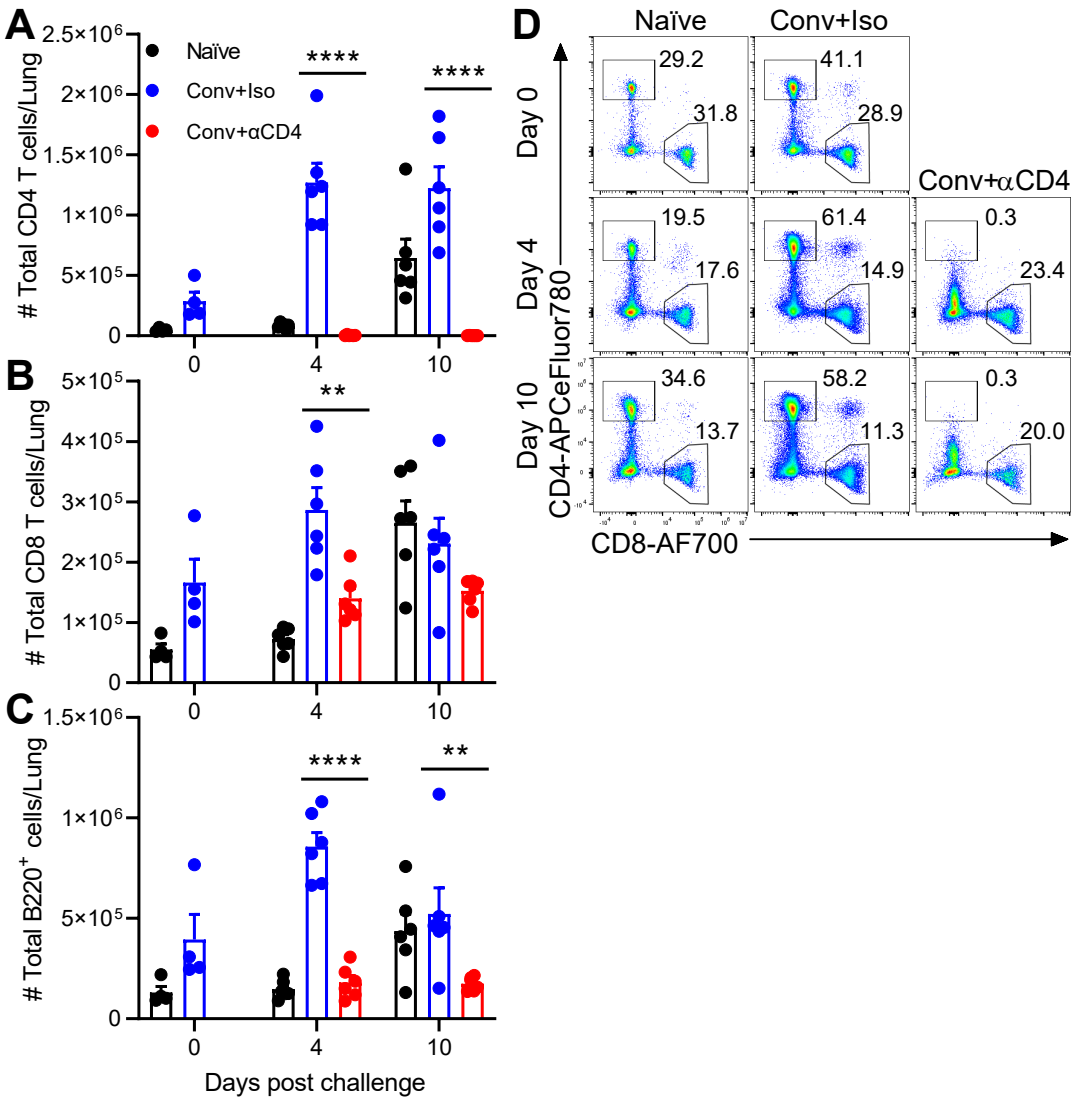

Figure 4.16 Anti-CD4 treatment significantly reduces CD4 T cells, CD8 T cells, and B220⁺ cells in the lungs of convalescent mice during *B. pertussis* re-infection.

Convalescent (conv) mice (70 days p.i.) were treated with an anti-CD4 antibody or isotype control administered i.p. (200 µg/mouse) and i.n. (50 µg/mouse) 5 and 1 day before and every 4 days after a secondary *B. pertussis* challenge. Lungs were harvested on the day of and 4 and 10 days after re-challenge from convalescent mice or from naïve control mice given a primary challenge on the same day. Cell suspensions were prepared from lungs and cells were stained for CD3, CD4, CD8 and B220 and analysed by flow cytometry. Absolute number of CD4⁺ T cells (A), CD8⁺ T cells (B), and B220⁺ cells (C) in the lungs, with representative flow cytometry plots of CD4 and CD8 populations, pre-gated on CD3⁺ cells (D). Data are mean ± SEM (n=4-6/group). $^{**}p < 0.01$, $^{****}p < 0.0001$ isotype control versus anti-CD4 treatment by two-way ANOVA followed by Sidak's post-test.

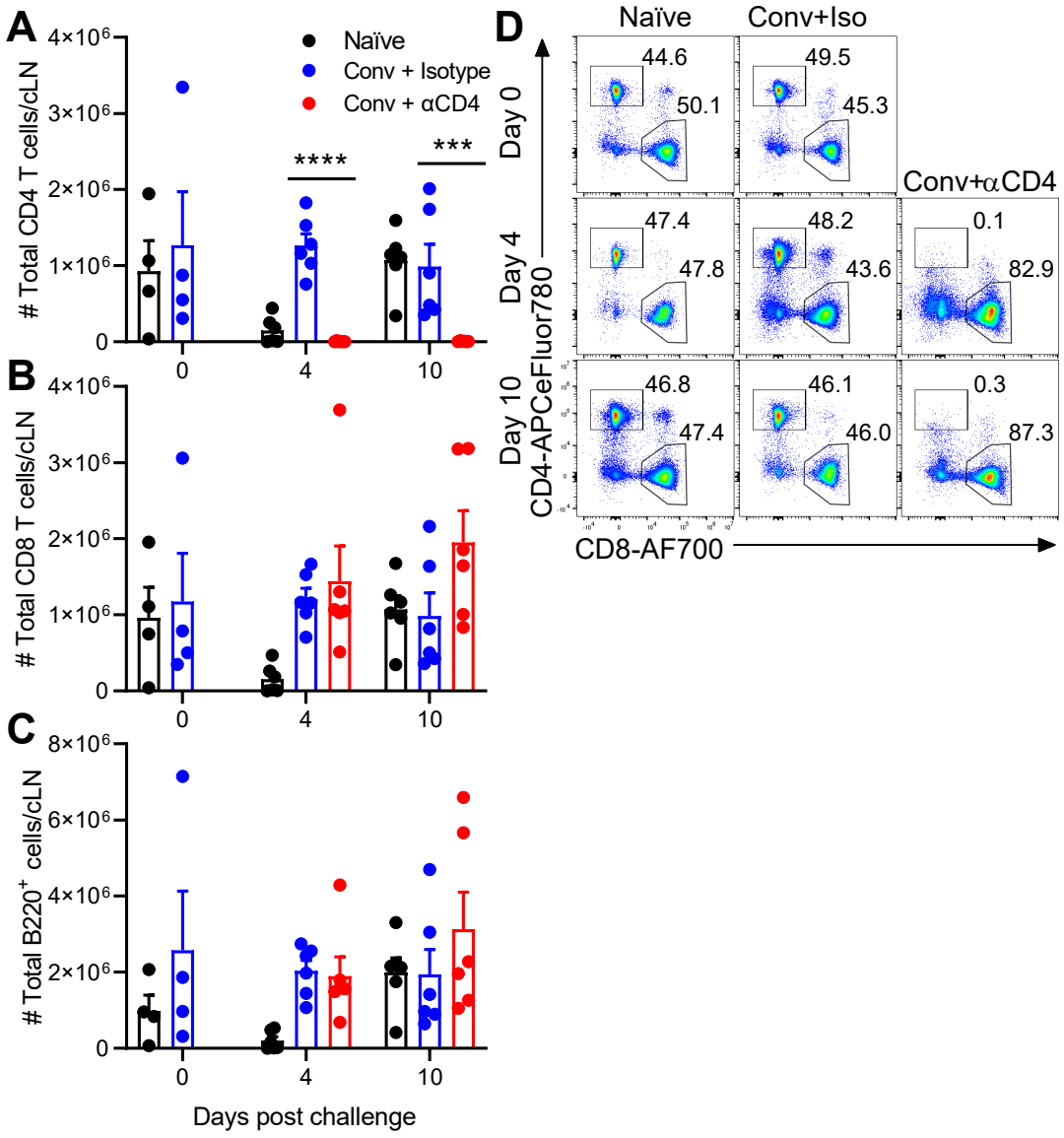

Figure 4.17 Anti-CD4 treatment significantly reduces CD4 T cells, but has no effect on CD8 T cell or B220⁺ cell numbers, in the cLNs during *B. pertussis* re-infection.

Convalescent (conv) mice (70 days p.i.) were treated with an anti-CD4 antibody or isotype control administered i.p. (200 µg/mouse) and i.n. (50 µg/mouse) 5 and 1 day before and every 4 days after a secondary *B. pertussis* challenge. cLNs were harvested on the day of and 4 and 10 days after re-challenge from convalescent mice or from naïve control mice given a primary challenge on the same day. Cell suspensions were prepared from cLNs and cells were stained for CD3, CD4, CD8 and B220, and analysed by flow cytometry. Absolute number of CD4⁺ T cells (A), CD8⁺ T cells (B), and B220⁺ cells (C) in the cLNs with representative flow cytometry plots of CD4 and CD8 populations, pre-gated on CD3⁺ cells (D). Data are mean ± SEM (n=4-6/group). ***p < 0.001, ****p < 0.0001 isotype control versus anti-CD4 treatment by two-way ANOVA followed by Sidak's post-test.

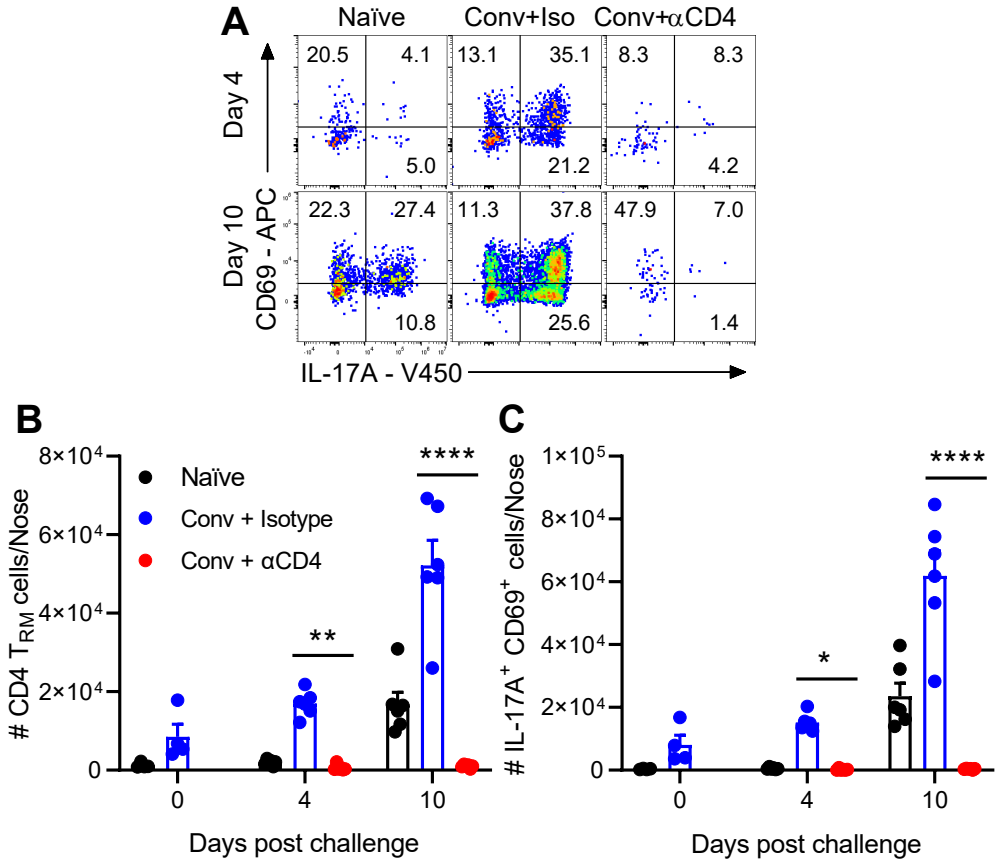

Figure 4.18 IL-17A-producing CD4 T_{RM} cells expand in the nasal cavity of convalescent mice during *B. pertussis* re-infection and are significantly reduced following anti-CD4 treatment.

Convalescent (conv) mice (70 days p.i.) were treated with an anti-CD4 antibody or isotype control administered i.p. (200 µg/mouse) and i.n. (50 µg/mouse) 5 and 1 day before and every 4 days after a secondary *B. pertussis* challenge. On the day of and 4 and 10 days after re-challenge, convalescent mice or naïve control mice given a primary challenge on the same day were treated with a fluorochrome-conjugated anti-CD45 antibody i.v. and euthanised 10 min later. Nasal tissue was harvested and mononuclear cells were isolated and stimulated with PMA (50 ng/ml), ionomycin (500 ng/ml), and brefeldin A (5 µg/ml) for 4 hours. Cells were stained for surface CD4, CD3, CD44, CD62L, CD69, CD103, and intracellular IL-17A and RORγT, and analysed by flow cytometry. Representative flow cytometry plots of IL-17A$^+$ CD4 T_{RM} cells ($CD4^+CD3^+CD45i.v.^-CD44^+CD62L^+CD69^+CD103^±$) in the nasal cavity (A). Absolute number of unstimulated CD4 T_{RM} cells in the nasal cavity (B). Absolute number of IL-17A-producing CD4 T_{RM} cells in the nasal cavity (C). Results shown are mean ± SEM (n=4-6/group). *p < 0.05, **p < 0.01, ****p < 0.0001 isotype control versus anti-CD4 treatment by two-way ANOVA followed by Sidak's post-test.

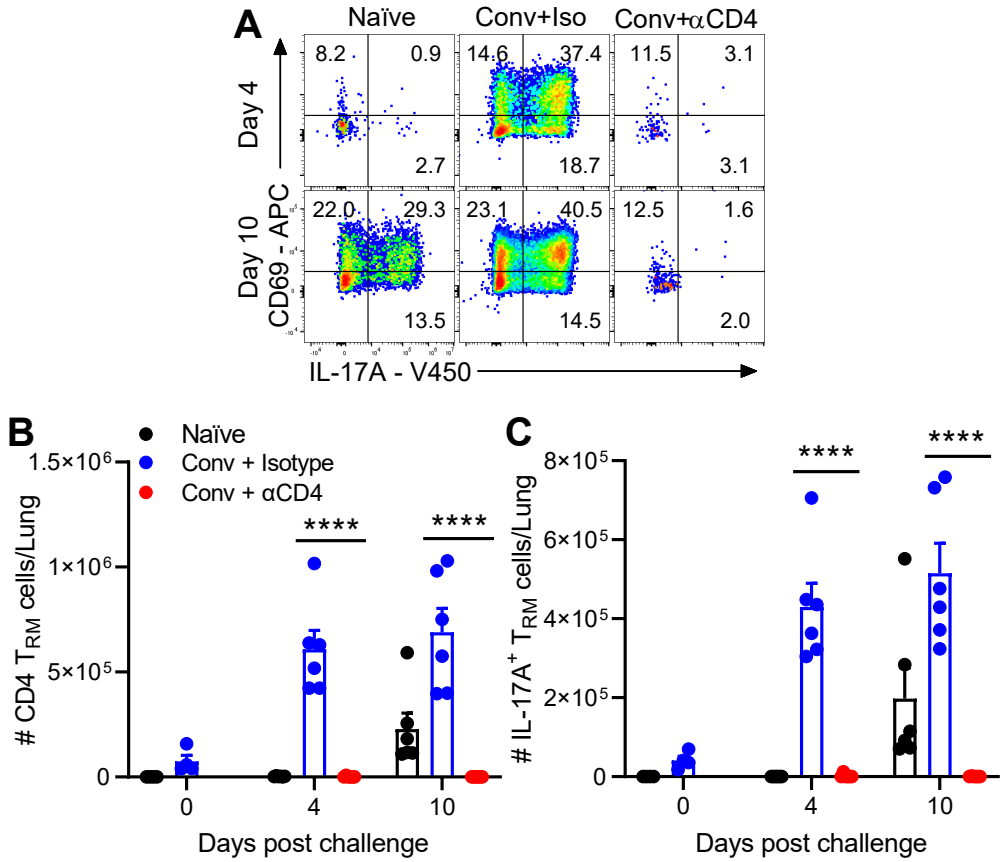

Figure 4.19 IL-17A-producing CD4 T_{RM} cells expand in the lungs of convalescent mice during *B. pertussis* re-infection and are significantly reduced following anti-CD4 treatment.

Convalescent (conv) mice (70 days p.i.) were treated with an anti-CD4 antibody or isotype control administered i.p. (200 µg/mouse) and i.n. (50 µg/mouse) 5 and 1 day before and every 4 days after a secondary *B. pertussis* challenge. On the day of and 4 and 10 days after re-challenge, convalescent mice or naïve control mice given a primary challenge on the same day were treated with a fluorochrome-conjugated anti-CD45 antibody i.v. and euthanised 10 min later. Lungs were harvested and mononuclear cells were isolated and stimulated with PMA (50 ng/ml), ionomycin (500 ng/ml), and brefeldin A (5 µg/ml) for 4 hours. Cells were stained for surface CD4, CD3, CD44, CD62L, CD69, CD103, and intracellular IL-17A, and analysed by flow cytometry. Representative flow cytometry plots of IL-17A$^+$ CD4 T_{RM} cells ($CD4^+CD3^+CD45i.v.^-CD44^+CD62L^+CD69^+CD103^\pm$) in the lungs (A). Absolute number of unstimulated CD4 T_{RM} cells in the lungs (B). Absolute number of IL-17A-producing CD4 T_{RM} cells in the lungs (C). Results shown are mean ± SEM (n=4-6/group). ****$p < 0.0001$ isotype control versus anti-CD4 treatment by two-way ANOVA followed by Sidak's post-test.

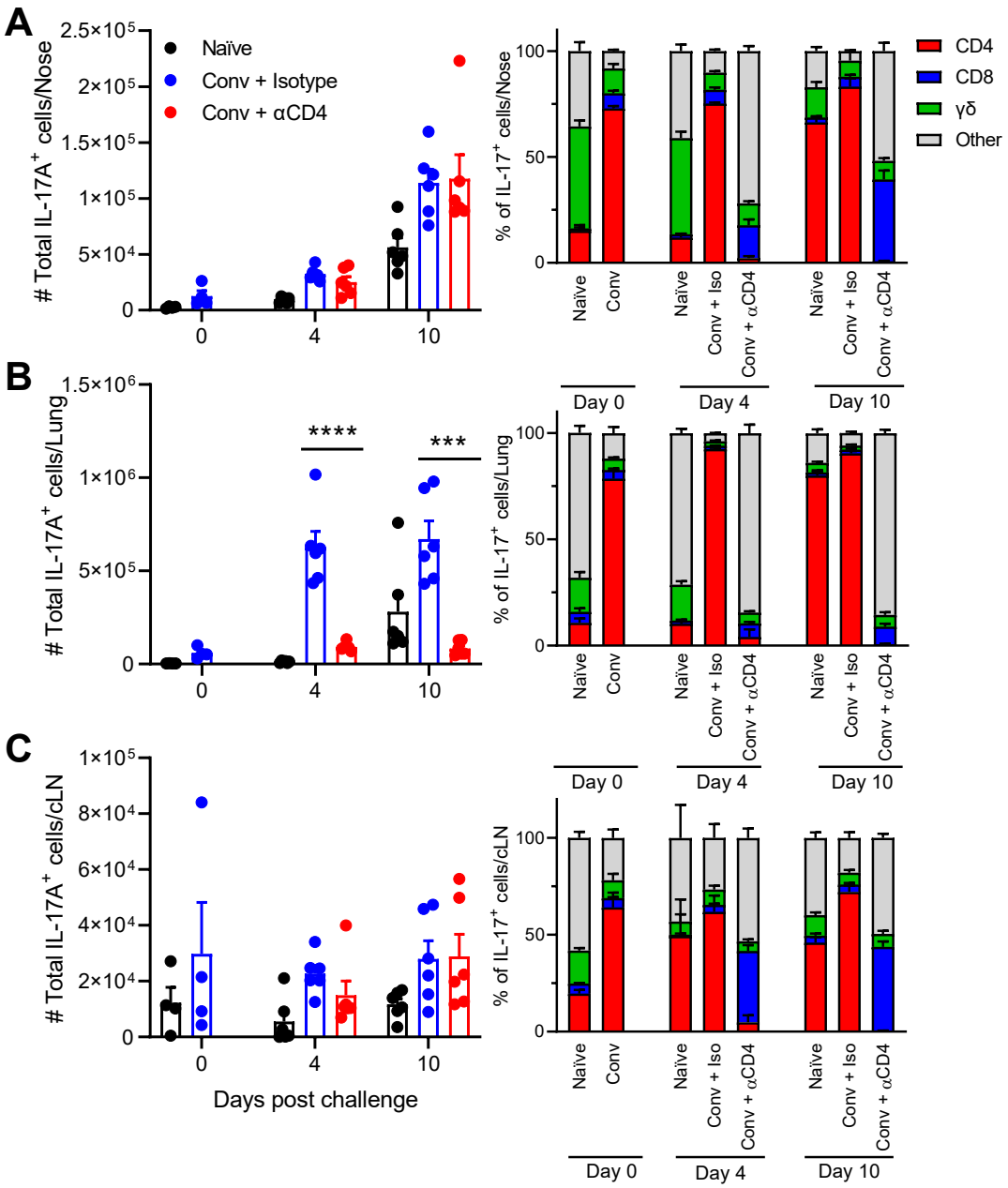

Figure 4.20 CD4 T cells are the dominant source of IL-17A in the nasal cavity, lungs, and cLNs of convalescent mice during *B. pertussis* re-infection.

Convalescent (conv) mice (70 days p.i.) were treated with an anti-CD4 antibody or isotype control administered i.p. (200 µg/mouse) and i.n. (50 µg/mouse) 5 and 1 day before and every 4 days after a secondary *B. pertussis* challenge. On the day of and day 4 and 10 post re-challenge, nasal tissue, lungs and cLNs were harvested from convalescent mice or naïve control mice given a primary challenge on the same day. Cell suspensions were prepared and cells were stimulated with PMA (50 ng/ml), ionomycin (500 ng/ml), and brefeldin A (5 µg/ml) for 4 hours. Cells were stained for surface CD3, CD4, CD8, γδ TCR, and intracellular IL-17A, and analysed by flow cytometry. Absolute numbers of IL-17A$^+$ cells, gated on the total live population, with frequencies of CD4$^+$, CD8$^+$, and γδ$^+$ cells, pre-gated the total IL-17A$^+$ cells in the nose (A), lungs (B), and cLNs (C). Data are mean ± SEM (n=4-6/group). ***p < 0.001, ****p < 0.0001, isotype control versus anti-CD4 treatment by two-way ANOVA followed by Sidak's post-test.

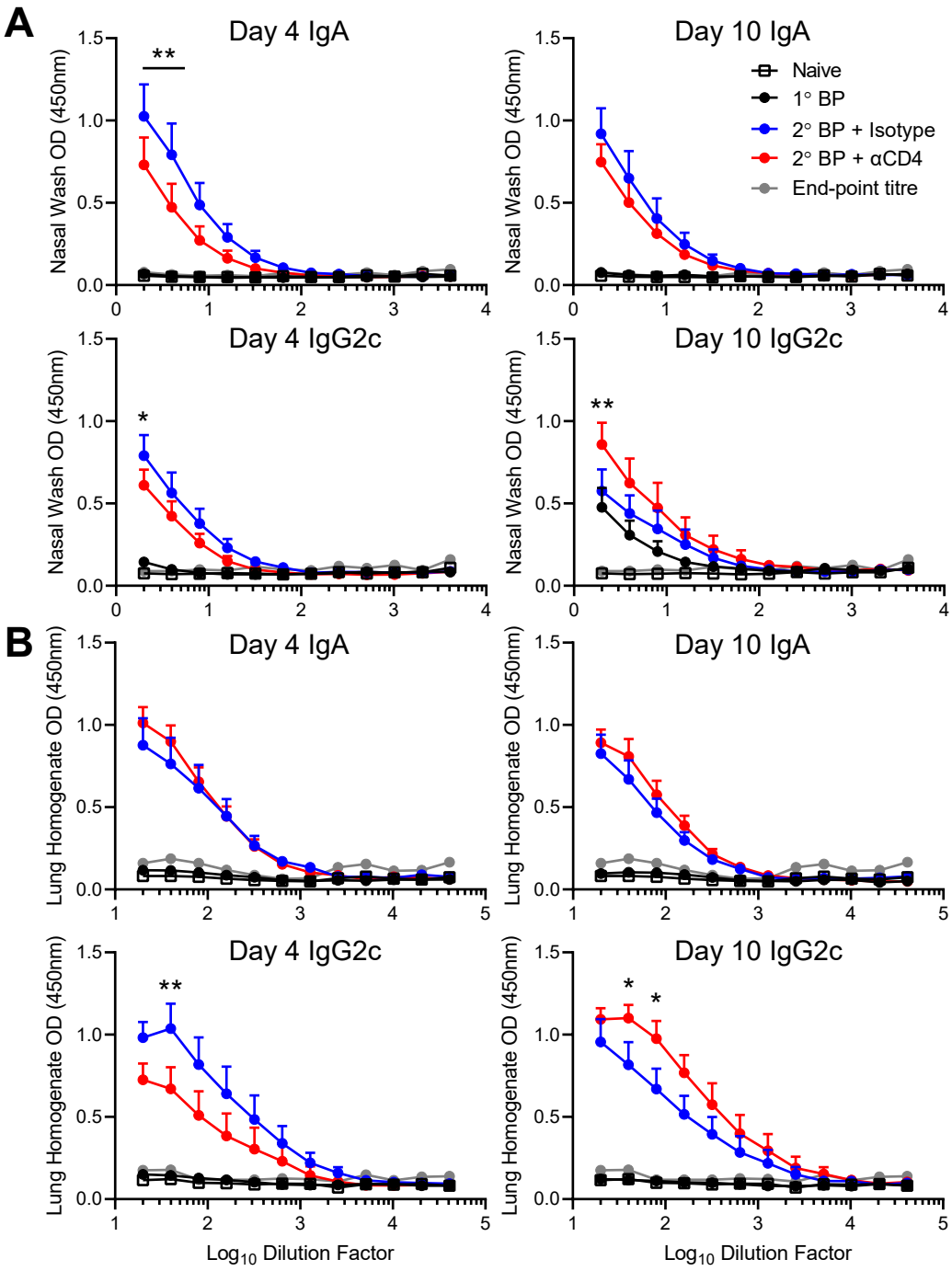
A
Day 4 IgA
Day 10 IgA
Day 4 IgG2c
Day 10 IgG2c
Nasal Wash OD (450nm)
Naive
1° BP
2° BP + Isotype
2° BP + αCD4
End-point titre
**
*
**
B
Day 4 IgA
Day 10 IgA
Day 4 IgG2c
Day 10 IgG2c
Lung Homogenate OD (450nm)
**
*
*
Log10 Dilution Factor
Log10 Dilution Factor

Figure 4.21 Effect of CD4 depletion on *B. pertussis*-specific IgA and IgG2c responses in the nasal wash and lung homogenates of convalescent mice.

Convalescent (conv) mice (70 days p.i.) were treated with an anti-CD4 antibody or isotype control administered i.p. (200 µg/mouse) and i.n. (50 µg/mouse) 5 and 1 day before and every 4 days after a secondary *B. pertussis* challenge. On the day of and 4 and 10 days after re-challenge, nasal washes and lung homogenates were harvested from convalescent mice or naïve control mice given a primary challenge on the same day. *B. pertussis*-specific IgA and IgG2c antibody responses were determined by ELISA on nasal washes (A) and lung homogenates (B) from individual mice. Results shown are mean ± SEM (n=4-6/group). *$p < 0.05$, **$p < 0.01$ isotype control versus anti-CD4 treatment by two-way ANOVA followed by Sidak's post-test.

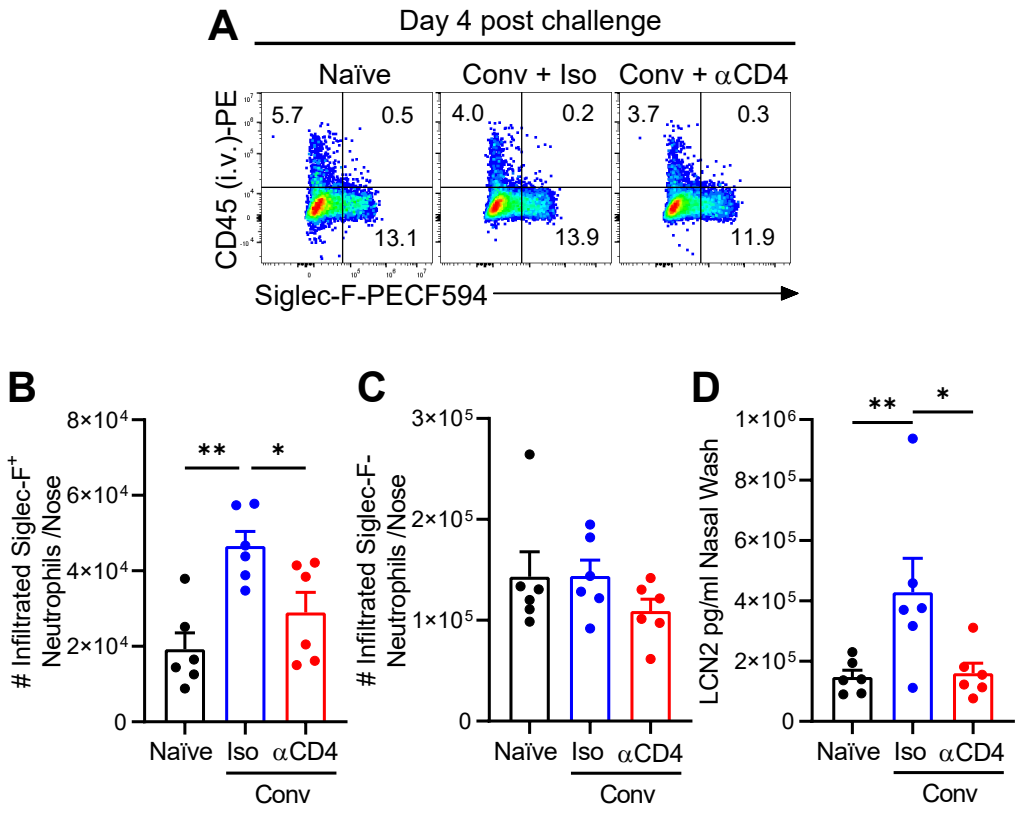

Figure 4.22 Depletion of CD4 T cells in convalescent mice significantly reduces Siglec-F⁺ neutrophils and LCN2 concentration the nasal cavity on day 4 post *B. pertussis* re-challenge.

Convalescent (conv) mice (70 days p.i.) were treated with an anti-CD4 antibody or isotype control administered i.p. (200 µg/mouse) and i.n. (50 µg/mouse) 5 and 1 day before and every 4 days after a secondary *B. pertussis* challenge. On day 4 post challenge, convalescent mice or naïve control mice given a primary challenge on the same day were treated with a fluorochrome-conjugated anti-CD45 antibody i.v. and euthanised 10 min later. Nasal tissue was harvested and mononuclear cells were isolated and stained for CD11b, Ly6G and Siglec-F, and analysed by flow cytometry. Representative flow cytometry plots (A) and absolute number of infiltrated (CD45 i.v.$^-$) Siglec-F$^+$ neutrophils (Ly6G$^+$CD11b$^+$) (B) and Siglec-F$^-$ neutrophils (C) in the nasal cavity. Nasal washes were collected on day 4 post challenge and LCN2 concentration was quantified by ELISA (D). Results shown are mean ± SEM (n=6 per group). *p < 0.05, **p < 0.01 by one-way ANOVA followed by Tukey's post-test.

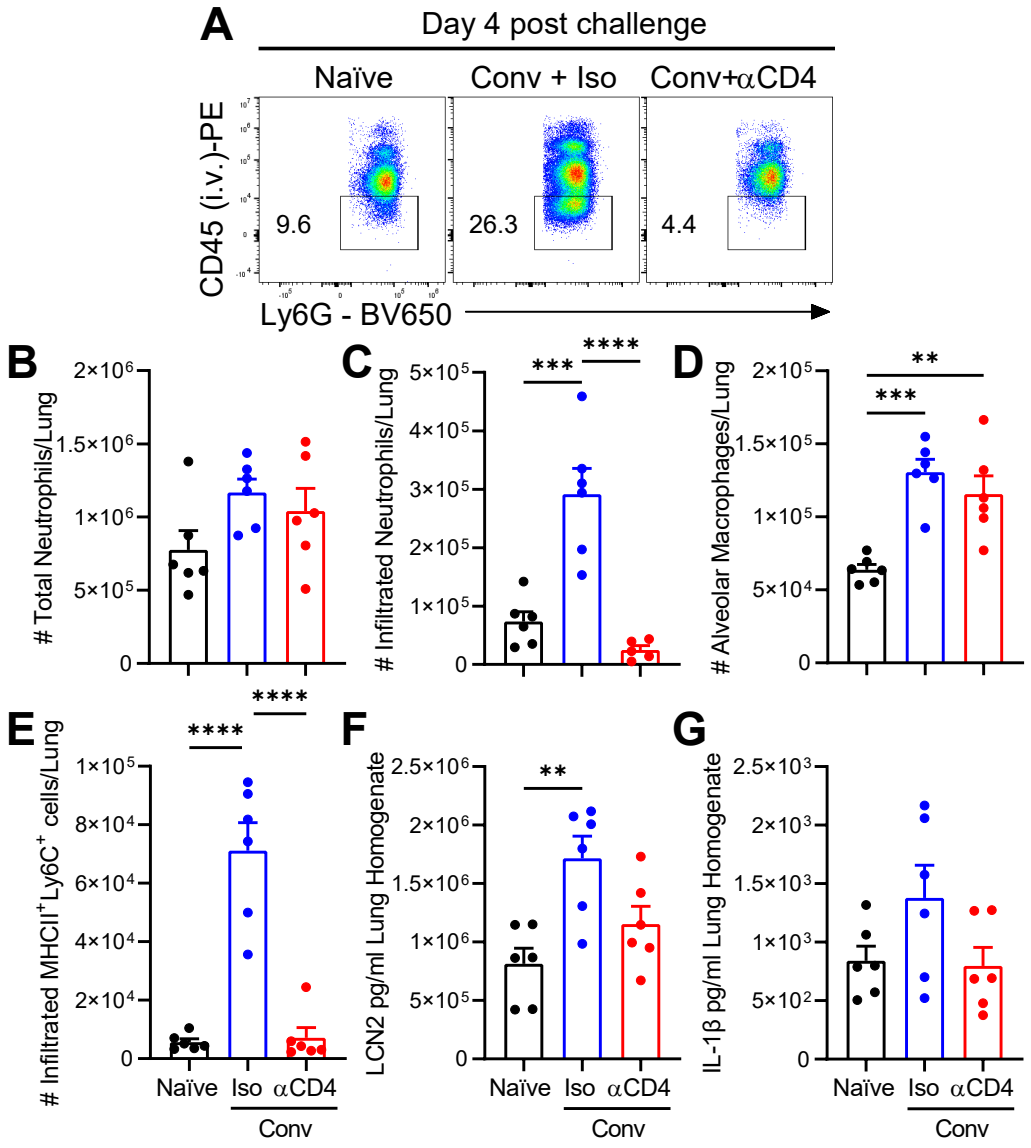

Figure 4.23 Depletion of CD4 T cells in convalescent mice decreases neutrophil and MHCII$^+$Ly6C$^+$ monocyte infiltration and reduces LCN2 and IL-1β concentrations in the lungs on day 4 post *B. pertussis* re-challenge.

Convalescent (conv) mice were treated with an anti-CD4 antibody or isotype control administered i.p. (200 µg/mouse) and i.n. (50 µg/mouse) 5 and 1 day before and every 4 days after a secondary *B. pertussis* challenge. On day 4 post challenge, convalescent mice or naïve control mice given a primary challenge on the same day were injected i.v. with a fluorochrome-conjugated anti-CD45 antibody and euthanised 10 min later. Lungs were harvested and mononuclear cells were isolated and stained for CD11b, CD11c, Ly6G, Ly6C, Siglec-F, and MHCII and analysed by flow cytometry. Representative flow cytometry plots (A) and absolute number of total neutrophils (Ly6G$^+$CD11b$^+$) (B) and lung-infiltrated (CD45 i.v.$^-$) neutrophils (C). Absolute number of alveolar macrophages (Siglec-F$^+$CD11c$^+$) (D) and lung-infiltrated MHCII$^+$Ly6C$^+$CD11b$^+$ monocytes (E). LCN2 (F) and IL-1β (G) concentrations in the lung homogenates on day 4 post re-infection, quantified by ELISA. Results shown are mean ± SEM (n=5-6 per group). $^{**}p < 0.01$, $^{***}p < 0.001$, $^{****}p < 0.0001$ by one-way ANOVA followed by Tukey's post-test.

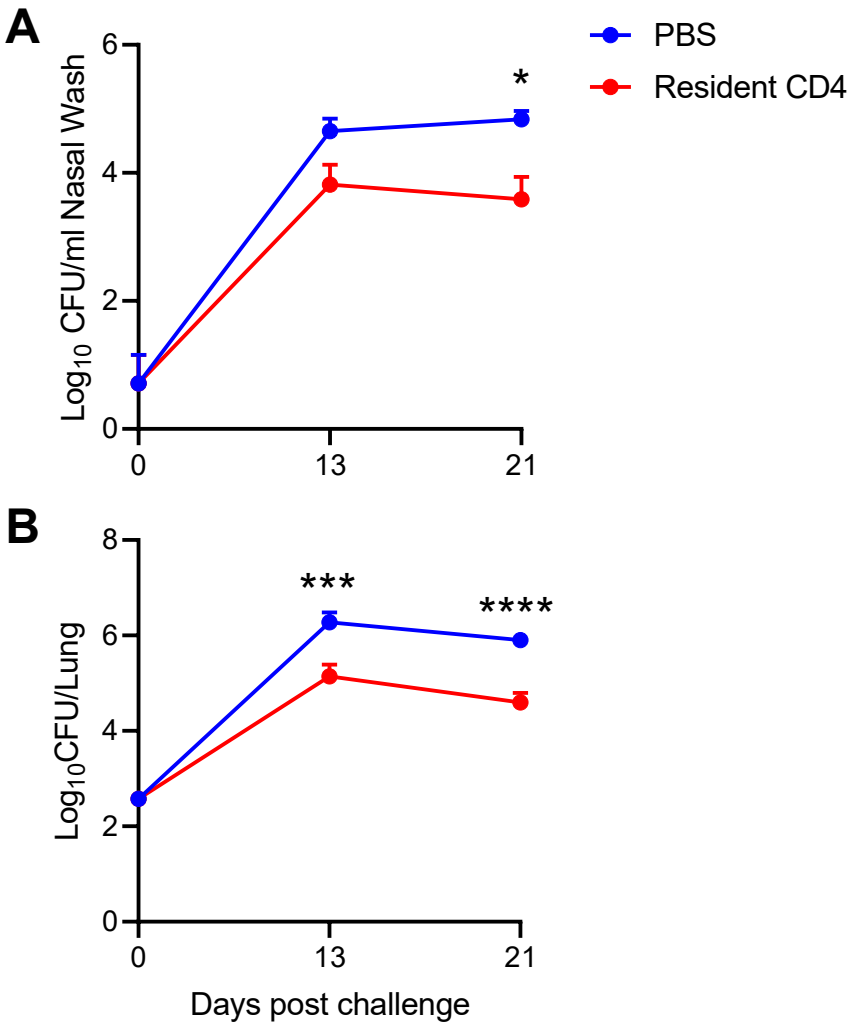

Figure 4.24 Transfer of lung- and nose-resident CD4 T cells isolated from convalescent mice confers protection against *B. pertussis* in the nasal cavity and lungs of naïve recipient mice.

CD45.2 mice on a C57BL/6 background were infected with *B. pertussis* and left to fully clear bacteria from respiratory tract. On day 60 post challenge, mice were injected i.v. with a fluorochrome-conjugated anti-CD45 antibody 10 min before euthanasia and lung- and nose-resident (CD45 i.v.$^-$) CD4 T cells were FACS purified from harvested lung and nasal tissue (pooled from n=15 mice). A mixture of lung- and nose-resident CD4 T cells was prepared at a ratio of 1:4 nose:lung CD4 T cells and 1 x 10^5 cells were injected i.p. to sublethally irradiated naïve CD45.1 mice. Control mice received an i.p. injection of PBS. Recipient mice were challenged with live *B. pertussis* 1 day later. The number of viable bacteria in the nasal cavity (A) and lungs (B) was estimated by performing CFU counts on serially diluted nasal washes and lung homogenates from individual mice on day 13 and 21 post challenge. Results shown are mean ± SEM CFU counts (n=3-4 mice per group). *p < 0.05, ***p < 0.001, ****p < 0.0001 PBS versus resident CD4 T cell recipients by two-way ANOVA followed by Sidak's post-test.

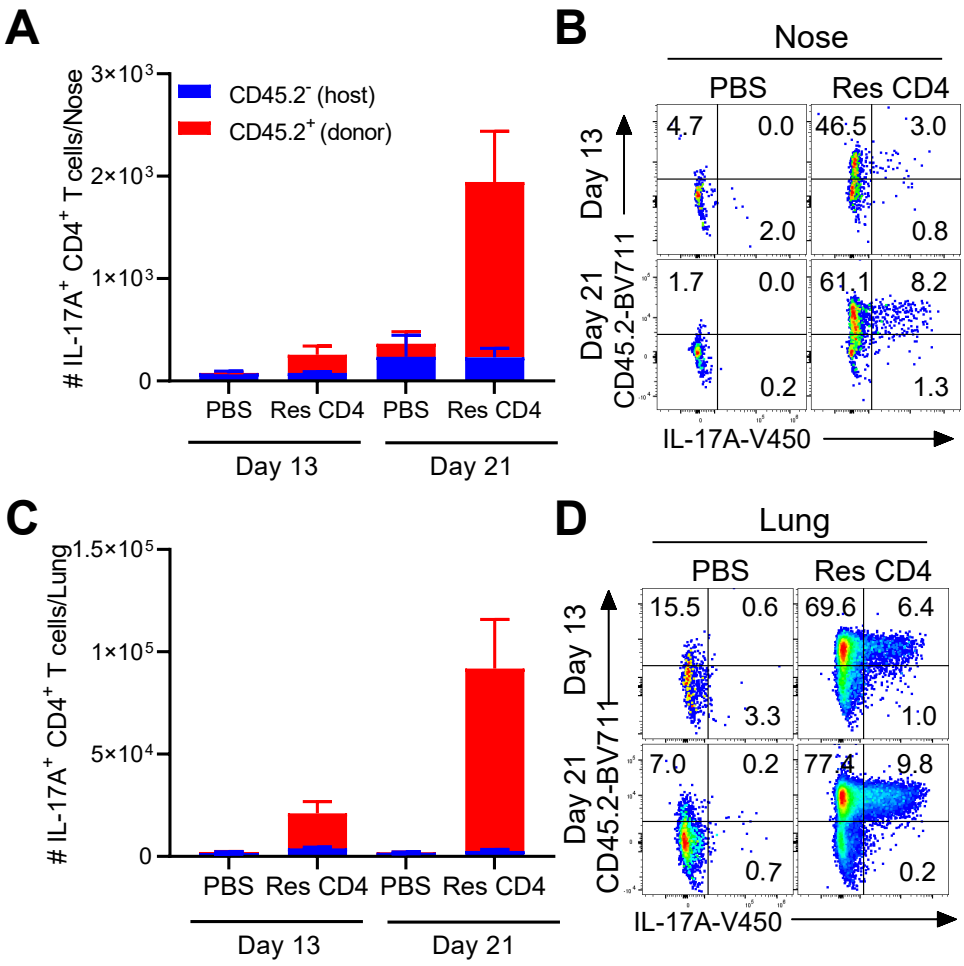

Figure 4.25 Donor CD4 T cells produce *B. pertussis*-specific IL-17A in the nasal cavity and lungs of recipient mice.

Combined lung- and nose-resident CD4 T cells from convalescent donor CD45.2 mice or PBS was transfered to naïve CD45.1 mice 1 day prior to *B. pertussis* challenge. Nasal tissue and lungs were harvested on day 13 and 21 post challenge. Cell suspensions were prepared from lung and nasal tissue and cells were stimulated with sBP (5 µg/ml) and anti-CD28 and anti-CD49d (both at 1 µg/ml) for 20 hours, with brefeldin A (5 µg/ml) added for the final 4 hours of culture. Absolute number (A) and representative flow cytometry plots (B) of IL-17A-producing CD45.2$^+$ (donor) and CD45.2$^-$ (host) CD4 T cells in the nasal cavity. Absolute number (C) and representative flow cytometry plots (D) of IL-17A-producing CD45.2$^+$ (donor) and CD45.2$^-$ (host) CD4 T cells in the lungs of recipient mice. Results shown are mean ± SEM (n=3-4 mice per group).

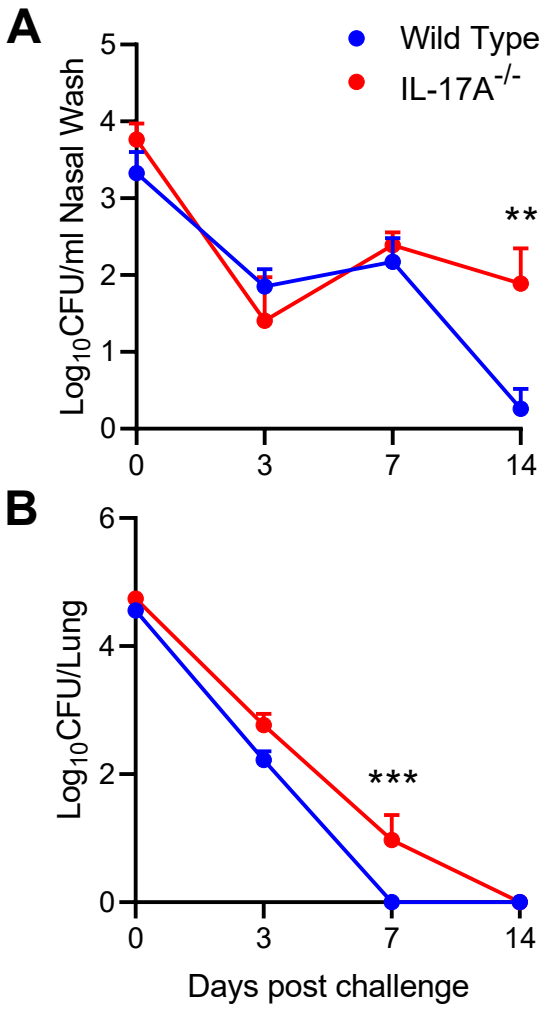

Figure 4.26 Delayed bacterial clearance from the nasal cavity and lungs of convalescent IL-17A$^{-/-}$ mice following secondary *B. pertussis* challenge.

WT and IL-17A$^{-/-}$ mice were challenged with *B. pertussis* and allowed to clear the infection from the respiratory tract. Once the infection had cleared (> 6 months), WT and IL-17A$^{-/-}$ mice were re-infected with live *B. pertussis* and nasal washes and lungs were harvested on day 3, 7, and 14 post re-challenge. The number of viable bacteria was estimated by performing CFU counts on serially diluted nasal washes (A) and lung homogenates (B) from individual mice. Results shown are mean ± SEM CFU counts (n=3-5 mice per group). $^{**}p < 0.01$, $^{***}p < 0.001$, WT versus IL-17A$^{-/-}$ by two-way ANOVA followed by Sidak's post-test. Experiment conducted in collaboration with Dr. Lisa Borkner at Trinity Biomedical Sciences Institute, Trinity College Dublin.

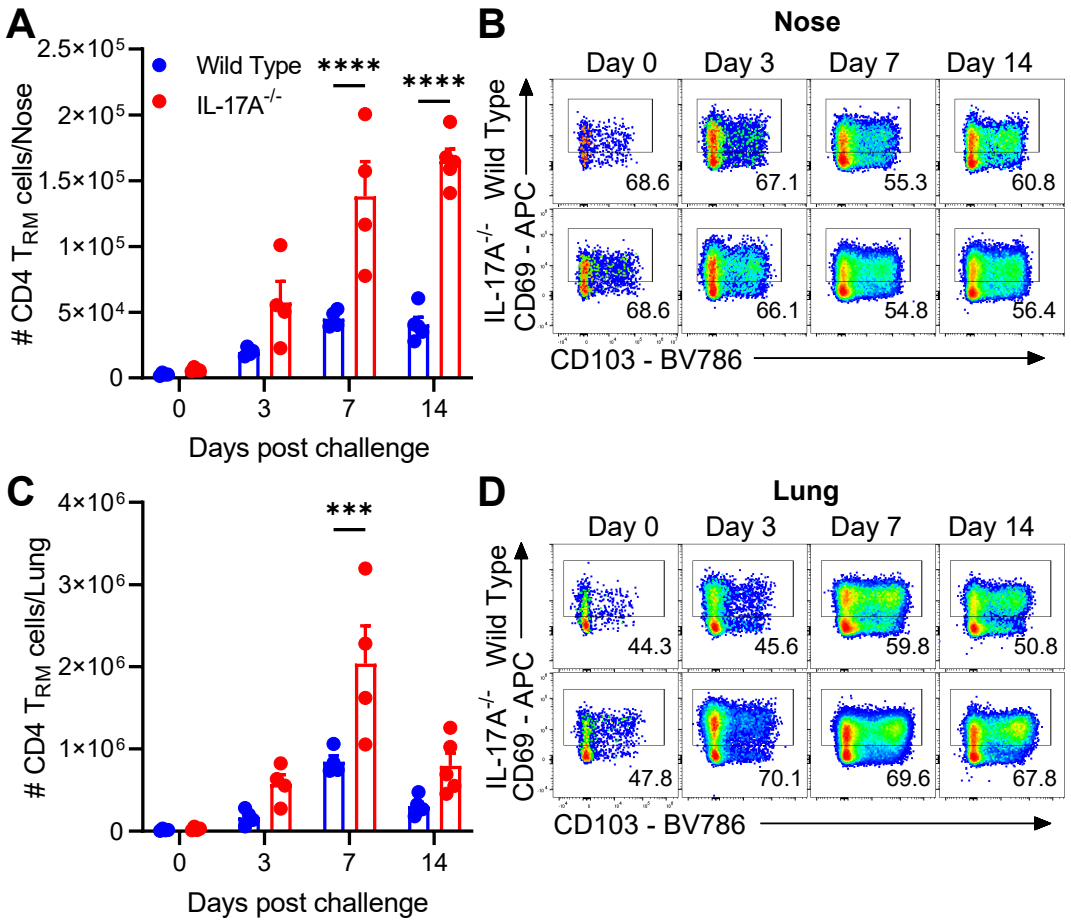

Figure 4.27 Convalescent IL-17A$^{-/-}$ mice have increased number of CD4 T_{RM} cells in the nasal cavity and lungs during re-infection with *B. pertussis*.

WT and IL-17A$^{-/-}$ mice were aerosol challenged with *B. pertussis* and allowed to clear the infection from the respiratory tract. Once the infection had cleared (> 6 months), WT and IL-17A$^{-/-}$ mice were re-infected with live *B. pertussis*. On the day of and 3, 7, and 14 days post re-challenge, WT and IL-17A$^{-/-}$ mice were injected i.v. with a fluorochrome-labelled anti-CD45 antibody and euthanised 10 min later. Cell suspensions were prepared from nasal tissue and lungs and cells were stained for CD4, CD3, CD44, CD62L, CD69 and CD103, and analysed by flow cytometry. Absolute number (A) with representative flow cytometry plots (B) of nasal CD4 T_{RM} cells ($CD4^+CD3^+CD44^+CD62L^-CD69^+CD103^{\pm}$) in WT and IL-17A$^{-/-}$ mice over the course of the infection. Absolute number (C) with representative flow cytometry plots (D) of CD4 T_{RM} cells in the lungs of WT and IL-17A$^{-/-}$ mice. Results shown are mean ± SEM (n=4/5 mice per group). ***p < 0.001, ****p < 0.0001 WT versus IL-17A$^{-/-}$ by two-way ANOVA followed by Sidak's post-test.

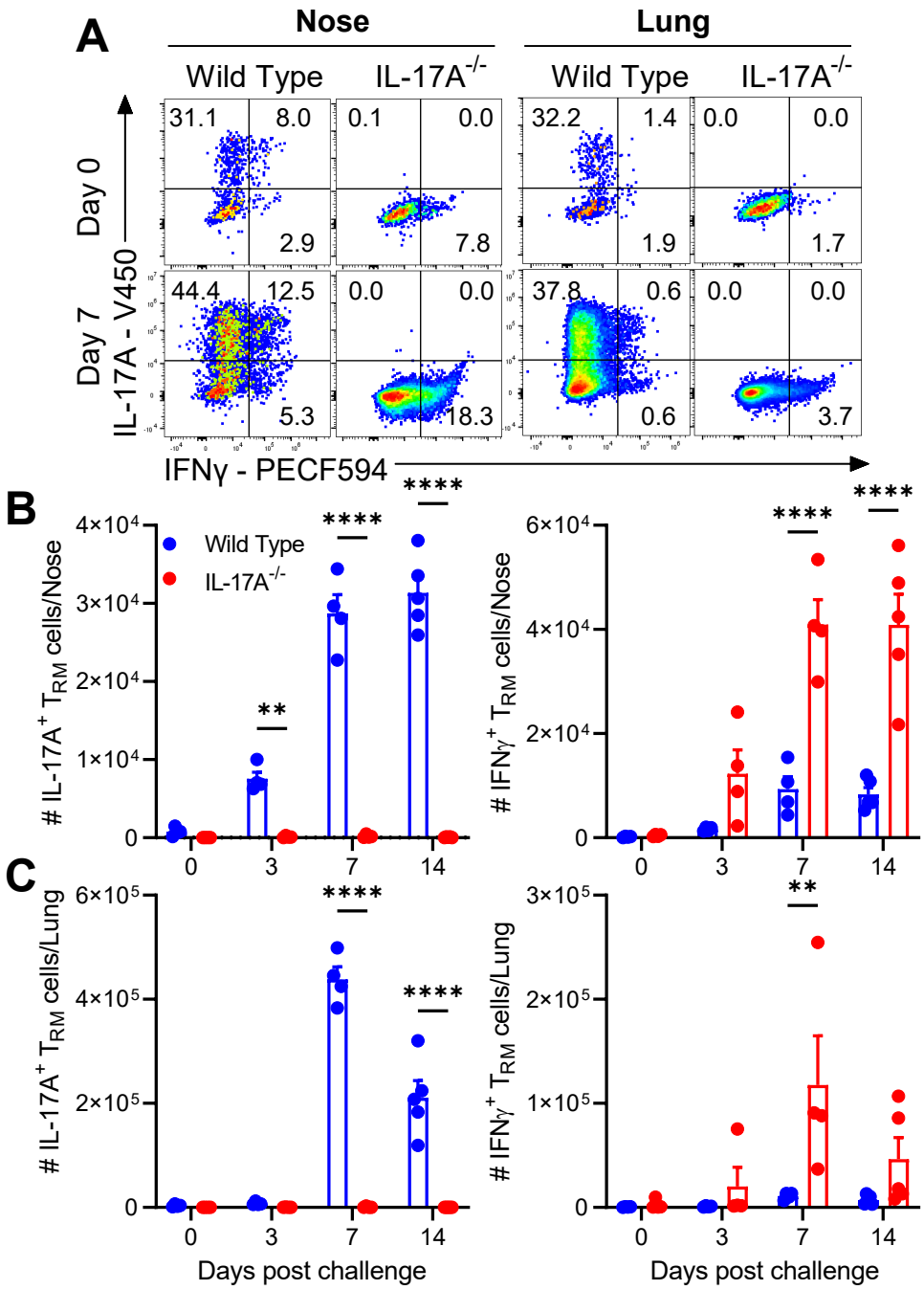
A
Nose
Lung
Wild Type
IL-17A-/-
Wild Type
IL-17A-/-
Day 0
Day 7
IL-17A - V450
IFNγ - PECF594
31.1
8.0
2.9
0.1
0.0
7.8
32.2
1.4
1.9
0.0
0.0
1.7
44.4
12.5
5.3
0.0
0.0
18.3
37.8
0.6
0.6
0.0
0.0
3.7
B
IL-17A+ TRM cells/Nose
IFNγ+ TRM cells/Nose
Wild Type
IL-17A-/-
C
IL-17A+ TRM cells/Lung
IFNγ+ TRM cells/Lung
Days post challenge
Days post challenge

Figure 4.28 Convalescent IL-17A$^{-/-}$ mice have significantly enhanced number of pathogen-specific IFNγ^{+} T_{RM} cells in the nasal cavity and lungs following *B. pertussis* re-infection.

WT and IL-17A$^{-/-}$ mice were aerosol challenged with *B. pertussis* and allowed to clear the infection from the respiratory tract. Once the infection had cleared (> 6 months), WT and IL-17A$^{-/-}$ mice were re-infected with live *B. pertussis*. On the day of and 3, 7, and 14 days post re-challenge, WT and IL-17A$^{-/-}$ mice were injected i.v. with a fluorochrome-labelled anti-CD45 antibody and euthanised 10 min later. Cell suspensions were prepared from nasal tissue and lungs and cells were stimulated with sBP (5 µg/ml) and anti-CD28 and anti-CD49d (both at 1 µg/ml) for 20 hours, with brefeldin A (5 µg/ml) added for the final 4 hours of culture. Cells were stained for surface CD4, CD3, CD44, CD62L, CD69, CD103, and intracellular IL-17A and IFNγ, and analysed by flow cytometry. Representative flow cytometry plots (A) and absolute number of *B. pertussis*-specific IL-17A^{+} and IFNγ^{+} CD4 T_{RM} cells in the nasal tissue (B) and lungs (C) of WT and IL-17A$^{-/-}$ mice. Results shown are mean ± SEM (n=4/5 mice per group). $^{**}p < 0.01$, $^{****}p < 0.0001$ WT versus IL-17A$^{-/-}$ by two-way ANOVA followed by Sidak's post-test.

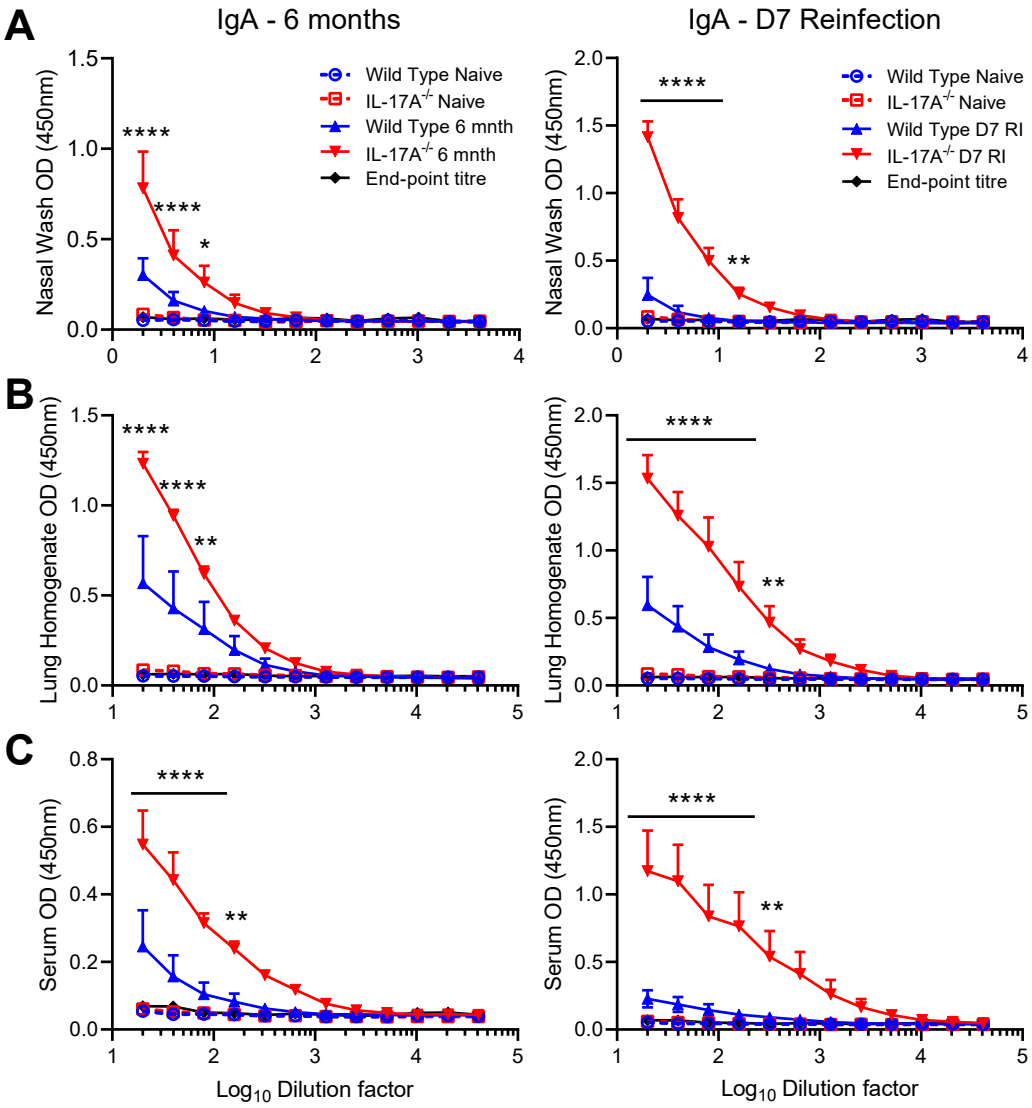

Figure 4.29 Convalescent IL-17A$^{-/-}$ mice have significantly higher *B. pertussis*-specific IgA prior to and during *B. pertussis* re-infection.

WT and IL-17A$^{-/-}$ mice were aerosol challenged with *B. pertussis* and allowed to clear the infection from the respiratory tract. Once the infection had cleared (> 6 months), WT and IL-17A$^{-/-}$ mice were re-infected with live *B. pertussis*. Nasal wash, lung homogenates, and serum was harvested from WT and IL-17A$^{-/-}$ mice on the day of (6 months post primary infection) and 7 days post re-challenge. *B. pertussis*-specific IgA was quantified in the nasal wash (A), lung homogenates (B), and serum (C) of WT and IL-17A$^{-/-}$ mice by ELISA. Data are mean ± SEM (n=4 mice per group). *p < 0.05, **p < 0.01, ****p < 0.0001 infected WT versus IL-17A$^{-/-}$ by two-way ANOVA followed by Sidak's post-test.

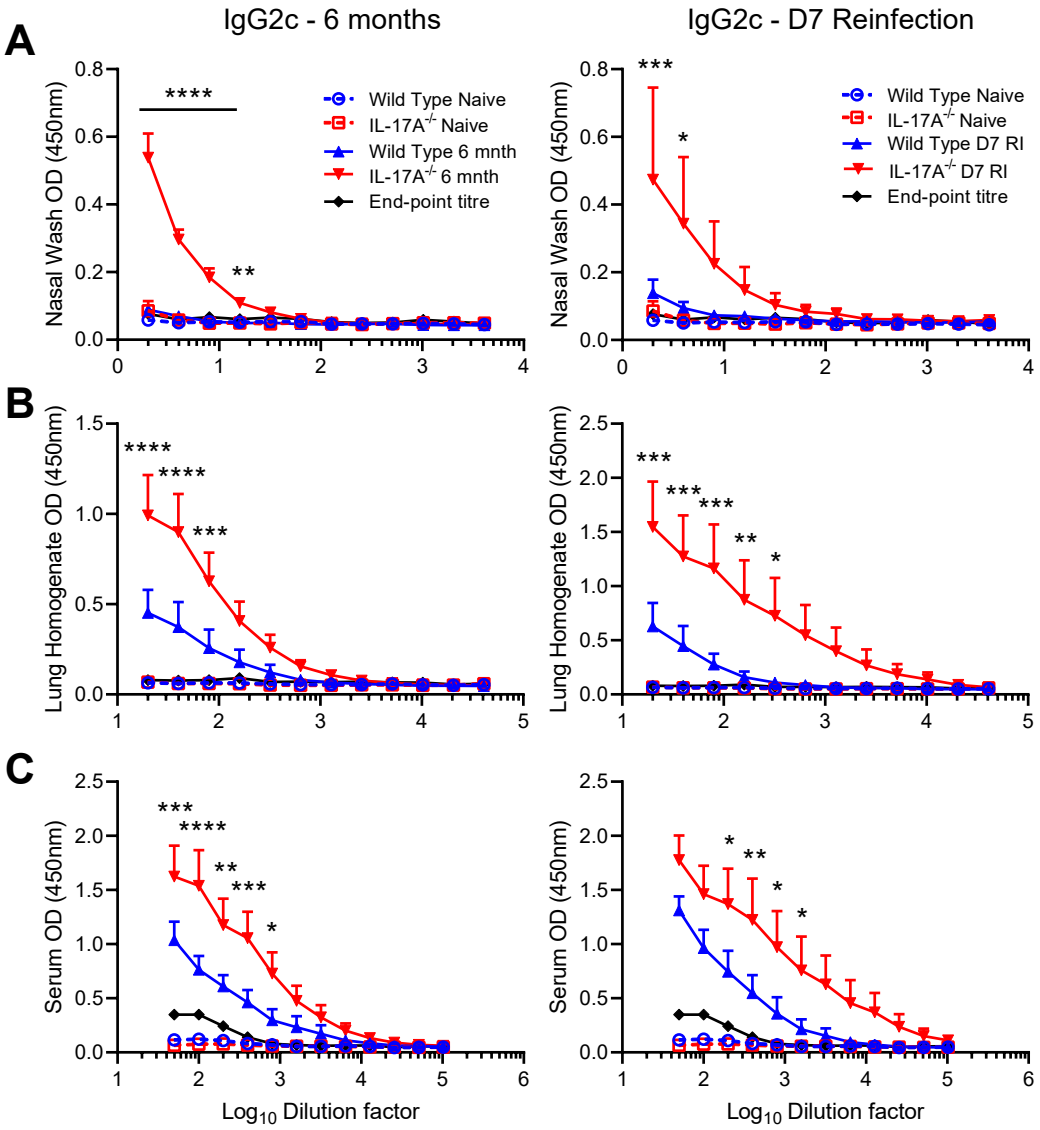

Figure 4.30 Convalescent IL-17A$^{-/-}$ mice have significantly higher *B. pertussis*-specific IgG2c prior to and during *B. pertussis* re-infection.

WT and IL-17A$^{-/-}$ mice were challenged with *B. pertussis* and allowed to clear the infection from the respiratory tract. Once the infection had cleared (> 6 months) WT and IL-17A$^{-/-}$ mice were re-infected with live *B. pertussis*. Nasal wash, lung homogenates, and serum was harvested from WT and IL-17A$^{-/-}$ mice on the day of (6 months post primary infection) and 7 day post re-challenge. *B. pertussis*-specific IgG2c was quantified in the nasal wash (A), lung homogenates (B), and serum (C) of WT and IL-17A$^{-/-}$ mice by ELISA. Data are mean ± SEM (n=4 mice per group). *p < 0.05, **p < 0.01, ***p < 0.001, ****p < 0.0001 infected WT versus IL-17A$^{-/-}$ by two-way ANOVA followed by Sidak's post-test.

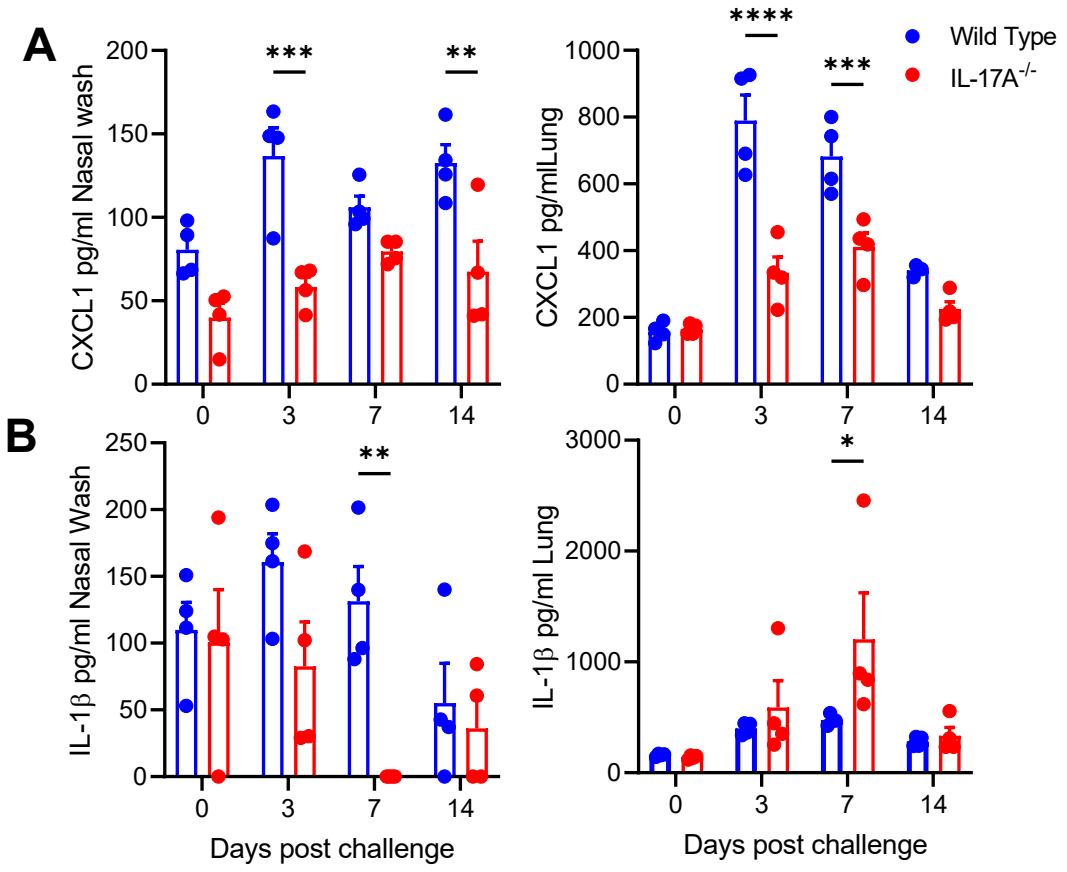

Figure 4.31 IL-17A$^{-/-}$ mice have significantly reduced CXCL1 concentration in the nasal wash and lung homogenates following re-infection with *B. pertussis*.

WT and IL-17A$^{-/-}$ mice were challenged with *B. pertussis* and allowed to clear the infection from the respiratory tract. Once the infection had cleared (> 6 months), WT and IL-17A$^{-/-}$ mice were re-infected with live *B. pertussis* and nasal washes and lungs were collected on the day of and 3, 7, and 14 days post challenge. CXCL1, and IL-1β concentrations in the nasal washes (A) and lung homogenates (B) of WT and IL-17A$^{-/-}$ mice were quantified by ELISA. . Results shown are mean ± SEM (n=4-5 mice per group). *p < 0.05, **p < 0.01, ***p < 0.001, ****p < 0.0001 WT versus IL-17A$^{-/-}$ by two-way ANOVA followed by Sidak's post-test.

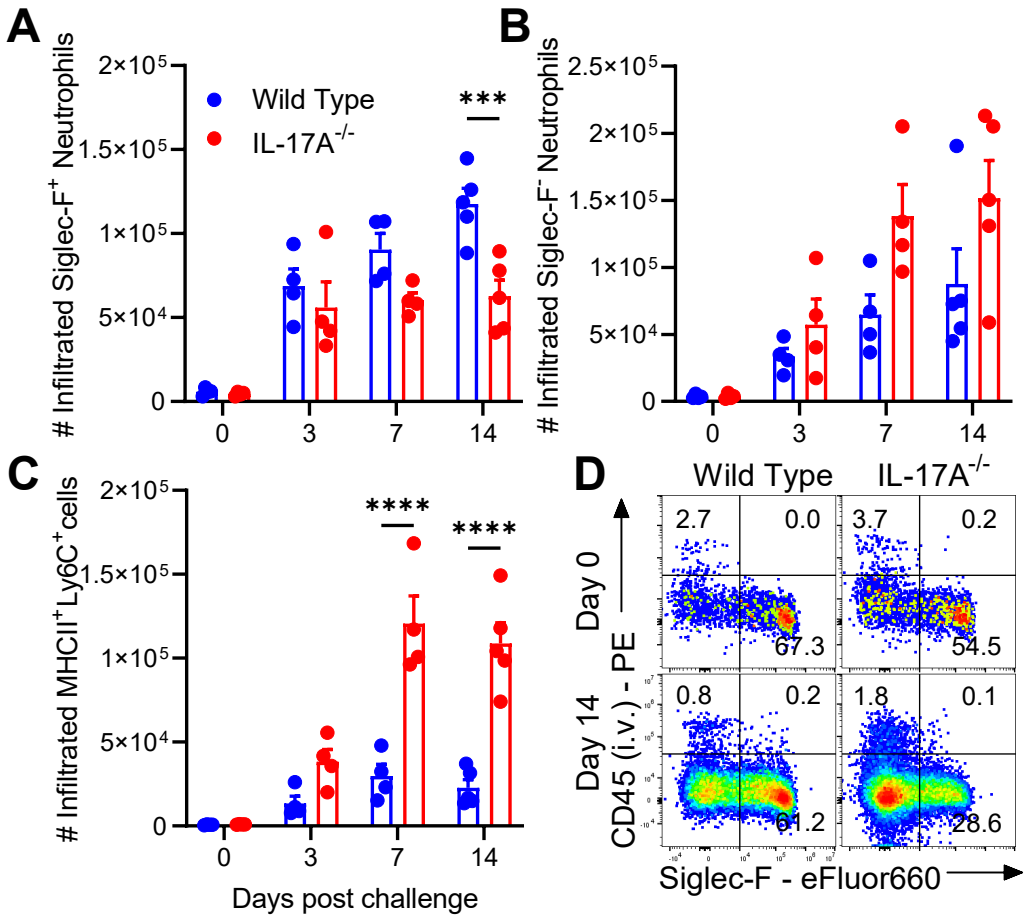

Figure 4.32 Reduced infiltration of Siglec-F$^+$ neutrophils into the nasal cavity of convalescent IL-17A$^{-/-}$ mice during *B. pertussis* re-infection.

WT and IL-17A$^{-/-}$ mice were challenged with *B. pertussis* and allowed to clear the infection from the respiratory tract. Once the infection had cleared (> 6 months), WT and IL-17A$^{-/-}$ mice were re-infected with live *B. pertussis*. On the day of and 3, 7, and 14 days post challenge, WT and IL-17A$^{-/-}$ mice were injected i.v. with a fluorochrome-labelled CD45 antibody 10 min prior to euthanasia. Nasal tissue was harvested and mononuclear cells were isolated and stained for CD11b, Ly6C, Ly6G, MHCII, and Siglec-F, and analysed by flow cytometry. Absolute number of infiltrated (CD45 i.v.$^-$) Siglec-F$^+$ neutrophils (Ly6G$^+$CD11b$^+$) (A) and conventional (Siglec-F$^-$) neutrophils (B). Absolute numbers of tissue-infiltrated MHCII$^+$Ly6C$^+$CD11b$^+$ monocytes in the nasal cavity (C). Representative flow cytometry plots of Siglec-F expression on tissue-infiltrated neutrophils on day 0 and 14 days post challenge. Results shown are mean ± SEM (n=4/5 mice per group). ***p < 0.001, ****p < 0.0001 WT versus IL-17A$^{-/-}$ by two-way ANOVA followed by Sidak's post-test.

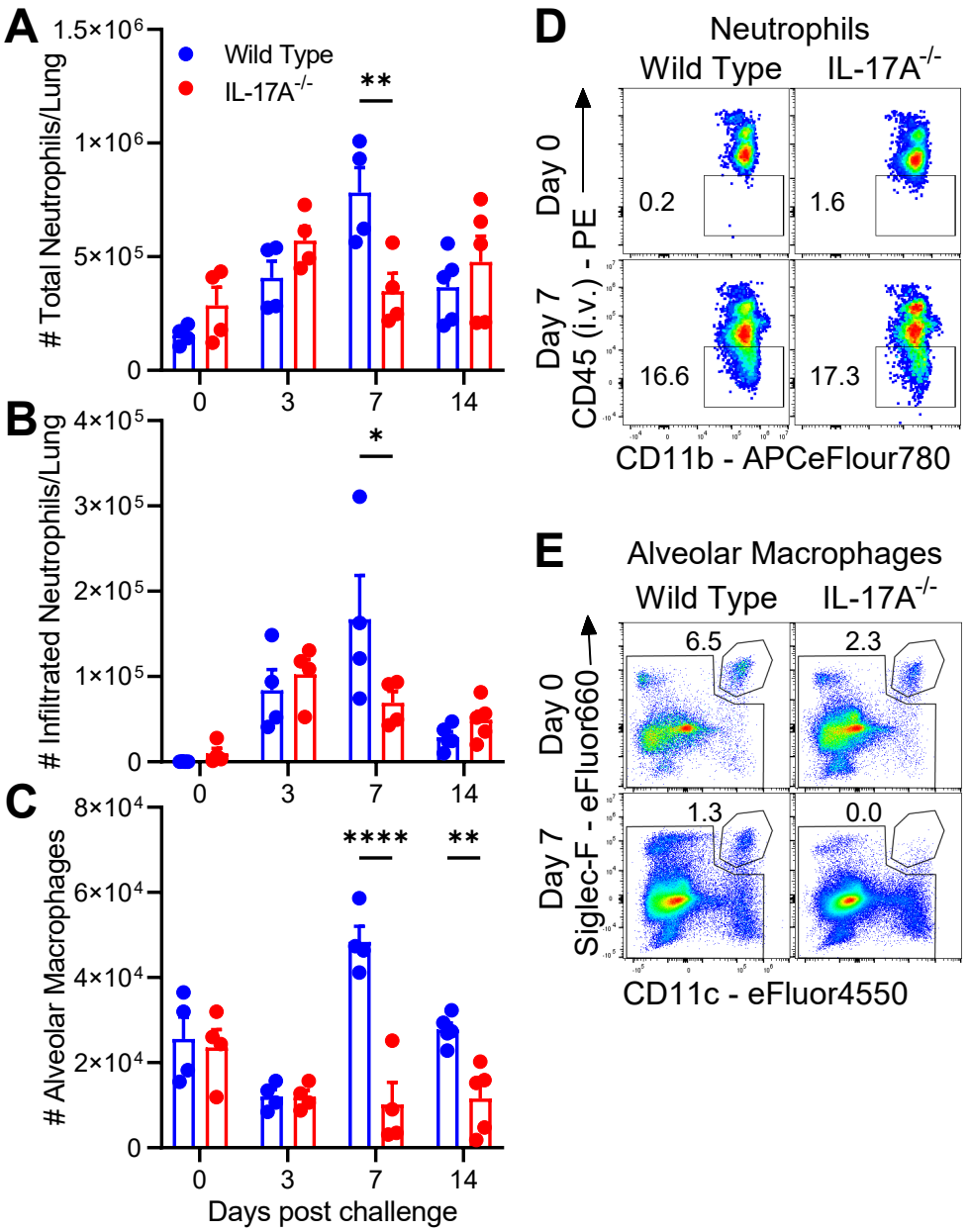

Figure 4.33 Reduced number of total neutrophils, tissue-infiltrated neutrophils, and alveolar macrophages in the lungs of convalescent IL-17A$^{-/-}$ following *B. pertussis* re-challenge.

WT and IL-17A$^{-/-}$ mice were challenged with *B. pertussis* and allowed to clear the infection from the respiratory tract. Once the infection had cleared (> 6 months), WT and IL-17A$^{-/-}$ mice were re-infected with live *B. pertussis*. On the day of and 3, 7, and 14 days post challenge, mice received an i.v. injection of a fluorochrome-conjugated CD45 antibody 10 min prior to euthanasia. Lungs were harvested and isolated mononuclear cells were stained for CD11c, CD11b, Siglec-F and Ly6G and analysed by flow cytometry. Absolute number of total neutrophils (Ly6G^{+}CD11b^{+}) (A), tissue-infiltrated (CD45i.v.$^{-}$) neutrophils (B), and alveolar macrophages (Siglec-F^{+}CD11c^{+}) (C) in the lungs of WT and IL-17A$^{-/-}$ mice, with representative flow cytometry plots of lung-infiltrating neutrophils (CD11b^{+}Ly6G^{+}) (D) and alveolar macrophages (E). Results shown are mean ± SEM (n=4/5 mice per group). *p < 0.05, **p < 0.01, ****p < 0.0001 WT versus IL-17A$^{-/-}$ by two-way ANOVA followed by Sidak's post-test.

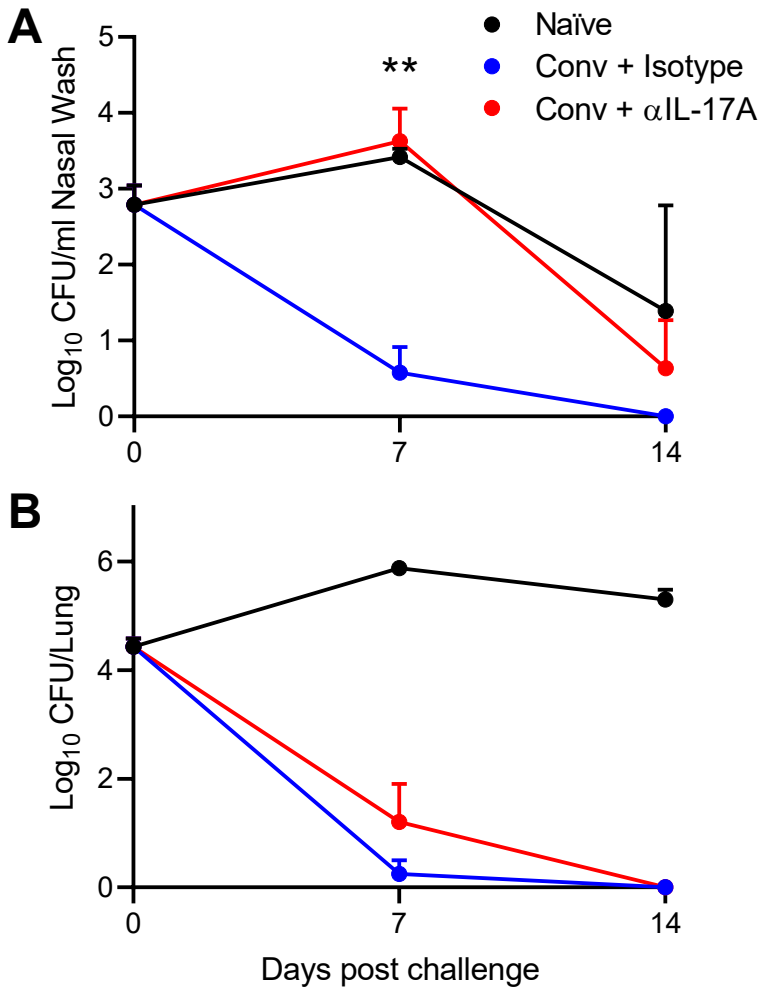

Figure 4.34 Neutralisation of IL-17A during *B. pertussis* re-infection delays bacterial clearance from the nasal cavity, but not lungs, of convalescent mice.

C57BL/6 mice were infected with *B. pertussis* and allowed to clear the infection. Convalescent mice (> 6 months p.i.) were injected i.p. with 200 µg of a neutralising anti-IL-17A antibody or isotype control from one day before and every 3 days after re-infection with *B. pertussis*. The number of viable bacteria in the nasal cavity (A) and lungs (B) was estimated by performing CFU counts on serially diluted nasal washes and lung homogenates from convalescent mice or naïve control mice given a primary challenge on the same day. Results shown are mean ± SEM CFU counts (n=3-4 mice per group). $^{**}p < 0.01$ isotype control versus anti-IL-17A treatment by two-way ANOVA followed by Sidak's post-test. Experiment conducted in collaboration with Dr. Lisa Borkner at Trinity Biomedical Sciences Institute, Trinity College Dublin.

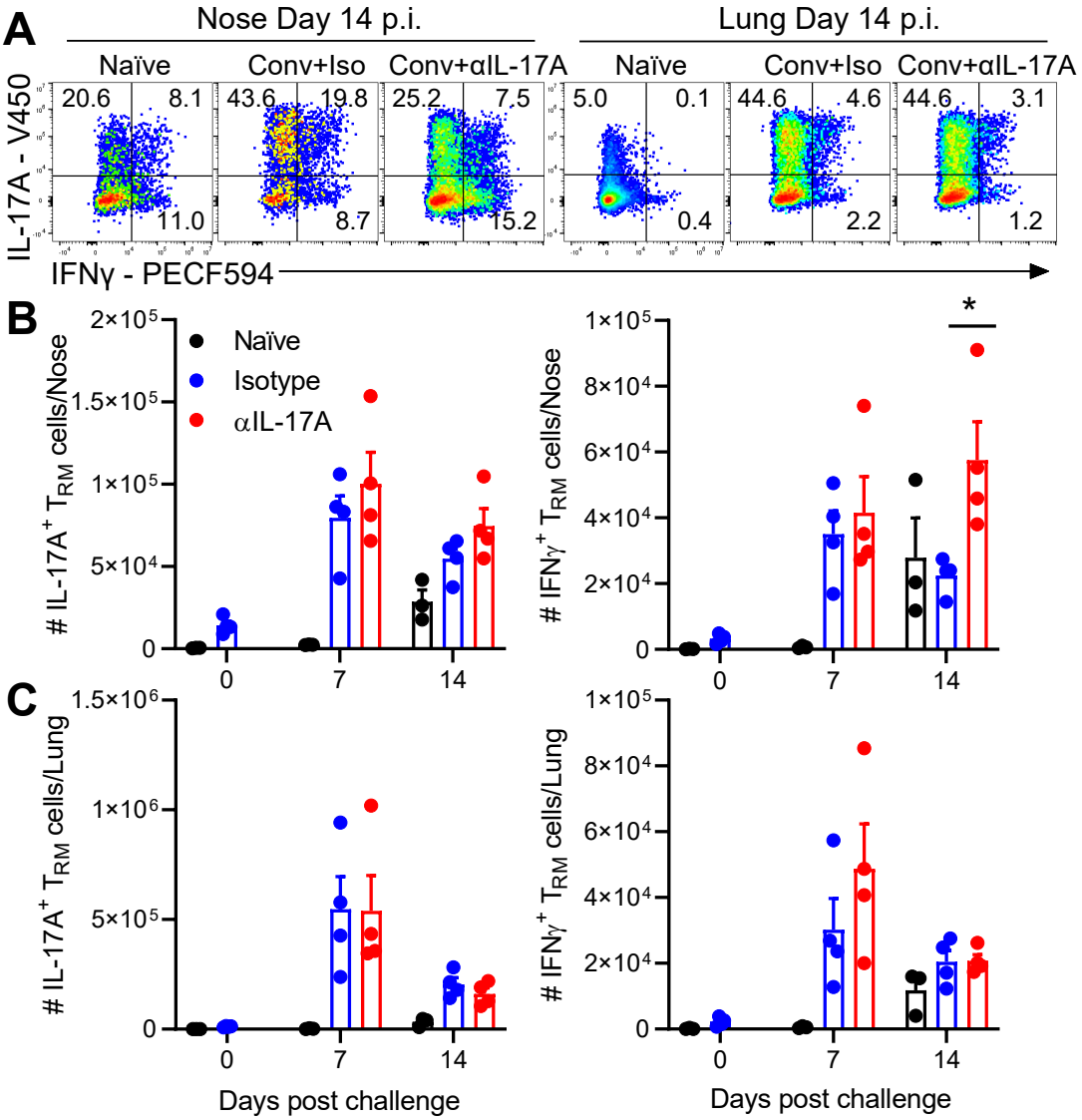

Figure 4.35 Neutralisation of IL-17A during *B. pertussis* re-infection enhances the number of *B. pertussis*-specific IFNγ⁺ CD4 T_{RM} cells in the nasal cavity of convalescent mice.

C57BL/6 mice that were previously infected with *B. pertussis* were treated with a neutralising anti-IL-17A antibody or isotype control (200 µg/mouse) one day before and every 3 days after re-infection with *B. pertussis*. On the day of and 7 and 14 days after re-challenge, convalescent mice or naïve control mice given a primary challenge on the same day were injected i.v. with a fluorochrome-conjugated anti-CD45 antibody and euthanised 10 min later. Nasal tissue and lungs were harvested and mononuclear cells were isolated and stimulated with sBP (5 µg/ml) and anti-CD28 and anti-CD49d (both at 1 µg/ml) for 20 hours, with brefeldin A (5 µg/ml) added for the final 4 hours of culture. Cells were stained for surface CD4, CD3, CD44, CD62L, CD69, CD103, and intracellular IL-17A and IFNγ, and analysed by flow cytometry. Representative flow cytometry plots of IL-17A⁺ and IFNγ⁺ CD4 T_{RM} cells in the nasal cavity and lungs on day 14 post challenge (A). Absolute number of IL-17A⁺ and IFNγ⁺ CD4 T_{RM} cells in the nasal cavity (B) and lungs (C). Results shown are mean ± SEM (n=3-4 mice per group). *$p < 0.05$, Isotype control versus anti-IL-17A treatment by two-way ANOVA followed by Sidak's post-test.

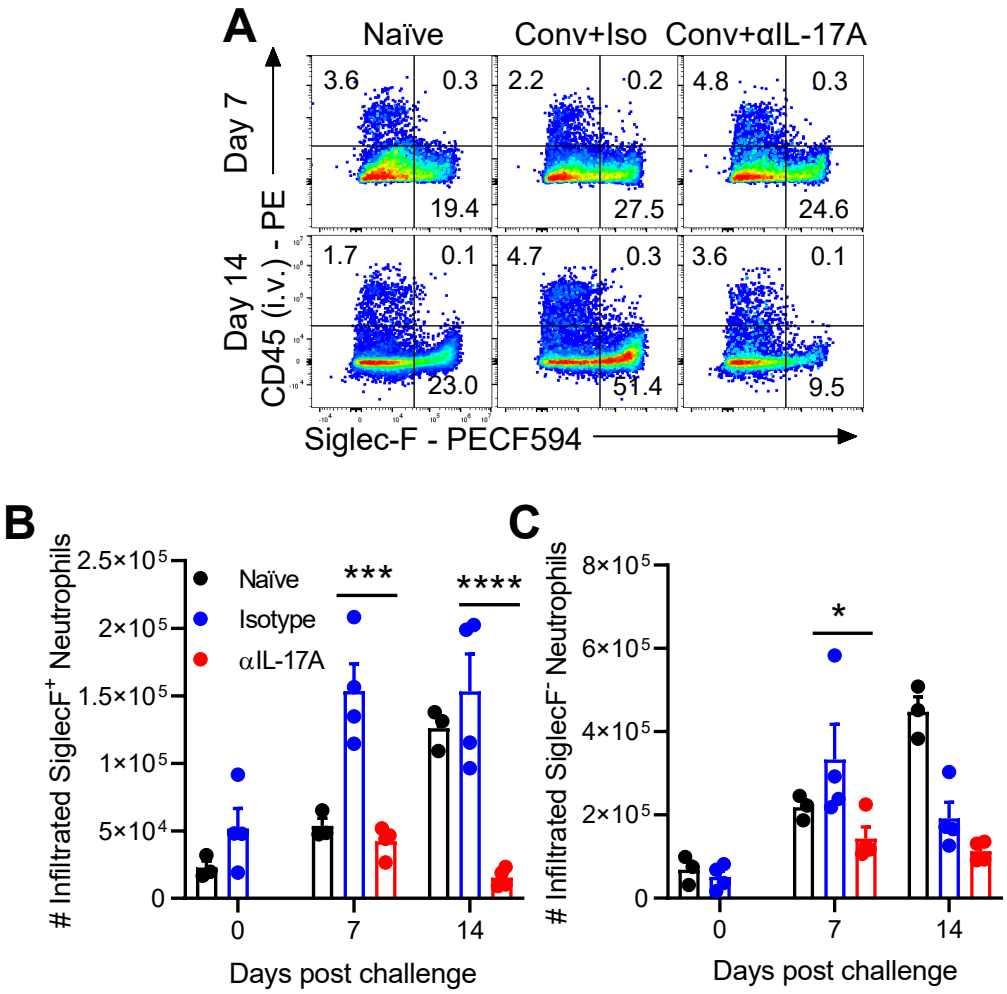

Figure 4.36 Reduced neutrophil infiltration into the nasal cavity of convalescent mice treated with an anti-IL-17A antibody during a secondary *B. pertussis* infection.

C57BL/6 mice that were previously infected with *B. pertussis* were treated with a neutralising anti-IL-17A antibody or isotype control (200 µg/mouse) one day before and every 3 days after re-infection with *B. pertussis*. On the day of and 7 and 14 days after re-challenge, convalescent mice or naïve control mice given a primary challenge on the same day were treated with a fluorochrome-conjugated anti-CD45 antibody i.v. and euthanised 10 min later. Nasal tissue was harvested and mononuclear cells were isolated and stained for CD11b, Ly6G and Siglec-F, and analysed by flow cytometry. Representative flow cytometry plots (A) and absolute numbers of infiltrated (CD45 i.v.$^-$) Siglec-F$^+$ (B) and Siglec-F$^-$ (C) neutrophils (Ly6G$^+$CD11b$^+$) in the nasal cavity. Data are mean ± SEM (n=3-4/group). *$p < 0.05$, ***$p < 0.001$, ****$p < 0.0001$ isotype control versus anti-IL-17A treatment by two-way ANOVA followed by Sidak's post-test.

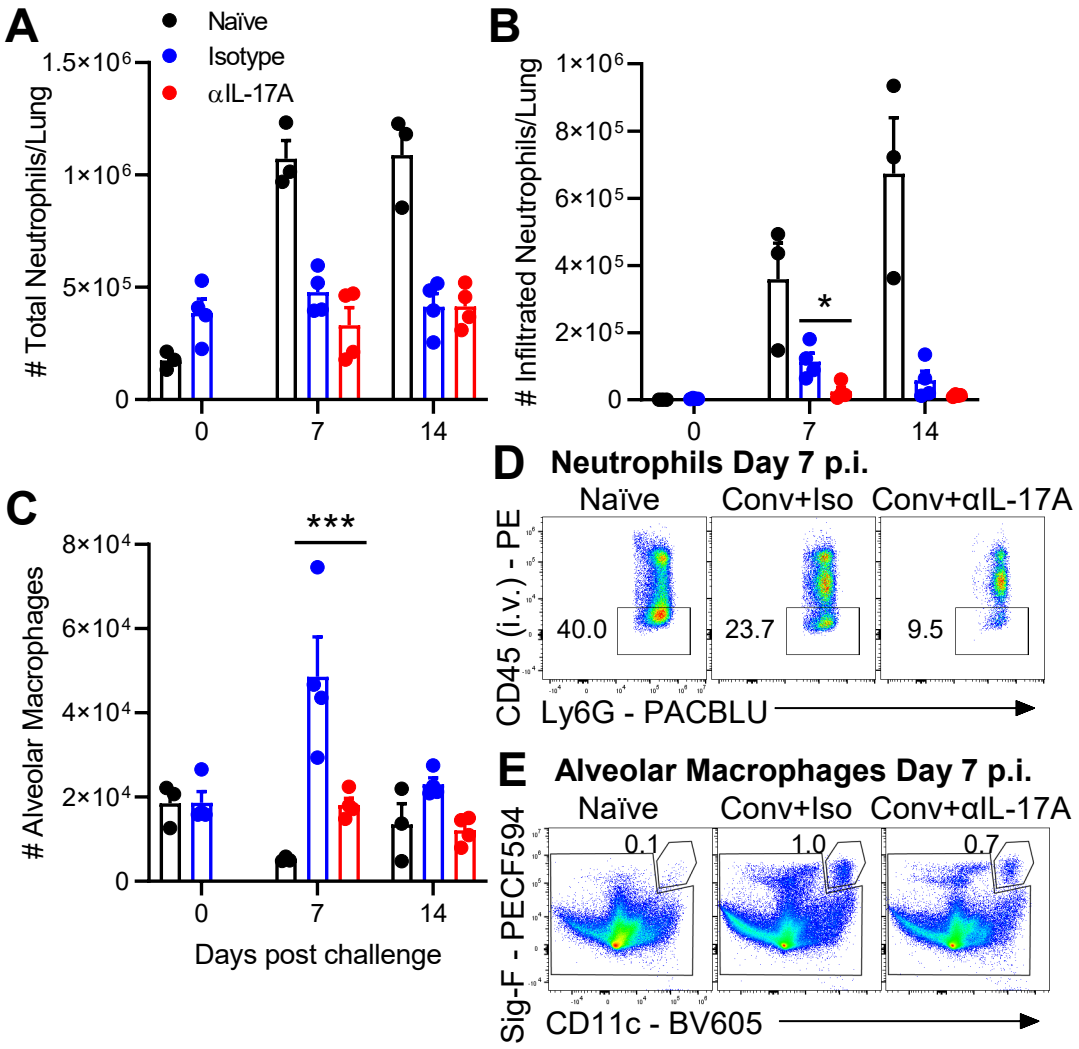

Figure 4.37 Treatment of convalescent mice with an anti-IL-17A antibody during *B. pertussis* re-infection reduces the number of lung-infiltrated neutrophils and alveolar macrophages.

C57BL/6 mice that were previously infected with *B. pertussis* were treated with a neutralising anti-IL-17A antibody or isotype control (200 µg/mouse) one day before and every 3 days after re-infection with *B. pertussis*. On the day of and 7 and 14 days after re-challenge, convalescent mice or naïve control mice given a primary challenge on the same day were treated with a fluorochrome-conjugated anti-CD45 antibody i.v. and euthanised 10 min later. Lungs were harvested and mononuclear cells were isolated and stained for CD11b, CD11c, Siglec-F and Ly6G and analysed by flow cytometry. Absolute number of total neutrophils ($Ly6G^+CD11b^+$) (A), tissue-infiltrated ($CD45\ i.v.^-$) neutrophils (B), and alveolar macrophages ($Siglec\text{-}F^+CD11c^+$) (C) in the lungs. Representative flow cytometry plots of lung-infiltrated neutrophils (D) and alveolar macrophages (E) on day 7 post challenge. Data are mean ± SEM (n=3-4/group). $^*p < 0.05$, $^{***}p < 0.001$ isotype control versus anti-IL-17A treatment by two-way ANOVA followed by Sidak's post-test.

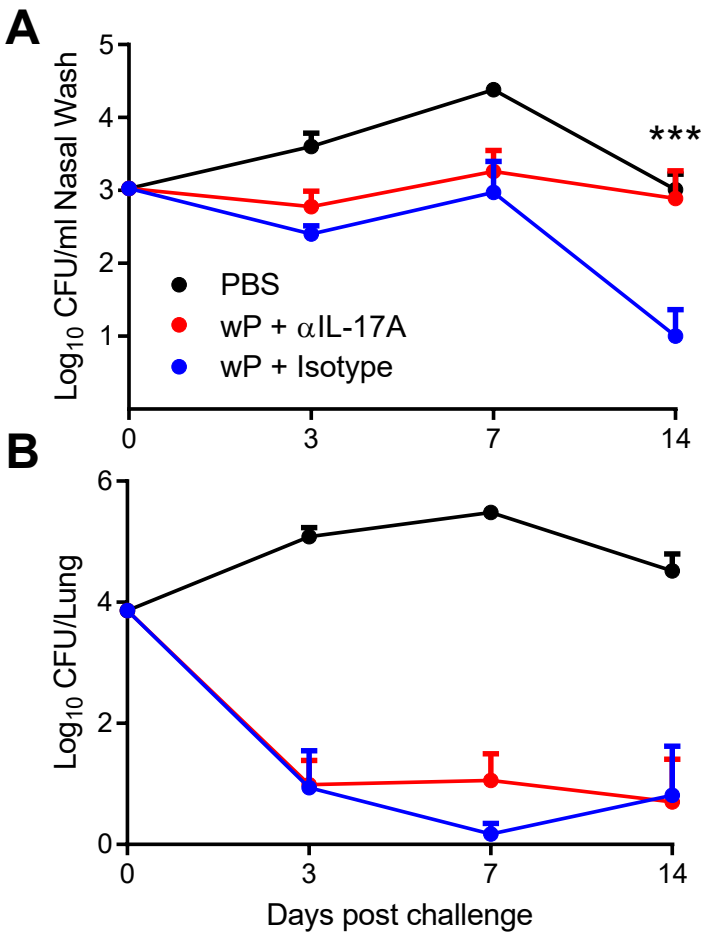

Figure 4.38 Neutralisation of IL-17A in mice immunised with a wP vaccine significantly delays clearance of *B. pertussis* from the nasal cavity.

C57BL/6 mice were immunised i.p. with 1/20th human dose of wP vaccine twice (-6 and -2 weeks). Naïve control mice were injected i.p. with PBS. Mice immunised with a wP vaccine were treated i.p. with 100 µg of a neutralising anti-IL-17A antibody or isotype control one day before and every 3 days after *B. pertussis* challenge. Nasal washes (A) and lungs (B) were collected on days 3, 7, and 14 post challenge and CFU counts were enumerated. Data are mean ± SEM (n=3-4 per group). ***$p < 0.001$ isotype control versus anti-IL-17A treatment by two-way ANOVA followed by Sidak's post-test.

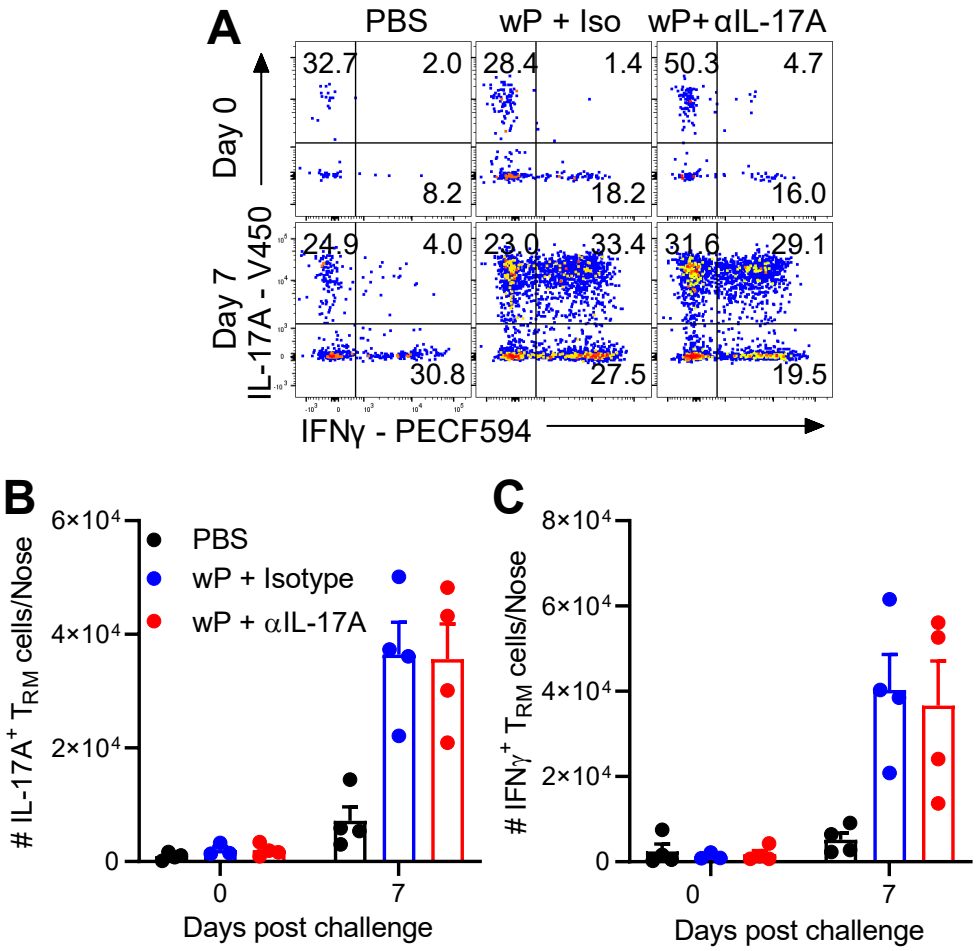

Figure 4.39 Expansion of nasal IL-17A$^+$ and IFNγ$^+$ CD4 T_{RM} cells in mice immunised with a wP vaccine is not impaired by anti-IL-17A treatment during *B. pertussis* infection.

C57BL/6 mice were immunised i.p. with 1/20th human dose of wP twice (-6 and -2 weeks). wP-immunised mice were injected i.p. with 100 µg of a neutralising anti-IL-17A antibody or isotype control one day before and every 3 days after *B. pertussis* challenge. Naïve control mice were injected i.p. with PBS and also infected with *B. pertussis*. On the day of and 7 days after challenge a fluorochrome-conjugated anti-CD45 antibody was administered i.v. and mice were euthanised 10 min later. Cell suspensions were prepared from nasal tissue and cells were stimulated with PMA (50 ng/ml), ionomycin (500 ng/ml), and brefeldin A (5 µg/ml) for 4 hours. Cells were stained for surface CD4, CD3, CD44, CD69, CD103, and intracellular IL-17A and IFNγ, and analysed by flow cytometry. Representative flow cytometry plots (A) and absolute number of IL-17A$^+$ (B) and IFNγ$^+$ (C) CD4 T_{RM} cells (CD4$^+$CD3$^+$CD45i.v.$^-$CD44$^+$CD69$^+$CD103$^\pm$) in the nasal tissue. Data are mean ± SEM (n=3-4 mice per group). No significance detected between isotype control versus anti-IL-17A treatment by two-way ANOVA followed by Sidak's post-test.

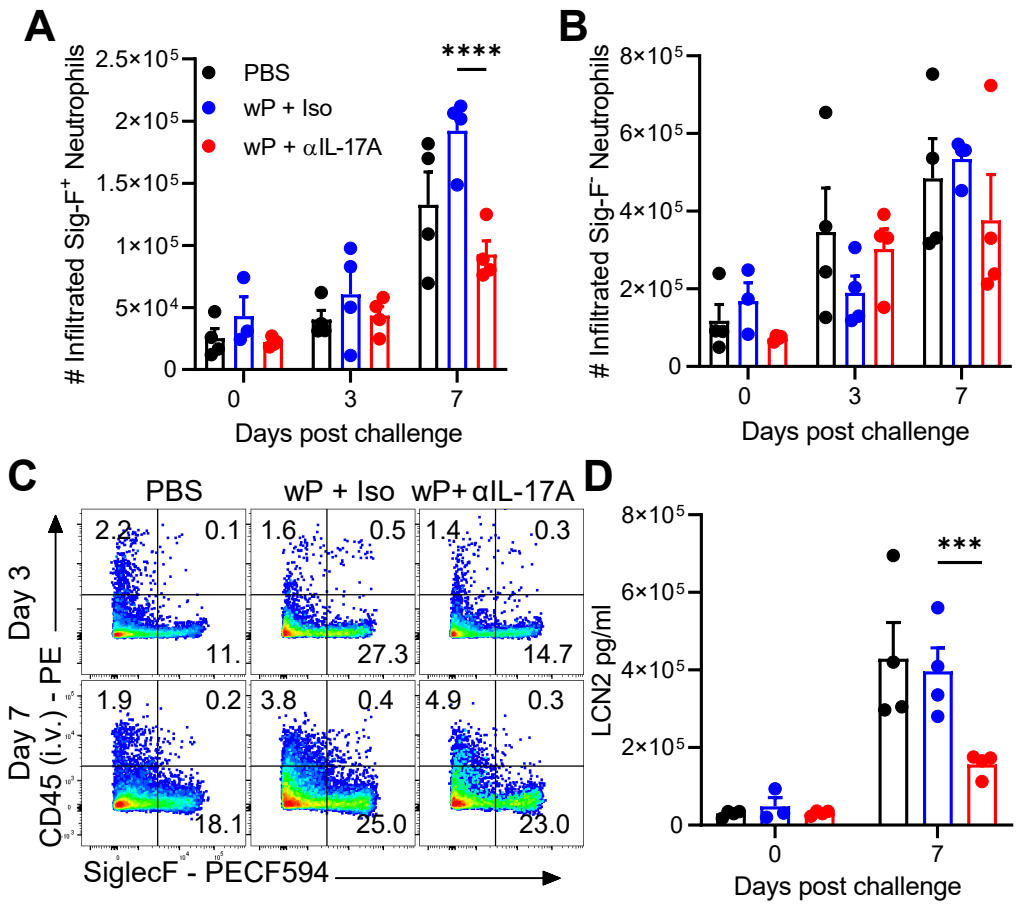

Figure 4.40 Neutralisation of IL-17A in mice immunised with a wP vaccine significantly reduces Siglec-F$^+$ neutrophil recruitment and LCN2 concentrations in the nasal cavity during *B. pertussis* infection.

C57BL/6 mice were immunised i.p. with 1/20th human dose of wP twice (-6 and -2 weeks). wP-immunised mice were injected i.p. with 100 µg of a neutralising anti-IL-17A antibody or isotype control one day before and every 3 days after *B. pertussis* challenge. Naïve control mice were injected i.p. with PBS and also infected with *B. pertussis*. On the day of and 3 and 7 days after challenge, a fluorochrome-conjugated anti-CD45 antibody was administered i.v. and mice were euthanised 10 min later. Nasal tissue was harvested and mononuclear cells were isolated and stained for CD11b, Ly6G, and Siglec-F, and analysed by flow cytometry. Absolute number of tissue-infiltrated (CD45 i.v.$^-$) Siglec-F$^+$ (A) and Siglec-F$^-$ (B) neutrophils (Ly6G$^+$CD11b$^+$) in the nasal tissue with representative flow cytometry plots (C). LCN2 concentration was quantified in nasal washes by ELISA (D). Data are mean ± SEM (n=3/4 per group). ***p < 0.001, ****p < 0.0001 isotype control versus anti-IL-17A treatment by two-way ANOVA followed by Sidak's post-test

Chapter 5: Bystander activation of CD4 T_{RM} cells induced by previous infection with *B. pertussis*

5.1 Introduction

The results from chapter 3 and 4 demonstrated that CD4 T_{RM} cells accumulate in the nasal cavity and lungs following *B. pertussis* infection, where they remain poised to sense and rapidly respond to re-infection with *B. pertussis*. However, there is emerging evidence that T_{RM} cells can exert their sensing and alarming functions in response to unrelated pathogens through a mechanism known as 'bystander activation' [348]. Classically, activation and differentiation of CD4 T cells requires three signals. Signal one consists of the TCR, alongside the CD4 co-receptor, engaging with the antigen-MHC class II complex presented by APCs [136]. Binding of co-stimulatory molecules expressed on APCs to co-stimulatory receptors on T cells is required as the second signal to prevent T cell anergy [349]. The cytokine milieu produced by APCs, as well as other innate immune cells, provide the third signal that influences the differentiation of naïve T cells into one of several T helper cell lineages [350]. However, it has been shown that the cytokine milieu generated during infection with an unrelated pathogen can directly activate effector and memory T cells independent of TCR engagement, in what is termed bystander activation [351, 352].

TCR-independent bystander activation has been well characterised for non-conventional lymphocytes which reside in peripheral tissues, such as ILCs and γδ T cells. ILCs are enriched at mucosal surfaces and can be divided into ILC1, ILC2, and ILC3 subsets based on their lineage-defining transcription factors and the signature cytokines they produce [353, 354]. ILCs lack antigen-specific receptors, however respond rapidly to cytokine stimulation, with ILC1s producing IFNγ in response to IL-12 and IL-18, ILC2s producing IL-5 and IL-13 in response to IL-33, IL-25, and TSLP, and ILC3s generating IL-17 and IL-22 following stimulation with IL-1β and IL-23 [353]. γδ T cells are another non-conventional T lymphocyte population which are activated by cytokines. Previous research from the Mills' lab demonstrated that IL-23 in combination with either IL-1β or IL-18 induces IL-17A production from γδ T cells, independent of TCR engagement [223, 224].

For bystander activation of conventional T cells, the majority of research has focused on CD8 T cells. Bystander activation of CD8 T cells was first described *in vivo* by Tough and colleagues, who found that injection of either Poly I:C or LPS into mice induced proliferation of memory CD8 T cells, and that this was mediated indirectly by type I IFN produced by APCs in response to Poly I:C or LPS [234]. Raue and colleagues further demonstrated that LCMV-specific memory CD8 T cells produced effector cytokines, such as IFNγ, in response to LPS-induced IL-12 and IL-18 *in vivo* [355]. Furthermore,

combinations of IL-18, IL-12, IL-2, IL-7, IL-15, IL-33, and TNF have been shown to induce IFNγ production from splenic LCMV-specific CD8 T cells [356]. Bystander activation of human CD8 T cells has also been reported in patients with infectious diseases. CD8 T cells specific for Epstein-Barr virus, cytomegalovirus, and influenza virus are activated during primary human immunodeficiency virus-1 (HIV) infection [352, 357]. Whilst the majority of studies have examined CD8 T cells which are found in circulation or secondary lymphoid organs, there is emerging evidence that tissue-resident CD8 T cells can also be activated in a TCR-independent manner. Lung CD8 T_{RM} cells have been shown to produce IFNγ in response to inhaled heat-killed *Salmonella enterica*, *S. aureus*, and LPS, and that this was mediated by IL-12/IL-18 signalling. Furthermore, direct stimulation of purified lung CD8 T_{RM} cells with IL-12 and IL-18 induced IFNγ production independent of TCR engagement [348].

The data surrounding bystander activation of CD4 T cells is more limited [233]. There is emerging evidence that the mechanism of TCR-independent activation of memory CD4 T cells is similar to that seen with ILC3s and γδ T cells, with IL-1 family cytokines, such as IL-1β and IL-18, synergising with STAT activators, such as IL-12 and IL-23, to induce IL-17A from CD4 T cells *in vitro* [243]. Research from the Mills' lab demonstrated that IL-1β in combination with IL-23 induced IL-17 production from splenic $CD3^+$ cells in the absence of TCR engagement [222]. Lalor and colleagues demonstrated that *M. tuberculosis*-stimulated BMDCs promoted IL-17A and IFNγ production from CD4 T cells isolated from the spleens of naïve mice, and that this was significantly reduced following the addition of a caspase-1 inhibitor, which prevents the cleavage of IL-1β and IL-18 into their active form, demonstrating that this effect was mediated in part by cytokine signalling. Furthermore, IL-23 in combination with IL-1β or IL-18 induced IL-17 production from purified splenic CD4 T cells *in vitro* [223]. A study by Lee and colleagues showed that memory-like CD4 T cells isolated from secondary lymphoid organs produced IL-17A in response to IL-1β and IL-23 stimulation in the presence of IL-7 [250]. Bystander activation has also been reported in human CD4 T cells. Human DCs primed with Gram-negative bacteria such *K. pneumoniae* and *E. coli* were found to induce IL-17A from human memory, but not naïve, CD4 T cells. As these are commonly encountered pathogens, the reactivation of pathogen-specific memory T cells cannot be ruled out. However, it was also demonstrated that muramyl dipeptide, a peptidoglycan derivative expressed by many bacterial species, could induce IL-17A production from human memory CD4 T cells indirectly via NOD2 activation in DCs and subsequent IL-1β and IL-23 production [358]. Furthermore, IL-1β and IL-23 have been shown to induce IL-17A and IFNγ production from human IL-1R1^{high} memory CD4 T cells [250]. As with CD8

T cells, the majority of research on TCR-independent activation of CD4 T cells has focused on cells found within the circulation or secondary lymphoid organs. Bystander activation of CD4 T_{RM} cells has not been well characterised.

The objective of this study was to assess if nasal and lung CD4 T_{RM} cells induced following natural infection with *B. pertussis* can be activated in a bystander manner. The hypothesis being tested was that pro-inflammatory cytokines, such as IL-1β, IL-23, and IL-18, generated by innate immune cells in response to unrelated pathogens and PAMPs can directly activate CD4 T_{RM} cells, independent of TCR engagement. The specific mechanisms by which bystander activation of CD4 T_{RM} cells occurs and the influence of bystander activation on the subsequent immune response in the nasal cavity was also examined.

5.2 Results

5.2.1 CD4 T_{RM} cells induced during B. pertussis infection produce IL-17A and IFNγ in response to cytokine stimulation.

In order to investigate if CD4 T_{RM} cells induced following *B. pertussis* infection can be activated in a TCR-independent manner, isolated mononuclear cells from the nasal cavity and lungs of naïve and convalescent (> 60 days post *B. pertussis* challenge) mice were stimulated with combinations of IL-1β, IL-23, IL-18, and IL-12. Cells were also stimulated with sBP and anti-CD28 and anti-CD49d to confirm the presence of pathogen-specific CD4 T_{RM} cells. Intracellular IL-17A and IFNγ production by total $CD3^+$ cells and by CD4 T_{RM} cells ($CD4^+CD3^+CD45i.v.^-CD44^+CD69^+CD103^±$) was assessed by flow cytometry.

$CD4^-CD3^+$ cells from the nasal tissue (Figure 5.1 *A, B*) and lungs (Figure 5.2 *A, B*) of naïve and convalescent mice produced IL-17A following *in vitro* stimulation with IL-23 in combination with IL-1β or IL-18, demonstrating the presence of an 'innate-like' IL-17A-producing $CD3^+$ T cell population in the nose and the lungs of mice. However, an increase in the frequency of IL-17A-producing $CD4^+CD3^+$ T cells following *in vitro* stimulation with combinations of IL-23, IL-1β, and IL-18 was only observed in the nasal tissue (Figure 5.1 *C*) and lungs (Figure 5.2 *C*) of convalescent mice.

An examination of intracellular IL-17A and IFNγ production by CD4 T_{RM} cells ($CD4^+CD3^+CD45i.v.^-CD44^+CD69^+CD103^±$) revealed that CD4 T_{RM} cells from the nasal tissue (Figure 5.3 *A, B*) and lungs (Figure 5.4 *A, B*) of convalescent mice produced the highest levels of IL-17A in response to *in vitro* stimulation with IL-23 in combination with IL-1β or IL-18. CD4 T_{RM} cells from the nasal tissue (Figure 5.3 *A, B*) and lungs (Figure 5.4 *A, B*) of naïve mice did not produce detectable levels of IL-17A in response to stimulation with Th17-polarising cytokines. However, IL-12 in combination with IL-18 induced an increase in the frequency of $IFNγ^+$ CD4 T_{RM} cells in the lungs (Figure 5.4 *C*) of naïve and convalescent mice. These findings suggest that TCR-independent IL-17A production by CD4 T_{RM} cells is unique to convalescent mice.

To confirm that tissue-resident CD4 T cells induced following infection with *B. pertussis* can produce effector cytokines independent of TCR engagement, circulating ($CD45\ i.v.^+$) or resident ($CD45\ i.v.^-$) CD4 T cells were isolated from the nasal tissue or lungs of convalescent mice and stimulated with combinations of IL-1β, IL-23, IL-18, IL-12, in the presence or absence of IL-7, which enhances the survival and maintenance of memory

T cells [359, 360]. Cells were also stimulated with anti-CD3 and anti-CD28 which served as a positive control for TCR-dependent responses. The concentration of IL-17A and IFNγ in the supernatants after 48 hours was quantified by ELISA. IL-23 in combination with IL-1β or IL-18 promoted IL-17A production from nose-resident (CD45 i.v.$^-$) CD4 T cells when cultured in the presence of IL-7. Furthermore, the combination of IL-12 and IL-18 induced IFNγ production from nose-resident CD4 T cells when IL-7 was added to culture (Figure 5.5 *B*). IL-7 alone did not promote IL-17A or IFNγ production (Figure 5.5 *A*).

IL-23 in combination with IL-1β or IL-18 induced IL-17A production from tissue-resident (CD45 i.v.$^-$), but not circulating (CD45 i.v.$^+$), CD4 T cells isolated from the lungs of convalescent mice when cultured in the presence of IL-7 (Figure 5.6 *A*). Additionally, IL-12 and IL-18 synergised with IL-7 to promote IFNγ production from both resident and circulating lung CD4 T cells (Figure 5.6 *B*). These results demonstrate that CD4 T_{RM} cells induced following *B. pertussis* infection can produce IL-17A and IFNγ in response to cytokine stimulation, independent of TCR engagement.

5.2.2 Nose- and lung-resident CD4 T cells express high levels of the IL-18 receptor.

Given that combinations of IL-1β, IL-18, and IL-23 can promote non-specific IL-17A production from nasal and lung CD4 T_{RM} cells, this study next investigated cell surface expression of the receptors for these cytokines on tissue-resident CD4 T cells. Expression of IL-18Rα (CD218a) was significantly higher on tissue-resident CD4 T cells in the nasal tissue and lungs of convalescent mice compared with CD4 T cells from naïve mice. However, IL-18Rα expression was low on spleen CD4 T cells in both naïve and convalescent mice (Figure 5.7 *A, B*). Furthermore, expression of both IL-23R and IL-1RI (CD121a) was low on CD4 T cells in the nasal tissue, lungs, and spleens of naïve and convalescent mice (Figure 5.7 *C, D*).

5.2.3 Nose- and lung-resident CD4 T cells induced following B. pertussis infection produce IL-17A in response to unrelated pathogens and PAMPs in vitro.

To investigate if tissue-resident CD4 T cells can produce IL-17A and IFNγ in response to unrelated pathogens and PAMPs, CD4 T cells isolated from the lungs and nasal tissue of convalescent mice were stimulated with *E. coli*-derived LPS, heat-killed *M. tuberculosis,* heat-killed *S. aureus*, Poly I:C, or sBP, which served as a pathogen-specific

control, in the presence or absence of BMDCs. After 48 hours supernatants were collected and concentration of IL-17A and IFNγ in supernatants was quantified by ELISA. Of the unrelated pathogens and PAMPs examined, *E. coli*-derived LPS induced the highest concentration of IL-17A from nose-resident (CD45 i.v.$^-$) CD4 T cells when co-cultured with BMDCs. IFNγ production by nose-resident CD4 T cells was not detected. Stimulation of BMDCs or CD4 T cells alone failed to induce detectable levels of IL-17A or IFNγ, indicating that unrelated pathogens and PAMPS do not act directly on tissue-resident CD4 T cells, but rather indirectly via innate immune cells (Figure 5.8 *A, B*). Additionally, *E. coli*-derived LPS, heat-killed *M. tuberculosis*, heat-killed *S. aureus*, and poly I:C induced IL-17A, but not IFNγ, production from lung-resident (CD45 i.v.$^-$) CD4 T cells when co-cultured with BMDCs. Circulating (CD45 i.v.$^+$) CD4 T cells isolated from the lungs of convalescent mice did not produce IL-17A following stimulation with unrelated pathogens and PAMPs, suggesting that this phenomenon is exclusive to tissue-resident CD4 T cells (Figure 5.9 *A, B*). Furthermore, conditioned medium from BMDCs previously stimulated with LPS and poly I:C promoted IL-17A production from nose-resident CD4 T cells isolated from convalescent mice. Interestingly, conditioned medium from BMDCs stimulated with LPS, heat-killed *M. tuberculosis*, heat-killed *S. aureus*, and poly I:C, promoted IFNγ production from nose-resident CD4 T cells, contrasting to results seen when using the co-culture system (Figure 5.10 *A, B*).

Assessment of innate cytokine production by BMDCs revealed that *E. coli*-derived LPS, heat-killed *M. tuberculosis,* heat-killed *S. aureus*, and sBP induced IL-1β production from BMDCs. *E. coli*-derived LPS and *S. aureus* promoted IL-12p70 secretion, whereas only *E. coli*-derived LPS and sBP induced IL-23 production from BMDCs (Figure 5.11 *A, B*). As LPS and sBP induced the highest concentrations of IL-17A from nose- and lung-resident CD4 T cells when co-cultured with BMDCs, these results suggest that IL-23 may be a key mediator of bystander activation of CD4 T_{RM} cells.

5.2.4 Bystander activation of nose- and lung-resident CD4 T cells is mediated by IL-12/IL-23 signalling in vitro.

To assess if LPS-induced IL-17A production from nose and lung-resident CD4 T cells is mediated by cytokines such as IL-23, CD4 T cells isolated from the nasal tissue or lungs of convalescent mice were co-cultured with BMDCs and stimulated with *E. coli*-derived LPS or sBP in the presence of an anti-IL-12p40 antibody, an anti-MHCII antibody, or an isotype control antibody. Both IL-12 and IL-23 contain a common p40 subunit, thus an

antibody targeting p40 neutralises both cytokines. After 48 hours of culture supernatants were collected and the concentration of IL-17A in supernatants was quantified by ELISA. *E. coli*-derived LPS induced IL-17A from nose-resident (Figure 5.12 *A*) and lung-resident (Figure 5.12 *B*) CD4 T cells isolated from convalescent mice when co-cultured with BMDCs, and this was significantly reduced by the addition of an anti-IL-12p40 antibody, but not by an anti-MHCII antibody, suggesting that this response is mediated by cytokines and not by TCR engagement with the MHC complex. In contrast, addition of an anti-IL-12p40 antibody or an anti-MHCII antibody reduced sBP-induced IL-17A production from nose and lung-resident CD4 T cells, demonstrating that the pathogen-specific response to sBP is mediated both by cytokines and TCR engagement (Figure 5.12 *A*, *B*). IL-17A production by circulating (CD45 i.v.$^+$) CD4 T cells isolated from the lungs of convalescent mice in response to LPS was much lower to that produced by tissue-resident CD4 T cells isolated from the same lung samples, suggesting that bystander activation is a feature of tissue-resident CD4 T cells (Figure 5.12 *B*).

5.2.5 CD4 T_{RM} cells rapidly produce IL-17A following intranasal challenge with E. coli-derived LPS in vivo.

In order to investigate if CD4 T_{RM} cells are susceptible to bystander activation *in vivo, E. coli*-derived LPS or PBS was administered i.n. to convalescent mice or naïve control mice. *E. coli*-derived LPS induced a significant increase in the number of IL-17A$^+$ CD4 T_{RM} cells in the nasal cavity of convalescent mice within 4 hours. Furthermore, *E. coli*-derived LPS also promoted an increase in the number of nasal IFNγ$^+$ CD4 T_{RM} cells in convalescent mice, however the absolute numbers of IFNγ$^+$ cells are low (< 100 cells). No increase in IL-17A$^+$ or IFNγ$^+$ CD4 T_{RM} cells was detected in naïve mice following LPS administration (Figure 5.13 *A, B, D*). The effect of i.n. administration of LPS on nose-resident γδ T cells was also examined as these cells can be activated in a TCR-independent manner [224]. LPS promoted IL-17A production from nose-resident γδ T cells in naïve and convalescent mice, with a significant increase observed in naïve mice (Figure 5.13 *C, E*). *E. coli*-derived LPS also induced a significant increase in the number of IL-17A$^+$, but not IFNγ$^+$, CD4 T_{RM} cells in the lungs of convalescent mice, however, the effect was not as striking as that seen in the nasal tissue (Figure 5.14 *A, B, D*). Furthermore, LPS promoted IL-17A production from lung-resident γδ T cells in naïve and convalescent mice, with a significant increase observed in convalescent mice (Figure 5.14 *C, E*).

As bystander activation of T cells is thought to be a rapid response [233], LPS-induced activation of CD4 T_{RM} cells was examined 4 and 24 hours after i.n. administration. LPS promoted a significant increase in the number of IL-17A$^+$ CD4 T_{RM} in the nasal tissue (Figure 5.15 *A*-*C*) and lungs (Figure 5.16 *A*-*C*) of convalescent mice within 4 hours, however, this was less obvious after 24 hours. In contrast, a significant increase in the number of IFNγ$^+$ CD4 T_{RM} cells was detected only in in the nasal tissue (Figure 5.15 *A*-*C*) and lungs (Figure 5.16 *A*-*C*) of naïve mice 24 hours after i.n. administration of LPS. Together, these results demonstrate that CD4 T_{RM} cells induced following infection with *B. pertussis* rapidly produce IL-17A in response to a PAMP derived from an unrelated pathogen *in vivo*.

5.2.6 LPS-induced IL-17A production from CD4 T_{RM} cells in convalescent mice is mediated by IL-12/IL-23 signalling in vivo.

In order to investigate if IL-17A production by CD4 T_{RM} cells in response to *E. coli*-derived LPS is mediated by IL-23/IL-12 signalling *in vivo*, convalescent mice were treated with a neutralising anti-IL-12p40 antibody or an isotype control antibody one day prior to and during i.n. administration of *E. coli*-derived LPS. LPS promoted IL-17A production from CD4 T_{RM} cells and γδ T cells in the nasal cavity (Figure 5.17 *A*-*D*) and lungs (Figure 5.18 *A*-*D*) of convalescent mice, and this was significantly reduced in mice treated with an anti-IL-17A antibody. These results demonstrate that IL-17A production by CD4 T_{RM} cells in response to LPS is mediated partly by IL-12/IL-23 signalling *in vivo*.

5.2.7 CD4 T_{RM} cells induced following previous infection with B. pertussis produce IL-17A in response to K. pneumoniae in vitro.

Having shown that non-specific IL-17A production by CD4 T_{RM} cells is partly mediated by IL-23/IL-12 signalling, it was next investigated if another pathogen could promote IL-23 production by myeloid cells and consequently induce non-specific activation of CD4 T_{RM} cells. *K. pneumoniae* is a Gram-negative bacterium that is part of the *Enterobacteriaceae* family and is known to colonise mucosal surfaces, such as the nasopharynx [361]. In the current study heat-killed *K. pneumoniae* induced IL-23, IL-1β, and IL-12p70 production from BMDCs in a dose-dependent manner (Figure 5.19).

It was next investigated if heat-killed *K. pneumoniae*-activated BMDCs could stimulate CD4 T_{RM} cells in a bystander manner *in vitro*. Isolated CD4 T cells from nasal tissue and

lungs of convalescent mice were co-cultured with BMDCs and stimulated with heat-killed *K. pneumoniae* in the presence of either an anti-IL-1β antibody, an anti-IL-23p19 antibody, an anti-IL-12p40 antibody, or an isotype control antibody. After 48 hours supernatants were collected and the concentration of IL-17A in supernatants was quantified by ELISA. Stimulation of BMDCs with heat-killed *K. pneumoniae* induced IL-17A production from nose- (Figure 5.20) and lung-resident (Figure 5.21) CD4 T cells in a dose-dependent manner. Addition of an anti-IL-1β antibody, an anti-IL-23p19 antibody, or an anti-IL-12p40 antibody significantly reduced IL-17A production by nose- and lung-resident CD4 T cells following co-culture with BMDCs stimulated with *K. pneumoniae* (Figure 5.20; Figure 5.21). The findings presented in this study demonstrate that *K. pneumoniae* can promote non-specific IL-17A production from CD4 T_{RM} cells *in vitro*, and this is mediated in part by Th17-polarising cytokines produced by BMDCs.

5.2.8 CD4 T_{RM} cells induced following B. pertussis infection produce IL-17A in response to heat-killed K. pneumoniae in vivo.

It was next examined if CD4 T_{RM} cells generated following infection with *B. pertussis* can produce IL-17A in response to heat-killed *K. pneumoniae in vivo*. I.n. administration of heat-killed *K. pneumoniae* promoted a significant increase in the number of IL-17A$^+$, but not IFNγ$^+$, CD4 T_{RM} cells in the nasal tissue (Figure 5.22 *A*-*C*) and lungs (Figure 5.23 *A*-*C*) of convalescent mice. The differences in innate cell recruitment to the nasal cavity between naïve and convalescent mice in response to *K. pneumoniae* was also investigated. Convalescent mice had significantly more neutrophils in the nasal cavity following i.n. administration of heat-killed *K. pneumoniae* compared with naïve mice. There was no significant difference in the number of Ly6C$^+$CD11b$^+$ monocytes between naïve and convalescent mice following heat-killed *K. pneumoniae* challenge (Figure 5.24 *A*-*C*). An examination of the location of neutrophils within the nasal tissue revealed that the number of tissue-infiltrated (CD45 i.v.$^-$) neutrophils was significantly higher in convalescent mice following i.n. administration of heat-killed *K. pneumoniae* (Figure 5.25 *A*-*C*). Taken together, these results demonstrate that CD4 T_{RM} cells induced during a previous infection with *B. pertussis* can produce non-specific IL-17A in response to *K. pneumoniae*, and this is accompanied by enhanced neutrophil infiltration into the nasal cavity of convalescent mice.

5.3 Discussion

This study has generated the novel finding that CD4 T_{RM} cells that accumulate in the nasal cavity and lungs following *B. pertussis* infection are susceptible to bystander activation both *in vitro* and *in vivo*. The results presented in this chapter demonstrated that CD4 T_{RM} cells can execute their sensing and alarming function in response to unrelated pathogens and PAMPs, and that this is mediated indirectly by cytokines produced by innate immune cells. Initial activation and expansion of CD4 T cells is classically thought to be strictly controlled by three signals. Engagement of the TCR with the antigen-MHC II complex presented by APCs and activation of co-stimulatory receptors expressed on T cells comprise signal 1 and 2, respectively. The third signal is provided by the cytokine milieu generated by APCs and other innate immune cells [126]. However, the results presented in this chapter demonstrated that the cytokine milieu alone can activate CD4 T_{RM} cells, revealing an alternative pathway of CD4 T_{RM} cell activation in the absence of classical recognition of antigens by TCRs.

The results of the present study showed that CD4 T_{RM} cells generated following *B. pertussis* infection can be activated by cytokines in a manner similar to that observed with γδ T cells and ILC3s. Consistent with previous studies [223, 250, 362], IL-1 family cytokines such as IL-1β and IL-18 synergised with STAT activators such as IL-12 and IL-23 to induce non-specific IL-17A and IFNγ production from lung- and nose-resident CD4 T cells. However, unlike the aforementioned studies [223, 250, 362] which reported these findings in CD4 T cells isolated from secondary lymphoid tissue, this study identified the previously unknown ability of tissue-resident CD4 T cells isolated from the nasal cavity and lungs to produce non-specific IL-17A and IFNγ in response to cytokine stimulation, independent of TCR engagement. A study by Ge and colleagues [348] found that memory CD8 T cells located in the lung parenchyma were more susceptible to bystander activation than memory CD8 T cells found in the lung vasculature. In agreement with this, results presented in this study revealed that lung-resident CD4 T cells isolated from convalescent mice had a greater propensity for IL-17A production in response to cytokine stimulation compared with circulating CD4 T cells purified from the same lung samples, demonstrating that non-specific IL-17A production from CD4 T cells is particular to those found within the parenchyma.

Despite responding to IL-1β and IL-23, expression of the receptors for these cytokines on tissue-resident CD4 T cells in the nasal cavity and lung was low. In contrast, high expression of the receptor for IL-18 was reported on tissue-resident CD4 T cells in the lung and nasal tissue of convalescent, but not naïve, mice. Interestingly, IL-18 receptor

expression has previously been associated with innate-like capacities of CD4 T cells. Pham et al. reported that IL-18R expression, in addition to death receptor 3 expression, on murine CD4 Th1 cells was required for optimal IFNγ production in response to non-cognate stimulation [246]. IL-18Rα expression also identified a major population of human memory CD4 T cells enriched in barrier tissue, such as the nasal polyps, with innate lymphocyte functionality, capable of producing cytokines, including IFNγ, TNF, IL-6, IL-5, IL-13, GM-CSF, and IL-22, in response to combinations of IL-12, IL-18, IL-15 and TNF-like cytokine 1A (TL1a) [363].

In addition to direct stimulation by cytokines, the findings presented in this study demonstrated that the Gram-negative bacterium, *K. pneumoniae*, and the TLR4 ligand, LPS, induced IL-17A from nose and lung CD4 T_{RM} cells *in vitro* when co-cultured with BMDCs, and *in vivo*. It must be noted that although *B. pertussis* is also a Gram-negative bacterium, *Bordetella* endotoxins exhibit structural variability between other Gram-negative bacteria, with *B. pertussis* endotoxins lacking a serospecific O polysaccharide, and is referred to as lipooligosaccharide (LOS) [292, 364]. The ability of *K. pneumoniae* and *E. coli*-derived LPS to induce non-specific IL-17A production from nose- and lung-resident CD4 T cells was associated with their capacity to induce IL-23 production from BMDCs. Non-specific IL-17A production by nose- and lung-resident CD4 T cells by Gram-negative bacteria or their components is consistent with findings in human memory CD4 T cells. Van Beelen and colleagues reported that IL-17A production by human memory CD4 T cells when co-cultured with DCs was highest in response to Gram-negative bacteria, including *K. pneumoniae* and *E. coli* [358]. Although there are some reports of CD4 T cells expressing PRRs, such as TLR4 [365], the data presented here demonstrated that innate immune cells were required for bystander activation as direct stimulation of purified nose or lung CD4 T cells in the absence of BMDCs failed to induce detectable levels of either IL-17A or IFNγ. Furthermore blocking IL-23/IL-12 signalling both *in vitro* and *in vivo* significantly reduced IL-17A production from nose- and lung-resident CD4 T cells, indicating that cytokine signalling is an important mediator of this phenomenon. In contrast, blocking MHC II did not reduced non-specific IL-17A production by tissue-resident CD4 T cells, suggesting that any potential cross-reactivity between shared epitopes of seemingly unrelated pathogens does not contribute to this.

Unlike pathogen-specific responses, which can take days to develop, bystander activation of memory T cells is a rapid response [366, 367]. The results from this study are in agreement with this; the highest levels of IL-17A production by nose and lung CD4 T_{RM} cells *in vivo* was detected within 4 hours of i.n. administration of LPS, and declined after 24 hours.

The results presented in this study have revealed that bystander activation of CD4 T_{RM} cells is accompanied by an amplified immune response to an unrelated pathogen, as demonstrated by increased neutrophil recruitment to the nasal cavity of convalescent mice in response to *K. pneumoniae*. *K. pneumoniae* is a Gram-negative opportunistic pathogen that can asymptomatically colonise mucosal surfaces without causing pathology. However, *K. pneumoniae* can disseminate from the mucosa to other tissues and cause life threatening infections, ranging from pneumonia to sepsis, in susceptible individuals [368, 369]. The immune response to *K. pneumoniae* has similarities to that seen in *B. pertussis* infection, such as the induction of a Th17 response and neutrophil recruitment to the respiratory tract [326, 370]. In the present study, i.n. administration of heat-killed *K. pneumoniae* induced non-specific IL-17A production from nasal CD4 T_{RM} cells in convalescent mice, and this was accompanied by significantly enhanced neutrophil infiltration into the nasal tissue compared with mice not previously infected with *B. pertussis*. The phenomenon of innate immune memory, which can be described as altered innate immune responses evoked by repeated insults [371], may contribute to the increased neutrophil infiltration seen in mice previously infected with *B. pertussis*. However, non-specific IL-17A produced by CD4 T_{RM} cells in response to heat-killed *K. pneumoniae* may also contribute to this observation. The results presented in this study complement those seen by Ge et al. who demonstrated that bystander activation of lung CD8 T_{RM} cells enhanced neutrophil recruitment to the airways and subsequently attenuated the severity of bacterial pneumonia in mice. As neutrophils have been implicated in host defence against *K. pneumoniae* [372], it is possible that bystander activation of *B. pertussis*-specific CD4 T_{RM} cells could confer non-specific protection against *K. pneumoniae* infection by accelerating neutrophil influx into the respiratory tract. Bystander activation of T cells has been shown to be protective in other infection models. Memory CD8 T cells specific for ovalbumin protein produced IFNγ after infection of mice with *L. monocytogenes*, and this was associated with enhanced bacterial clearance of *L. monocytogenes* from the spleen and liver [238]. Non-specific activation of CD4 T cells has also been implicated in enhancing bacterial clearance following *Salmonella, Chlamydia,* and *Brucella* infection [246].

Overall, the experiments conducted in this study demonstrated that nasal and lung CD4 T_{RM} cells induced following *B. pertussis* infection are susceptible to bystander activation, highlighting an additional mechanism by which these cells can be activated in the absence of TCR engagement. Stimulation with Th17-polarising cytokines induced IL-17 production from nose- and lung-resident CD4 T cells. Furthermore, BMDCs stimulated with unrelated pathogens and PAMPs promoted non-specific IL-17A production from

lung and nose CD4 T_{TM} cells, and this was found to be mediated indirectly by cytokine signalling. Additionally, bystander activation of CD4 T_{RM} cells *in vivo* is accompanied by enhanced innate immune responses, as evident by the increased neutrophil infiltration into the nasal cavity of convalescent mice in response to an unrelated pathogen, *K. pneumoniae*. Due to their capacity to rapidly respond to previously encountered pathogens and to unrelated pathogens, CD4 T_{RM} cells represent an important link between innate and adaptive responses at mucosal surfaces.

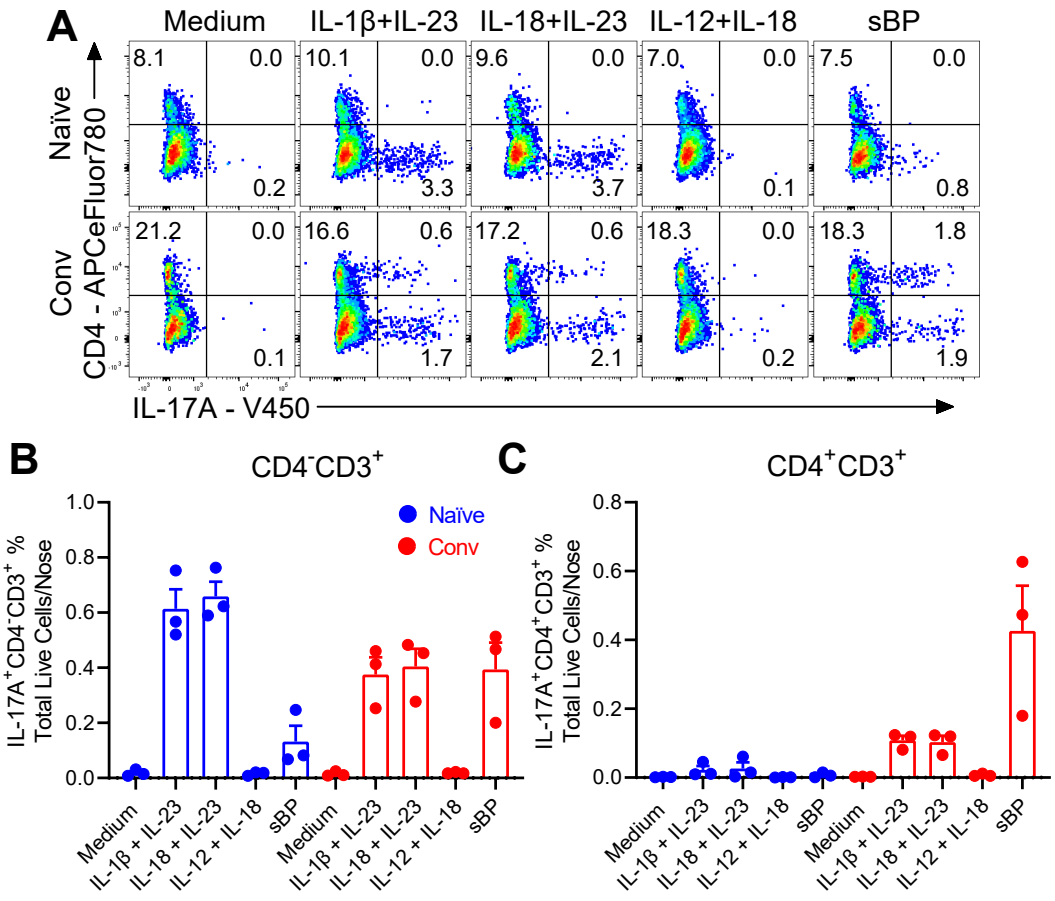

Figure 5.1 CD4 T cells from the nasal tissue of mice previously infected with *B. pertussis* produce IL-17A in response to Th17-polarising cytokines.

C57BL/6 mice were infected with live *B. pertussis*. Once infection had cleared (> 60 days p.i.), nasal tissue was harvested from convalesvent (conv) and naïve control mice. Mononuclear cells were isolated and pooled from 8 mice/group and stimulated in triplicate ($0.9x10^6$ cells/ml) with combinations of IL-1β, IL-23, IL-18, IL-12 (all at 10 ng/ml) or sBP (5 µg/ml) with anti-CD28 and anti-CD49d (both at 1 µg/ml) or medium alone for 20 hours. Brefeldin A (5 µg/ml) was added for the final 4 hours of culture. Cells were stained for surface CD3 and CD4, and intracellular IL-17A, and analysed by flow cytometry. Representative flow cytometry plots (A) and frequencies of IL-17A-producing $CD4^-$ (B) and $CD4^+$ (C) cells, gated on total $CD3^+$ cells, and expressed as a frequency of total live cells. Data are mean ± SEM of pooled data from three independent experiments, with each dot representing the average of three technical replicates from one independent experiment.

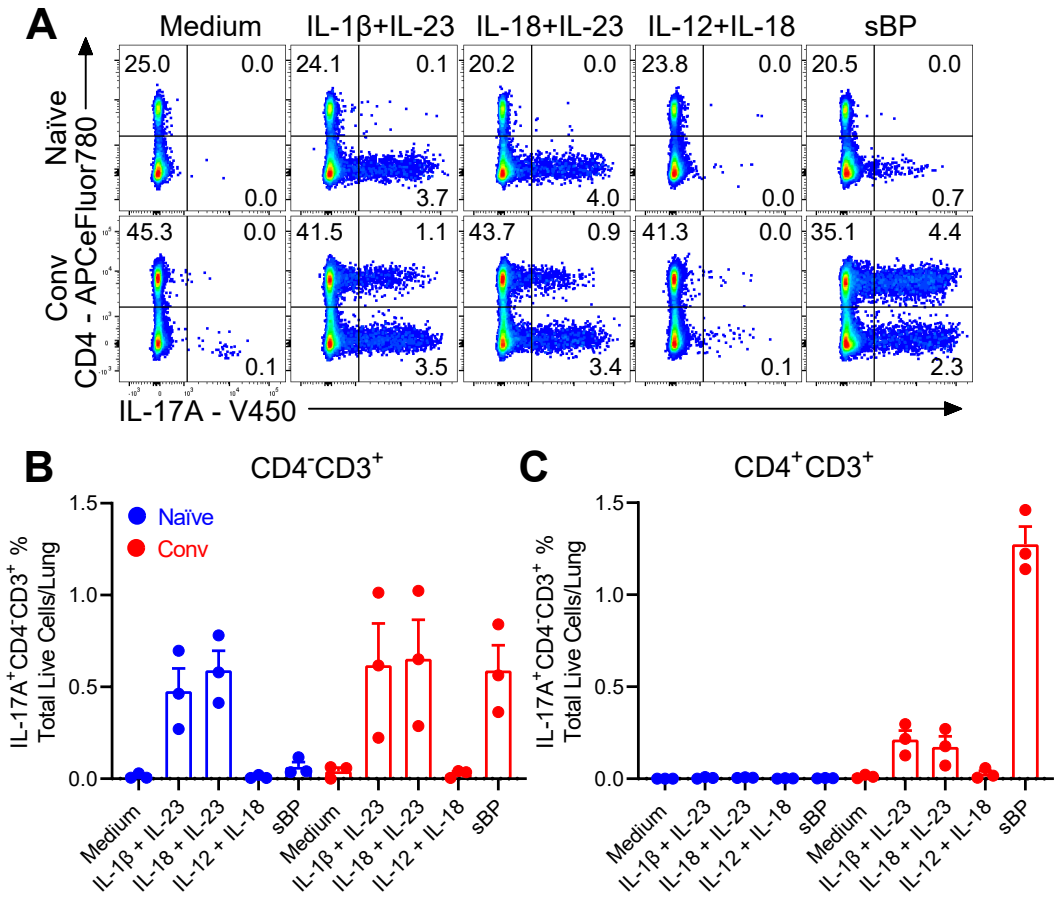

Figure 5.2 CD4 T cells from the lungs of mice previously infected with *B. pertussis* produce IL-17A in response to Th17-polarising cytokines.

C57BL/6 mice were infected with live *B. pertussis*. Once infection had cleared (> 60 days p.i.), lungs were harvested from convalescent (conv) and naïve control mice. Mononuclear cells were isolated from lungs and cells were pooled from 8 mice/group and stimulated in triplicate ($2.8x10^6$ cells/ml) with combinations of IL-1β, IL-23, IL-18, IL-12 (all at 10 ng/ml), or sBP (5 μg/ml) with anti-CD28 and anti-CD49d (both at 1 μg/ml) or medium alone for 20 hours. Brefeldin A (5 μg/ml) was added for the final 4 hours of culture. Cells were stained for surface CD3 and CD4, and intracellular IL-17A, and analysed by flow cytometry. Representative flow cytometry plots (A) and frequencies of IL-17A-producing $CD4^-$ (B) and $CD4^+$ (C) cells, gated on total $CD3^+$ cells, and expressed as a frequency of total live cells. Data are mean ± SEM of pooled data from three independent experiments, with each dot representing the average of three technical replicates from one independent experiment.

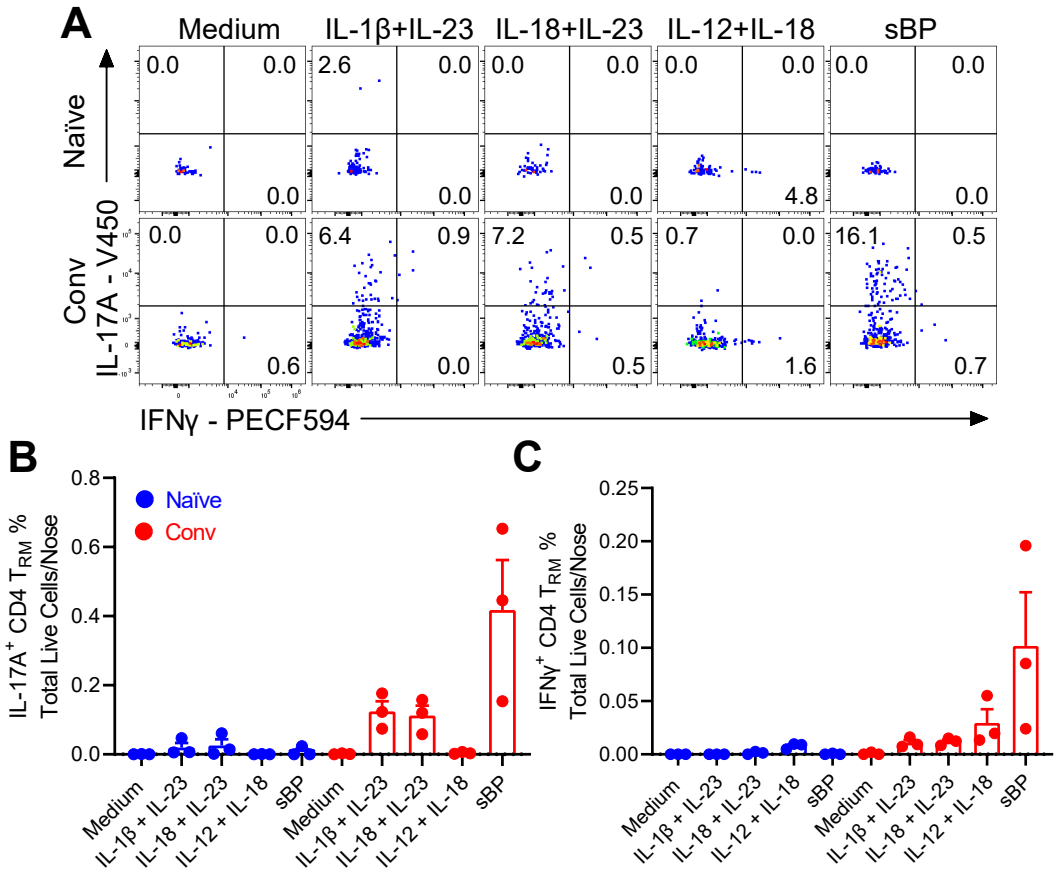

Figure 5.3 CD4 T_{RM} cells from the nasal tissue of mice previously infected with *B. pertussis* produce IL-17A in response to cytokine stimulation only.

C57BL/6 mice were infected with live *B. pertussis*. Once infection had cleared (> 60 days p.i.) convalescent (conv) and naïve control mice were injected i.v. with a fluorochrome-conjugated anti-CD45 antibody 10 min prior to euthanasia. Nasal tissue was harvested from naïve and convalescent mice. Mononuclear cells were isolated and pooled from each group of mice (n=8/group) and stimulated in triplicate ($0.9x10^6$ cells/ml) with combinations of IL-1β, IL-23, IL-18, IL-12 (all at 10 ng/ml) or sBP (5 µg/ml) with anti-CD28 and anti-CD49d (both at 1 µg/ml), or medium alone for 20 hours, with brefeldin A (5 µg/ml) added for the final 4 hours of culture. Cells were stained with antibodies specific for CD4, CD3, CD44, CD69, CD103, and intracellular IL-17A and IFNγ, and analysed by flow cytometry. Representative flow cytometry plots (A) and relative frequencies of IL-$17A^+$ (B) and $IFN\gamma^+$ (C) CD4 T_{RM} cells ($CD4^+CD3^+CD45i.v.^-CD44^+CD69^+CD103^\pm$), expressed as a percentage of total live cells. Data are mean ± SEM of pooled data from three independent experiments, with each dot representing the average of three technical replicates from one independent experiment.

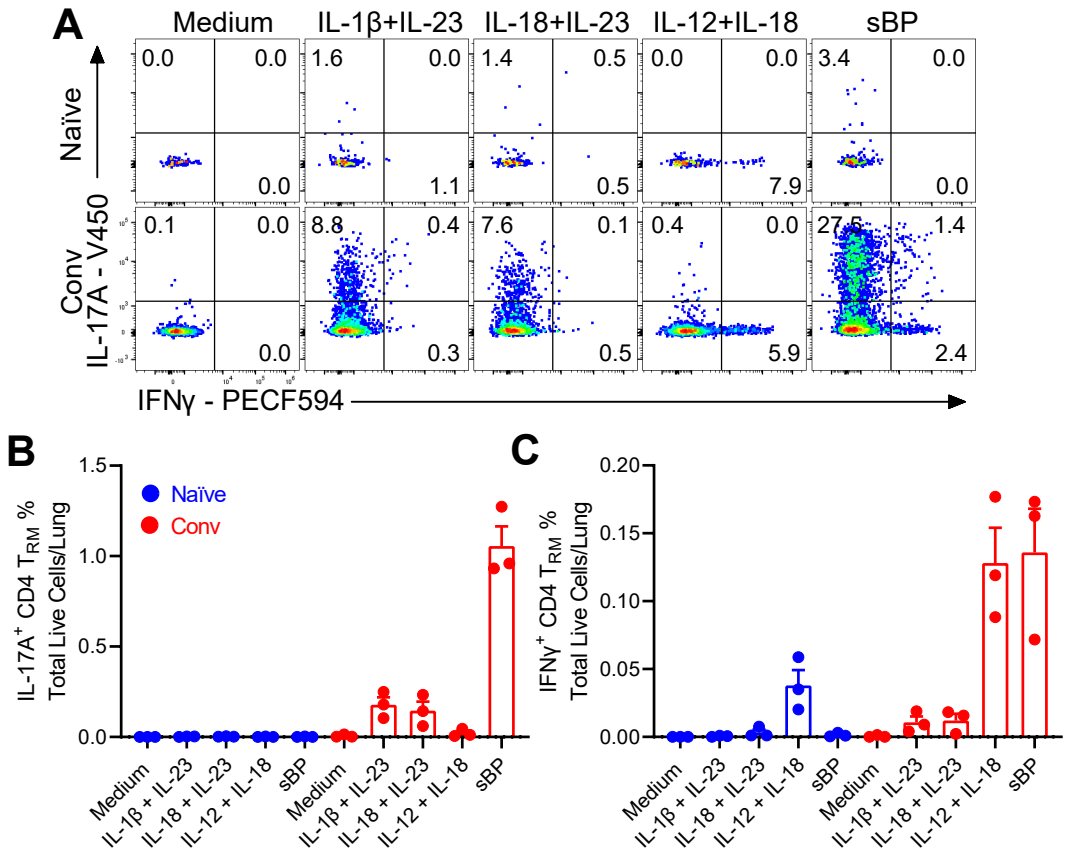

Figure 5.4 CD4 T_{RM} cells from the lungs of mice previously infected with *B. pertussis* produce IL-17A and IFNγ in response to cytokine stimulation only.

C57BL/6 mice were infected with live *B. pertussis*. Once infection had cleared (> 60 days p.i.) convalescent (conv) and naïve control mice were injected i.v. with a fluorochrome-conjugated anti-CD45 antibody and euthanised 10 min later. Lung mononuclear cells were isolated and pooled from each group of mice (n=8/group) and stimulated in triplicate ($2.8x10^6$ cells/ml) with combinations of IL-1β, IL-23, IL-18, IL-12 (all at 10 ng/ml) or sBP (5 µg/ml) with anti-CD28 and anti-CD49d (both at 1 µg/ml), or medium alone for 20 hours, with brefeldin A (5 µg/ml) added for the final 4 hours of culture. Cells were stained with antibodies specific for CD4, CD3, CD44, CD69, CD103, and intracellular IL-17A and IFNγ, and analysed by flow cytometry. Representative flow cytometry plots (A) and relative frequencies of IL-17A$^+$ (B) and IFNγ$^+$ (C) CD4 T_{RM} (CD4$^+$CD3$^+$CD45i.v.$^-$ CD44$^+$CD69$^+$CD103$^\pm$) cells, expressed as a percentage of total live cells. Data are mean ± SEM of pooled data from three independent experiments, with each dot representing the average of three technical replicates from one independent experiment.

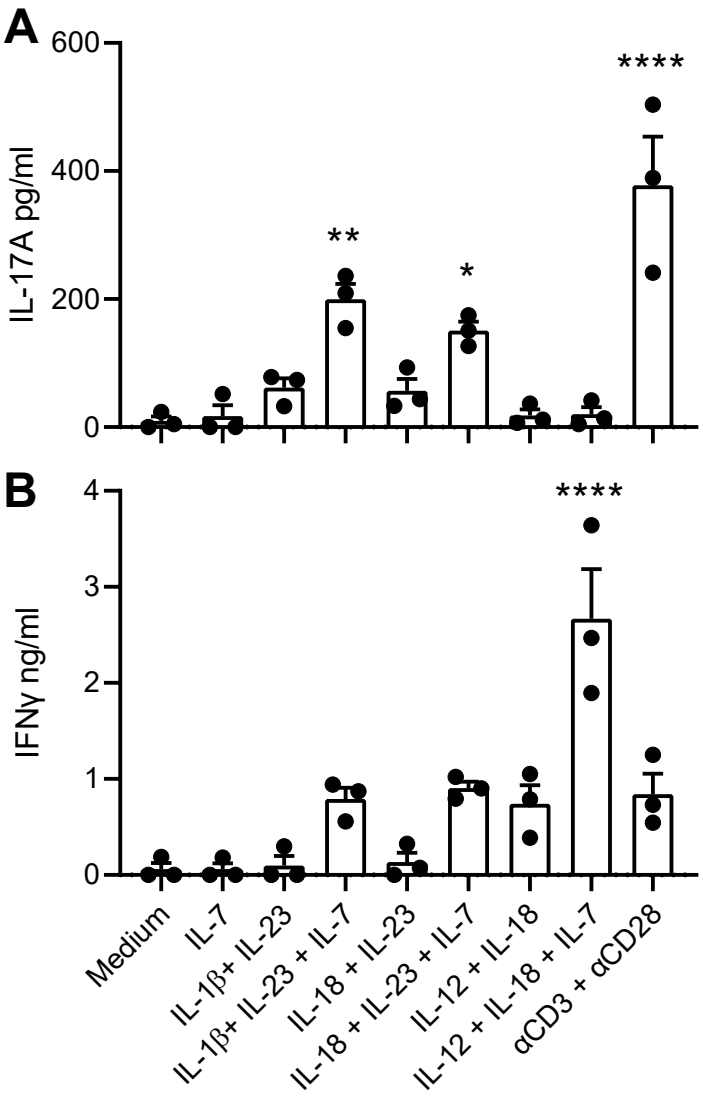

Figure 5.5 Nose-resident CD4 T cells from convalescent mice produce IL-17A and IFNγ in response to Th1- and Th17-polarising cytokines in the presence of IL-7, without TCR activation.

C57BL/6 mice were infected with live *B. pertussis*. Once infection had cleared (> 60 days p.i.) mice were injected i.v. with a fluorochrome-conjugated anti-CD45 antibody 10 min prior to euthanasia. Nose-resident (CD45 i.v.$^-$) CD4$^+$CD3$^+$ T cells were FACS purified from pooled nasal tissue and stimulated in triplicate (1.7x10^4 cells/ml) with combinations of IL-1β, IL-23, IL-18, IL-12 (all at 10 ng/ml) in the presence or absence of IL-7 (10 ng/ml) or with anti-CD3 and anti-CD28 (both at 1 µg/ml) or medium alone. After 72 hours IL-17A (A) and IFNγ (B) concentrations in supernatants were quantified by ELISA. Data represent mean concentration ± SEM for n=3 independent experiments, with each dot representing the average of three technical replicates from one independent experiment. *$p < 0.05$, **$p < 0.05$. ****$p < 0.0001$ versus medium treated control by one-way ANOVA followed by Dunnett's post hoc analysis.

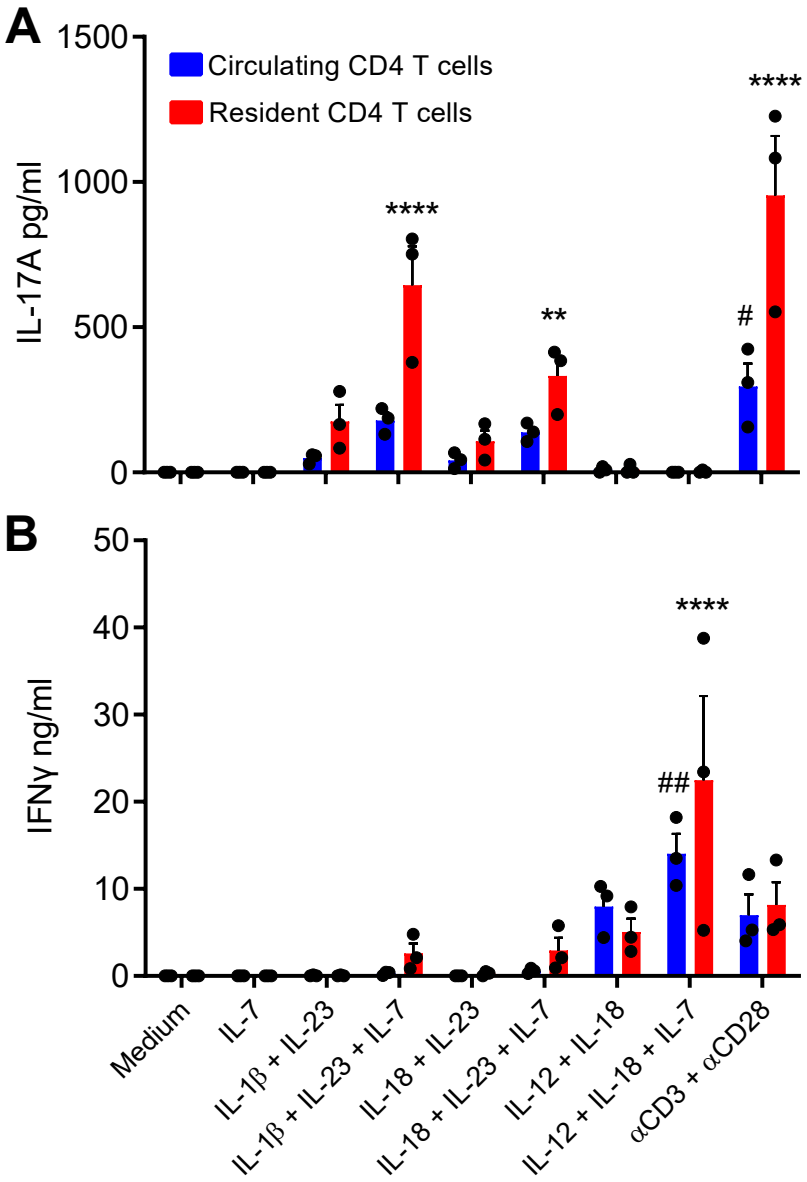

Figure 5.6 Lung-resident, but not circulating, CD4 T cells from convalescent mice produce IL-17A in response to Th17-polarising cytokines in the presence of IL-7, without TCR activation.

C57BL/6 mice were infected with live *B. pertussis*. Once infection had cleared (> 60 days p.i.) mice were injected i.v. with a fluorochrome-conjugated anti-CD45 antibody 10 min prior to euthanasia. Lung-resident (CD45 i.v.$^-$) and circulating (CD45 i.v.$^+$) CD4$^+$CD3$^+$ T cells were FACS purified from pooled lungs and stimulated in triplicate (5.2x10^4 cells/ml) with combinations of IL-1β, IL-23, IL-18, IL-12 (all at 10 ng/ml) in the presence or absence of IL-7 (10 ng/ml) or with anti-CD3 and anti-CD28 (both at 1 µg/ml) or medium alone. After 72 hours IL-17A (A) and IFNγ (B) concentrations in supernatants were quantified by ELISA. Data represent mean concentration ± SEM for n=3 independent experiments, with each dot representing the average of three technical replicates from one independent experiment. #p < 0.05, ##p < 0.01 versus medium control for circulating CD4 cells; **p < 0.01, ****p < 0.0001 versus medium control for resident CD4 cells by two-way ANOVA with Dunnett's multiple comparisons test.

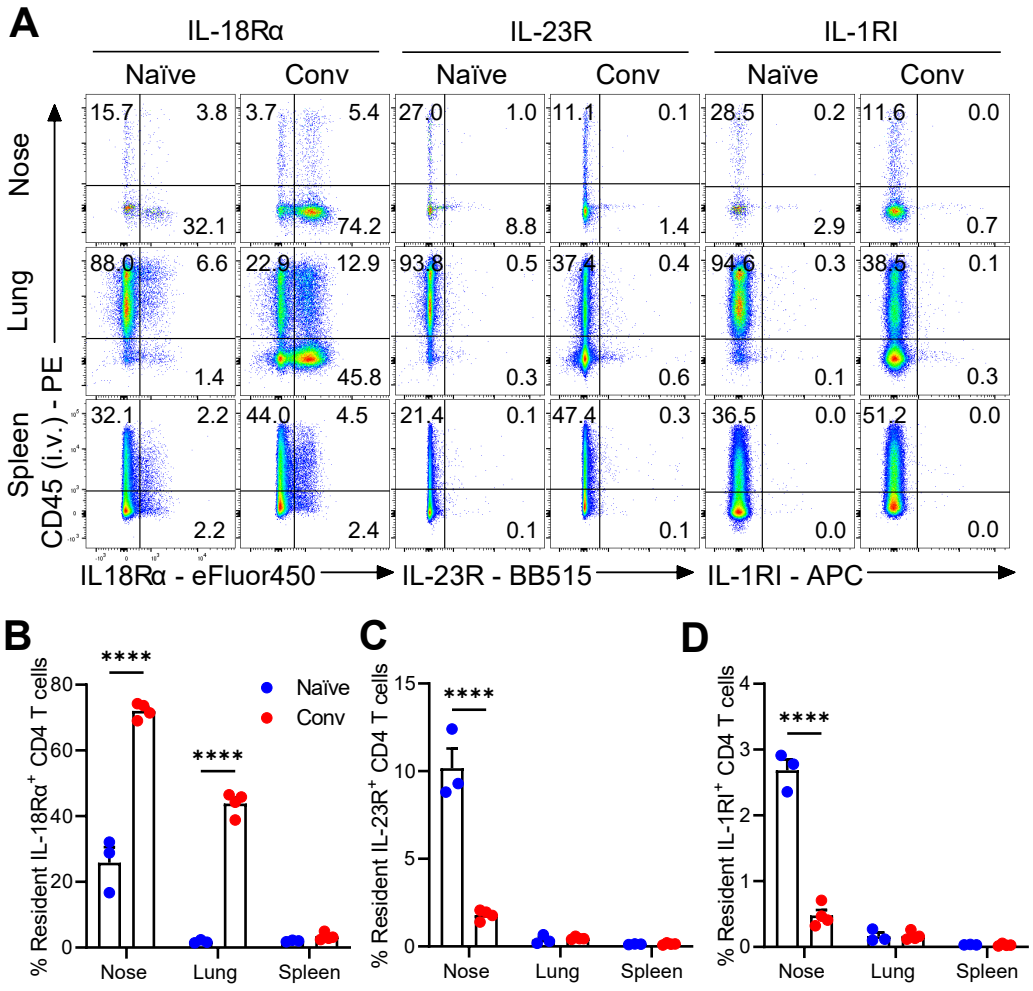

Figure 5.7 Lung- and nose-resident CD4 T cells induced following infection with *B. pertussis* express high levels of IL-18Rα but low levels of IL-23R and IL-1RI.

C57BL/6 mice were infected with live *B. pertussis*. Once infection had cleared (> 60 days p.i.) convalescent (conv) and naïve control mice were injected i.v. with a fluorochrome-conjugated anti-CD45 antibody 10 min prior to euthanasia. Nasal tissue, lungs, and spleens were harvested and isolated mononuclear cells were stained for surface CD4, CD3, IL-18R, IL-23R, and IL-1R, and analysed by flow cytometry. Representative flow cytometry plots (A) and relative frequencies of tissue-resident (CD45 i.v.$^-$) IL-18R$^+$ (B), IL-23R$^+$ (C), and IL-1RI$^+$ (D) CD4 T cells, gated on total CD4$^+$CD3$^+$ cells. Results shown are mean ± SEM (n=3/4 mice per group). ****p < 0.0001 naïve versus convalescent mice by two-way ANOVA with Sidak's multiple comparisons test.

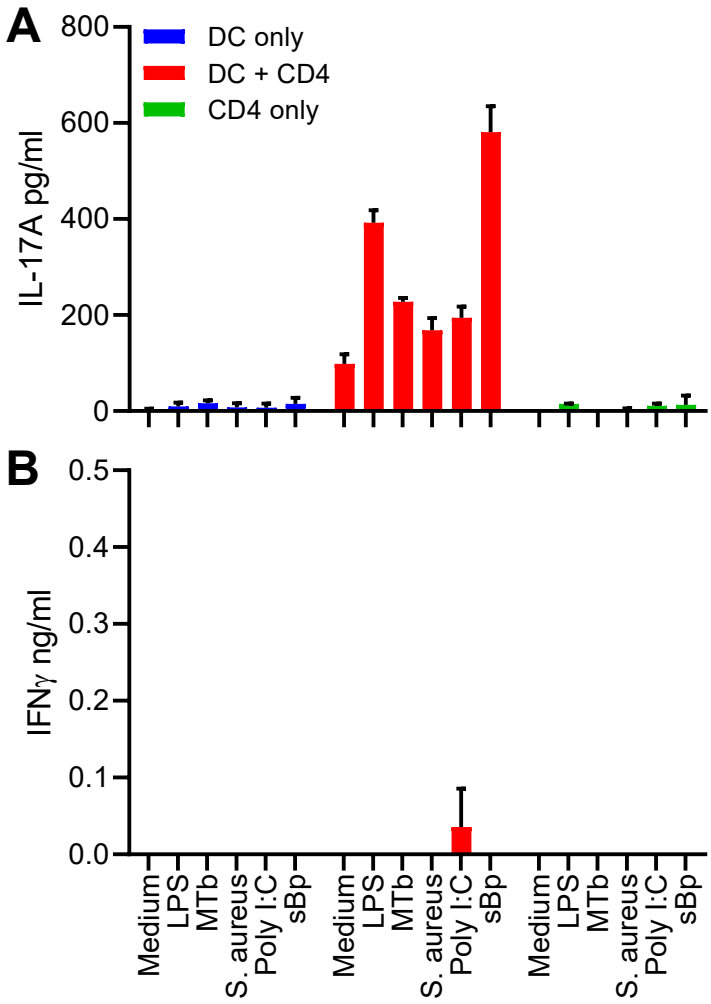

Figure 5.8 PAMPs or pathogens induce IL-17A production from nose-resident CD4 T cells when cultured in the presence of BMDCs.

C57BL/6 mice were infected with live *B. pertussis*. Once infection had cleared (> 60 days p.i.) mice were injected i.v. with a fluorochrome-conjugated anti-CD45 antibody 10 min before euthanasia. Nose-resident (CD45 i.v.$^{-}$) $CD4^{+}CD3^{+}$ T cells were FACS purified from pooled nasal tissue and cultured ($1.6x10^{4}$ cells/ml) in the presence or absence of BMDCs ($0.8x10^{6}$ cells/ml) and stimulated with *E. coli*-derived LPS (100 ng/ml), heat-killed *M. Tuberculosis* (MTb; 10 µg/ml), heat-killed *S. aureus* (10 µg/ml), Poly I:C (50 µg/ml), sBP (5 µg/ml) or medium alone. After 48 hours IL-17A (A) and IFNγ (B) concentrations in supernatants were quantified by ELISA. Data presented are means ± SD for duplicate culture and representative of one independent experiment.

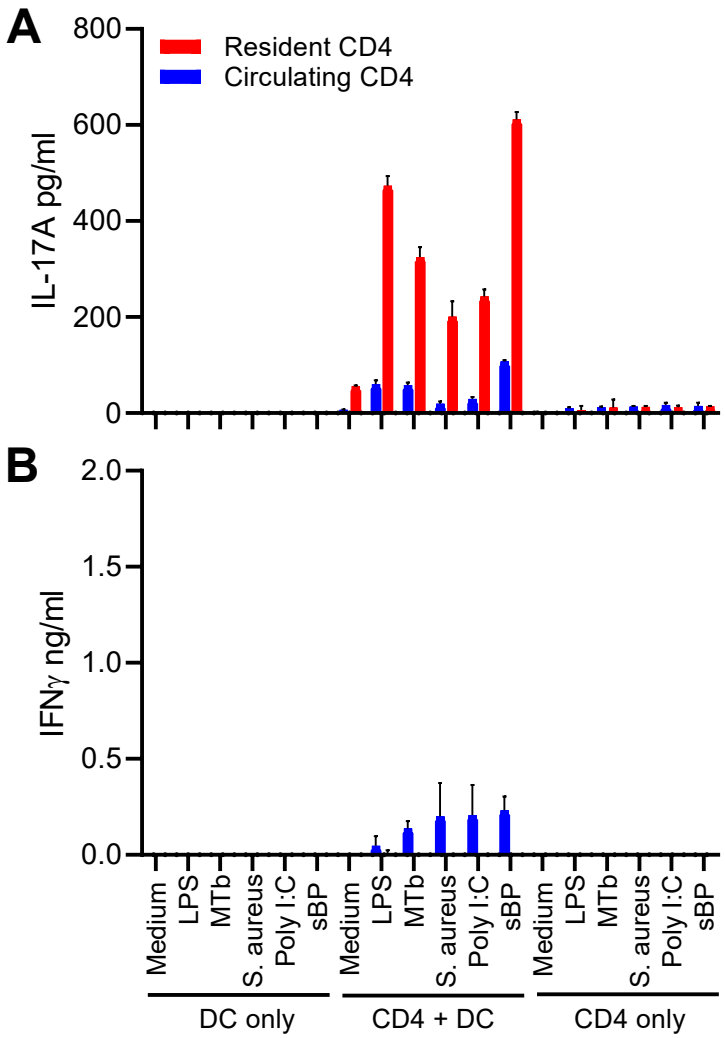

Figure 5.9 Tissue-resident, but not circulating, lung CD4 T cells from convalescent mice produce IL-17A is response to PAMPs or pathogens in the presence of BMDCs.

C57BL/6 mice were infected with live *B. pertussis*. Once infection had cleared (> 60 days p.i.) mice were injected i.v. with a fluorochrome-conjugated anti-CD45 antibody and euthanised 10 min later. Lung-resident (CD45 i.v.$^-$) and circulating (CD45 i.v.$^+$) CD4$^+$CD3$^+$ T cells were FACS purified from pooled lungs and cultured (3.7x10^4 cells/ml) in the presence or absence of BMDCs (0.8x10^6 cells/ml) and stimulated with *E. coli*-derived LPS (100 ng/ml), heat-killed *M. tuberculosis* (MTb; 10 µg/ml), heat-killed *S. aureus* (10 µg/ml), Poly I:C (50 µg/ml), sBP (5 µg/ml) or medium alone. After 48 hours IL-17A (A) and IFNγ (B) concentrations in supernatants were quantified by ELISA. Data presented are means ± SD for triplicate culture and representative if one independent experiment.

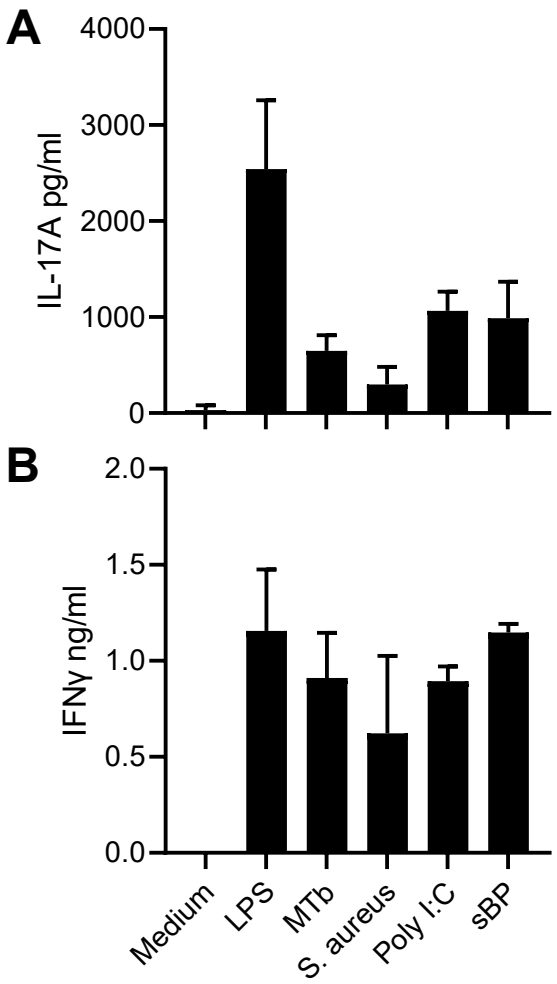

Figure 5.10 Conditioned medium from BMDCs stimulated with PAMPs or pathogens induce IL-17A and IFNγ production from nose-resident CD4 T cells from convalescent mice.

BMDCs from C57BL/6 mice were stimulated ($0.8x10^6$ cells/ml) with *E. coli*-derived LPS (100 ng/ml), heat-killed MTb (10 µg/ml), heat-killed *S. aureus* (10 µg/ml), Poly I:C (50 µg/ml), sBP (5 µg/ml) or medium alone. After 24 hours supernatants were collected and transferred on to nose-resident (CD45 i.v.$^-$) $CD4^+CD3^+$ T cells ($0.16x10^5$ cells/ml) FACS purified from pooled nasal tissue of convalescent mice C57BL/6 mice. After 72 hours IL-17A (A) and IFNγ (B) concentrations in supernatants were quantified by ELISA. Data presented are means ± SD for triplicate culture and representative of one independent experiment.

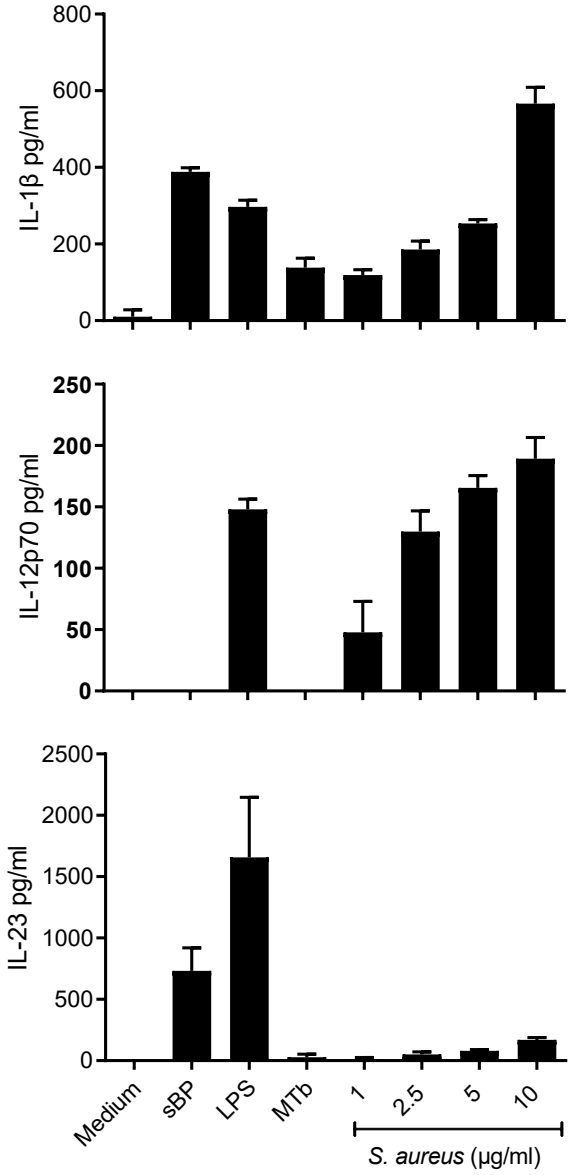

Figure 5.11 Heat-killed *S. aureus* or *M. tuberculosis* fail to induce IL-23 from BMDCs.

BMDCs from C57BL/6 mice were stimulated ($0.8x10^6$ cells/ml) with sBP (5 µg/ml), *E. coli*-derived LPS (100 ng/ml), heat-killed *M. tuberculosis* (MTb; 10 µg/ml), heat-killed *S. aureus* (1-10 µg/ml) or medium alone. After 24 hours supernatants were harvested and IL-1β, IL-12p70, and IL-23 concentrations were quantified by ELISA. Data are means ± SD for triplicate culture and representative of one independent experiment.

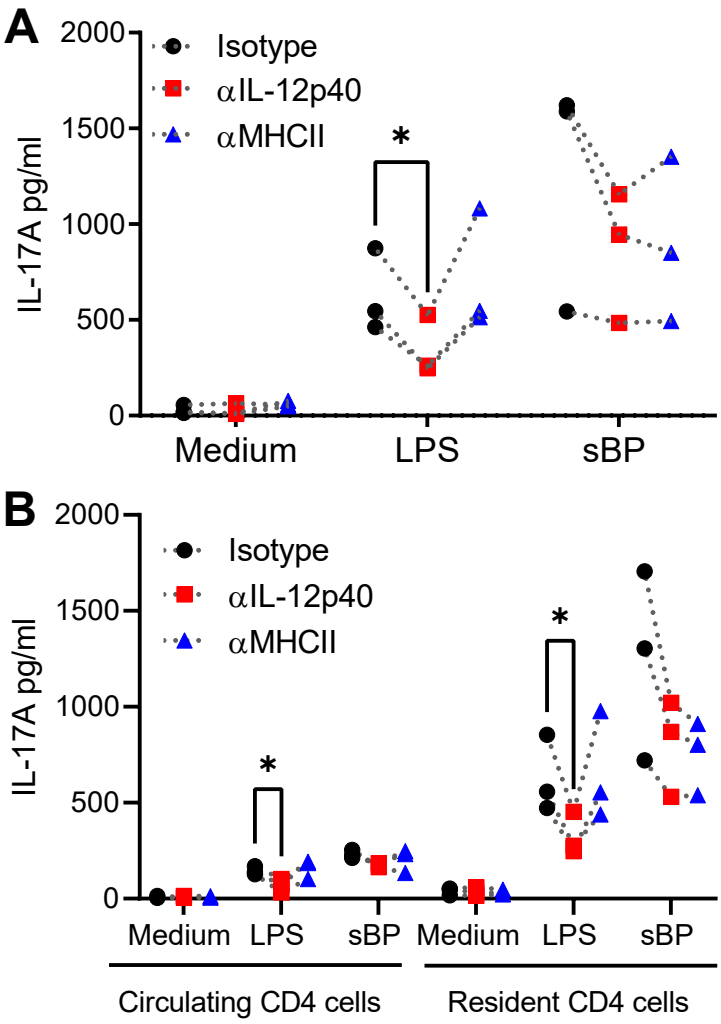

Figure 5.12 Anti-IL-12p40, but not anti-MHCII, significantly reduces LPS-induced IL-17A production from nose- and lung-resident CD4 T cells co-cultured with BMDCs.

C57BL/6 mice were infected with live *B. pertussis*. Once infection had cleared (> 60 days p.i.) mice were injected i.v. with a fluorochrome-conjugated anti-CD45 antibody 10 min before euthanasia. Nose-resident (CD45 i.v.$^-$) $CD4^+CD3^+$ T cells were FACS purified from pooled nasal tissue of convalescent mice. Lung-resident (CD45 i.v.$^-$) or circulating (CD45 i.v.$^+$) $CD4^+CD3^+$ T cells were FACS purified from pooled lungs of convalescent mice. Isolated nose ($0.2x10^5$ cells/ml) or lung ($0.3x10^6$ cells/ml) CD4 T cells were co-cultured with BMDCs ($0.8x10^6$ cells/ml) and stimulated with *E. coli*-derived LPS (100 ng/ml), sBP (5 µg/ml), or medium alone in the presence of either anti-IL-12p40 antibody (10 µg/ml), anti-MHCII antibody (2 µg/ml), or isotype control (10 µg/ml). After 48 hours, IL-17A production by nose (A) or lung (B) CD4 T cells quantified by ELISA on cell supernatants. Data presented are mean ± SEM for n=3 independent experiments, with each dot representing the average of three technical replicates from one independent experiment. *$p < 0.05$ versus isotype control by repeated measures two-way ANOVA followed by Dunnett's post-hoc analysis.

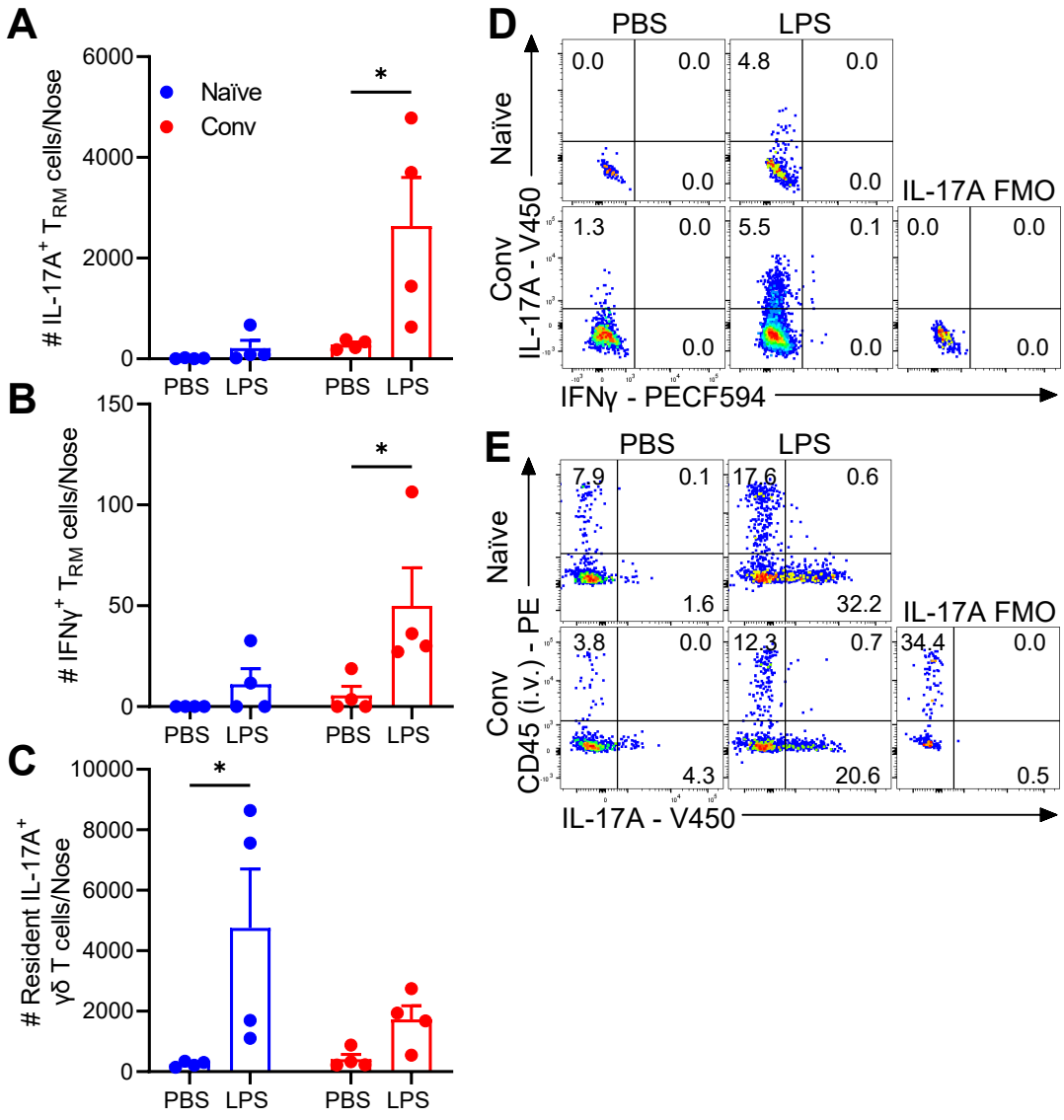

Figure 5.13 Intranasal delivered *E. coli* LPS induces IL-17A production from nasal CD4 T_{RM} cells and γδ T cells in convalescent mice *in vivo*.

E. coli-derived LPS (1 µg/mouse) or PBS was administered i.n. to convalescent (conv) mice (> 60 days post-*B. pertussis* infection) or to naïve control mice. After 4 hours a fluorochrome-conjugated anti-CD45 antibody was administered i.v. and mice were euthanised 10 min later. Nasal tissue was harvested and incubated with brefeldin A (5 µg/ml) for 1 hour during tissue digestion stage. Mononuclear cells were isolated and stained for surface CD4, CD3, γδ TCR, CD44, CD69, CD103, and intracellular IL-17A and IFNγ, and analysed by flow cytometry. Absolute number of IL-17A$^+$ (A) and IFNγ$^+$ (B) CD4 T_{RM} cells (CD4$^+$CD3$^+$CD45i.v.$^-$CD44$^+$CD69$^+$CD103$^\pm$), and IL-17A$^+$ tissue-resident (CD45 i.v.$^-$) γδ T cells (γδ$^+$CD3$^+$) (C) in the nasal cavity of naïve and convalescent mice. Representative flow cytometry plots of cytokine producing CD4 T_{RM} cells (D) and γδ T cells (E) in the nasal cavity of naïve and convalescent mice. Results shown are mean ± SEM (n=4 mice per group). *p < 0.05 PBS versus LPS treatment by two-way ANOVA with Sidak's multiple comparisons test.

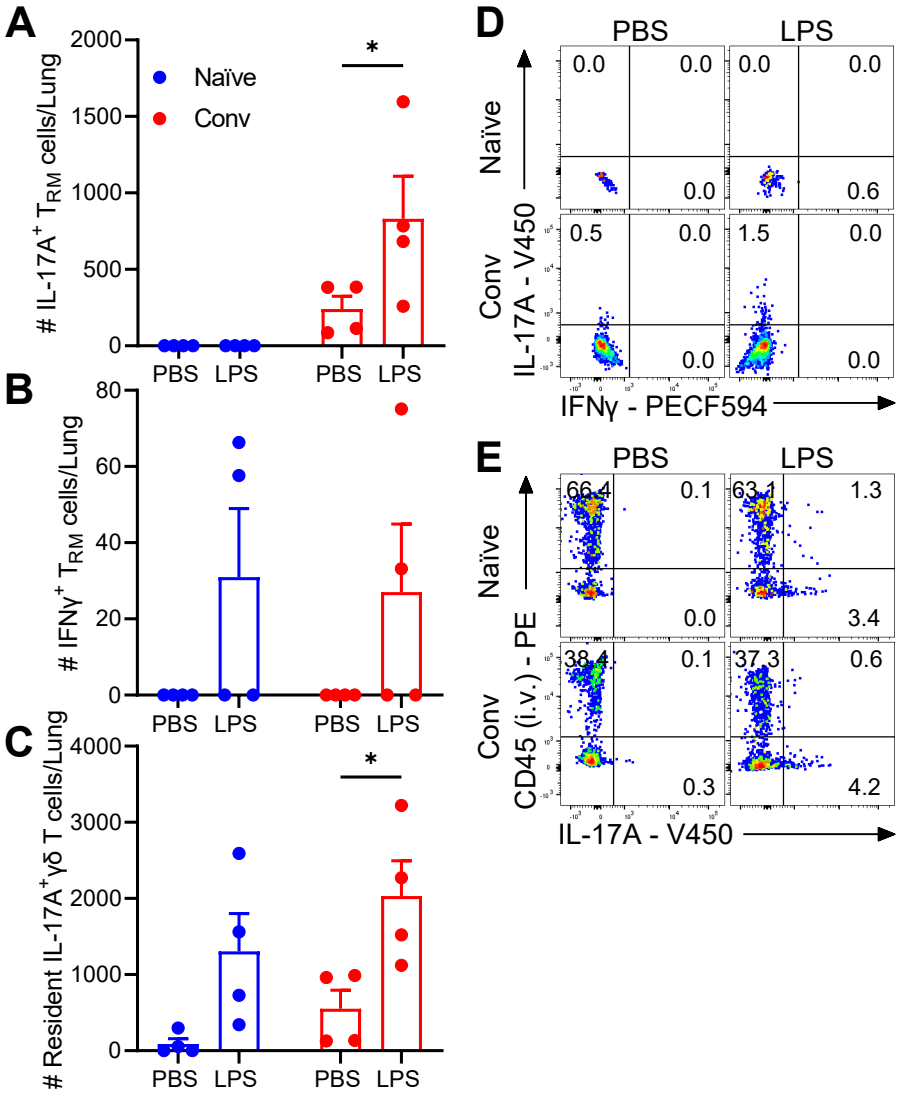

Figure 5.14 Intranasal *E. coli* LPS induces IL-17A production from lung CD4 T_{RM} cells and γδ T cells in convalescent mice *in vivo*.

E. coli-derived LPS (1 µg/mouse) or PBS was administered i.n. to convalescent (conv) C57BL/6 mice (> 60 days post-*B. pertussis* infection) or to naïve control mice. After 4 hours a fluorochrome-conjugated anti-CD45 antibody was administered i.v. and mice were euthanised 10 min later. Lungs were harvested and incubated with brefeldin A (5 µg/ml) for 1 hour during tissue digestion stage. Mononuclear cells were isolated and stained for surface CD4, CD3, γδ TCR, CD44, CD69, CD103, and intracellular IL-17A and IFNγ, and analysed by flow cytometry. Absolute numbers of IL-17A$^+$ (A) and IFNγ$^+$ (B) CD4 T_{RM} cells (CD4$^+$CD3$^+$CD45i.v.$^-$CD44$^+$CD69$^+$CD103$^\pm$), and IL-17A$^+$ tissue-resident (CD45 i.v.$^-$) γδ T cells (γδ$^+$CD3$^+$) (C) in the lungs of naïve and convalescent mice. Representative flow cytometry plots of cytokine producing CD4 T_{RM} cells (D) and γδ T cells (E). Results shown are mean ± SEM (n=4 mice per group). *p < 0.05 PBS versus LPS treatment by two-way ANOVA followed by Sidak's post-test.

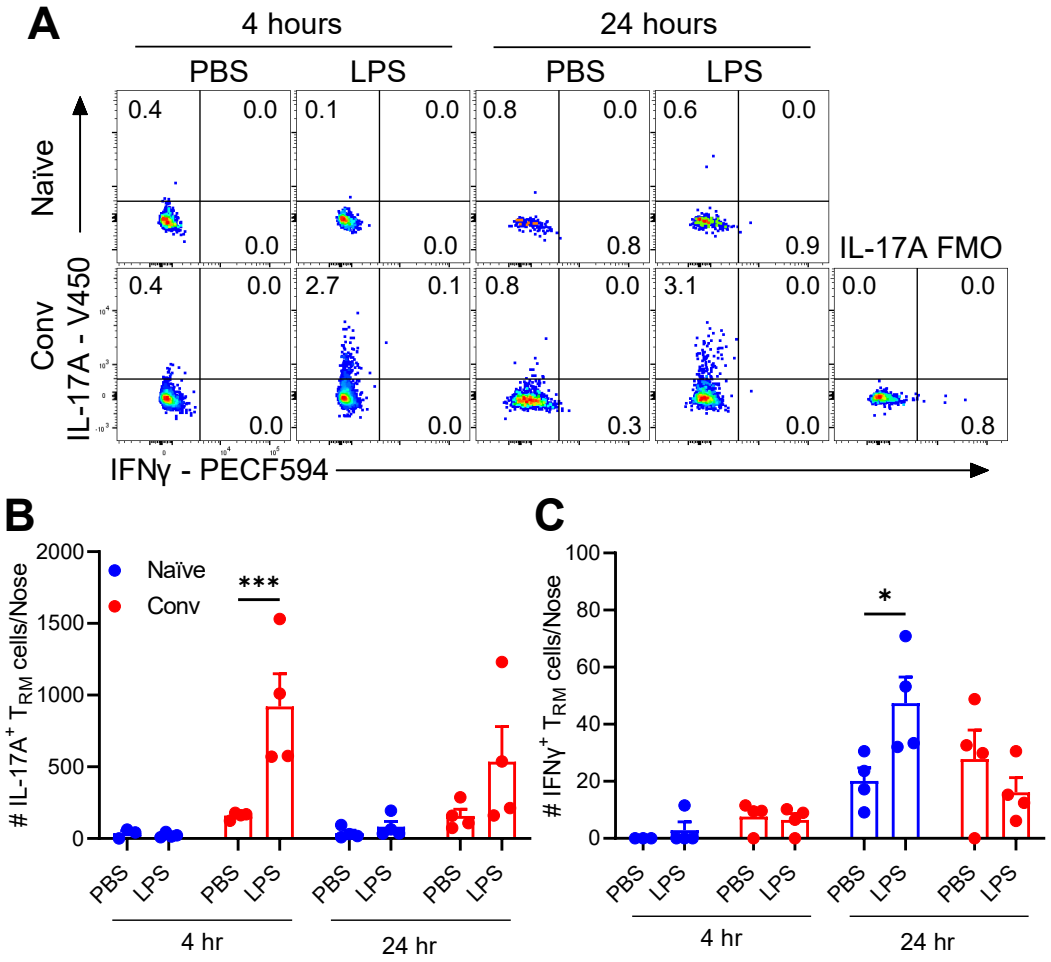

Figure 5.15 Intranasal delivered *E. coli* LPS induces IL-17A production from nasal CD4 T_{RM} cells at 4 and 24 hours post challenge.

E. coli-derived LPS (1 µg/mouse) or PBS was administered i.n. to convalescent (conv) C57BL/6 mice (> 60 days post-*B. pertussis* infection) or to naïve control mice. A fluorochrome-conjugated anti-CD45 antibody was administered i.v. to mice 4 hours or 24 hours post LPS challenge and mice were euthanised 10 min later. Nasal tissue was harvested and incubated with brefeldin A (5 µg/ml) for 1 hour during tissue digestion stage. Mononuclear cells were isolated and stained for surface CD4, CD3, γδ TCR, CD44, CD69, CD103, and intracellular IL-17A and IFNγ, and analysed by flow cytometry. Representative flow cytometry plots (A) and absolute number of IL-17A$^+$ (B) and IFNγ$^+$ (C) CD4 T_{RM} cells (CD4$^+$CD3$^+$CD45i.v.$^-$CD44$^+$CD69$^+$CD103$^\pm$) in the nasal cavity 4 hours and 24 hours after LPS administration. Results shown are mean ± SEM (n=4 mice per group). *$p < 0.05$, ***$p < 0.001$ PBS versus LPS treatment by two-way ANOVA followed by Sidak's post-test.

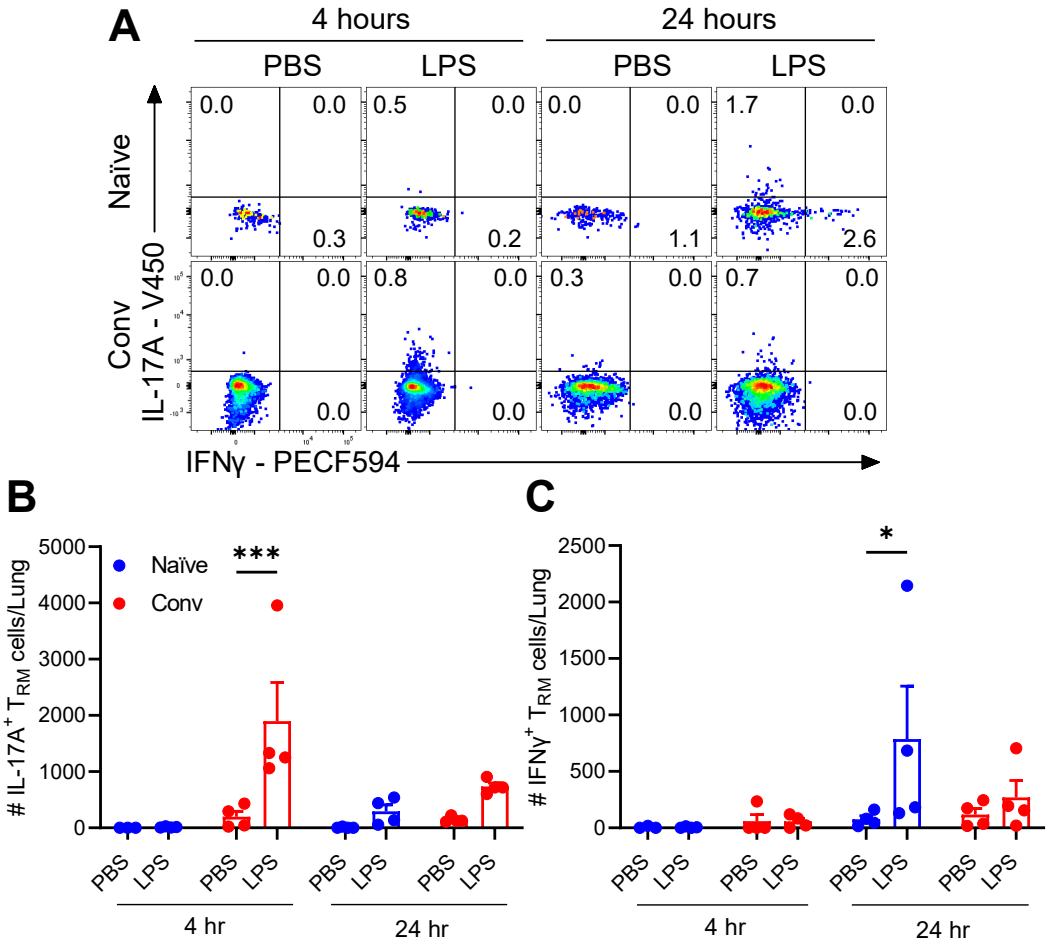

Figure 5.16 Intranasal delivered *E. coli* LPS induces IL-17A production from nasal CD4 T_{RM} cells at 4 hours but not 24 hours post challenge.

E. coli-derived LPS (1 µg/mouse) or PBS was administered i.n. to convalescent (conv) C57BL/6 mice (>60 days post-*B. pertussis* infection) or to naïve control mice. After 4 hours a fluorochrome-conjugated anti-CD45 antibody was administered i.v. and mice were euthanised 10 min later. Lungs were harvested and incubated with brefeldin A (5 µg/ml) for 1 hour during tissue digestion stage. Mononuclear cells were isolated and stained for surface CD4, CD3, γδ TCR, CD44, CD69, CD103, and intracellular IL-17A and IFNγ, and analysed by flow cytometry. Representative flow cytometry plots (A) and absolute numbers of IL-17A$^+$ (B) and IFNγ$^+$ (C) CD4 T_{RM} cells (CD4$^+$CD3$^+$CD45i.v.$^-$ CD44$^+$CD69$^+$CD103$^\pm$) from naïve and convalescent mice. Data are mean ± SEM (n=4 mice per group). *$p < 0.05$, ***$p < 0.001$ PBS versus LPS treatment by two-way ANOVA followed by Sidak's post-test.

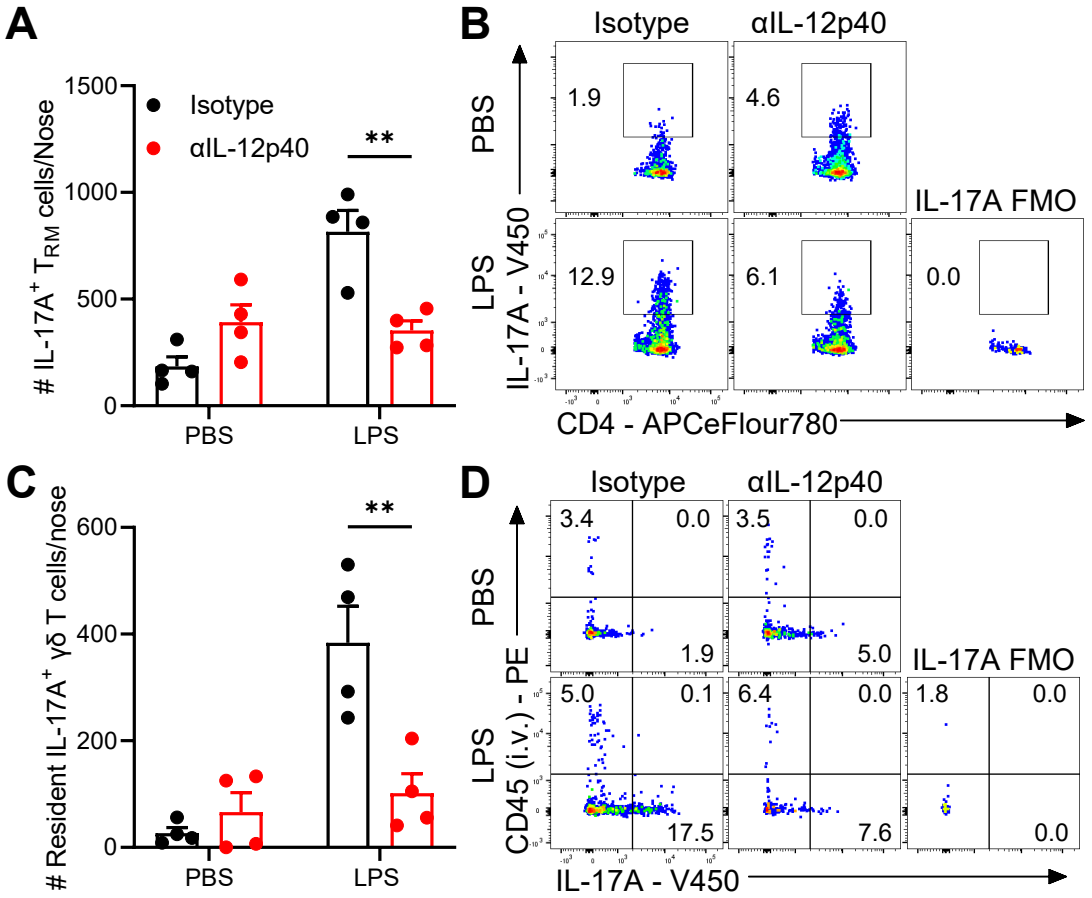

Figure 5.17 LPS-induced IL-17A production from nasal CD4 T_{RM} cells and γδ T cells is significantly reduced by treatment with a neutralising anti-IL-12p40 antibody *in vivo*.

Convalescent C57BL/6 mice (> 60 days post *B. pertussis* infection) were injected i.p. with a neutralising anti-IL-12p40 antibody (200 µg/mouse) or isotype control. *E. coli*-derived LPS (5 µg/mouse) or PBS was administered i.n. to convalescent mice 24 hours later together with an additional i.n. dose of anti-IL-12p40 antibody (50 µg/mouse) or isotype control. After 4 hours a fluorochrome-conjugated anti-CD45 antibody was administered i.v. and mice were euthanised 10 min later. Nasal tissue was harvested and incubated with brefeldin A (5 µg/ml) for 1 hour during tissue digestion stage. Mononuclear cells were isolated and stained for surface expression of CD4, CD3, γδ TCR, CD44, CD62L, CD69, CD103, and intracellular IL-17A, and analysed by flow cytometry. Absolute number (A) and representative flow cytometry plots (B) of IL-17A$^+$ CD4 T_{RM} cells (CD4$^+$CD3$^+$CD45i.v.$^-$CD44$^+$CD69$^+$CD103$^\pm$). Absolute number (C) and representative flow cytometry plots (D) of nose-resident IL-17A$^+$ γδ T cells. Results shown are mean ± SEM (n=4 mice per group). $^{**}p < 0.01$ isotype control versus anti-IL-12p40 treatment by two-way ANOVA with Sidak's multiple comparisons test.

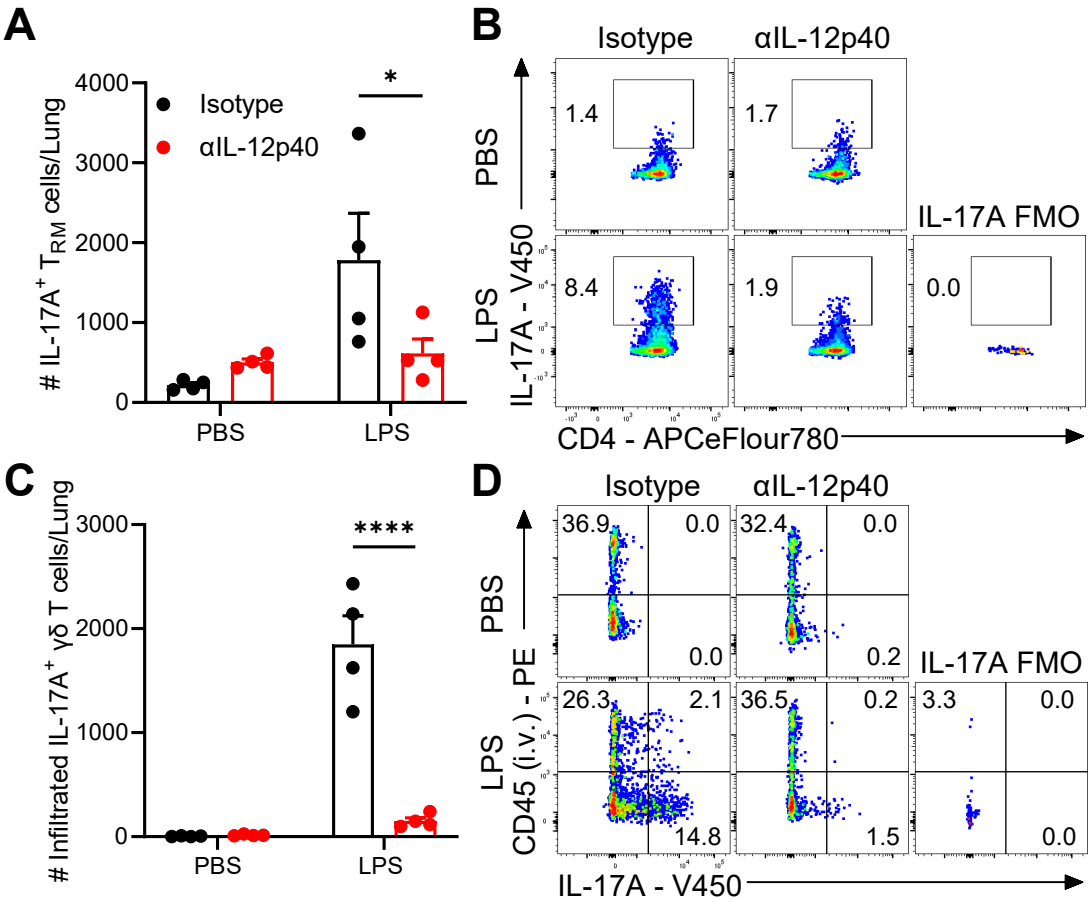

Figure 5.18 LPS-induced IL-17A production from lung CD4 T_{RM} cells and γδ T cells is significantly reduced by treatment with a neutralising anti-IL-12p40 *in vivo*.

Convalescent C57BL/6 mice (> 60 days post *B. pertussis* infection) were injected i.p. with a neutralising anti-IL-12p40 antibody (200 µg/mouse) or isotype control. *E. coli*-derived LPS (5 µg/mouse) or PBS was administered i.n. to convalescent mice 24 hours later together with an additional i.n. dose of anti-IL-12p40 antibody (50 µg/mouse) or isotype control. After 4 hours a fluorochrome-conjugated anti-CD45 antibody was administered i.v. and mice were euthanised 10 min later. Lungs were harvested and incubated with brefeldin A (5 µg/ml) for 1 hour during tissue digestion stage. Mononuclear cells were isolated and stained for surface expression of CD4, CD3, γδ TCR, CD44, CD62L, CD69, CD103, and intracellular IL-17A, and analysed by flow cytometry. Absolute number (A) and representative flow cytometry plots (B) of IL-17A$^+$ CD4 T_{RM} cells (CD4$^+$CD3$^+$CD45i.v.$^-$CD44$^+$CD69$^+$CD103$^\pm$). Absolute number (C) and representative flow cytometry plots (D) of lung-resident IL-17A$^+$ γδ T cells. Results shown are mean ± SEM (n=4 mice per group). *p < 0.05, ****p < 0.0001 isotype control versus anti-IL-12p40 treatment by two-way ANOVA followed by Sidak's multiple comparisons post-test.

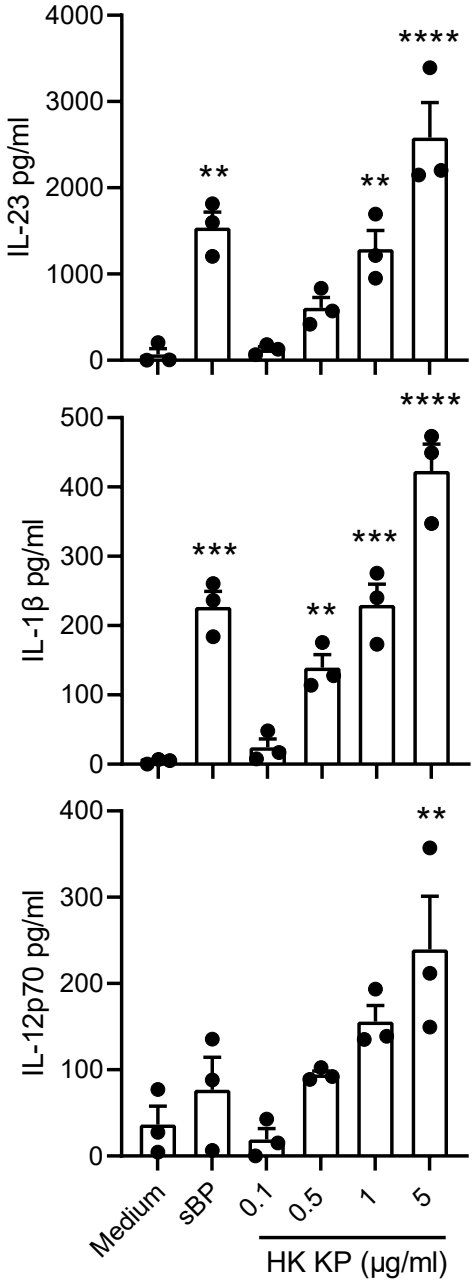

Figure 5.19 Heat-killed *K. pneumoniae* induces IL-23, IL-1β, and IL-12p70 production from BMDCs in a dose-dependent manner.

BMDCs from C57BL/6 mice were stimulated with sBP (5 μg/ml), heat-killed *K. pneumoniae* (HK KP; 0.1 – 5 μg/ml) or medium alone. After 24 hours supernatants were harvested and IL-23, IL-1β, and IL-12p70 concentrations were quantified by ELISA. Data represent mean concentration ± SEM for n=3 independent experiments, with each dot representing the average of three technical replicates from one independent experimen. *$p < 0.05$, **$p < 0.01$, ***$p < 0.001$, ****$p < 0.0001$ versus medium control by one-way ANOVA followed by Dunnett's post-test.

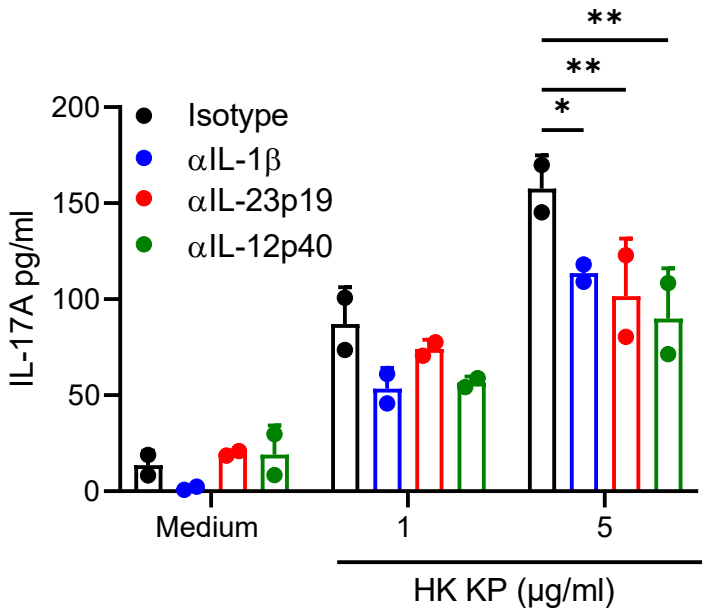

Figure 5.20 Heat-killed *K. pneumoniae* induces dose-dependent IL-17A production from nose-resident CD4 T cells co-cultured with BMDCs, which is significantly reduced by anti-IL-1β, anti-IL-23p19, and anti-IL-12p40.

C57BL/6 mice were infected with live *B. pertussis*. Once infection had cleared (> 60 days p.i.) mice were injected i.v. with a fluorochrome-conjugated anti-CD45 antibody and euthanised 10 min later. Nose-resident (CD45 i.v.$^-$) CD4$^+$CD3$^+$ T cells were FACS purified from pooled nasal tissue of convalescent mice. Nose-resident CD4 T cells ($0.7x10^4$ cells/ml) were co-cultured with BMDCs ($0.8x10^6$ cells/ml) and stimulated with heat-killed *K. pneumoniae* (HK KP; 1 - 5 µg/ml) or medium alone in the presence of either anti-IL-1β, anti-IL23p19, anti-IL-12p40 or isotype control (all at 10 µg/ml). After 48 hours IL-17A concentration in supernatants was quantified by ELISA. Data represent mean data ± SEM from two independent experiments, with each dot representing the average of three technical replicates from one independent experiment. *$p < 0.05$, **$p < 0.01$ versus isotype control by two-way ANOVA followed by Dunnett's multiple comparisons test.

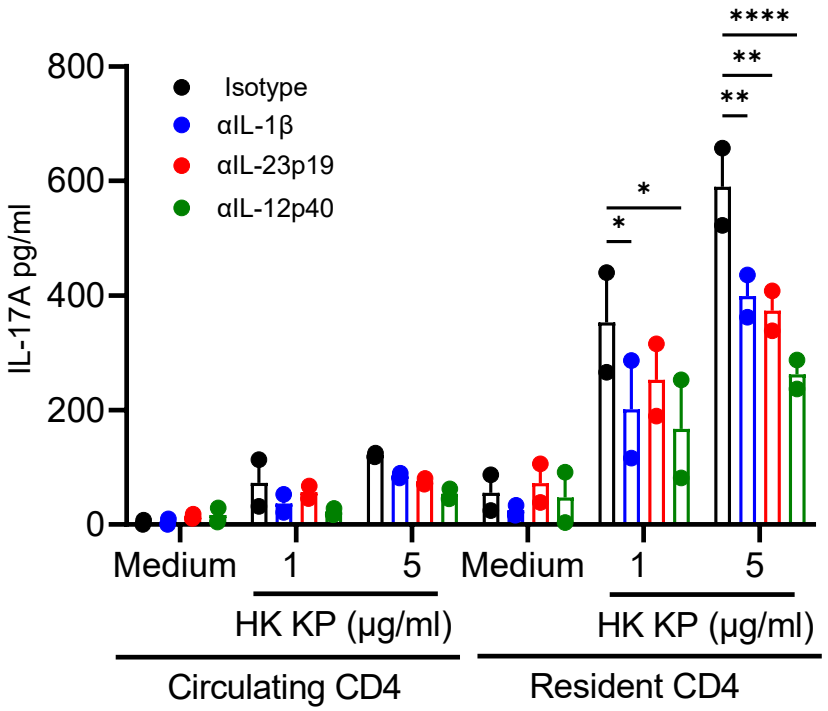

Figure 5.21 Heat-killed *K. pneumoniae* induces dose-dependent IL-17A production from lung-resident CD4 T cells co-cultured with BMDCs, which is significantly reduced by anti-IL-1β, anti-IL-23p19, and anti-IL-12p40.

C57BL/6 mice were infected with live *B. pertussis*. Once infection had cleared (> 60 days p.i.) mice were injected i.v. with a fluorochrome-conjugated anti-CD45 antibody 10 min prior to euthanasia. Lung-resident (CD45 i.v.$^-$) and circulating (CD45 i.v.$^+$) CD4$^+$CD3$^+$ T cells were FACS purified from pooled lungs of convalescent mice. Cell yield was normalised between resident and circulating CD4 cells (3.2x10^4 cells/ml) and co-cultured with BMDCs (0.8x10^6 cells/ml). Cells were stimulated with heat-killed *K. pneumoniae* (HK KP; 1 - 5 μg/ml) or medium alone in the presence of either anti-IL-1β, anti-IL23p19, anti-IL-12p40 or isotype control (all at 10 μg/ml). After 48 hours IL-17A concentrations in supernatants was quantified by ELISA. Data are mean ± SEM of pooled data from two independent experiments, with each dot representing the average of three technical replicates from one independent experiment. *$p < 0.05$, **$p < 0.01$, ****$p < 0.0001$ versus isotype control by two-way ANOVA followed by Dunnett's multiple comparisons test.

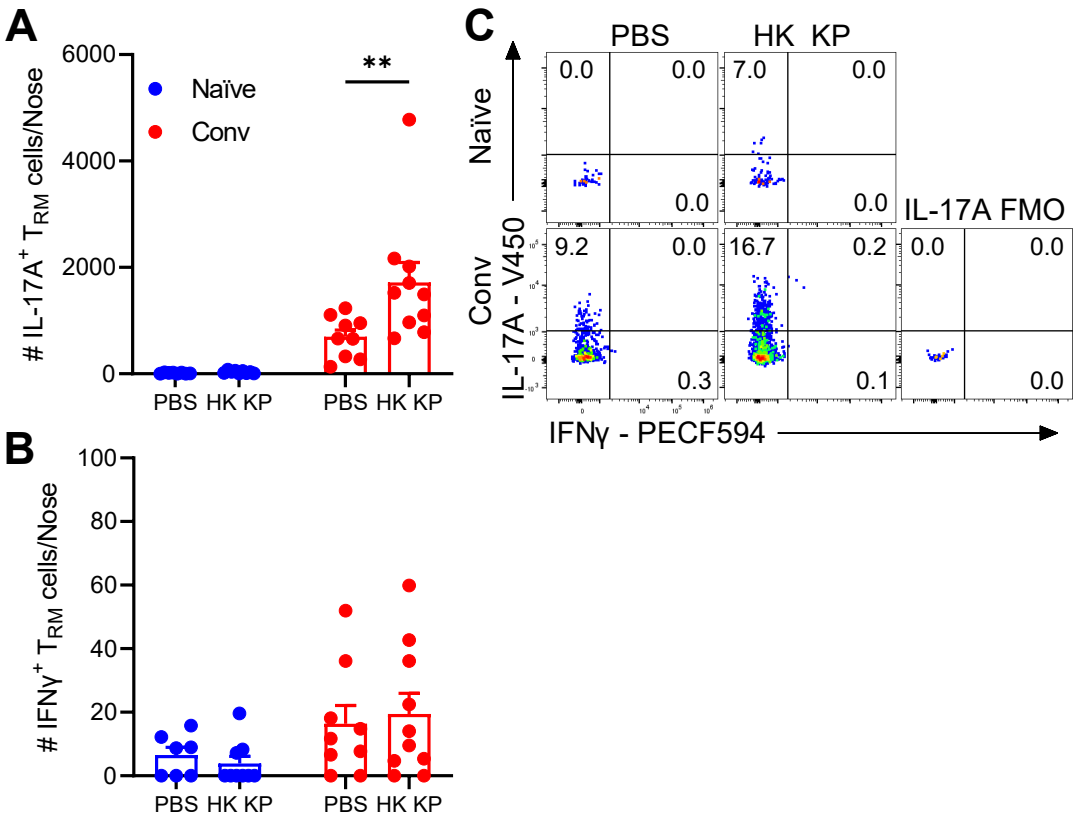

Figure 5.22 Heat-killed *K. pneumoniae* induces IL-17A production from CD4 T_{RM} cells in the nasal cavity of convalescent mice previously infected with *B. pertussis*.

C57BL/6 mice were infected with live *B. pertussis*. Once infection had cleared (> 60 days p.i.) heat-killed *K. pneumoniae* (HK KP; 10 µg/mouse) or PBS was administered i.n. to convalescent (conv) mice or naïve control mice. After 4 hours a fluorochrome-conjugated anti-CD45 antibody was administered i.v. and mice were euthanised 10 min later. Nasal tissue was harvested and incubated with brefeldin A (5 µg/ml) for 1 hour during tissue digestion stage. Mononuclear cells were isolated and stained for the surface markers CD4, CD3, CD44, CD62L, CD69, CD103, and intracellular IL-17A and IFNγ, and analysed by flow cytometry. Absolute number of IL-17A$^+$ (A) and IFNγ$^+$ (B) CD4 T_{RM} cells (CD4$^+$CD3$^+$CD45i.v.$^-$CD44$^+$CD62L$^-$CD69$^+$CD103$^\pm$), with representative flow cytometry plots (C) in the nasal tissue of naïve and convalescent mice following i.n. PBS or HK KP. Results are combined from two independent experiments. Data shown are mean ± SEM (n=8-10 mice per group). $^{**}p < 0.01$ PBS versus HK KP treatment by two-way ANOVA followed by Sidak's multiple comparisons post-test.

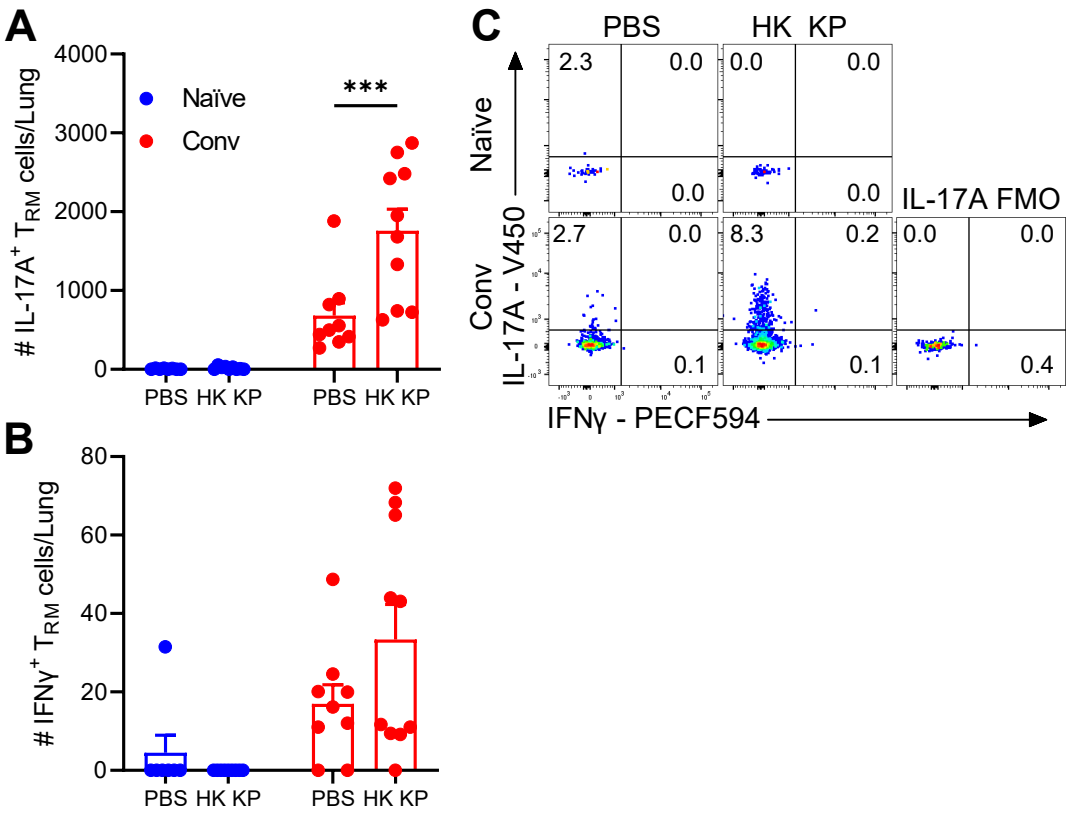

Figure 5.23 Heat-killed *K. pneumoniae* promotes IL-17A production from CD4 T_{RM} cells in the lungs of convalescent mice previously infected with *B. pertussis*.

C57BL/6 mice were infected with live *B. pertussis*. Once infection had cleared (> 60 days p.i.) heat-killed *K. pneumoniae* (HK KP; 10 µg/mouse) or PBS was administered i.n. to convalescent (conv) mice or naïve control mice. After 4 hours a fluorochrome-conjugated anti-CD45 antibody was administered i.v. and mice were euthanised 10 min later. Lungs were harvested and incubated with brefeldin A (5 µg/ml) for 1 hour during tissue digestion stage. Mononuclear cells were isolated and stained for the surface markers CD4, CD3, CD44, CD62L, CD69, CD103, and intracellular IL-17A and IFNγ, and analysed by flow cytometry. Absolute numbers of IL-17A$^+$ (A) and IFNγ$^+$ (B) CD4 T_{RM} cells (CD4$^+$CD3$^+$CD45i.v.$^-$CD44$^+$CD62L$^-$CD69$^+$CD103$^\pm$), with representative flow cytometry plots (C) in the lungs of naïve and convalescent mice following i.n. PBS or HK KP. Results are combined from two independent experiments. Data shown are mean ± SEM (n=8-10 mice per group). ***$p < 0.001$ PBS versus HK KP treatment by two-way ANOVA followed by Sidak's multiple comparisons post-test.

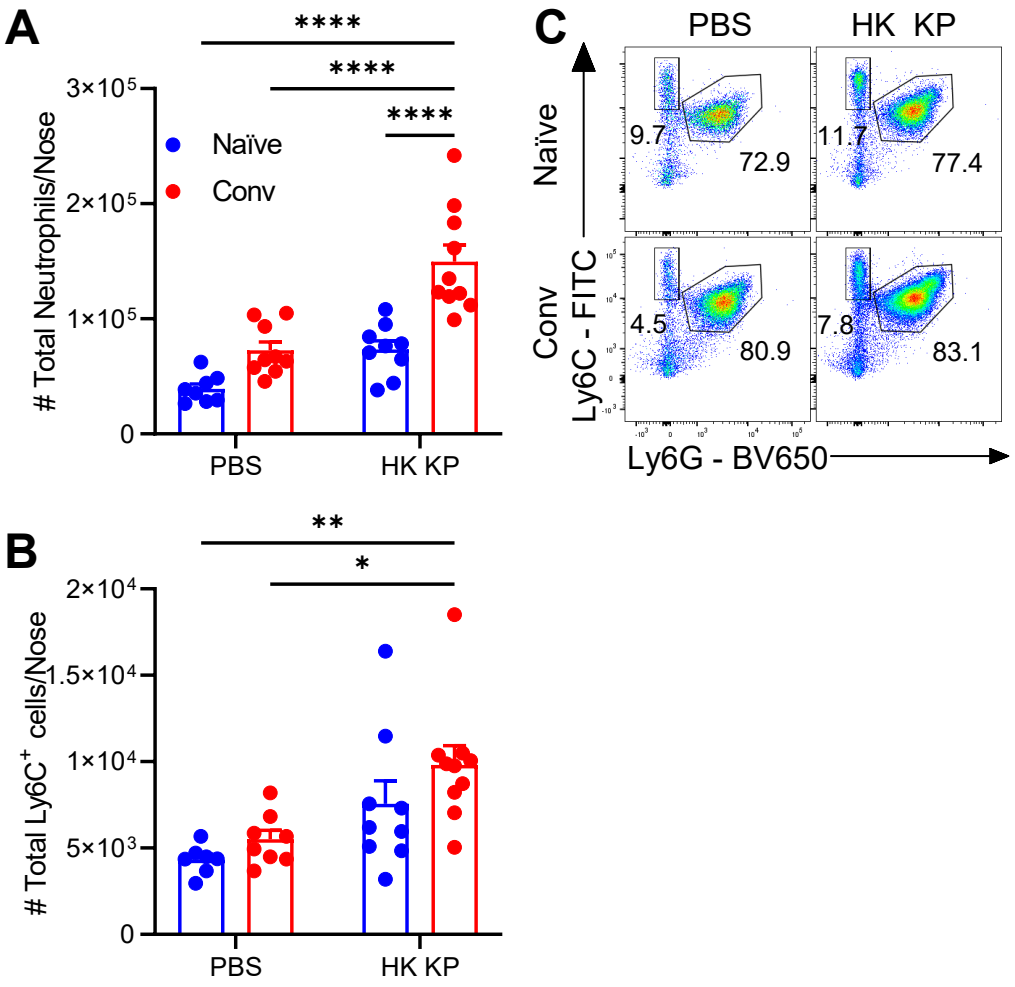

Figure 5.24 Convalescent mice previously infected with *B. pertussis* have enhanced neutrophil numbers in the nasal cavity following heat-killed *K. pneumoniae* challenge.

C57BL/6 mice were infected with live *B. pertussis*. Once infection had cleared (> 60 days p.i.) heat-killed *K. pneumoniae* (HK KP; 10 µg/mouse) or PBS was administered i.n. to convalescent (conv) mice or naïve control mice. Nasal tissue was harvested 4 hours later and isolated mononuclear cells were stained with antibodies specific for Ly6C, Ly6G, and CD11b and analysed by flow cytometry. Absolute numbers of total neutrophils ($Ly6G^+CD11b^+$) (A) and $Ly6C^+CD11b^+$ monocytes (B) with representative flow cytometry plots (C) in the nasal tissue. Results are combined from two independent experiments. Data shown are mean ± SEM (n=8-10 mice per group). *$p < 0.05$, **$p < 0.01$, ****$p < 0.0001$ by two-way ANOVA followed by Tukey's multiple comparisons post-test.

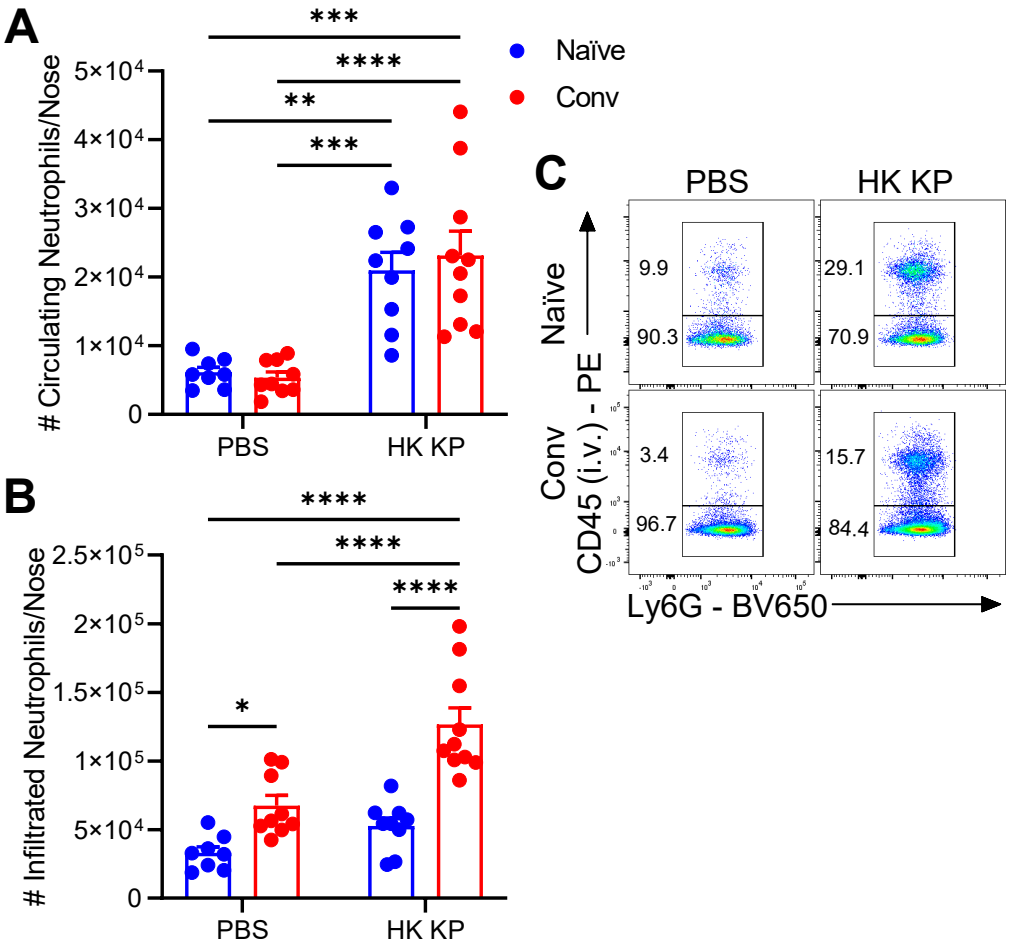

Figure 5.25 Enhanced neutrophil infiltration into the nasal cavity of convalescent mice following heat-killed *K. pneumoniae* challenge.

C57BL/6 mice were infected with live *B. pertussis*. Once infection had cleared (> 60 days p.i.) *K. pneumoniae* (HK KP; 10 µg/mouse) or PBS was administered i.n. to convalescent (conv) mice or naïve control mice. After 4 hours a fluorochrome-conjugated anti-CD45 antibody was administered i.v. and mice were euthanised 10 min later. Nasal tissue was harvested and isolated mononuclear cells were stained for surface Ly6G and CD11b for analysis by flow cytometry. Absolute numbers of circulating (CD45 i.v.$^+$) (A) and tissue-infiltrated (CD45 i.v.$^-$) (B) neutrophils in the nasal tissue, with representative flow cytometry plots (C). Results are combined from two independent experiments. Data shown are mean ± SEM (n=8-10 mice per group). *p < 0.05, **p < 0.01, ***p < 0.001, ****p < 0.0001 by two-way ANOVA followed by Tukey's multiple comparisons post-test.

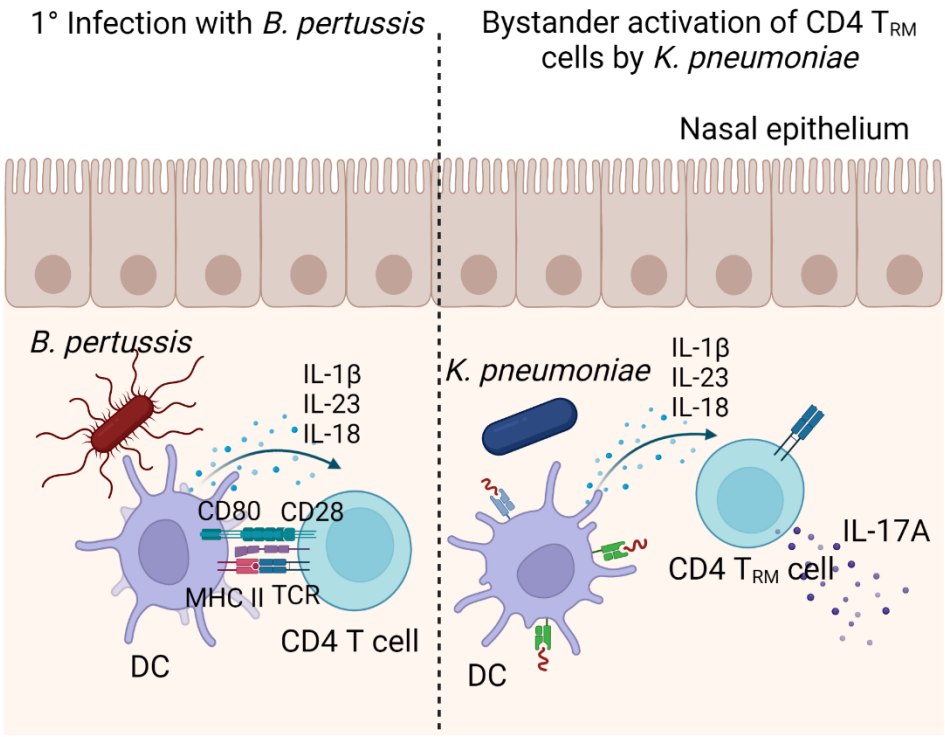

Figure 5.26 Proposed mechanism of bystander activation of CD4 T_{RM} cells induced following *B. pertussis* infection.

A primary infection with *B. pertussis* promotes the accumulation of IL-17A-producing CD4 T_{RM} cells in the nasal tissue. Exposure to an unrelated pathogen, *K. pneumoniae*, induces pro-inflammatory cytokine production, including IL-23, IL-1β, and IL-18, from innate immune cells such as DCs. The pro-inflammatory cytokines act directly on *B. pertussis*-specific CD4 T_{RM} cells in the nasal tissue and promote IL-17A production by CD4 T_{RM} cells, independent of TCR engagement.

Chapter 6 : Bystander activation of CD4 T_{RM} cells induced by intranasal immunisation with a wP vaccine

6.1 Introduction

The results from chapter 5 demonstrated that nasal and lung CD4 T_{RM} cells induced following natural infection with *B. pertussis* produced IL-17A in response to direct stimulation by cytokines, or indirectly following exposure to DCs stimulated with unrelated pathogens or PAMPs. The objective of this study was to investigate if vaccine-induced CD4 T_{RM} cells were also susceptible to bystander activation and if non-specific activation of CD4 T_{RM} cells could enhance immunity to an unrelated pathogen, a term broadly described as 'heterologous immunity' [373].

Research from the Mills' lab demonstrated that wP, but not the aP, vaccines induced long-lived IL-17A-producing CD4 T_{RM} cells in the nasal cavity and lungs of mice, and that this correlated with sustained protection against *B. pertussis* in the nasal cavity [194]. Furthermore, BPZE1, a live attenuated *B. pertussis* vaccine for nasal administration, conferred long-lived protection against *B. pertussis* infection in a murine model, and this was associated with the vaccines ability to induce IL-17A-producing CD4 T_{RM} cells in the nasal mucosa [286].

The aim of vaccination is to generate specific and long-lived adaptive immune responses against a pathogen, which protect against re-exposure to that pathogen [373]. However, there is emerging evidence that vaccines can elicit non-specific or heterologous effects, and generate immune responses to unrelated pathogens [374]. Non-specific protective effects have been observed for multiple vaccines, including the Bacillus Calmette-Guerin (BCG), smallpox, measles and oral polio vaccines, with studies demonstrating that these vaccines reduce the incidence of disease and/or mortality from infections caused by unrelated pathogens [375]. The measles vaccine was shown to reduced all-cause child mortality after the age of vaccination and until 3 - 5 years of age by 30-86% in different studies across several low-income countries [376]. This is much greater than the proportion of deaths attributed to acute measles disease. The off-target effects of vaccines have also been utilised in clinical settings, with intravesical BCG used as a treatment for non-invasive bladder cancer [377].

Although heterologous effects have been reported for multiple vaccines, the underlying mechanisms remain elusive. One potential mechanism is T cell cross-reactivity. The specific nature of adaptive immunity has centred on the theory of clonal selection, where individual T cells are specific for a single peptide-MHC molecule. However, this theory has been questioned on the basis that the number of theoretical TCRs needed for effective immunity would require recognition of $>10^{15}$ potential foreign peptides, whereas in reality there are estimated to be $<10^{8}$ distinct TCRs in the human naïve T cell pool.

This has led to the theory of T cell cross-reactivity, where an individual TCR can recognise more than one distinct peptide-MHC ligand. Heterologous immunity mediated by T cell cross-reactivity is often observed amongst closely related pathogens [373, 378].

Another potential mechanism underlying vaccine-induced heterologous immunity is the concept of innate immune training, where the innate immune system is reprogrammed after challenge to induce enhanced protection against reinfection in a T and B cell-independent manner [374]. The BCG vaccine against *M. tuberculosis* has been shown to induce trained innate immunity. Monocytes isolated from healthy volunteers produced significantly higher levels of pro-inflammatory cytokines in response to unrelated bacterial and fungal pathogens or PAMPS following BCG vaccination. These effects persisted for up to three months post-vaccination and were mediated in-part by epigenetic reprogramming of monocytes [379]. Interestingly, BCG vaccination has also been reported to augment non-specific T cell responses in healthy volunteers, with enhanced IFNγ and IL-17 production in response to unrelated pathogens, such as *C. albicans* and *S. aureus,* observed up to one year post BCG vaccination [380]. This leads to a third potential mechanism for vaccine-induced heterologous immunity, where vaccine-induced T cells can respond non-specifically to unrelated pathogens through TCR-independent mechanisms.

Heterologous immunity has also been observed in *B. pertussis* vaccines, however the mechanisms underlying this phenomenon are unclear. A wP vaccine has been shown to confer moderate protection against *B. parapertussis*, a closely related species to *B. pertussis* which causes a milder whooping cough-like disease, in the trachea and lungs of mice. [381]. Similarly, BPZE1 conferred protection against *B. parapertussis* and this was shown to be mediated by CD4 T cells [382]. BPZE1 has also been shown to promote protective effects in a range of infectious models in animals, including *S. pneumoniae*, influenza A, and respiratory syncytial virus (RSV), and inflammatory conditions including OVA-induced allergic airway inflammation and dinitrochlorobenzene (DNCB)-induced contact hypersensitivity (CHS) [383-386]. The mechanism of protection conferred by BPZE1 varied depending on the model used. For influenza A infection, OVA-induced airway inflammation, and DNCB-induced CHS, BPZE1 was shown to confer protection by reducing pro-inflammatory cytokines, including IL-1β and IL-6 [384, 386]. In contrast, BPZE1 conferred protection against RSV infection in mice by IL-17-dependent mechanisms [385].

Since bystander activation of CD4 T_{RM} cells may be a key mediator of vaccine-induced heterologous immunity, the objective of this study was to investigate if vaccine-induced

CD4 T_{RM} cells can be activated in a bystander manner. Due to the ability of a wP vaccine to induce a robust CD4 T_{RM} cell population in the nasal cavity and lungs [194], a wP vaccine was used in this study. However, there is emerging evidence that the route of immunisation can affect the induction of T_{RM} cells at mucosal surfaces and their susceptibility to bystander activation. The studies demonstrating heterologous immunity afforded by BPZE1 administered the vaccine via the i.n. route. Therefore the influence of the route of vaccine delivery on the capacity of vaccine-induced CD4 T_{RM} cells to TCR-independent activation was also addressed in this study. Finally, this study assessed if immunisation with a pertussis vaccine could confer non-specific immune protection against an unrelated pathogen. The results presented in chapter 5 revealed that *K. pneumoniae* promoted non-specific IL-17A production from nasal CD4 T_{RM} cells generated following natural *B. pertussis* infection. Therefore, a *K. pneumoniae* infection model was used to examine if a wP vaccine can generate non-specific protective immunity to an unrelated pathogen.

6.2 Results

6.2.1 Intranasal delivery of a wP vaccine confers protective immunity against B. pertussis in the nasal cavity.

In order to investigate if the route of wP vaccine delivery influenced the immune response to *B. pertussis* in the nasal cavity, C57BL/6 mice were immunised either i.n. or i.p. twice at 0 and 4 weeks with a wP vaccine, or with PBS as a control, and were aerosol challenged with *B. pertussis* 2 weeks later. There was no difference in clearance of *B. pertussis* from the lungs between the mice immunised by the i.n. or i.p. route. However, mice immunised with a wP vaccine by the i.n. route had significantly less CFU counts in the nasal wash on day 3 post challenge and in the nasal tissue on days 3 and 7 post challenge (Figure 6.1 *A*-*C*). Assessment of T cell responses in the nasal cavity revealed that mice immunised by the i.n. route exhibited elevated numbers of total CD4 T_{RM} cells ($CD4^+CD3^+CD45i.v.^-CD44^+CD62L^-CD69^+CD103^±$) and *B. pertussis*-specific IL-17A$^+$ and IFNγ$^+$ CD4 T_{RM} cells day of and 7 days post *B. pertussis* challenge (Figure 6.2 *A*-*E*). Furthermore, when compared with the i.p. route, mice immunised by the i.n. route had enhanced infiltration (CD45 i.v.$^-$) of Siglec-F$^+$ neutrophils into the nasal tissue on the day of and 7 days post *B. pertussis* challenge (Figure 6.3 *A*-*C*). In contrast, mice immunised by the i.p. route had significantly more infiltrated (CD45 i.v.$^-$) Ly6C$^+$MHCII$^+$ monocytes in the nasal cavity on day 7 post challenge (Figure 6.3 *D, E*).

Assessment of T cell responses in the lungs revealed that mice immunised by the i.n. route had a marked increase in the number of total CD4 T_{RM} cells and *B. pertussis*-specific IL-17A$^+$ CD4 T_{RM} cells (Figure 6.4 *A*-*C*). In contrast, mice immunised by the i.p. route had significantly more *B. pertussis*-specific IFNγ$^+$ CD4 T_{RM} cells in the lungs on day 7 post challenge, suggesting that the route of vaccine delivery influences the subsequent T cell responses in the lungs (Figure 6.4 *D*). Mice immunised by the i.n. route exhibited the highest number of alveolar macrophages in the lungs on day 7 post challenge (Figure 6.5 *A, B*). In contrast, mice immunised by the i.p. route had reduced numbers of total neutrophils and tissue-infiltrated (CD45 i.v.$^+$) neutrophils in the lungs compared with mice immunised by the i.n. route or PBS-immunised control mice on day 7 post challenge (Figure 6.5 *C*-*E*). Overall, the results from this study demonstrate that i.n. delivery of a wP vaccine is more effective than i.p. delivery in promoting protective immunity against nasal infection with *B. pertussis*.

6.2.2 Intranasal delivery of a wP vaccine induces CD4 T_{RM} cells that produce IL-17A following cytokine stimulation, independent of TCR engagement.

Having established that i.n. delivery of a wP vaccine induces a substantial population of *B. pertussis*-specific CD4 T_{RM} cells in the nasal cavity, it was next investigated if vaccine-induced CD4 T_{RM} cells can be activated in a TCR-independent manner and if the route of vaccine delivery can influence their capacity for bystander activation. C57BL/6 mice were immunised either i.n. or i.p. twice at 0 and 4 weeks with a wP vaccine. PBS was administered i.n. and i.p. to naïve control mice. Nasal tissue and lungs were harvested 2 weeks later and isolated mononuclear cells were stimulated with combinations of IL-1β, IL-23, IL-18, and IL-12. Cells were also stimulated with sBP and anti-CD28 and anti-CD49d to confirm the presence of pathogen-specific CD4 T_{RM} cells. Intracellular IL-17A and IFNγ production by CD4 T_{RM} cells ($CD4^+CD3^+CD45i.v.^-CD44^+CD69^+CD103^±$) was analysed by flow cytometry. CD4 T_{RM} cells from the nasal cavity (Figure 6.6 *A, B*) and lungs (Figure 6.7 *A, B*) of mice immunised with a wP vaccine by the i.n. route produced the highest levels of $IL\text{-}17A^+$ following *in vitro* stimulation with IL-23 in combination with IL-1β or IL-18. In contrast, IFNγ production by CD4 T_{RM} cells was detected in the lungs (Figure 6.7 *A, C*) of mice immunised by the i.p. or the i.n. route following *in vitro* stimulation with IL-12 and IL-18. Combined, these results demonstrate that CD4 T_{RM} cells generated following immunisation with a wP vaccine can be activated by cytokines, and that the route of vaccine delivery to induce T_{RM} cells influences this response.

6.2.3 CD4 T_{RM} cells induced following i.n. immunisation with a wP vaccine produce IL-17A in response to K. pneumoniae in vitro.

Having shown that vaccine-induced CD4 T_{RM} cells can be activated by cytokines alone, it was next investigated if CD4 T_{RM} cells could be activated in a bystander manner by an unrelated pathogen, *K. pneumoniae*. C57BL/6 mice were immunised either i.n. or i.p. twice at 0 and 4 weeks with a wP vaccine. Convalescent mice previously infected with *B. pertussis* were included as a positive control. Naïve control mice were treated with PBS. Nasal tissue and lungs were harvested 2 weeks after the last immunisation or 60 days post *B. pertussis* challenge. Isolated mononuclear cells were co-cultured with BMDCs and stimulated with heat-killed *K. pneumoniae* or sBP, and intracellular IL-17A and IFNγ production by CD4 T_{RM} cells ($CD4^+CD3^+CD45i.v.^-CD44^+CD69^+CD103^±$) was analysed by flow cytometry. CD4 T_{RM} cells from the nasal tissue (Figure 6.8 *A, B*) and lungs (Figure 6.9 *A, B*) of mice immunised with a wP vaccine by the i.n. route or mice

previously infected with *B. pertussis* produced the highest levels of IL-17A$^+$ following stimulation with heat-killed *K. pneumoniae* or sBP. A significant increase in the frequency of IFNγ$^+$ CD4 T_{RM} cells following stimulation with heat-killed *K. pneumoniae* was only observed in cells isolated from the nasal cavity of mice immunised by the i.n. route (Figure 6.8 *B*). CD4 T_{RM} cells from the lungs of mice immunised by the i.p. route exhibited a moderate increase in IFNγ production following stimulation with heat-killed *K. pneumoniae* (Figure 6.9 *B, C*). These results demonstrate that CD4 T_{RM} cells induced by a wP vaccine can be activated by an unrelated pathogen, however the type of response appeared to be influenced by the route of immunisation.

To confirm if IL-17A production by vaccine-induced tissue-resident CD4 T cells in response to an unrelated pathogen or PAMP is mediated by cytokines, circulating (CD45 i.v.$^+$) and tissue-resident (CD45 i.v.$^-$) CD4 T cells were isolated from the lungs of mice immunised twice with an i.n. wP vaccine and co-cultured with BMDCs. Cells were stimulated with *E. coli*-derived LPS, heat-killed *K. pneumoniae*, or sBP in the presence of an anti-IL-12p40 antibody, an anti-MHC II antibody, or an isotype control antibody. After 48 hours supernatants were collected and the concentration of IL-17A in the supernatants was quantified by ELISA. *E. coli*-derived LPS and heat-killed *K. pneumoniae* promoted IL-17A production from lung-resident, but not circulating, CD4 T cells when co-cultured with BMDCs, and this was reduced by the addition of an anti-IL-12p40 antibody (Figure 6.10). Addition of an anti-MHCII antibody caused a small reduction in LPS-induced IL-17A production, but not to the same extent as the anti-IL-12p40 antibody, and had no effect on heat-killed *K. pneumoniae*-induced IL-17A production. Addition of an anti-IL-12p40 antibody or an anti-MHC II reduced sBP-mediated IL-17A production from lung-resident CD4 T cells, indicating that the response to sBP is mediated by both cytokines and TCR engagement. These results demonstrate that PAMPs, such as *E. coli*-derived LPS, and unrelated pathogens, such as *K. pneumoniae,* can promote IL-17A production from CD4 T_{RM} cells generated following i.n. administration of a wP vaccine, and this is mediated in-part by IL-12/IL-23 signalling.

6.2.4 E. coli-derived LPS promotes IL-17A production from vaccine-induced CD4 T_{RM} cells in vivo and this is accompanied by enhanced neutrophil recruitment to the nasal cavity.

It was next investigated if vaccine-induced CD4 T_{RM} cells were susceptible to bystander activation *in vivo*. As CD4 T_{RM} cells generated following i.n. delivery of a wP vaccine had

a greater propensity for IL-17A production *in vitro* compared with cells from mice given the vaccine by the i.p. route, the i.n. route was utilised. C57BL/6 mice were immunised i.n. twice at 0 and 4 weeks with a wP vaccine. Naïve control mice received PBS by the i.n. route. *E. coli*-derived LPS or PBS was administered i.n. to mice 2 weeks after the second immunisation. Interestingly, IL-17A-producing CD4 T_{RM} cells were detected in the nasal tissue of unchallenged wP-immunised mice, suggesting CD4 T_{RM} cells are still producing IL-17A in the nasal cavity up to 2 weeks post immunisation. However, i.n. administration of *E. coli*-derived LPS promoted a significant increase in the number of IL-17A$^+$ CD4 T_{RM} cells in the nasal cavity of wP-immunised mice. No significant increase in nasal IFNγ$^+$ CD4 T_{RM} cells was detected following i.n. administration of LPS (Figure 6.11 *A*-*C*). Nose-resident γδ T cells in naïve and wP-immunised mice produced IL-17A following i.n. administration of LPS, however a significant increase was only observed in wP-immunised mice (Figure 6.11 *D, E*). The differences in innate cell recruitment between naïve and immunised mice in response to LPS was also examined. Mice immunised with a wP vaccine had the greatest number of total neutrophils in the nasal cavity following i.n. administration of LPS, however, there was no significant difference in the number of Ly6C$^+$CD11b$^+$ monocytes between naïve and immunised mice following LPS challenge (Figure 6.12 *A*-*C*). When the location of neutrophils within the nasal tissue was investigated, wP-immunised mice had significantly more tissue-infiltrated (CD45 i.v.$^-$) neutrophils in the nasal tissue compared with naïve mice following i.n. administration of LPS (Figure 6.13 *A*-*C*). Combined, these results demonstrate that vaccine-induced nasal CD4 T_{RM} cells are capable of producing IL-17A in response to *E. coli*-derived LPS *in vivo*, and this is accompanied by enhanced neutrophil infiltration into the nasal cavity.

6.2.5 Heat-killed K. pneumoniae promotes IL-17A production from vaccine-induced CD4 T_{RM} cells in vivo and this is accompanied by enhanced neutrophil recruitment to the nasal cavity.

To examine if an unrelated pathogen can promote IL-17A production from vaccine-induced CD4 T_{RM} cells *in vivo,* heat-killed *K. pneumoniae* or PBS was administered i.n. to mice previously immunised (prime/boost) with an i.n. wP vaccine or to naïve control mice. I.n. administration of heat-killed *K. pneumoniae* promoted a significant increase in the number of IL-17A$^+$ and IFNγ$^+$ CD4 T_{RM} cells in the nasal cavity of wP-immunised mice. (Figure 6.14 *A*- *C*). Furthermore, a significant increase in the number of nose-resident IL-17A$^+$ γδ T cells was observed in wP-immunised mice following i.n. administration of heat-killed *K. pneumoniae* (Figure 6.14 *D, E*). The differences in innate

cell recruitment between naïve and immunised mice in response to *K. pneumoniae* was also examined. Mice immunised with a wP vaccine had the greatest number of total neutrophils and $Ly6C^{+}CD11b^{+}$ monocytes in the nasal cavity following i.n. administration of heat-killed *K. pneumoniae* (Figure 6.15 *A*-*C*). An examination of the location of neutrophils within the nasal tissue revealed that wP-immunised mice had a significantly higher number of circulating (CD45 i.v.$^{+}$) and tissue-infiltrated (CD45 i.v.$^{-}$) neutrophils in the nasal cavity compared with naïve mice following i.n. administration of heat-killed *K. pneumoniae* (Figure 6.16 *A*-*C*). Taken together, these findings indicate that vaccine-induced nasal CD4 T_{RM} cells produce non-specific IL-17A in response to heat-killed *K. pneumoniae in vivo,* and this is associated with enhanced neutrophil infiltration into the nasal cavity.

6.2.6 Neutralisation of IL-17A reduces neutrophil infiltration and cytokine, chemokine, and AMP production in the nasal cavity of the wP immunised mice challenged with heat-killed K. pneumoniae.

To examine if the enhanced neutrophil recruitment observed in wP immunised mice in response to heat-killed *K. pneumoniae* is mediated by IL-17A, mice immunised with a wP vaccine were treated with an anti-IL17A antibody or an isotype control antibody one day prior to and during i.n. administration of heat-killed *K. pneumoniae*. Heat-killed *K. pneumoniae* was also administered to naïve control mice. wP-immunised mice treated with the isotype control antibody exhibited a marked increase in the absolute number and frequency of total neutrophils (Figure 6.17 *A*-*C*) and tissue-infiltrated (CD45 i.v.$^{-}$) neutrophils (Figure 6.17 *D, E*) in the nasal cavity compared with naive mice following i.n. administration of heat-killed *K. pneumoniae*. Treatment of wP-immunised mice with an anti-IL-17A antibody moderately reduced the absolute number and significantly reduced the frequency of total neutrophils (Figure 6.17 *A*-*C*) and tissue-infiltrated (CD45 i.v.$^{-}$) neutrophils (Figure 6.17 *D, E*) in the nasal cavity following challenge with heat-killed *K. pneumoniae*.

It was next examined if treatment of wP-immunised mice with an anti-IL-17A antibody affected chemokine, cytokine, and AMP production following i.n. administration of heat-killed *K. pneumoniae*. wP-immunised mice treated with the isotype control antibody had increased LCN2, CXCL1, and IL-1β concentrations in the nasal wash compared with naive control mice following i.n. administration of heat-killed *K. pneumoniae*, and this was significantly reduced following treatment with a neutralising anti-IL-17A antibody

(Figure 6.18). These findings demonstrate that enhanced neutrophil infiltration and increased cytokine, chemokine, and AMP production observed in wP-immunised mice following i.n. administration of heat-killed *K. pneumoniae* is mediated partly by IL-17A.

6.2.7 Immunisation with a wP vaccine confers non-specific protective immunity to K. pneumoniae.

IL-17A plays a protective role in host defence against *K. pneumoniae* [387]. Having demonstrated that nasal CD4 T_{RM} cells induced following i.n. immunisation with a wP vaccine can produce IL-17A in response to heat-killed *K. pneumoniae in vivo*, it was next investigated if i.n. immunisation with a wP vaccine could generate non-specific protective immunity to *K. pneumoniae*. C57BL/6 mice were immunised i.n. twice at 0 and 4 weeks with a wP vaccine and were infected i.n. with live *K. pneumoniae* ($1x10^6$ CFU/mouse) 2 weeks after the second immunisation. Compared with naïve mice, mice immunised with a wP vaccine had significantly less CFU counts in the nasal wash and nasal tissue at 24 hours and 5 days post *K. pneumoniae* challenge (Figure 6.19 *A*-*B*). An examination of the innate immune response revealed that mice immunised with a wP vaccine had significantly increased concentration of CXCL1 in the nasal wash and enhanced number of circulating (CD45 i.v.$^+$) neutrophils in the nasal tissue compared with naïve control mice 4 hours post-*K. pneumoniae* challenge (Figure 6.20 *A*-*B*). Tissue-infiltrated (CD45 i.v.$^-$) neutrophils were markedly higher in the wP-immunised mice both prior to and post *K. pneumoniae* challenge, and this pre-existing resident neutrophil population may also contribute to clearance of *K. pneumoniae* from the nasal cavity (Figure 6.20 *C*-*D*). Taken together, the results presented in this study demonstrate that i.n. immunisation with a wP vaccine confers non-specific protective immunity to *K. pneumoniae* in the nasal cavity.

6.3 Discussion

This study demonstrated that CD4 T_{RM} cells induced following i.n. immunisation with a wP vaccine can produce IL-17A in response to Th17-polarising cytokines and to DCs stimulated with unrelated pathogens and PAMPs *in vitro* and *in vivo.* Bystander activation of vaccine-induced CD4 T_{RM} cells was accompanied by an amplified immune response to unrelated pathogens and PAMPs in the nasal cavity. Furthermore, the results also demonstrated that i.n. delivery of a wP vaccine could confer non-specific protection to an unrelated pathogen, *K. pneumoniae*.

The results from this chapter showed that i.n. immunisation with a wP vaccine conferred protection against nasal infection with *B. pertussis* which was superior to that generated by i.p. delivery of the same vaccine, and this was accompanied by increased *B. pertussis*-specific IL-17A$^+$ CD4 T_{RM} cells and Siglec-F$^+$ neutrophils in the nasal mucosa. Current pertussis vaccines are delivered intramuscularly (i.m.), however, there is emerging evidence that i.n. administration of *B. pertussis* vaccines confer improved protection. Not only does i.n. immunisation offer the advantage of ease of administration over conventional needle-based injections, but i.n. vaccination also induces robust mucosal and systemic immunity similar to that conferred by natural infection [388].

Early research studies in humans showed that i.n. delivery of the wP vaccine as a nasal spray induced antigen-specific T cell responses in healthy volunteers [389]. Despite these promising results, i.n. immunisation with wP vaccines was not followed up [388]. Murine models have demonstrated that i.n. delivery of an aP vaccine formulated with a novel adjuvant called LP-GMP, which consists of a combination of a STING and a TLR2 agonist, conferred enhanced protection against *B. pertussis* in the nasal cavity compared with parenteral delivery of the same vaccine [291]. A study by Wolf and colleagues demonstrated that i.n. immunisation of mice with an aP vaccine without any adjuvants also promoted protection against *B. pertussis* in the nasal cavity [390]. BPZE1, which promotes long-term immunity in the nasal cavity in murine [286] and non-human primate models [285], is the first i.n. *B. pertussis* vaccine to reach phase 2 of clinical trials [388].

In addition to promoting enhanced mucosal immunity against *B.* pertussis, i.n. delivery of the wP vaccine induced CD4 T_{RM} cells capable of producing IL-17A non-specially in response to Th17-polarising cytokines *in vitro.* Furthermore, CD4 T_{RM} cells induced following i.n. immunisation with a wP vaccine produced non-specific IL-17A in response to *E. coli*-derived LPS and heat-killed *K. pneumoniae in vivo*. This was accompanied by enhanced neutrophil recruitment and increased CXCL1, IL-1β, and LCN2 production in the nasal cavity, which was significantly reduced following antibody-mediated

neutralisation of IL-17A. This suggests that IL-17A generated during the bystander activation of vaccine-induced CD4 T_{RM} cells can enhance immune responses to an unrelated pathogen. These results complement findings by Schnoeller and colleagues, who found that i.n. immunisation with BPZE1 conferred heterologous protection during a RSV infection. This was associated with the expansion of IL-17A producing lung-resident CD4 T cells and enhanced neutrophil recruitment to the lungs. The protective effect of BPZE1 on RSV was ablated following antibody-mediated neutralisation of IL-17 [385].

Experiments presented in this chapter demonstrated that i.n. immunisation with a wP vaccine conferred non-specific protective immunity to *K. pneumoniae* in the nasal cavity, and this was accompanied by enhanced CXCL1 and circulating neutrophils in the nose. CXCL1 production and neutrophil recruitment is enhanced by IL-17A, which has been shown to contribute to host defence against *K. pneumoniae* [323, 387]. It is possible that nonspecific IL-17A generated during the bystander activation of CD4 T_{RM} cells contributes to accelerated clearance of *K. pneumoniae* from the nasal cavity. However, further studies, such as depletion of CD4 T cells or neutralisation of IL-17A, are required to confirm the role of wP vaccine-induced CD4 T_{RM} cells in non-specific protective immunity against *K. pneumoniae*.

In addition to immunoprotective effects, bystander activation of CD4 T_{RM} cells may also promote pathological effects. T cell activation is considered to be highly regulated in order to prevent excessive inflammation, which may be detrimental during infection or lead to the development of autoimmune disease. Bystander activation of CD4 T cells has been shown to contribute to tissue damage during infection. A study by Gangappa and colleagues demonstrated that non-specific activation of OVA-specific CD4 T cells contributed to the development of ocular lesions during ocular HSV infection in mice [391]. Bystander activation of CD4 T cells has also been implicated in the development of autoimmune diseases. A study by Lee et al. demonstrated that unrelated OVA-specific memory-like Th17 cells contributed to the development of EAE, a murine model of multiple sclerosis, by infiltrating the CNS and producing IL-17A and IFNγ in an IL-1 receptor-dependent manner [250]. Many industrialised countries switched to the aP vaccine due to adverse effects associated with the wP vaccine. The reactogenicity of the wP vaccine is attributed to the high endotoxin content in these vaccines, which is highly inflammatory [1]. Consequently, excessive inflammation generated during bystander activation in individuals primed with a wP vaccine may be detrimental. Therefore, it is worth investigating bystander activation of CD4 T_{RM} cells induced by next-generation pertussis vaccines that exhibit a better safety profile.

Overall, the experiments from this study demonstrated that i.n. administration of a wP vaccine generated CD4 T_{RM} cells capable of producing pathogen-specific and nonspecific IL-17A, which is a key mediator of mucosal immunity in the nasal cavity. I.n. administration of a wP vaccine promoted superior protection against *B. pertussis* infection in the nose compared with i.p. delivery of the same vaccine. Furthermore, i.n. administration of a wP vaccine conferred non-specific protection against *K. pneumoniae* in the nasal cavity. The induction of broader heterologous T cell responses following vaccination may be beneficial in protecting against unrelated respiratory pathogens and against evolving *B. pertussis* strains that are able to escape immunity generated by current aP vaccines.

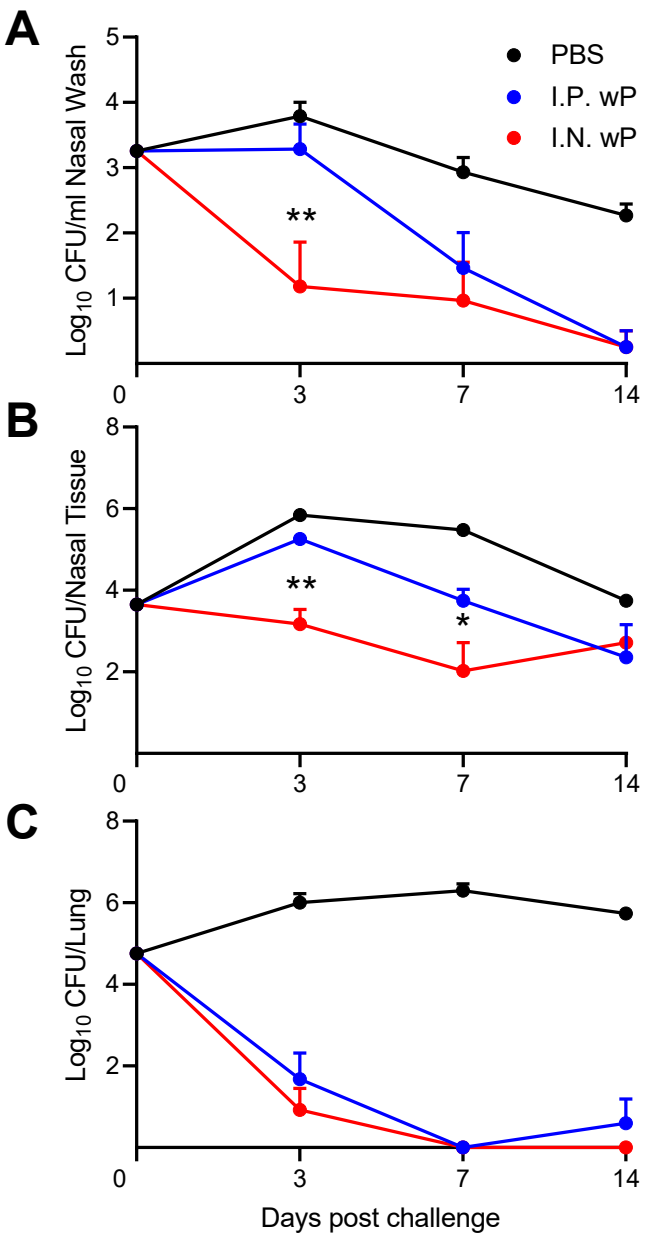

Figure 6.1 Intranasal immunisation with a wP vaccine significantly enhances clearance of *B. pertussis* from the nasal cavity.

C57BL/6 mice were immunised i.n. or i.p. twice (0 and 4 weeks) with a wP vaccine (1/20th human dose). Mice were aerosol challenged with live *B. pertussis* 2 weeks after the last immunisation and nasal washes, nasal tissue, and lungs were harvested from immunised or PBS-treated naïve control mice 3, 7, and 14 days post challenge. The number of viable bacteria in the nasal wash (A), digested nasal tissue (B), and lungs (C) was estimated by performing CFU counts on serially diluted nasal washes, nasal tissue, and lung homogenates from individual mice. Results shown are mean ± SEM CFU counts (n=4 mice per group). *$p < 0.05$, ** $p < 0.01$ i.n. versus i.p. immunisation by two-way ANOVA followed by Sidak's post-test.

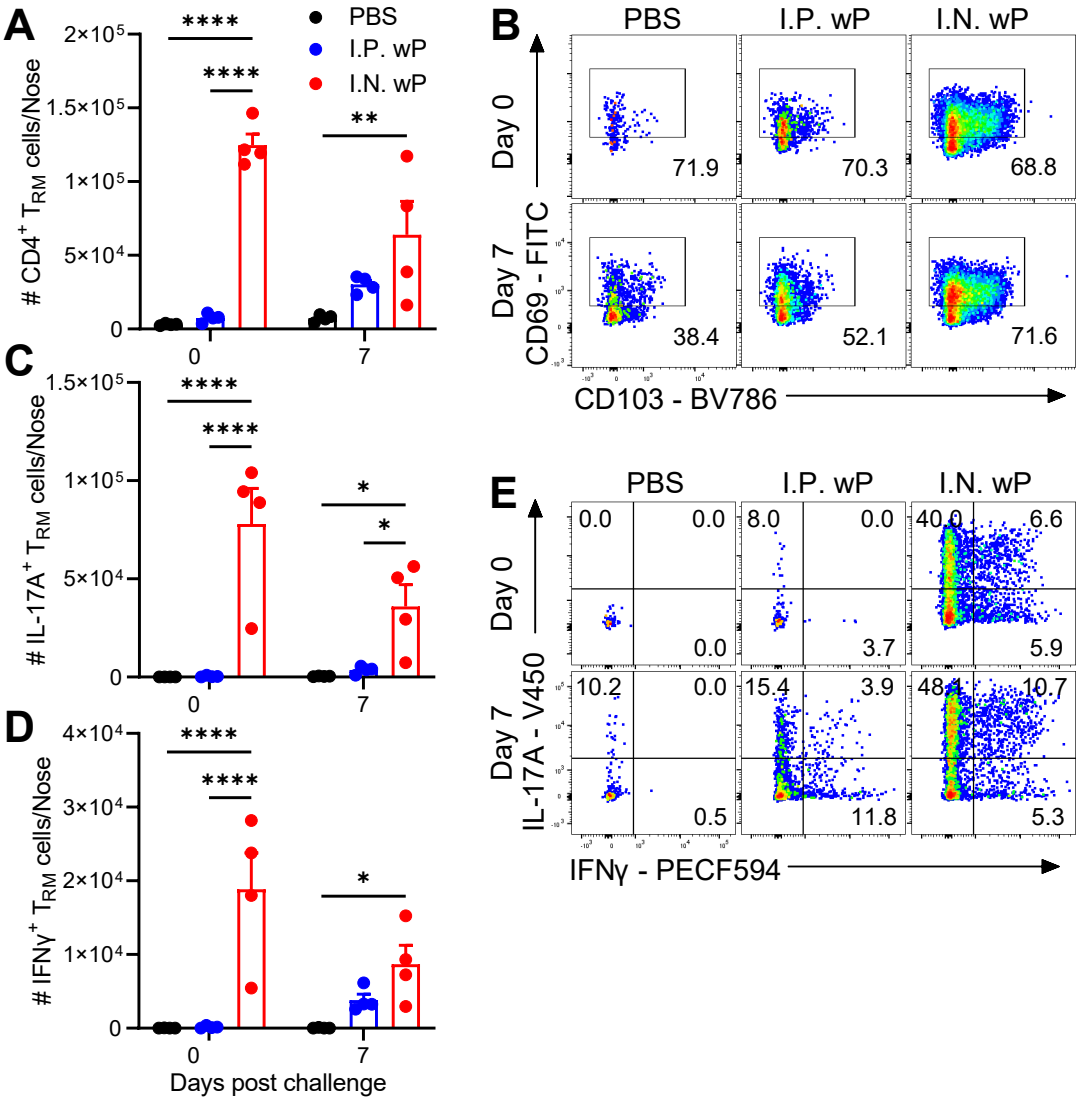

Figure 6.2 Enhanced CD4 T_{RM} cells, as well as *B. pertussis*-specific IL-17A$^+$ and IFNγ$^+$ CD4 T_{RM} cells, in the nasal cavity of mice immunised with an intranasal wP vaccine.

C57BL/6 mice were immunised i.n. or i.p. twice (0 and 4 weeks) with a wP vaccine (1/20th human dose) or with PBS as a control. Mice were aerosol challenged 2 weeks after the last immunisation with live *B. pertussis*. On the day of or 7 days post challenge, mice received an i.v. injection of fluorochrome-labelled anti-CD45 antibody and euthanised 10 min later. Nasal tissue was harvested and mononuclear cells were isolated and stained for CD4, CD3, CD44, CD62L, CD69, and CD103 and analysed by flow cytometry. Absolute number (A) and representative flow cytometry plots (B) of unstimulated CD4 T_{RM} cells (CD4$^+$CD3$^+$CD45i.v.$^-$CD44$^+$CD62L$^-$CD69$^+$CD103$^\pm$) in the nasal cavity. Nasal mononuclear cells were stimulated with sBP (5 μg/ml) and anti-CD28 and anti-CD49d (both at 1 μg/ml) for 20 hr, with brefeldin A (5 μg/ml) added for the final 4 hours of culture. Intracellular IL-17A and IFNγ production by CD4 T_{RM} cells was analysed by flow cytometry. Absolute number of IL-17A$^+$ (C) and IFNγ$^+$ (D) CD4 T_{RM} cells in the nasal cavity, with representative flow cytometry plots (E). Results shown are mean ± SEM (n=4 mice per group). *p < 0.05, ****p < 0.0001 by two-way ANOVA followed by Tukey's post-hoc test.

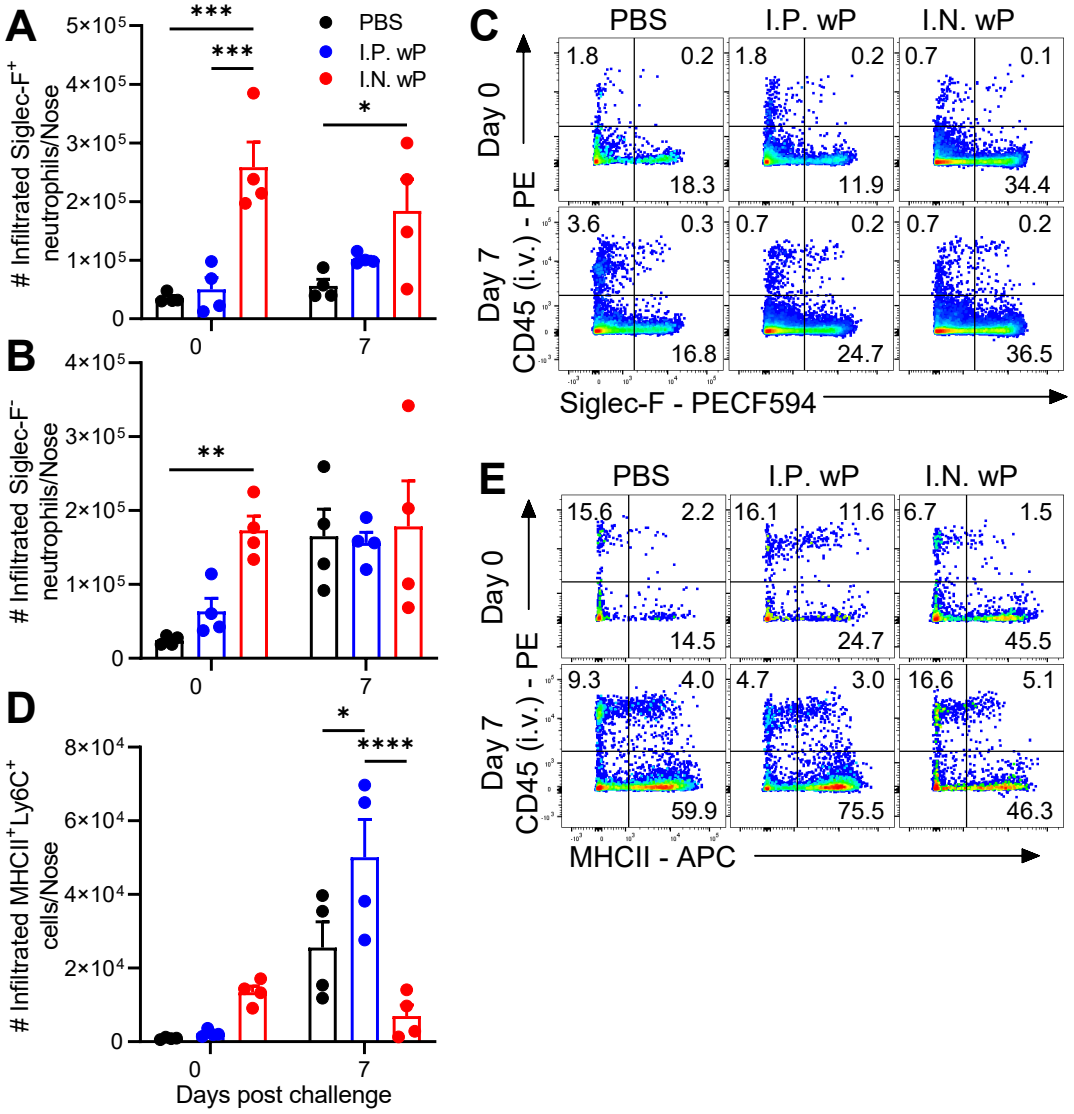

Figure 6.3 Mice immunised with an intranasal wP vaccine have increased Siglec-F⁺ neutrophils in the nasal cavity before and during *B. pertussis* infection.

C57BL/6 mice were immunised i.n. or i.p. twice (0 and 4 weeks) with a wP vaccine (1/20th human dose) or with PBS as a control. Mice were aerosol challenged 2 weeks after the last immunisation with live *B. pertussis*. On the day of or 7 days post challenge, mice received an i.v. injection of fluorochrome-labelled anti-CD45 antibody and euthanised 10 min later. Nasal tissue was harvested and mononuclear cells were isolated and stained with antibodies specific for CD11b, Ly6G, Ly6C, MHCII, and Siglec-F, and analysed by flow cytometry. Absolute number of tissue-infiltrated (CD45 i.v.$^{-}$) Siglec-F^{+} (A) and Siglec-F^{-} (B) neutrophils (Ly6G^{+}CD11b^{+}) in the nasal cavity, with representative flow cytometry plots (C). Absolute number (D) and representative flow cytometry plots (E) of tissue-infiltrated MHCII^{+}Ly6C^{+}CD11b^{+} monocytes in the nasal cavity. Data are mean ± SEM (n=4 mice per group). *p < 0.05, **p < 0.01, ***p < 0.001, ****p < 0.0001 by two-way ANOVA followed by Tukey's multiple comparisons test.

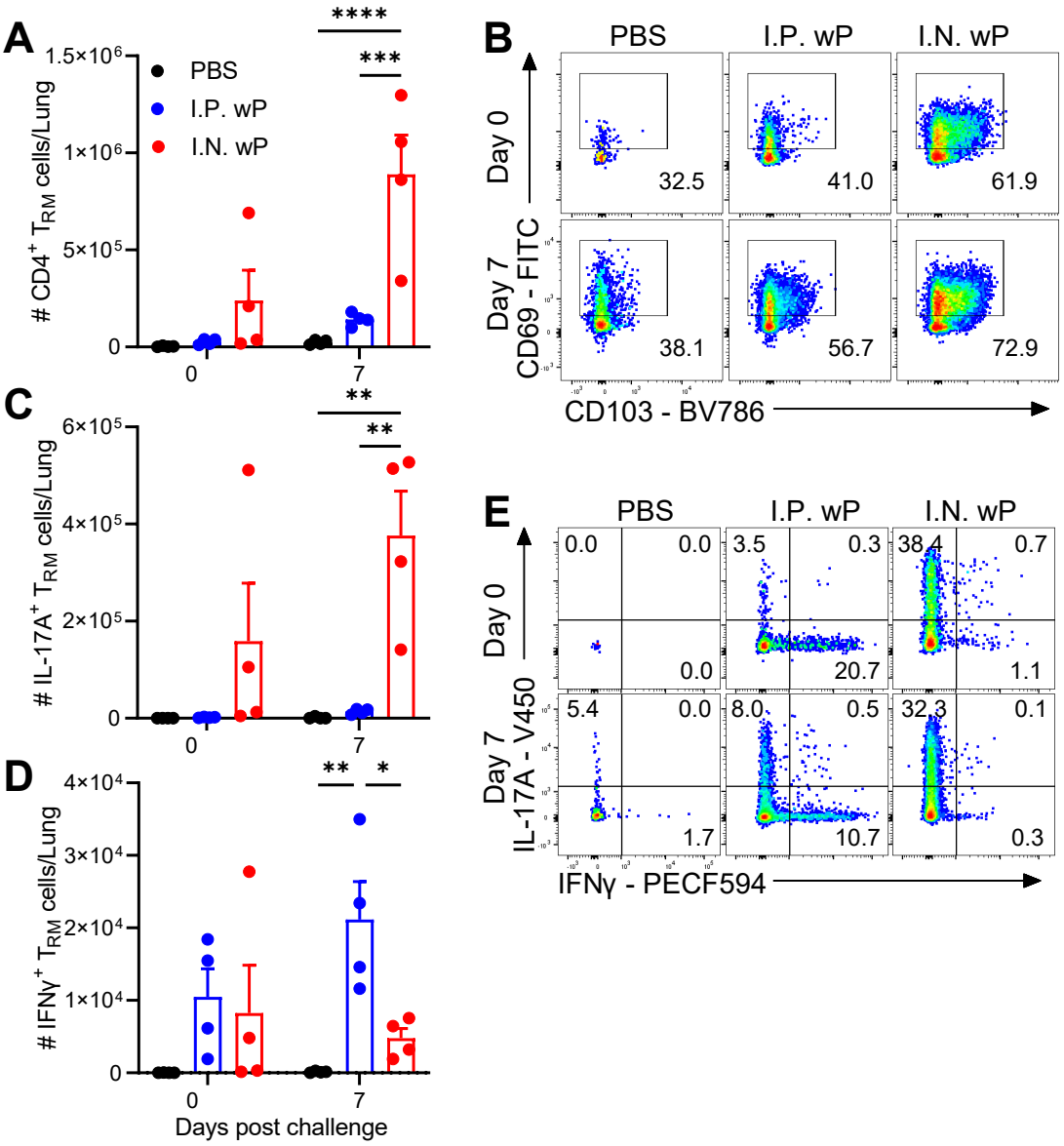
A
1.5×10^6
1×10^6
5×10^5
0
CD4+ TRM cells/Lung
PBS
I.P. wP
I.N. wP
****
***
0
7
B
PBS
I.P. wP
I.N. wP
Day 0
Day 7
CD69 - FITC
32.5
41.0
61.9
38.1
56.7
72.9
CD103 - BV786
C
6×10^5
4×10^5
2×10^5
0
IL-17A+ TRM cells/Lung
**
**
0
7
D
4×10^4
3×10^4
2×10^4
1×10^4
0
IFNγ+ TRM cells/Lung
**
*
0
7
Days post challenge
E
PBS
I.P. wP
I.N. wP
Day 0
Day 7
IL-17A - V450
0.0
0.0
0.0
0.0
3.5
0.3
20.7
38.4
0.7
1.1
5.4
0.0
1.7
8.0
0.5
10.7
32.3
0.1
0.3
IFNγ - PECF594

Figure 6.4 Intranasal immunisation with a wP vaccine enhances the number of IL-17A$^+$ CD4 T_{RM} cells, whereas intraperitoneal immunisation enhances the number of IFNγ$^+$ CD4 T_{RM} cells, in the lungs.

C57BL/6 mice were immunised i.n. or i.p. twice (0 and 4 weeks) with a wP vaccine (1/20th human dose) or with PBS as a control. Mice were aerosol challenged 2 weeks after the last immunisation with live *B. pertussis*. On the day of or 7 days post challenge, mice received an i.v. injection of fluorochrome-labelled anti-CD45 antibody and euthanised 10 min later. Lungs were harvested and mononuclear cells were isolated and stained for CD4, CD3, CD44, CD62L, CD69, and CD103, and analysed by flow cytometry. Absolute number (A) and representative flow cytometry plots (B) of unstimulated CD4 T_{RM} cells (CD4$^+$CD3$^+$CD45i.v.$^-$CD44$^+$CD62L$^-$CD69$^+$CD103$^\pm$) in the lungs. Isolated mononuclear cells were stimulated with sBP (5 μg/ml) and anti-CD28 and anti-CD49d (both at 1 μg/ml) for 20 hr, with brefeldin A (5 μg/ml) added for the final 4 hours of culture. Intracellular IL-17A and IFNγ production by CD4 T_{RM} cells was analysed by flow cytometry. Absolute number of IL-17A$^+$ (C) and IFNγ$^+$ (D) CD4 T_{RM} cells in the lungs, with representative flow cytometry plots (E). Results shown are mean ± SEM (n=4 mice per group). *p < 0.05, **p < 0.01, ***p < 0.001, ****p < 0.0001 by two-way ANOVA followed by Tukey's multiple comparisons test.

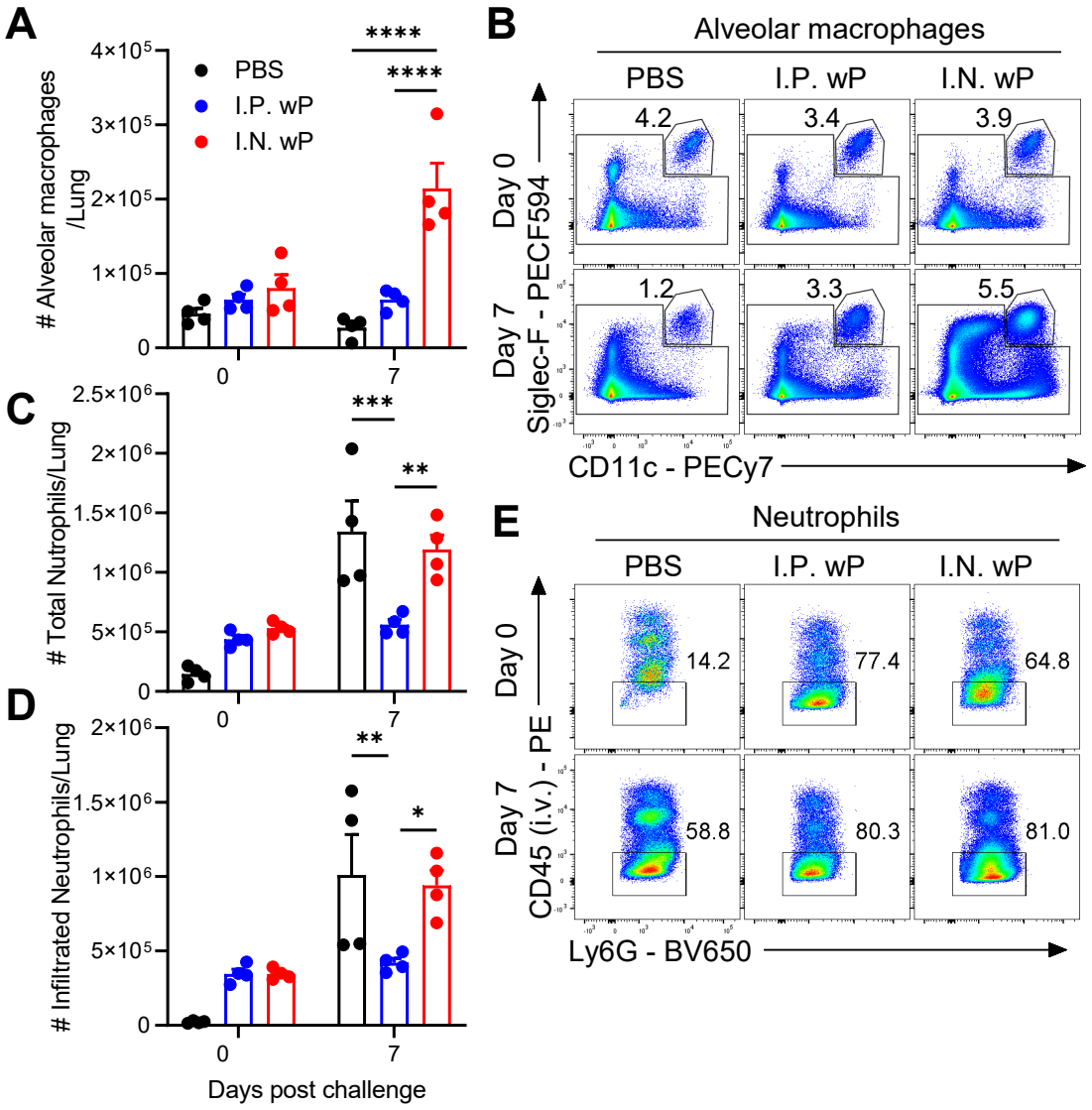

Figure 6.5 Intranasal immunisation with a wP vaccine significantly enhances the number of alveolar macrophages and infiltrated neutrophils in the lungs during *B. pertussis* infection.

C57BL/6 mice were immunised i.n. or i.p. twice (0 and 4 weeks) with a wP vaccine (1/20th human dose) or with PBS as a control. Mice were aerosol challenged 2 weeks after the last immunisation with live *B. pertussis*. On the day of or 7 days post challenge, mice received an i.v. injection of fluorochrome-labelled anti-CD45 antibody and euthanised 10 min later. Lungs were harvested and mononuclear cells were isolated and stained for surface CD11b, CD11c, Ly6G, and Siglec-F, and analysed by flow cytometry. Absolute number of alveolar macrophages (Siglec-F$^+$CD11c$^+$) (A) with representative flow cytometry plots (B) in the lungs. Absolute number of total (C) and lung-infiltrated (CD45 i.v.$^-$) (D) neutrophils (Ly6G$^+$CD11b$^+$) with representative flow cytometry plots (E). Data are mean ± SEM (n=4 mice per group). *p < 0.05, **p < 0.01, ***p < 0.001 ****p < 0.0001 by two-way ANOVA followed by Tukey's multiple comparisons test.

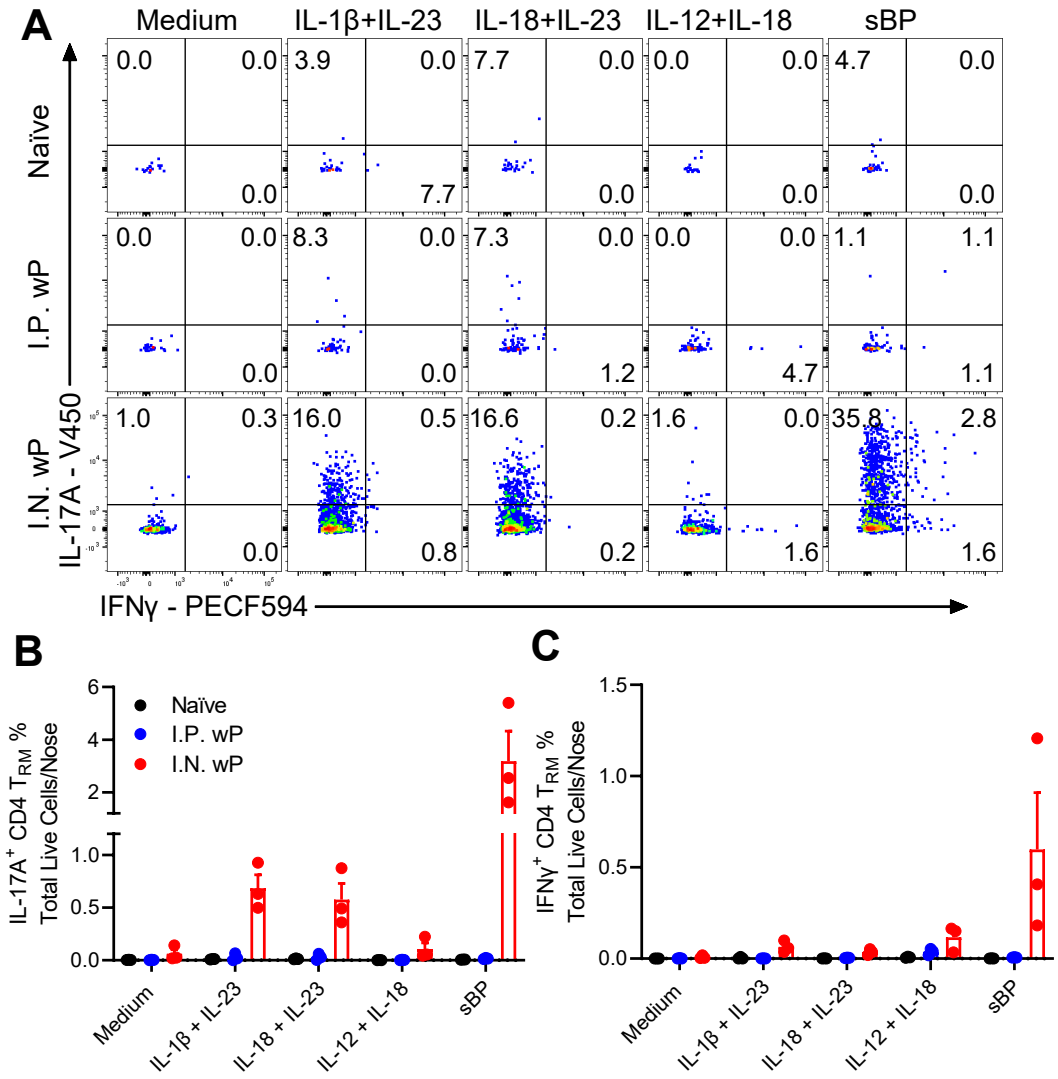

Figure 6.6 Nasal CD4 T_{RM} cells induced by intranasal immunisation with a wP vaccine produce IL-17A in response to cytokine stimulation.

C57BL/6 mice were immunised i.n. or i.p. twice (0 and 4 weeks) with a wP vaccine (1/20th human dose). Immunised mice and naïve control mice were injected i.v. with a fluorochrome-conjugated anti-CD45 antibody 2 weeks after the last immunisation and mice were euthanised 10 min later. Mononuclear cells were isolated from nasal tissue and pooled from immunised and naïve control mice (n=8/group). Cells were stimulated in triplicate (0.5x10^6 cells/ml) with combinations of IL-1β, IL-23, IL-18, IL-12 (all at 10 ng/ml) or sBP (5 µg/ml) with anti-CD28 and anti-CD49d (both at 1 µg/ml), or with medium alone for 20 hours. Brefeldin A (5 µg/ml) was added for the final 4 hours of culture. Cells were stained for the surface markers CD4, CD3, CD44, CD69, CD103, and intracellular IL-17A and IFNγ, and analysed by flow cytometry. Representative flow cytometry plots (A) and relative frequencies of IL-17A$^+$ (B) and IFNγ$^+$ (C) CD4 T_{RM} cells (CD4$^+$CD3$^+$CD45i.v.$^-$CD44$^+$CD69$^+$CD103$^\pm$), expressed as a percentage of live cells. Data are mean ± SEM of pooled data from three independent experiments, with each dot representing the average of three technical replicates from one independent experiment.

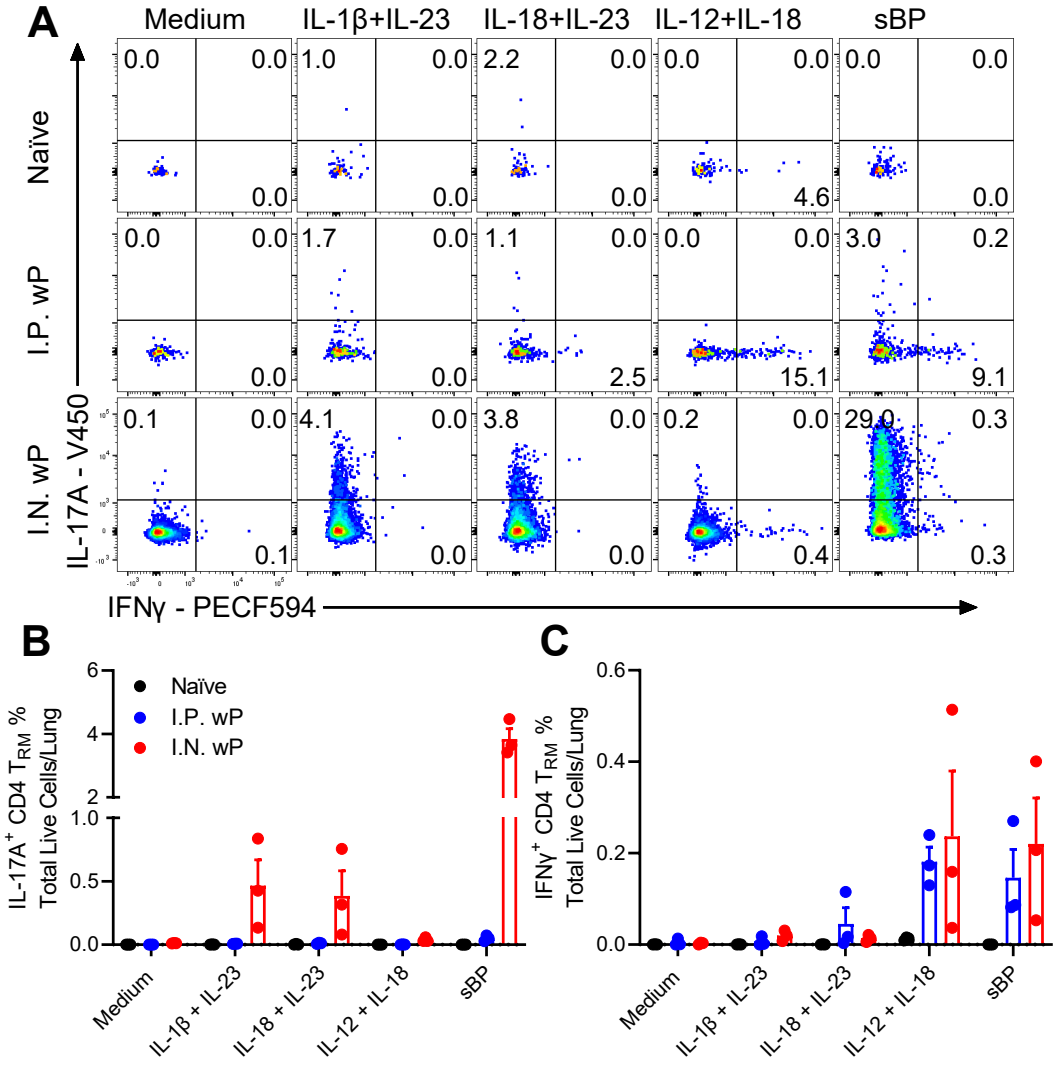

Figure 6.7 Lung CD4 T_{RM} cells induced by intranasal immunisation produce IL-17A, whereas lung CD4 T_{RM} cells generated following intraperitoneal immunisation produce IFNγ, in response to cytokine stimulation.

C57BL/6 mice were immunised i.n. or i.p. twice (0 and 4 weeks) with a wP vaccine (1/20th human dose). Immunised mice and naïve control mice were injected i.v. with a fluorochrome-conjugated anti-CD45 antibody 2 weeks after the last immunisation and mice were euthanised 10 min later. Mononuclear cells were isolated from the lungs and pooled from immunised and naïve control mice (n=8/group). Cells were stimulated in triplicate (2.5x10^6 cells/ml) with combinations of IL-1β, IL-23, IL-18, IL-12 (all at 10 ng/ml) or sBP (5 μg/ml) with anti-CD28 and anti-CD49d (both at 1 μg/ml), or with medium alone for 20 hours. Brefeldin A (5 μg/ml) was added for the final 4 hours of culture. Cells were stained for the surface markers CD4, CD3, CD44, CD69, CD103, and intracellular IL-17A and IFNγ, and analysed by flow cytometry. Representative flow cytometry plots (A) and relative frequencies of IL-17A$^+$ (B) and IFNγ$^+$ (C) CD4 T_{RM} cells (CD4$^+$CD3$^+$CD45i.v.$^-$ CD44$^+$CD69$^+$CD103$^\pm$) in the lungs, expressed as a percentage of live cells. Data are mean ± SEM of pooled data from three independent experiments, with each dot representing the average of three technical replicates from one independent experiment.

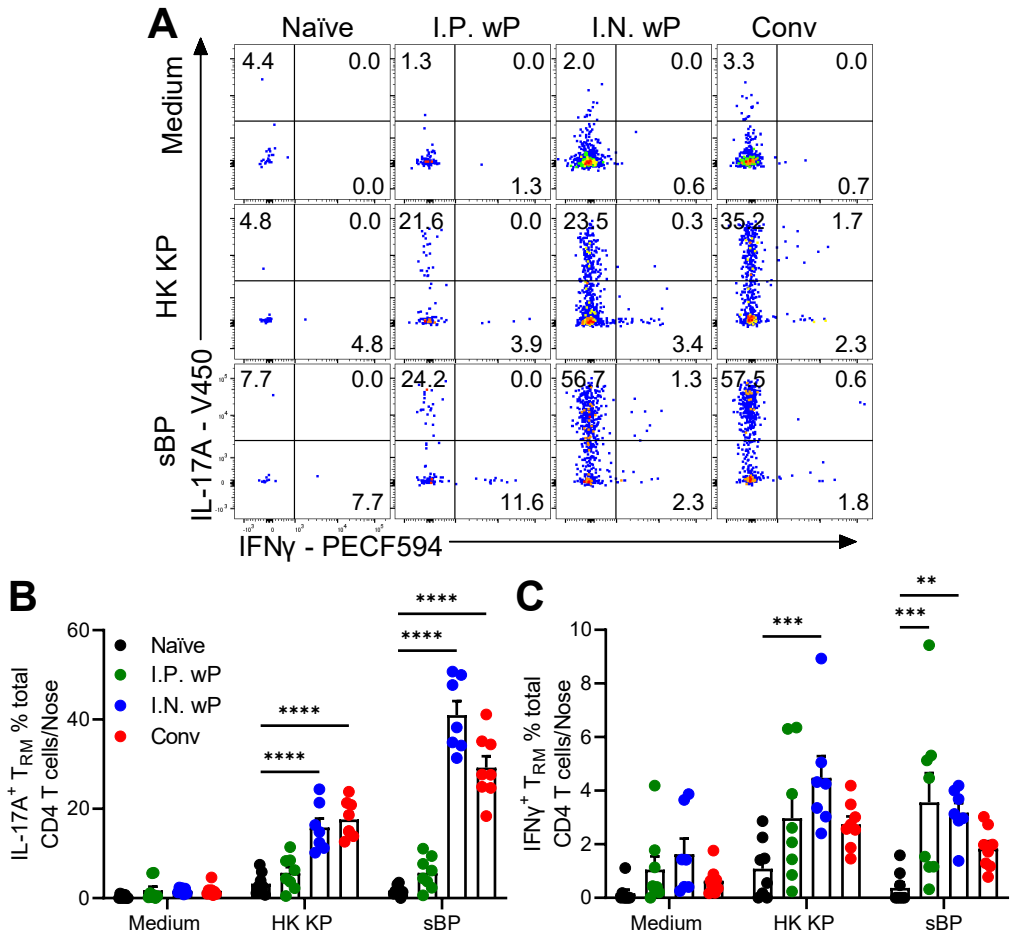

Figure 6.8 Nasal CD4 T_{RM} cells induced by intranasal administration of a wP vaccine or by natural infection with *B. pertussis* produce IL-17A in response to heat-killed *K. pneumoniae*.

C57BL/6 mice were immunised i.n. or i.p. twice (0 and 4 weeks) with a wP vaccine (1/20th human dose) or mice were infected with *B. pertussis* and allowed to recover. Immunised mice, convalescent (conv) mice, or naïve control mice were injected i.v. with a fluorochrome-conjugated anti-CD45 antibody 2 weeks after the last immunisation or 60 days post infection, and mice were euthanised 10 min later. Nasal mononuclear cells ($0.2x10^6$ cells/ml) were co-cultured with BMDCs ($0.5x10^6$ cells/ml) and stimulated with heat-killed *K. pneumoniae* (HK KP; 5 µg/ml), sBP (5 µg/ml), or medium alone for 20 hours, with brefeldin A (5 µg/ml) added for the final 4 hours of culture. Cells were stained for the surface markers CD4, CD3, CD44, CD69, CD103, and intracellular IL-17A and IFNγ, and analysed by flow cytometry. Representative flow cytometry plots (A) and relative frequencies of IL-17A$^+$ (B) and IFNγ$^+$ (C) nasal CD4 T_{RM} cells (CD4$^+$CD3$^+$CD45i.v.$^-$CD44$^+$CD69$^+$CD103$^\pm$). Results are combined from two independent experiments. Data are mean ± SEM (n=7/8 mice per group). $^{**}p < 0.01$, $^{***}p < 0.001$, $^{****}p < 0.0001$ versus naive control by two-way ANOVA followed by Dunnett's multiple comparisons test.

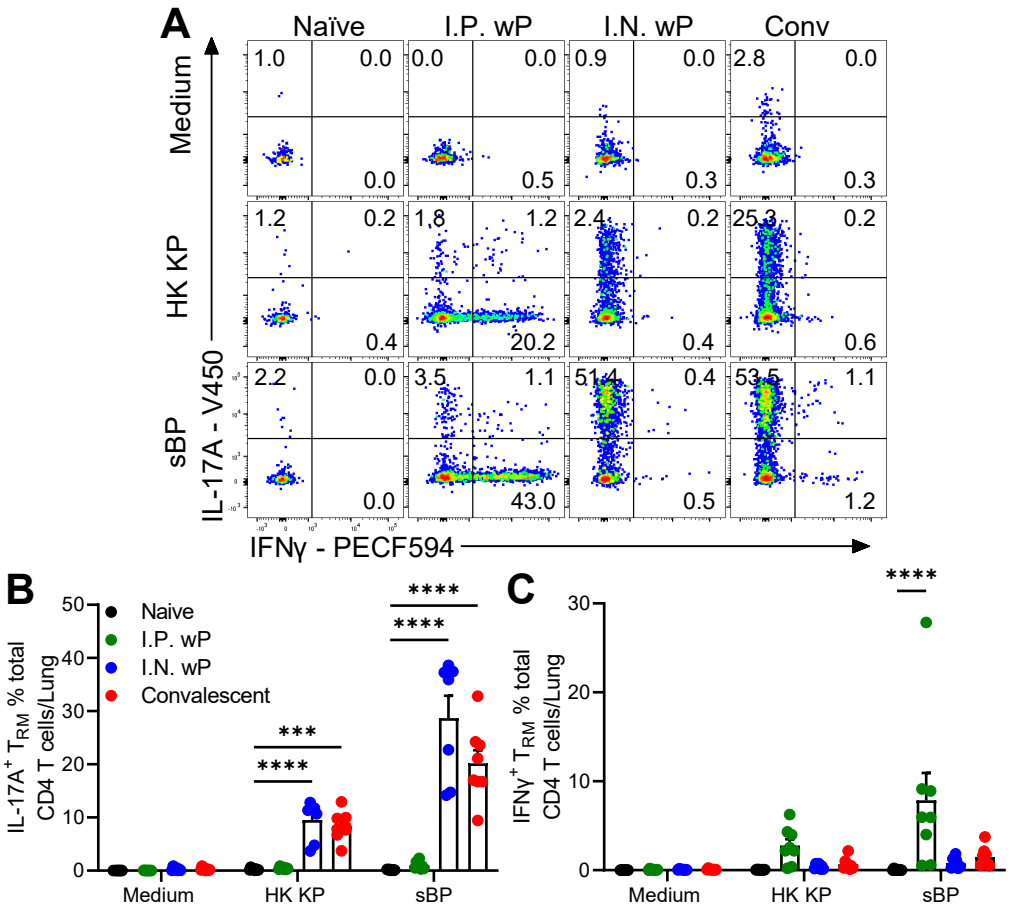

Figure 6.9 Lung CD4 T_{RM} cells induced by intranasal administration of a wP vaccine or by natural infection with *B. pertussis* produce IL-17A in response to heat-killed *K. pneumoniae*.

C57BL/6 mice were immunised i.n. or i.p. twice (0 and 4 weeks) with a wP vaccine ($1/20^{th}$ human dose) or mice were infected with *B. pertussis* and allowed to recover. Immunised mice, convalescent (conv) mice, or naïve control mice were injected i.v. with a fluorochrome-conjugated anti-CD45 antibody 2 weeks after the last immunisation or 60 days post infection, and mice were euthanised 10 min later. Lung mononuclear cells ($1x10^6$ cells/ml) were co-cultured with BMDCs ($0.5x10^6$ cells/ml) and stimulated with heat-killed *K. pneumoniae* (HK KP; 5 µg/ml), sBP (5 µg/ml), or medium alone for 20 hours, with brefeldin A (5 µg/ml) added for the final 4 hours of culture. Cells were stained for the surface markers CD4, CD3, CD44, CD69, CD103, and intracellular IL-17A and IFNγ, and analysed by flow cytometry. Representative flow cytometry plots (A) and relative frequencies of IL-17A$^+$ (B) and IFNγ$^+$ (C) lung CD4 T_{RM} cells (CD4$^+$CD3$^+$CD45i.v.$^-$ CD44$^+$CD69$^+$CD103$^\pm$). Results are combined from two independent experiments. Data are mean ± SEM (n=7/8 mice per group). ***p < 0.001, ****p < 0.0001 versus naive control by two-way ANOVA followed by Dunnett's multiple comparisons test.

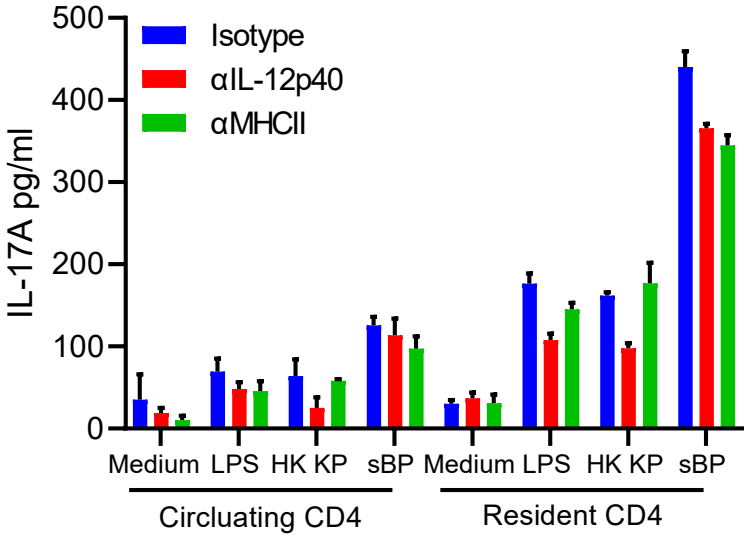

Figure 6.10 *E. coli* LPS and heat-killed *K. pneumoniae* induce IL-17A production from lung-resident CD4 T cells from wP-immunised mice co-cultured with BMDCs, and this is reduced in the presence of anti-IL-12p40.

C57BL/6 mice were immunised i.n. twice (0 and 4 weeks) with a wP vaccine (1/20th human dose). Mice were injected i.v. with a fluorochrome-conjugated anti-CD45 antibody 2 weeks after second immunisation and euthanised 10 min later. Lung-resident (CD45 i.v.$^{-}$) CD4^{+}CD3^{+} T cells were FACS purified from pooled lungs and cell yield was normalised between resident and circulating CD4 cells and co-cultured with BMDCs. Cells were stimulated with *E. coli*-derived LPS (100 ng/ml), *K. pneumoniae* (HK KP; 1 µg/ml), sBP (5 µg/ml) or medium alone in the presence of either anti-IL-12p40 (10 µg/ml), anti-MHCII (2 µg/ml), or isotype control (10 µg/ml). After 48 hours concentration of IL-17A in the supernatants was quantified by ELISA. Data presented are means ± SD and are representative of one independent experiment performed in triplicate culture.

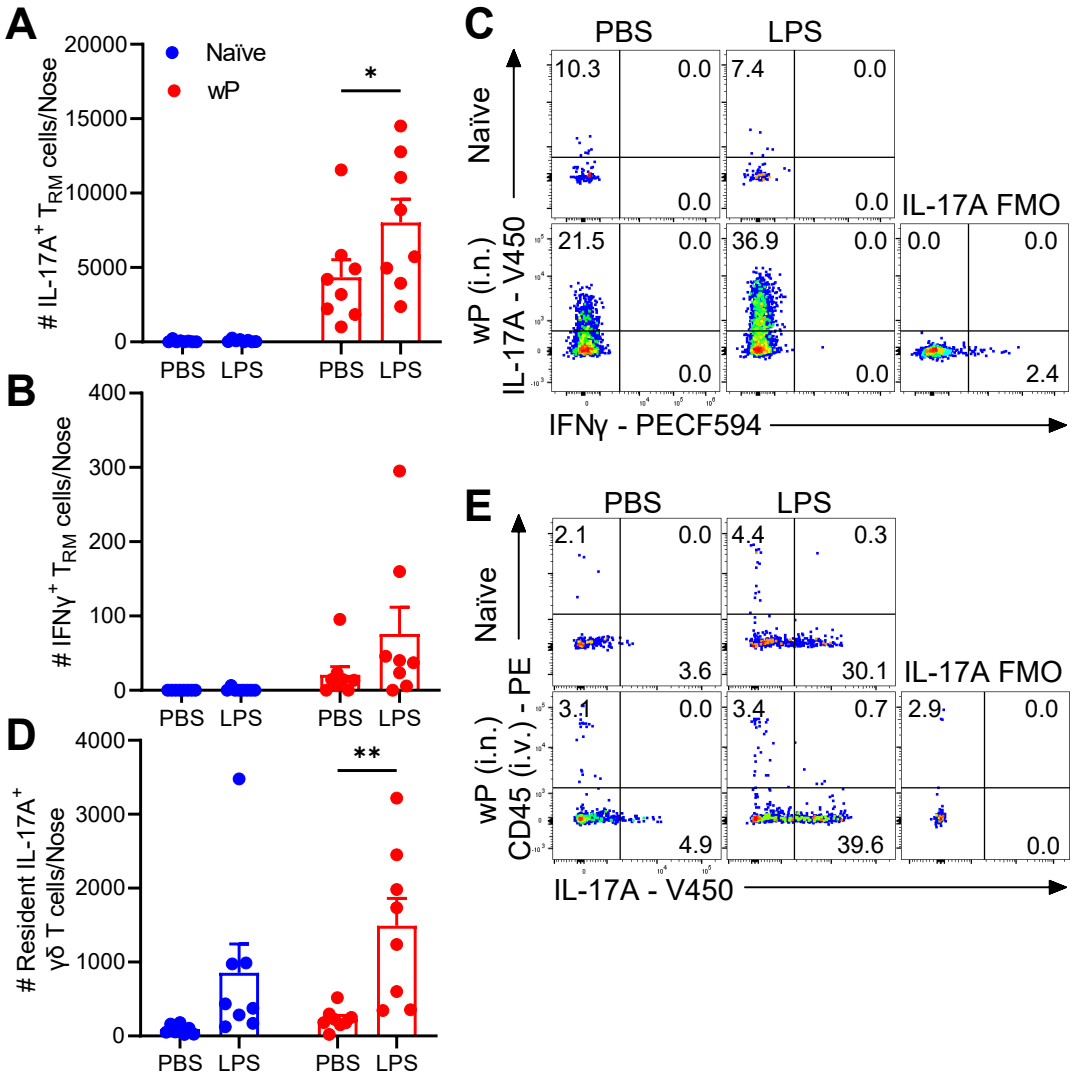

Figure 6.11 CD4 T_{RM} cells induced following intranasal immunisation with a wP vaccine produce IL-17A in response to *E. coli* LPS *in vivo*.

C57BL/6 mice were immunised i.n. twice (0 and 4 weeks) with a wP vaccine (1/20th human dose). *E. coli*-derived LPS (5 µg/mouse) or PBS was administered i.n. to mice 2 weeks after the last immunisation or to naïve control mice. After 4 hours a fluorochrome-conjugated anti-CD45 antibody was administered i.v. and mice were euthanised 10 min later. Nasal tissue was harvested and incubated with brefeldin A (5 µg/ml) for 1 hour during tissue digestion stage. Mononuclear cells were isolated and stained with antibodies specific for surface CD4, CD3, γδ TCR, CD44, CD62L, CD69, CD103, and intracellular IL-17A and IFNγ, and analysed by flow cytometry. Absolute number of IL-17A$^+$ (A) and IFNγ$^+$ (B) CD4 T_{RM} cells (CD4$^+$CD3$^+$CD45i.v.$^-$CD44$^+$CD62L$^-$CD69$^+$CD103$^\pm$), with representative flow cytometry plots in the nasal tissue (C). Absolute number of nose-resident (CD45 i.v.$^-$) IL-17A$^+$ γδ T cells (D) in the nasal cavity with representative flow cytometry plots (E). Results are combined from two independent experiments. Results shown are mean ± SEM (n=8 mice per group). *p < 0.05, **p < 0.01 PBS versus LPS treatment by two-way ANOVA followed by Sidak's multiple comparisons post-test.

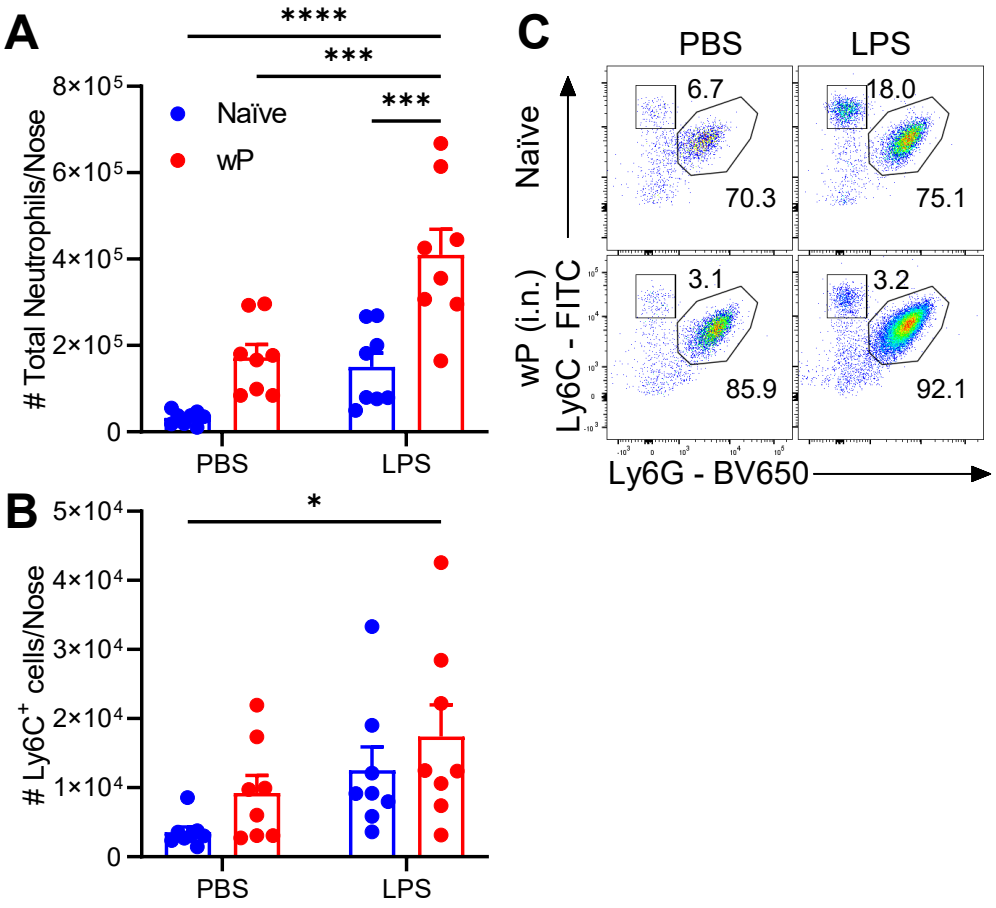

Figure 6.12 Mice immunised with an intranasal wP vaccine have increased number of neutrophils in the nasal cavity following intranasal *E. coli* LPS challenge.

C57BL/6 mice were immunised i.n. twice (0 and 4 weeks) with a wP vaccine (1/20th human dose). *E. coli*-derived LPS (5 µg/mouse) or PBS was administered i.n. to mice 2 weeks after the last immunisation or to naïve control mice. After 4 hours nasal tissue was harvested and mononuclear cells were isolated and stained for surface Ly6G, Ly6C and CD11b and analysed by flow cytometry. Absolute number of total neutrophils (A) and Ly6C^{+}CD11b^{+} monocytes (B), with representative flow cytometry plots (C) in the nasal tissue. Results are combined from two independent experiments. Data are mean ± SEM (n=8 mice per group). *p < 0.05, ***p < 0.001, ****p < 0.0001 by two-way ANOVA with Tukey's multiple comparisons test.

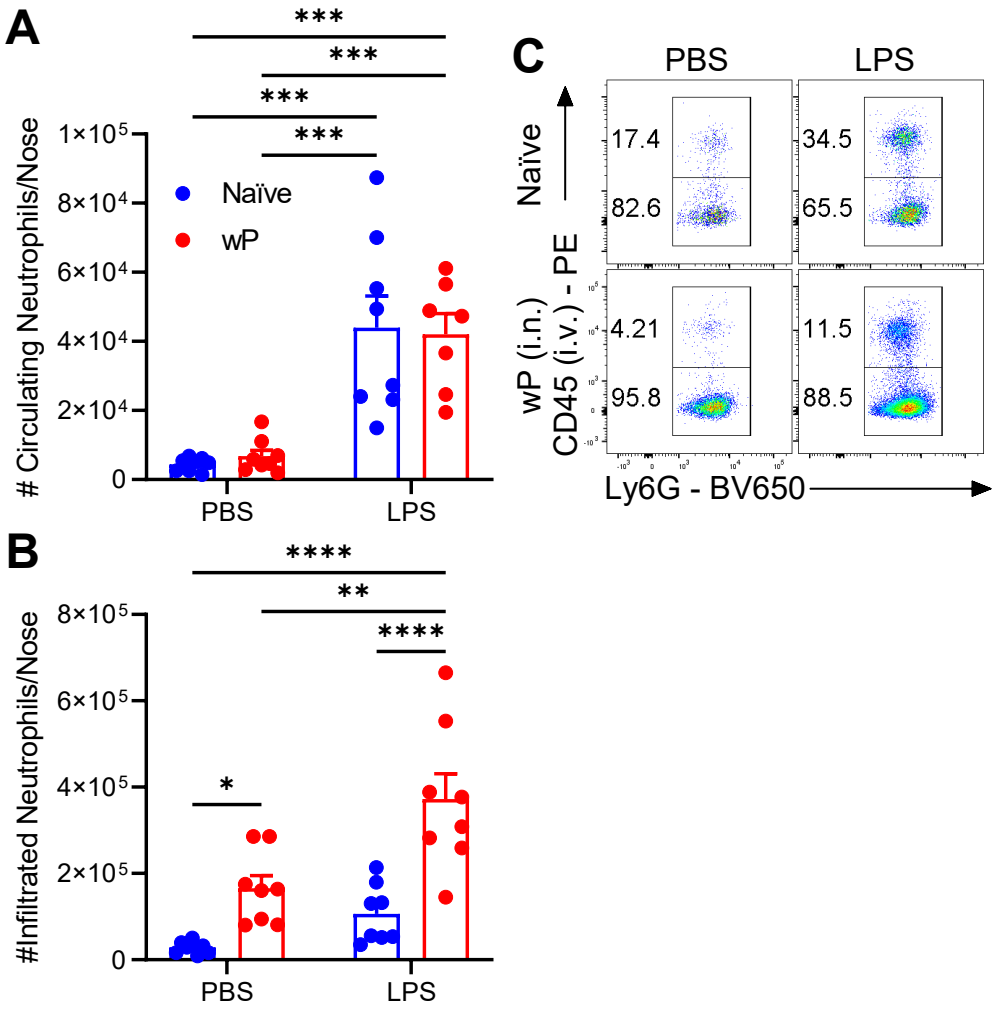

Figure 6.13 Enhanced neutrophil infiltration into the nasal tissue of wP-immunised mice following intranasal LPS challenge.

C57BL/6 mice were immunised i.n. twice (0 and 4 weeks) with a wP vaccine (1/20th human dose). *E. coli*-derived LPS (5 µg/mouse) or PBS was administered i.n. to mice 2 weeks after the last immunisation or to naïve control mice. After 4 hours a fluorochrome-conjugated anti-CD45 antibody was administered i.v. and mice were euthanised 10 min later. Nasal tissue was harvested and mononuclear cells were isolated and stained for surface Ly6G and CD11b, and analysed by flow cytometry. Absolute numbers of circulating (CD45 i.v.$^{+}$) (A) and tissue-infiltrated (CD45 i.v.$^{-}$) (B) neutrophils in the nasal tissue, with representative flow cytometry plots (C). Results are combined from two independent experiments. Data shown are mean ± SEM (n=7-8 mice per group). *p < 0.05, **p < 0.01, ***p < 0.001, ****p < 0.0001 by two-way ANOVA followed by Tukey's multiple comparisons post-test.

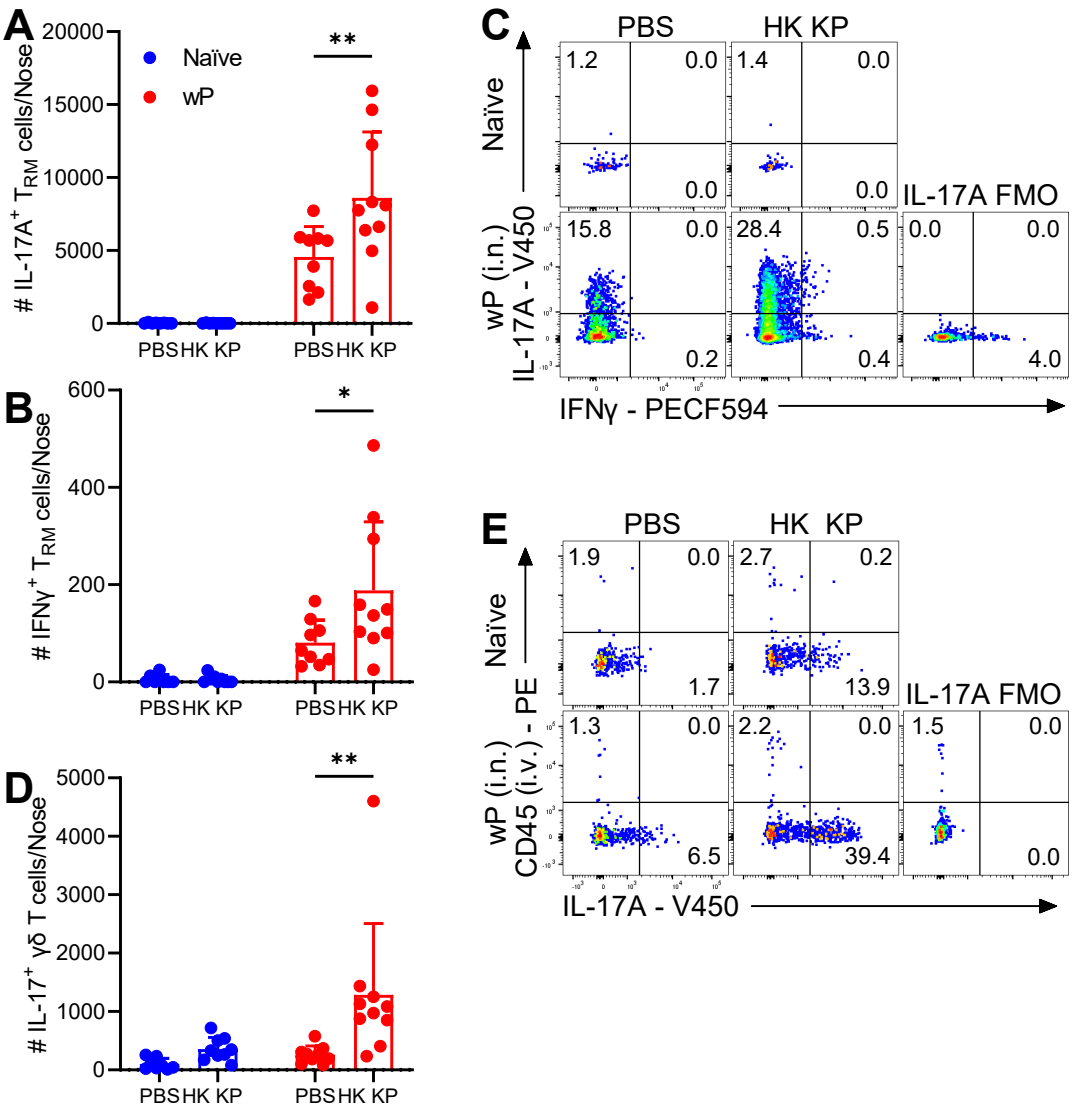

Figure 6.14 CD4 T_{RM} cells induced following intranasal immunisation with a wP vaccine produce IL-17A in response to intranasal heat-killed *K. pneumoniae* challenge *in vivo*.

C57BL/6 mice were immunised i.n. twice (0 and 4 weeks) with a wP vaccine (1/20th human dose). Heat-killed *K. pneumoniae* (HK KP; 10 µg/mouse) or PBS was administered i.n. to mice 2 weeks after the last immunisation or to naïve control mice. After 4 hours a fluorochrome-conjugated anti-CD45 antibody was administered i.v. and mice were euthanised 10 min later. Nasal tissue was harvested and incubated with brefeldin A (5 µg/ml) for 1 hour during tissue digestion stage. Nasal mononuclear cells were isolated and stained with antibodies specific for the surface markers CD4, CD3, γδ TCR, CD44, CD62L, CD69, CD103, and for intracellular IL-17A and IFNγ, and analysed by flow cytometry. Absolute numbers of IL-17A$^+$ (A) and IFNγ$^+$ (B) CD4 T_{RM} cells (CD4$^+$CD3$^+$CD45i.v.$^-$CD44$^+$CD62L$^-$CD69$^+$CD103$^\pm$), with representative flow cytometry plots (C) in the nasal tissue. Absolute number of nose-resident (CD45 i.v.$^-$) IL-17A$^+$ γδ T cells in the nasal cavity (D) with representative flow cytometry plots (E). Results are combined from two independent experiments. Results shown are mean ± SEM (n=8 – 10 mice per group). *p < 0.05, **p < 0.01 PBS versus HK KP treatment by two-way ANOVA with Sidak's multiple comparisons test.

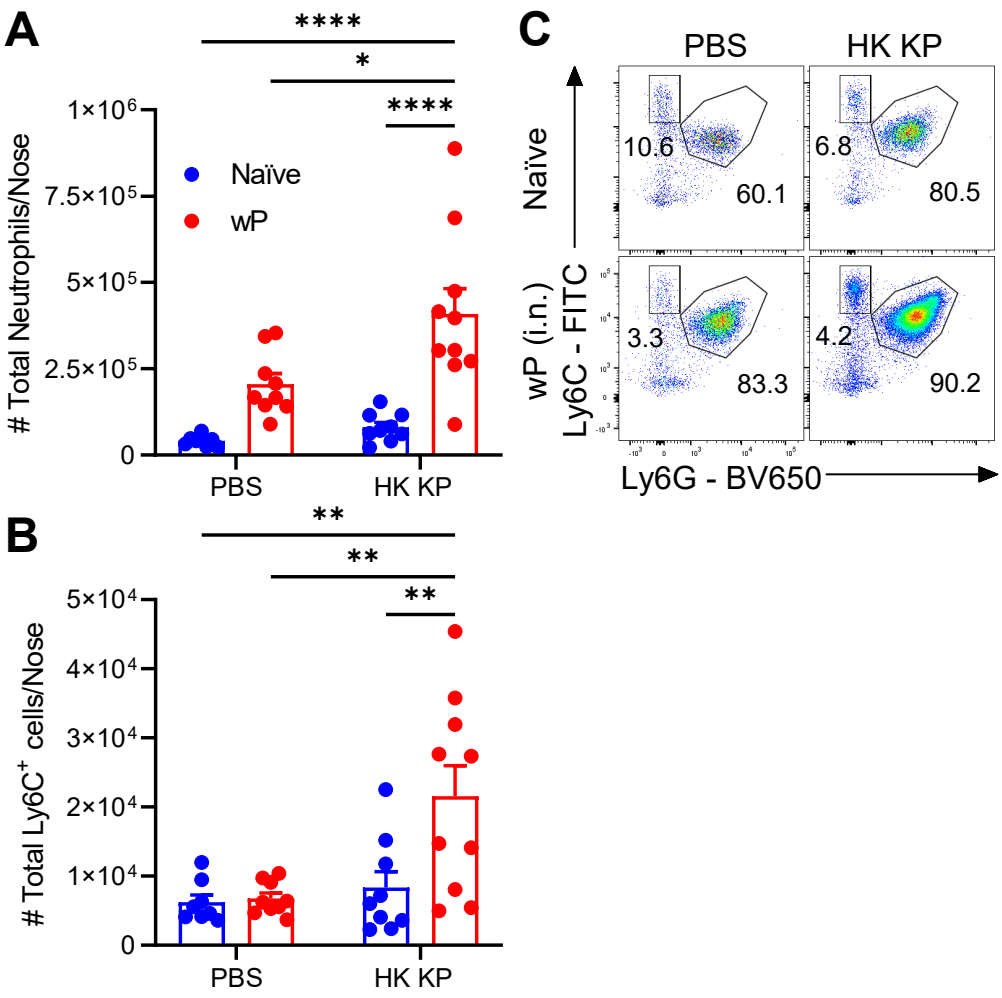

Figure 6.15 wP-immunised mice have increased neutrophil and Ly6C⁺CD11b⁺ monocyte numbers in the nasal cavity following heat-killed *K. pneumoniae* challenge.

C57BL/6 mice were immunised i.n. twice (0 and 4 weeks) with a wP vaccine (1/20th human dose). Heat-killed *K. pneumoniae* (HK KP; 10 µg/mouse) or PBS was administered i.n. to mice 2 weeks after the last immunisation or to naïve control mice. After 4 hours nasal tissue was harvested and isolated mononuclear cells were stained for surface Ly6G, Ly6C and CD11b, and analysed by flow cytometry. Absolute numbers of total neutrophils (Ly6G⁺CD11b⁺) (A) and Ly6C⁺CD11b⁺ monocytes (B), with representative flow cytometry plots in the nasal tissue (C). Results are combined from two independent experiments. Data are mean ± SEM (n=8-10 mice per group). *$p < 0.05$, **$p < 0.01$, ****$p < 0.0001$ by two-way ANOVA followed by Tukey's post-test.

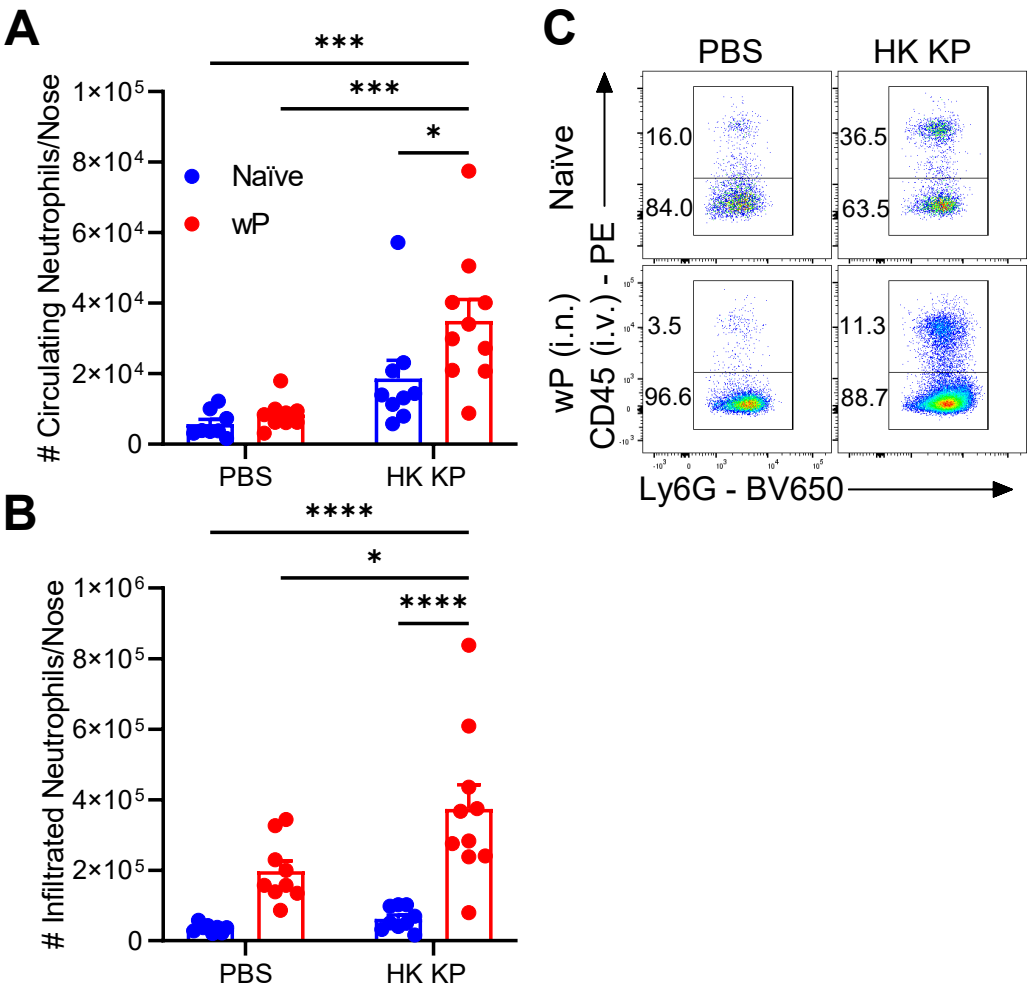

Figure 6.16 Mice immunised with an intranasal wP vaccine have increased number of circulating and nose-infiltrated neutrophils following heat-killed *K. pneumoniae* challenge.

C57BL/6 mice were immunised i.n. twice (0 and 4 weeks) with a wP vaccine (1/20th human dose). Heat-killed *K. pneumoniae* (HK KP; 10 µg/mouse) or PBS was administered i.n. to mice 2 weeks after the last immunisation or to naïve control mice. After 4 hours nasal tissue was harvested and isolated mononuclear cells were stained for surface Ly6G and CD11b, and analysed by flow cytometry. Absolute numbers of circulating (CD45 i.v.$^{+}$) (A) and tissue-infiltrated (CD45 i.v.$^{-}$) (B) neutrophils in the nasal tissue, with representative flow cytomety plots (C). Results are combined from two independent experiments. Data shown are mean ± SEM (n=8-10 mice per group). *p < 0.05, ***p < 0.001, ****p < 0.0001 by two-way ANOVA followed by Tukey's multiple comparisons post-test.

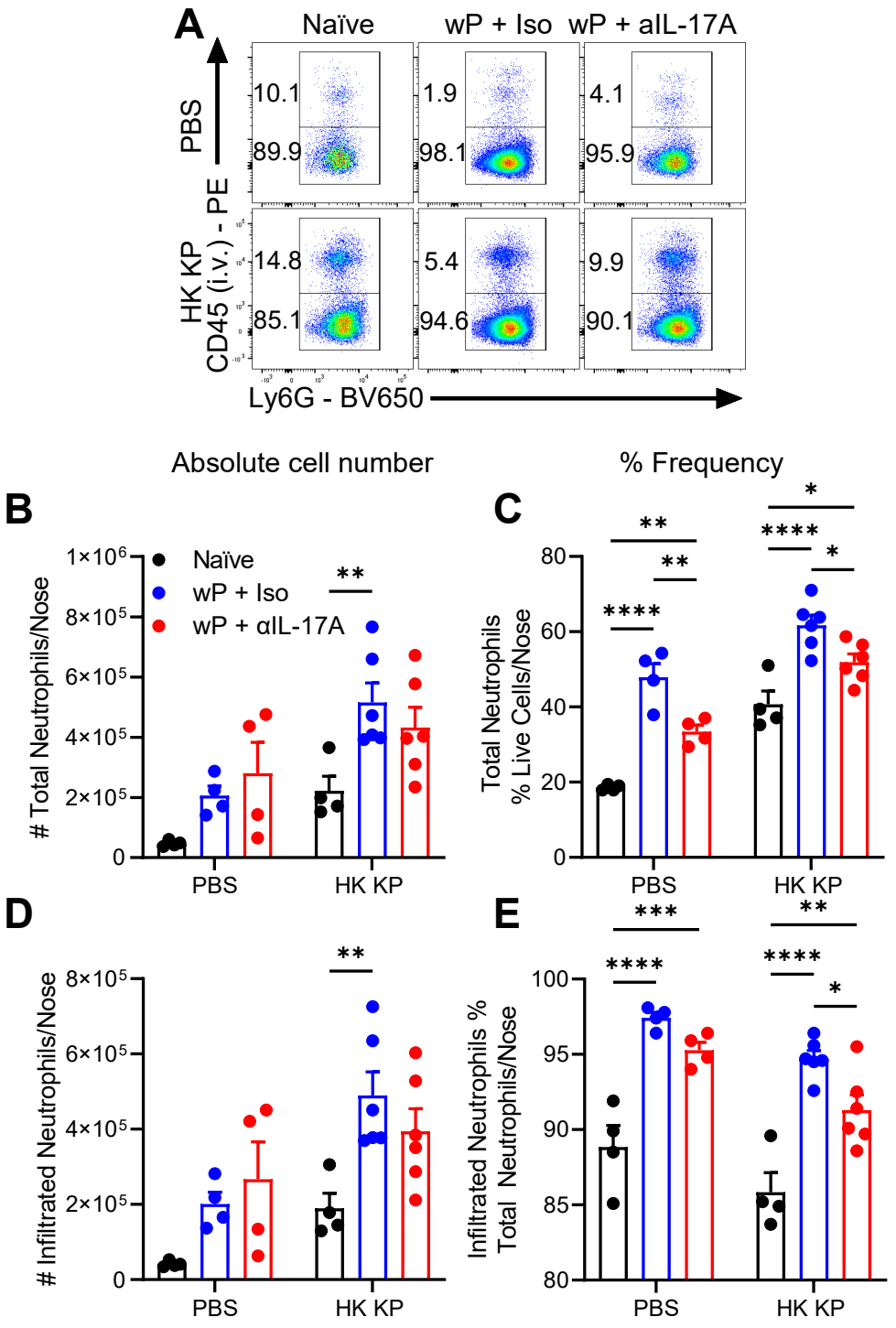
A
Naïve
wP + Iso
wP + aIL-17A
PBS
HK KP
CD45 (i.v.) - PE
Ly6G - BV650
10.1
89.9
1.9
98.1
4.1
95.9
14.8
85.1
5.4
94.6
9.9
90.1
Absolute cell number
% Frequency
B
Total Neutrophils/Nose
Naïve
wP + Iso
wP + αIL-17A
C
Total Neutrophils
% Live Cells/Nose
D
Infiltrated Neutrophils/Nose
E
Infiltrated Neutrophils %
Total Neutrophils/Nose
PBS
HK KP

Figure 6.17 Neutralisation of IL-17A reduces the frequency of total neutrophils and tissue-infiltrated neutrophils in the nasal cavity of wP-immunised mice following heat-killed *K. pneumoniae* challenge.

C57BL/6 mice were immunised i.n. twice (0 and 4 weeks) with a wP vaccine (1/20th human dose). Mice were injected i.p. with a neutralising anti-IL-17A antibody (200 µg/mouse) or isotype control 2 weeks after the last immunisation. Heat-killed *K. pneumoniae* (HK KP; 10 µg/mouse) or PBS was administered i.n. to mice 24 hours later together with an additional i.n. dose of anti-IL-17A (50 µg/mouse) or isotype control. After 4 hours a fluorochrome-conjugated anti-CD45 antibody was administered i.v. and mice were euthanised 10 min later. Nasal tissue was harvested and mononuclear cells were isolated and stained for surface CD11b and Ly6G, and analysed by flow cytometry. Representative flow cytometry plots of circulating (CD45 i.v.$^{+}$) and tissue-infiltrating (CD45 i.v.$^{-}$) neutrophils (Ly6G^{+}CD11b^{+}) in the nasal cavity (A). Absolute number (B) and relative frequency (C) of total neutrophils in the nose. Absolute number (D) and relative frequency (E) of tissue-infiltrated (CD45 i.v.$^{-}$) neutrophils. Results shown are mean ± SEM (n=4-6 mice per group). *$p < 0.05$, **$p < 0.01$, ***$p < 0.001$, ****$p < 0.0001$ by two-way ANOVA followed by Tukey's post-test.

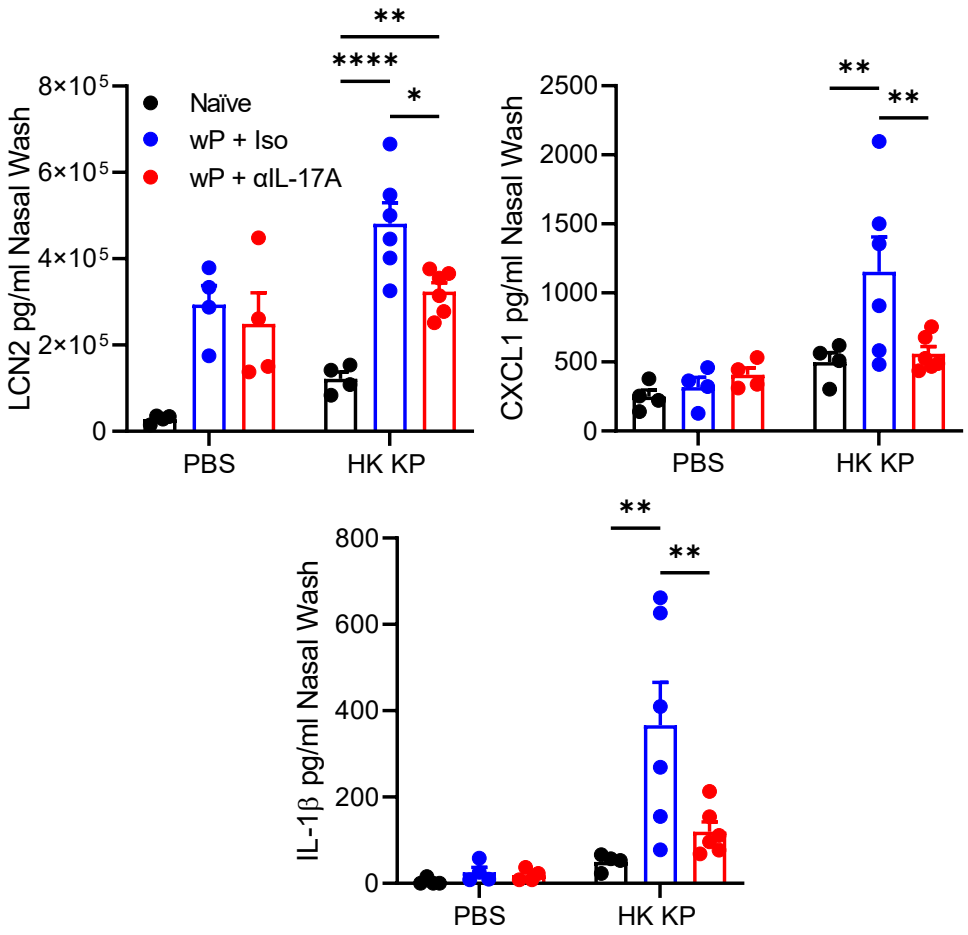

Figure 6.18 Neutralisation of IL-17A significantly reduces the concentration of LCN2, CXCL1, and IL-1β in the nasal wash of wP-immunised mice following heat-killed *K. pneumoniae* challenge.

C57BL/6 mice were immunised i.n. twice (0 and 4 weeks) with a wP vaccine (1/20th human dose). Mice were injected i.p. with a neutralising anti-IL-17A antibody (200 µg/mouse) or isotype control 2 weeks after the last immunisation. Heat-killed *K. pneumoniae* (HK KP; 10 µg/mouse) or PBS was administered i.n. to mice 24 hours later together with an additional dose of anti-IL-17A (50 µg/mouse) or isotype control. After 4 hours nasal washes were harvested and LCN2, CXCL1, and IL-1β concentrations were quantified by ELISA. Data are mean ± SEM (n=4-6 mice per group). *p < 0.05, **p < 0.01, ****p < 0.0001 naïve versus isotype versus anti-IL-17A treatment by two-way ANOVA followed by Tukey's post-test.

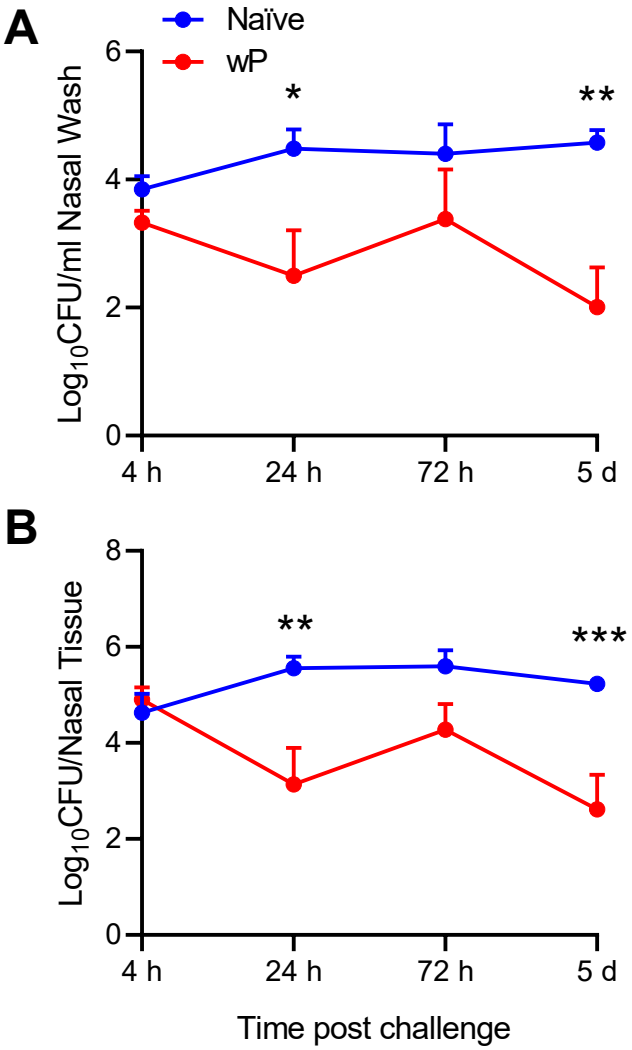

Figure 6.19 Intranasal immunisation with a wP vaccine significantly enhances clearance of *K. pneumoniae* from the nasal cavity.

C57BL/6 mice were immunised i.n. twice (0 and 4 weeks) with a wP vaccine (1/20th human dose) or with PBS as a control. Mice were infected with live *K. pneumoniae* i.n. (1x10^6 CFU/mouse) 2 weeks after the last immunisation. Nasal washes and nasal tissue were harvested from immunised mice and PBS-treated naïve control mice 4 h, 24 h, 72 h, and 5 days post challenge. The number of viable bacteria in the nasal wash (A) and digested nasal tissue (B) was estimated by performing CFU counts on serially diluted nasal washes and nasal homogenates from individual mice. Results are combined from two independent experiments. Results shown are mean ± SEM CFU counts (n=9-10 mice per group). *p < 0.05, **p < 0.01, ***p < 0.001 naïve versus immunised mice by two-way ANOVA followed by Sidak's post-test. Experiment conducted in collaboration with Dr. Jenny Mannion at Trinity Biomedical Sciences Institute, Trinity College Dublin.

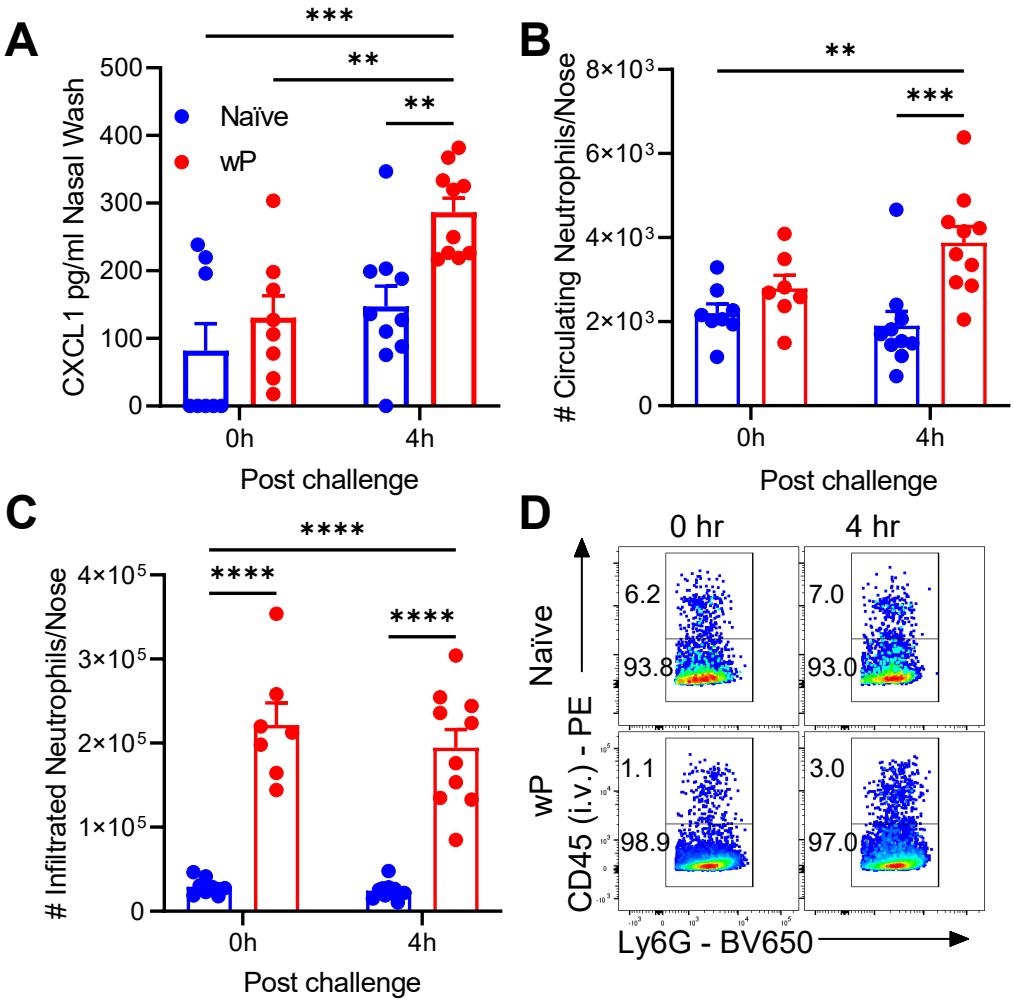

Figure 6.20 Mice immunised i.n. with a wP vaccine have enhanced CXCL1 concentration and circulating neutrophil numbers in the nasal cavity following live *K. pneumoniae* challenge.

C57BL/6 mice were immunised i.n. twice (0 and 4 weeks) with a wP vaccine (1/20th human dose). Immunised mice and naïve control mice were challenged with live *K. pneumoniae* i.n. (1x10^6 CFU/mouse) 2 weeks after the last immunisation. At the time of and 4 hours after *K. pneumoniae* challenge a fluorochrome-conjugated anti-CD45 antibody was administered i.v. and mice were euthanised 10 min later. Nasal washes were collected and concentration of CXCL1 was quantified by ELISA (A). Nasal tissue was harvested and mononuclear cells were isolated and stained for surface CD11b and Ly6G for analysis by flow cytometry. Absolute numbers of circulating (CD45 i.v.$^+$) (B) and tissue-infiltrated (CD45 i.v.$^-$) (C) neutrophils in the nasal cavity, with representative flow cytometry plots (D). Results are combined from two independent experiments. Results shown are mean ± SEM (n=7-10 mice per group). **$p < 0.01$, ***$p < 0.001$, ****$p < 0.0001$ by two-way ANOVA with Tukey's multiple comparisons test.

Chapter 7: General Discussion

7. General Discussion

Despite high vaccine coverage, whooping cough remains a major public health concern, with over 24 million pertussis cases and 160,700 deaths from pertussis estimated in children younger than 5 years in 2014. Pertussis is endemic in all countries and epidemic cycles occur every 2-5 years, even after the implementation of effective vaccination programmes [392]. Many industrialised countries introduced the aP vaccine in their paediatric immunisation schedule in the mid-1990s due to the frequency of local and systemic adverse events associated with use of the wP vaccine [17]. However, multiple outbreaks of pertussis have been reported in countries that use aP vaccines. There are a number of potential reasons for the resurgence of pertussis. These include improved diagnostic methodology and disease awareness, genetic evolution of circulating *B. pertussis* strains to escape vaccine-induced immunity, and waning immunity following vaccination [393]. However, emerging evidence suggests that current aP vaccines fail to induce sterilising immunity in the nasal cavity and this may contribute to asymptomatic transmission of *B. pertussis* amongst the general population [28]. It is clear that improved pertussis vaccines with the capacity to induce long-lasting mucosal immunity in the upper respiratory tract are required to prevent future pertussis outbreaks. However, in order to help inform the design of next-generation pertussis vaccines, the mechanisms of protective immunity against *B. pertussis* in the nasal mucosa must be understood.

Mathematical modelling, longitudinal surveillance studies, and non-human primate models have provided evidence of asymptomatic transmission of *B. pertussis*, indicating that the characteristic paroxysmal cough is not necessary for effective transmission of disease [28, 279, 394]. The relationship between nasal carriage and asymptomatic transmission has been described for multiple other pathogens, including *S. aureus, S. pneumoniae* and severe acute respiratory syndrome coronavirus 2 (SARS-CoV-2). Up to 30% of the human population are asymptomatically and permanently colonised with *S. aureus*, however *S. aureus* remains a frequent cause of serious infections with high morbidity, mortality, and healthcare-associated costs [395]. *S. pneumoniae* is a leading cause of community-acquired pneumonia, meningitis, and sinusitis. The transmission rate of *S. pneumoniae* is directly influenced by the carriage rate in a given population, with up to 70% of young children reported to carry *S. pneumoniae* in their nasopharynx [396, 397]. Furthermore, nasal carriage and asymptomatic transmission SARS-CoV-2 was a major contributing factor for the global spread of the COVID-19 pandemic, which has resulted in over 500 million infections globally with > 6 million deaths worldwide [398, 399]. When considering immunity to respiratory pathogens, the immune response in the nasal cavity has often been overlooked, however it is now clear that prevention of

infection at this site is critical for control of community acquired infections against a range of respiratory pathogens.

The generation of T_{RM} cells has been shown to be an essential aspect of long-term protective immunity at mucosal surfaces. Previous research from the Mills' lab has shown that protection against *B. pertussis* infection in the nasal cavity is associated with the induction of IL-17A-producing CD4 T_{RM} cells [194, 297]. The results from the current study demonstrated that IL-17A secreted by CD4 T_{RM} cells plays a critical role in clearance of *B. pertussis* from the nasal cavity following primary infection and is a key mediator of acquired immunity against secondary infection by promoting chemokine production and recruitment of Siglec-F$^+$ neutrophils to the nasal mucosa. IL-17-producing pathogen-specific CD4 T_{RM} cells accumulated in the nasal tissue during infection with *B. pertussis* and these T_{RM} cells expanded locally following re-infection with *B. pertussis*. Mice treated with a depleting anti-CD4 antibody or mice lacking IL-17A had significantly impaired clearance of a primary or secondary infection of the nose with *B. pertussis* and this was accompanied by reduced CXCL1 and delayed recruitment of Siglec-F$^+$ neutrophils.

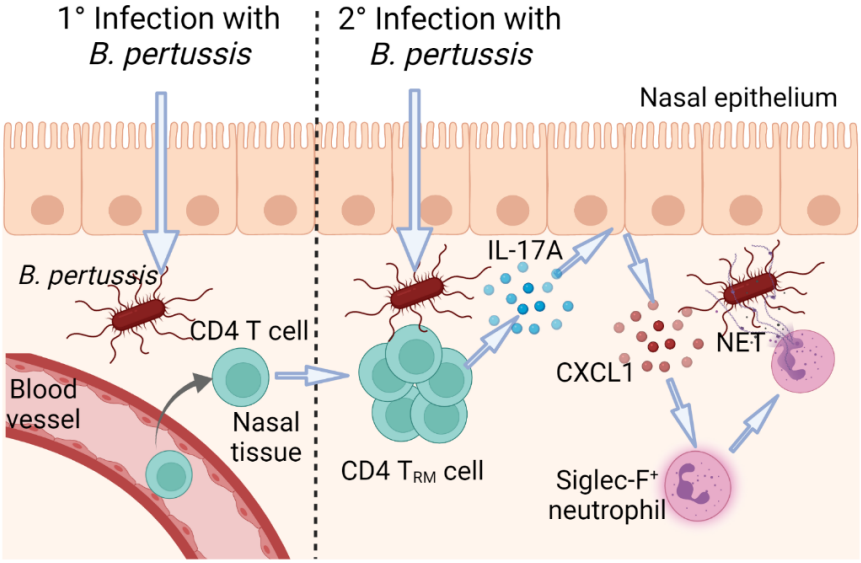

Figure 7.1 Proposed mechanism of how IL-17A-producing CD4 T_{RM} cells mediate acquired protective immunity against *B. pertussis* in the nasal cavity.

CD4 T_{RM} cells accumulate in the nasal tissue during a primary infection with *B. pertussis*. CD4 T_{RM} cells rapidly expand during a secondary infection with *B. pertussis* and produce IL-17A. IL-17A interacts with the IL-17R which is expressed on multiple cell types, including epithelial cells. Activation of the IL-17R induces CXCL1 secretion from epithelial cells, which promotes the recruitment of Siglec-F$^+$ neutrophils to the nasal mucosa. Siglec-F$^+$ neutrophils may contribute to clearance of *B. pertussis* from the nasal cavity by the formation of NETs.

During an inflammatory response to infection, IL-17A interacts with the IL-17R expressed on a range of non-immune cells, such as epithelial cells and mesothelial cells, to promote chemokine, AMP, and matrix metalloproteinase production. Chemokines subsequently promote the recruitment of other immune cells, such as neutrophils, to the site of inflammation where they contribute to pathogen clearance by a range of mechanisms including ROS production and NET formation [400]. Previous research from the Mills' lab showed increased mRNA expression of *Cxcl1* in the peritoneum tissue of mice following i.p. injection of IL-17A. Furthermore, mesothelial cells secreted CXCL1 when stimulated with IL-17A and this was enhanced by addition of TNF [307]. The results of the present study are in agreement with this, and demonstrated that i.n. administration of IL-17A induces increased *Cxcl1* mRNA expression in the nasal tissue.

IL-17A has been implicated in neutrophil recruitment in multiple infection models. Infection of IL-17A$^{-/-}$ mice with uropathogenic *E. coli* significantly reduced neutrophil recruitment to the bladder in a murine urinary tract infection model [401]. Moreover, systemic *C. albicans* challenge of mice with defective IL-17 receptor signalling was associated with reduced survival, increased fungal burden in the kidneys, and reduced mobilisation and influx of peripheral neutrophils into infected organs [402]. A role of IL-17A in neutrophil recruitment to the nasal tissues has also been described in humans. Increased numbers of IL-17A^{+} T cells were found in nasal polyp tissue from patients with chronic rhinosinusitis compared with tissues from healthy mucosa, and this correlated with enhanced neutrophil infiltration. Furthermore, homogenates from polyp tissues with high IL-17 promoted neutrophil migration *in vitro* [403]. In addition to promoting neutrophil mobilisation to the site of inflammation, IL-17A can act directly on human [404] and murine [307] neutrophils expressing IL-17RA, which is a common subunit shared by IL-17 receptors. IL-17A promotes the secretion of AMPs, including β-defensins, S100A8, and LCN2, from neutrophils in response to acute pathogen invasion [405]. Furthermore, IL-17A enhances intracellular killing of *B. pertussis* by neutrophils [146].

In the present study, Siglec-F^{+} neutrophil influx into the nasal cavity during *B. pertussis* infection mirrored the expansion of *B. pertussis*-specific CD4 T_{RM} cells in the nasal cavity and their recruitment was significantly reduced in the absence of IL-17A or CD4 T cells. Siglec-F^{+} neutrophils were recruited almost exclusively to the nasal tissue, with only a small expansion observed in the lungs during *B. pertussis* infection. Siglec-F^{+} neutrophils were not found in the NALT, spleen, or bone marrow. This is consistent with previous studies, which also failed to detect Siglec-F^{+} neutrophils in these tissues, nor were they detected in the peripheral blood, cLNs, colon, and small intestine [316, 318, 320]. Since neutrophils and eosinophil arose from a common granulocyte-monocyte progenitor

[406], it is possible that Siglec-F$^+$ neutrophils may be a hybrid neutrophil/eosinophil population. However, studies have demonstrated that Siglec-F$^+$ neutrophils expand in GATA-deficient mice which lack eosinophils, suggesting that Siglec-F$^+$ neutrophils are a distinct population from eosinophils [320, 407]. Furthermore, Matsui and colleagues demonstrated that Siglec-F$^+$ neutrophils induced in the nose in an allergic rhinitis model were morphologically similar to neutrophils, exhibiting a multi-lobed nucleus and lacked eosinophilic granules in the cytosol [316]. Purinergic receptor signalling has been implicated in Siglec-F expression by neutrophils, with adenosine 5'-triphosphate (ATP), a ubiquitous DAMP, sufficient to induce Siglec-F expression on lung neutrophils *in vivo* [317]. It is possible that ATP, or another DAMP, generated as a consequence of *B. pertussis* infection could promote Siglec-F expression on neutrophils entering the nasal cavity during infection. To our knowledge, this is the first study to describe a role of Siglec-F$^+$ neutrophils in protective immunity against infection with a bacterial pathogen. Siglec-F$^+$ neutrophils were found to have a greater capacity for NET formation, which may contribute to clearance of *B. pertussis* from the nasal cavity, however, more studies are required to establish a role of NETosis in *B. pertussis* infection. As results presented in this study demonstrated that Siglec-F$^+$ neutrophils directly contribute to clearance of *B. pertussis* from the nasal cavity, strategies to promote their recruitment should be considered in future vaccine design.

Animal models have proven to be an invaluable tool in the study of the immune response to *B. pertussis* infection and vaccination. *B. pertussis* is an obligate human pathogen that infects other species only under experimental conditions [408]. The primary aim of an animal model is to replicate the features of a human disease. Multiple *B. pertussis* animal models have been described, including rat, leporine, canine, and porcine models [408-410]. Non-human primate models come closest to recapitulating the characteristic clinical signs of pertussis observed in humans [409, 411]. Warfel and colleagues developed a baboon model which exhibits typical pertussis symptoms, including a paroxysmal cough, leucocytosis, and the development of a *B. pertussis*-specific T cell and humoral immune responses [176, 412]. A key feature of the baboon model is the capacity of *B. pertussis* to transmit from infected animals to naïve cage-mates, which is imperative when assessing vaccine efficacy [28]. However, a major disadvantage of using baboon models is the high housing costs, limited availability, and requirement of special facilities for biocontainment since *B. pertussis* is an airborne human pathogen [28]. Rhesus macaque models were used to study pertussis in the 1920s-1930s, however limited experimental details are available. A recent study by Jiang *et al.* described a model using infant rhesus macaques which developed typical whooping

cough, leucocytosis, and inter-animal transmission following aerosol infection with *B. pertussis*. Due to lower housing costs and increased availability, rhesus macaques are a promising alternative to baboons [413].

Mouse models are the most widely used model to study natural and vaccine induced immunity to *B. pertussis* [409]. Mouse models exhibit many features of the human disease, such as leucocytosis and immune suppression. The disease is persistent in mice, lasting 4-8 weeks. Clearance of *B. pertussis* from the respiratory tract is accompanied by a robust *B. pertussis*-specific immune response which mirrors that induced in humans following infection or immunisation [414]. Natural infection with *B. pertussis* or immunisation with a wP vaccine induces a Th1/Th17 immune response in humans, whereas immunisation with an aP vaccines was found to induce a predominant Th2 immune response [273-275]. This Th1/Th2 dichotomy following priming with a wP or an aP vaccine has been replicated in murine models [268], demonstrating that a mouse model can serve as a useful tool for studying natural and vaccine-induced immunity to *B. pertussis.* Mouse models provide additional benefits, such as the ease of obtaining samples to study cell populations, including T_{RM} cells, which are restricted to tissues not easily accessible in humans. Furthermore, the use of genetically modified mice or neutralising or depleting antibodies permit the study or specific immune mechanisms in a controlled manner. However, one major disadvantage of the mouse model is that mice infected with *B. pertussis* do not display the characteristic paroxysmal cough, as mice do not cough, and fail to transmit disease to other mice [408].

There is no standardised *B. pertussis* mouse model, with different mouse strains, such as BALB/c, C57BL/6, C3H/HeJ, NIH, Swiss, and white albino mice, used across studies [409]. However, the genetic background of mice used can greatly influence the immune response to *B. pertussis*, with BALB/c more prone to a Th2 response, whereas C57BL/6 mice are more prone to a Th1 response [415]. Furthermore, different routes of *B. pertussis* infection are also used. The intracerebral injection model, which results in lethal infection, was originally used as the gold standard to assess the potency of the wP vaccine [408]. However, i.n. administration or aerosol exposure are now the most common methods used for *B. pertussis* infection of mice. The i.n. method involves dropping a solution of bacteria on the nares of the mouse and waiting for it to inhale the bacteria, however considerable variability in this method has been reported [409, 414]. The aerosol challenge method utilises a nebulizer to deliver an aerosol of bacteria to mice in a confined chamber. The aerosol challenge method results in less variation in bacterial load administered and delivers the bacteria deeper into the lungs of mice [414]. Two recently published studies have described a method to recapitulate the catarrhal

stage of *B. pertussis* upper respiratory tract infection in mice. The early highly transmissible catarrhal stage of disease, which is characterised by non-specific symptoms such as nasal congestion, rhinorrhoea, and low-grade fever in humans, is bypassed in mouse models of *B. pertussis*. Both studies administered a low volume (5 µl) of *B. pertussis* i.n. to mice with defective TLR4 signalling. The rationale of using mice with defective TLR4 responses is that the modified lipo-oligosaccharides of *B. pertussis* are less stimulatory at the TLR4/MD2 receptor complexes in humans than in mice. This adaptation contributes to innate immune evasion by *B. pertussis* in humans and facilitates nasal colonisation. These studies reported nasopharyngeal colonisation with *B. pertussis*, accompanied by rhinosinusitis, bacterial shedding during the early stages of infection, and transmission to naïve co-housed mice [416, 417].

Furthermore, de Graaf and colleagues have reported asymptomatic colonisation with *B. pertussis* in a human challenge model. Healthy volunteers were i.n. inoculated with escalating doses of a fully virulent *B. pertussis* strain, with subjects subsequently treated with azithromycin from day 14 post challenge to limit development of symptoms [258]. An effective human challenge model may be beneficial in studying the early stages of infection and evaluating the effectiveness of next generation pertussis vaccines in preventing infection, overcoming limitations associated with animal models [418].

Animal models have highlighted that the induction of a Th17 response in the nasal cavity is required to induce sterilising immunity in the upper respiratory tract. The results from this study showed that neutralisation of IL-17A ablates protective immunity in the nasal cavity of mice primed by natural infection or by immunisation with a wP vaccine. Third generation pertussis vaccines currently in development are employing multiple strategies, such as adjusting adjuvant formulations or the use of OMVs, to induce IL-17A-producing CD4 T_{RM} cells in the nasal cavity [289, 291]. However, a simple yet effective solution could be modifying the route of vaccine delivery from the conventionally used i.m. route to the i.n. route. I.n. vaccines are less invasive and promote long-lasting mucosal immunity. I.m. injections elicit a systemic humoral reaction to a vaccine, mediated by B cells and antibody production [419]. As the nasal mucosa is often the initial site of infection, i.n. immunisation can generate an adaptive immune response similar to that seen following natural infection. It has been postulated that antigen localisation to the nasal mucosa during i.n. administration is required for the accumulation of protective T_{RM} at this site [37].

The results from this study demonstrated that i.n. immunisation with a wP vaccine was superior to i.p. delivery of the vaccine at inducing *B. pertussis*-specific IL-17A$^+$ CD4 T_{RM}

cells in the nasal mucosa and promoting rapid bacterial clearance from the nasal cavity. This is not exclusive to wP vaccines, with a study by Boehm and colleagues demonstrated that i.n. immunisation with an aP vaccine conferred enhanced bacterial clearance in the nasal cavity and this was accompanied by increased CD4 T_{RM} cell numbers and IL-17A production in the lungs [390]. However, the study by Boehm et al. did not examine the induction of CD4 T_{RM} cells in the nasal cavity. The induction of CD4 T_{RM} cells following i.n. vaccination has been demonstrated in other models. I.n. immunisation with a pneumococcal whole-cell vaccine was found to induce protective IL-17A-producing CD4 T_{RM} cells in the nasal mucosa, with protection against *S. pneumoniae* completely abrogated following treatment with a depleting anti-CD4 antibody [337]. I.n. vaccines are currently being developed for SARS-CoV-2, with a single dose of an i.n., but not an i.m., adenoviral-vectored trivalent COVID-19 vaccine shown to induce protective mucosal immunity against SAR-CoV2. Protection induced by the i.n. vaccine was associated with the generation of mucosal antibody responses and antigen-specific IFNγ^+ CD8 T_{RM} cells in the lungs [420].

In addition to providing enhanced localised protection in the nasal cavity, i.n. immunisation can also confer protection in distal mucosal sites, in line with the long-standing notion of the 'common mucosal immune system', whereby an immune response can be generated at a mucosal site following the administration of antigen to a distal mucosal site [421]. I.n. administration of an experimental HIV vaccine was found to induce an antigen-specific mucosal CD8 T cells and IgA and IgG responses in the genital tissue of mice [422]. Many i.n. vaccines are still in the developmental stages, however i.n. live attenuated influenza vaccines (LIAV) have been approved for use in multiple countries, with FluMist Quadrivalent available in the United States [423], and Fluenz Tetra approved for use in children aged 2 to 17 years in Ireland [424]. I.n. influenza vaccines are generally considered safe and efficacious, nonetheless adverse effects have been reported, with the withdrawal of the Nasaflu vaccine in Switzerland due to a strong link between the vaccine and development of Bell's palsy [425].

The present study demonstrated that CD4 T_{RM} cells generated following natural infection with *B. pertussis* or by i.n. immunisation with a wP vaccine could be activated in a bystander manner and produce IL-17A independent of TCR engagement. Non-specific IL-17A production was not apparent in CD4 T_{RM} cell generated by i.p. immunisation, suggesting that the priming of an immune response in the nasal tissue is necessary for this phenomenon. Bystander activation of CD4 T_{RM} cells was mediated by the Th17-polarising cytokines IL-1β, IL-23, and IL-18, and mirrored the mechanisms of activation of non-conventional lymphocytes, such as γδ T calls and ILC3s, which are also enriched

at mucosal barrier tissues [224, 227, 346]. As T_{RM} cells are embedded in sites frequently exposed to pathogens, bystander activation of CD4 T_{RM} cells may be beneficial to the host by enhancing local alarming functions and antimicrobial activity to help combat antigenically unrelated pathogens. Enhanced antimicrobial responses associated with bystander activation of nasal CD4 T_{RM} was observed in the current study, with increased neutrophil influx into the nasal cavity and AMP, cytokine, and chemokine production observed following exposure to an unrelated pathogen or a PAMP in mice previously infected with *B. pertussis* or primed with a wP vaccine. This enhanced 'innate syle' immune response was diminished following neutralisation of IL-17A, demonstrating that IL-17A generated during the bystander activation of CD4 T_{RM} cells contributes to this effect. These findings complement a study by Ge et al. which showed that non-specific IFNγ production by OVA-specific lung CD8 T_{RM} cells in response to heat-killed *S. aureus* or heat-killed Salmonella Typhimurium was accompanied by enhanced neutrophil recruitment to the lungs. Treatment with a depleting anti-CD8 antibody reversed this effect, showing that the enhanced neutrophil influx in response to an unrelated pathogen was dependent on bystander activation of pre-existing CD8 T_{RM} cells [348]. Due to their capacity to respond to previously encountered pathogens as well as unrelated pathogens, T_{RM} cells represent an important link between innate and adaptive responses at mucosal surfaces.

Results presented in this study demonstrated that CD4 T_{RM} cells induced following i.n. immunisation with a wP vaccine could produce non-specific IL-17A in response to heat-killed *K. pneumoniae*, and that i.n. priming with a wP vaccine conferred non-specific protection against a live infection with *K. pneumoniae*. These findings suggest that bystander activation of T_{RM} cells may be an underlying mechanism of vaccine-induced heterologous immunity. Heterologous immunity is the immune response that occurs in response to a pathogen if the host has previously been infected or immunised with an unrelated pathogen [426]. Non-specific protective effects have been observed for multiple vaccines, including BCG, smallpox, measles and oral polio vaccines [375]. In addition to potentially conferring protection against unrelated pathogens, heterologous immunity may also confer enhanced protection against circulating strains of pathogens that are constantly evolving to evade vaccine-induced immunity. Employing vaccine strategies that promote broader T cell responses may be of particular benefit in controlling the increasing incidence of pertussis. In contrast to the wP vaccine, which contains more than 3000 antigens, the aP vaccine contains no more than 5 purified *B. pertussis* antigens [9]. Since the introduction of the aP vaccine in the mid-1990s, circulating *B. pertussis* strains have evolved drastically, with many strains now lacking

expression of the aP vaccine component PRN [427]. The evolution of circulating *B. pertussis* strains to evade aP vaccine-induced immunity is thought to be one of the major contributing factor to increased pertussis incidence [428] . The findings presented in this study demonstrated that i.n. administration of a wP vaccine induced T_{RM} cells capable of broader, non-specific responses. The induction of broader T cell responses following i.n. administration of a vaccine has also been demonstrated with a live-attenuated influenza vaccine (FluMist). I.n. administration of a FluMist to mice was superior to the injectable version of the vaccine (Fluzone) at generating lung CD4 T_{RM} cells and virus specific CD8 T_{RM} cells which mediated heterosubtypic protection to multiple non-vaccine influenza strains [282]. Therefore, the route of administration and susceptibility of vaccine-induced CD4 T_{RM} to bystander activation should be considered in the development of next-generation pertussis vaccines.

In addition to enhancing their sensing and alarming functions, bystander activation of CD4 T_{RM} cells may be a potential mechanism by which these cells persist long-term in peripheral tissues in the absence of cognate antigens. Homeostatic cytokines such as IL-7 and IL-15 have been implicated in the maintenance of central and effector memory T cells, however the factors that maintain T_{RM} cells within tissues remain undefined [429]. There is emerging evidence that local inflammatory cues regulate the persistence of T_{RM} cells in peripheral tissues. A study by Bergsbaken et al. demonstrated that IL-12 and type I IFN produced by intestinal macrophages during a local infection was required for the maintenance of CD8 T_{RM} cells in the intestine [430]. Furthermore, chemokines such as CCL5 produced by a local network of macrophages have been implicated in the maintenance of vaginal CD4 T_{RM} cells [431]. Additionally, the persistence of lung CD4 T_{RM} cells induced following immunisation with heat-killed *K. pneumoniae* was shown to be mediated by IL-7 produced by lymphatic endothelial cells [210].

Current aP vaccines are inadequate at preventing outbreaks of pertussis due to their failure to induce sterilising immunity in the nasal cavity. There is a clear need for improved pertussis vaccines capable of inducing long-lasting mucosal immunity. The results from the current study have helped clarify the mechanisms of protective immunity against *B. pertussis* in the upper respiratory tract. The present study demonstrated that CD4 T_{RM} cells are key mediators of protective immunity in the nasal cavity. CD4 T_{RM} cells are the predominant source of IL-17A, which plays an essential role in clearance of *B. pertussis* from the nasal cavity during primary and secondary infection by promoting chemokine production and recruitment of Siglec-F^{+} neutrophils. Furthermore, results from the current study demonstrated CD4 T_{RM} cells induced following natural infection or immunisation are susceptible to bystander activation, highlighting an additional

mechanism by which these cells can be activated in the absence of TCR engagement. The data presented in this thesis suggests that next generation pertussis vaccines should employ strategies, such as i.n. immunisation, to promote the induction of IL-17-producing T_{RM} cells that recruit Siglec-F^{+} neutrophils in the nasal mucosa in order to generate long-lasting mucosal immunity required to control transmission of *B. pertussis*.

Chapter 8: Bibliography

1. Dias, W.O., et al., *An improved whole cell pertussis vaccine with reduced content of endotoxin.* Hum Vaccin Immunother, 2013. **9**(2): p. 339-48.
2. Cherry, J.D., *The History of Pertussis (Whooping Cough); 1906–2015: Facts, Myths, and Misconceptions.* Current Epidemiology Reports, 2015. **2**(2): p. 120-130.
3. Mattoo, S. and J.D. Cherry, *Molecular pathogenesis, epidemiology, and clinical manifestations of respiratory infections due to Bordetella pertussis and other Bordetella subspecies.* Clin Microbiol Rev, 2005. **18**(2): p. 326-82.
4. Dewan, K.K., et al., *Acellular Pertussis Vaccine Components: Today and Tomorrow.* Vaccines (Basel), 2020. **8**(2).
5. Pichichero, M.E., W.J. Hoeger, and J.R. Casey, *Azithromycin for the treatment of pertussis.* Pediatr Infect Dis J, 2003. **22**(9): p. 847-9.
6. WHO. *Pertussis*. 2022 [cited 2022 March 18]; Available from: https://www.who.int/health-topics/pertussis#tab=tab_1.
7. HSE, *Tdap Vaccination during Pregnancy - Frequently asked Questions for Health Professionals*. 2020.
8. Cherry, J.D., *Pertussis in the preantibiotic and prevaccine era, with emphasis on adult pertussis.* Clin Infect Dis, 1999. **28**(Suppl 2): p. S107-11.
9. Cherry, J.D., *The 112-Year Odyssey of Pertussis and Pertussis Vaccines-Mistakes Made and Implications for the Future.* J Pediatric Infect Dis Soc, 2019. **8**(4): p. 334-341.
10. Patterson, J., et al., *Adverse events following primary and secondary immunisation with whole-cell pertussis: a systematic review protocol.* BMJ Open, 2017. **7**(1): p. e012945.
11. Kulenkampff, M., J.S. Schwartzman, and J. Wilson, *Neurological complications of pertussis inoculation.* Arch Dis Child, 1974. **49**(1).
12. Bellman, M.H., E.M. Ross, and D.L. Miller, *Infantile spasms and pertussis immunisation.* Lancet, 1983. **321**(8332): p. 1031-1034.
13. Moore, D.L., et al., *Lack of evidence of encephalopathy related to pertussis vaccine: active surveillance by IMPACT, Canada, 1993-2002.* Pediatr Infect Dis J, 2004. **23**(6): p. 568-71.
14. Gale, J.L., et al., *Risk of serious acute neurological illness after immunization with diphtheria-tetanus-pertussis vaccine. A population-based case-control study.* JAMA, 1994. **271**(1): p. 37-41.
15. Sato, Y., M. Kimura, and H. Fukumi, *Development of a pertussis component vaccine in Japan.* Lancet, 1984. **1**(8369): p. 122-6.
16. WHO. *Immunization coverage*. 2022 [cited 2022 March 18]; Available from: https://www.who.int/news-room/fact-sheets/detail/immunization-coverage.
17. Esposito, S., et al., *Pertussis Prevention: Reasons for Resurgence, and Differences in the Current Acellular Pertussis Vaccines.* Front Immunol, 2019. **10**: p. 1344.
18. HPSC, *Pertussis in Ireland, 2012*. 2012.
19. Mooi, F.R., N.A. Van Der Maas, and H.E. De Melker, *Pertussis resurgence: waning immunity and pathogen adaptation - two sides of the same coin.* Epidemiol Infect, 2014. **142**(4): p. 685-94.
20. Wendelboe, A.M., et al., *Duration of immunity against pertussis after natural infection or vaccination.* Pediatr Infect Dis J, 2005. **24**(5 Suppl): p. S58-61.
21. Klein, N.P., et al., *Waning protection following 5 doses of a 3-component diphtheria, tetanus, and acellular pertussis vaccine.* Vaccine, 2017. **35**(26): p. 3395-3400.
22. Zerbo, O., et al., *Acellular Pertussis Vaccine Effectiveness Over Time.* Pediatrics, 2019. **144**(1).
23. Martin, S.W., et al., *Pertactin-negative Bordetella pertussis strains: evidence for a possible selective advantage.* Clin Infect Dis, 2015. **60**(2): p. 223-7.

24. Zeddeman, A., et al., *Investigations into the emergence of pertactin-deficient Bordetella pertussis isolates in six European countries, 1996 to 2012.* Euro Surveill, 2014. **19**(33): p. 20881.
25. Hegerle, N., et al., *Evolution of French Bordetella pertussis and Bordetella parapertussis isolates: increase of Bordetellae not expressing pertactin.* Clin Microbiol Infect, 2012. **18**(9): p. E340-6.
26. Lam, C., et al., *Rapid increase in pertactin-deficient Bordetella pertussis isolates, Australia.* Emerg Infect Dis, 2014. **20**(4): p. 626-33.
27. Otsuka, N., et al., *Prevalence and genetic characterization of pertactin-deficient Bordetella pertussis in Japan.* PLoS One, 2012. **7**(2): p. e31985.
28. Warfel, J.M., L.I. Zimmerman, and T.J. Merkel, *Acellular pertussis vaccines protect against disease but fail to prevent infection and transmission in a nonhuman primate model.* Proc Natl Acad Sci U S A, 2014. **111**(2): p. 787-92.
29. HPSC, *Annual Epidemiological Report for Pertussis: Pertussis in Ireland, 2018*. 2019.
30. Chaplin, D.D., *Overview of the immune response.* J Allergy Clin Immunol, 2010. **125**(2 Suppl 2): p. S3-23.
31. Medzhitov, R. and C.A.J. Janeway, *Innate immunity: impact on the adaptive immune response.* Curr Opin Immunol, 1997. **9**(1): p. 4-9.
32. Medzhitov, R., P. Preston-Hurlburt, and C.A.J. Janeway, *A human homologue of the Drosophila Toll protein signals activation of adaptive immunity.* Nature, 1997. **388**(6640): p. 394-7.
33. Amarante-Mendes, G.P., et al., *Pattern Recognition Receptors and the Host Cell Death Molecular Machinery.* Front Immunol, 2018. **9**: p. 2379.
34. Medzhitov, R., *Pattern recognition theory and the launch of modern innate immunity.* J Immunol, 2013. **191**(9): p. 4473-4.
35. Galeas-Pena, M., N. McLaughlin, and D. Pociask, *The role of the innate immune system on pulmonary infections.* Biol Chem, 2019. **400**(4): p. 443-456.
36. Barnes, M.G. and A.A. Weiss, *BrkA protein of Bordetella pertussis inhibits the classical pathway of complement after C1 deposition.* Infect Immun, 2001. **69**(5): p. 3067-72.
37. Nelson, S.A. and A.J. Sant, *Potentiating Lung Mucosal Immunity Through Intranasal Vaccination.* Front Immunol, 2021. **12**: p. 808527.
38. Vielle, N.J., et al., *The Human Upper Respiratory Tract Epithelium Is Susceptible to Flaviviruses.* Front Microbiol, 2019. **10**: p. 811.
39. Bustamante-Marin, X.M. and L.E. Ostrowski, *Cilia and Mucociliary Clearance.* Cold Spring Harb Perspect Biol, 2017. **9**(4).
40. Jongerius, I., et al., *Complement evasion by Bordetella pertussis: implications for improving current vaccines.* J Mol Med (Berl), 2015. **93**(4): p. 395-402.
41. Parker, D. and A. Prince, *Innate immunity in the respiratory epithelium.* Am J Respir Cell Mol Biol, 2011. **45**(2): p. 189-201.
42. Yougbare, I., et al., *Anti-FIM and Anti-FHA Antibodies Inhibit Bordetella pertussis Growth and Reduce Epithelial Cell Inflammation Through Bacterial Aggregation.* Front Immunol, 2020. **11**: p. 605273.
43. Belcher, C.E., et al., *The transcriptional responses of respiratory epithelial cells to Bordetella pertussis reveal host defensive and pathogen counter-defensive strategies.* Proc Natl Acad Sci U S A, 2000. **97**(25): p. 13847-52.
44. Malandra, A., et al., *Bordetella Adenylate Cyclase Toxin Elicits Airway Mucin Secretion through Activation of the cAMP Response Element Binding Protein.* Int J Mol Sci, 2021. **22**(16).
45. Hasan, S., et al., *Bordetella pertussis Adenylate Cyclase Toxin Disrupts Functional Integrity of Bronchial Epithelial Layers.* Infect Immun, 2018. **86**(3).

46. Lamberti, Y., et al., *Bordetella pertussis entry into respiratory epithelial cells and intracellular survival.* Pathog Dis, 2013. **69**(3): p. 194-204.
47. Huan, Y., et al., *Antimicrobial Peptides: Classification, Design, Application and Research Progress in Multiple Fields.* Front Microbiol, 2020. **11**: p. 582779.
48. Shah, N.R., R.E. Hancock, and R.C. Fernandez, *Bordetella pertussis lipid A glucosamine modification confers resistance to cationic antimicrobial peptides and increases resistance to outer membrane perturbation.* Antimicrob Agents Chemother, 2014. **58**(8): p. 4931-4.
49. Merle, N.S., et al., *Complement System Part I - Molecular Mechanisms of Activation and Regulation.* Front Immunol, 2015. **6**(262).
50. Barnes, M.G. and A.A. Weiss, *Activation of the complement cascade byBordetella pertussis.* FEMS Microbiology Letters, 2003. **220**(2): p. 271-275.
51. Dunkelberger, J.R. and W.C. Song, *Complement and its role in innate and adaptive immune responses.* Cell Res, 2010. **20**(1): p. 34-50.
52. Marr, N., R.A. Luu, and R.C. Fernandez, *Bordetella pertussis binds human C1 esterase inhibitor during the virulent phase, to evade complement-mediated killing.* J Infect Dis, 2007. **195**(4): p. 585-8.
53. Mayadas, T.N., X. Cullere, and C.A. Lowell, *The multifaceted functions of neutrophils.* Annu Rev Pathol, 2014. **9**: p. 181-218.
54. Rosales, C., *Neutrophil: A Cell with Many Roles in Inflammation or Several Cell Types?* Front Physiol, 2018. **9**: p. 113.
55. de Oliveira, S., E.E. Rosowski, and A. Huttenlocher, *Neutrophil migration in infection and wound repair: going forward in reverse.* Nat Rev Immunol, 2016. **16**(6): p. 378-91.
56. Manley, H.R., M.C. Keightley, and G.J. Lieschke, *The Neutrophil Nucleus: An Important Influence on Neutrophil Migration and Function.* Front Immunol, 2018. **9**: p. 2867.
57. Sollberger, G., D.O. Tilley, and A. Zychlinsky, *Neutrophil Extracellular Traps: The Biology of Chromatin Externalization.* Dev Cell, 2018. **44**(5): p. 542-553.
58. Cowland, J.B. and N. Borregaard, *Granulopoiesis and granules of human neutrophils.* Immunol Rev, 2016. **273**(1): p. 11-28.
59. Summers, C., et al., *Neutrophil kinetics in health and disease.* Trends Immunol, 2010. **31**(8): p. 318-24.
60. El-Benna, J., et al., *Priming of the neutrophil respiratory burst: role in host defense and inflammation.* Immunol Rev, 2016. **273**(1): p. 180-93.
61. Sawant, K.V., et al., *Chemokine CXCL1-Mediated Neutrophil Trafficking in the Lung: Role of CXCR2 Activation.* J Innate Immun, 2015. **7**(6): p. 647-58.
62. Ley, K., et al., *Getting to the site of inflammation: the leukocyte adhesion cascade updated.* Nat Rev Immunol, 2007. **7**(9): p. 678-89.
63. Lefort, C.T. and K. Ley, *Neutrophil arrest by LFA-1 activation.* Front Immunol, 2012. **3**: p. 157.
64. Alvites, R.D., et al., *The Nasal Cavity of the Rat and Mouse-Source of Mesenchymal Stem Cells for Treatment of Peripheral Nerve Injury.* Anat Rec (Hoboken), 2018. **301**(10): p. 1678-1689.
65. Tecchio, C., A. Micheletti, and M.A. Cassatella, *Neutrophil-derived cytokines: facts beyond expression.* Front Immunol, 2014. **5**: p. 508.
66. Nordenfelt, P. and H. Tapper, *Phagosome dynamics during phagocytosis by neutrophils.* J Leukoc Biol, 2011. **90**(2): p. 271-84.
67. Brinkmann, V., et al., *Neutrophil extracellular traps kill bacteria.* Science, 2004. **303**(5663): p. 1532-5.
68. Vorobjeva, N.V. and B.V. Chernyak, *NETosis: Molecular Mechanisms, Role in Physiology and Pathology.* Biochemistry (Mosc), 2020. **85**(10): p. 1178-1190.

69. Papayannopoulos, V. and A. Zychlinsky, *NETs: a new strategy for using old weapons.* Trends Immunol, 2009. **30**(11): p. 513-21.
70. Dancey, J.T., et al., *Neutrophil kinetics in man.* J Clin Invest, 1976. **58**(3): p. 705-15.
71. Pillay, J., et al., *In vivo labeling with 2H2O reveals a human neutrophil lifespan of 5.4 days.* Blood, 2010. **116**(4): p. 625-7.
72. Wang, J., *Neutrophils in tissue injury and repair.* Cell Tissue Res, 2018. **371**(3): p. 531-539.
73. Bratton, D.L. and P.M. Henson, *Neutrophil clearance: when the party is over, clean-up begins.* Trends Immunol, 2011. **32**(8): p. 350-7.
74. Eby, J.C., et al., *Review of the neutrophil response to Bordetella pertussis infection.* Pathog Dis, 2015. **73**(9): p. ftv081.
75. Kirimanjeswara, G.S., et al., *Pertussis toxin inhibits neutrophil recruitment to delay antibody-mediated clearance of Bordetella pertussis.* J Clin Invest, 2005. **115**(12): p. 3594-601.
76. Andreasen, C. and N.H. Carbonetti, *Role of neutrophils in response to Bordetella pertussis infection in mice.* Infect Immun, 2009. **77**(3): p. 1182-8.
77. Fedele, G., et al., *Invasion of Dendritic Cells, Macrophages and Neutrophils by the Bordetella Adenylate Cyclase Toxin: A Subversive Move to Fool Host Immunity.* Toxins (Basel), 2017. **9**(10).
78. do Vale, A., D. Cabanes, and S. Sousa, *Bacterial Toxins as Pathogen Weapons Against Phagocytes.* Front Microbiol, 2016. **7**: p. 42.
79. Guermonprez, P., et al., *The adenylate cyclase toxin of Bordetella pertussis binds to target cells via the alpha(M)beta(2) integrin (CD11b/CD18).* J Exp Med, 2001. **193**(9): p. 1035-44.
80. Confer, D.L. and J.W. Eaton, *Phagocyte impotence caused by an invasive bacterial adenylate cyclase.* Science, 1982. **217**(4563): p. 948-50.
81. Cerny, O., et al., *cAMP Signaling of Adenylate Cyclase Toxin Blocks the Oxidative Burst of Neutrophils through Epac-Mediated Inhibition of Phospholipase C Activity.* J Immunol, 2017. **198**(3): p. 1285-1296.
82. Eby, J.C., M.C. Gray, and E.L. Hewlett, *Cyclic AMP-mediated suppression of neutrophil extracellular trap formation and apoptosis by the Bordetella pertussis adenylate cyclase toxin.* Infect Immun, 2014. **82**(12): p. 5256-69.
83. Locht, C., L. Coutte, and N. Mielcarek, *The ins and outs of pertussis toxin.* FEBS J, 2011. **278**(23): p. 4668-82.
84. Andreasen, C. and N.H. Carbonetti, *Pertussis toxin inhibits early chemokine production to delay neutrophil recruitment in response to Bordetella pertussis respiratory tract infection in mice.* Infect Immun, 2008. **76**(11): p. 5139-48.
85. Rosenberg, H.F., K.D. Dyer, and P.S. Foster, *Eosinophils: changing perspectives in health and disease.* Nat Rev Immunol, 2013. **13**(1): p. 9-22.
86. Ondari, E., et al., *Eosinophils and Bacteria, the Beginning of a Story.* Int J Mol Sci, 2021. **22**(15).
87. LeMessurier, K.S. and A.E. Samarasinghe, *Eosinophils: Nemeses of Pulmonary Pathogens?* Curr Allergy Asthma Rep, 2019. **19**(8): p. 36.
88. DeChatelet, L.R., et al., *Comparison of intracellular bactericidal activities of human neutrophils and eosinophils.* Blood, 1978. **52**(3): p. 609-617.
89. Yousefi, S., et al., *Catapult-like release of mitochondrial DNA by eosinophils contributes to antibacterial defense.* Nat Med, 2008. **14**(9): p. 949-53.
90. Ueki, S., et al., *Eosinophil extracellular DNA trap cell death mediates lytic release of free secretion-competent eosinophil granules in humans.* Blood, 2013. **121**(11): p. 2074-83.

91. Rubin, K. and S. Glazer, *The pertussis hypothesis: Bordetella pertussis colonization in the etiology of asthma and diseases of allergic sensitization.* Med Hypotheses, 2018. **120**: p. 101-115.
92. Gestal, M.C., et al., *Disrupting Bordetella Immunosuppression Reveals a Role for Eosinophils in Coordinating the Adaptive Immune Response in the Respiratory Tract.* Microorganisms, 2020. **8**(11).
93. Wolf, A.A., et al., *The Ontogeny of Monocyte Subsets.* Front Immunol, 2019. **10**: p. 1642.
94. Ginhoux, F. and S. Jung, *Monocytes and macrophages: developmental pathways and tissue homeostasis.* Nat Rev Immunol, 2014. **14**(6): p. 392-404.
95. Geissmann, F., S. Jung, and D.R. Littman, *Blood Monocytes Consist of Two Principal Subsets with Distinct Migratory Properties.* Immunity, 2003. **19**(1): p. 71-82.
96. Guilliams, M., et al., *Dendritic cells, monocytes and macrophages: a unified nomenclature based on ontogeny.* Nat Rev Immunol, 2014. **14**(8): p. 571-8.
97. Schaeffer, L.M. and A.A. Weiss, *Pertussis toxin and lipopolysaccharide influence phagocytosis of Bordetella pertussis by human monocytes.* Infect Immun, 2001. **69**(12): p. 7635-41.
98. Ahmad, J.N., et al., *Bordetella Adenylate Cyclase Toxin Inhibits Monocyte-to-Macrophage Transition and Dedifferentiates Human Alveolar Macrophages into Monocyte-like Cells.* mBio, 2019. **10**(5).
99. Murray, P.J. and T.A. Wynn, *Protective and pathogenic functions of macrophage subsets.* Nat Rev Immunol, 2011. **11**(11): p. 723-37.
100. van Furth, R. and Z.A. Cohn, *The origin and kinetics of mononuclear phagocytes.* J Exp Med, 1968. **128**(3): p. 415-35.
101. Davies, L.C., et al., *Tissue-resident macrophages.* Nat Immunol, 2013. **14**(10): p. 986-95.
102. Allard, B., A. Panariti, and J.G. Martin, *Alveolar Macrophages in the Resolution of Inflammation, Tissue Repair, and Tolerance to Infection.* Front Immunol, 2018. **9**(1777).
103. Guilliams, M., et al., *Alveolar macrophages develop from fetal monocytes that differentiate into long-lived cells in the first week of life via GM-CSF.* J Exp Med, 2013. **210**(10): p. 1977-92.
104. Hu, G. and J.W. Christman, *Editorial: Alveolar Macrophages in Lung Inflammation and Resolution.* Front Immunol, 2019. **10**: p. 2275.
105. Schyns, J., F. Bureau, and T. Marichal, *Lung Interstitial Macrophages: Past, Present, and Future.* J Immunol Res, 2018. **2018**: p. 5160794.
106. Bernard, N.J., et al., *A critical role for the TLR signaling adapter Mal in alveolar macrophage-mediated protection against Bordetella pertussis.* Mucosal Immunol, 2015. **8**(5): p. 982-92.
107. Carbonetti, N.H., et al., *Pertussis toxin targets airway macrophages to promote Bordetella pertussis infection of the respiratory tract.* Infect Immun, 2007. **75**(4): p. 1713-20.
108. Coleman, M.M., et al., *Alveolar macrophages contribute to respiratory tolerance by inducing FoxP3 expression in naive T cells.* Am J Respir Cell Mol Biol, 2013. **48**(6): p. 773-80.
109. Li, Z., et al., *FOXP3+ regulatory T cells and their functional regulation.* Cell Mol Immunol, 2015. **12**(5): p. 558-65.
110. Mills, K.H., et al., *Cell-mediated immunity to Bordetella pertussis: role of Th1 cells in bacterial clearance in a murine respiratory infection model.* Infect Immun, 1993. **61**(2): p. 399-410.
111. McGuirk, P. and K.H. Mills, *Direct anti-inflammatory effect of a bacterial virulence factor: IL-10-dependent suppression of IL-12 production by filamentous hemagglutinin from Bordetella pertussis.* Eur J Immunol, 2000. **30**(2): p. 415-22.

112. Hellwig, S.M., et al., *Evidence for an intracellular niche for Bordetella pertussis in broncho-alveolar lavage cells of mice.* FEMS Immunol Med Microbiol, 1999. **26**(3-4): p. 203-7.
113. Friedman, R.L., et al., *Uptake and intracellular survival of Bordetella pertussis in human macrophages.* Infect Immun, 1992. **60**(11): p. 4578-85.
114. Cabeza-Cabrerizo, M., et al., *Dendritic Cells Revisited.* Annu Rev Immunol, 2021. **39**: p. 131-166.
115. Musumeci, A., et al., *What Makes a pDC: Recent Advances in Understanding Plasmacytoid DC Development and Heterogeneity.* Front Immunol, 2019. **10**: p. 1222.
116. Joffre, O., et al., *Inflammatory signals in dendritic cell activation and the induction of adaptive immunity.* Immunol Rev, 2009. **227**(1): p. 234-47.
117. Dalod, M., et al., *Dendritic cell maturation: functional specialization through signaling specificity and transcriptional programming.* EMBO J, 2014. **33**(10): p. 1104-16.
118. Steinman, R.M. and Z.A. Cohn, *Identification of a novel cell type in peripheral lymphoid organs of mice. I. Morphology, quantitation, tissue distribution.* J Exp Med, 1973. **137**(5): p. 1142-62.
119. Worbs, T., S.I. Hammerschmidt, and R. Forster, *Dendritic cell migration in health and disease.* Nat Rev Immunol, 2017. **17**(1): p. 30-48.
120. Swiecki, M. and M. Colonna, *The multifaceted biology of plasmacytoid dendritic cells.* Nat Rev Immunol, 2015. **15**(8): p. 471-85.
121. Hampton, H.R. and T. Chtanova, *Lymphatic Migration of Immune Cells.* Front Immunol, 2019. **10**: p. 1168.
122. Dunne, P.J., et al., *CD11c+CD8alpha+ dendritic cells promote protective immunity to respiratory infection with Bordetella pertussis.* J Immunol, 2009. **183**(1): p. 400-10.
123. Janeway, C.A., Jr. , et al., *Immunobiology: The Immune System in Health and Disease. 5th edition*. 2001, New York: Garland Science.
124. Andersen, M.H., et al., *Cytotoxic T cells.* J Invest Dermatol, 2006. **126**(1): p. 32-41.
125. Redhead, K., et al., *Effective immunization against Bordetella pertussis respiratory infection in mice is dependent on induction of cell-mediated immunity.* Infect Immun, 1993. **61**(8): p. 3190-8.
126. Tai, Y., et al., *Molecular Mechanisms of T Cells Activation by Dendritic Cells in Autoimmune Diseases.* Front Pharmacol, 2018. **9**: p. 642.
127. Embgenbroich, M. and S. Burgdorf, *Current Concepts of Antigen Cross-Presentation.* Front Immunol, 2018. **9**(1643).
128. Mariuzza, R.A., P. Agnihotri, and J. Orban, *The structural basis of T-cell receptor (TCR) activation: An enduring enigma.* J Biol Chem, 2020. **295**(4): p. 914-925.
129. Birnbaum, M.E., et al., *Molecular architecture of the alphabeta T cell receptor-CD3 complex.* Proc Natl Acad Sci U S A, 2014. **111**(49): p. 17576-81.
130. Lafferty, K.J., L. Andrus, and S.J. Prowse, *Role of lymphokine and antigen in the control of specific T cell responses.* Immunol Rev, 1980. **51**(279-314).
131. Sharpe, A.H., *Mechanisms of costimulation.* Immunol Rev, 2009. **229**(1): p. 5-11.
132. Frauwirth, K.A. and C.B. Thompson, *Activation and inhibition of lymphocytes by costimulation.* Journal of Clinical Investigation, 2002. **109**(3): p. 295-299.
133. Halle, S., O. Halle, and R. Forster, *Mechanisms and Dynamics of T Cell-Mediated Cytotoxicity In Vivo.* Trends Immunol, 2017. **38**(6): p. 432-443.
134. Zhang, N. and M.J. Bevan, *CD8(+) T cells: foot soldiers of the immune system.* Immunity, 2011. **35**(2): p. 161-8.
135. Dirix, V., et al., *Both CD4(+) and CD8(+) lymphocytes participate in the IFN-gamma response to filamentous hemagglutinin from Bordetella pertussis in infants, children, and adults.* Clin Dev Immunol, 2012. **2012**: p. 795958.

136. Luckheeram, R.V., et al., *CD4(+)T cells: differentiation and functions.* Clin Dev Immunol, 2012. **2012**: p. 925135.
137. Ruterbusch, M., et al., *In Vivo CD4(+) T Cell Differentiation and Function: Revisiting the Th1/Th2 Paradigm.* Annu Rev Immunol, 2020. **38**: p. 705-725.
138. Geginat, J., et al., *Plasticity of human CD4 T cell subsets.* Front Immunol, 2014. **5**: p. 630.
139. Trinchieri, G., S. Pflanz, and R.A. Kastelein, *The IL-12 family of heterodimeric cytokines: new players in the regulation of T cell responses.* Immunity, 2003. **19**(5): p. 641-4.
140. Afkarian, M., et al., *T-bet is a STAT1-induced regulator of IL-12R expression in naive CD4+ T cells.* Nat Immunol, 2002. **3**(6): p. 549-57.
141. Teng, M.W., et al., *IL-12 and IL-23 cytokines: from discovery to targeted therapies for immune-mediated inflammatory diseases.* Nat Med, 2015. **21**(7): p. 719-29.
142. Fedele, G., et al., *Bordetella pertussis-infected human monocyte-derived dendritic cells undergo maturation and induce Th1 polarization and interleukin-23 expression.* Infect Immun, 2005. **73**(3): p. 1590-7.
143. Spensieri, F., et al., *Bordetella pertussis inhibition of interleukin-12 (IL-12) p70 in human monocyte-derived dendritic cells blocks IL-12 p35 through adenylate cyclase toxin-dependent cyclic AMP induction.* Infect Immun, 2006. **74**(5): p. 2831-8.
144. Ryan, M., et al., *Bordetella pertussis respiratory infection in children is associated with preferential activation of type 1 T helper cells.* J Infect Dis, 1997. **175**(5): p. 1246-50.
145. Mascart, F., et al., *Bordetella pertussis infection in 2-month-old infants promotes type 1 T cell responses.* J Immunol, 2003. **170**(3): p. 1504-9.
146. Ross, P.J., et al., *Relative contribution of Th1 and Th17 cells in adaptive immunity to Bordetella pertussis: towards the rational design of an improved acellular pertussis vaccine.* PLoS Pathog, 2013. **9**(4): p. e1003264.
147. Barbic, J., et al., *Role of gamma interferon in natural clearance of Bordetella pertussis infection.* Infect Immun, 1997. **65**(12): p. 4904-8.
148. Mahon, B.P., et al., *Atypical disease after Bordetella pertussis respiratory infection of mice with targeted disruptions of interferon-gamma receptor or immunoglobulin mu chain genes.* J Exp Med, 1997. **186**(11): p. 1843-51.
149. Kak, G., M. Raza, and B.K. Tiwari, *Interferon-gamma (IFN-gamma): Exploring its implications in infectious diseases.* Biomol Concepts, 2018. **9**(1): p. 64-79.
150. Mahon, B.P. and K.H. Mills, *Interferon-gamma mediated immune effector mechanisms against Bordetella pertussis.* Immunol Lett, 1999. **68**(2-3): p. 213-7.
151. Huang, G., Y. Wang, and H. Chi, *Regulation of TH17 cell differentiation by innate immune signals.* Cell Mol Immunol, 2012. **9**(4): p. 287-95.
152. Ivanov, II, et al., *The orphan nuclear receptor RORgammat directs the differentiation program of proinflammatory IL-17+ T helper cells.* Cell, 2006. **126**(6): p. 1121-33.
153. Yang, X.O., et al., *T helper 17 lineage differentiation is programmed by orphan nuclear receptors ROR alpha and ROR gamma.* Immunity, 2008. **28**(1): p. 29-39.
154. Veldhoen, M., et al., *TGFbeta in the context of an inflammatory cytokine milieu supports de novo differentiation of IL-17-producing T cells.* Immunity, 2006. **24**(2): p. 179-89.
155. Bettelli, E., et al., *Reciprocal developmental pathways for the generation of pathogenic effector TH17 and regulatory T cells.* Nature, 2006. **441**(7090): p. 235-8.
156. Volpe, E., et al., *A critical function for transforming growth factor-beta, interleukin 23 and proinflammatory cytokines in driving and modulating human T(H)-17 responses.* Nat Immunol, 2008. **9**(6): p. 650-7.
157. Nurieva, R., et al., *Essential autocrine regulation by IL-21 in the generation of inflammatory T cells.* Nature, 2007. **448**(7152): p. 480-3.
158. McGeachy, M.J., et al., *The interleukin 23 receptor is essential for the terminal differentiation of interleukin 17-producing effector T helper cells in vivo.* Nat Immunol, 2009. **10**(3): p. 314-24.

159. Chen, K. and J.K. Kolls, *Interluekin-17A (IL17A).* Gene, 2017. **614**: p. 8-14.
160. Gu, C., L. Wu, and X. Li, *IL-17 family: cytokines, receptors and signaling.* Cytokine, 2013. **64**(2): p. 477-85.
161. Gaffen, S.L., *Structure and signalling in the IL-17 receptor family.* Nat Rev Immunol, 2009. **9**(8): p. 556-67.
162. Chang, S.H. and C. Dong, *A novel heterodimeric cytokine consisting of IL-17 and IL-17F regulates inflammatory responses.* Cell Res, 2007. **17**(5): p. 435-40.
163. Herjan, T., et al., *IL-17-receptor-associated adaptor Act1 directly stabilizes mRNAs to mediate IL-17 inflammatory signaling.* Nat Immunol, 2018. **19**(4): p. 354-365.
164. Chang, S.H. and C. Dong, *Signaling of interleukin-17 family cytokines in immunity and inflammation.* Cell Signal, 2011. **23**(7): p. 1069-75.
165. Ye, P., et al., *Requirement of interleukin 17 receptor signaling for lung CXC chemokine and granulocyte colony-stimulating factor expression, neutrophil recruitment, and host defense.* J Exp Med, 2001. **194**(4): p. 519-27.
166. Cho, J.S., et al., *IL-17 is essential for host defense against cutaneous Staphylococcus aureus infection in mice.* J Clin Invest, 2010. **120**(5): p. 1762-73.
167. Huang, W., et al., *Requirement of interleukin-17A for systemic anti-Candida albicans host defense in mice.* J Infect Dis, 2004. **190**(3): p. 624-31.
168. Schwarzenberger, P., et al., *IL-17 stimulates granulopoiesis in mice: use of an alternate, novel gene therapy-derived method for in vivo evaluation of cytokines.* J Immunol, 1998. **161**(11): p. 6383-9.
169. Yu, J.J., et al., *An essential role for IL-17 in preventing pathogen-initiated bone destruction: recruitment of neutrophils to inflamed bone requires IL-17 receptor-dependent signals.* Blood, 2007. **109**(9): p. 3794-802.
170. Jones, C.E. and K. Chan, *nterleukin-17 stimulates the expression of interleukin-8, growth-related oncogene-alpha, and granulocyte-colony-stimulating factor by human airway epithelial cells.* Am J Respir Cell Mol Biol, 2002. **26**(6): p. 748-53.
171. Shen, F., et al., *Identification of common transcriptional regulatory elements in interleukin-17 target genes.* J Biol Chem, 2006. **281**(34): p. 24138-48.
172. Flo, T.H., et al., *Lipocalin 2 mediates an innate immune response to bacterial infection by sequestrating iron.* Nature, 2004. **432**(7019): p. 917-21.
173. Kao, C.Y., et al., *IL-17 markedly up-regulates beta-defensin-2 expression in human airway epithelium via JAK and NF-kappaB signaling pathways.* J Immunol, 2004. **173**(5): p. 3482-91.
174. Dunne, A., et al., *Inflammasome activation by adenylate cyclase toxin directs Th17 responses and protection against Bordetella pertussis.* J Immunol, 2010. **185**(3): p. 1711-9.
175. Andreasen, C., D.A. Powell, and N.H. Carbonetti, *Pertussis toxin stimulates IL-17 production in response to Bordetella pertussis infection in mice.* PLoS One, 2009. **4**(9): p. e7079.
176. Warfel, J.M. and T.J. Merkel, *Bordetella pertussis infection induces a mucosal IL-17 response and long-lived Th17 and Th1 immune memory cells in nonhuman primates.* Mucosal Immunol, 2013. **6**(4): p. 787-96.
177. Walker, J.A. and A.N.J. McKenzie, *TH2 cell development and function.* Nat Rev Immunol, 2018. **18**(2): p. 121-133.
178. Zhu, J., *T helper 2 (Th2) cell differentiation, type 2 innate lymphoid cell (ILC2) development and regulation of interleukin-4 (IL-4) and IL-13 production.* Cytokine, 2015. **75**(1): p. 14-24.
179. McGuirk, P. and K.H. Mills, *A regulatory role for interleukin 4 in differential inflammatory responses in the lung following infection of mice primed with Th1- or Th2-inducing pertussis vaccines.* Infect Immun, 2000. **68**(3).

180. Debock, I. and V. Flamand, *Unbalanced Neonatal CD4(+) T-Cell Immunity.* Front Immunol, 2014. **5**: p. 393.
181. Sojka, D.K., Y.H. Huang, and D.J. Fowell, *Mechanisms of regulatory T-cell suppression - a diverse arsenal for a moving target.* Immunology, 2008. **124**(1): p. 13-22.
182. Brady, M.T., et al., *Fasciola hepatica suppresses a protective Th1 response against Bordetella pertussis.* Infect Immun, 1999. **67**(10): p. 5372-8.
183. Schmitt, E.G. and C.B. Williams, *Generation and function of induced regulatory T cells.* Front Immunol, 2013. **4**: p. 152.
184. Vignali, D.A., L.W. Collison, and C.J. Workman, *How regulatory T cells work.* Nat Rev Immunol, 2008. **8**(7): p. 523-32.
185. Romano, M., et al., *Past, Present, and Future of Regulatory T Cell Therapy in Transplantation and Autoimmunity.* Front Immunol, 2019. **10**: p. 43.
186. Chen, W., et al., *Conversion of peripheral CD4+CD25- naive T cells to CD4+CD25+ regulatory T cells by TGF-beta induction of transcription factor Foxp3.* J Exp Med, 2003. **198**(12): p. 1875-86.
187. Walker, L.S., *Treg and CTLA-4: two intertwining pathways to immune tolerance.* J Autoimmun, 2013. **45**: p. 49-57.
188. McGuirk, P., C. McCann, and K.H. Mills, *Pathogen-specific T regulatory 1 cells induced in the respiratory tract by a bacterial molecule that stimulates interleukin 10 production by dendritic cells: a novel strategy for evasion of protective T helper type 1 responses by Bordetella pertussis.* J Exp Med, 2002. **195**(2): p. 221-31.
189. Coleman, M.M., et al., *The immunoregulatory role of CD4(+) FoxP3(+) CD25(-) regulatory T cells in lungs of mice infected with Bordetella pertussis.* FEMS Immunol Med Microbiol, 2012. **64**(3): p. 413-24.
190. Higgins, S.C., et al., *Toll-like receptor 4-mediated innate IL-10 activates antigen-specific regulatory T cells and confers resistance to Bordetella pertussis by inhibiting inflammatory pathology.* J Immunol, 2003. **171**(6): p. 3119-27.
191. Crotty, S., *T follicular helper cell differentiation, function, and roles in disease.* Immunity, 2014. **41**(4): p. 529-42.
192. Krishnaswamy, J.K., et al., *Determination of T Follicular Helper Cell Fate by Dendritic Cells.* Front Immunol, 2018. **9**: p. 2169.
193. Farber, D.L., et al., *Immunological memory: lessons from the past and a look to the future.* Nat Rev Immunol, 2016. **16**(2): p. 124-8.
194. Wilk, M.M., et al., *Immunization with whole cell but not acellular pertussis vaccines primes CD4 TRM cells that sustain protective immunity against nasal colonization with Bordetella pertussis.* Emerg Microbes Infect, 2019. **8**(1): p. 169-185.
195. MacLeod, M.K., et al., *CD4 memory T cells: what are they and what can they do?* Semin Immunol, 2009. **21**(2): p. 53-61.
196. Pepper, M. and M.K. Jenkins, *Origins of CD4(+) effector and central memory T cells.* Nat Immunol, 2011. **12**(6): p. 467-71.
197. Sallusto, F., et al., *Two subsets of memory T lymphocytes with distinct homing potentials and effector functions.* Nature, 1999. **401**(6754): p. 708-12.
198. Sallusto, F., J. Geginat, and A. Lanzavecchia, *Central memory and effector memory T cell subsets: function, generation, and maintenance.* Annu Rev Immunol, 2004. **22**: p. 745-63.
199. Carbone, F.R., *Tissue-Resident Memory T Cells and Fixed Immune Surveillance in Nonlymphoid Organs.* J Immunol, 2015. **195**(1): p. 17-22.
200. Masopust, D., et al., *Preferential localization of effector memory cells in nonlymphoid tissue.* Science, 2001. **291**: p. 2413-7.
201. Klonowski, K.D., et al., *Dynamics of blood-borne CD8 memory T cell migration in vivo.* Immunity, 2004. **20**(5): p. 551-62.

202. Nguyen, Q.P., et al., *Origins of CD4(+) circulating and tissue-resident memory T-cells.* Immunology, 2019. **157**(1): p. 3-12.
203. Anderson, K.G., et al., *Intravascular staining for discrimination of vascular and tissue leukocytes.* Nat Protoc, 2014. **9**(1): p. 209-22.
204. Mackay, L.K., et al., *Cutting edge: CD69 interference with sphingosine-1-phosphate receptor function regulates peripheral T cell retention.* J Immunol, 2015. **194**(5): p. 2059-63.
205. Matloubian, M., et al., *Lymphocyte egress from thymus and peripheral lymphoid organs is dependent on S1P receptor 1.* Nature, 2004. **427**(6972): p. 355-60.
206. Teijaro, J.R., et al., *Cutting edge: Tissue-retentive lung memory CD4 T cells mediate optimal protection to respiratory virus infection.* J Immunol, 2011. **187**(11): p. 5510-4.
207. Glennie, N.D., et al., *Skin-resident memory CD4+ T cells enhance protection against Leishmania major infection.* J Exp Med, 2015. **212**(9): p. 1405-14.
208. Romagnoli, P.A., et al., *Differentiation of distinct long-lived memory CD4 T cells in intestinal tissues after oral Listeria monocytogenes infection.* Mucosal Immunol, 2017. **10**(2): p. 520-530.
209. Shin, H. and A. Iwasaki, *A vaccine strategy that protects against genital herpes by establishing local memory T cells.* Nature, 2012. **491**(7424): p. 463-7.
210. Amezcua Vesely, M.C., et al., *Effector TH17 Cells Give Rise to Long-Lived TRM Cells that Are Essential for an Immediate Response against Bacterial Infection.* Cell, 2019. **178**(5): p. 1176-1188 e15.
211. Kumar, B.V., et al., *Human Tissue-Resident Memory T Cells Are Defined by Core Transcriptional and Functional Signatures in Lymphoid and Mucosal Sites.* Cell Rep, 2017. **20**(12): p. 2921-2934.
212. Snyder, M.E., et al., *Generation and persistence of human tissue-resident memory T cells in lung transplantation.* Sci Immunol, 2019. **4**(33): p. eaav5581.
213. Watanabe, R., et al., *Human skin is protected by four functionally and phenotypically discrete populations of resident and recirculating memory T cells.* Sci Transl Med, 2015. **7**(279): p. 279ra39.
214. Clark, R.A., et al., *Skin effector memory T cells do not recirculate and provide immune protection in alemtuzumab-treated CTCL patients.* Sci Transl Med, 2012. **18**(117): p. 117ra7.
215. Blanc, C.A., et al., *Sphingosine-1-phosphate receptor antagonism enhances proliferation and migration of engrafted neural progenitor cells in a model of viral-induced demyelination.* Am J Pathol, 2015. **185**(10): p. 2819-32.
216. Wilk, M.M., et al., *Lung CD4 Tissue-Resident Memory T Cells Mediate Adaptive Immunity Induced by Previous Infection of Mice with Bordetella pertussis.* J Immunol, 2017. **199**(1): p. 233-243.
217. Dubois, V., et al., *Suppression of mucosal Th17 memory responses by acellular pertussis vaccines enhances nasal Bordetella pertussis carriage.* NPJ Vaccines, 2021. **6**(1): p. 6.
218. Tomas, J., et al., *PTX Instructs the Development of Lung-Resident Memory T Cells in Bordetella pertussis Infected Mice.* Toxins (Basel), 2021. **13**(9).
219. Kotas, M.E. and R.M. Locksley, *Why Innate Lymphoid Cells?* Immunity, 2018. **48**(6): p. 1081-1090.
220. Chien, Y.H., C. Meyer, and M. Bonneville, *gammadelta T cells: first line of defense and beyond.* Annu Rev Immunol, 2014. **32**: p. 121-55.
221. Van Kaer, L., et al., *Innate, innate-like and adaptive lymphocytes in the pathogenesis of MS and EAE.* Cell Mol Immunol, 2019. **16**(6): p. 531-539.
222. Sutton, C., et al., *A crucial role for interleukin (IL)-1 in the induction of IL-17-producing T cells that mediate autoimmune encephalomyelitis.* J Exp Med, 2006. **203**(7): p. 1685-91.

223. Lalor, S.J., et al., *Caspase-1-processed cytokines IL-1beta and IL-18 promote IL-17 production by gammadelta and CD4 T cells that mediate autoimmunity.* J Immunol, 2011. **186**(10): p. 5738-48.
224. Sutton, C.E., et al., *Interleukin-1 and IL-23 induce innate IL-17 production from gammadelta T cells, amplifying Th17 responses and autoimmunity.* Immunity, 2009. **31**(2): p. 331-41.
225. Ribot, J.C., N. Lopes, and B. Silva-Santos, *gammadelta T cells in tissue physiology and surveillance.* Nat Rev Immunol, 2021. **21**(4): p. 221-232.
226. Bertotto, A., et al., *Gamma delta T cells are decreased in the blood of children with Bordetella pertussis infection.* Acta Paediatr, 1997. **86**(1): p. 114-5.
227. Misiak, A., et al., *IL-17-Producing Innate and Pathogen-Specific Tissue Resident Memory gammadelta T Cells Expand in the Lungs of Bordetella pertussis-Infected Mice.* J Immunol, 2017. **198**(1): p. 363-374.
228. Abel AM, et al., *Natural Killer Cells: Development, Maturation, and Clinical Utilization.* Front Immunol, 2018. **9**(1869).
229. Byrne, P., et al., *Depletion of NK cells results in disseminating lethal infection with Bordetella pertussis associated with a reduction of antigen-specific Th1 and enhancement of Th2, but not Tr1 cells.* Eur J Immunol, 2004. **34**(9): p. 2579-88.
230. den Hartog, G., et al., *Bordetella pertussis induces IFN-gamma production by NK cells resulting in chemo-attraction by respiratory epithelial cells.* J Infect Dis, 2020.
231. Kroes, M.M., et al., *Activation of Human NK Cells by Bordetella pertussis Requires Inflammasome Activation in Macrophages.* Front Immunol, 2019. **10**: p. 2030.
232. Whiteside, S.K., et al., *Bystander T Cells: A Balancing Act of Friends and Foes.* Trends Immunol, 2018. **39**(12): p. 1021-1035.
233. Lee, H.G., M.Z. Cho, and J.M. Choi, *Bystander CD4(+) T cells: crossroads between innate and adaptive immunity.* Exp Mol Med, 2020. **52**(8): p. 1255-1263.
234. Tough, D.F., P. Borrow, and J. Sprent, *Induction of bystander T cell proliferation by viruses and type I interferon in vivo.* Science, 1996. **272**(5270): p. 1947-50.
235. Tough, D.F., S. Sun, and J. Sprent, *T cell stimulation in vivo by lipopolysaccharide (LPS).* J Exp Med, 1997. **185**(12): p. 2089-94.
236. Alves, N.L., et al., *IL-15 induces antigen-independent expansion and differentiation of human naive CD8+ T cells in vitro.* Blood, 2003. **102**(7): p. 2541-6.
237. Berg, R.E., C.J. Cordes, and J. Forman, *Contribution of CD8+ T cells to innate immunity: IFN-gamma secretion induced by IL-12 and IL-18.* Eur J Immunol, 2002. **32**(10): p. 2807-16.
238. Berg, R.E., et al., *Memory CD8+ T cells provide innate immune protection against Listeria monocytogenes in the absence of cognate antigen.* J Exp Med, 2003. **198**(10): p. 1583-93.
239. Soudja, S.M., et al., *Inflammatory monocytes activate memory CD8(+) T and innate NK lymphocytes independent of cognate antigen during microbial pathogen invasion.* Immunity, 2012. **37**(3): p. 549-62.
240. Chen, H.D., et al., *Memory CD8+ T cells in heterologous antiviral immunity and immunopathology in the lung.* Nat Immunol, 2001. **2**(11): p. 1067-76.
241. Marsland, B.J., et al., *Bystander suppression of allergic airway inflammation by lung resident memory CD8+ T cells.* Proc Natl Acad Sci U S A, 2004. **101**(16): p. 6117-21.
242. Unutmaz, D., P. Pileri, and S. Abrignani, *Antigen-independent activation of naive and memory resting T cells by a cytokine combination.* J Exp Med, 1994. **180**(3): p. 1159-64.
243. Guo, L., et al., *IL-1 family members and STAT activators induce cytokine production by Th2, Th17, and Th1 cells.* Proc Natl Acad Sci U S A, 2009. **106**(32): p. 13463-8.
244. Suwannasaen, D., et al., *Bystander T cells in human immune responses to dengue antigens.* BMC Immunol, 2010. **11**(47).

245. Srinivasan, A., et al., *Innate immune activation of CD4 T cells in salmonella-infected mice is dependent on IL-18.* J Immunol, 2007. **178**(10): p. 6342-9.
246. Pham, O.H., et al., *T cell expression of IL-18R and DR3 is essential for non-cognate stimulation of Th1 cells and optimal clearance of intracellular bacteria.* PLoS Pathog, 2017. **13**(8): p. e1006566.
247. Nogai, A., et al., *Lipopolysaccharide injection induces relapses of experimental autoimmune encephalomyelitis in nontransgenic mice via bystander activation of autoreactive CD4+ cells.* J Immunol, 2005. **175**(2): p. 959-66.
248. Guo, L., et al., *Innate immunological function of TH2 cells in vivo.* Nat Immunol, 2015. **16**(10): p. 1051-9.
249. Nian, H., et al., *Characterization of autoreactive and bystander IL-17+ T cells induced in immunized C57BL/6 mice.* Invest Ophthalmol Vis Sci, 2012. **53**(2): p. 897-905.
250. Lee, H.G., et al., *Pathogenic function of bystander-activated memory-like CD4(+) T cells in autoimmune encephalomyelitis.* Nat Commun, 2019. **10**(1): p. 709.
251. Edwards, S.C., S.C. Higgins, and K.H.G. Mills, *Respiratory infection with a bacterial pathogen attenuates CNS autoimmunity through IL-10 induction.* Brain Behav Immun, 2015. **50**: p. 41-46.
252. Melchers, F., *Checkpoints that control B cell development.* J Clin Invest, 2015. **125**(6): p. 2203-10.
253. Nothelfer, K., P.J. Sansonetti, and A. Phalipon, *Pathogen manipulation of B cells: the best defence is a good offence.* Nat Rev Microbiol, 2015. **13**(3): p. 173-84.
254. Akkaya, M., K. Kwak, and S.K. Pierce, *B cell memory: building two walls of protection against pathogens.* Nat Rev Immunol, 2020. **20**(4): p. 229-238.
255. Hoffman, W., F.G. Lakkis, and G. Chalasani, *B Cells, Antibodies, and More.* Clin J Am Soc Nephrol, 2016. **11**(1): p. 137-54.
256. Schroeder, H.W., Jr. and L. Cavacini, *Structure and function of immunoglobulins.* J Allergy Clin Immunol, 2010. **125**(2 Suppl 2): p. S41-52.
257. Higgs, R., et al., *Immunity to the respiratory pathogen Bordetella pertussis.* Mucosal Immunol, 2012. **5**(5): p. 485-500.
258. de Graaf, H., et al., *Controlled Human Infection With Bordetella pertussis Induces Asymptomatic, Immunizing Colonization.* Clin Infect Dis, 2020. **71**(2): p. 403-411.
259. Storsaeter, J., et al., *Levels of anti-pertussis antibodies related to protection after household exposure to Bordetella pertussis.* Vaccine, 1998. **16**(20): p. 1907-16.
260. Cherry, J.D., et al., *A search for serologic correlates of immunity to Bordetella pertussis cough illnesses.* Vaccine, 1998. **16**(20): p. 1901-6.
261. Goodman, Y.E., A.J. Wort, and F.L. Jackson, *Enzyme-linked immunosorbent assay for detection of pertussis immunoglobulin A in nasopharyngeal secretions as an indicator of recent infection.* J Clin Microbiol, 1981. **13**(2): p. 286-92.
262. Tuomanen, E.I., et al., *Characterization of antibody inhibiting adherence of Bordetella pertussis to human respiratory epithelial cells.* J Clin Microbiol, 1984. **20**(2): p. 167-70.
263. Hellwig, S.M., et al., *Immunoglobulin A-mediated protection against Bordetella pertussis infection.* Infect Immun, 2001. **69**(8): p. 4846-50.
264. Halperin, S.A., et al., *Is pertussis immune globulin efficacious for the treatment of hospitalized infants with pertussis? No answer yet.* Pediatr Infect Dis J, 2007. **26**(1): p. 79-81.
265. Lucchesi, P.F. and A.C. LaBoccetta, *Whooping cough treated with pertussis immune serum, human; report on a controlled series of 52 patients under 1 year of age.* Am J Dis Child, 1949. **77**(1): p. 15-24.
266. Granström, M., et al., *Specific immunoglobulin for treatment of whooping cough.* Lancet, 1991. **338**(8777): p. 1230-3.

267. Wolfe, D.N., et al., *Comparative role of immunoglobulin A in protective immunity against the Bordetellae.* Infect Immun, 2007. **75**(9): p. 4416-22.
268. Barnard, A., et al., *Th1/Th2 cell dichotomy in acquired immunity to Bordetella pertussis: variables in the in vivo priming and in vitro cytokine detection techniques affect the classification of T-cell subsets as Th1, Th2 or Th0.* Immunology, 1996. **87**(3): p. 372-80.
269. Mills, K.H., et al., *A murine model in which protection correlates with pertussis vaccine efficacy in children reveals complementary roles for humoral and cell-mediated immunity in protection against Bordetella pertussis.* Infect Immun, 1998. **66**(2): p. 594-602.
270. Wilk, M.M. and K.H.G. Mills, *CD4 TRM Cells Following Infection and Immunization: Implications for More Effective Vaccine Design.* Front Immunol, 2018. **9**(1860).
271. Higgins, S.C., et al., *TLR4 mediates vaccine-induced protective cellular immunity to Bordetella pertussis: role of IL-17-producing T cells.* J Immunol, 2006. **177**(11): p. 7980-9.
272. Choy, D.F., et al., *TH2 and TH17 inflammatory pathways are reciprocally regulated in asthma.* Sci Transl Med, 2015. **7**(301): p. 301ra129.
273. Ausiello, C.M., et al., *Vaccine- and antigen-dependent type 1 and type 2 cytokine induction after primary vaccination of infants with whole-cell or acellular pertussis vaccines.* Infect Immun, 1997. **65**(6): p. 2168-74.
274. Ryan, M., et al., *Distinct T-cell subtypes induced with whole cell and acellular pertussis vaccines in children.* Immunology, 1998. **93**(1): p. 1-10.
275. Ryan, E.J., et al., *Booster immunization of children with an acellular pertussis vaccine enhances Th2 cytokine production and serum IgE responses against pertussis toxin but not against common allergens.* Clin Exp Immunol, 2000. **121**(2): p. 193-200.
276. Le, T., et al., *Immune responses and antibody decay after immunization of adolescents and adults with an acellular pertussis vaccine: the APERT Study.* J Infect Dis, 2004. **190**(3).
277. Witt, M.A., P.H. Katz, and D.J. Witt, *Unexpectedly limited durability of immunity following acellular pertussis vaccination in preadolescents in a North American outbreak.* Clin Infect Dis, 2012. **54**(12): p. 1730-5.
278. Chisholm, R.H., et al., *Implications of asymptomatic carriers for infectious disease transmission and control.* R Soc Open Sci, 2018. **5**(2): p. 172341.
279. Althouse, B.M. and S.V. Scarpino, *Asymptomatic transmission and the resurgence of Bordetella pertussis.* BMC Med, 2015. **13**: p. 146.
280. Craig, R., et al., *Asymptomatic Infection and Transmission of Pertussis in Households: A Systematic Review.* Clin Infect Dis, 2020. **70**(1): p. 152-161.
281. da Silva Antunes, R., et al., *Th1/Th17 polarization persists following whole-cell pertussis vaccination despite repeated acellular boosters.* J Clin Invest, 2018. **128**(9): p. 3853-3865.
282. Zens, K.D., J.K. Chen, and D.L. Farber, *Vaccine-generated lung tissue-resident memory T cells provide heterosubtypic protection to influenza infection.* JCI Insight, 2016. **1**(10).
283. Fan, X., et al., *Intrapulmonary Vaccination Induces Long-lasting and Effective Pulmonary Immunity Against Staphylococcus aureus Pneumonia.* J Infect Dis, 2021. **224**(5): p. 903-913.
284. Xu, N., et al., *Vaccine-induced gastric CD4(+) tissue-resident memory T cells proliferate in situ to amplify immune response against Helicobacter pylori insult.* Helicobacter, 2019. **24**(5): p. e12652.
285. Mielcarek, N., et al., *Live attenuated B. pertussis as a single-dose nasal vaccine against whooping cough.* PLoS Pathog, 2006. **2**(7): p. e65.
286. Solans, L., et al., *IL-17-dependent SIgA-mediated protection against nasal Bordetella pertussis infection by live attenuated BPZE1 vaccine.* Mucosal Immunol, 2018. **11**(6): p. 1753-1762.

287. Jahnmatz, M., et al., *Safety and immunogenicity of the live attenuated intranasal pertussis vaccine BPZE1: a phase 1b, double-blind, randomised, placebo-controlled dose-escalation study.* The Lancet Infectious Diseases, 2020. **20**(11): p. 1290-1301.
288. Balhuizen, M.D., E.J.A. Veldhuizen, and H.P. Haagsman, *Outer Membrane Vesicle Induction and Isolation for Vaccine Development.* Front Microbiol, 2021. **12**: p. 629090.
289. Zurita, M.E., et al., *A Pertussis Outer Membrane Vesicle-Based Vaccine Induces Lung-Resident Memory CD4 T Cells and Protection Against Bordetella pertussis, Including Pertactin Deficient Strains.* Front Cell Infect Microbiol, 2019. **9**: p. 125.
290. Chasaide, C.N. and K.H.G. Mills, *Next-Generation Pertussis Vaccines Based on the Induction of Protective T Cells in the Respiratory Tract.* Vaccines (Basel), 2020. **8**(4).
291. Allen, A.C., et al., *Sustained protective immunity against Bordetella pertussis nasal colonization by intranasal immunization with a vaccine-adjuvant combination that induces IL-17-secreting TRM cells.* Mucosal Immunol, 2018. **11**(6): p. 1763-1776.
292. Marr, N., et al., *Variability in the lipooligosaccharide structure and endotoxicity among Bordetella pertussis strains.* J Infect Dis, 2010. **202**(12): p. 1897-906.
293. Caro, V., V. Bouchez, and N. Guiso, *Is the Sequenced Bordetella pertussis strain Tohama I representative of the species?* J Clin Microbiol, 2008. **46**(6): p. 2125-8.
294. Boivin, G., et al., *Durable and controlled depletion of neutrophils in mice.* Nat Commun, 2020. **11**(1): p. 2762.
295. Pizzolla, A., et al., *Resident memory CD8+ T cells in the upper respiratory tract prevent pulmonary influenza virus infection.* Sci Immunol, 2017. **2**(12): p. eaam6970.
296. Zharkova, O., et al., *A Flow Cytometry-Based Assay for High-Throughput Detection and Quantification of Neutrophil Extracellular Traps in Mixed Cell Populations.* Cytometry A, 2019. **95**(3): p. 268-278.
297. Borkner, L., et al., *IL-17 mediates protective immunity against nasal infection with Bordetella pertussis by mobilizing neutrophils, especially Siglec-F(+) neutrophils.* Mucosal Immunol, 2021. **14**(5): p. 1183-1202.
298. Gill, C., P. Rohani, and D.M. Thea, *The relationship between mucosal immunity, nasopharyngeal carriage, asymptomatic transmission and the resurgence of Bordetella pertussis.* F1000Res, 2017. **6**: p. 1568.
299. Solans, L. and C. Locht, *The Role of Mucosal Immunity in Pertussis.* Front Immunol, 2018. **9**: p. 3068.
300. Jameson, S.C. and D. Masopust, *Understanding Subset Diversity in T Cell Memory.* Immunity, 2018. **48**(2): p. 214-226.
301. Mueller, S.N. and L.K. Mackay, *Tissue-resident memory T cells: local specialists in immune defence.* Nat Rev Immunol, 2016. **16**(2): p. 79-89.
302. Schreiner, D. and C.G. King, *CD4+ Memory T Cells at Home in the Tissue: Mechanisms for Health and Disease.* Front Immunol, 2018. **9**: p. 2394.
303. McGeachy, M.J. and D.J. Cua, *Th17 cell differentiation: the long and winding road.* Immunity, 2008. **28**(4): p. 445-53.
304. Lu, Y.J., et al., *Interleukin-17A mediates acquired immunity to pneumococcal colonization.* PLoS Pathog, 2008. **4**(9): p. e1000159.
305. Archer, N.K., J.M. Harro, and M.E. Shirtliff, *Clearance of Staphylococcus aureus nasal carriage is T cell dependent and mediated through interleukin-17A expression and neutrophil influx.* Infect Immun, 2013. **81**(6): p. 2070-5.
306. Warfel, J.M., L.I. Zimmerman, and T.J. Merkel, *Comparison of Three Whole-Cell Pertussis Vaccines in the Baboon Model of Pertussis.* Clin Vaccine Immunol, 2016. **23**(1): p. 47-54.
307. McGinley, A.M., et al., *Interleukin-17A Serves a Priming Role in Autoimmunity by Recruiting IL-1beta-Producing Myeloid Cells that Promote Pathogenic T Cells.* Immunity, 2020. **52**(2): p. 342-356 e6.

308. Mitsdoerffer, M., et al., *Proinflammatory T helper type 17 cells are effective B-cell helpers.* Proc Natl Acad Sci U S A, 2010. **107**(32): p. 14292-7.
309. Chiba, K., et al., *FTY720, a novel immunosuppressant, induces sequestration of circulating mature lymphocytes by acceleration of lymphocyte homing in rats. I. FTY720 selectively decreases the number of circulating mature lymphocytes by acceleration of lymphocyte homing.* J Immunol, 1998. **160**(10): p. 5037-44.
310. Xiong, H., et al., *Innate Lymphocyte/Ly6C(hi) Monocyte Crosstalk Promotes Klebsiella Pneumoniae Clearance.* Cell, 2016. **165**(3): p. 679-89.
311. Crocker, P.R., J.C. Paulson, and A. Varki, *Siglecs and their roles in the immune system.* Nat Rev Immunol, 2007. **7**(4): p. 255-66.
312. Kiwamoto, T., et al., *The role of lung epithelial ligands for Siglec-8 and Siglec-F in eosinophilic inflammation.* Curr Opin Allergy Clin Immunol, 2013. **13**(1): p. 106-11.
313. Kirby, A.C., M.C. Coles, and P.M. Kaye, *Alveolar macrophages transport pathogens to lung draining lymph nodes.* J Immunol, 2009. **183**(3): p. 1983-9.
314. Gicheva, N., et al., *Siglec-F is a novel intestinal M cell marker.* Biochem Biophys Res Commun, 2016. **479**(1): p. 1-4.
315. Bolden, J.E., et al., *Identification of a Siglec-F+ granulocyte-macrophage progenitor.* J Leukoc Biol, 2018. **104**(1): p. 123-133.
316. Matsui, M., et al., *A novel Siglec-F(+) neutrophil subset in the mouse nasal mucosa exhibits an activated phenotype and is increased in an allergic rhinitis model.* Biochem Biophys Res Commun, 2020. **526**(3): p. 599-606.
317. Shin, J.W., et al., *A unique population of neutrophils generated by air pollutant-induced lung damage exacerbates airway inflammation.* J Allergy Clin Immunol, 2021.
318. Pfirschke, C., et al., *Tumor-Promoting Ly-6G(+) SiglecF(high) Cells Are Mature and Long-Lived Neutrophils.* Cell Rep, 2020. **32**(12): p. 108164.
319. Stadtmann, A. and A. Zarbock, *CXCR2: From Bench to Bedside.* Front Immunol, 2012. **3**: p. 263.
320. Ogawa, K., et al., *Frontline Science: Conversion of neutrophils into atypical Ly6G(+) SiglecF(+) immune cells with neurosupportive potential in olfactory neuroepithelium.* J Leukoc Biol, 2021. **109**(3): p. 481-496.
321. Tsai, W.C., et al., *CXC chemokine receptor CXCR2 is essential for protective innate host response in murine Pseudomonas aeruginosa pneumonia.* Infect Immun, 2000. **68**(7): p. 4289-96.
322. Tateda, K., et al., *Chemokine-dependent neutrophil recruitment in a murine model of Legionella pneumonia: potential role of neutrophils as immunoregulatory cells.* Infect Immun, 2001. **69**(4): p. 2017-24.
323. Ye, P., et al., *Requirement of interleukin 17 receptor signaling for lung CXC chemokine and granulocyte colony-stimulating factor expression, neutrophil recruitment, and host defense.* J Exp Med, 2001. **194**(4): p. 519-27.
324. Ajendra, J., et al., *IL-17A both initiates, via IFNgamma suppression, and limits the pulmonary type-2 immune response to nematode infection.* Mucosal Immunol, 2020. **13**(6): p. 958-968.
325. Onishi, R.M. and S.L. Gaffen, *Interleukin-17 and its target genes: mechanisms of interleukin-17 function in disease.* Immunology, 2010. **129**(3): p. 311-21.
326. Ye, P., et al., *Interleukin-17 and lung host defense against Klebsiella pneumoniae infection.* Am J Respir Cell Mol Biol, 2001. **25**(3): p. 335-40.
327. Li, Y., L. Jin, and T. Chen, *The Effects of Secretory IgA in the Mucosal Immune System.* Biomed Res Int, 2020. **2020**: p. 2032057.
328. Jaffar, Z., et al., *Cutting edge: lung mucosal Th17-mediated responses induce polymeric Ig receptor expression by the airway epithelium and elevate secretory IgA levels.* J Immunol, 2009. **182**(8): p. 4507-11.

329. Christensen, D., et al., *Vaccine-induced Th17 cells are established as resident memory cells in the lung and promote local IgA responses.* Mucosal Immunol, 2017. **10**(1): p. 260-270.
330. Ciric, B., et al., *IL-23 drives pathogenic IL-17-producing CD8+ T cells.* J Immunol, 2009. **182**(9): p. 5296-305.
331. Marshall, J.S., et al., *An introduction to immunology and immunopathology.* Allergy Asthma Clin Immunol, 2018. **14**(Suppl 2): p. 49.
332. Schenkel, J.M. and D. Masopust, *Tissue-resident memory T cells.* Immunity, 2014. **41**(6): p. 886-97.
333. Pan, Y. and T.S. Kupper, *Metabolic Reprogramming and Longevity of Tissue-Resident Memory T Cells.* Front Immunol, 2018. **9**: p. 1347.
334. Kamran, P., et al., *Parabiosis in mice: a detailed protocol.* J Vis Exp, 2013(80).
335. Zhi, L., et al., *FTY720 blocks egress of T cells in part by abrogation of their adhesion on the lymph node sinus.* J Immunol, 2011. **187**(5): p. 2244-51.
336. Florido, M., et al., *Pulmonary immunization with a recombinant influenza A virus vaccine induces lung-resident CD4(+) memory T cells that are associated with protection against tuberculosis.* Mucosal Immunol, 2018. **11**(6): p. 1743-1752.
337. O'Hara, J.M., et al., *Generation of protective pneumococcal-specific nasal resident memory CD4(+) T cells via parenteral immunization.* Mucosal Immunol, 2020. **13**(1): p. 172-182.
338. Gu, Z.W., Y.X. Wang, and Z.W. Cao, *Neutralization of interleukin-17 suppresses allergic rhinitis symptoms by downregulating Th2 and Th17 responses and upregulating the Treg response.* Oncotarget, 2017. **8**(14): p. 22361-22369.
339. Ferreira, M.C., et al., *Interleukin-17-induced protein lipocalin 2 is dispensable for immunity to oral candidiasis.* Infect Immun, 2014. **82**(3): p. 1030-5.
340. Archer, N.K., et al., *Interleukin-17A (IL-17A) and IL-17F Are Critical for Antimicrobial Peptide Production and Clearance of Staphylococcus aureus Nasal Colonization.* Infect Immun, 2016. **84**(12): p. 3575-3583.
341. Zeng, B., et al., *ILC3 function as a double-edged sword in inflammatory bowel diseases.* Cell Death Dis, 2019. **10**(4): p. 315.
342. Lu, B., et al., *IL-17 production by tissue-resident MAIT cells is locally induced in children with pneumonia.* Mucosal Immunol, 2020. **13**(5): p. 824-835.
343. Wu, Z., et al., *CD3(+)CD4(-)CD8(-) (Double-Negative) T Cells in Inflammation, Immune Disorders and Cancer.* Front Immunol, 2022. **13**: p. 816005.
344. Godfrey, D.I., et al., *The biology and functional importance of MAIT cells.* Nat Immunol, 2019. **20**(9): p. 1110-1128.
345. Rha, M.S., et al., *IL-17A-producing sinonasal MAIT cells in patients with chronic rhinosinusitis with nasal polyps.* J Allergy Clin Immunol, 2022. **149**(2): p. 599-609 e7.
346. Yang, D., et al., *The Role of Group 3 Innate Lymphoid Cells in Lung Infection and Immunity.* Front Cell Infect Microbiol, 2021. **11**: p. 586471.
347. Bayes, H.K., N.D. Ritchie, and T.J. Evans, *Interleukin-17 Is Required for Control of Chronic Lung Infection Caused by Pseudomonas aeruginosa.* Infect Immun, 2016. **84**(12): p. 3507-3516.
348. Ge, C., et al., *Bystander Activation of Pulmonary Trm Cells Attenuates the Severity of Bacterial Pneumonia by Enhancing Neutrophil Recruitment.* Cell Rep, 2019. **29**(13): p. 4236-4244 e3.
349. Smith-Garvin, J.E., G.A. Koretzky, and M.S. Jordan, *T cell activation.* Annu Rev Immunol, 2009. **27**: p. 591-619.
350. Zhu, J., H. Yamane, and W.E. Paul, *Differentiation of effector CD4 T cell populations (*).* Annu Rev Immunol, 2010. **28**: p. 445-89.

351. Maurice, N.J., A.K. Taber, and M. Prlic, *The Ugly Duckling Turned to Swan: A Change in Perception of Bystander-Activated Memory CD8 T Cells.* J Immunol, 2021. **206**(3): p. 455-462.
352. Lee, H., S. Jeong, and E.C. Shin, *Significance of bystander T cell activation in microbial infection.* Nat Immunol, 2022. **23**(1): p. 13-22.
353. Panda, S.K. and M. Colonna, *Innate Lymphoid Cells in Mucosal Immunity.* Front Immunol, 2019. **10**: p. 861.
354. McGinty, J.W. and J. von Moltke, *A three course menu for ILC and bystander T cell activation.* Curr Opin Immunol, 2020. **62**: p. 15-21.
355. Raue, H.P., et al., *Activation of virus-specific CD8+ T cells by lipopolysaccharide-induced IL-12 and IL-18.* J Immunol, 2004. **173**(11): p. 6873-81.
356. Freeman, B.E., et al., *Regulation of innate CD8+ T-cell activation mediated by cytokines.* Proc Natl Acad Sci U S A, 2012. **109**(25): p. 9971-6.
357. Doisne, J.M., et al., *CD8+ T cells specific for EBV, cytomegalovirus, and influenza virus are activated during primary HIV infection.* J Immunol, 2004. **173**(4): p. 2410-8.
358. van Beelen, A.J., et al., *Stimulation of the intracellular bacterial sensor NOD2 programs dendritic cells to promote interleukin-17 production in human memory T cells.* Immunity, 2007. **27**(4): p. 660-9.
359. Kondrack, R.M., et al., *Interleukin 7 regulates the survival and generation of memory CD4 cells.* J Exp Med, 2003. **198**(12): p. 1797-806.
360. Boise, L.H., et al., *Growth factors can enhance lymphocyte survival without committing the cell to undergo cell division.* Proc Natl Acad Sci U S A, 1995. **92**(12): p. 5491-5.
361. Martin, R.M. and M.A. Bachman, *Colonization, Infection, and the Accessory Genome of Klebsiella pneumoniae.* Front Cell Infect Microbiol, 2018. **8**: p. 4.
362. Chakir, H., et al., *"Bystander polarization" of CD4+ T cells: activation with high-dose IL-2 renders naive T cells responsive to IL-12 and/or IL-18 in the absence of TCR ligation.* Eur J Immunol, 2003. **33**(7): p. 1788-98.
363. Holmkvist, P., et al., *A major population of mucosal memory CD4+ T cells, coexpressing IL-18Ralpha and DR3, display innate lymphocyte functionality.* Mucosal Immunol, 2015. **8**(3): p. 545-58.
364. Fedele, G., et al., *Lipopolysaccharides from Bordetella pertussis and Bordetella parapertussis differently modulate human dendritic cell functions resulting in divergent prevalence of Th17-polarized responses.* J Immunol, 2008. **181**(1): p. 208-16.
365. Reynolds, J.M., et al., *Toll-like receptor 4 signaling in T cells promotes autoimmune inflammation.* Proc Natl Acad Sci U S A, 2012. **109**(32): p. 13064-9.
366. Kim, T.S. and E.C. Shin, *The activation of bystander CD8(+) T cells and their roles in viral infection.* Exp Mol Med, 2019. **51**(12): p. 1-9.
367. Lertmemongkolchai, G., et al., *Bystander activation of CD8+ T cells contributes to the rapid production of IFN-gamma in response to bacterial pathogens.* J Immunol, 2001. **166**(2): p. 1097-105.
368. Bengoechea, J.A. and J. Sa Pessoa, *Klebsiella pneumoniae infection biology: living to counteract host defences.* FEMS Microbiol Rev, 2019. **43**(2): p. 123-144.
369. Opoku-Temeng, C., et al., *Innate Host Defense against Klebsiella pneumoniae and the Outlook for Development of Immunotherapies.* J Innate Immun, 2021: p. 1-15.
370. Xiong, H., et al., *Distinct Contributions of Neutrophils and CCR2+ Monocytes to Pulmonary Clearance of Different Klebsiella pneumoniae Strains.* Infect Immun, 2015. **83**(9): p. 3418-27.
371. Netea, M.G., et al., *Defining trained immunity and its role in health and disease.* Nat Rev Immunol, 2020. **20**(6): p. 375-388.

372. Hirche, T.O., et al., *Myeloperoxidase plays critical roles in killing Klebsiella pneumoniae and inactivating neutrophil elastase: effects on host defense.* J Immunol, 2005. **174**(3): p. 1557-65.
373. Agrawal, B., *Heterologous Immunity: Role in Natural and Vaccine-Induced Resistance to Infections.* Front Immunol, 2019. **10**: p. 2631.
374. Saadatian-Elahi, M., et al., *Heterologous vaccine effects.* Vaccine, 2016. **34**(34): p. 3923-30.
375. Cauchi, S. and C. Locht, *Non-specific Effects of Live Attenuated Pertussis Vaccine Against Heterologous Infectious and Inflammatory Diseases.* Front Immunol, 2018. **9**: p. 2872.
376. Aaby, P., et al., *Non-specific beneficial effect of measles immunisation: analysis of mortality studies from developing countries.* BMJ, 1995. **311**(7003): p. 481-5.
377. Redelman-Sidi, G., M.S. Glickman, and B.H. Bochner, *The mechanism of action of BCG therapy for bladder cancer--a current perspective.* Nat Rev Urol, 2014. **11**(3): p. 153-62.
378. Sewell, A.K., *Why must T cells be cross-reactive?* Nat Rev Immunol, 2012. **12**(9): p. 669-77.
379. Kleinnijenhuis, J., et al., *Bacille Calmette-Guerin induces NOD2-dependent nonspecific protection from reinfection via epigenetic reprogramming of monocytes.* Proc Natl Acad Sci U S A, 2012. **109**(43): p. 17537-42.
380. Kleinnijenhuis, J., et al., *Long-lasting effects of BCG vaccination on both heterologous Th1/Th17 responses and innate trained immunity.* J Innate Immun, 2014. **6**(2): p. 152-8.
381. David, S., R. van Furth, and F.R. Mooi, *Efficacies of whole cell and acellular pertussis vaccines against Bordetella parapertussis in a mouse model.* Vaccine, 2004. **22**(15-16): p. 1892-8.
382. Feunou, P.F., J. Bertout, and C. Locht, *T- and B-cell-mediated protection induced by novel, live attenuated pertussis vaccine in mice. Cross protection against parapertussis.* PLoS One, 2010. **5**(4): p. e10178.
383. Belcher, T., et al., *Live attenuated Bordetella pertussis vaccine candidate BPZE1 transiently protects against lethal pneumococcal disease in mice.* Vaccine, 2022. **40**(11): p. 1555-1562.
384. Li, R., et al., *Attenuated Bordetella pertussis protects against highly pathogenic influenza A viruses by dampening the cytokine storm.* J Virol, 2010. **84**(14): p. 7105-13.
385. Schnoeller, C., et al., *Attenuated Bordetella pertussis vaccine protects against respiratory syncytial virus disease via an IL-17-dependent mechanism.* Am J Respir Crit Care Med, 2014. **189**(2): p. 194-202.
386. Li, R., et al., *Attenuated Bordetella pertussis BPZE1 protects against allergic airway inflammation and contact dermatitis in mouse models.* Allergy, 2012. **67**(10): p. 1250-8.
387. Chen, K., et al., *IL-17 Receptor Signaling in the Lung Epithelium Is Required for Mucosal Chemokine Gradients and Pulmonary Host Defense against K. pneumoniae.* Cell Host Microbe, 2016. **20**(5): p. 596-605.
388. Dubois, V. and C. Locht, *Mucosal Immunization Against Pertussis: Lessons From the Past and Perspectives.* Front Immunol, 2021. **12**: p. 701285.
389. Berstad, A.K., et al., *Induction of antigen-specific T cell responses in human volunteers after intranasal immunization with a whole-cell pertussis vaccine.* Vaccine, 2000. **18**(22): p. 2323-30.
390. Wolf, M.A., et al., *Intranasal Immunization with Acellular Pertussis Vaccines Results in Long-Term Immunity to Bordetella pertussis in Mice.* Infect Immun, 2021. **89**(3): p. e00607-20.
391. Gangappa, S., S.P. Deshpande, and B.T. Rouse, *Bystander activation of CD4+ T cells accounts for herpetic ocular lesions.* Invest Ophthalmol Vis Sci, 2000. **41**(2): p. 453-9.
392. Yeung, K.H.T., et al., *An update of the global burden of pertussis in children younger than 5 years: a modelling study.* The Lancet Infectious Diseases, 2017. **17**(9): p. 974-980.

393. Lapidot, R. and C.J. Gill, *The Pertussis resurgence: putting together the pieces of the puzzle.* Trop Dis Travel Med Vaccines, 2016. **2**: p. 26.
394. Gill, C.J., et al., *Asymptomatic Bordetella pertussis infections in a longitudinal cohort of young African infants and their mothers.* Elife, 2021. **10**.
395. Sakr, A., et al., *Staphylococcus aureus Nasal Colonization: An Update on Mechanisms, Epidemiology, Risk Factors, and Subsequent Infections.* Front Microbiol, 2018. **9**: p. 2419.
396. Regev-Yochay, G., et al., *Nasopharyngeal carriage of Streptococcus pneumoniae by adults and children in community and family settings.* Clin Infect Dis, 2004. **38**(5): p. 632-9.
397. Henderson, F.W., et al., *Nasopharyngeal carriage of antibiotic-resistant pneumococci by children in group day care.* J Infect Dis, 1988. **157**(2): p. 256-63.
398. WHO. *WHO Coronavirus (COVID-19) Dashboard*. 2022 [cited 2022 April 26]; Available from: https://covid19.who.int/.
399. Zhang, C., et al., *Asymptomatic Transmissibility Calls for Implementing a Zero-COVID Strategy to End the Current Global Crisis.* Frontiers in Cellular and Infection Microbiology, 2022. **12**.
400. Song, X., et al., *The roles and functional mechanisms of interleukin-17 family cytokines in mucosal immunity.* Cell Mol Immunol, 2016. **13**(4): p. 418-31.
401. Sivick, K.E., et al., *The innate immune response to uropathogenic Escherichia coli involves IL-17A in a murine model of urinary tract infection.* J Immunol, 2010. **184**(4): p. 2065-75.
402. Huang, W., et al., *Requirement of interleukin-17A for systemic anti-Candida albicans host defense in mice.* J Infect Dis, 2004. **190**(3): p. 624-31.
403. Yu, S., et al., *Local IL-17 positive T cells are functionally associated with neutrophil infiltration and their development is regulated by mucosal microenvironment in nasal polyps.* Inflamm Res, 2021. **70**(1): p. 139-149.
404. Tenland, E., et al., *Innate Immune Responses after Airway Epithelial Stimulation with Mycobacterium bovis Bacille-Calmette Guerin.* PLoS One, 2016. **11**(10): p. e0164431.
405. Zhao, J., et al., *The role of interleukin-17 in tumor development and progression.* J Exp Med, 2020. **217**(1).
406. Kwok, I., et al., *Combinatorial Single-Cell Analyses of Granulocyte-Monocyte Progenitor Heterogeneity Reveals an Early Uni-potent Neutrophil Progenitor.* Immunity, 2020. **53**(2): p. 303-318 e5.
407. Calcagno, D.M., et al., *SiglecF(HI) Marks Late-Stage Neutrophils of the Infarcted Heart: A Single-Cell Transcriptomic Analysis of Neutrophil Diversification.* J Am Heart Assoc, 2021. **10**(4): p. e019019.
408. Elahi, S., J. Holmstrom, and V. Gerdts, *The benefits of using diverse animal models for studying pertussis.* Trends Microbiol, 2007. **15**(10): p. 462-8.
409. Cimolai, N., *Non-primate animal models for pertussis: back to the drawing board?* Appl Microbiol Biotechnol, 2022. **106**(4): p. 1383-1398.
410. Elahi, S., et al., *Infection of newborn piglets with Bordetella pertussis: a new model for pertussis.* Infect Immun, 2005. **73**(6): p. 3636-45.
411. Zimmerman, L.I., et al., *Histopathology of Bordetella pertussis in the Baboon Model.* Infect Immun, 2018. **86**(11).
412. Warfel, J.M., et al., *Nonhuman primate model of pertussis.* Infect Immun, 2012. **80**(4): p. 1530-6.
413. Jiang, W., et al., *Infant rhesus macaques as a non-human primate model of Bordetella pertussis infection.* BMC Infect Dis, 2021. **21**(1): p. 407.
414. Mills, K.H. and V. Gerdts, *Mouse and pig models for studies of natural and vaccine-induced immunity to Bordetella pertussis.* J Infect Dis, 2014. **209 Suppl 1**: p. S16-9.

415. Mosley, Y.C., F. Lu, and H. HogenEsch, *Differences in innate IFNgamma and IL-17 responses to Bordetella pertussis between BALB/c and C57BL/6 mice: role of gammadeltaT cells, NK cells, and dendritic cells.* Immunol Res, 2017. **65**(6): p. 1139-1149.
416. Holubova, J., et al., *The Fim and FhaB adhesins play a crucial role in nasal cavity infection and Bordetella pertussis transmission in a novel mouse catarrhal infection model.* PLoS Pathog, 2022. **18**(4): p. e1010402.
417. Soumana, I.H., et al., *Modeling the catarrhal stage of Bordetella pertussis upper respiratory tract infections in mice.* Dis Model Mech, 2022. **dmm.049266**.
418. Merkel, T.J., *Toward a Controlled Human Infection Model of Pertussis.* Clin Infect Dis, 2020. **71**(2): p. 412-414.
419. Chavda, V.P., et al., *Intranasal vaccines for SARS-CoV-2: From challenges to potential in COVID-19 management.* Drug Discov Today, 2021. **26**(11): p. 2619-2636.
420. Afkhami, S., et al., *Respiratory mucosal delivery of next-generation COVID-19 vaccine provides robust protection against both ancestral and variant strains of SARS-CoV-2.* Cell, 2022. **185**(5): p. 896-915 e19.
421. Mestecky, J., *The common mucosal immune system and current strategies for induction of immune responses in external secretions.* J Clin Immunol, 1987. **7**(4): p. 265-76.
422. Gherardi, M.M., et al., *Induction of HIV immunity in the genital tract after intranasal delivery of a MVA vector: enhanced immunogenicity after DNA prime-modified vaccinia virus Ankara boost immunization schedule.* J Immunol, 2004. **172**(10): p. 6209-20.
423. Grohskopf, L.A., et al., *Prevention and Control of Seasonal Influenza with Vaccines.* MMWR Recomm Rep, 2016. **65**(5): p. 1-54.
424. HSE. *Children's flu vaccine*. 2021 2021 Nov 2021 [cited 2022 March 18]; Available from: https://www2.hse.ie/screening-and-vaccinations/flu-vaccine/children/.
425. Xu, H., et al., *Intranasal vaccine: Factors to consider in research and development.* Int J Pharm, 2021. **609**: p. 121180.
426. Welsh, R.M.F., R. S., *Pathogenic epitopes, heterologous immunity and vaccine design.* Nat Rev Microbiol, 2007. **5**(7): p. 555-63.
427. Kroes, M.M., et al., *Bordetella pertussis-infected innate immune cells drive the anti-pertussis response of human airway epithelium.* Sci Rep, 2022. **12**(1): p. 3622.
428. Lesne, E., et al., *Acellular Pertussis Vaccines Induce Anti-pertactin Bactericidal Antibodies Which Drives the Emergence of Pertactin-Negative Strains.* Front Microbiol, 2020. **11**: p. 2108.
429. Takamura, S., *Niches for the Long-Term Maintenance of Tissue-Resident Memory T Cells.* Front Immunol, 2018. **9**(1214).
430. Bergsbaken, T., M.J. Bevan, and P.J. Fink, *Local Inflammatory Cues Regulate Differentiation and Persistence of CD8(+) Tissue-Resident Memory T Cells.* Cell Rep, 2017. **19**(1): p. 114-124.
431. Iijima, N. and A. Iwasaki, *T cell memory. A local macrophage chemokine network sustains protective tissue-resident memory CD4 T cells.* Science, 2014. **346**(6205): p. 93-8.